

Novel nanostructured lipid carriers based on Ω -3 polyunsaturated fatty acids and TAT peptide for neurodegenerative disease treatment

Lipido-garraiatzaile nanoegituratu berriak Ω -3 gantz-azido poliinsaturatuetan eta TAT peptidotan oinarritutakoak gaixotasun neurodegeneratiboak tratatzeko

Sara Hernando Revilla

Vitoria-Gasteiz, 2020

NanoBioCel group

Laboratory of Pharmaceutics, School of Pharmacy

University of the Basque Country (UPV/EHU)

ACKNOWLEDGEMENTS FOR THE FINANCIAL SUPPORT

This doctoral thesis has been funded by the 'Ministerio de Economía y Competitividad' (SAF2013-42347-R, RTC-2015-3542-1), the University of the Basque Country (UPV/EHU; UFI 11/32), Basque Government (Saiotek S-PE13UN048, Consolidated Groups IT 907-16) and FEDER funds.

Sara Hernando Revilla gratefully acknowledges the predoctoral grant provided by the Basque Government.

ACKNOWLEDGEMENTS TO THE EDITORIALS

Authors thank the editorials for granting permission to reuse the published articles in this thesis. The published versions can be accessed at the following links:

Hernando S et al. *Nanomedicine (Lond)* 2016 May;11(10):1267-85. (Appendix 1)

<https://doi.org/10.2217/nnm-2016-0019>.

Hernando S et al. (Ed.), *Drug and Gene Delivery to the Central Nervous System for Neuroprotection*. 2017 © Springer International Publishing, Switzerland, pp. 57-87. (Appendix 2)

https://doi.org/10.1007/978-3-319-57696-1_3

Hernando S et al. *Curr Drug Deliv* 2018;15(9):1218-1220 (Appendix 3)

<https://doi.org/10.2174/1567201815666180510103747>

Hernando S et al. *Mol Neurobiol* 2018 Jan;55(1):145-155 (Appendix 4)

<https://doi.org/10.1007/s12035-017-0728-7>

Hernando S et al. *Neurobiol Dis* 2019 Jan;121:252-262. (Appendix 5)

<https://doi.org/10.1016/j.nbd.2018.10.001>.

Hernando, S. et al *Pharmaceutics* 2020, 12, 928. (Appendix 6)

<https://doi.org/10.3390/pharmaceutics12100928>

The last experimental work derived from this doctoral thesis (Appendix 7) has been sent to *Acta Biomaterialia* international journal.

Agradecimientos

El final de un ciclo, el final de un proyecto profesional y también personal que no podría haber sido posible sin todas las personas que me han acompañado y dado fuerzas durante este camino. No quisiera dejar pasar la oportunidad de utilizar estas líneas para expresar el profundo agradecimiento que siento a todas las personas que me han acompañado durante este camino.

En primer lugar, a mis directoras de tesis por darme la oportunidad de comenzar con esta tesis doctoral y por confiar en mí más de lo que yo muchas veces lo he hecho. Manoli, gracias por tu clarividencia y pragmatismo que han hecho las decisiones difíciles mucho más fáciles. A Rosa, por estar siempre disponible para contestar todas mis dudas, por buscar siempre la mejor respuesta para mi futuro profesional.

A Enara, porque tengo muy claro que sin ti esta tesis no habría llegado a su fin. Gracias por acompañarme en este camino, por darme apoyo técnico y moral cuando más lo necesitaba. De la misma manera, al resto de investigadores y profesores del departamento, por tener siempre palabras amables y preguntar sobre mis avances. Pero en especial, gracias a las chicas de la tercera planta de la facultad por todos los cafés compartidos; a Lorena, Amaia, Claudia y como no, a Aiala. Gracias en especial también a Ixaso por todo lo que me has enseñado en este tiempo, por estar siempre disponible a ayudarme. Igualmente, a Ainho y Mari por hacer los momentos difíciles mucho más fáciles, por estar siempre ahí para escuchar mis miserias y alegrías. Gracias por los momentos compartidos dentro y fuera del labo.

Gracias al laboratorio de Neurociencias del Centro de Investigación 12 de octubre de Madrid y en especial a la Dra. Eva Carro por darme la oportunidad de formarme en su laboratorio. Gracias al resto de personas del grupo de investigación de los que aprendí mucho en mis inicios en la investigación. De la misma manera, quisiera agradecer a la Dra. Luisa Ugedo y al resto de investigadores del grupo de Neurofarmacología por darme la oportunidad de aprender en un campo diferente al mío durante los meses que estuve ahí. Pero especialmente a Elena, no sólo por esos meses, sino por los años de carrera y todo lo que ha venido después. Gracias por

las conversaciones interminables divagando sobre la ciencia y nuestro futuro, por estar siempre disponible cuando necesitaba desahogarme.

Finally, thank you to Dr Anna Herland from Karolinska Institutet for the opportunity of complete my scientific and personal training. Thank to all your collaborators for the welcoming environment and for the technical and personal support I receive from all them. Special thanks to Xenia, my Greek, crazy and always cheerful girl. Thanks for all your support in and out of the lab.

Y como no, gracias a todas las personas que fuera del labo me habéis acompañado durante este tiempo, por demostrarme que lo verdaderamente importante no puede esperar a lo simplemente urgente. Gracias a mis amigas, Jani, Janire, Marta, Mai, Kris, Sandra, Goiu, por preguntar siempre por cómo estaba y cómo lo llevaba; por obligarme a desconectar y darme fuerzas y ánimos para llegar hasta el final. Por supuesto, gracias enormes a los menesianos. A Rafa y Natxo por ayudarme a no perder el foco. A Oscar, Enrique y Joaquín por el tiempo en Chile, porque fuisteis un oasis en el ecuador de la tesis. A Sandra, Sofi, Amaia, Imanol, Asier, Eneko, Diego, Edu, Javi y un largo etc., gracias por todos los mensajes para levantarme el ánimo, por todas las cañas compartidas que me han ayudado a resetear y continuar con energía todo este tiempo.

Y, por último, gracias de corazón a mi familia, a la cercana y a la más lejana (aunque sea solo geográficamente) por preocuparos e interesaros por mi trabajo y por mí durante todo este tiempo. En especial a mis padres, por dejarme ser sin juzgarme. Por acompañarme en mis decisiones sin cuestionarme y por enseñarme que el trabajo bien hecho es tu mejor carta de presentación, sin fuegos artificiales ni grandilocuencias. A mis hermanas, Cris y María, mis segundas madres, por estar siempre disponibles para hablar, por conocerme mejor que yo misma y por aguantar como nadie mis enfados e inoportunidades. A Jon y a Ander, porque de una manera u otras también me habéis acompañado en este camino. Gracias por el regalo de sobrinas y sobrinos que me habéis dado que me han servido como mi válvula de escape y anclaje al mundo real, al importante.

Gracias a todos de corazón.

A todos ellos va dedicada esta tesis doctoral.

“Creamos a fuerza de fuerzas. Crear es sacudir la inercia, mantener a pulso la libertad, nadar a contracorriente, cuidar el estilo, decir una palabra amable, defender un derecho, inventar un chiste, hacer un regalo, reírse de uno mismo, tomarse muy en serio las cosas serias... burlarse del destino; es decir, de la rutina, de la maldad, del tedio”.

H. Josu Fernández-Olabarrieta

Glossary

6-OHDA: 6-hydroxydopamine

α -syn: alpha-synuclein

Ω -3: omega-3

Ω -6: omega-6

A β : amyloid beta

ABC: avidin-biotin-peroxidase complex

AchE: acetylcholinesterase

AD: alzheimer's disease

ANOVA: analysis of variances

ARE: antioxidant response element

BBB: blood brain barrier

BDNF: brain derived neurotrophic factor

BMECs: brain microvascular endothelial cells

BrdU: bromodeoxyuridine

BSA: bovine serum albumine

BuChE: butyrylcholinesterase

CCK-8: cell counting Kit-8

CL: cardioplin

CMC: carboxymethylcellulose

CNS: central nervous system

CNTF: ciliary neurotrophic factor

CPP: cell penetrating peptide

CS: chitosan

CSF: cerebrospinal fluid

DA: dopamine

DAB: 3,3'-diaminobenzidine

DAPI: 4',6-diamidino-2-phenylindole

DDS: drug delivery system

DiD: 1,1'-dioctadecyl-3,3,3',3'-tetramethylindodicarbocyanine perchlorate

DHA: docohexaenoic acid

DHAH: hydroxilated derivate of docohexaenoic acid

DLS: dynamic light scattering

DMEM: dulbecco's modified eagle medium

DMSO: dimethyl sulfoxide

DNase: deoxyribonuclease I from bovine pancreas

DPBS: dulbecco's phosphate-buffered saline

DPX: depex mounting medium

ECM: extracellular matrix

EDC: 1-ethyl-3-(3-dimethylaminopropyl) carbodiimide hydrochloride

EE: encapsulation efficiency

ELISA: enzyme-linked immunosorbent assay

EPA: eicosapentaenoic acid

FBS: fetal bovine serum

FGF: fibroblast growth factor

GDNF: glial derived neurotrophic factor

GF: growth factor

GFP: green fluorescent protein

GFAP: glial fibrillary acidic protein

HBSS: hank's balanced salt solution

hESFM: human endothelial serum free medium

hiPSCs: human induced pluripotent stem cells

HO-1: hemoxygenase 1

Iba-1: ionizing calcium-binding adaptor molecule 1

ICV: intracerebroventricular

IF: immunofluorescence

IGF-I: insulin growth factor-I

IgG: immunoglobuline G

IHC: immunohistochemistry

IL-6: interleukin-6

IL-8: interleukin-8

IL-1 β : interleukin- 1 β

iNOS: inducible nitric oxide synthase

i.n.: intranasal

IOD: integrated optical density

i.p.: intraperitoneally

I.V: intravenous

KPBS: potassium phosphate buffered saline

LDH: lactate dehydrogenase

L-DOPA: levodopa

LNC: lipid core nanocapsules

LPS: lipopolysaccharide

MP: microparticle

MPTP: 1-methyl-4-phenyl-1,2,3,6-tetrahydropyridine

mSOD: superoxide dismutase

MRI: magnetic resonance imaging

MS: microsphere

MTT: 3-(4,5-Dimethylthiazol-2-yl)-2,5-Diphenyltetrazolium Bromide

NADPH: nicotinamide adenine dinucleotide phosphate

ND: neurodegenerative disease

NGF: nerve growth factor

NGS: normal goat serum

NLC: nanostructured lipid carrier

NP: nanoparticle

Nrf2: nuclear factor erythroid 2-related factor 2

NS: nanosphere

NT-3: neurotrophin

NTF: neurotrophic factor

NVU: neurovascular unit

ON: overnight

PB: phosphate buffer

PBCA: poly n-butylcyanoacrylate

PBS: phosphate buffer saline

PD: parkinson's disease

PDI: polydispersity index

PEG: polyethylene glycol

PET: positron emission tomography

PFA: paraformaldehyde

P-gp: P-glycoprotein

PLGA: poly lactide-co-glycolide

P/S: penicillin/streptomycin

PUFAs: polyunsaturated fatty acids

RA: retinoic acid

ROS: reactive oxygen species

RT: room temperature

SEM: standard error of mean

SD: standard deviation

SLN: solid lipid nanoparticle

SN: substantia nigra

SNpc: substantia nigra pars compacta

ST: striatum

sulfo-NHS: N-Hydroxysulfosuccinimide

TAT: transactivator of transcription

TEER: trans-epithelial electrical resistance

TEM: transmission electron microscopy

Tf: transferrin

TH: tyrosine hydroxylase

TNF: tumor necrosis factor α

VEGF: vascular endothelial growth factor

WGA: wheat germ agglutinin

ZO-1: zonula occludens-1

Index

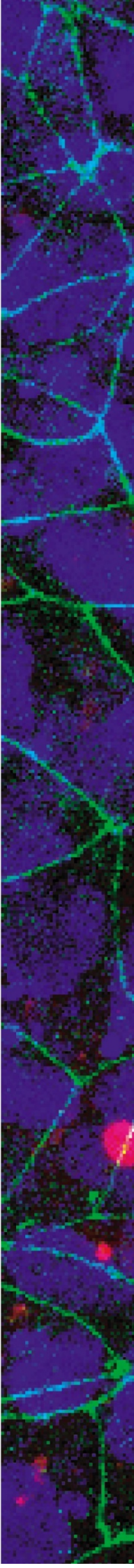
ENGLISH VERSION

Chapter 1.....	31
INTRODUCTION	31
1. State of the art	3
2. Methodology	10
2.1. NLCs preparation	10
2.2. NLC characterization: particle size, zeta potential, morphology and encapsulation efficiency	11
2.3. Animal models	13
2.4. Behavioral test in animal models of PD	15
2.5. In vitro models and bioactivity assays in different cell culture models	16
2.6. Immunohistochemistry and immunofluorescence techniques	23
2.7. RTqPCR	25
2.8. Multiplex assay	25
2.9. Statistical analysis and figures	26
3. Hypothesis and Objectives	27
4. Results and discussion	29
5. Bibliography	46
Chapter 2.....	53
CONCLUSIONS	53
Chapter 3.....	57
APPENDIXES	57
Advances in nanomedicine for the treatment of Alzheimer's and Parkinson's diseases.....	59
Nanotechnology based approaches for neurodegenerative disorders: diagnosis and treatment.....	91
The role of lipid nanoparticles and its surface modification in reaching the brain: an approach for neurodegenerative diseases treatment	133
Intranasal administration of TAT conjugated lipid nanocarriers loading GDNF for Parkinson's Disease	143
Beneficial effects of n-3 polyunsaturated fatty acids administration in a partial lesion model of Parkinson's disease: the role of glia and NRF2 regulation	167
Nanostructured lipid carriers made of Ω -3 polyunsaturated fatty acids: <i>In vitro</i> evaluation of emerging nanocarriers to treat neurodegenerative diseases	195
Dual effect of TAT functionalized DHAH lipid nanoparticles with neurotrophic factors in human BBB and microglia cultures	231

EUSKERAZKO BERTSIOA

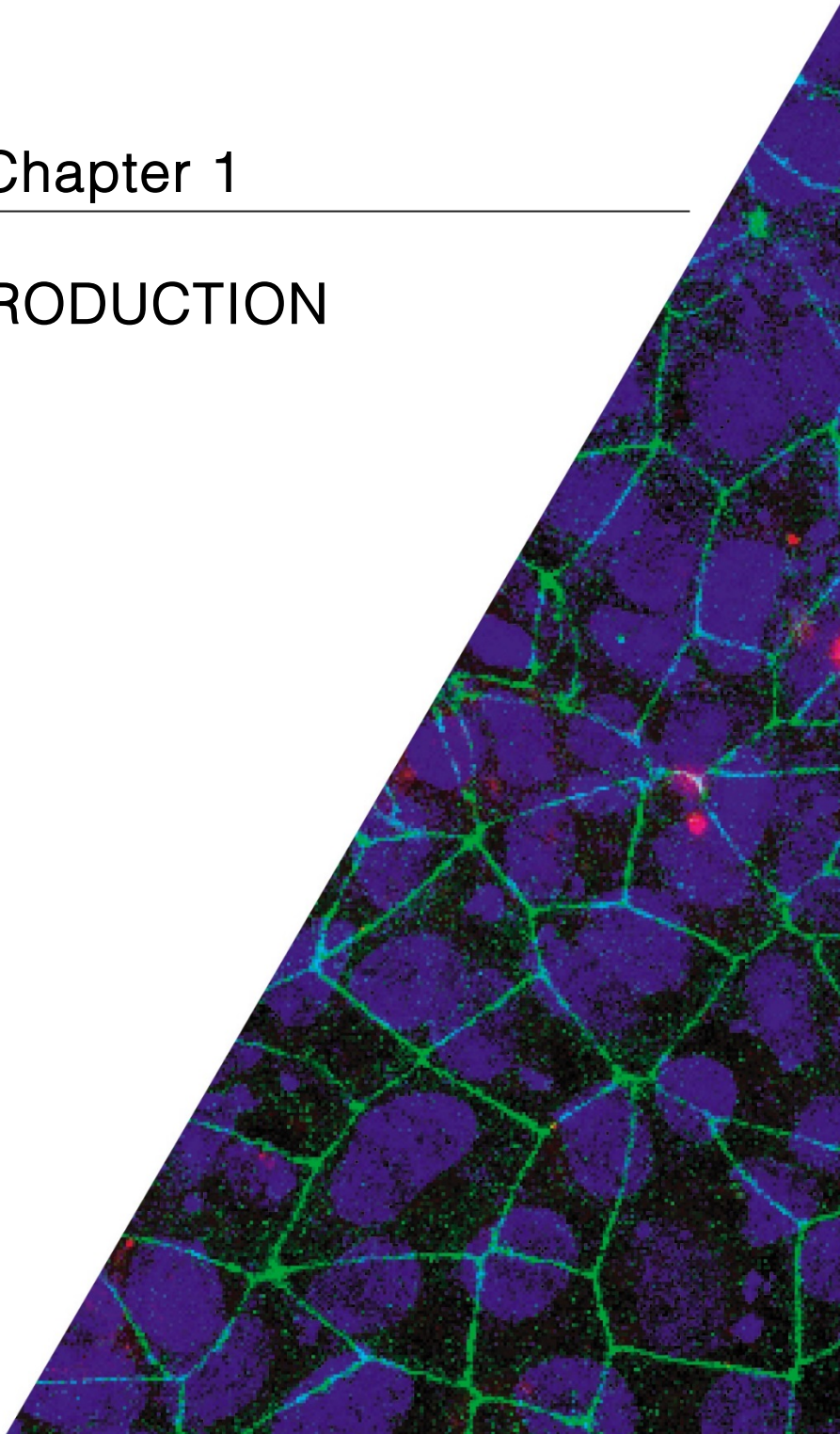
1. Kapituluua	271
SARRERA	271
1. Sarrera	273
2. Metodoak	280
2.1 NLCen ekoizpena.....	280
2.2 NLCen karakterizazioa: partikulen tamaina, zeta potentziala, morfologia eta kapsularazte eraginkortasuna.....	281
2.3 Animalia ereduak	283
2.4. Entsegu lokomotoriak PD-ko animalia ereduetan.....	285
2.5 In vitro ereduak eta kultibo zelularrak	286
2.6 Immunohistokimika eta immunofluoresentzia teknikak	292
2.7 RTqPCR.....	295
2.8 Multiplex saioa	295
2.9 Anlisi estatistikoa eta irudiak	295
3. Hipotesi eta helburuak.....	296
4. Emaitzak eta eztabaida	298
2. Kapituluua	317
ONDORIOAK	317

ENGLISH VERSION



Chapter 1

INTRODUCTION



1. State of the art

Neurodegenerative diseases (NDs) are complex neurological conditions with different clinical features but common progressive loss of brain functions. In addition, they exhibit selective loss of neurons within the central nervous system (CNS) [1]. The different circuits affected during major NDs result in distinct clinical symptoms varying from memory loss, motor tremor, postural instability or loss of muscular control. Although they exhibit different clinical features, they share common hallmarks and mechanism of neurodegeneration such as deposit of insoluble proteins, mitochondrial dysfunction, stress granules and synaptic dysfunction, that together with oxidative stress and neuroinflammation contribute to final neuronal loss and neurodegeneration [2,3] (Figure 1). NDs are multifactorial diseases with plenty causes and risk factors, however; among all of them, ageing itself is by far the predominant risk factor for NDs [4]. The most common NDs, Alzheimer' disease (AD) and Parkinson's disease (PD) are predominantly observed in elderly individuals affecting 43.7 and 6.1 million people, respectively, worldwide [5,6]. Since ageing is expecting to continue, its prevalence will continue increasing becoming in a serious economic burden and public health problem.

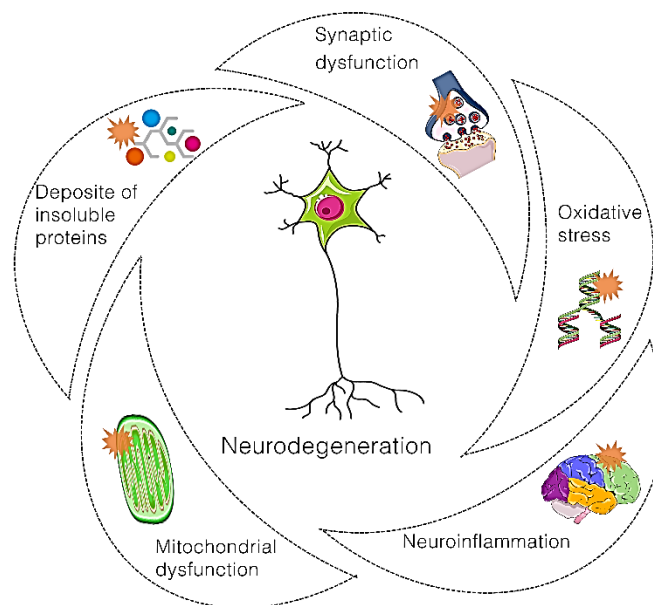


Figure 1. Different hallmarks of neurodegeneration.

Current therapies are far from optimal, treating the symptomatology of the disease but without handling the undergoing neuronal damage or preventing it. Despite the

public health problem such NDs constitute, in the clinical practice there are few therapeutic alternatives to treat the symptomatology of these diseases. For example, in the case of AD, the therapy involves two major classes of drugs: cholinesterase inhibitors and memantine, with no or small clinical benefits and the lack of positive effect on disease progression for both of them. Similar is the case for PD in which the administration of L-dopa or dopamine agonists show positive effects replacing the dopamine depletion and treating motor symptomatology, without tackle the non-movement disorder symptoms. This lack of overall positive effect on the clinic, together with the presence of systemic side effects has prompted the patients to abandon their therapies [7,8]. Therefore, there is an urgent need of new drug candidates that could slow down the progression of the disease. In this line, scientists and pharmaceutical industry moved away from classical targets of pharmacotherapy to focus on disease-modifying treatments. Among others, the use of neurotrophic factors (NTF) has gained the attention of the scientific community due to their neuroregenerative and neuroprotective properties acting on growth, proliferation and differentiation of neuronal cells. Despite the incomplete understanding of the mechanism of action of NTF in neurological diseases, *in vitro* and *in vivo* experiments of different pathologies aim to obtain therapeutic efficacy on neuronal survival, thus, decreasing the symptomatology of the disease. Among different growth factors (GF), glial derived neurotrophic factor (GDNF) is known to be the gold standard NTF for PD, showing important effects on dopaminergic and motor neuronal survival. Moreover, vascular endothelial growth factor (VEGF) has noted as one of the best candidate for ND treatment since it improves neuronal growth and neuroprotection. Moreover, it promotes angiogenesis and endothelial cell development tackling the neurovascular toxicity related to AD [9,10].

Most of the new developed therapies have focused on restoring neuronal loss to modify the course of the disease. Nonetheless, in the last years it has been known that the pathogenesis of NDs is more complex than thought and the neurocentric-based therapies might not be enough to treat these diseases due to the contribution of non-neuronal cells in NDs, mainly consist of glia. The subtypes of mature CNS glia are astrocytes, oligodendrocytes and microglia [11,12]. Among all of them, microglia is the key causative factor of neuroinflammation leading to neurodegeneration. As seen in Figure 2, microglia is activated by direct or indirect pathways that led to the release of cytokines and/or proteases, the activation of

excitotoxic pathways and oxidative stress. This response turn into more neurodegeneration with neuronal death and toxic substance accumulation, therefore, becoming in an endless process. This self- perpetuating degenerative process occurs within the area of neurodegeneration highlighting the link between neuroinflammation and neuronal loss [13,14].

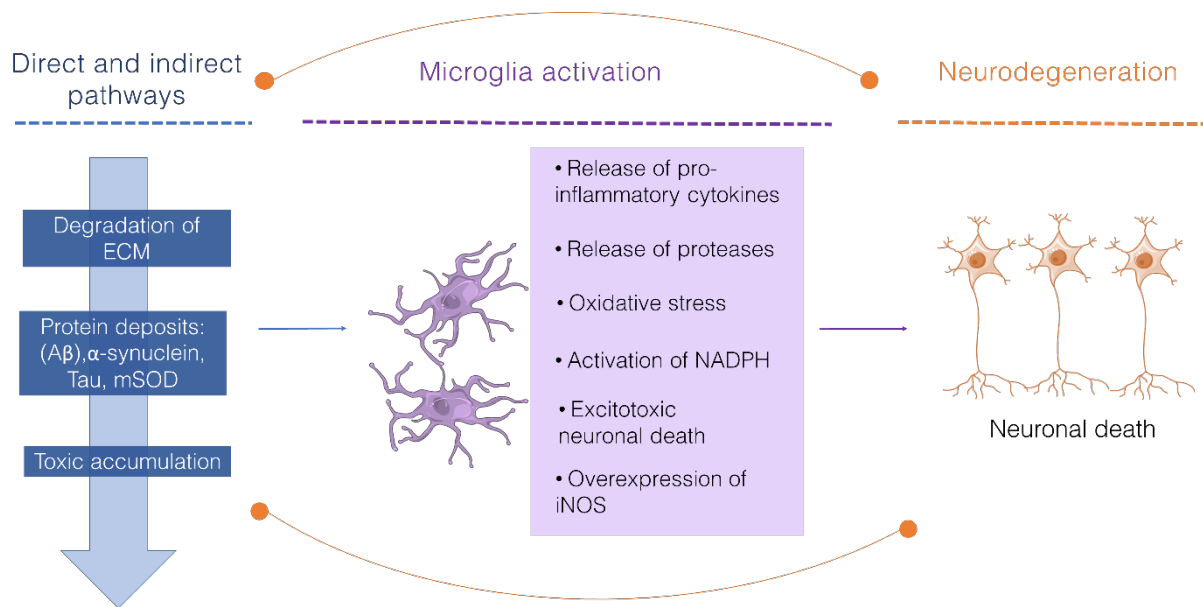


Figure 2. Role of microglia activation and neurodegeneration: an endless process. (ECM: extracellular matrix; mSOD: superoxide dismutase; NADPH: nicotinamide adenine dinucleotide phosphate; iNOS: inducible nitric oxide synthase)

The complexity of NDs with the undergoing neuronal loss, neuroinflammation and oxidative stress needs the combination of different therapies that could treat the diverse degenerative mechanism present in these neurological conditions. In the last years, new natural compounds with an active role in oxidative stress and neuroinflammation have been disclosed as future therapeutic options. Different phytochemicals have been identified as promising therapeutic agents in NDs management; resveratrol, curcumin or polyunsaturated fatty acids (PUFAs) are such examples. Although their mechanism of action is not clear to date, it is a proven fact that they exhibit a neuroprotective effect through their anti-oxidative and anti-inflammatory properties [15].

However, one of the biggest challenges to obtain an effective therapy for NDs is the pass of most of the molecules across the blood brain barrier (BBB) (Figure 3).

This dynamic barrier regulates the flow of substances and neurotoxic molecules into the brain, therefore, limiting the efficacy of new therapies. The BBB is composed by highly specialized endothelial cells, named as brain microvascular endothelial cells (BMECs), pericytes and astrocytes that together constitute the neurovascular unit (NVU) conferring unique properties to this dynamic barrier [16,17].

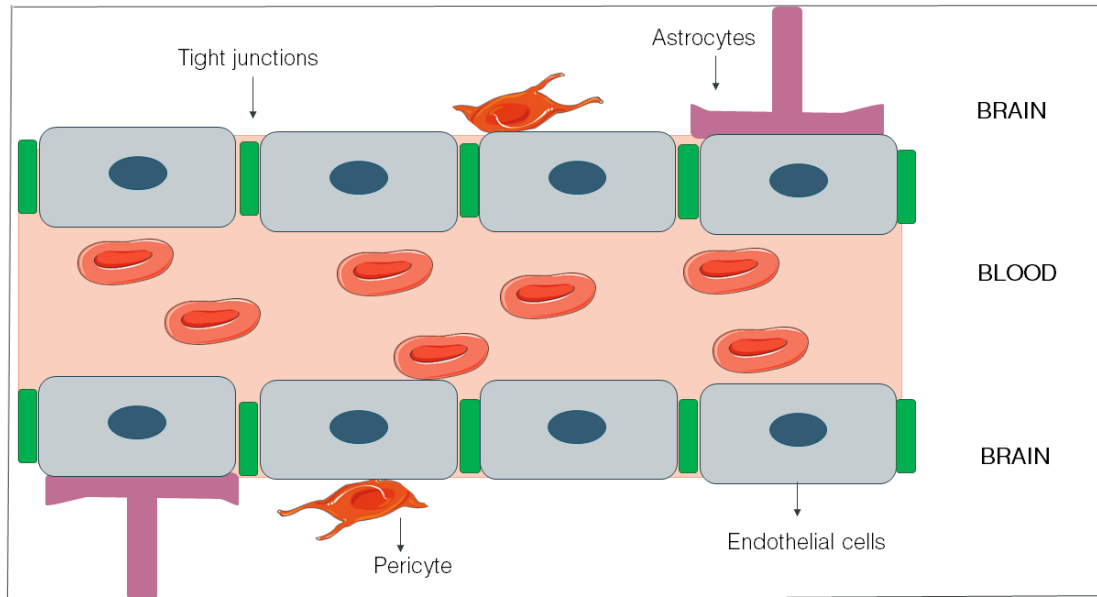


Figure 3. Schematic representation of the blood brain barrier (BBB) and other components of the neurovascular unit (NVU).

In order to pass through the BBB, different strategies have been described in the last years. These strategies involve direct and indirect methods to cross this barrier. (See also an extended chapter describing different methods to pass across BBB [18], Appendix 2 of this doctoral thesis). The direct or invasive techniques include surgical methods to administer drugs directly into the brain, and the disruption of the BBB to open it. Meanwhile, the indirect or noninvasive techniques comprise non-aggressive approaches to access into the brain, without affecting the barrier integrity. These non-invasive techniques include alternative systemic administration routes, like intranasal, the combination of the drug with cell penetrating peptides (CPP) and/or the encapsulation of the drugs within nanotechnology based drug delivery systems (DDS). DDS englobe a range of nanosized drug carriers with the ability to target specifically the brain, protect the drug from enzymatic degradation and improve their bioavailability increasing their pass through BBB [19]. (See here a review about the use of nanomedicine for the treatment of NDs such as PD and AD [20]; Appendix 1 of this doctoral thesis (Figure

4)). One of the most widely used and studied DDS are nanoparticles (NPs). NPs are solid particles in which the active compound is dissolved, entrapped or encapsulated, or to which the active principle is absorbed or attached. Moreover, different administration routes can be used to administer them. Among other materials, natural or synthetic polymers and lipids have been employed in NPs development [21]. Actually, in the last years numerous research groups have combined the use of NPs with well-known treatments or recently appeared therapeutic approaches, such as, the previous mentioned GFs and phytochemicals [22-25]. All these studies support the use of NPs offering better features over traditional formulations such as; protecting the molecule from degradation or increasing the half-life of the therapeutic molecules, therefore, limiting multiple dosing, and decreasing side effects [26]. Among others, the nanostructured lipid carriers (NLCs) are unstructured solid lipid matrix, made of a mixture of a lipid blend (solid and liquid lipids) and an aqueous phase containing surfactants [27]. In addition, they have gained much attention due to their lack of toxicity, high drug loading capacity of both hydrophobic and hydrophilic compounds, and a natural tendency to pass across the BBB [28].

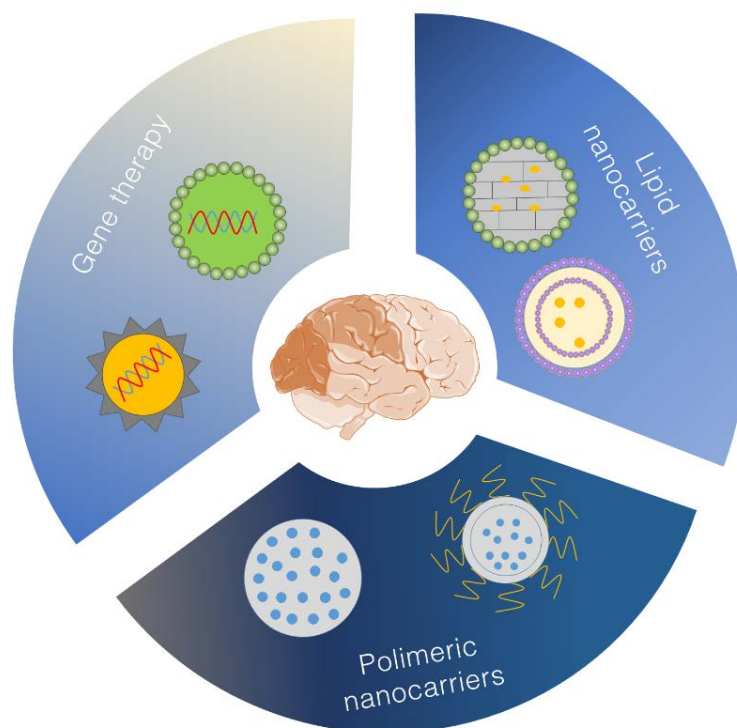


Figure 4. Nanomedicine tools to target the CNS and treat NDs.

In addition, the surface of NPs can be functionalized to control their interaction with the BBB and neurons in order to increase their access into the CNS. These surface-engineered NPs can be modified with multiple ligands enhancing their targeting ability without affecting any other physiological event [29]. Among other ligands, polyethylene glycol (PEG) is one of the most used ones, however, in the last years new glycoproteins, polysaccharides or peptides have appeared as promising ligands to specially target CNS. (For further information, see also an extended review about lipid NPs surface modification in [30], Appendix 3 of this doctoral thesis). CPP or chitosan (CS) are such examples. CS is a cationic polysaccharide that exhibits singular chemical and biological characteristics, for example: biocompatibility, low toxicity, and biodegradability, with positive results enhancing the delivery of different therapeutics into the brain [31]. Regarding CPP, they are short amphipathic and cationic peptides that unlike most peptides are rapidly internalized across cell membrane, which make them perfect to attach to NP surface for increasing their entry into different types of cells and therefore, maximize the therapeutic concentration of the drug and its efficacy [32].

Up until now, most of the lipids used for NLC lipid matrix formation were inert excipients, without any active role in preventing or treating diseases [33]. Indeed, only few studies have described the use of functional lipids that could play an active role i.e. Ω -9 oleic acid incorporated into a NLC formulation for dermal applications [34]. Other kind of functional lipids are PUFAs. As pointed out before, among other phytochemicals, they have been raised as a new promising approach to treat or prevent NDs. Omega-3 (Ω -3) and omega-6 (Ω -6) fatty acids are the two major classes of PUFAS [35,36]. Ω -3 PUFAs are essential nutrients in the development and functioning of brain and visual system. Among all of them, docohexaenoic acid (DHA) constitutes over 90% of the Ω -3 PUFAs and 10–20% of total lipids in the brain [37]. Although the exact mechanism by which these compounds exert their therapeutic effect is already unknown, different *in vitro* and *in vivo* studies have demonstrated their effects on neuroprotection, neuroinflammation, neurogenesis, release of neurotransmitters and gene expression [38]. Furthermore, they have exhibited positive results improving memory in animal models of AD, sensory motor tests in PD animal models or inhibiting amyloid- β fibrils both *in vitro* and *in vivo* [39-41]. Moreover, the epidemiological studies published in the last years have probed the positive effect of PUFAs supplementation decreasing the risk for developing PD

or AD [42,43]. This positive effect was confirmed in clinical trials in which the supplementation with DHA and other related Ω -3 fatty acids decreased the cognitive decline in patients with mild to moderate AD or decrease the inflammatory status of these NDs reducing depressive symptoms, among others [44-47]. Overall, these positive effects support their use as functional lipids that could early manage some symptoms of the disease altering their natural progression, both as a treatment itself or as co-adjuvant to boost a synergistic therapy [48].

Nonetheless, all the efforts made by the scientific community and the pharmaceutical industry to obtain an effective treatment for NDs have resulted in fail drug candidates in clinical trials, in phase II and III, showing no translation research from bench to clinic [49,50]. The unreliable prediction of different neurotherapeutics is a result of a deficient understanding of the disease, the lack of reliable biomarkers, and last but not least, because of the lack of disease models that could accurately mimic the human disease condition. Therefore, all these failures have disclosed the need for *in vitro* models that could really mimic the conditions of human brain in NDs, becoming in a useful tool for drug screening. The development of new *in vitro* models within a human context might hopefully bridge the gap between current preclinical animal models and humans. Among different *in vitro* approaches to generate brain-on-chip platforms, the onset of human induced pluripotential stem cells (hiPSCs) provides the researchers the adequate tool to model the nervous system and retain the ability to work in human brain context [51,52]. As pointed out before, one of the key aspect for succeeding in NDs treatment is the pass through the BBB. That is why; the generation of BMCEs differentiated from hiPSC has become essential to study the toxicity and transport rate of new drugs and nanotherapeutics. This new *in vitro* tool might reduce animal use for preclinical drug testing, while offering higher reliability for human translation [53,54]. Although, as seen in Figure 3, microglia is not part of NVU, it definitely participate in important processes controlled by the NVU; regulating the BBB during health and injury. Indeed, as seen before, microglia is in communication with neurons and it is involved in the undergoing neuroinflammation in NDs. Moreover, it contributes to the disruption of BBB generating an aberrant cellular infiltration, increasing the levels of pro-inflammatory cytokines, proteases and free radicals [55]. Actually, the microglia and BBB are in constant bi-directional communication and alterations in any of those cellular systems is related with NDs pathophysiology. This dynamic BBB-microglia

interaction is present during the neuroinflammation ongoing in NDs and may represent a target for future therapeutic approaches [56].

To sum up, the complexity of NDs makes necessary the combination of different strategies and molecules to target the CNS and treat the different pathologies related to neurodegenerative disorders. The rise of nanomedicine has opened the opportunity to combine different strategies that could constitute a feasible solution. Indeed, the combination of different neurotherapeutics within a nanoformulation, together with its surface modification to target the brain, may open a new perspective for NDs treatment efficacy.

2. Methodology

2.1. NLCs preparation

NLCs were prepared using melt-emulsification technique, previously developed by our research group [31]. Firstly, a mixture of solid and liquid lipids (Precirol ATO® 5 (Gattefosé, France) and Mygliol® (Sasol, Germany GmbH) or different kind of PUFAs (Medalchemistry, Spain) were chosen to form the lipid matrix of NLCs. The solid and liquid lipid ratio varied from 2.5% to 1.5% for solid lipid and in the case of liquid lipid, it varied from 0.25% to 1.25% (Table 1). The lipid phase was melted 5°C above its melting point (56°C). Then, an aqueous solution containing the surfactant combination of Tween 80 (3%, w/v) and Poloxamer 188 (2%, w/v) (Panreac, Spain) was heated at the same temperature to be added to the lipid phase under continuous stirring during 60 second at 50W (Bradson® Sonifier 250). The resulted emulsion was maintained with magnetic stirring during 15 minutes (min) at room temperature (RT). Then, it was immediately cooled at 4-8°C overnight to obtain the NLCs formation due to lipid solidification. NLCs surface was modified just with CS (Novamatrix, Norway) or CS and TAT (ChinaPeptides). For the surface modification with CS, the NLC dispersion was added dropwise to an equal volume (4 ml) of a CS solution (0.5%, w/v) under continuous agitation at RT for 20 min. After the coating process, the NLC dispersion was centrifuged in Amicon filters (Amicon, "Ultracel-100k", Millipore, USA) at 2,500 rpm (MIXTASEL, P Selecta, Spain) for 15 min, washed three times with Milli Q water and lyophilized for 42 h (LyoBeta 15, Telstar, Spain). TAT peptide was covalently linked to CS by a surface activation method [57]. Briefly, 250µl of EDC (1-ethyl-3-(3-dimethylaminopropyl) carbodiimide hydrochloride)

(Millipore Sigma Life Sciences, Germany) in solution (1mg/ml) and 250µl of sulfo NHS (N-Hydroxysulfosuccinimide) (Millipore Sigma Life Sciences, Germany) in 0.02M phosphate buffer saline (PBS) (1mg/ml) were added dropwise to a 4 ml CS solution (0.5% w/v, in PBS 0.02M) under magnetic stirring (2 h at RT). After CS activation, TAT coupling was performed. To start with, 250µl of the TAT solution (1mg/ml) in PBS (0.02M; 7.4 pH) was added dropwise to the activated CS, under gentle agitation. The TAT-CS solution was maintained under agitation another 4h at RT and then incubated 4°C overnight. On the day after, the NLCs were coated with CS-TAT; NLC dispersion previously prepared was added dropwise to the CS-TAT solution under continuous agitation for 20 min at RT. After the coating process, CS-TAT-NLC nanoformulation was centrifuged and lyophilized as previously pointed out. Finally, the NTF; GDNF or VEGF (Peprotech, UK) were loaded in the previously developed lipid formulation at a concentration of 0.125% or 0.15% (w/w). Depending the Study, different concentration of GF was used. Additionally, in order to incorporate a fluorescent tracer into the nanoformulation, the lipophilic dye DiD (1,1'-Dioctadecyl-3,3',3',3'-Tetramethylindodicarbocyanine Perchlorate) (Termofisher Scientific, Spain) was incorporated into the NLC formulation at a concentration of 0.5% (w/w). These formulations were elaborated following previously described protocol, but including the related GF or dye, depending on the formulation, in the lipid phase prior to the sonication process. All the different formulation used along this doctoral thesis have been summarized in Table 1, regarding the solid and lipid liquid rate, the entrapped molecule and their use in the different studies (Study I, Study III and Study IV).

2.2. NLC characterization: particle size, zeta potential, morphology and encapsulation efficiency

The mean particle size (Z-average diameter) and the polydispersity index (PDI) and the zeta potential were measured by Dynamic Light Scattering (DLS), through Laser Doppler micro-electrophoresis (Malvern® Zetasizer Nano ZS, Model Zen 3600; Malvern instruments Ltd, UK). Three replicate analyses were performed for each formulation. The data are represented as the mean \pm SD. NP surface characteristics and morphology were examined by transmission electron microscopy (TEM) (JEOL JEM 1400 Plus). The encapsulation efficiency (EE) of the NLCs was determined by an indirect method in which we measured the non-encapsulated GF presente

Table 1. Composition of the different NLCs used along this doctoral thesis.

STUDY	FORMULATION	PRECIROL ATO5 @ % (w/v)	LIQUID LIPID (%) (w/v)		SURFACE MODIFICATION	ENTRAPPED MOLECULE (%) w/v	ANIMAL OR CELL MODEL
Study I	CS-NLC-blank	2.5	Mygliol @	0.25	CS	-	In vivo MPTP animal model
	CS-NLC-GDNF	2.5	Mygliol @	0.25	CS	GDNF (0.15)	
	CS-NLC-TAT-GDNF	2.5	Mygliol @	0.25	CS and TAT	GDNF (0.15)	
Study III	Mygliol-NLC	2.5	Mygliol @	0.25	-	-	Only physicochemical chracterization. Not functional assays
		2		0.75	-	-	
		1.75		1	-	-	
		1.5		1.25	-	-	
	DHA-NLC	2.5	DHA	0.25	-	-	
		2		0.75	-	-	
		1.75		1	-	-	
		1.5		1.25	-	-	
	DHA-EE-NLC	2.5	DHA-EE	0.25	-	-	
		2		0.75	-	-	
		1.75		1	-	-	
		1.5		1.25	-	-	
	DHA-TG-NLC	2.5	DHA-TG	0.25	-	-	
		2		0.75	-	-	
		1.75		1	-	-	
		1.5		1.25	-	-	
Mygliol-NLC	1.75	Mygliol @	1	CS and TAT	-	Primary neuron and microglia cell culture	
DHAH-NLC	1.75	DHAH	1	CS and TAT	-		
Study IV	CS-NLC-DiD	1.75	DHAH	1	CS	DiD	hIPSCs derived BMCECs
	TAT-CS-NLC-DiD	1.75	DHAH	1	CS and TAT	DiD	
	Mygliol-NLC	1.75	Mygliol @	1	CS and TAT	-	HMC3 microglia cell line
	DHAH-NLC	1.75	DHAH	1	CS and TAT	-	
	DHAH-NLC- GDNF	1.75	DHAH	1	CS and TAT	GDNF (0.125)	
	DHAH-NLC- VEGF	1.75	DHAH	1	CS and TAT	VEGF (0.125)	

the supernatant obtained after the filtration/centrifugation process described in 2.1 section. The EE (%) of the different GF was determined by ELISA (Enzyme-Linked ImmunoSorbent Assay) technique using the following equation:

$$EE (\%) = \frac{\text{total GF amount added} - \text{free amount of GF}}{\text{total GF amount added}} \times 100$$

The absence of DiD release from NLC in transport buffer was assessed in previous studies and thus, not included within the present work [31].

2.3. Animal models

2.3.1. MPTP animal model and treatment

Nine week-old male C57BL/6J mice supplied from Charles River Laboratory (Charles River, L'Arbresle, France) were employed to produce the MPTP parkinsonian model (Study I). Mice were housed in standard conditions with a constant temperature of 22°C, a 12-h dark/light cycle and *ad libitum* access to water and food. All experimental procedures were performed in compliance with the Ethical Committee of Animal Welfare (CEBA) at the PROEX 343/14. In study I 53 mice were used, five of which were treated with the saline solution as negative control. The other 48 were treated with the MPTP toxic (30 mg/kg) (Millipore Sigma Life Sciences, Germany) intraperitoneally (i.p) administered at 24 h intervals during five consecutive days in order to obtain a PD animal model. At the same time the lesion protocol was initiated, the animals were divided into 6 groups (n=6) receiving the following treatments (Table 2) on alternate days during 3 weeks. The intranasal administration route was used to administer the different treatments. The final dose of GDNF after three weeks treatment was 2.5µg per each animal group. Animals' locomotor activity was evaluated every week of the study during four weeks. Once the study finished, all mice were euthanized and tissue was collected for future immunohistochemical evaluation.

Table 2. Different experimental groups to perform the in vivo assay in Study I.

GROUP	TREATMENT	MPTP (+/-)
Control	Saline solution (NaCl 0.9% w/v)	-
MPTP	Saline solution(NaCl 0.9% w/v)	+
GDNF	2.5 µg GDNF in NaCl solution	+
CS-NLC blank	CS-NLC	+
CS-NLC-GDNF	CS-NLC-GDNF (2.5 µg GDNF)	+
CS-NLC-TAT-GDNF	CS-NLC-TAT-GDNF(2.5 µg GDNF)	+

2.3.2. 6-OHDA rat lesion model and treatments

32 male albino Sprague-Dawley rats (170-220 g) were housed in groups of four under standard laboratory conditions ($22 \pm 1^\circ\text{C}$, $55 \pm 5\%$ relative humidity, and 12:12 h light/dark cycle) with food and water provided ad libitum (Study II). Experimental protocols were reviewed and approved by the Local Ethical Committee for Animal Research of the University of the Basque Country (UPV/EHU, CEEA, ref.ES48/054000/6069). All the experiments were performed in accordance with the European Community Council Directive on "The Protection of Animals Used for Scientific Purposes" (2010/63/EU) and with Spanish Law (RD 53/2013) for the care and use of laboratory animals. To obtain the 6-OHDA (6-hydroxydopamine) PD animal model, the following protocol was employed [25]. Thirty min before 6-OHDA (Termofisher Scientific, Spain) injection, the rats were pre-treated with desipramine (25mg/kg, intraperitoneal (i.p)), and then, they were anesthetized with isoflurane inhalation (1.5-2%) and mounted on a Kopf stereotaxic instrument to perform the lesion [25]. Four weeks before the 6-OHDA injection was administered to the animals, they were divide in four different groups depending the treatment they will receive (n=8) (Table 3). The treatments were daily administered intragastrically through a gavage. After the striatal lesion with 6-OHDA was made, they continued the treatment 15 weeks more. Moreover, every two weeks different behavioral tests were performed to check the effectiveness of the administered PUFAs. After that period, rats were euthanized and tissue was collected for future immunohistochemical studies.

Table 3. Different experimental groups to perform the *in vivo* assay in Study II. (CMC: carboxymethylcellulose; DHA: docohexaenoic acid; DHAH-EE: ethyl ester from of hydroxilated DHA).

GROUP	TREATMENT	6-OHDA
Saline	Saline solution (0.9% w/v)	+
Vehicle	Aqueous solution with 0.5% (w/v) of CMC and 0.05% (w/v) of Tween 80	+
DHA	DHA formulated in vehicle aqueous solution	+
DHAH	DHAH-EE formulated in vehicle aqueous solution	+

2.4. Behavioral test in animal models of PD

2.4.1. Rotarod Test

Locomotor activity of mice was assessed in a Rotarod apparatus (Figure 5A) (Ugo Basile, Italy) with increasing acceleration. The mouse head was directed against the direction of rotation, so that the mouse had to progress forward to avoid falling. Mice were submitted to five consecutive trials with an interval of 30 min between them. The tested ended when the animal fell or after a maximum of 5 min. The time spent on the rotating rod was recorded for each animal and trial. However, only the results from the fifth trial for each animal were used for statistical comparisons. The other four trials were discarded since they were pre-training sessions to familiarize the mice with the procedure. All animals were tested in the locomotor activity assay before they were lesioned with MPTP and after the lesion, every week during four consecutive weeks.

2.4.2. Cylinder test

Forelimb use asymmetry was assessed using the cylinder test every two weeks during 15 weeks. The first trial was done three weeks after the lesion with the toxic was made (2.3.2 section), once the lesion was established. Rats were individually placed in a 20 cm diameter glass cylinder and allowed to explore freely (Figure 5B). Mirrors were placed behind the cylinder to allow a 360° view of the exploratory activity. Each animal was left in place until at least 20 supporting front paw touches were done on the walls of the cylinder. The session was videotaped and later analyzed. Touches performed with the contralateral (injured side) or ipsilateral (uninjured side) front limb were counted and data are expressed as the percentage of ipsilateral placement, calculated as the following equation:

$$\% \textit{ ipsilateral touches} = \frac{\textit{ ipsilateral paw placement}}{\textit{ ipsilateral+contralateral paw placement}} * 100$$

2.4.3. Amphetamine induced rotational test

Three week after inducing the 6-OHDA lesion, the rats were tested in the amphetamine induced rotational test. This test was repeated once every two weeks. For this purpose, D-amphetamine (5 mg/kg in 0.9% NaCl; Sigma-Aldrich, St. Louis, USA) was i.p administered and, after 15 min of latency, in an individual cage for each animal, the total number of full ipsilateral rotations were recorded for 90 min with an automated rotameter (Multicounter LE3806; Harvard Apparatus, Holliston, MA, USA) (Figure 5B). The results are expressed as the percentage of ipsilateral turns per minute.

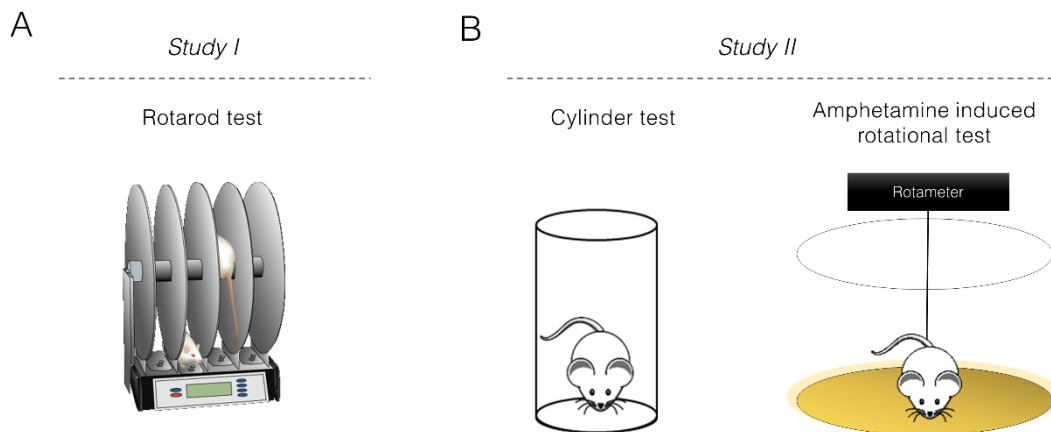


Figure 5. Schematic representation of the different locomotor tests performed along this doctoral thesis. (A) Rotarod test was performed in experimental *Study I*/(B) Cylinder test and amphetamine induced rotational test were performed in *Study II*.

2.5. In vitro models and bioactivity assays in different cell culture models

2.5.1. Primary dopaminergic neuron cell culture

Dopaminergic neuronal cultures were prepared from Wistar rat embryos at 15, 16 or 17 days of gestation (E15-E17) for the third experimental study of this doctoral thesis. Animal procedures were reviewed and approved by the Local Ethical Committee for Animal Research of the University of the Basque Country (UPV/EHU, CEEA, ref. M20/2017/019). All of the experiments were performed in accordance with the European Community Council Directive on "The Protection of Animals Used for Scientific Purposes" (2010/63/EU) and with Spanish Law (RD 53/2013) for the care and use of laboratory animals. In order to obtain primary dopaminergic cell

cultures, the following protocols were followed with slightly modifications [58,59] (Figure 6A). Pregnant rats were euthanized and, under no aseptic conditions, removed the whole brain from the rat embryos and maintained on ice in a petri dish (10 cm \emptyset) with HBSS (Hank's Balanced Salt Solution) (Gibco[®] by Life Technologies, Spain) for removing the blood vessels and meninges. Then, the ventral portion of the mesencephalic flexure was selected following *Gaven et al.* protocol [60]. After collecting the brain areas of interest, tissue was incubated with Trypsin (Gibco[®] by Life Technologies, Spain) at 37°C during 15 min under aseptic conditions. Then, it was also incubated with DNase (deoxyribonuclease I from bovine pancreas (DNase I) (Millipore Sigma Life Sciences, Germany) for 30 seconds and after that time, the trypsin was inactivated and the tissue was washed twice with DMEM (Dulbecco's Modified Eagle Medium) GlutaMAX[™] FBS (fetal bovine serum) (10%), P/S (penicillin/streptomycin) (Gibco[®] by Life Technologies, Spain). After that, the tissue was mechanically dissociated by several passages through a 5 mL and 2 mL pipette. Finally, the cell suspension was passed through a 100 μ m Nylon strainer and centrifuged for obtaining cell pellet. Cell pellet was resuspended in Neurobasal Medium supplemented with 0.5 mM glutamine, 1% antibiotic (P/S) and 3 % B27 (Gibco[®] by Life Technologies, Spain) and cells were seeded for future functional studies.

2.5.1.1. Cell viability assay

The obtained cell suspension in 2.5.1 section was seeded at 40×10^3 cells/well density in poly-l-lysine-precoated 96-well culture plates. Dopaminergic cells were maintained during 7-10 days before performing the experiments and the medium was changed every 3 days, if necessary. At determined time point, the media from the cells was removed and new fresh media was added with the different nanoparticles concentrations, DHAH-NLCs or Mygliol- NLCs, (Table 1, Study III) (100, 75, 50, 25, 12.5 and 5 μ M) for 24 or 48h. The concentration (μ M) is referred to the quantity of DHAH present in the NLC formulation. For dosing Mygliol NPs, an equal amount of NLCs was used as internal control to show the difference between using a functional lipid such as DHAH versus an inert lipid such as Mygliol[®]. Afterwards, the viability was assessed using CCK-8 kit following manufacturer's protocol. Cell viability for each condition is represented in percentage regarding to control positive (C⁺) where no treatment was added to the cell media.

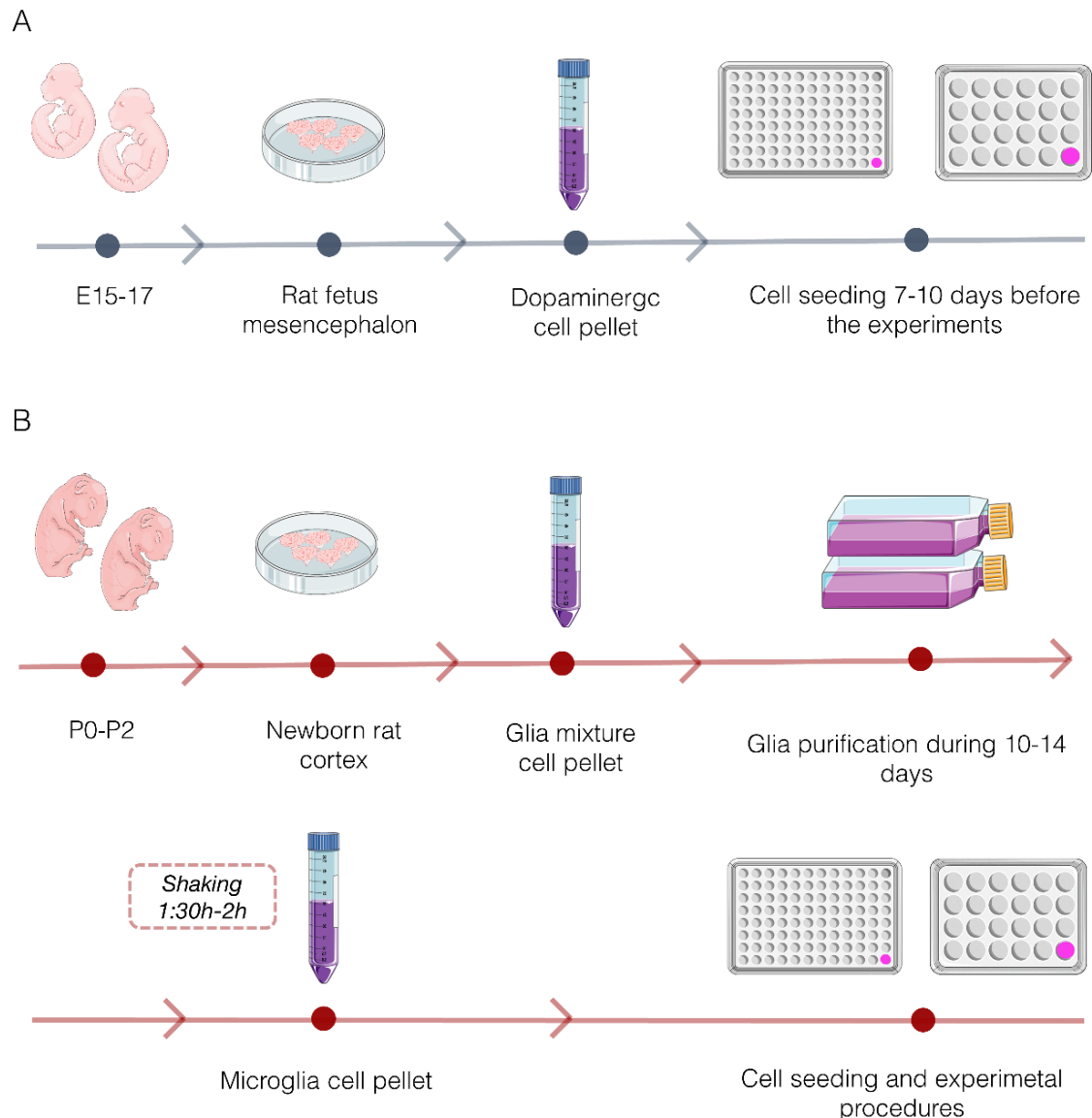


Figure 6. Schematic representation of primary cell culture protocols. (A) Primary dopaminergic neuron culture isolation and seeding. (B) Primary microglia cell culture isolation and seeding.

2.5.1.2. 6-OHDA toxicity assay: *in vitro* neurotoxicity model

Cell suspension (2.5.1 section) was seeded at 40×10^3 cells/well density in poly-l-lysine-precoated 96-well culture plates. Dopaminergic cell culture was maintained during 7-10 days, changing the media if necessary every 3 days. After that time, the media was removed and different concentrations of 6-OHDA toxin were added (500, 100, 50, 25, 10 and $5\mu\text{M}$) during 24 h to correlate neurotoxin concentration to cell viability. As positive control (C^+) we just changed the media and for negative control (C^-) DMSO (dimethyl sulfoxide) 10% was added. To assess cell viability, after 24 h incubation with 6-OHDA neurotoxin the media was removed and the cells were fixed with 3.7% paraformaldehyde (PFA) (Panreac, Spain) for 10 min and then, washed

three times in PBS. DAPI (4',6-diamidino-2-phenylindole) (Termofisher Scientific, Spain) staining (1:1000) in PBS during 15 min was used to determine viable cells. The data are expressed as the percentage of C⁺ group with no treatment, which was set as 100%.

2.5.1.3. *Neuroprotective assay*

Similar as before, cells were seed at 40×10^3 cells/well density and incubated during 7-10 days and then, treated with DHAH-NLCs or Mygliol NLCs (50, 25 and 12.5 μ M) 24 h before the 6-OHDA neurotoxin was added to the culture. 24 h after, the media was removed and fresh media was added with a final concentration of 25 μ M 6-OHDA neurotoxin and the previously tested concentrations for NLCs (50, 25 and 12.5 μ M). To assess the neuroprotective effect of DHAH-NLCs against 6-OHDA neurotoxin, the media was removed 24 h later and cells were fixed and incubated with DAPI as described in 2.5.1.2 section.

2.5.2. *Primary microglia cell culture*

Microglia neuronal cultures were prepared from Wistar rat puppets from day 0 to 2 (P0-P2) to carry out the third experimental study of this doctoral thesis. Animal procedures were reviewed and approved by the Local Ethical Committee for Animal Research of the University of the Basque Country (UPV/EHU, CEEA, ref. M20/2017/035). All the experiments were performed in accordance with the European Community Council Directive on "The Protection of Animals Used for Scientific Purposes" (2010/63/EU) and with Spanish Law (RD 53/2013) for the care and use of laboratory animals. Primary microglia cell cultures were obtained following *Chen et al.* protocol with slightly modifications [61] (Figure 6B). Puppet's brains were removed and kept on ice in a Petri dish (10 cm \emptyset) for removing the meninges and select the brain area of interest. Then, brain cortex was collected and incubated with trypsin for 15 min at 37°C. The tissue was incubated with DNase for 30 seconds and afterwards, the trypsin was inactivated and tissue was washed twice with DMEM GluatMAX™ FBS 10%, P/S. Finally, the tissue was mechanically dissociated by several passages through a 5 mL and 2 mL pipette and then, passed through a 70 μ m Nylon strainer and centrifuged for obtaining cell pellet. The obtained pellet was resuspended in DMEM GlutaMAX™ FBS 15%, P/S and incubated in poly-l-lysine coated flask at 37°C in a humidified 5% CO₂ atmosphere. After 3 days, full media was changed to DMEM GlutaMAX™ FBS 10%, P/S. After this,

half media changes were done every 2-3 days for maintaining this glia mixture culture during 10-14 days. To perform microglia cell isolation, flask media was removed and replaced with DMEM GlutaMAX™ FBS 15% P/S 24 h before the isolation started. Then, the flasks were put in a shaker at 250 rpm during 1:30-2 h to detach microglia cells from astroglia layer. After that time, primary microglia cells were removed from the flask, resuspended in complete DMEM with FBS 15%, and seeded in poly-L-lysine–precoated 96-well culture plates for different studies.

2.5.2.1. Cell viability assay

Microglia cell viability assay was performed similar to the one described in 2.5.1.1 section. However, in this case, microglia cells were seeded at 50×10^3 cells/well density. 24 h after cell attachment, the media was removed and the cells were incubated during 24 or 48 h with the different concentrations of NLCs as previously pointed out. Then, the viability CCK-8 test was performed following manufacturer's protocol.

2.5.2.2. Pro-inflammatory cytokine release quantification: TNF- α , IL-1 β and IL-6

DHAH-NLCs anti-inflammatory effect against LPS (lipopolysaccharide) was studied in microglia primary cells. To perform the assay, cells were pre-treated for 24 h with DHAH-NLCs and Mygliol-NLCs at different concentrations (50 μ M, 25 μ M, and 12.5 μ M) or just media change. After that treatment, media was removed and cells were incubated for other 24 h with LPS 50ng/ml, and the different concentrations of the nanoparticles. After that 24 h, cell media supernatant was collected and stored at -80°C. The levels of TNF- α , IL-1 β and IL-6 were analyzed with ELISA assay (Peprotech (UK)). The total amount of cytokine release was normalized according to cell viability measured with CCK-8 assay at the same time point.

2.5.3. BMCEs differentiation protocol: BBB model

In the Study IV of this doctoral thesis, BMCEs were differentiated from hiPSCs to generate a human BBB model. For that purpose, hiPSC were cultured in Matrigel (Corning®, USA) coated six-well plates (1mg/ml) with mTeSR™1 medium (STEMCELL Technologies, France). The protocol followed is similar to the one described by *Neal et al.*, but with slight modifications [62].

One day before the differentiation started (D-1) the media was removed, cells were washed with DPBS (Dulbecco's Phosphate-Buffered Saline) and 500 μ l of TrypLE (Gibco[®] by Life Technologies, Sweden) was added to each well. After 5 min incubation, it was diluted 1:5 in mTeSR media, centrifuged 3 min at 200 rcf and resuspended in mTeSR media with ROCK inhibitor (Y-27632 dihydrochloride) (Bio-Techne, USA) (10 μ M). hiPSCs were seeded into Matrigel coated six-well plates at 16K/cm² cell density. 24 h later, the mTeSR media was removed and changed with E6 media (Essential 6[™] medium) (Gibco[®] by Life Technologies, Sweden) daily during four days (D0-D3). Then, the media was changed to hESFM media (human endothelial serum free medium) (Gibco[®] by Life Technologies, Sweden) supplemented with B27 1X, FGF (fibroblast growth factor) (Bio-Techne, USA) 20 ng/ml and RA (all-trans retinoic acid) (Millipore Sigma Life Sciences, Germany) 10 μ M called as, hESFM complete media. Cells were maintained in this media during two consecutive days without media change. After that period, the media was removed, cells were washed and incubated with TrypLE for 20 min to 30 min until a single cell suspension was formed. Cells were collected via centrifugation and plated, also referred to as subculturing, onto substrates coated in a mixture of 400 μ g/mL collagen IV and 100 μ g/mL fibronectin (Millipore Sigma Life Sciences, Germany) seeding 3.3 10⁵ cells in each Transwell[™] with hESFM complete media. 24 h after sub-culturing, TEER was measured using STX2 chopstick electrodes and an EVOM2 voltohmmeter (World Precision Instruments). This procedure was also repeated at 48 h. 24 h before the cells were used for any functional assay the media was changed with hESFM with B27, but no bFGF nor RA was added. Cells were used for permeability functional assay 24 h after the removal of bFGF and RA.

2.5.3.1. NLC transport across BMCEs differentiated from hiPSC

Transport of NLCs across *BMCEs* of BBB *in vitro* model was studied quantitatively by fluorescence measurement (Plate Reader Infinite M1000, Tecan, Switzerland) and qualitatively by confocal laser scanning microscopy (LSM 710), for which DiD ($\lambda_{em} = 644$ nm, $\lambda_{ex} = 685$ nm) labeled NLCs were employed. The transport of the different NLCs was evaluated in BMECs 48 h after seeding on Transwell[™] inserts as explained in 2.5.3 section. Inserts with TEER values above 3000 Ω cm² were selected to conduct the transport studies. The experiments were conducted at 37°C by adding a volume of 100 μ l at 1 mg/ml NLC (CS-NLC-DiD or TAT-CS-NLC-DiD, Table 1) concentration in hESFM with B27 on the apical side of the inserts. At

different time points (0 min, 30 min, 1 h, 1 h 30 min and 2 h), a sample aliquot of 50 μ l was collected from the basolateral side and 50 μ l of fresh media was added to the same chamber. The NLC concentration was determined by fluorescence measurement (Plate Reader Infinite M1000, Tecan, Switzerland). The relative fluorescent signal was correlated to standard linear curve (125-0 μ g/ml in serial dilutions). The NLC transport rate is expressed as mean of transported NLCs in percentage \pm SEM. After transport experiments, cell monolayers were fixed in PFA 4% for subsequent staining and imaging.

2.5.4. HMC3 microglia cell culture

2.5.4.1. HMC3 cell line viability assay

HMC3 cells were maintained in DMEM/F12 (Gibco[®] by Life Technologies, Sweden) medium containing 10% of FBS under standardized conditions (95% relative humidity, 5% CO₂, 37°C) (Study IV). To evaluate the non-toxic and most effective dose to work, alamarBlue[™] assay was carried out. Cells were seeded at a density of 10K/cm² for 24h to allow cell attachment. The day after, different doses of NLCs of four different kind of formulations were added (DHAH-NLC, Mygliol-NLC, DHAH-NLC-GDNF and DHAH-NLC VEGF, Table 1) during 24 and 48 h. Afterwards, the viability was assessed using alamarBlue[™] kit, following manufacturer's protocol. Cell viability for each condition is represented in percentage regarding to control negative where no treatment was added to the cell media, which was set as 100%. For control positive, cells were treated with DMSO 10% at least for 24h.

2.5.4.2. HMC3 activation with LPS

Cells were seeded at 10K/ cm² or 15K/ cm², depending on the subsequent assay done with those cells, Multiplex assay to check cytokine level or RT-qPCR to determine the genes involve in the neuroinflammatory process, respectively. Two different conditions were tested in this assay. In the first one (condition A) we incubated the cells with the NPs (Table 1) during 24 h after cell attachment. The NLC concentration was previously established with alamarBlue[™] assay and was set at 25 μ m for the functional lipid (DHAH) and 25ng/ml for the GF, (for Mygliol-NLC an equal dose of NLCs in mg/ml was used as internal control). In this condition, for control groups we had Control⁺ (LPS 100ng/ml during 24 h) and Control⁻ with just media. In the second condition (condition B) after seeding the cells for 24 h, cells were pre-treated during other 24 h with the four different NLC formulation (Table 1).

After that time, LPS (100ng/ml) and different NPs were incubated for additional 24 h. For Control, daily media change was performed. 24 h later, cell supernatant was collected for Multiplex assay (2.8 section) or cells were lysate for RNA extraction (2.7 section).

2.6. Immunohistochemistry and immunofluorescence techniques

2.6.1. *Immunohistochemistry*

2.6.1.1. *Peroxidase technique*

As previously explained, animals going under behavioral tests (Study I and Study II) were sacrificed after finishing the study. Different immunohistochemistry assays were performed in these two different studies. Tyrosine hydroxylase (TH) immunohistochemistry assay was performed in both of them, and nuclear factor erythroid 2-related factor 2 (Nrf2) assay was only performed in Study II, with the animals going through PUFAs treatment. The protocol followed in both cases was similar. Indeed, after being sacrificed, the brain tissue was collected, fixed and brain areas of interest, striatum (ST) and substantia nigra (SN) were selected to perform immunohistochemical studies (Table 4). Brain slices were washed with different kind of buffers. Hereafter, endogenous peroxidases were quenched during 15-30 min. After rinsing, slices were blocked and permeabilized during 1 h. After that time, they were incubated with the primary antibody, TH or Nrf2 overnight under constant agitation at 4°C. The day after they were incubated with the secondary antibody, incubated with ABC kit (Palex, Spain) and visualized with DAB chromogen. Finally, slices were mounted on gelatin-coated slides, dehydrated, and mounted with fixed DPX medium (BDH Gum ®, UK). A schematic representation of the reagents and steps followed in this technique have been summarized in Table 4.

2.6.1.2. *Immunofluorescence technique*

For studying Iba1 and GFAP microglia and astroglia markers the followed protocol and technique was different to the previously explained one. After rising ST and SN brain areas of interest, fixed brain sections were blocked and permeabilized in PB. Then, they were incubated with the primary antibodies overnight at 4°C.

Table 4. Summary of the different techniques and immunohistochemistry assays performed (Study I and Study II). PB: phosphate buffer; BSA: bovine serum albumine, TH: tyrosine hydroxylase, ON: overnight, KPBS: potassium phosphate buffered saline; NGS: normal goat serum; KPBST: potassium phosphate buffered saline with 1% of Triton; Nrf2: nuclear factor erythroid 2-related factor 2; Iba-1: ionizing calcium-binding adaptor molecule 1; GFAP: glial fibrillary acidic protein; DAPI: 4',6-diamidino-2-phenylindole.

Peroxidase technique				
	<i>Endogenous peroxidase quenching</i>	<i>Blocking and permeabilize</i>	<i>Primary antibody</i>	<i>Second antibody</i>
Study I	1% (v/v) H ₂ O ₂ and 1% (v/v) ethanol Panreac (Spain) in PB, 15 min, RT.	2% (w/v) of BSA (Millipore Sigma Life Sciences, Germany), 0.5% (v/v) Triton-X (Millipore Sigma Life Sciences, Germany) in PB solution.	rabbit polyclonal anti-TH (1:2000) (Millipore Sigma Life Sciences, Germany) in BSA 0.1% (w/v), Triton-X 0.5% (v/v), ON, 4°C.	secondary biotinylated antibody (1:250) (Palex, Spain), in PB, 1 h, RT.
Study II	1% (v/v) H ₂ O ₂ and 10% (v/v) methanol (Panreac, Spain) in KPBS, 30 min, RT.	5% (v/v) NGS (Palex, Spain) and 1% (v/v) Triton X-100 (Millipore Sigma Life Sciences, German with KPBS, 1h, RT	rabbit polyclonal anti-TH (1:1000) (Millipore Sigma Life Sciences, Germany) or primary rabbit polyclonal antibody anti- Nrf2 (Abcam, UK) (1:400) in in 5% NGS (v/v) KPBST at RT ON, 4°C	secondary biotinylated goat anti-rabbit IgG (1:200), 2.5% NGS (v/v) in KPBST, 2 h, RT.
Immunofluorescence technique				
	<i>Blocking and permeabilize</i>	<i>Primary antibody</i>	<i>Second antibody</i>	<i>DAPI incubation</i>
Study I	2% (w/v) BSA solution and 0.5% (w/v) Triton-X in PB, 1 h, RT.	polyclonal rabbit anti- Iba-1 (1:1000, Wako) in BSA 0.1% (w/v), Triton-X 0.5% (v/v), ON, 4°C.	anti-rabbit Alexa Fluor IgG 488 (1:1000) (Termofisher Scientific (Spain) with 0.1% (w/v) BSA and 0.1% Triton-X (v/v) in PB, 2 h RT.	The slices were mounted with Vectashiel® with DAPI (Vector Laboratories, Spain)
Study II	2% (w/v) BSA solution and 0.5% (w/v) Triton-X in PB, 1 h, RT.	polyclonal rabbit ant-ilba1 (1:1000) (Synaptic Systems , Germany) or for mouse anti GFAP (1:400) (Termofisher Scientific, Spain) in BSA 0.1% (w/v), Triton-X 0.5% (v/v), ON, 4°C..	anti-rabbit Alexa Fluor IgG 488 (1:1000); anti-mouse Alexa Fluor IgG 488 (1:1000) (Termofisher Scientific, Spain) with 0.1% (w/v) BSA and 0.1% Triton-X (v/v) in PB, 2 h, RT.	DAPI (1:10.000) (Termofisher Scientific, Spain) and mounted in coverslips with FluoroMount™ (Millipore Sigma Life Sciences, Germany)

The following day, brain slices were incubated with the secondary antibody for 2 h. Then, the slices were washed, incubated with DAPI to stain the nucleus, and mounted with mounting media. (If the DAPI staining was not performed the mounting media was with DAPI). In table 4 a schematic representation of the different buffers and antibodies have been summarized.

2.6.2. Immunofluorescence in cells

In the case of BMCEs, ZO-1 (zonula occludens-1) staining was performed to check the reliability of our BBB human model with the presence of ZO-1 marker. The immunofluorescence (IF) was carried out directly into Transwell® inserts. After fixing and washing the cells, they were blocked for a minimum of 1 h at RT in DPBS with 10% goat serum and 0.1% Triton X-100 (Millipore Sigma Life Sciences, Germany) in DPBS. After three rinsing steps, cells were then incubated with ZO-1 primary antibody (1:100) with 1% goat serum and 0.01% Triton X-100 in DPBS overnight at 4°C. The following day, cells were incubated with the secondary antibody, anti-mouse IgG1 (γ1), CF™488A antibody (Millipore Sigma Life Sciences, Germany) (1:1000) in DPBS with 1% goat serum and 0.01% Triton X-100 during 1 h at RT. After three rinsing steps, the fixed cells were incubated in DAPI. Hereafter, the insert was cut and mounted with ProLong™ Glass Antifade Mountant (Invitrogen™ by ThermoFisher Scientific, Sweden) on glass slides.

2.7. RTqPCR

Total RNA isolation of HMC3 microglia cell line (2.5.4.2 section) and purification was performed using High pure RNA isolation Kit (Roche®, Switzerland), following manufacturer's instructions. Subsequently, RNA quantity and quality was assessed by NanoDrop™ 1000 Spectrophotometer (Thermo Scientific). cDNA synthesis was performed using High-Capacity RNA-to-cDNA™ Kit (Thermo Scientific, Sweden) according to manufacturer's instructions. TaqMan Master Mix was used together with TaqMan Assays (Thermo Scientific, Sweden) to amplify relevant genes, and run on QuantStudio™ 5 Flex Real-Time PCR System in 96 well plate and running samples in duplicate. Relative gene expression was computed by the delta Ct method using as a reference gene glyceraldehyde 3-phosphate dehydrogenase (GAPDH).

2.8. Multiplex assay

Cytokine levels of cell culture supernatant (2.5.4.2 section) were measured on the U-Plex MSD electrochemiluminescence multi-spot assay platform (MesoScale

Diagnostics, Rockville USA). MSD assays was performed according to the manufacturer's instructions. MSD testing was conducted in a single laboratory by a single technician at the SciLifeLab (Stockholm, Sweden).

2.9. Statistical analysis and figures

Experimental data were analyzed using the computer program GraphPad Prism (v. 6.01, GraphPad Software, Inc.) P values < 0.05 were considered as statistically significant. All graphs were done with GraphPad Prism (v. 6.01, GraphPad Software, Inc.). All figures were created using Servier Medical Art templates, which are licensed under a Creative Commons Attribution 3.0 Unported License <https://smart.servier.com> .

3. Hypothesis and Objectives

Neurodegenerative diseases are complex neurological conditions with increasing prevalence as life expectancy rises and without effective treatment slowing down the progression of the disease. In order to obtain a successful therapy, the research has focused mainly on disease-modifying strategies. Among others, GFs have been displayed as a feasible therapeutic option since they enhance cell differentiation, promote neurogenesis and axonal growth. However, increasing evidence suggest that NDs pathogenesis is not restricted to the neuronal compartment but strongly interacts with glia. Actually, microglia is known to be a key player in the neuroinflammation undergoing in NDs and its modulation may be an useful tool to treat NDs. That is why, in the last years other kind of molecules such as PUFAs have been considered as good candidates to manage the inflammation and oxidative stress present in NDs.

In the case of GF, the key aspect to obtain an effective treatment in NDs is their lack of brain targeting due to the presence of BBB. In an attempt to overcome it, different strategies have been develop in the last years. One of most studied ones is the use of nanotechnology based DDS to target and treat CNS related disorders. Among all of them, NLC are unstructured lipid matrix, made of a mixture of lipid blend (solid and liquid lipids) and an aqueous phase containing surfactants. These lipid nanocarriers are made by inert lipids without any effective role in the treatment or prevention of the disease. However, in the last years, different functional lipids have been incorporated to the lipid matrix of NLC, so the nanocarrier itself could exhibit beneficial effects. Moreover, the surface of the NLC can be modified with different peptides and polysaccharides to specifically target the brain. Therefore, increasing the concentration of the therapeutics in the brain and enhancing their ability to treat NDs.

Bearing all this information in mind, the main objective of the present thesis is the development of NLC composed of functional lipids, and surface modified with different moieties, to target and treat CNS related disorders. To accomplish this purpose, four specific objectives are considered:

1. To develop, characterize and *in vivo* study the effect of intranasally administered CS-TAT surface modified NLC to target the brain and increase

the therapeutic effect of GDNF in Parkinson's disease animal model [63]. (Study I can be seen in Appendix 4 of this thesis).

2. To study the effect of functional lipids such as DHA and DHAH in the 6-OHDA rat model of Parkinson's disease, regarding their ability to act on dopaminergic system, neuroinflammation and oxidative stress [40]. (Study II can be seen in Appendix 5 of this thesis).
3. To develop and characterize NLC composed of DHAH functional lipid, retaining its ability to act as neuroprotective and anti-inflammatory agent in primary cell culture models [64] (Study III can be seen in Appendix 6 of this thesis).
4. To develop and characterize NLC composed of DHAH functional lipid and entrapping GDNF or VEGF neurotherapeutics to become in a simultaneously integrated boost treatment for NDs related pathogenesis in *in vitro* cell cultures mimicking human context as an alternative to animal models (Study IV can be seen in Appendix 7 of this thesis).

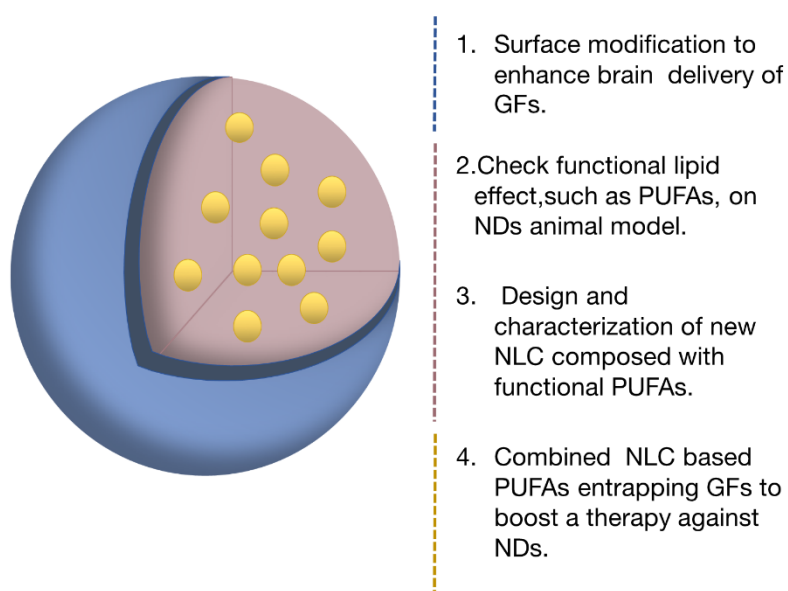


Figure 7. Schematic representation of the objectives of the present doctoral thesis. (NLC: nanostructured lipid carriers; GF: growth factors; PUFA: polyunsaturated fatty acids; ND: neurodegenerative diseases).

4. Results and discussion

As pointed out before, PD is the second most common NDs. PD is a complex neurodegenerative condition that is characterized by resting tremor, bradykinesia, rigidity, and postural instability. Despite all the effort made by the scientific community in the last years, up until now there is no treatment able of slowing down the progression of the disease [65,66]. NTF therapy, more concretely GDNF, has the potential to act as a disease modifying treatment. Although the controversial about its effects in recent clinical trials, it still remains as the gold standard NTF for PD treatment [67,68]. One of the most challenging aspect to complete the clinical translation of GDNF is the lack of an effective carrier and administration route. Regarding this aspect, in previous studies conducted by our research group, we successfully develop polymeric micro and nanospheres encapsulating GDNF to restore locomotor activity in PD animal model [69,70]. However, the invasive administration route employed, intrastriatal administration, limits their use in clinical application. Therefore, the development of new nanocarriers that could be administered through alternative administrations routes remains necessary.

In the first study of this doctoral thesis, we aim to generate a functional carrier modified with CS and TAT that successfully deliver GDNF in mice's brains through intranasal administration. The intranasal administration brings the opportunity to target the brain through a non-invasive technique as previously pointed out. To obtain that goal, modifications on NP surface can be done. A recent study conducted by our research group showed that the surface modification of NLC with CS successfully deliver GDNF in lesioned rat and restored the motor symptomatology [25]. In the present study, we did not only change the surface with CS but also with TAT to enhance brain targeting of GDNF neurotherapeutic. TAT molecule has been used to boost the delivery of peptides in the brain through the intranasal administration [71,72] and the results obtained in this doctoral thesis support that data.

The formulation of NLC coated with CS and TAT and entrapping GDNF (CS-NLC-TAT-GDNF) exhibited positive zeta values ($+21.9 \pm 1.8$ mV), indicating that TAT and CS coating process was successfully perform. The EE of GDNF was high, around 87% for both formulations entrapping GDNF (CS-NLC-GDNF and CS-NLC-TAT-GDNF). Moreover, the size of the particles, (205.9 ± 6.3 nm) (PDI 0.275 ± 0.02)

makes them suitable for intranasal administration [31]. The administration of this nanoformulation to MPTP injured animal model of PD restored the locomotor activity, being the group with the best results since the beginning of the study (191.8 ± 21.9 ; $*p < 0.05$) and maintaining this positive effect until the end of the study (176.4 ± 38.8 ; $*p < 0.05$) Figure 8A. This beneficial effect was confirmed with immunohistological evaluation. As seen in Figure 8B-D, the administration of CS-NLC-TAT-GDNF increased the positive TH fibers in ST (141.18 ± 5.68 ; $****p < 0.05$) and TH⁺ cells (%) in SN (91.46 ± 7.54 ; $****p < 0.05$), two of the main brain areas affected in PD. This effect was also seen for CS-NLC-GDNF nanoformulation but with slightly worse results, highlighting the effectiveness of TAT targeting the brain and increasing the therapeutic concentration of GDNF.

Moreover, recently it has been highlighted the therapeutic effect of GDNF modulating microglial activation process in the disease. As previously explained, microglia is a key factor in the neuroinflammation undergoing in NDs and its modulation could be beneficial in NDs treatment. In the last few years, different studies in primary microglia cell cultures and PD animal models demonstrated the effect of GDNF decreasing the release of proinflammatory and neurotoxic molecules [73-75]. In this assay, we also conclude that the administration of GDNF may not only have a protective effect on neurons, but may also modulate microglial activities to exert its therapeutic effect. The data obtained in this research is in line with those studies. Indeed, the administration of CS-NLC-TAT-GDNF nanoformulation decreased the microglial activation (confirmed with Iba-1⁺ cells (%)) present after MPTP administration with values similar to Control for both ST ($99.43.0 \pm 4.25$; $****p < 0.0001$) and SN (107.0 ± 6.2 ; $****p < 0.0001$) (Figure 9). The GDNF administration in solution did not decrease the activation of microglial cells. Therefore, the present results confirm the suitability of the developed nanocarrier CS and TAT modified to increase brain levels of GDNF to exert its therapeutic effect; restoring motor activity, increasing TH expression in both brain areas of interest, and furthermore, decreasing the microgliosis related to PD.

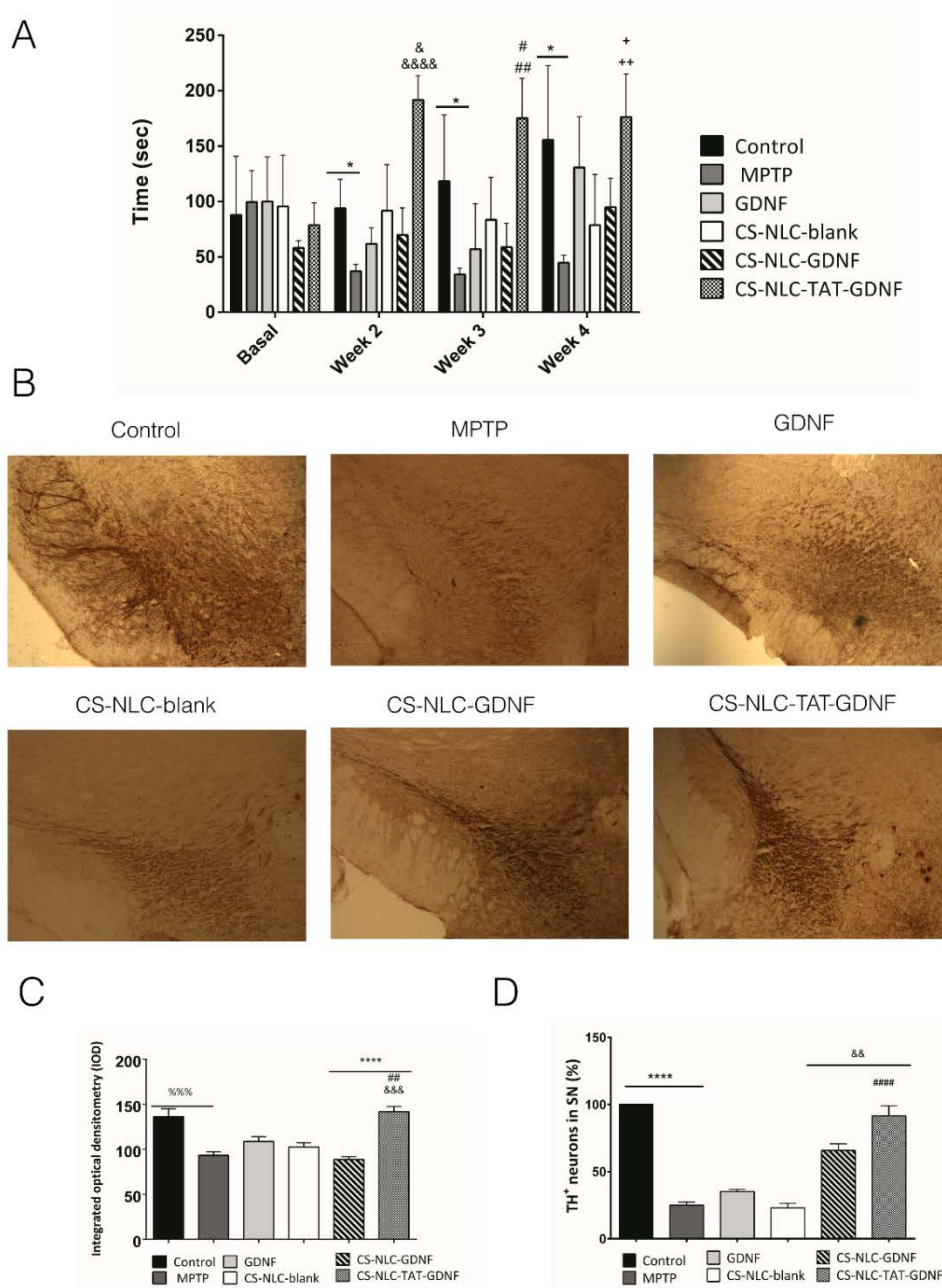


Figure 8. (A) Locomotor activity. (* $p < 0.05$ Control vs MPTP; &&&& $p < 0.0001$ CS-NLC-TAT-GDNF vs MPTP; & $p < 0.05$ CS-NLCTAT- GDNF vs CS-NLC-blank, CS-NLC-GDNF; ## $p < 0.05$ CS-NLCTAT- GDNF vs MPTP; # $p < 0.05$ CS-NLC-TAT-GDNF vs CS-NLC-blank; ++ $p < 0.01$ CS-NLC-TAT-GDNF vs MPTP, CS-NLC-blank; + $p < 0.05$ CS-NLC-TAT-GDNF vs CS-NLC-GDNF), Student's t test. (B) Representative photomicrographs of TH immunostaining in SN in all mice groups. (C) The integrated optical density (IOD) of TH⁺ fibers in the ST. (%%% $p < 0.05$ Control vs MPTP; **** $p < 0.05$ CS-NLC-TAT-GDNF vs MPTP, CS-NLC-GDNF; &&& $p < 0.05$ CS-NLS-TAT-GDNF vs CS-NLC blank; ## $p < 0.05$ CS-NLC-TAT GDNF vs GDNF, One-way ANOVA). (D) TH⁺ neurons in SN (%) (**** $p < 0.05$ Control vs MPTP; #### $p < 0.05$ CS-NLCTAT- GDNF vs MPTP, GDNF and CS-NLC-blank; && $p < 0.05$ CS-NLCTAT- GDNF vs CS-NLC-GDNF, One-way ANOVA) The data are shown as the mean \pm SEM.

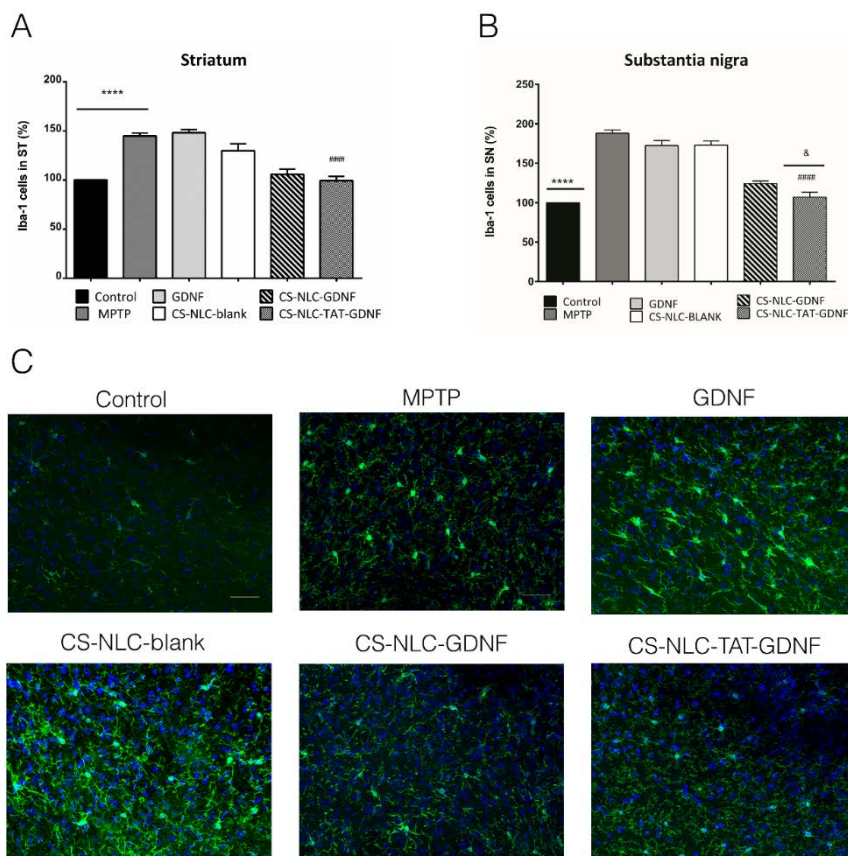


Figure 9. (A) Graphic representation of Iba-1⁺ cells in ST (****p < 0.0001 MPTP vs Control; #####p < 0.0001 CS-NLC-TAT-GDNF vs MPTP and GDNF. (B) Graphic representation of Iba-1⁺ cells in SN (****p < 0.001 MPTP vs Control, #####p < 0.0001 CSNLC- TAT-GDNF vs MPTP, GDNF and CS-NLC-blank; &p < 0.05 CSNLC- TAT-GDNF vs CS-NLC-GDNF (Student's t test). The data are shown as the mean \pm SEM. (C) Representative Iba-1 immunophotographs in the SN. (Scale bar 50 μ M).

In the second step of this doctoral thesis, we continue studying different treatments that could manage the neuroinflammation present in NDs, and more concretely in PD. Among other molecules, the use of functional lipids such as PUFA have gained attention due to their beneficial role in the prevention and/or treatment of the disease. Although it is not known the exact mechanism by which they exert their beneficial effects, they have shown positive results modulating the pathological hallmarks of the disease: oxidative stress, neuroinflammation, mitochondrial dysfunction and excitotoxicity [36,39]. Moreover, recent epidemiological studies together with animal studies in AD and PD animal models support their use as a co-adjuvant treatment [43,76,77]. Among different functional lipids, in the second experimental study of this doctoral thesis we focus on DHA and its hydroxylated derivate DHAH. The chronic administration of these two functional lipids, before and after 6-OHDA neurotoxic lesion, showed a trend to improve the behavioral activity of

the animals going through DHA and DHAH daily treatment. Despite the positive effect shown, we were not able to detect statistical significance (Two-way Anova) at any of the session performed along 15 weeks for neither of the two different behavioral test performed, amphetamine induced behavioral test and cylinder test. In previous studies with chronic administration of n-3 PUFAs, similar results were observed; without a statistical difference in behavioral tests [78,79] (Figure 10 A-D). Nonetheless, the recovery trend saw in behavioral tests was confirmed with TH immunohistochemistry studies, supporting the beneficial effect of these functional lipids. The DHAH supplementation increased the density of TH⁺ fibers (%) (41.01 ± 2.93), showing higher values when compared to DHA group (29.34 ± 3.03). This difference was higher when compared to saline group, almost doubling the values (23.33 ± 2.68) (Figure 10 E-F). Accordingly, the TH⁺ nigral neurons were higher in this experimental group (31.0 ± 3.32) with similar but worse result for DHA treated group (24.48 ± 3.17). In this case, the group going through DHAH treatment showed three time higher TH⁺ nigral neurons when compared to saline group (10.70 ± 1.89) (Figure 10 G-H).

Furthermore, PUFAs are known to have an anti-inflammatory effect [80]. That is why; we can hypothesize that its administration may decrease the reactive gliosis and target the neuroinflammation present in PD [81]. In the present study we confirmed the ability of PUFA to decrease the astrogliosis and microgliosis present in the 6-OHDA animal model of the disease. The GFAP marker for astroglia was decreased after DHA (143.4 ± 18.4) (115.2 ± 3.3) and DHAH (129.0 ± 8.4) (129.1 ± 8.4) treatment in both brain areas of interest, ST and SN, respectively (Figure 11 A-B, E). Moreover, as in the previous study, we did also check the effect of these functional lipids in microglia activation. In this case, the daily treatment with DHA decreased the microgliosis present after the 6-OHDA toxic, both in ST (142.7 ± 11.8) and in SN (122.8 ± 7.59) (Figure 11 C-D). This decrease in Iba-1⁺ cells was more evident after DHAH treatment with values similar to control in ST (110.4 ± 9.2) and SN (113.6 ± 3.8). Indeed, the exogenous administration of DHA reducing astrogliosis and microgliosis has been previously described in both *in vitro* and *in vivo* studies with different models of neuroinflammation [82-85]. Overall, the results obtained in this study are in line with previous publications with PUFAs treatment administration and revealed a higher positive effect of DHAH supplementation decreasing astroglia and microglia positive cells. Therefore, normalizing the activity of glia in PD injured brain.

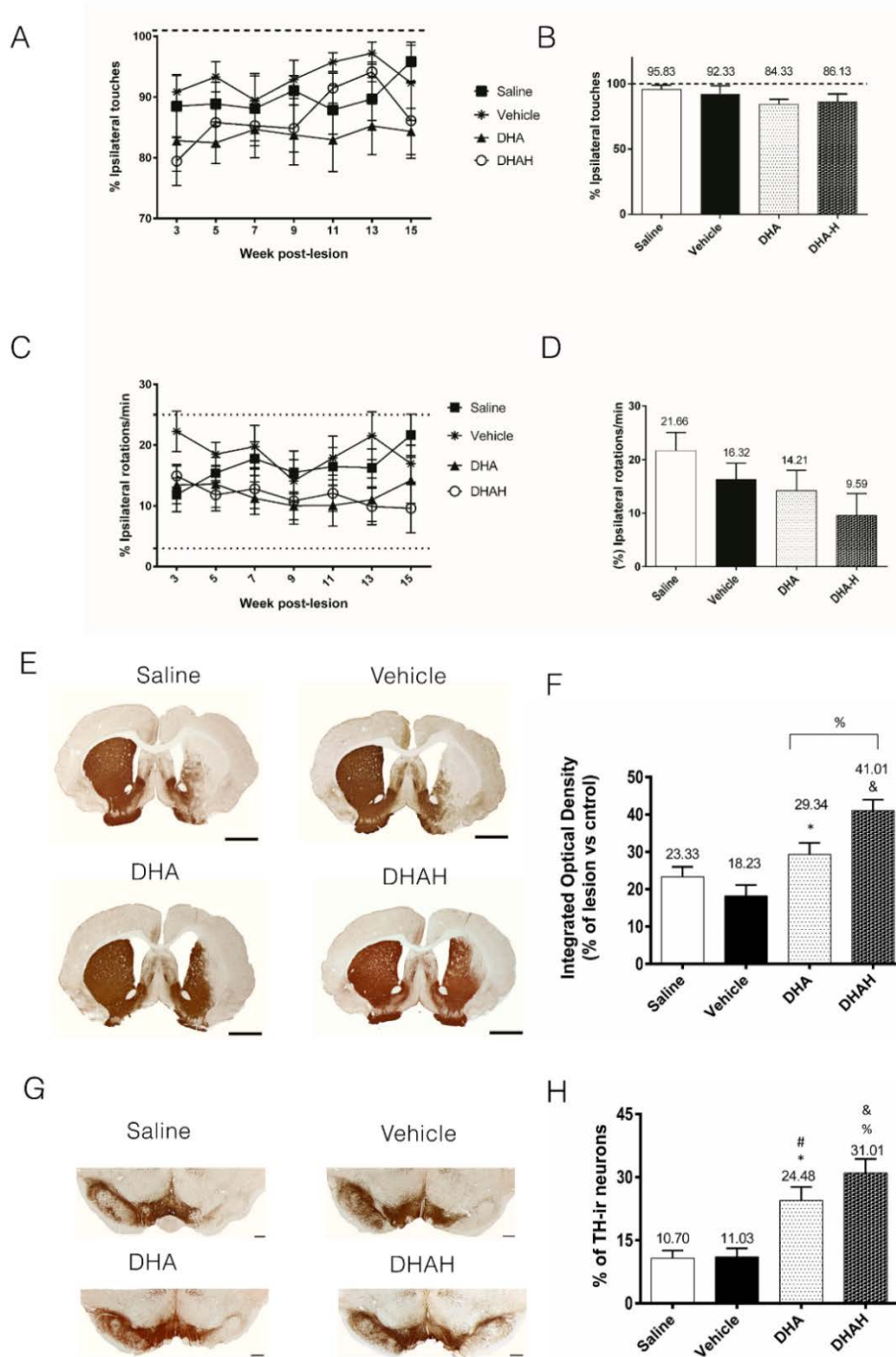


Figure 10. (A) Graphical representation of the evolution on amphetamine induced rotations during the study. (B) Graphical representation of the data obtained at week 15 (C) Graphical representation of the evolution on the cylinder test. (D) Graphical representation of the data obtained at week (p>0.05, Two-way ANOVA, Tukey's multiple comparisons test) (E) Representative photomicrographs of TH-immunostained ST (scale bar 2mm). (F) Graph depicts the integrated optical density (IOD) of TH⁺ fibers in ST. The data are shown as the mean \pm SEM. (*p<0.05 DHA vs Vehicle, &p<0.0001 DHAH vs Saline and Vehicle, %p<0.01 DHAH vs DHA), One-way ANOVA, Tukey's multiple comparisons test). (G) Representative photomicrographs of TH immunostain in SN (scale bar 500µm). (H) TH⁺ neurons in SN (%). The data are shown as the mean \pm SEM. (&p<0.05 DHA vs vehicle, *p<0.01 DHA vs saline, &p<0.0001 DHAH vs saline %p<0.001 DHAH vs vehicle), One-way ANOVA, Tukey's multiple comparisons test.

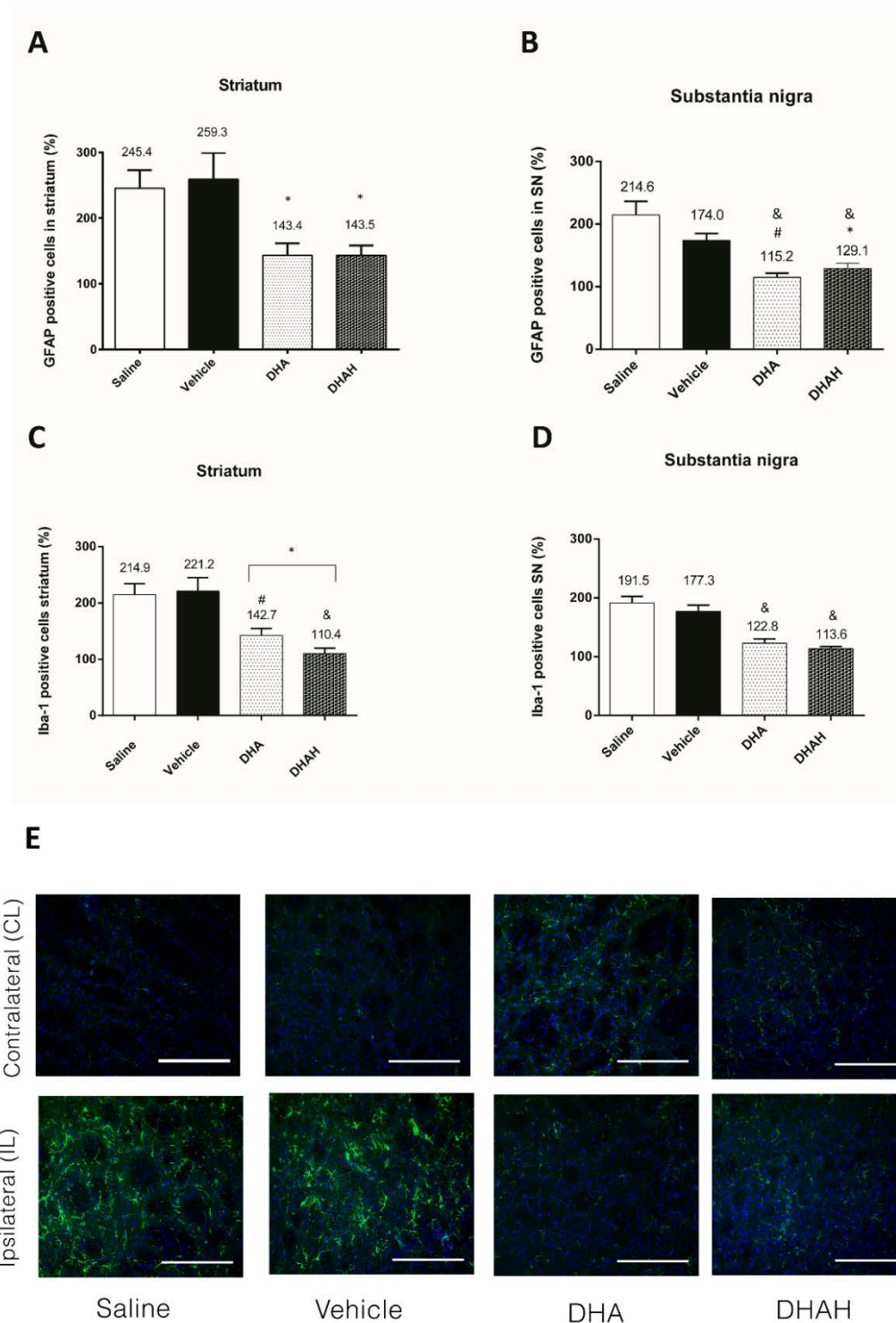


Figure 11. (A) GFAP⁺ cells in the striatum of all rat groups (%). ($*p < 0.05$ DHA vs saline and vehicle) ($*p < 0.05$ vs saline and vehicle). (B) GFAP⁺ cells in SN of all rat groups (%). ($*p < 0.0001$ DHA vs saline, $\#p < 0.01$ DHA vs vehicle) ($*p < 0.0001$ DHAH vs saline, $*p < 0.05$ DHAH vs vehicle). The data are shown as the mean \pm SEM (One-way ANOVA Tukey's multiple comparisons test) (C) Iba-1⁺ cells in the striatum of all rat groups (%). ($*p < 0.01$ DHA vs saline and vehicle) ($*p < 0.0001$ DHAH vs saline and vehicle) ($*p < 0.05$ DHAH vs DHA). (D) Iba-1 cells in SN of all rat groups (%). ($*p < 0.0001$ DHA vs saline, and vehicle) ($*p < 0.0001$ DHAH vs saline and vehicle), unpaired Student's t-test. The data are shown as the mean \pm SEM. (E) Representative GFAP immunophotographs in ST (scale bar 10 μ m). Blue stained for nucleus and green stained for GFAP⁺ cells.

Finally, we studied the effect of these functional lipids on the anti-oxidative pathway (ARE/Nrf2). Indeed, oxidative stress is a hallmark of PD and therefore, the antioxidant therapy has been proposed as a reasonable therapeutic approach [86]. The activation of Nrf2 pathway seen after 6-OHDA exposure was decreased after DHAH administration with similar values for ST (115.3 ± 6.6) and SN (120.6 ± 4.8) (Figure 12). In this case, DHA administration decrease Nrf2⁺ cells in both brain areas of interest. However, it was not statistically significant, different from what seen in different cell cultures or animal models of neuroinflammation [87,88]. In summary, all the results obtained in this second experimental study support the use of DHAH as a functional lipid since it exhibited positive effect on dopaminergic system, neuroinflammation and oxidative stress.

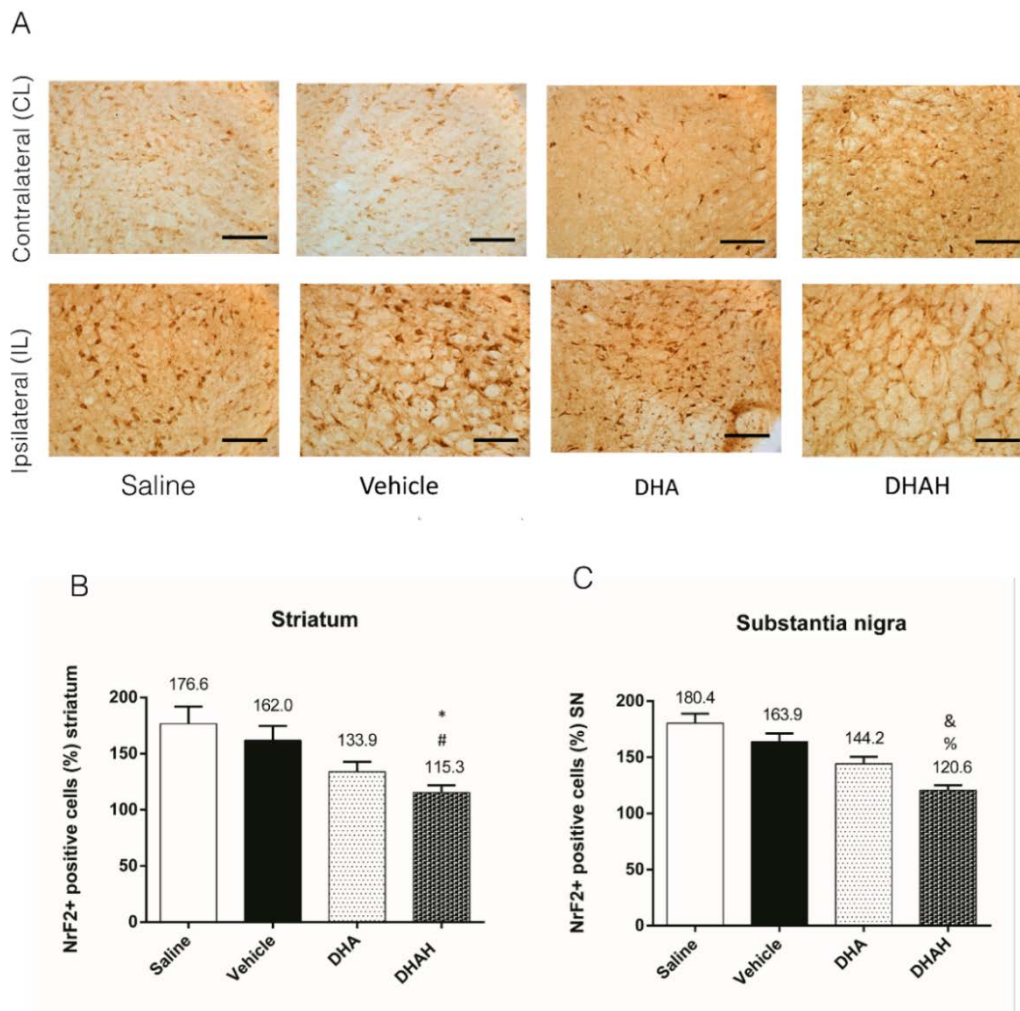


Figure 12. (A) Representative Nrf2 immunophotographs of all rat groups in the SN (sale bar $2\mu\text{m}$) (B) Nrf2⁺ cells in the striatum of all rat groups (%). (# $p < 0.01$ DHAH vs saline; * $p < 0.05$ DHAH vs vehicle). (C) Nrf2⁺ cells in SN of all rat groups (%). (& $p < 0.0001$ DHAH vs saline) (% $p < 0.001$ DHAH vs vehicle), The data are shown as the mean \pm SEM. (One-way ANOVA, Tukey's multiple comparisons test).

Once we demonstrated the suitability of DHAH as a functional lipid modulating the inflammation and oxidative stress present in NDs, we design a third experimental study to develop a new NLC formulation that includes DHAH in the lipid matrix of the nanoformulation.

All the developed nanoformulations (Table 1) were between 50-90 nm in size, with a PDI value below 0.5 indicating a homogenous suspension. The selected solid: liquid lipid ratio for the two different lipids, Mygliol and DHAH, was in the ratio normally used for NLCs preparation [27]. The resulted NPs were similar in size, around 100 nm, and exhibited positive zeta values, due to the successful CS coating process. The TEM images showed that the NPs were uniform in morphology and size dispersion (Figure 13).

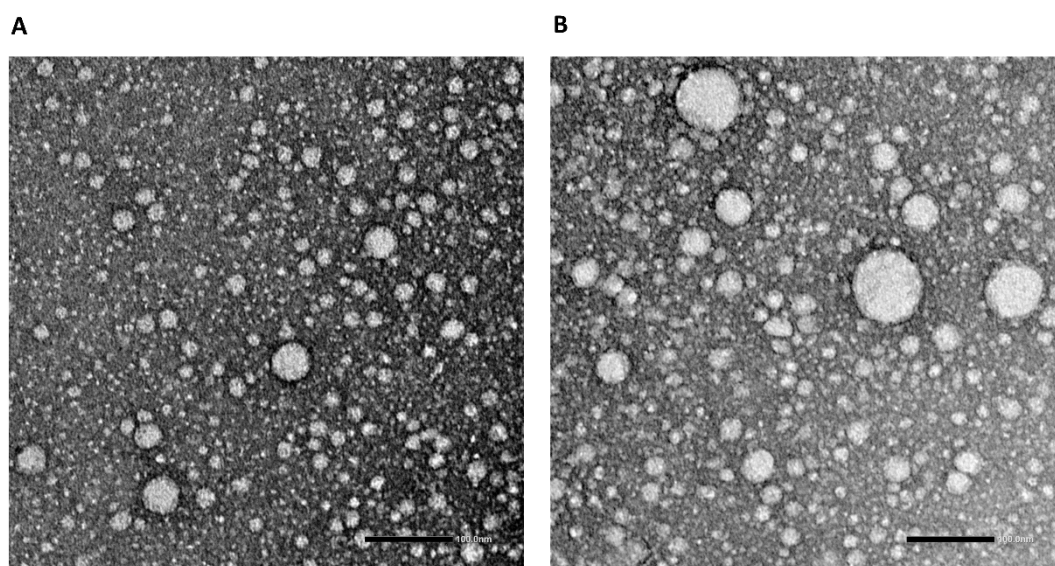


Figure 13. TEM photographs of NLC (scale bar 100 nm). (A) DHAH-NLCs (B) Mygliol-NLCs.

In this third experimental study, different studies were performed in *in vitro* primary cell cultures to assess the effectiveness of these nanoformulations retaining DHAH beneficial properties. To start with, the developed DHAH based NLC were tested in primary dopaminergic neuron cultures. First of all, both nanoformulations showed to be safe at all tested concentrations (100 μ M, 75 μ M, 50 μ M, 25 μ M, 12.5 μ M and 5 μ M) with a viability up to 70% and showing better values for DHAH-NLCs at 48h in primary dopaminergic neurons (Figure 14A-B). In addition, to check the effectiveness of DHAH-NLCs as neuroprotective agent, we treat dopaminergic cell cultures before and after the incubation with 25 μ M 6-OHDA neurotoxin. DHAH-NLCs

showed to be effective protecting the cells from the neurotoxin compared to Mygliol-NLCs (Figure 15A, E). These data are in line with previous publications regarding the DHA neuroprotective effect in neuron cell cultures [89,90]. Then, demonstrating that the neuroprotective effect known about DHAH and confirmed in the previous study, (Study II) was maintained after its incorporation to NLC lipid matrix.

On the other hand, as before, we aim to check the ability of our new develop nanoformulation decreasing the neuroinflammation undergoing in NDs. Firstly, we check the safety of both nanoformulations (DHAH-NLC and Mygliol-NLC) for all the previous cited concentrations in primary microglia cell cultures. In this assay, the DHAH-NLCs showed to be safe at any of the tested concentrations with a viability up to 70%, in contrast to Mygliol-NLCs where the highest concentrations decreased cell viability (Figure 14C-D).

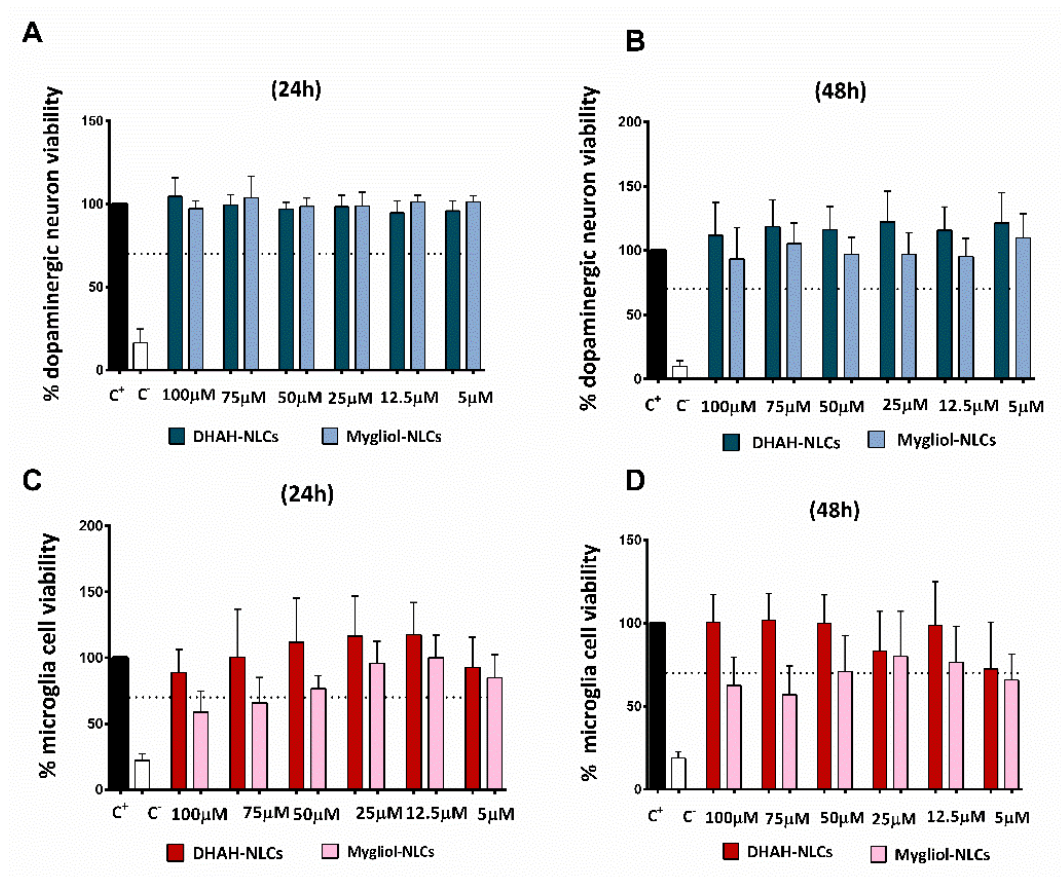


Figure 14. (A) Dopaminergic neuron viability at 24h (B) Dopaminergic neuron viability at 48h. (C) Microglia cell viability at 24h (D) Microglia cell viability at 48h. In all cases, different concentration of DHAH-NLCs and Mygliol-NLCs were tested. (The graphs shows the results of three biological replicates media \pm SEM).

Once we determined the concentrations to continue working with, we incubate these different nanoformulations with primary microglia cells activated with LPS *stimuli*, the gold standard *stimuli* for generating reactive gliosis and activate the neuroinflammation cascade. [91-93]. The addition of LPS at 50 ng/ml concentration promoted the release of pro-inflammatory cytokines at similar levels to previously published articles [92]. This upregulation was reverted with the addition of DHAH-NLCs. Therefore, the ability of DHAH to decrease neuroinflammation was maintained in DHAH-NLCs, obtaining pro-inflammatory cytokine levels similar to C⁻ in IL-6 and IL-1 β , and decreasing TNF- α almost to the half for any of the tested concentrations (Figure 15B-D). The ability of other PUFAs such as DHA or EPA (eicosapentaenoic acid) for decreasing the pro-inflammatory cytokine levels has been previously described [94]. Thus, this study enforces the use of these kind of functional lipid formulated in NLCs as an emerging tool to treat the undergoing inflammatory process in NDs. Altogether, these results highlight that this new developed nanocarrier can constitute a new therapeutic tool for treating NDs. The DHAH-NLCs were similar in size, PDI, zeta values and TEM morphology to previously developed NLCs. Moreover, they exhibited neuroprotective effects in a cell culture model of dopaminergic neurons, and anti-inflammatory properties decreasing pro-inflammatory cytokine levels in microglia primary cell cultures.

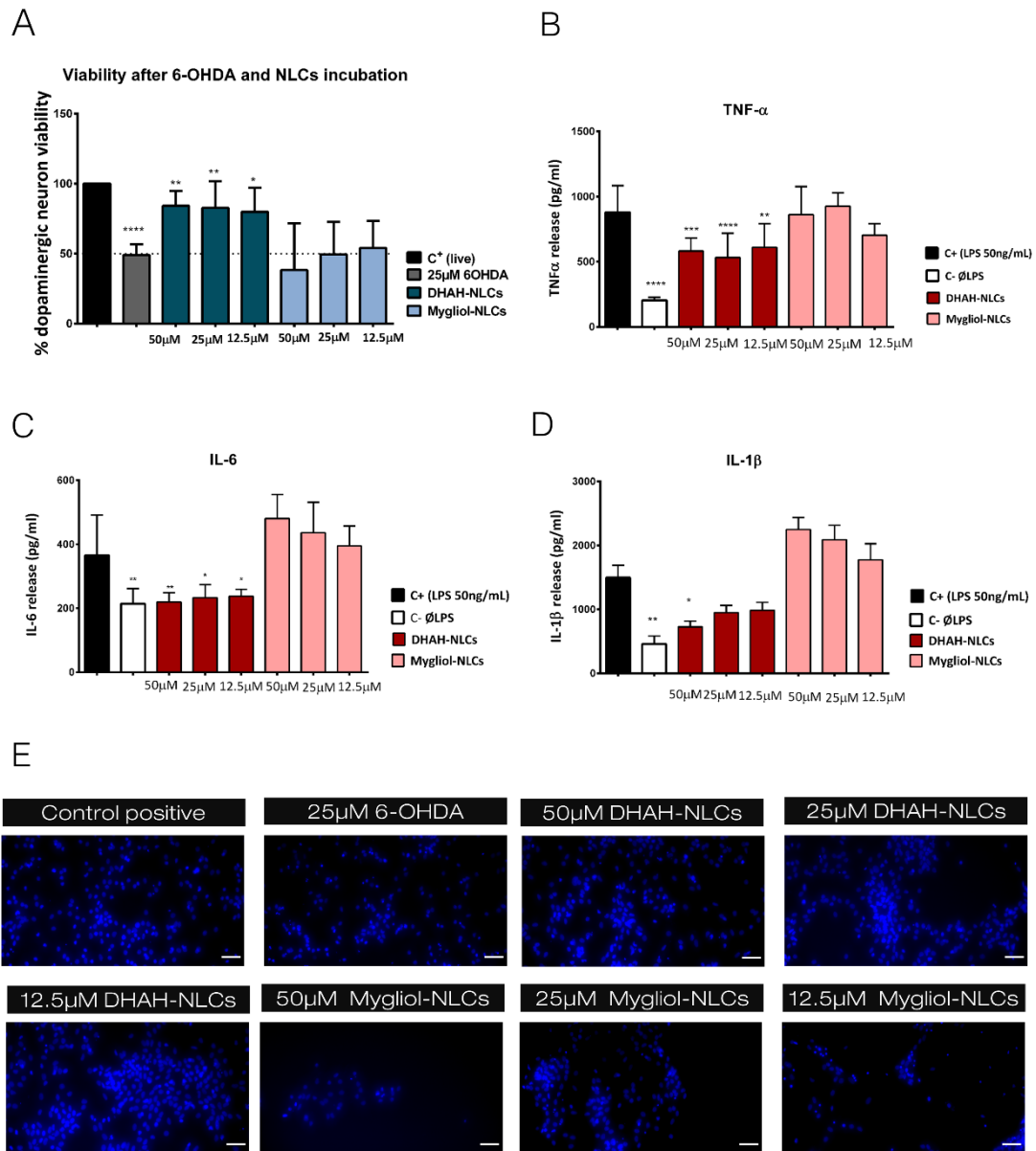


Figure 15. (A) Graphic representation of the neuroprotective effect of DHAH-NLCs. (** $p < 0.01$ 25 μ M 6-OHDA vs 50 μ M DHAH-NLCs and 25 μ M DHAH-NLCs, * $p < 0.05$ 25 μ M 6-OHDA vs 12.5 μ M DHAH-NLCs), One-way ANOVA. (B) Graphic representation of TNF- α values (pg/ml) for all the different tested concentrations and formulations. (**** $p < 0.0001$ C⁺ vs C⁻ and 25 μ M DHAH-NLCs, *** $p < 0.001$ C⁺ vs 50 μ M DHAH-NLCs, ** $p < 0.01$ C⁺ vs 12.5 μ M DHAH-NLCs), One-way ANOVA (C) Graphic representation of IL-6 values (pg/ml) for all the different tested concentrations and formulations. (** $p < 0.01$ C⁺ vs C⁻ and 50 μ M DHAH-NLCs, * $p < 0.05$ C⁺ vs 25 μ M DHAH-NLCs and 12.5 μ M DHAH-NLCs), One-way ANOVA. (D) Graphic representation of IL-1 β values (pg/ml) for all the different tested concentrations and formulations. (** $p < 0.01$ C⁺ vs C⁻ and * $p < 0.05$ C⁺ vs 50 μ M DHAH-NLCs), One-way ANOVA. (E) Representative fluorescence images of neuroprotective assay with DAPI staining. (Scale bar 50 μ M).

Among the different models to mimic the human BBB, BMCEs derived from hiPSCs are good candidates for drug permeability screening through BBB and preclinical studies [96,97]. The TEER values obtained in this study, around $3000 \Omega \times \text{cm}^2$ (Figure 16A) confirmed the suitability of this model for permeability studies of small and large molecules [98]. In this research, we showed that the administration of TAT modified NLC enabled the pass of this lipid nanoformulation across the BMCEs as seen in Figure 16B quantitatively and in Figure 16C qualitatively. The surface modification of the NP with a peptide such as TAT, commonly used for increase the pass of different molecules across cell membranes [99], enhanced the pass of these NPs across this BBB *in vitro* model. Although other permeability studies with functionalized NP have exhibited better results [100-103], they were carried out in bEnd.3D cell model or in primary HBMCEs with significantly lower TEER values, around $200 \Omega \times \text{cm}^2$, resulting in bad reliability with the clinical data and the obtained permeability values [104,105]. Therefore, the present permeability study is more reliable due to the human BBB model used and confirm the suitability of TAT surface modification to reach the brain.

Finally, in the last experimental study (Study IV) of this doctoral thesis we check whether the combination of this new safe and effective nanocarrier (DHAH-NLC) with different therapeutic molecules such as GDNF or VEGF, could become an emerging tool to treat in a synergistic manner the clinic associated to NDs. Moreover, we studied the pass of this new developed nanocarrier through BMCEs in a human BBB *in vitro* model. Although nanotechnology based DDS have exhibited promising results, all pharmaceutical treatments require rigorous preclinical studies to assess their toxicity and efficacy. The development of organ-on-chip approaches provide test platforms that incorporate human relevant physiological context, maybe reliable for prediction of drug effects [52,95].

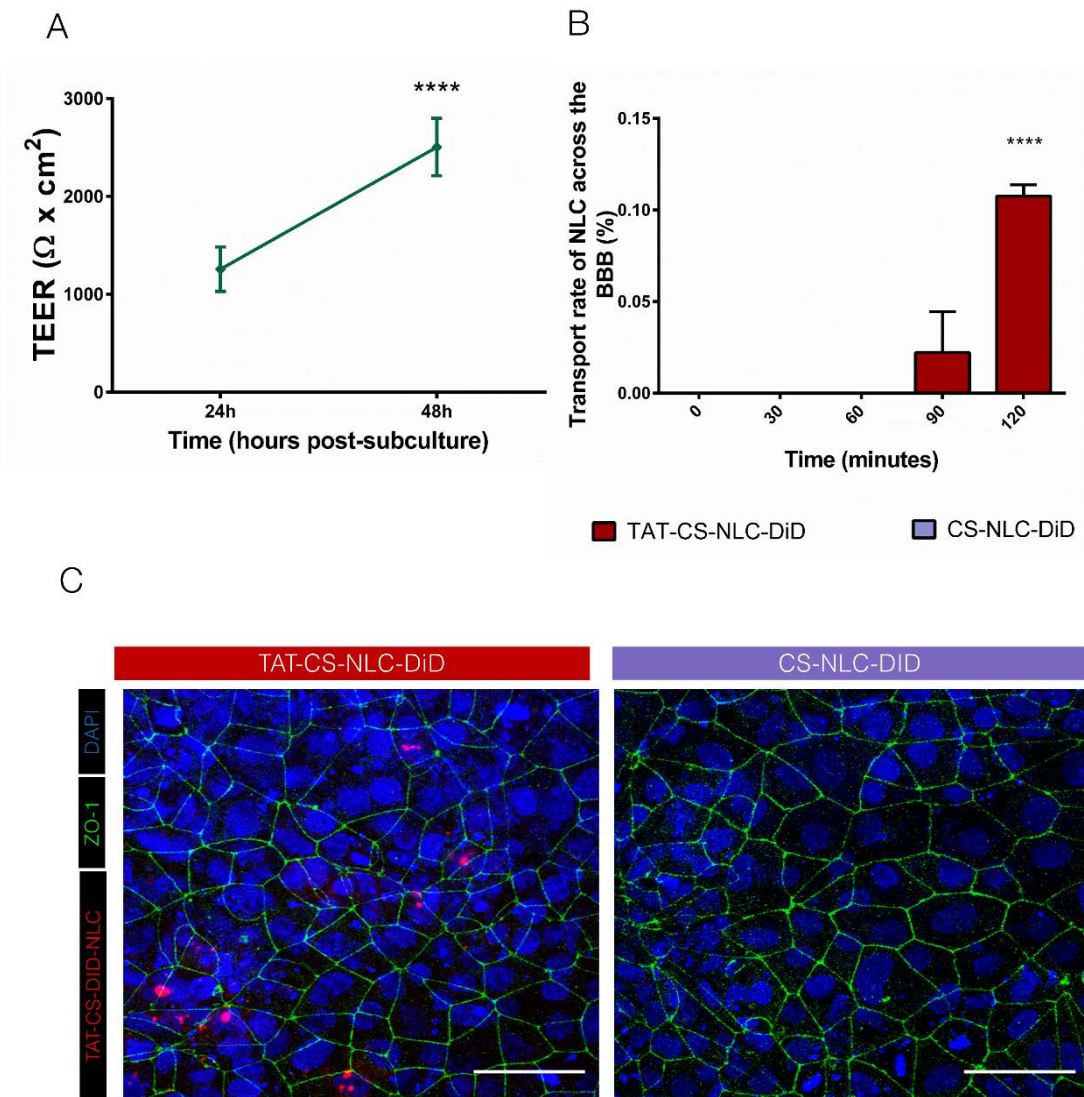


Figure 16. (A) TEER values after subculture into Transwell® at two different time points, 24 h and 48 h. (**** $p < 0.0001$ TEER values at 24 h vs. TEER values at 48 h). (B) Graphic representation of the percentage of the NLCs passing through BMCEs. (**** $p > 0.0001$ TAT-CS-DiD-NLC vs CS-DiD-NLC, One way ANOVA) at 2 h. (C) Immunofluorescence images: ZO-1 and DAPI staining where TAT-CS-DiD-NLCs can be qualitatively detected in BMCEs. (scale bar 50 μM).

On the other hand, as explained before, microglia has raised as key causative factor amplifying ongoing neuronal damage [106]. Furthermore, studies in microglia revealed as a key aspect to understand the NVU during health and disease. In this experimental study, we aim to revert the neuroinflammation generated after LPS *stimuli* in human microglial HMC3 cell line, a good experimental model to study the implications of neuroinflammation in human brain context. Before LPS *stimuli*, we incubated our new develop nanoformulations with this microglia cell model. None of

the tested nanoformulations showed to alter the pro-inflammatory pattern of this cell line (Figure 17 A-C and Figure 18 A-C), therefore we can conclude that the neuroinflammatory status generated after LPS is the result of the incubation with this *stimuli*, not because the incubation with the different NLCs. The generated inflammatory status was decreased after the treatment with DHAH composed NLCs; however, this effect was not seen with Mygliol-NLC (Figure 17 E-G and Figure 18 D-F). This data highlights the potential anti-inflammatory effect of our new nanoformulation composed with DHAH functional lipid, remarking that the potential anti-inflammatory effect already known about Ω -3 fatty acids [94,107] is maintained when formulated in NLC lipid matrix. In an attempt to see a synergic effect between GDNF or VEGF and DHAH, we develop DHAH-NLC-GDNF and DHAH-NLC-VEGF to co-administer both therapeutics. Despite the beneficial effect already known about GDNF and VEGF in microglia [73,108] (Figure 9), we could not see a synergistic effect (Figure 17 E-G and Figure 18 D-F). Although a decrease in the inflammatory state can be seen, VEGF nor GDNF did not improve the results obtained after DHAH-NLC treatment. Actually, the published works are not conclusive about the effect of VEGF in activated microglia [109] and regarding GDNF, a recent study suggest that the effect of this GF regulating microglia might be because the activation of an endogenous anti-oxidative system, not because the decrease of pro-inflammatory makers such as TNF- α or IL-6 [110].

This hypothesis is in line with our data. In fact, the anti-oxidative pathway NR2/HO-1 was studied in this research since it has been raised as an emerging target against oxidative stress and neuroinflammation in NDs [111]. As shown in Figure 17H, the treatment with DHAH-NLC-GDNF increased the expression of this gene even in an inflammatory context. The ability of DHAH to boost this pathway has been already described in a previous work conducted in hemiparkinsonian rats [40] (Figure 12). Although HO-1 gene expression was increased for all the DHAH nanoformulations (Figure 17H), only the co-administration with GDNF presented statically significant results. The effect of GDNF activating the anti-oxidative system in microglia is manifested in these results and support recent evidences in this line [110,112].

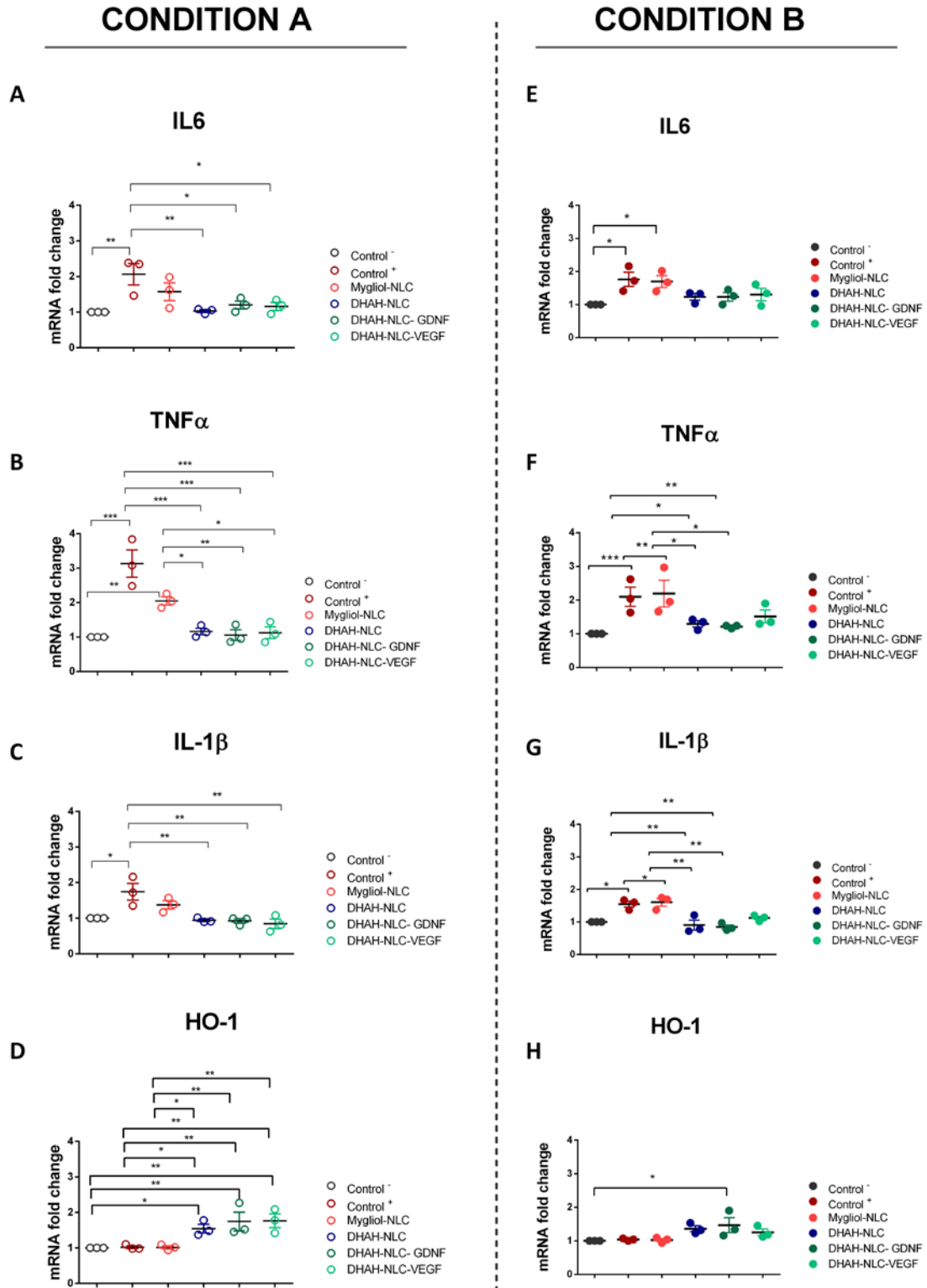


Figure 17. Gene expression analysis (RT-qPCR). mRNA fold change was used for graphical representation and Δ CT values statistical analysis using GAPDH as house keeping gene. (A) IL6 (B) TNF- α (C) IL-1 β and (D) HO-1 for condition A. (E) IL6 (F) TNF- α (G) IL-1 β and (H) HO-1 for condition B. *p<0.05 ** p<0.01 *** p<0.001, One- Way ANOVA.

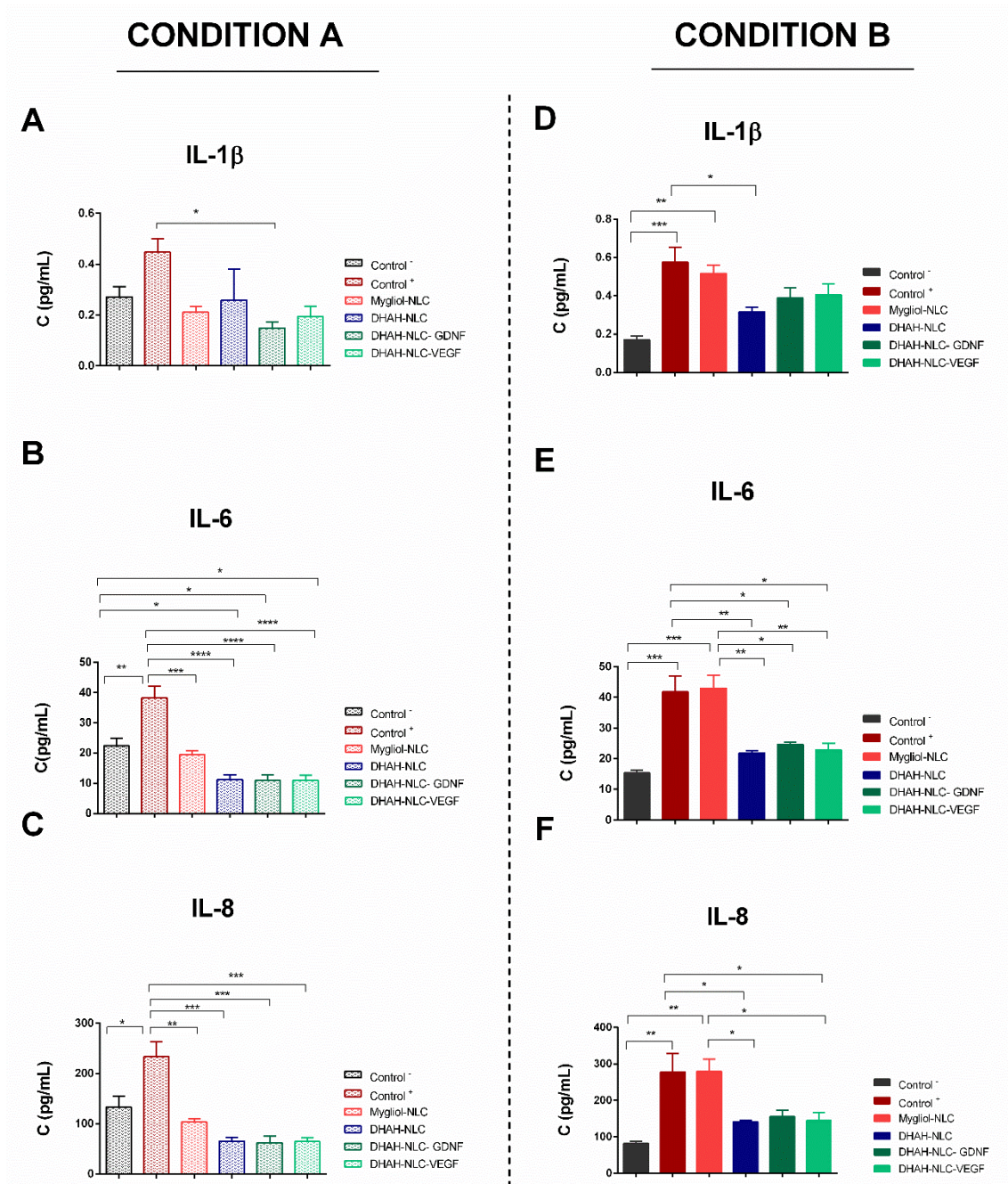


Figure 18. Multiplex assay values. (A) IL-1 β (B) IL-6 and (C) IL-8 for condition A. (D) IL-1 β (E) IL-6 and (F) IL-8 for condition B. * $p < 0.05$ ** $p < 0.01$ *** $p < 0.001$, **** $p < 0.0001$; One- Way ANOVA.

To sum up, the present study support the use of TAT functionalized NLCs as an effective tool to pass across BBB and target the brain treating the related CNS disorders. Moreover, the NLCs composed with DHAH functional lipid showed positive effects modulating the undergoing inflammation and oxidative stress present in NDs in human microglia cell line. This beneficial effect was enhanced with the co-administration with GDNF, enabling a targeted synergistic strategy to treat the BBB-microglia interaction present during neuroinflammation in different NDs.

5. BIBLIOGRAPHY

- [1] M. Katsuno, K. Sahashi, Y. Iguchi, A. Hashizume, Preclinical progression of neurodegenerative diseases, *Nagoya J. Med. Sci.* 80 (2018) 289-298.
- [2] L. Gan, M.R. Cookson, L. Petrucelli, A.R. La Spada, Converging pathways in neurodegeneration, from genetics to mechanisms, *Nat. Neurosci.* 21 (2018) 1300-1309.
- [3] A. Xie, J. Gao, L. Xu, D. Meng, Shared mechanisms of neurodegeneration in Alzheimer's disease and Parkinson's disease, *Biomed. Res. Int.* 2014 (2014) 648740.
- [4] Y. Hou, X. Dan, M. Babbar, Y. Wei, S.G. Hasselbalch, D.L. Croteau, V.A. Bohr, Ageing as a risk factor for neurodegenerative disease, *Nat. Rev. Neurol.* 15 (2019) 565-581.
- [5] GBD 2016 Dementia Collaborators, Global, regional, and national burden of Alzheimer's disease and other dementias, 1990-2016: a systematic analysis for the Global Burden of Disease Study 2016, *Lancet Neurol.* 18 (2019) 88-106.
- [6] GBD 2016 Parkinson's Disease Collaborators., Global, regional, and national burden of Parkinson's disease, 1990-2016: a systematic analysis for the Global Burden of Disease Study 2016. *Lancet Neurol.* 17 (2018) 939-953.
- [7] R. Briggs, S.P. Kennelly, D. O'Neill, Drug treatments in Alzheimer's disease, *Clin. Med. (Lond).* 16 (2016) 247-253.
- [8] W. Oertel, J.B. Schulz, Current and experimental treatments of Parkinson disease: A guide for neuroscientists, *J. Neurochem.* 139 Suppl 1 (2016) 325-337.
- [9] S.J. Allen, J.J. Watson, D.K. Shoemark, N.U. Barua, N.K. Patel, GDNF, NGF and BDNF as therapeutic options for neurodegeneration, *Pharmacol. Ther.* 138 (2013) 155-175.
- [10] V. Echeverria, G.E. Barreto, M. Avila-Rodriguezc, V.V. Tarasov, G. Aliev, Is VEGF a Key Target of Cotinine and Other Potential Therapies Against Alzheimer Disease? *Curr. Alzheimer Res.* 14 (2017) 1155-1163.
- [11] V.H. Perry, J.A. Nicoll, C. Holmes, Microglia in neurodegenerative disease, *Nat. Rev. Neurol.* 6 (2010) 193-201.
- [12] A.D. Greenhalgh, S. David, F.C. Bennett, Immune cell regulation of glia during CNS injury and disease, *Nat. Rev. Neurosci.* 21 (2020) 139-152.
- [13] M.L. Block, L. Zecca, J.S. Hong, Microglia-mediated neurotoxicity: uncovering the molecular mechanisms, *Nat. Rev. Neurosci.* 8 (2007) 57-69.
- [14] S. Hickman, S. Izzy, P. Sen, L. Morsett, J. El Khoury, Microglia in neurodegeneration, *Nat. Neurosci.* 21 (2018) 1359-1369.
- [15] J. Wang, Y. Song, Z. Chen, S.X. Leng, Connection between Systemic Inflammation and Neuroinflammation Underlies Neuroprotective Mechanism of Several Phytochemicals in Neurodegenerative Diseases, *Oxid Med. Cell. Longev.* 2018 (2018) 1972714.
- [16] J. Keaney, M. Campbell, The dynamic blood-brain barrier, *FEBS J.* 282 (2015) 4067-4079.
- [17] R. Daneman, A. Prat, The blood-brain barrier, *Cold Spring Harb Perspect. Biol.* 7 (2015) a020412.
- [18] Hernando S, Herran E, Pedraz JL, Igartua M, Hernandez RM, Nanotechnology Based Approaches for Neurodegenerative Disorders: Diagnosis and Treatment, in: Sharma H. S et al. (Ed.), Drug and Gene Delivery to the Central Nervous System for Neuroprotection. Springer International Publishing, Switzerland, 2017, pp. 57-87.

- [19] E. Garbayo, A. Estella-Hermoso de Mendoza, M.J. Blanco-Prieto, Diagnostic and therapeutic uses of nanomaterials in the brain, *Curr. Med. Chem.* 21 (2014) 4100-4131.
- [20] S. Hernando, O. Gartzandia, E. Herran, J.L. Pedraz, M. Igartua, R.M. Hernandez, Advances in nanomedicine for the treatment of Alzheimer's and Parkinson's diseases, *Nanomedicine (Lond)*. 11 (2016) 1267-1285.
- [21] A. Babazadeh, F. Mohammadi Vahed, S.M. Jafari, Nanocarrier-mediated brain delivery of bioactives for treatment/prevention of neurodegenerative diseases, *J. Controlled Release*. 321 (2020) 211-221.
- [22] G. da Rocha Lindner, D. Bonfanti Santos, D. Colle, E.L. Gasnhar Moreira, R. Daniel Prediger, M. Farina, N.M. Khalil, R. Mara Mainardes, Improved neuroprotective effects of resveratrol-loaded polysorbate 80-coated poly(lactide) nanoparticles in MPTP-induced Parkinsonism, *Nanomedicine (Lond)*. 10 (2015) 1127-1138.
- [23] S. Sharma, S. Lohan & R. S. R. Murthy, Formulation and characterization of intranasal mucoadhesive nanoparticulates and thermo-reversible gel of levodopa for brain delivery, *Drug Dev Ind Pharm.* 7 (2013) 869-78.
- [24] B. Shah, D. Khunt, H. Bhatt, M. Misra, H. Padh, Application of quality by design approach for intranasal delivery of rivastigmine loaded solid lipid nanoparticles: Effect on formulation and characterization parameters, *Eur J Pharm Sci.* 78 (2015) 54-66.
- [25] O. Gartzandia, E. Herrán, J.A. Ruiz-Ortega, C. Miguelez, M. Igartua, J.V. Lafuente, J.L. Pedraz, L. Ugedo, R.M. Hernández, Intranasal administration of chitosan-coated nanostructured lipid carriers loaded with GDNF improves behavioral and histological recovery in a partial lesion model of Parkinson's disease, *J Biomed Nanotechnol.* 12 (2016) 1-11.
- [26] F. Re, M. Gregori, M. Masserini, Nanotechnology for neurodegenerative disorders, *Maturitas.* 73 (2012) 45-51.
- [27] A. Beloqui, M.Á Solinís, A. Rodríguez-Gascón, A.J. Almeida, V. Prétat, Nanostructured lipid carriers: Promising drug delivery systems for future clinics, *Nanomedicine*.12 (2016) 143-161.
- [28] M. Inês Teixeira, C.M. Lopes, M. Helena Amaral, P.C. Costa, Current insights on lipid nanocarrier-assisted drug delivery in the treatment of neurodegenerative diseases, *Eur J Pharm Biopharm.* 149 (2020) 192-217.
- [29] D. Singh, H. Kapahi, M. Rashid, A. Prakash, A.B. Majeed, N. Mishra, Recent prospective of surface engineered Nanoparticles in the management of Neurodegenerative disorders, *Artif. Cells Nanomed Biotechnol.* 44 (2016) 780-791.
- [30] J.L. Pedraz, M. Igartua, R. Maria, S. Hernando, The role of lipid nanoparticles and its surface modification in reaching the brain: an approach for neurodegenerative diseases treatment, *Curr. Drug Deliv.* 15 (2018) 1218-1220.
- [31] O. Gartzandia, E. Herran, J.L. Pedraz, E. Carro, M. Igartua, R.M. Hernandez, Chitosan coated nanostructured lipid carriers for brain delivery of proteins by intranasal administration, *Colloids Surf. B Biointerfaces.* 134 (2015) 304-313.
- [32] G. Guidotti, L. Brambilla, D. Rossi, Cell-Penetrating Peptides: From Basic Research to Clinics, *Trends Pharmacol. Sci.* 38 (2017) 406-424.
- [33] B.K. Nanjwade, D.J. Patel, R.A. Udhani, F.V. Manvi, Functions of lipids for enhancement of oral bioavailability of poorly water-soluble drugs, *Sci. Pharm.* 79 (2011) 705-727.
- [34] Y. Agrawal, K.C. Petkar, K.K. Sawant, Development, evaluation and clinical studies of Acitretin loaded nanostructured lipid carriers for topical treatment of psoriasis, *Int J Pharm.* 401 (2010) 93-102.

[35] F.C. Frédéric Calon, Can we prevent Parkinson's disease with n-3 polyunsaturated fatty acids? *Future Lipidol.* 3 (2) (2008) 133-137.

[36] O. Kerdiles, S. Layé, F. Calon, Omega-3 polyunsaturated fatty acids and brain health: Preclinical evidence for the prevention of neurodegenerative diseases, *Trends Food Sci Technol.* 69 (2017) 203-213.

[37] J.T. Brenna, G. Diau, The influence of dietary docosahexaenoic acid and arachidonic acid on central nervous system polyunsaturated fatty acid composition, *Prostaglandins Leukot Essent Fatty Acids.* 77 (2007) 247-250.

[38] R.P. Bazinet, S. Laye, Polyunsaturated fatty acids and their metabolites in brain function and disease, *Nat. Rev. Neurosci.* 15 (2014) 771-785.

[39] M. Hashimoto, S. Hossain, A. Al Mamun, K. Matsuzaki, H. Arai, Docosahexaenoic acid: one molecule diverse functions, *Crit. Rev. Biotechnol.* 37 (2017) 579-597.

[40] S. Hernando, C. Requejo, E. Herran, J.A. Ruiz-Ortega, T. Morera-Herreras, J.V. Lafuente, L. Ugedo, E. Gainza, J.L. Pedraz, M. Igartua, R.M. Hernandez, Beneficial effects of n-3 polyunsaturated fatty acids administration in a partial lesion model of Parkinson's disease: The role of glia and NRF2 regulation, *Neurobiol Dis.* 121 (2019) 252-262.

[41] C. Boudrault, R.P. Bazinet, D.W.L. Ma, Experimental models and mechanisms underlying the protective effects of n-3 polyunsaturated fatty acids in Alzheimer's disease, *J Nutr Biochem.* 20 (2009) 1-10.

[42] E.E. Devore, F. Grodstein, F.J. van Rooij, A. Hofman, B. Rosner, M.J. Stampfer, J.C. Witteman, M.M. Breteler, Dietary intake of fish and omega-3 fatty acids in relation to long-term dementia risk, *Am. J. Clin. Nutr.* 90 (2009) 170-176.

[43] L.M. de Lau, M. Bornebroek, J.C. Witteman, A. Hofman, P.J. Koudstaal, M.M. Breteler, Dietary fatty acids and the risk of Parkinson disease: the Rotterdam study, *Neurology.* 64 (2005) 2040-2045.

[44] M. Taghizadeh, O.R. Tamtaji, E. Dadgostar, R. Daneshvar Kakhaki, F. Bahmani, J. Abolhassani, M.H. Aarabi, E. Kouchaki, M.R. Memarzadeh, Z. Asemi, The effects of omega-3 fatty acids and vitamin E co-supplementation on clinical and metabolic status in patients with Parkinson's disease: A randomized, double-blind, placebo-controlled trial, *Neurochem Int.* 108 (2017) 183-189.

[45] H. Soininen, A. Solomon, P.J. Visser, S.B. Hendrix, K. Blennow, M. Kivipelto, T. Hartmann, LipiDiDiet clinical study group, 24-month intervention with a specific multinutrient in people with prodromal Alzheimer's disease (LipiDiDiet): a randomised, double-blind, controlled trial, *Lancet Neurol.* 16 (2017) 965-975.

[46] S. Andrieu, S. Guyonnet, N. Coley, C. Cantet, M. Bonnefoy, S. Bordes, L. Bories, M.N. Cufi, T. Dantoine, J.F. Dartigues, F. Desclaux, A. Gabelle, Y. Gasnier, A. Pesce, K. Sudres, J. Touchon, P. Robert, O. Rouaud, P. Legrand, P. Payoux, J.P. Caubere, M. Weiner, I. Carrie, P.J. Ousset, B. Vellas, MAPT Study Group, Effect of long-term omega 3 polyunsaturated fatty acid supplementation with or without multidomain intervention on cognitive function in elderly adults with memory complaints (MAPT): a randomised, placebo-controlled trial, *Lancet Neurol.* 16 (2017) 377-389.

[47] Y. Freund-Levi, M. Eriksdotter-Jonhagen, T. Cederholm, H. Basun, G. Faxen-Irving, A. Garlind, I. Vedin, B. Vessby, L.O. Wahlund, J. Palmblad, Omega-3 fatty acid treatment in 174 patients with mild to moderate Alzheimer disease: OmegAD study: a randomized double-blind trial, *Arch. Neurol.* 63 (2006) 1402-1408.

[48] R. Avallone, G. Vitale, M. Bertolotti, Omega-3 Fatty Acids and Neurodegenerative Diseases: New Evidence in Clinical Trials, *Int. J. Mol. Sci.* 20 (2019) 10.3390/ijms20174256.

- [49] C.W. Olanow, K. Kieburtz, A.H. Schapira, Why have we failed to achieve neuroprotection in Parkinson's disease? *Ann. Neurol.* 64 Suppl 2 (2008) S101-10.
- [50] L.S. Schneider, F. Mangialasche, N. Andreasen, H. Feldman, E. Giacobini, R. Jones, V. Mantua, P. Mecocci, L. Pani, B. Winblad, M. Kivipelto, Clinical trials and late-stage drug development for Alzheimer's disease: an appraisal from 1984 to 2014, *J. Intern. Med.* 275 (2014) 251-283.
- [51] A. Slanzi, G. Iannoto, B. Rossi, E. Zenaro, G. Constantin, In vitro Models of Neurodegenerative Diseases, *Front. Cell. Dev. Biol.* 8 (2020) 328.
- [52] B. Miccoli, D. Braeken, Y.E. Li, Brain-on-a-chip Devices for Drug Screening and Disease Modeling Applications, *Curr. Pharm. Des.* 24 (2018) 5419-5436.
- [53] E.W. Esch, A. Bahinski, D. Huh, Organs-on-chips at the frontiers of drug discovery, *Nat. Rev. Drug Discov.* 14 (2015) 248-260.
- [54] E.S. Lippmann, A. Al-Ahmad, S.P. Palecek, E.V. Shusta, Modeling the blood-brain barrier using stem cell sources, *Fluids Barriers CNS.* 10 (2013) 2-8118-10-2.
- [55] W. Eldahshan, S.C. Fagan, A. Ergul, Inflammation within the neurovascular unit: Focus on microglia for stroke injury and recovery, *Pharmacol. Res.* 147 (2019) 104349.
- [56] H. Thurgur, E. Pinteaux, Microglia in the Neurovascular Unit: Blood-Brain Barrier-microglia Interactions After Central Nervous System Disorders, *Neuroscience.* 405 (2019) 55-67.
- [57] S.P. Egusquiaguirre, C. Manguán-García, L. Pintado-Berninches, L. Iarriccio, D. Carbajo, F. Albericio, M. Royo, J.L. Pedraz, R.M. Hernández, R. Perona, M. Igartua, Development of surface modified biodegradable polymeric nanoparticles to deliver GSE24.2 peptide to cells: A promising approach for the treatment of defective telomerase disorders, *Eur J Pharm Biopharm.* 91 (2015) 91-102.
- [58] M. Weinert, T. Selvakumar, T.S. Tierney, K.N. Alavian, Isolation, culture and long-term maintenance of primary mesencephalic dopaminergic neurons from embryonic rodent brains, *J. Vis. Exp.* (96). doi (2015) 10.3791/52475.
- [59] S.D. Skaper, M. Barbierato, V. Ferrari, M. Zusso, L. Facci, Culture of Rat Mesencephalic Dopaminergic Neurons and Application to Neurotoxic and Neuroprotective Agents, *Methods Mol. Biol.* 1727 (2018) 107-118.
- [60] F. Gaven, P. Marin, S. Claeyssen, Primary culture of mouse dopaminergic neurons, *J. Vis. Exp.* (91):e51751. doi (2014) e51751.
- [61] Chen, X., Zhang, Y., Sadadcharam, G., Cui, W. and Wang, J. H., Isolation, Purification, and Culture of Primary Murine Microglia Cells. *Bio-protocol.* 3(1): e314. (2013) 10.21769/BioProtoc.314.
- [62] E.H. Neal, N.A. Marinelli, Y. Shi, P.M. McClatchey, K.M. Balotin, D.R. Gullett, K.A. Hagerla, A.B. Bowman, K.C. Ess, J.P. Wikswo, E.S. Lippmann, A Simplified, Fully Defined Differentiation Scheme for Producing Blood-Brain Barrier Endothelial Cells from Human iPSCs, *Stem Cell. Reports.* 12 (2019) 1380-1388.
- [63] S. Hernando, E. Herran, J. Figueiro-Silva, J.L. Pedraz, M. Igartua, E. Carro, R.M. Hernandez, Intranasal Administration of TAT-Conjugated Lipid Nanocarriers Loading GDNF for Parkinson's Disease, *Mol. Neurobiol.* 55 (2018) 145-155.
- [64] S. Hernando, E. Herran, R.M. Hernandez, M. Igartua, Nanostructured Lipid Carriers Made of Omega-3 Polyunsaturated Fatty Acids: In Vitro Evaluation of Emerging Nanocarriers to Treat Neurodegenerative Diseases, *Pharmaceutics.* 12 (2020) 10.3390/pharmaceutics12100928.
- [65] L.V. Kalia, S.K. Kalia, A.E. Lang, Disease-modifying strategies for Parkinson's disease, *Mov. Disord.* 30 (2015) 1442-1450.

- [66] L.V. Kalia, A.E. Lang, Parkinson's disease, *The Lancet*. 386 896-912.
- [67] J.R. Evans, R.A. Barker, Neurotrophic factors as a therapeutic target for Parkinson's disease, *Expert Opin. Ther. Targets*. 12 (2008) 437-447.
- [68] A. Kirkeby, R.A. Barker, Parkinson disease and growth factors - is GDNF good enough? *Nat. Rev. Neurol*. 15 (2019) 312-314.
- [69] E. Herrán, J.Á Ruiz-Ortega, A. Aristieta, M. Igartua, C. Requejo, J.V. Lafuente, L. Ugedo, J.L. Pedraz, R.M. Hernández, In vivo administration of VEGF- and GDNF-releasing biodegradable polymeric microspheres in a severe lesion model of Parkinson's disease, *Eur J Pharm Biopharm*. 85 (2013) 1183-1190.
- [70] Herran,E, Requejo C, Ruiz-Ortega JA. et al, Increased antiparkinson efficacy of the combined administration of VEGF- and GDNF-loaded nanospheres in a partial lesion model of Parkinson's disease, *International Journal of Nanomedicine*. 9(1) (2014) 2677-2687.
- [71] T. Kanazawa, F. Akiyama, S. Kakizaki, Y. Takashima, Y. Seta, Delivery of siRNA to the brain using a combination of nose-to-brain delivery and cell-penetrating peptide-modified nano-micelles, *Biomaterials*. 34 (2013) 9220-9226.
- [72] G. Lou, Q. Zhang, F. Xiao, Q. Xiang, Z. Su, Y. Huang, Intranasal TAT-haFGF Improves Cognition and Amyloid-beta Pathology in an AbetaPP/PS1 Mouse Model of Alzheimer's Disease, *J. Alzheimers Dis*. 51 (2016) 985-990.
- [73] S.M. Rocha, A.C. Cristovão, F.L. Campos, C.P. Fonseca, G. Baltazar, Astrocyte-derived GDNF is a potent inhibitor of microglial activation, *Neurobiol. Dis*. 47 (2012) 407-415.
- [74] U. Rickert, S. Grampp, H. Wilms, J. Spreu, F. Knerlich-Lukoschus, J. Held-Feindt, R. Lucius, Glial Cell Line-Derived Neurotrophic Factor Family Members Reduce Microglial Activation via Inhibiting p38MAPKs-Mediated Inflammatory Responses, *J. Neurodegener Dis*. 2014 (2014) 369468.
- [75] Y. Zhao, M.J. Haney, Y.S. Jin, O. Uvarov, N. Vinod, Y.Z. Lee, B. Langworthy, J.P. Fine, M. Rodriguez, N. El-Hage, A.V. Kabanov, E.V. Batrakova, GDNF-expressing macrophages restore motor functions at a severe late-stage, and produce long-term neuroprotective effects at an early-stage of Parkinson's disease in transgenic Parkin Q311X(A) mice, *J. Controlled Release*. 315 (2019) 139-149.
- [76] M. Bousquet, M. Saint-Pierre, C. Julien, N. Salem Jr, F. Cicchetti, F. Calon, Beneficial effects of dietary omega-3 polyunsaturated fatty acid on toxin-induced neuronal degeneration in an animal model of Parkinson's disease, *FASEB J*. 22 (2008) 1213-1225.
- [77] M. Bousquet, F. Calon, F. Cicchetti, Impact of omega-3 fatty acids in Parkinson's disease, *Ageing Research Reviews*. 10 (2011) 453-463.
- [78] A.S. Barros, R.Y.G. Crispim, J.U. Cavalcanti, R.B. Souza, J.C. Lemos, G. Cristino Filho, M.M. Bezerra, T.F.M. Pinheiro, S.M.M. de Vasconcelos, D.S. Macedo, G.S. de Barros Viana, L.M.V. Aguiar, Impact of the Chronic Omega-3 Fatty Acids Supplementation in Hemiparkinsonism Model Induced by 6-Hydroxydopamine in Rats, *Basic Clin. Pharmacol. Toxicol*. 120 (2017) 523-531.
- [79] K. Coulombe, M. Saint-Pierre, G. Cisbani, I. St-Amour, C. Gibrat, A. Giguère-Rancourt, F. Calon, F. Cicchetti, Partial neurorescue effects of DHA following a 6-OHDA lesion of the mouse dopaminergic system, *J Nutr Biochem*. 30 (2016) 133-142.
- [80] P.C. Calder, Marine omega-3 fatty acids and inflammatory processes: Effects, mechanisms and clinical relevance, *Biochimica et Biophysica Acta (BBA) - Molecular and Cell Biology of Lipids*. 1851 (2015) 469-484.
- [81] E.C. Hirsch, S. Hunot, Neuroinflammation in Parkinson's disease: a target for neuroprotection? *The Lancet Neurology*. 8 (2009) 382-397.

- [82] I. Paterniti, D. Impellizzeri, R. Di Paola, E. Esposito, S. Gladman, P. Yip, J.V. Priestley, A.T. Michael-Titus, S. Cuzzocrea, Docosahexaenoic acid attenuates the early inflammatory response following spinal cord injury in mice: in-vivo and in-vitro studies, *J. Neuroinflammation*. 11 (2014) 6-2094-11-6.
- [83] L.D. Harvey, Y. Yin, I.Y. Attarwala, G. Begum, J. Deng, H.Q. Yan, C.E. Dixon, D. Sun, Administration of DHA Reduces Endoplasmic Reticulum Stress-Associated Inflammation and Alters Microglial or Macrophage Activation in Traumatic Brain Injury, *ASN Neuro*. 7 (2015).
- [84] D. Heras-Sandoval, J. Pedraza-Chaverri, J.M. Perez-Rojas, Role of docosahexaenoic acid in the modulation of glial cells in Alzheimer's disease, *J. Neuroinflammation*. 13 (2016) 61-016-0525-7.
- [85] P.K. Chang, A. Khatchadourian, R.A. McKinney, D. Maysinger, Docosahexaenoic acid (DHA): a modulator of microglia activity and dendritic spine morphology, *J. Neuroinflammation*. 12 (2015) 34-015-0244-5.
- [86] S. Koppula, H. Kumar, S.V. More, B.W. Kim, I.S. Kim, D.K. Choi, Recent advances on the neuroprotective potential of antioxidants in experimental models of Parkinson's disease, *Int. J. Mol. Sci*. 13 (2012) 10608-10629.
- [87] A. Ozkan, H. Parlak, G. Tanriover, S. Dilmac, S.N. Ulker, I. Birsen, A. Agar, The protective mechanism of docosahexaenoic acid in mouse model of Parkinson: The role of heme oxygenase, *Neurochem Int*. 101 (2016) 110-119.
- [88] Y. Zhang, L. Liu, D. Sun, Y. He, Y. Jiang, K.W. Cheng, F. Chen, DHA protects against monosodium urate-induced inflammation through modulation of oxidative stress, *Food Funct*. 10 (2019) 4010-4021.
- [89] D. Cao, R. Xue, J. Xu, Z. Liu, Effects of docosahexaenoic acid on the survival and neurite outgrowth of rat cortical neurons in primary cultures, *J. Nutr. Biochem*. 16 (2005) 538-546.
- [90] P.Y. Wang, J.J. Chen, H.M. Su, Docosahexaenoic acid supplementation of primary rat hippocampal neurons attenuates the neurotoxicity induced by aggregated amyloid beta protein(42) and up-regulates cytoskeletal protein expression, *J. Nutr. Biochem*. 21 (2010) 345-350.
- [91] C. Fourrier, J. Remus-Borel, A.D. Greenhalgh, M. Guichardant, N. Bernoud-Hubac, M. Lagarde, C. Joffre, S. Laye, Docosahexaenoic acid-containing choline phospholipid modulates LPS-induced neuroinflammation in vivo and in microglia in vitro, *J. Neuroinflammation*. 14 (2017) 170-017-0939-x.
- [92] L. Lin, R. Desai, X. Wang, E.H. Lo, C. Xing, Characteristics of primary rat microglia isolated from mixed cultures using two different methods, *J. Neuroinflammation*. 14 (2017) 101-017-0877-7.
- [93] V. De Smedt-Peyrusse, F. Sargueil, A. Moranis, H. Harizi, S. Mongrand, S. Laye, Docosahexaenoic acid prevents lipopolysaccharide-induced cytokine production in microglial cells by inhibiting lipopolysaccharide receptor presentation but not its membrane subdomain localization, *J. Neurochem*. 105 (2008) 296-307.
- [94] S. Laye, A. Nadjar, C. Joffre, R.P. Bazinet, Anti-Inflammatory Effects of Omega-3 Fatty Acids in the Brain: Physiological Mechanisms and Relevance to Pharmacology, *Pharmacol. Rev*. 70 (2018) 12-38.
- [95] E.W. Esch, A. Bahinski, D. Huh, Organs-on-chips at the frontiers of drug discovery, *Nat. Rev. Drug Discov*. 14 (2015) 248-260.
- [96] H.C. Helms, N.J. Abbott, M. Burek, R. Cecchelli, P.O. Couraud, M.A. Deli, C. Forster, H.J. Galla, I.A. Romero, E.V. Shusta, M.J. Stebbins, E. Vandenhoute, B. Weksler, B. Brodin, In vitro models of the blood-brain barrier: An overview of commonly used brain endothelial cell culture models and guidelines for their use, *J. Cereb. Blood Flow Metab*. 36 (2016) 862-890.

[97] E.S. Lippmann, S.M. Azarin, J.E. Kay, R.A. Nessler, H.K. Wilson, A. Al-Ahmad, S.P. Palecek, E.V. Shusta, Derivation of blood-brain barrier endothelial cells from human pluripotent stem cells, *Nat. Biotechnol.* 30 (2012) 783-791.

[98] J.L. Mantle, L. Min, K.H. Lee, Minimum Transendothelial Electrical Resistance Thresholds for the Study of Small and Large Molecule Drug Transport in a Human in Vitro Blood-Brain Barrier Model, *Mol. Pharm.* 13 (2016) 4191-4198.

[99] L. Zou, Q. Peng, P. Wang, B. Zhou, Progress in Research and Application of HIV-1 TAT-Derived Cell-Penetrating Peptide, *J. Membr. Biol.* 250 (2017) 115-122.

[100] I. Papademetriou, E. Vedula, J. Charest, T. Porter, Effect of flow on targeting and penetration of angiopep-decorated nanoparticles in a microfluidic model blood-brain barrier, *PLoS One.* 13 (2018) e0205158.

[101] A. Cox, D. Vinciguerra, F. Re, R.D. Magro, S. Mura, M. Masserini, P. Couvreur, J. Nicolas, Protein-functionalized nanoparticles derived from end-functional polymers and polymer prodrugs for crossing the blood-brain barrier, *Eur. J. Pharm. Biopharm.* 142 (2019) 70-82.

[102] J.A. Loureiro, B. Gomes, G. Fricker, M.A.N. Coelho, S. Rocha, M.C. Pereira, Cellular uptake of PLGA nanoparticles targeted with anti-amyloid and anti-transferrin receptor antibodies for Alzheimer's disease treatment, *Colloids and Surfaces B: Biointerfaces.* 145 (2016) 8-13.

[103] B. Dos Santos Rodrigues, S. Lakkadwala, T. Kanekiyo, J. Singh, Development and screening of brain-targeted lipid-based nanoparticles with enhanced cell penetration and gene delivery properties, *Int. J. Nanomedicine.* 14 (2019) 6497-6517.

[104] D.J. Mc Carthy, M. Malhotra, A.M. O'Mahony, J.F. Cryan, C.M. O'Driscoll, Nanoparticles and the blood-brain barrier: advancing from in-vitro models towards therapeutic significance, *Pharm. Res.* 32 (2015) 1161-1185.

[105] Y. Zhou, Z. Peng, E.S. Seven, R.M. Leblanc, Crossing the blood-brain barrier with nanoparticles, *J. Control. Release.* 270 (2018) 290-303.

[106] R.M. Ransohoff, How neuroinflammation contributes to neurodegeneration, *Science.* 353 (2016) 777-783.

[107] E. Hjorth, M. Zhu, V.C. Toro, I. Vedin, J. Palmblad, T. Cederholm, Y. Freund-Levi, G. Faxen-Irving, L.O. Wahlund, H. Basun, M. Eriksdotter, M. Schultzberg, Omega-3 fatty acids enhance phagocytosis of Alzheimer's disease-related amyloid-beta42 by human microglia and decrease inflammatory markers, *J. Alzheimers Dis.* 35 (2013) 697-713.

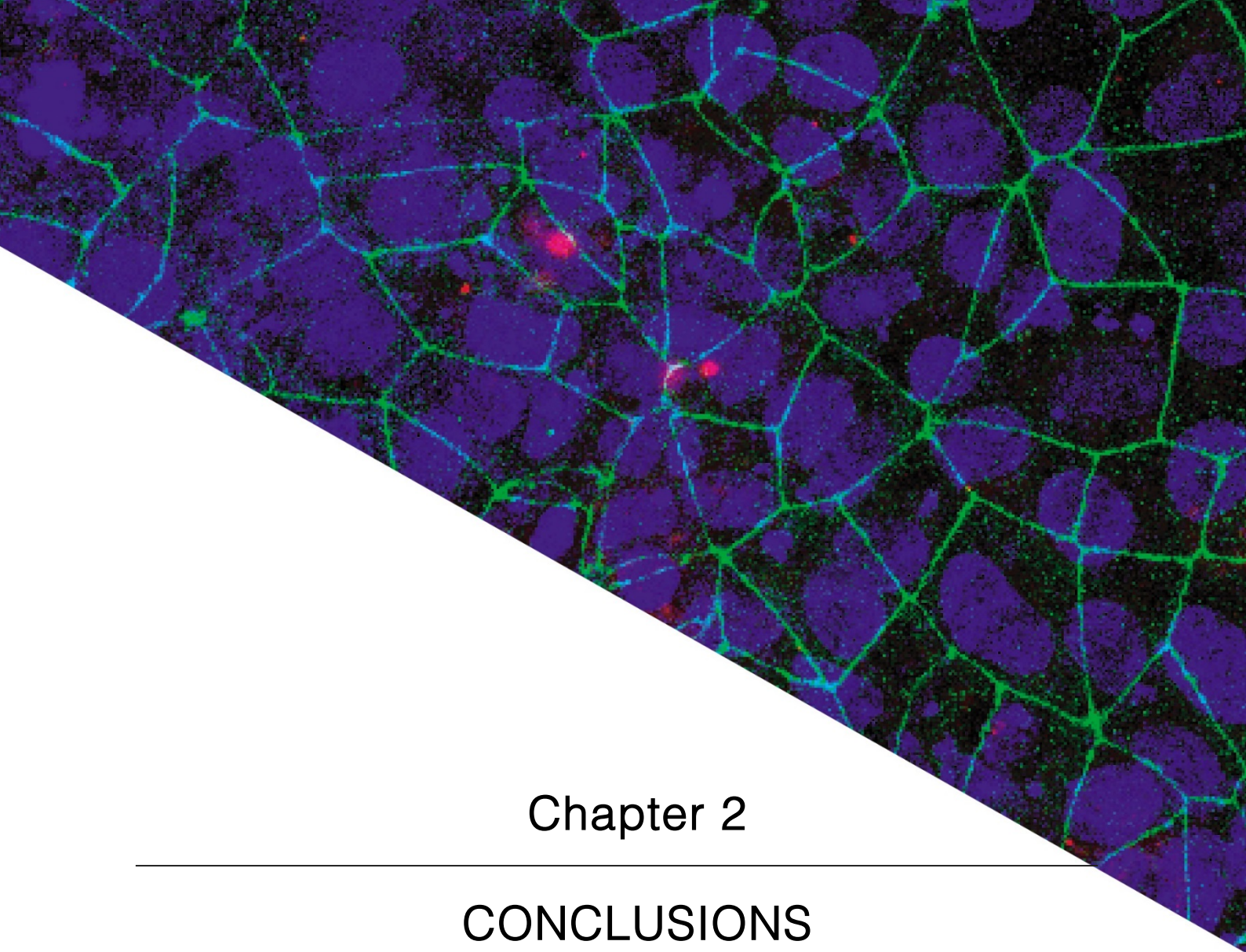
[108] Z. Xu, K. Han, J. Chen, C. Wang, Y. Dong, M. Yu, R. Bai, C. Huang, L. Hou, Vascular endothelial growth factor is neuroprotective against ischemic brain injury by inhibiting scavenger receptor A expression on microglia, *J. Neurochem.* 142 (2017) 700-709.

[109] J.M. Bain, L. Moore, Z. Ren, S. Simonishvili, S.W. Levison, Vascular endothelial growth factors A and C are induced in the SVZ following neonatal hypoxia-ischemia and exert different effects on neonatal glial progenitors, *Transl. Stroke Res.* 4 (2013) 158-170.

[110] Y.P. Chang, K.M. Fang, T.I. Lee, S.F. Tzeng, Regulation of microglial activities by glial cell line derived neurotrophic factor, *J. Cell. Biochem.* 97 (2006) 501-511.

[111] M. Sandberg, J. Patil, B. D'Angelo, S.G. Weber, C. Mallard, NRF2-regulation in brain health and disease: Implication of cerebral inflammation, *Neuropharmacology.* 79 (2014) 298-306.

[112] P. Yue, L. Gao, X. Wang, X. Ding, J. Teng, Pretreatment of glial cell-derived neurotrophic factor and geranylgeranylacetone ameliorates brain injury in Parkinson's disease by its anti-apoptotic and anti-oxidative property, *J. Cell. Biochem.* 119 (2018) 5491-5502.



Chapter 2

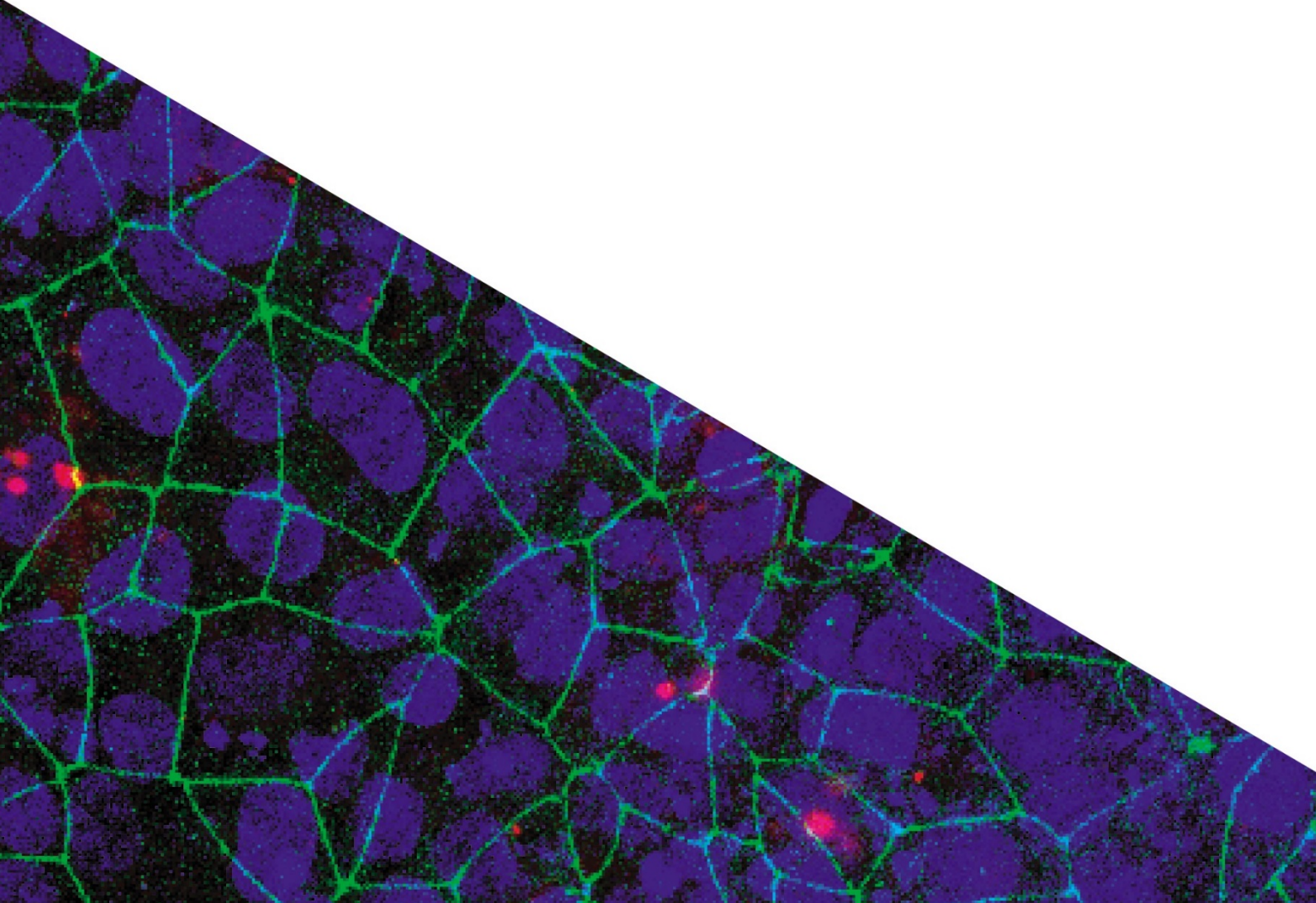
CONCLUSIONS

Based on the results obtained in the experimental studies, the main conclusions of this doctoral thesis are the following:

1. The developed CS and TAT surface modified NLCs with GDNF were successfully administered intranasally to a MPTP mouse model of PD, restoring its motor activity, increasing the TH expression in brain areas of interest, and decreasing the microgliosis related to the disease.
2. The daily oral administration of DHAH functional lipid to 6-OHDA rat model of PD showed a trend to improve the locomotor activity of lesioned animals. This effect was confirmed with positive effects on animals' dopaminergic system, increasing TH⁺ marker expression. Moreover, DHAH administration modulated the neuroinflammation and oxidative stress present in this PD animal model.
3. The NLCs developed using DHAH functional lipid and CS and TAT coating, were similar in size, Z potential and TEM images to previously developed NLCs. Additionally, these new nanocarriers retain the ability of DHAH functional lipid regarding its neuroprotective and anti-inflammatory properties in primary neuron and microglia cell cultures.
4. The functionalization of DHAH based nanoparticles with CS and TAT proved to be a useful tool to pass across BMCES derived from hiPSCs as *in vitro* human BBB model. The permeability results showed that this new nanoformulation is a good candidate to target and treat CNS related disorders.
5. The addition of DHAH functional lipid to NLC lipid matrix showed a positive effect modulating the underlying neuroinflammation and oxidative stress present in a human microglial cell line. This beneficial effect was enhanced when GDNF was encapsulated into the NLCs, and could constitute a promising synergistic therapy to target the CNS and treat BBB-microglia interactions present in NDs.

Chapter 3

APPENDIXES



Advances in nanomedicine for the treatment of Alzheimer's and Parkinson's diseases₁

Sara Hernando^{1,2,&}, Oihane Gartzandia^{1,2,&}, Enara Herran^{1,2}, Jose Luis Pedraz^{1,2}, Manoli Igartua^{1,2}, Rosa Maria Hernandez^{1,2,*}

¹NanoBioCel Group, Laboratory of Pharmaceutics, School of Pharmacy, University of the Basque Country (UPV/EHU), Vitoria-Gasteiz, 01006, Spain;

²Biomedical Research Networking Centre in Bioengineering, Biomaterials and Nanomedicine (CIBER-BBN), Vitoria-Gasteiz, 01006, Spain.

*Corresponding author: Rosa Maria Hernandez

&These two authors contribute equally to this research article

¹Published in: Nanomedicine (Lond) 2016

IF: 4.727 (Q1)

<https://doi.org/10.2217/nnm-2016-0019>

Cat: Nanoscience & Nanotechnology

ABSTRACT

Alzheimer's disease (AD) and Parkinson's disease (PD) are the most common neurodegenerative diseases (NDs) worldwide. Despite all the efforts made by the scientific community, current available treatments have limited effectiveness, without halting the progression of the disease. That is why, new molecules such as growth factors (GF), antioxidants and metal chelators have been raised as new therapeutical approaches. However, these molecules have difficulties to cross the blood brain barrier (BBB) limiting its therapeutic effect. The development of nanometric drug delivery systems (DDS) may permit a targeted and sustained release of old and new treatments offering a novel strategy to treat these neurodegenerative disorders. This review summarized the main investigated DDS as promising approaches to treat AD and PD.

Keywords: Alzheimer's disease • Parkinson's disease • nanotechnology • nanomedicine • drug delivery systems

1. INTRODUCTION

Neurodegenerative diseases (NDs) are characterized by a continuous structural and functional neuronal loss, usually correlated with neuronal death. Due to this deterioration, some cognitive, motor, emotional and sensory functions of patients are affected. Between different NDs, Alzheimer's disease (AD) and Parkinson's disease (PD) are the first and the second most common disorders, respectively [1]. AD is caused by an irreversible neuronal loss and vascular toxicity due to amyloid beta ($A\beta$) peptide extracellular deposition in senile plaques, together with neurofibrillary tangles of phosphorylated tau protein. The progressive loss of memory, deterioration of judgment decision, orientation to physical surrounding and language are the most important clinical hallmarks of this disease [2-5]. Regarding PD, it is pathologically characterized by the degeneration of midbrain dopaminergic neurons in the substantia nigra (SN), followed by the dopamine decrease in the striatum (ST). The parkinsonism is the set of clinical symptoms that characterize the disease, among which are bradykinesia, resting tremor, rigidity and postural instability [5,6]. As shown in Table 1, the approved and most commonly used treatments for AD are acetylcholinesterase inhibitors (tacrine, donepezil, rivastigmine, galantamine) and N-methyl-D-aspartate receptor antagonist (memantine). All of them are administered by the oral route, and rivastigmine can also be transdermally administered using patches. In relation to PD, current pharmacological therapies are based on dopaminergic drugs (Benserazide/Levodopa, Levodopa/Carbidopa, Levodopa/Carbidopa/Entacapone) administered by the oral route.

Table 1. Current pharmacological treatments for AD and PD.

ND	Drug	Mode of action
AD	Tacrine	Acetylcholinestrase inhibitors
	Donepezil	
	Rivastigmine	
	Galantamine	
PD	Memantine	N-methyl-D-aspartatereceptor antagonist
	Benserazide/Levodopa	Dopamimetic
	Levodopa/Carbidopa	
	Levodopa/Carbidopa/	
	Entacapon	

Nevertheless, it is important to note that the treatments mentioned above are only symptomatic, with a temporary effect, and without halting the progression of the disease [3]. Thereby, the researchers are making big efforts searching new therapies to address the neurodegenerative process.

2. NEW PROMISING MOLECULES FOR THE TREATMENT OF AD AND PD

Bearing in mind that nowadays the clinical treatments for AD and PD are mainly symptomatic, the development of new therapeutic options to address the main causes of neurodegenerative diseases are urgently needed. In this sense, in the last years new promising molecules such as neurotrophic factors (NTFs), antioxidant molecules and metal chelators have been considered promising approaches to attain this purpose.

Accordingly, growth factors (GFs) are a group of proteins which are able to improve the growth, proliferation and differentiation of neuronal cells, having also a significant role in tissue morphogenesis, cell differentiation, angiogenesis and neurite outgrowth [7-9]. Table 2 describes the main neurotrophic factors (NTFs) used to develop new therapies towards AD and PD, in order to address directly the progression of the disease.

On the other hand, it is commonly known that oxidative stress plays an important role in the pathophysiology of NDs such as AD and PD. Recent research works have

demonstrated that the products generated from free-radical mediated reactions are increased in NDs, being related with the hallmarks of these diseases [19-28]. Moreover, transition metals have been suggested to be responsible of neuronal damage in AD [20]. In an attempt to treat or prevent these NDs, both antioxidants and metal chelators have been raised as new treatment approaches. In the Table 3 it has been summarized the studied molecules and the outcome of their use in AD and PD.

Table 2. Different growth factors and their main functions in the central nervous system (CNS).

Growth factor	Main functions	Ref
Glial-derived neurotrophic factor (GDNF)	High specificity against dopaminergic neurons. Protective and trophic effects on noradrenergic neurons of the locus coeruleus.	[10,11]
Brain-derived neurotrophic factor (BDNF)	Important role in the normal development of the peripheral and CNS. Promotes the synaptic plasticity and survival of neurons in adult brains.	[12]
Nerve growth factor (NGF)	Promotes the survival, differentiation and maintenance of sympathetic and sensory neurons, having neuroprotective and repair functions.	[13]
Ciliary neurotrophic factor (CNTF)	Ability to support the survival and/or differentiation of sympathetic, sensory, or motor neurons.	[14]
Insulin growth factor-I (IGF-I)	Helps in the survival of neurons and rescue from neurotoxicity, stimulating also the neurogenesis and synaptogenesis.	[15]
Vascular endothelial growth factor (VEGF)	Stimulates angiogenesis and the development of endothelial cells. Enhances neuronal growth and survival, and axonal outgrowth.	[16,17]
Neurotrophin (NT-3)	Survival and differentiation of neurons, and in neurite growth.	[18]

Nevertheless, whatever the treatment, the clinical application of all of these new molecules is limited. Some of these drawbacks come after their *in vivo* administration, due to their short circulation half-life and rapid degradation rate [29]. Hence, high doses are required to obtain therapeutic levels in the brain, with the risk of suffering adverse systemic effects [30].

However, the main obstacle for most of the drugs to access the brain is the presence of the blood brain-barrier (BBB) (Figure 1), having big difficulties to cross

it, due to their unsuitable lipophilicity, molecular weight or charge. Thus, this barrier restricts the effective delivery and diffusion of therapeutic molecules to the CNS [31], maintaining CNS homeostasis and hindering the free penetration and diffusion of foreign components from the bloodstream to the brain [32].

Table 3. Antioxidants and metal chelators and their therapeutic functions in CNS.

Molecule	Main functions	Ref.
Resveratrol	Reduction in A β pathway and attenuation of cognitive decline.	[21]
	Upregulation of the antioxidant status and reduction of dopaminergic neuronal loss, improving the rotational behavior.	[22,23]
Curcumin	Increase of β -amyloid-degrading enzymes;	[24]
	Protection against oxidation and improvement of behavioral tests.	[25]
Catechins	Decrease in A β levels and plaques.	[24]
Metal chelators	49% decrease in A β deposition; inhibition of τ phosphorylation.	[26,27]
Coenzyme Q10	Protection of the nigrostriatal dopaminergic system; Delay of the symptomatology in PD patients.	[28]

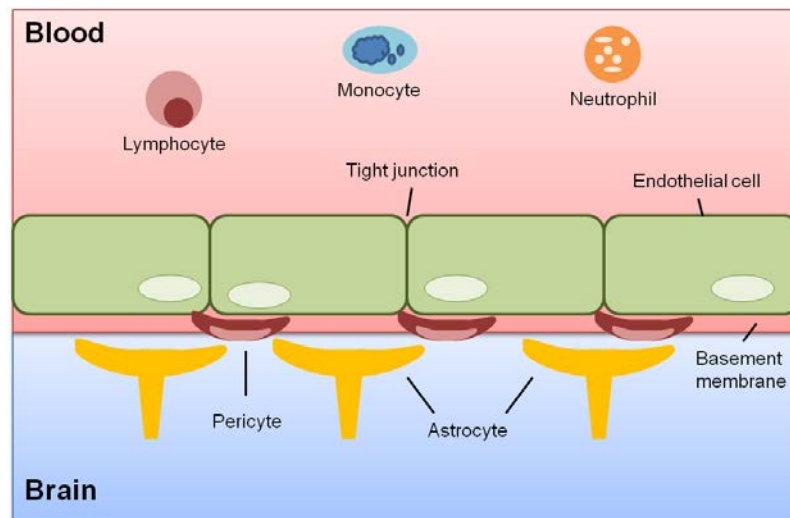


Figure 1. Schematic illustration of the BBB and its tight junction structure. The figure shows an irrigated blood vessel in the brain which forms the BBB. The BBB is formed by endothelial cells with tight junctions, surrounded by pericytes and astrocyte end-feet.

Therefore, over the years different strategies to access the brain have been developed, and the different approaches to cross or by-pass the BBB can be divided into invasive and non-invasive techniques (Figures 2 and 3) [32]. As shown

in Figure 2, the invasive techniques enclose surgical methods to administer drugs directly into the brain, and the disruption of the BBB to intentionally open it, while the non-invasive techniques showed in Figure 3 include non-aggressive approaches to access into the brain, such as the intranasal administration or the encapsulation of drugs within nanotechnological carriers.

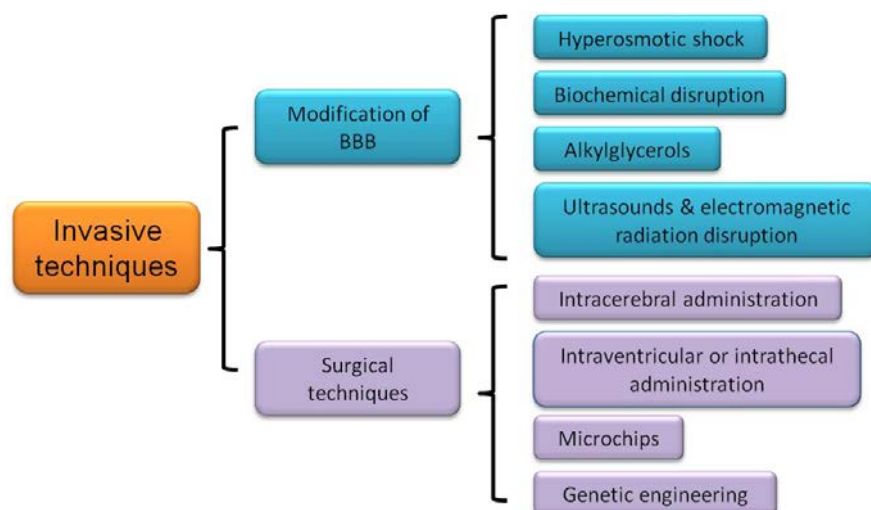


Figure 2. A schematic representation of the invasive techniques used to deliver drugs to the brain.

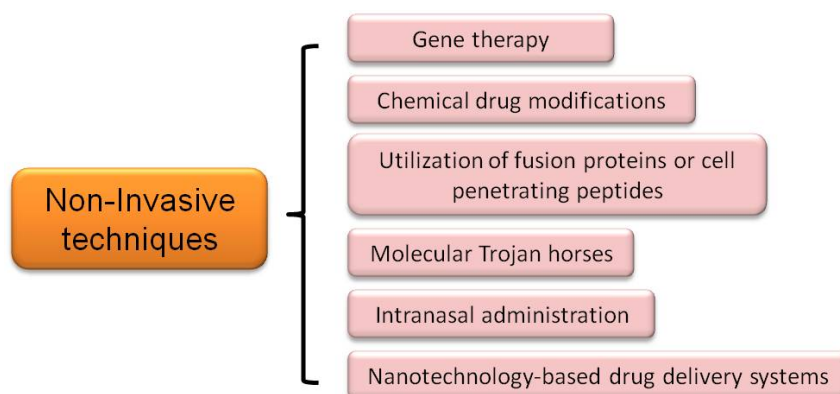


Figure 3. A schematic representation of the non-invasive techniques used to deliver drugs to the brain.

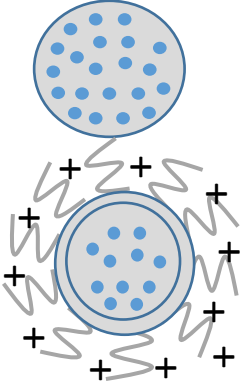
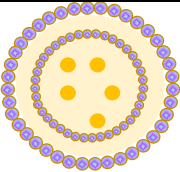
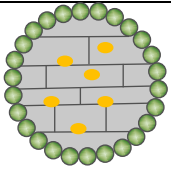
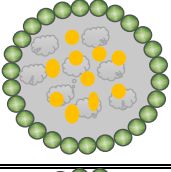
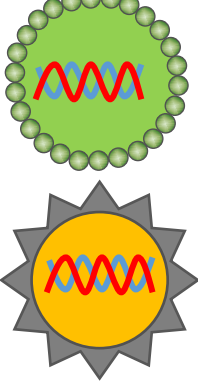
All in all, great efforts are being made by scientific community in the search of adequate technologies for brain targeting, and in the last years, the nanotechnology has appeared as a promising solution to deal with this challenge [31].

3. NANOTECHNOLOGY SOLUTIONS FOR NEURODEGENERATIVE DISEASES

Nanotechnology is an emerging field of science with promising physiochemical properties for the treatment of neurodegenerative diseases [33-35]. In this section

we have focused on describing the advances made in nanomedicine for the treatments of PD and AD, concretely. Table 4 summarized the drug delivery systems (DDS) mainly investigated for the administration of different drugs to treat NDs.

Table 4. Mainly used DDSs in the treatment of NDs.

Nanotechnology device	Schematic illustrations	Characteristics	Ref.
Polymeric (functionalized) nanoparticles (NP)		Microspheres and nanospheres are constituted of biodegradable and biocompatible materials. Therapeutic agents are entrapped in the colloidal matrix or coated on the surface by adsorption or conjugation. Moreover, ligands can be linked on the surface enhancing cell penetration. Polymer microcapsules and nanocapsules can be produced with different synthetic and natural monomers/polymers and with different preparation methods, their surface can be also functionalized for specific brain targeting.	[36-39]
(Nano)liposomes		Vesicles composed by concentric bilayers of phospholipid-based membranes. Its surface may be modified by targeting agents achieving transport across BBB.	[40]
Solid lipid nanoparticle (SLN)		Lipid nanocarriers formed by mono-di and tri glycerides, fatty acids, steroids and waxes and stabilized by various classes of emulsifiers.	[41]
Nanostructured lipid carrier (NLC)		Mixture of solid and liquid lipids with higher encapsulation efficiency and better release properties.	[42]
Gene therapy: viral and non viral vectors		Specific gene or DNA compacted carriers to target cells or tissues, entering to the nucleus to be expressed.	[43,44]

3.1 AD and nanotechnology.

3.1.1 DDSs to release acetylcholinesterase inhibitors and NMDA receptor antagonist.

Rivastigmine (RT) is a reversible inhibitor of both *acetylcholinesterase* (AChE) and *butyrylcholinesterase* (BuChE) which has low bioavailability due to its hydrophilic nature. The limited entry to the brain makes necessary frequent dosing worsening cholinergic side effects [41,45]. The application of DDSs to overcome these disadvantages could be suitable. For example, *Joshi et al.* prepared RT loaded poly lactide-co-glycolide (PLGA) and poly (n-butylcyanoacrylate) NP coated with polysorbate 80 (PBCA-80) to improve brain targeting.

Moreover, these NP provide sustained release, reducing dosing frequency and minimizing side effects. The results from the *Morris Water Maze (MWM) Test* showed the suitability of these nanoformulations regaining memory faster than RT solution in a scopolamine-induced amnesic mouse (Figure 4) [46]. Furthermore, PBCA nanoparticles have been developed with the aim of improving diagnostic imaging. For instance, *Kulkarni et al.* prepared PBCA loaded I-cloiquinol (CQ, 5-chloro-7-iodo-8-hydroxyquinoline) NPs, showing more efficient brain entry and rapid clearance, which are the ideal characteristics for in vivo imaging [47].

On the other hand, *Wilson et al* elaborated PBCA-80 NP for the targeted delivery of RT into the brain. They observed that the uptake of RT after intravenous administration of RT loaded PBCA-80 NP was 3.82 fold higher than the free drug [48]. Chitosan NP of RT have also been developed by *Naqpal et al.* in an attempt to increase this drug therapeutic efficacy and tolerance profile. The studies demonstrated the reduction of the toxicity as well as improved memory activity in RT chitosan NP treated mice compared with free RT [49].

In addition to the intravenous route, the nasal route has also been investigated to avoid first pass metabolism and distribution to non-targeted organs thus, decreasing peripheral side effects. The administration of RT chitosan NP via intranasal route has showed an increase in brain AChE concentrations, decreasing the levels at lungs or liver [45].

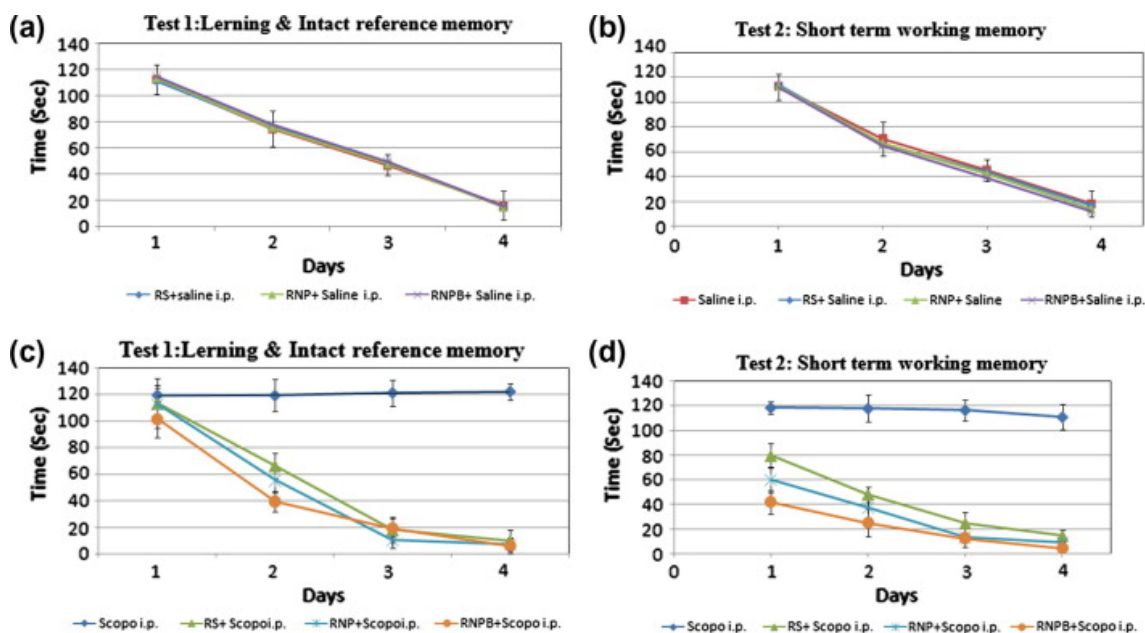


Figure 4. *Saline-treated mice*: (a) Test 1: learning and intact reference memory, (b) Test 2: short-term working memory. ($n = 4$); *scopolamine-treated mice*: (c) Test 1: learning and intact reference memory, and (d) Test 2: short-term working memory. ($n = 4$). Abbreviations: RS, RT solution; RNP, RT loaded PLGA NPs; RNPB, RT loaded PBCA NPs; ip, intraperitoneal; scop ip, scopolamine intraperitoneal. Reproduced with permission from [46].

SLN have also been studied as a new approach for intranasal delivery of RT. Despite the hydrophilic nature of RT, the SLN system enhances its diffusion across nasal membrane due to the lipidic nature of these nanosystems [41].

Regarding liposomal formulations, subcutaneous administration of RT loaded liposomes has been investigated. The pharmacodynamic study in MWM Test manifested overcoming effect of RT loaded liposomes to RT solution normalizing cognitive level [50].

Another commercialized inhibitor of AchE is donepezil. *In vivo* studies of donepezil loaded PLGA NP were carried out by *Bhavna et al.* They revealed that the brain accumulation of donepezil was higher when the drug was encapsulated in NP as it was confirmed in the gamma scintigraphic image. This donepezil loaded NP were coated with Tween 80 improving the opening of the tight junctions in BBB and inhibiting P-glycoprotein efflux system enhancing drug delivery to the brain [51].

Galantamine is also known for been a reversible, competitive, AchE inhibitor used in the treatment of AD. Nevertheless, its poor brain penetration results in lower bioavailability to the target organ. With the aim to improve these disadvantages, *Misra et al.* elaborated SLN loaded with galantamine. After *in vivo* administration,

injected nanoformulations presented higher bioavailability than the free drug. In addition, the nanoformulated galantamine improved behavioral deficits presented in treated rats when compared with the control group [52]. In this case the DDSs can also be functionalized to improve brain targeting. In an attempt to obtain it, *Mufamadi et al.* developed pegylated nanoliposomes for targeted delivery of galantamine. They studied the cellular uptake of functionalized galantamine loaded nanoliposomes in cell cultures, showing higher targeted delivery than non-functionalized liposomes [40].

Finally, *Laserra et al.* synthesized a codrug of the NMDA antagonist, memantine, and (R)- α -lipoic acid (LA-MEM) with neuroprotective properties. This codrug was loaded in SLN showing lack of toxicity in both N2a neuroblastoma cells (NB) and primary whole blood (PHWB) after using MTT (3-(4,5-Dimethylthiazol-2-yl)-2,5-Diphenyltetrazolium Bromide) and lactate dehydrogenase (LDH) assays [53].

3.1.2 DDSs to release GFs

Regarding GFs, our research group developed VEGF loaded PLGA nanospheres (NS) administered by craniotomy as a novel therapeutic approach to AD. *In vitro* studies in cortical neuronal cultures showed their effectiveness increasing cell viability and protecting neurons from A β induced toxicity. Furthermore, hippocampal neurogenesis was enhanced in APP/Ps1 mouse model treated group, which was confirmed with an increase in BrdU⁺ cells, specially in the dentate gyrus. Behavioral studies were also carried out to demonstrate the therapeutic effect of VEGF loaded NS. Mice treated with VEGF NS presented better results in T-maze test and object recognition test, with higher exploratory memory and an improvement in short-term memory, respectively, as shown in Figure 5 [54,55].

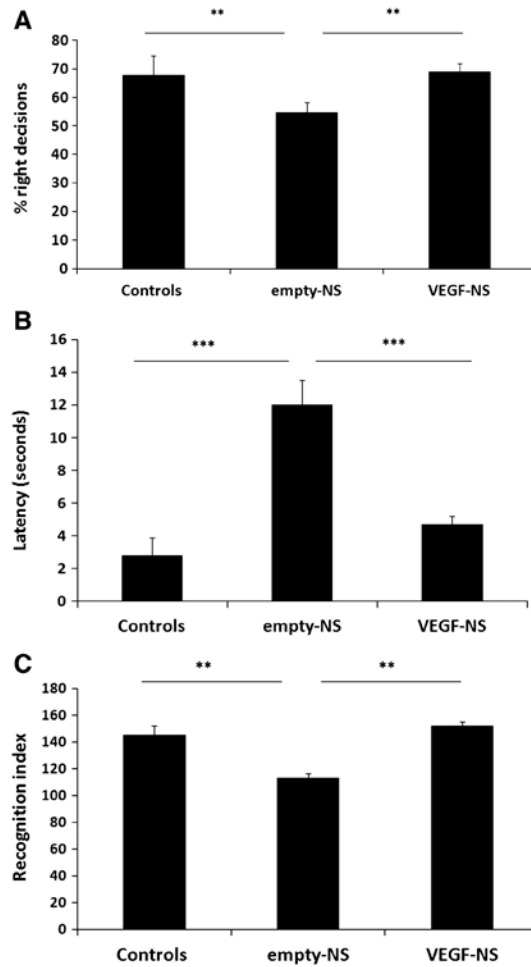


Figure 5. Behavioral cognition in control (non-transgenic) and in VEGF-NS and empty-NS treated APP/Ps1 mice groups. A. Correct decision percentage in the spontaneous alternation in the T-maze test; **p < 0.01, empty-NS vs. VEGF-NS and controls. B. Latencies in the spontaneous alternation in the T-maze; ***p < 0.001, empty-NS vs. VEGF-NS and controls. C. Recognition index, representing exploratory preference, obtained in the novel-object recognition task; **p < 0.01, empty-NS vs. VEGF-NS and controls. Data are expressed as mean \pm SEM (n = 10–11 per APP/Ps1 mice group, n = 8 per non-transgenic mice group). Reproduced with permission from [55].

A less invasive administration route, such as the intranasal administration, has also been studied to deliver GFs to the brain. *Zhang et al.* developed PEG-PLGA NP loaded with basic fibroblast growth factor (bFGF) and conjugated with *Solanum tuberosum lectin* (STL) which selectively binds to nasal epithelium, enhancing brain distribution of the formulations after intranasal administration. In these studies behavioral, histochemical and biochemical improvements were achieved when compared with the control group [56].

Along with GF, NGF loaded PBCA NP coated with polysorbate 80 have been developed by *Kurakhmaeva et al.* NGF-NP demonstrated their effectiveness reversing the scopolamine-induced amnesia in an AD mouse model [57,58]. NGF

was also encapsulated in cereport and transferrin functionalized liposomes by *Kuo et al.* They showed the ability of these liposomes to increase the permeability across BBB due to the fact that they increase the width of tight junction between cells and open the endothelial pores. In addition, the same research group encapsulated NGF along with curcumin in an attempt to obtain a synergistic effect. They developed wheat germ agglutinin (WGA)-conjugated and cardioplin (CL)-conjugated liposomes loaded these two drugs to rescue apoptotic neurons in AD. Surface WGA contributes enhancing the permeability of NGF and curcumin across the BBB. Moreover, CL protects SK-N-MC cells against neurotoxicity [59,60].

In AD, gene therapy has also been investigated to enhance targeted drug delivery into the brain. *Revilla et al.* developed lentiviral vectors engineered to overexpress GDNF as a promising tool to treat AD. The outcome of their studies demonstrated GFP (green fluorescent protein) and GDNF expression in transduced astrocytes, which were validated by localization with the astrocyte marker GFAP (glial fibrillary acidic protein). Furthermore, the neuroprotective effect of GDNF in hippocampus of 3xTg-AD mice was confirmed, as it improved spatial learning and memory (Figure 6) [61]. In another study, Sendai Virus Vector (SeV) mediated BDNF expression in hippocampal reduces neurons from synaptic degeneration, thus improving memory deficits in a Tg2576 mouse model of AD [58].

3.1.3 DDSs to release antioxidants and metal chelators.

As interesting and novel molecules to treat AD, antioxidants have also been encapsulated with the aim to enhance their low bioavailability and hydrophilic properties which limit their pass through BBB and consequently their therapeutic use. *Frezza et al.* developed resveratrol loaded lipid core nanocapsules (LNC) demonstrating their effectiveness to regain short-term and long-term memory. These promising outcomes might be due to the higher resveratrol brain concentration found in the brain of animals treated with this nano-DDS [62].

On the other hand, *Meng et al.* elaborated curcumin loaded NLC modified with lactoferrin. Biodistribution studies revealed the suitability of this nanoformulation enhancing brain uptake 2.78 times than non-modified NLC. *In vivo* studies revealed a reduction in the pathological damages in hippocampus of AD treated group [63]. In an attempt to obtain a synergistic effect, other research group encapsulated both antioxidant drugs (resveratrol and curcumin) in NLC. Nanoencapsulation increased

the stability of these two photosensible molecules, and enhanced the antioxidants activity in cell cultures [64].

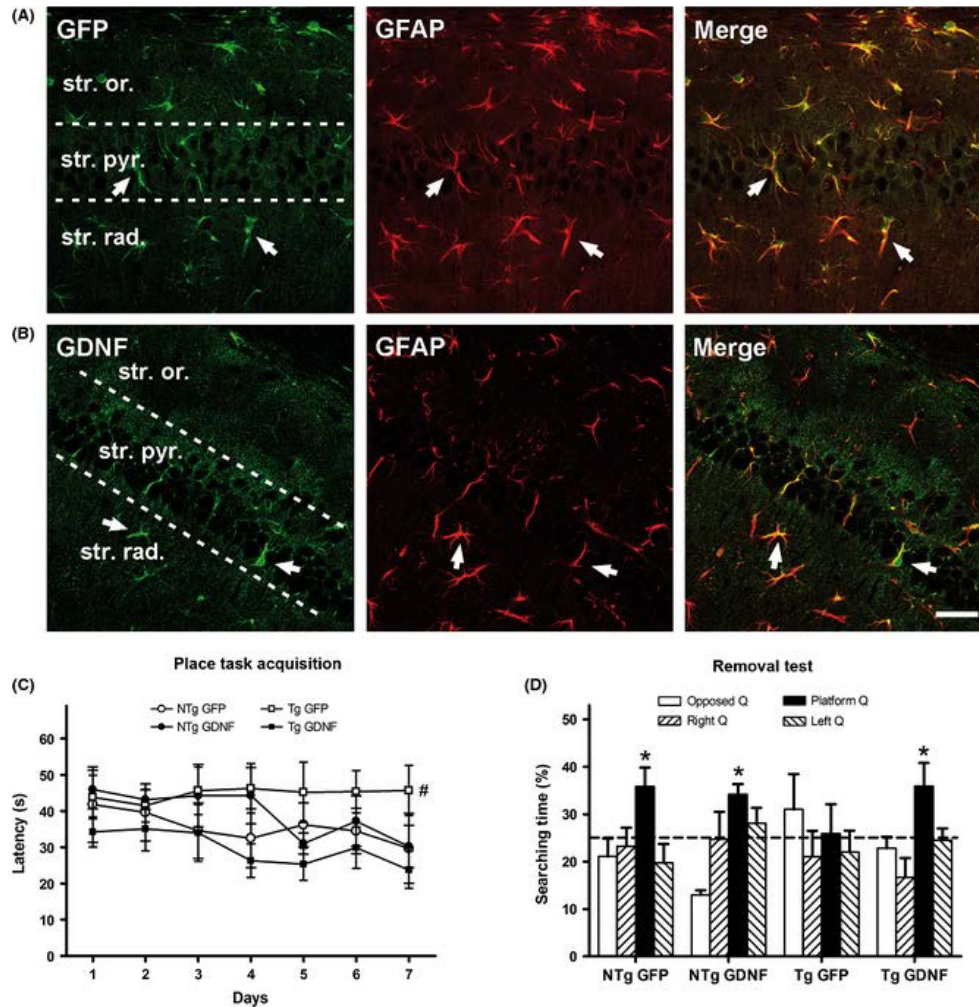


Figure 6. GDNF gene therapy and its effects on spatial learning and memory in the 3xTgAD mice. (A–B) Transgene expression of GFP and GDNF driven by lentiviral vectors stereotactically injected in the hippocampus. Both, GFP (A) and GDNF expression (B) in transduced astrocytes of the CA1 hippocampal area, were confirmed by co-localization with the astrocyte marker GFAP in the merge images for GFP plus GFAP and GDNF plus GFAP, respectively. Representative confocal images of double immunohistochemistry. Abbreviations: str. or., stratum oriens; str. pyr., stratum pyramidale; str. rad., stratum radiatum. Arrows indicate the same astrocyte cells along each row. Scale bar = 50 μ m. (C–D) Behavioral testing in the Morris water maze of 3xTgAD mice (Tg) and nontransgenic mice (NTg) treated with GFP or GDNF. (C) Latency to reach the escape platform during the 6 days of training indicating lower spatial learning in the Tg mice treated with GFP than in the other groups. (D) Time spent swimming in the platform quadrant of the pool (platform Q) when the platform was removed to test the retention of learning was different from chance in NTg mice and Tg mice treated with GDNF, but not in Tg-GFP mice. Dotted line indicates chance performance. Values are the mean \pm SEM, $n = 8-9$. Statistics: (C) $\#P < 0.01$ compared to the acquisition curve of NTg-GFP and Tg-GDNF; (D) $*P < 0.05$ compared to chance value; see text for details. Reproduced with permission from [61].

In the same way, catechins have also been encapsulated in nanolipidic particles to improve its physicochemical properties. In *vitro* studies carried out by *Smith et al.*, showed this nanoformulation ability to promote non-amyloidogenic processing of amyloid precursor protein (APP) by increasing α -secretase activity, thus preventing brain A β plaque formation [65].

About metal chelators for the treatment of AD, *Liu et al.* developed a NP conjugated with iron chelator which demonstrated its ability to protect cortical neurons from amyloid β -associated toxicity inhibiting amyloid β aggregation and neurotoxicity [66,67].

3.2 PD and nanotechnology

3.2.1 DDSs to release dopamine

As mentioned above, dopamine (DA) and dopaminergic treatments are the most commonly used therapies for PD. Nevertheless, the hydrophilic nature of DA together with its high hydrogen bonding potential limits its capability in terms of crossing BBB. Moreover, the systemic side effects such as nausea, hypotension, wearing on-off phenomena and dyskinesias restrict its therapeutic use [68,69].

Accordingly, *Trapani et al.* developed DA loaded chitosan NP in an attempt to overcome these limitations. The resulted NPs were suitable in terms of lack of toxicity and enhancing the transport across the BBB according to the studies carried out in the MDCKII-MDR1 cell line. *In vivo* biodistribution using microdialysis, showed that intraperitoneal administration of DA loaded chitosan NP increased the levels of this neurotransmitter in the striatum in a dose-dependent manner [70]. In order to avoid adverse side effects and increase the levels into the brain enhancing DA therapeutic efficacy, *Pillay et al.* designed an intracranial nano-enabled scaffold device (NESD) obtaining site specific delivery. The NESD was embedded in stable DA-loaded cellulose acetate phthalate (CAP) NP, showing a sustained release after implantation in the parenchyma of the frontal lobe of the Sprague-Dawley rat model [71]. Moreover, *López et al.* evaluated the use of nanostructured silica-DA reservoirs to reverse the rotational asymmetry induced by apomorphine in hemiparkinsonian rats. Neither dyskinesias nor other motor abnormalities were observed in animals after intrastriatal implantation of these implants [72].

Gene therapy has also been studied with the purpose of attaining the continuous production of DA in the CNS in a target-specific manner. *Jarraya et. al* demonstrated that injection of a tricistronic lentiviral vector, encoding the critical genes for DA synthesis, into the striatum increased extracellular concentrations of DA and restored motor deficits without associated dyskinesias or “ON”/“OFF” states in macaque monkeys [73].

3.2.2 DDSs to release levodopa

Levodopa is also a widely use treatment in clinical practice. In an attempt to improve brain uptake and eliminate carbidopa co-administration, *Sharma et. al* encapsulated levodopa in chitosan NP which were incorporated in a thermo-reversible Pluronic F127 gel for nose to brain delivery. *In vivo* studies demonstrated that the use of this nanoformulation increased levodopa percentage in the brain after intranasal administration. Despite these promising results, gel viscosity reduced NP uptake when it is compared with NP dispersed in saline solution, as they showed higher drug brain levels [74].

D'Aurizio et al. synthesized the prodrug levodopa- α -lipoic acid (LD-DA), a compound with lower susceptibility towards enzymatic conversion and hydrophilicity that facilitates its delivery to CNS. This compound was loaded in biodegradable PLGA MS in an attempt to obtain a depot system with a sustained release. Subcutaneous administration to rats demonstrated its ability optimizing levodopa pharmacokinetic profile, thus it could limit the associated motor syndrome side effect that accompanies PD treatment [75].

Current PD therapy also includes the co-administration of levodopa with benserazide. However, chronic administration of levodopa usually induced levodopa-induced dyskinesias (LID). Given that it has been demonstrated that continuous DA stimulation reduces LID, *Ren et al.* developed levodopa/benserazide loaded PLGA-MS to achieve a sustained release of this drug along time. The pharmacodynamic study revealed a decrease in apomorphine- induced turns (Figure 7) and improved stepping of the lesioned forepaw in PD rat model. Furthermore, western blot analysis exhibited a reduction in the levels of PD biochemical markers such as Δ fosB, phosphorylated dopamine or c-AMP-regulated phosphoprotein after the administration of this nanosystem [76]. These results are consistent with *Yang et al.* where Levodopa/benserazide loaded PLGA-

NP significantly reduced dyskinesias in a 6-OHDA animal model of PD as well as biochemical markers in western blot study [77].

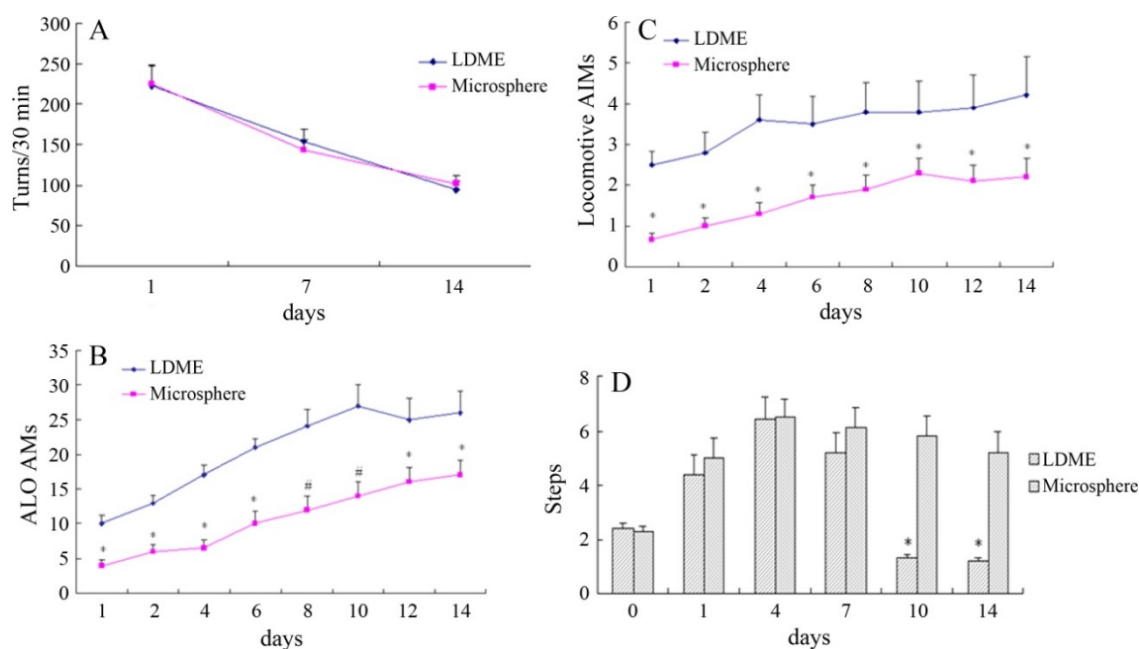


Figure 7. Comparison of motor response of 6-OHDA-lesioned rats treated with subcutaneous pulsatile levodopa methyl ester (LDME) *versus* LDME released from biodegradable microspheres over a two-week period; (A) pulsatile *versus* microsphere administration of LDME in 6-OHDA-lesioned rats show no differences in apomorphine-induced rotations; (B) and (C) Levodopa/benserazide-loaded biodegradable microspheres reduced dyskinesia expression in levodopa-treated rats. (B) $*P < 0.05$, $\#P < 0.01$ *versus* Levodopa. (C) $*P < 0.05$; (D) levodopa/benserazide-loaded biodegradable microspheres improved motor performance in levodopa-treated rats. $*P < 0.01$ *versus* levodopa. Reproduced with permission from [76].

3.3.3 DDSs to release dopaminergic agonist

Rotigotine is a non-ergoline agonist of DA receptors for the therapy of PD which has an extensive first pass metabolism showing low bioavailability through oral administration. Wang *et al.* developed rotigotine loaded PLGA MS which exhibited a sustained release and higher brain levels. Its therapeutic effects were evaluated in 6-OHDA rat model decreasing the dyskinesias associated with levodopa pulsatile treatment [78]. This formulation was then chronically intramuscularly administered during 3 months to Cynomolgus monkeys and Sprague-Dawley rats in order to assess its *in vivo* toxicity, highlighting the lack of toxicity of this formulation [79,80].

Another non-ergoline agonist of DA receptors is ropirinole. Transdermal delivery of ropirinole has been studied by Azeem *et al.* They demonstrated the suitability of

an oil based nanocarrier system enhancing the bioavailability of ropirinole as well as restoring biochemical changes in PD rat model [81]. Moreover, *Chandrakantsing et al.* with the aim of using a less invasive administration route, developed ropirinole loaded SLN as intranasal carriers with suitable pharmacokinetic results and no severe damage on the integrity of nasal mucosa [82].

Esposito et al. developed SLN as delivery systems for bromocriptine, an ergoline agonist of DA receptors. These lipid carriers prolonged the half-life of bromocriptine with suitable pharmacodynamic outcomes as they decreased akinesias in 6-OHDA hemiparkinsonian rats [83]. Not only akinesia but also catalepsia and oxidative stress levels have been improved in the research work developed by *Shadab et al.* Moreover, gamma scintigraphy imaging has demonstrated the capacity of bromocriptine loaded chitosan NP for drug targeted brain delivery [37].

Finally, apomorphine is a non-narcotic derivative of morphine which is used in the treatment of patients with advanced PD. PLGA based NP were used for the encapsulation of this drug, improving the physiochemical characteristics of the molecule and obtaining a sustained release according to *in vitro* studies [36]. Apomorphine loaded SLN were developed by *Tsai et al.* for oral administration. This nanosystem enhanced the brain uptake of the drug in the striatum as well as its bioavailability [84].

3.3.4 DDSs to release GFs

Jollivet et al. were the first ones to propose DDSs to release NTFs in order to treat neurodegenerative disorders. They designed PLGA MS to release GDNF directly into the brain in a partial lesioned rat model of PD. The outcomes of these studies revealed the suitability of this formulation after intrastriatal administration to stimulate the axonal regeneration of mesencephalic dopaminergic neurons, which are affected in PD. Moreover, the brain implantation of GDNF-PLGA-MS increased TH⁺ fibers (Figure 8) and neuronal density in the striatum and substantia nigra which was accompanied by functional improvement in the lesioned animals [85,86].

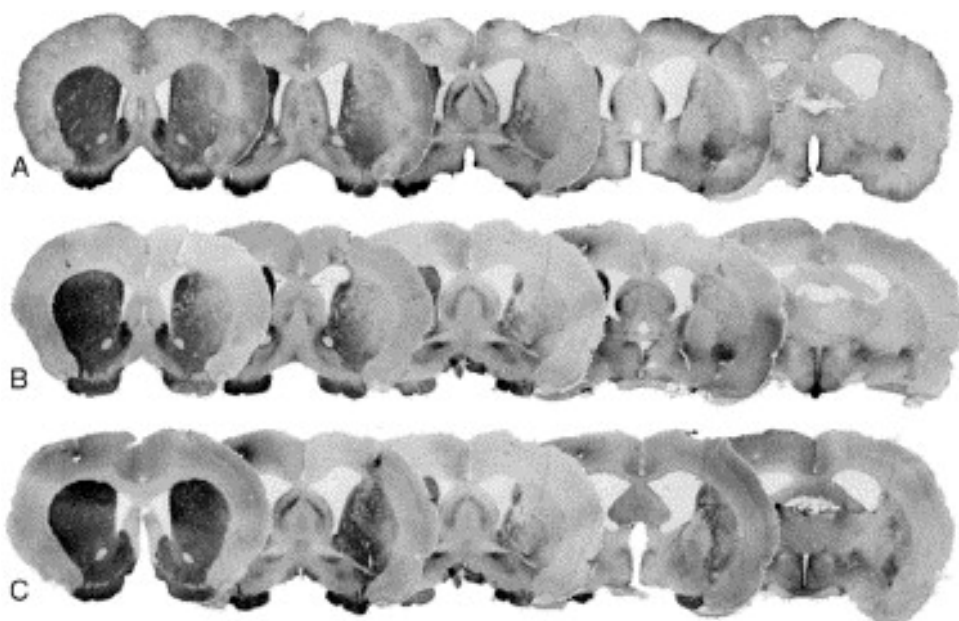


Figure 8. Photomicrographs of striatal TH-ir fibers. Five sections, which were used for optical density (OD) measurements, are shown. The two-sites lesion induced an extensive dorsolateral and caudal lesion in the non-treated rat (A). Blank MS implantation induced an increase of the fibers density (B) whereas GDNF-loaded MS induced a stronger reinnervation (C). Reproduced with permission from [85].

These results are consistent with *Garbayo et al.* published work, which confirmed the capability of PLGA MS to release this biologically active NTF in both *in vivo* and *in vitro* studies. Moreover, GDNF treated animals showed an improvement in amphetamine-induced rotational asymmetry test and in immunohistochemical analysis with an increase in the density of TH+ fibers at the striatal level. They could also confirm an increase in dopaminergic striatal neurons and long-term neuroprotection and neurorestoration by GDNF-MS [87,88].

With the aim of regulating the GDNF release from MP, *Gujral et al.* developed PLGA/collagen MS that encapsulated GDNF fused with a collagen binding protein. Only when collagenase penetrates into the MS through its porous surface, is the collagen phase degraded. Then, the GDNF should be de-link from the collagen and diffuse out of the MS. *In vitro* studies after PLGA formulation administration, demonstrated the differentiation of neuronal progenitor cells into mature neurons, which are promising results for the treatment of PD [89].

The co-administration of GDNF with other NTFs has also been studied in order to investigate the synergistic effects of these molecules after the administration into the brain. For example, *Lampe et al.* investigated the brain administration of BDNF and

GDNF loaded PLGA MS within a degradable PEG-based hydrogel. This approach allowed a different release profile for both grow factors decreasing the microglial response related with sham brain surgeries [90].

In a different study, our research group demonstrated the neuroregenerative potential of PLGA MS and NP encapsulating VEGF, GDNF and their combination on severely and partially lesioned rat models. The results of these works proved the biological activities of encapsulated NTFs in both *in vitro* and *in vivo* studies. Behavioral and immunohistochemical tests were improved in the treated 6-OHDA lesioned rats as shown in Figure 9, due to the synergistic effect of NTF, permitting a reduction of the dose by a half [91-93].

Although GDNF is one of the most studied NTF for the treatment of PD, other similar molecules have also been encapsulated to improve its bioavailability. NGF loaded PBCA NPs were able to reduce the basic symptoms of PD in a MPTP (1-methyl-4-phenyl-1,2,3,6-tetrahydropyridine) rat mode[94]. Besides this, gelatin NLC encapsulating bFGF has been studied as a novel approach to target the brain via nasal administration. The intranasal NLCs improved rotational behavior, monoamine neurotransmitter levels and TH expression in *in vitro* and *in vivo* studies without any adverse effects on the integrity of nasal mucosa [95].

Finally, as in AD, gene therapy has also been considered as a potential approach for the treatment of PD [44]. In an attempt to obtain this main goal, adenoviral-mediated GDNF gene transfer has been studied in a rat model of PD. *Kozlowski et al.* results revealed the suitability of this nanosystem increasing the number of dopaminergic neurons in the substantia nigra and maintaining functional connections to the striatum [96]. In addition, *Chen et al.* research work reinforces these outcomes since they could demonstrate the protective effect of GDNF gene transfer after intracerebral administration. Moreover, adenoviral (Ad) GDNF treated animals showed an improvement in behavioral tests and an increase in the survival of TH+ cells [97]. Not only has been demonstrated the effectiveness of Ad vectors in mouse models, but also, studies in non-human primate models of PD have been performed. *Eslamboli et al* and *Eberling et al.* showed that Ad-GDNF enhanced DA activity in the striatum, which was associated with clinical improvements without adverse effects in MPTP and 6-OHDA primate models of PD, respectively [98,99]. Moreover, the investigation led by *Kordower et al.* demonstrated that the delivery of

neurturin, a GDNF analog, via Ad vectors provided structural and functional neuroprotection and neurorestoration in MPTP-treated monkeys without histological pathology [100].

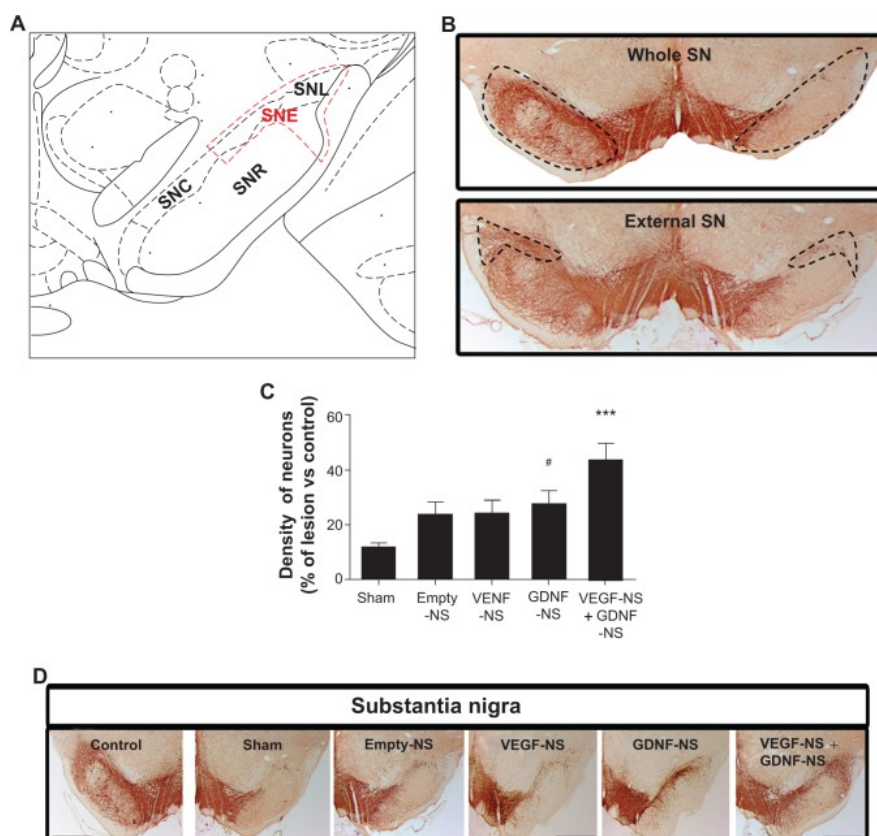


Figure 9. Histological evaluation of the treatments in the SN. (A) Schematic illustration of the SN with the “external SN” delimited. This area is topologically related to the lesioned area of striatum and includes SNL, a part of the SNR, and half of the SNC. (B) Picture of whole SN and delimited “external SN”. Scale bar =1 mm. (C) Density of dopaminergic neurons in “external SN”. The results are expressed as a percentage of lesioned hemisphere compared to the non-lesioned one (control). Data are shown as the mean \pm standard error of the mean ($n=6-8$) ($\#P<0.05$ GDNF NS group versus sham group; $***P<0.001$ VEGF NS and GDNF NS group versus sham and empty NS groups). (D) Photomicrographs of SN immunostained for tyrosine hydroxylase from a representative intact hemisphere (control) and 6-OHDA lesioned hemispheres from the different experimental groups. Scale bar =1 mm. Abbreviations: 6-OHDA, 6-hydroxydopamine; GDNF, glial cell line-derived neurotrophic factor; NS, nanospheres; SN, substantia nigra; SNC, SN pars compacta; SNL, SN lateral; SNR, SN pars reticulata; SNE, SN externa; VEGF, vascular endothelial growth factor. Reproduced with permission from [92].

However, due to the risk of viral gene therapy associated with immunogenicity and safety, safer and effective non viral gene delivery vectors have been developed [43]. A neurotensin polyplex carrier was elaborated for delivering GDNF gene into nigral dopamine neurons of hemiparkinsonian rats with stereotaxic procedures. RT-

PCR and western blot analysis confirmed that GDNF was correctly transfected in the substantia nigra reducing PD symptoms [101]. In order to improve transfection efficiency of nonviral gene vectors, different modifications on their surface have been made. For instance, *Chung-Fang et al.* developed intravenous GDNF plasmid DNA using Trojan horse liposomes (THLs) targeted with a monoclonal antibody (MAb) to the rat transferring receptor (TfR). They observed an increase in the concentrations of GDNF in the substantia nigra, which resulted in a reduction in apomorphine-induced rotations with different doses of encapsulated GF (Figure 10) and an increase in striatal TH enzyme activity [102].

Furthermore, *Huang et al.* proposed a lactoferrin-modified vector which was demonstrated to be effective for brain gene delivery of GDNF. Neuroprotective effects of these NPs were assayed in 6-OHDA lesioned rats and in rotenone-induced chronic PD model. *In vivo* studies revealed its capability for improving locomotor activity, reducing dopaminergic neuronal loss and enhancing monoamine neurotransmitter levels with multiple intravenous administrations and without brain toxicity [103,104].

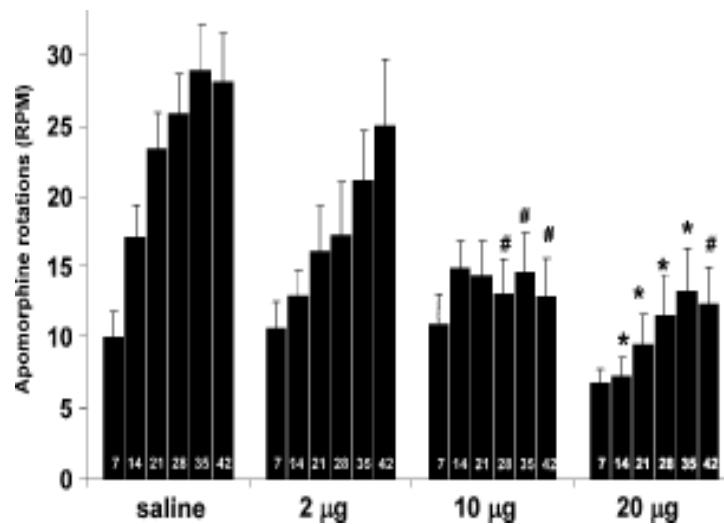


Figure 10. Apomorphine-induced rotation, measured in r.p.m., in rats with experimental PD, and treated intravenously with saline, or TfRMAb-targeted THLs carrying 2, 10 or 20 µg/rat of encapsulated pTHpro-GDNF plasmid DNA. The THLs were given on day 0, and rotation behaviour was measured at 7, 14, 21, 28, 35 and 42 days after the single intravenous injection of THLs. The rats were lesioned with intra-cerebral 6-hydroxydopamine 14 days before THL administration. Statistical differences were determined by ANOVA with Tukey's post-hoc correction; difference from saline control: # $p < 0.05$; * $p < 0$. Reproduced with permission from [102].

3.3.5 DDSs to release other molecules.

Although there are scientific studies supporting the use of coenzyme Q10 to treat PD, the results derived from clinical trials are inconclusive. It may be due to the low solubility, bioavailability and brain penetration of this molecule. In an attempt to overcome these all drawbacks, *Sikorska et al.* developed a nanomicellar formulation of coenzyme Q10 and tested its effectiveness in a mouse MPTP model. The outcomes of this investigation revealed the therapeutic effect of coenzyme Q10 via oral administration offsetting the neurotoxicity before and after MPTP injection. This was confirmed by cell counts, analyses of striatal dopamine levels and improved animals' motor skills on behavioral tests [105].

The antioxidant effect of resveratrol has also been enhanced after being loaded in liposomes. The behaviors, TH⁺ cells, apoptotic cells, ROS level and antioxidant capacity were determined in *in vivo* studies, showing resveratrol liposome more favorable effects than free resveratrol [106]. Resveratrol has also been loaded in Vitamin E nanoemulsion to improve its pharmacological activities. Pharmacokinetic studies showed a higher concentration of the drug in the brain with the nanoemulsion, which was consistent with higher antioxidant activity evaluated by DPPH (2,2-diphenyl-1-picrylhydrazyl) assay [107].

4. CONCLUSIONS AND FUTURE OUTLOOK

Current available therapies to treat AD and PD are only symptomatic without modifying the progression of these diseases. This fact, along with the difficulty of researching the pathways that cause NDs, drives the need for the development of new therapeutic alternatives to address the problem of these NDs.

Given this difficult situation, in the last years, not only the standardized drugs, but also new molecules such as growth factors, metal chelators and antioxidants have been investigated in order to study their potential activity in the restoration and promotion of neuronal processes. However, the physicochemical properties of these molecules make difficult their pass across the BBB to the brain, limiting their effectiveness and clinical application *in vivo*.

Therefore, there is a critical need to develop new DDSs to overcome these drawbacks with the aim of obtaining targeted drug delivery and a sustained release profile of the above mentioned drugs into the brain. The rapid progression of the

nanomedicine in the neuroscience area, is giving rise to design different nanometric formulations that permit the encapsulation of the drugs, protecting them against the enzymatic degradation and helping to reach therapeutic drug concentrations into the CNS after their *in vivo* administration.

The results presented in this review support the use of nanotechnology as a promising approach to control the release of old and new drugs for the treatment of AD and PD. Nevertheless, not only further studies of the properties of these nanocarriers, but also more preclinical test are needed to assess the therapeutic use and safety values of this nanocarriers for future applications in human clinical trials.

5. FINANCIAL & COMPETING INTERESTS DISCLOSURE

This project was partially supported by the 'Ministerio de Economía y Competitividad' (SAF2013-42347-R), the University of the Basque Country (UPV/EHU; UFI 11/32), Basque Government (Saiotek S-PE13UN048), (GIC IT 794/13) and FEDER funds. The authors have no other relevant affiliations or financial involvement with any organization or entity with a financial interest in or financial conflict with the subject matter or materials discussed in the manuscript apart from those disclosed. No writing assistance was utilized in the production of this manuscript.

EXECUTIVE SUMMARY
<p>NEW PROMISING MOLECULES FOR THE TREATMENT OF AD AND PD</p> <ul style="list-style-type: none"> • In the last years new molecules such as neurotrophic factors (NTFs), antioxidant molecules and metal chelators have been considered promising approaches to address the main causes of NDs. • Growth factors are a group of proteins which are able to improve the growth, proliferation and differentiation of neuronal cells. • Antioxidants have been raised as new treatment approaches to address the oxidative stress produced in AD and PD. • The main obstacle for most of these drugs to access into the brain is the presence of the BBB, therefore, different strategies have been developed to cross or by-pass this barrier.
<p>NANOTECHNOLOGY SOLUTIONS FOR NEURODEGENERATIVE DISEASES.</p> <ul style="list-style-type: none"> • Nanotechnology is an emerging field of science with promising physiochemical properties for the treatment of neurodegenerative diseases. • Different nanotechnology devices have been studied such as, polymeric nanoparticles, liposomes, SLN, NLC or gene therapy. • DDSs have been developed to release currently available treatments, growth factors, antioxidants and metal chelators for the treatment of AD and PD.
<p>CONCLUSIONS AND FUTURE OUTLOOK</p> <ul style="list-style-type: none"> • There is a critical need to develop new DDSs with the aim of obtaining targeted drug delivery and a sustained release profile of the therapeutic drugs into the brain. • The results presented in this review support the use of nanotechnology as a promising approach to control the release of old and new drugs for the treatment of AD and PD.

6. REFERENCES

1. Foster ER: Themes from the special issue on neurodegenerative diseases: what have we learned, and where can we go from here? *Am. J. Occup. Ther.* 68(1), 6-8 (2014).
2. Desai AK GG: Diagnosis and treatment of Alzheimer's disease. *Neurology* 64, S34-9 (2005).
3. Citron M.: Alzheimer's disease: strategies for disease modification. *Nat. Rev Drug Discov*, 387-398 (2010).
4. John Hardy KC: Amyloid at the blood vessel wall. *Nature Medicine* 12, 756-757 (2006).
5. Nussbaum RL, Ellis CE: Alzheimer's Disease and Parkinson's Disease. *N. Engl. J. Med.* 348(14), 1356-1364 (2003).
6. Linzasoro G: A global view of Parkinson's disease pathogenesis: Implications for natural history and neuroprotection. *Parkinsonism Relat. Disord.* 15(6), 401-405 (2009).

7. Ciesler J, Sari Y: Neurotrophic Peptides: Potential Drugs for Treatment of Amyotrophic Lateral Sclerosis and Alzheimer's disease. *Open J. Neurosci.* 3, 2 (2013).
8. Levy YS1, Gilgun-Sherki Y, Melamed E, Offen D: Therapeutic potential of neurotrophic factors in neurodegenerative diseases. *BioDrugs* 19, 97-127 (2005).
9. Vivian Y. Poon, Sojoong Choi and Mikyoung Park: Growth factors in synaptic function. *Front Synaptic Neurosci* 5, (2013).
10. Allen SJ, Watson JJ, Shoemark DK, Barua NU, Patel NK: GDNF, NGF and BDNF as therapeutic options for neurodegeneration. *Pharmacol. Ther.* 138(2), 155-175 (2013).
11. Lapchak PA, Gash DM, Jiao S, Miller PJ, Hilt D: Glial Cell Line-Derived Neurotrophic Factor: A Novel Therapeutic Approach to Treat Motor Dysfunction in Parkinson's Disease. *Exp. Neurol.* 144(1), 29-34 (1997).
12. Ventriglia M, Zanardini R, Bonomini C *et al.*: Serum brain-derived neurotrophic factor levels in different neurological diseases. *Biomed. Res. Int.* 901082 (2013).
13. Sofroniew MV, Howe CL, Mobley WC: Nerve growth factor signaling, neuroprotection, and neural repair. *Annu. Rev. Neurosci.* 24, 1217-1281 (2001).
14. Sendtner M, Carroll P, Holtmann B, Hughes RA, Thoenen H.: Ciliary neurotrophic factor. *J Neurobiol* 11, 1436-1453 (1994).
15. Liu X, Fawcett JR, Thorne RG, DeFor TA, Frey II WH: Intranasal administration of insulin-like growth factor-I bypasses the blood-brain barrier and protects against focal cerebral ischemic damage. *J. Neurol. Sci.* 187(1-2), 91-97 (2001).
16. Carmeliet P, Storkebaum E: Vascular and neuronal effects of VEGF in the nervous system: implications for neurological disorders. *Semin. Cell Dev. Biol.* 13(1), 39-53 (2002).
17. Storkebaum E, Lambrechts D, Carmeliet P: VEGF: once regarded as a specific angiogenic factor, now implicated in neuroprotection. *Bioessays* 26(9), 943-954 (2004).
18. Coppola V, Kucera J, Palko ME *et al.*: Dissection of NT3 functions in vivo by gene replacement strategy. *Development* 128(21), 4315-4327 (2001).
19. Wang X, Wang W, Li L, Perry G, Lee H, Zhu X: Oxidative stress and mitochondrial dysfunction in Alzheimer's disease. *Biochimica et Biophysica Acta (BBA) - Molecular Basis of Disease* 1842(8), 1240-1247 (2014).
20. Lovell MA, Robertson JD, Teesdale WJ, Campbell JL, Markesbery WR: Copper, iron and zinc in Alzheimer's disease senile plaques. *J. Neurol. Sci.* 158(1), 47-52 (1998).
21. Teng Ma, Meng-Shan Tan, Jin-Tai Yu, and Lan Tan: Resveratrol as a Therapeutic agent for Alzheimer's Disease. *Biomed Research International* (2014).
22. Khan MM, Ahmad A, Ishrat T *et al.*: Resveratrol attenuates 6-hydroxydopamine-induced oxidative damage and dopamine depletion in rat model of Parkinson's disease. *Brain Res.* 1328, 139-151 (2010).

23. Wang Y, Xu H, Fu Q, Ma R, Xiang J: Protective effect of resveratrol derived from *Polygonum cuspidatum* and its liposomal form on nigral cells in Parkinsonian rats. *J. Neurol. Sci.* 304(1–2), 29-34 (2011).
24. Stefani M, Rigacci S: Beneficial properties of natural phenols: Highlight on protection against pathological conditions associated with amyloid aggregation. *Biofactors* 40(5), 482-493 (2014).
25. Khuwaja G, Khan MM, Ishrat T *et al.*: Neuroprotective effects of curcumin on 6-hydroxydopamine-induced Parkinsonism in rats: Behavioral, neurochemical and immunohistochemical studies. *Brain Res.* 1368, 254-263 (2011).
26. Cherny RA, Atwood CS, Xilinas ME *et al.*: Treatment with a Copper-Zinc Chelator Markedly and Rapidly Inhibits β -Amyloid Accumulation in Alzheimer's Disease Transgenic Mice. *Neuron* 30(3), 665-676 (2001).
27. Guo C, Wang P, Zhong M *et al.*: Deferoxamine inhibits iron induced hippocampal tau phosphorylation in the Alzheimer transgenic mouse brain. *Neurochem. Int.* 62(2), 165-172 (2013).
28. Shults CW: Therapeutic role of coenzyme Q10 in Parkinson's disease. *Pharmacol. Ther.* 107(1), 120-130 (2005).
29. Begley DJ: Delivery of therapeutic agents to the central nervous system: the problems and the possibilities. *Pharmacol. Ther.* 104(1), 29-45 (2004).
30. Mathias NR, Hussain MA: Non-invasive systemic drug delivery: developability considerations for alternate routes of administration. *J. Pharm. Sci.* 99(1), 1-20 (2010).
31. Wong HL, Wu XY, Bendayan R: Nanotechnological advances for the delivery of CNS therapeutics. *Adv. Drug Deliv. Rev.* 64(7), 686-700 (2012).
32. Tajés M, Ramos-Fernandez E, Weng-Jiang X *et al.*: The blood-brain barrier: structure, function and therapeutic approaches to cross it. *Mol. Membr. Biol.* 31(5), 152-167 (2014).
33. Re F, Gregori M, Masserini M: Nanotechnology for neurodegenerative disorders. *Maturitas* 73(1), 45-51 (2012).
34. Modi G, Pillay V, Choonara YE: Advances in the treatment of neurodegenerative disorders employing nanotechnology. *Ann. N. Y. Acad. Sci.* 1184(1), 154-172 (2010).
35. Roney C, Kulkarni P, Arora V *et al.*: Targeted nanoparticles for drug delivery through the blood-brain barrier for Alzheimer's disease. *J. Controlled Release* 108(2–3), 193-214 (2005).
36. Regnier-Delplace C, Thillaye du Boullay O, Siepmann F *et al.*: PLGA microparticles with zero-order release of the labile anti-Parkinson drug apomorphine. *Int. J. Pharm.* 443(1–2), 68-79 (2013).
37. Md S, Khan RA, Mustafa G *et al.*: Bromocriptine loaded chitosan nanoparticles intended for direct nose to brain delivery: Pharmacodynamic, Pharmacokinetic and Scintigraphy study in mice model. *Eur J Pharm Sci* 48(3), 393-405 (2013).
38. Kreuter J: Drug delivery to the central nervous system by polymeric nanoparticles: What do we know? *Adv. Drug Deliv. Rev.* 71, 2-14 (2014).

39. Musyanovych A, Landfester K: Polymer Micro- and Nanocapsules as Biological Carriers with Multifunctional Properties. *Macromol Biosci.* 14(4), 458-477 (2014).
40. Mufamadi MS, Choonara YE, Kumar P *et al.*: Ligand-functionalized nanoliposomes for targeted delivery of galantamine. *Int. J. Pharm.* 448(1), 267-281 (2013).
41. Shah B, Khunt D, Bhatt H, Misra M, Padh H: Application of quality by design approach for intranasal delivery of rivastigmine loaded solid lipid nanoparticles: Effect on formulation and characterization parameters. *Eur J Pharm Sci* 78, 54-66 (2015).
42. Müller RH, Radtke M, Wissing SA: Nanostructured lipid matrices for improved microencapsulation of drugs. *Int. J. Pharm.* 242(1-2), 121-128 (2002).
43. Schlachetzki F, Zhang Y, Boado RJ, Pardridge WM.: Gene therapy of the brain: the trans-vascular approach. *Neurology* 62, 1275-1281 (2004).
44. Giridhar Murlidharan, Richard J. Samulski, and Aravind Asokan: Biology of adeno-associated viral vectors in the central nervous system. *Mol Neurosci* 7(76) (2014).
45. Fazil M, Md S, Haque S *et al.*: Development and evaluation of rivastigmine loaded chitosan nanoparticles for brain targeting. *Eur J Pharm Sci* 47(1), 6-15 (2012).
46. Joshi SA, Chavhan SS, Sawant KK: Rivastigmine-loaded PLGA and PBCA nanoparticles: Preparation, optimization, characterization, in vitro and pharmacodynamic studies. *Eur J Pharm Biopharm* 76(2), 189-199 (2010).
47. Kulkarni PV, Roney CA, Antich PP, Bonte FJ, Raghu AV, Aminabhavi TM: Quinoline-n-butylcyanoacrylate-based nanoparticles for brain targeting for the diagnosis of Alzheimer's disease. *Wiley Interdiscip Rev Nanomed Nanobiotechnol* 2(1), 35-47 (2010).
48. Wilson B, Samanta MK, Santhi K, Kumar KPS, Paramakrishnan N, Suresh B: Poly(n-butylcyanoacrylate) nanoparticles coated with polysorbate 80 for the targeted delivery of rivastigmine into the brain to treat Alzheimer's disease. *Brain Res.* 1200, 159-168 (2008).
49. Nagpal K, Singh SK, Mishra DN: Optimization of brain targeted chitosan nanoparticles of Rivastigmine for improved efficacy and safety. *Int. J. Biol. Macromol.* 59, 72-83 (2013).
50. Ismail MF, ElMeshad AN, Salem NA-H: Potential therapeutic effect of nanobased formulation of rivastigmine on rat model of Alzheimer's disease. *Int J Nanomedicine.*, 393-406 (2013).
51. Bhavna , Shadab Md , Mushir Ali , Sanjula Baboota , Jasjeet Kaur Sahni , Aseem Bhatnagar , Javed Ali: Preparation, characterization, in vivo biodistribution and pharmacokinetic studies of donepezil-loaded PLGA nanoparticles for brain targeting. *Drug Dev Ind Pharm* 40 (2014).
52. Shubham Misra , Kanwaljit Chopra , V. R. Sinha , Bikash Medhi: Galantamine-loaded solid-lipid nanoparticles for enhanced brain delivery: preparation, characterization, in vitro and in vivo evaluations. *Drug delivery* (2015).
53. Laserra S, Basit A, Sozio P *et al.*: Solid lipid nanoparticles loaded with lipoyl-memantine codrug: Preparation and characterization. *Int. J. Pharm.* 485(1-2), 183-191 (2015).

54. Herrán E, Pérez-González R, Igartua M, Pedraz JL, Carro E, Hernández RM: VEGF-releasing biodegradable nanospheres administered by craniotomy: A novel therapeutic approach in the APP/Ps1 mouse model of Alzheimer's disease. *J. Controlled Release* 170(1), 111-119 (2013).
55. Herran E, Perez- Gonzalez R, Igartua M, Pedraz J.L, Carro E and Hernandez R.M: Enhanced Hippocampal Neurogenesis in APP/Ps1 Mouse Model of Alzheimer's Disease After Implantation of VEGF-loaded PLGA Nanospheres. *Curr Alzheimer Res* 12(10), 932-940 (2015).
56. Zhang C, Chen J, Feng C *et al.*: Intranasal nanoparticles of basic fibroblast growth factor for brain delivery to treat Alzheimer's disease. *Int. J. Pharm.* 461(1–2), 192-202 (2014).
57. Kamila B. Kurakhmaeva , Irma A. Djindjikhshvili , Valery E. Petrov , Vadim U. Balabanyan , Tatiana A. Voronina , Sergey S. Trofimov , Jörg Kreuter , Svetlana Gelperina , David Begley , Renad N. Alyautdin: Brain targeting of nerve growth factor using poly(butyl cyanoacrylate) nanoparticles. *J Drug Target* 17(8) (2009).
58. Iwasaki Y, Negishi T, Inoue M, Tashiro T, Tabira T, Kimura N: Sendai virus vector-mediated brain-derived neurotrophic factor expression ameliorates memory deficits and synaptic degeneration in a transgenic mouse model of Alzheimer's disease. *J. Neurosci. Res.* 90(5), 981-989 (2012).
59. Yung-Chih Kuo CL: Rescuing apoptotic neurons in Alzheimer's disease using wheat germ agglutinin-conjugated and cardiolipin-conjugated liposomes with encapsulated nerve growth factor and curcumin. *Int J Nanomedicine.* (2015).
60. Kuo Y, Chou P: Neuroprotection Against Degeneration of SK-N-MC Cells Using Neuron Growth Factor-Encapsulated Liposomes with Surface Cereport and Transferrin. *J. Pharm. Sci.* 103(8), 2484-2497 (2014).
61. Revilla S, Ursulet S, Álvarez-López MJ *et al.*: Lenti-GDNF Gene Therapy Protects Against Alzheimer's Disease-Like Neuropathology in 3xTg-AD Mice and MC65 Cells. *CNS Neuroscience & Therapeutics* 20(11), 961-972 (2014).
62. L. Frozza R, Bernardi A, Juliana B., B. Meneghetti A, Matté A, Battastini A, Pohlmann A, Guterres S, Salbego C: Neuroprotective Effects of Resveratrol Against A β Administration in Rats are Improved by Lipid-Core Nanocapsules. *Molecular Neurobiology* 47(3), 1066-1080 (2013).
63. Meng F, Asghar S, Gao S *et al.*: A novel LDL-mimic nanocarrier for the targeted delivery of curcumin into the brain to treat Alzheimer's disease. *Colloids and Surfaces B: Biointerfaces* 134, 88-97 (2015).
64. Coradini K, Lima FO, Oliveira CM *et al.*: Co-encapsulation of resveratrol and curcumin in lipid-core nanocapsules improves their in vitro antioxidant effects. *Euro J Pharm Biopharm* 88(1), 178-185 (2014).
65. Smith A, Giunta B, Bickford PC, Fountain M, Tan J, Shytle RD: Nanolipidic particles improve the bioavailability and α -secretase inducing ability of epigallocatechin-3-gallate (EGCG) for the treatment of Alzheimer's disease. *Int. J. Pharm.* 389(1–2), 207-212 (2010).
66. Liu G, Men P, Harris PLR, Rolston RK, Perry G, Smith MA: Nanoparticle iron chelators: A new therapeutic approach in Alzheimer disease and other neurologic disorders associated with trace metal imbalance. *Neurosci. Lett.* 406(3), 189-193 (2006).
67. Liu G, Men P, Kudo W, Perry G, Smith MA: Nanoparticle–chelator conjugates as inhibitors of amyloid- β aggregation and neurotoxicity: A novel therapeutic approach for Alzheimer disease. *Neurosci. Lett.* 455(3), 187-190 (2009).

68. Garbayo E, Ansorena E, Blanco-Prieto MJ: Drug development in Parkinson's disease: From emerging molecules to innovative drug delivery systems. *Maturitas* 76(3), 272-278 (2013).
69. Rascol O, Goetz C, Koller W, Poewe W, Sampaio C: Treatment interventions for Parkinson's disease: an evidence based assessment. *The Lancet* 359(9317), 1589-1598 (2002).
70. Trapani A, De Giglio E, Cafagna D *et al.*: Characterization and evaluation of chitosan nanoparticles for dopamine brain delivery. *Int. J. Pharm.* 419(1-2), 296-307 (2011).
71. Pillay S, Pillay V, Choonara YE *et al.*: Design, biometric simulation and optimization of a nano-enabled scaffold device for enhanced delivery of dopamine to the brain. *Int. J. Pharm.* 382(1-2), 277-290 (2009).
72. López T, Bata-García J L, Esquivel D, et al: Treatment of Parkinson's disease: nanostructured sol-gel silica-dopamine reservoirs for controlled drug release in the central nervous system. *Int J Nanomedicine*. 2011(6), 19-31 (2010).
73. B Jarraya B, Boulet S, Ralph G.S *et al.*: Dopamine Gene Therapy for Parkinson's Disease in a Nonhuman Primate Without Associated Dyskinesia. *Sci Translational Medicine* 1(2ra4) (2009).
74. Sharma S, Lohan S & Murthy R.S.R: Formulation and characterization of intranasal mucoadhesive nanoparticulates and thermo-reversible gel of levodopa for brain delivery. *Drug Dev Ind Pharm* (2013).
75. D'Aurizio E, Sozio P, Cerasa L. S, Vacca M, Brunetti L, Orlando G, Chiavaroli A, Kok R. J, Hennink W. E, and Di Stefano A: Biodegradable Microspheres Loaded with an Anti-Parkinson Prodrug: An in Vivo Pharmacokinetic Study. *Mol Pharm* 8(6) (2011).
76. Ren T, Yang X, Wu N, Cai Y, Liu Z, Yuan W: Sustained-release formulation of levodopa methyl ester/benserazide for prolonged suppressing dyskinesia expression in 6-OHDA-lesioned rats. *Neurosci. Lett.* 502(2), 117-122 (2011).
77. Yang X, Zheng R, Cai Y, Liao M, Yuan W, Liu Z: Controlled-release levodopa methyl ester/benserazide-loaded nanoparticles ameliorate levodopa-induced dyskinesia in rats. *Int J Nanomedicine.*, 2077-2086 (2012).
78. Wang A, Wang L, Sun K, Liu W, Sha C, Li Y.: Preparation of rotigotine-loaded microspheres and their combination use with L-DOPA to modify dyskinesias in 6-OHDA-lesioned rats. *Pharm Res* (2012).
79. Ye L, Guan X, Tian J *et al.*: Three-month subchronic intramuscular toxicity study of rotigotine-loaded microspheres in SD rats. *Food Chem Toxicol* 56, 81-92 (2013).
80. Tian J, Du G, Ye L *et al.*: Three-month subchronic intramuscular toxicity study of rotigotine-loaded microspheres in Cynomolgus monkeys. *Food Chem Toxicol* 52, 143-152 (2013).
81. Azeem A, Talegaonkar S, Negi LM, Ahmad FJ, Khar RK, Iqbal Z: Oil based nanocarrier system for transdermal delivery of ropinirole: A mechanistic, pharmacokinetic and biochemical investigation. *Int. J. Pharm.* 422(1-2), 436-444 (2012).
82. Pardeshi CV, Rajput PV, Belgamwar VS, Tekade AR, Surana SJ.: Novel surface modified solid lipid nanoparticles as intranasal carriers for ropinirole hydrochloride: application of factorial design approach. *Drug delivery*, 47-56 (2013).

83. Esposito L, Fantin M, Marti M, Drechsler M, Paccamiccio L, Mariani P, Sivieri E, Lain F, Menegatti E et al.: Solid lipid nanoparticles as delivery systems for bromocriptine. *Pharm Res* 25(7) (2008).
84. Tsai M, Huang Y, Wu P et al.: Oral apomorphine delivery from solid lipid nanoparticles with different monostearate emulsifiers: Pharmacokinetic and behavioral evaluations. *J. Pharm. Sci.* 100(2), 547-557 (2011).
85. Jollivet C, Aubert-Pouessel A, Clavreul A et al.: Long-term effect of intra-striatal glial cell line-derived neurotrophic factor-releasing microspheres in a partial rat model of Parkinson's disease. *Neurosci. Lett.* 356(3), 207-210 (2004).
86. Jollivet C, Aubert-Pouessel A, Clavreul A et al.: Striatal implantation of GDNF releasing biodegradable microspheres promotes recovery of motor function in a partial model of Parkinson's disease. *Biomaterials* 25(5), 933-942 (2004).
87. Garbayo E, Montero-Menei CN, Ansorena E, Lanciego JL, Aymerich MS, Blanco-Prieto MJ: Effective GDNF brain delivery using microspheres—A promising strategy for Parkinson's disease. *J. Controlled Release* 135(2), 119-126 (2009).
88. Garbayo E, Ansorena E, Lanciego JL, Blanco-Prieto MJ, Aymerich MS: Long-term neuroprotection and neurorestoration by glial cell-derived neurotrophic factor microspheres for the treatment of Parkinson's disease. *Movement Disorders* 26(10), 1943-1947 (2011).
89. Gujral C, Minagawa Y, Fujimoto K, Kitano H, Nakaji-Hirabayashi T: Biodegradable microparticles for strictly regulating the release of neurotrophic factors. *J. Controlled Release* 168(3), 307-316 (2013).
90. Lampe KJ, Kern DS, Mahoney MJ, Bjugstad KB: The administration of BDNF and GDNF to the brain via PLGA microparticles patterned within a degradable PEG-based hydrogel: Protein distribution and the glial response. *Journal of Biomedical Materials Research Part A* 96A(3), 595-607 (2011).
91. Herrán E, Ruiz-Ortega JÁ, Aristieta A et al.: In vivo administration of VEGF- and GDNF-releasing biodegradable polymeric microspheres in a severe lesion model of Parkinson's disease. *Eur J Pharm Biopharm* 85(3, Part B), 1183-1190 (2013).
92. Herran E, Requejo C, Ruiz-Ortega JA. et al: Increased antiparkinson efficacy of the combined administration of VEGF- and GDNF-loaded nanospheres in a partial lesion model of Parkinson's disease. *Int J Nanomedicine.* 9(1), 2677-2687 (2014).
93. C. Requejo, J.A. Ruiz-Ortega, H. Bengoetxea et al.: Topographical Distribution of Morphological Changes in a Partial Model of Parkinson's Disease—Effects of Nanoencapsulated Neurotrophic Factors Administration. *Molecular Neurobiology* 52(2), 846-858 (2015).
94. Kamila B. Kurakhmaeva, Irma A. Djindjhashvilib, Valery E. et al: Brain targeting of nerve growth factor using poly(butyl cyanoacrylate) nanoparticles. *J Drug Targeting* 17(8), 564-574 (2009).
95. Zhao Y, Li X, Lu C et al.: Gelatin nanostructured lipid carriers-mediated intranasal delivery of basic fibroblast growth factor enhances functional recovery in hemiparkinsonian rats. *Nanomedicine* 10(4), 755-764 (2014).
96. Kozlowski DA, Connor B, Tillerson JL, Schallert T, Bohn MC: Delivery of a GDNF Gene into the Substantia Nigra after a Progressive 6-OHDA Lesion Maintains Functional Nigrostriatal Connections. *Exp. Neurol.* 166(1), 1-15 (2000).

97. Chen X, Liu W, Guoyuan Y *et al.*: Protective effects of intracerebral adenoviral-mediated GDNF gene transfer in a rat model of Parkinson's disease. *Parkinsonism Relat. Disord.* 10(1), 1-7 (2003).
98. Eslamboli A, Georgievska B, Ridley RM *et al.*: Continuous Low-Level Glial Cell Line-Derived Neurotrophic Factor Delivery Using Recombinant Adeno-Associated Viral Vectors Provides Neuroprotection and Induces Behavioral Recovery in a Primate Model of Parkinson's Disease. *J Neurosci* 25(4), 769-777 (2005).
99. Jamie L. Eberling, Adrian P. Kells, Philip Pivrotto *et al.*: Functional effects of AAV2-GDNF on the dopaminergic nigrostriatal pathway in parkinsonian rhesus monkeys. *Hum Gene Ther* 20(5), 511-518 (2009).
100. Kordower JH, Herzog CD, Dass B *et al.*: Delivery of neurturin by AAV2 (CERE-120)-mediated gene transfer provides structural and functional neuroprotection and neurorestoration in MPTP-treated monkeys. *Ann. Neurol.* 60(6), 706-715 (2006).
101. Gonzalez-Barrios J A, Lindahl M, Bannon M J *et al.*: Neurtensin polyplex as an efficient carrier for delivering the human GDNF gene into nigral dopamine neurons of hemiparkinsonian rats. *Mol Ther* 14(6), 857-865 (2006).
102. Xia C, Boado RJ, Zhang Y, Chu C, Pardridge WM: Intravenous glial-derived neurotrophic factor gene therapy of experimental Parkinson's disease with Trojan horse liposomes and a tyrosine hydroxylase promoter. *J. Gene Med.* 10(3), 306-315 (2008).
103. Huang R, Han L, Li J *et al.*: Neuroprotection in a 6-hydroxydopamine-lesioned Parkinson model using lactoferrin-modified nanoparticles. *J. Gene Med.* 11(9), 754-763 (2009).
104. Huang R, Ke W, Liu Y *et al.*: Gene therapy using lactoferrin-modified nanoparticles in a rotenone-induced chronic Parkinson model. *J. Neurol. Sci.* 290(1-2), 123-130 (2010).
105. Sikorska M, Lanthier P, Miller H *et al.*: Nanomicellar formulation of coenzyme Q10 (Ubisol-Q10) effectively blocks ongoing neurodegeneration in the mouse 1-methyl-4-phenyl-1,2,3,6-tetrahydropyridine model: potential use as an adjuvant treatment in Parkinson's disease. *Neurobiol. Aging* 35(10), 2329-2346 (2014).
106. Wang Y, Xu H, Fu Q, Ma R, Xiang J: Protective effect of resveratrol derived from *Polygonum cuspidatum* and its liposomal form on nigral cells in Parkinsonian rats. *J. Neurol. Sci.* 304(1-2), 29-34 (2011).
107. Pangeni R, Sharma S, Mustafa G *et al.*: Vitamin E loaded resveratrol nanoemulsion for brain targeting for the treatment of Parkinson's disease by reducing oxidative stress. *Nanotechnology* 25(48) (2014).

Nanotechnology based approaches for neurodegenerative disorders: diagnosis and treatment ²

Sara Hernando^{1,2}, Enara Herran^{1,2}, Jose Luis Pedraz^{1,2}, Manoli Igartua^{1,2}, Rosa Maria Hernandez^{1,2,*}

¹NanoBioCel Group, Laboratory of Pharmaceutics, School of Pharmacy, University of the Basque Country (UPV/EHU), Vitoria-Gasteiz, 01006, Spain;

²Biomedical Research Networking Centre in Bioengineering, Biomaterials and Nanomedicine (CIBER-BBN), Vitoria-Gasteiz, 01006, Spain.

*Corresponding author: R.M. Hernández

² Published in Drug and Gene Delivery to the Central Nervous System for Neuroprotection (2017). Sharma H., Muresanu D., Sharma A. (eds) Springer, Cham.
https://doi.org/10.1007/978-3-319-57696-1_3

ABSTRACT

Nanotechnology has been raised as a promising alternative for the diagnosis and treatment of different neurodegenerative disorders (ND). Among NDs, Alzheimer's disease (AD) and Parkinson's disease (PD) represent the most common neurodegenerative disorders worldwide. The early diagnoses of AD and PD together with a successful treatment hampering the neurodegenerative process are priority objectives for the scientific community. Although new treatment strategies and diagnostic methods have been proposed, reach the brain is one of the most challenging tasks in modern medicine. At present, the formulation of different nanomedicine devices has shown several advantages to cross the BBB, offering novel diagnosis and treatment approaches. Therefore, this chapter focuses on nanotechnology solutions for AD and PD diagnosis and treatment.

Keywords: Alzheimer's disease • Parkinson's disease • nanotechnology • nanomedicine • drug delivery systems

1. INTRODUCTION

Nanotechnology is a field of science which employs materials and devices in the nanometer scale. In the last years, numerous studies have proposed nanomedicine as a promising approach for the treatment and diagnosis of neurodegenerative disorders since they can be effective avoiding some drug delivery problems, enhancing drugs accessibility to target areas or improving specificity and selectivity for diagnostic criteria [1-3]. In this section, we have focus on describing different nanotechnology systems used for the diagnosis and treatment of AD and PD, concretely (Figure 1).

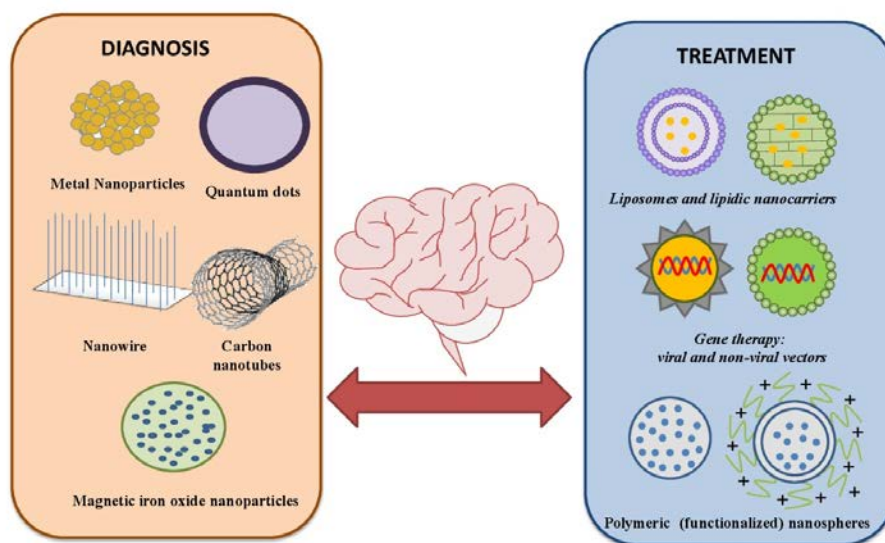


Figure 1. Nanotechnology devices for diagnosis and treatment.

2. CHALLENGES AND NEW STRATEGIES FOR CNS DELIVERY: THE BLOOD BRAIN BARRIER

One of the most challenging obstacles for an effective treatment of central nervous system (CNS) related disorders is the low efficiency penetration of drugs to CNS due to the presence of the blood brain barrier (BBB). The BBB is a dynamic barrier which protects the brain against invading organism and unwanted substances. Physiologically it is constituted by endothelial cells, extracellular base membrane, adjoining pericytes, astrocytes and microglia, which are all the integral parts of the BBB supporting system (Figure 2) [16].

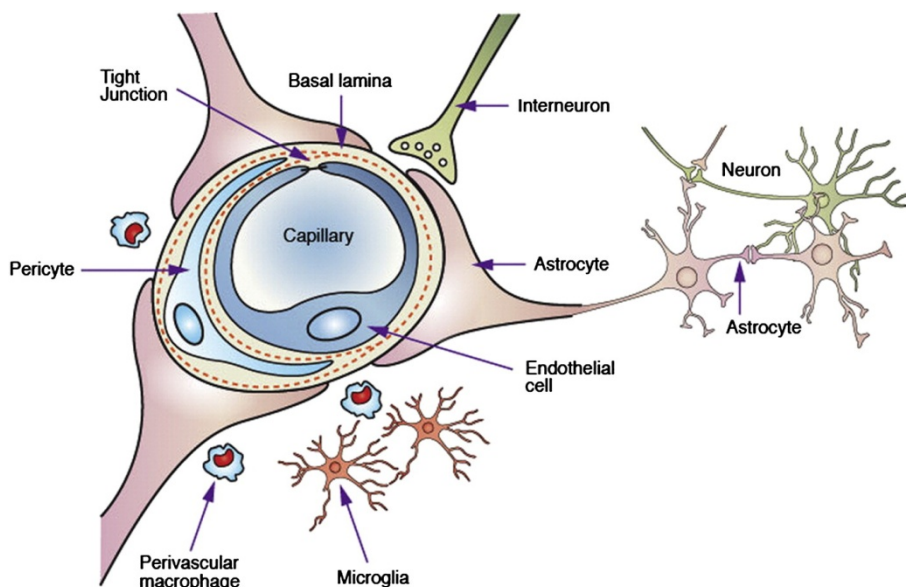


Figure 2. Schematic representation of the blood brain barrier (BBB) and other components of a neurovascular unit (NVU). Reproduced with permission from [16].

To enter the brain, drugs can take different routes, however, the BBB have also some mechanisms for their elimination. In figure 3, there have been summarized the different uptake routes and elimination strategies that occur in the BBB.

On the one hand, small hydrophilic compounds with a mass lower than 150 Da and highly hydrophobic compounds with a mass lower than 400-600 Da are able to cross the BBB by passive diffusion. Even so, polar solutes have difficulties to cross the BBB and reach the brain due to the presence of tight junctions [17]. In any case, most of the therapeutic molecules pass the BBB by specific receptor mediated or vesicular mechanisms. Receptor mediated transcytosis is the main route used for

the uptake of macromolecules. In this sense, systems including transferring or insulin receptor have been developed in order to enhance brain targeting using this route [16]. Adsorptive-mediated transcytosis, also known as pynocytosis is another well establish route for crossing the BBB. In this regard, pynocytosis based drug delivery systems have also been studied. These systems involve either cationic proteins or cell penetrating peptides such as Tat-derived and Syn-B vectors [18]. Finally, cell-mediated transcytosis, “Trojan horse” model is a recently described route for drug transport across the BBB. In this transport route, the molecules interact with immune cells such as monocytes or macrophages to cross the BBB [19]. Furthermore, it would also be pointed out the presence of the P-glycoprotein (P-gp) pump in the BBB as an obstacle for entering to the brain. This P-gp system is the main efflux mechanism for the expulsion of several molecules including pharmaceuticals [20].

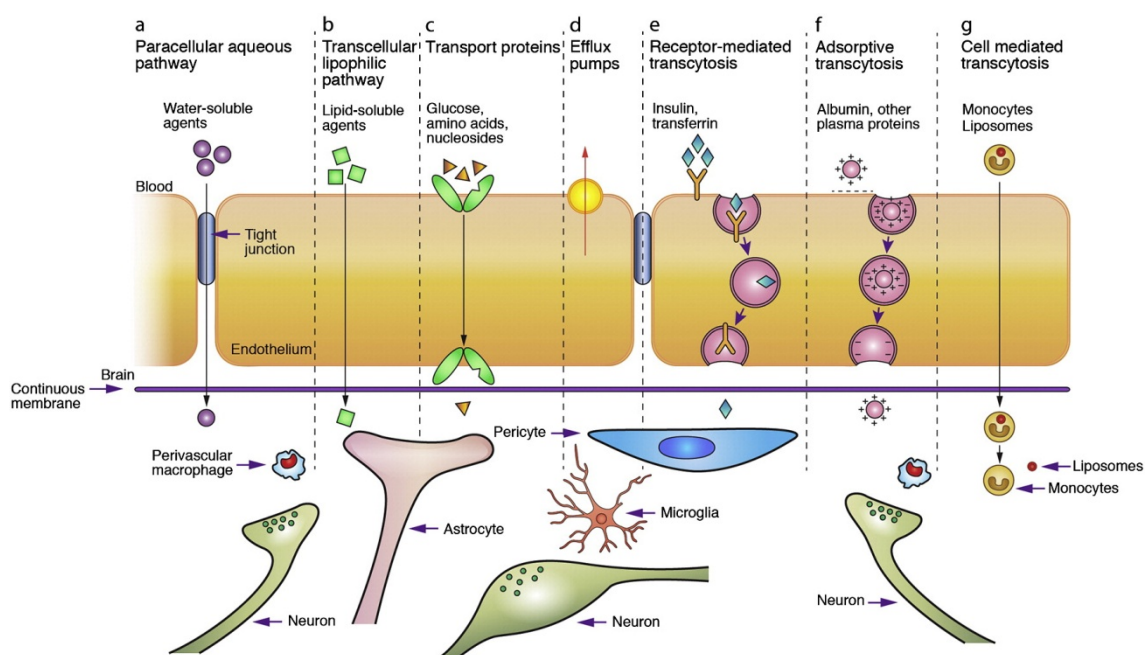


Figure 3: Transport routes across the BBB. Reproduced with permission from [16].

Table 1. Nanotechnology devices as drug delivery systems (DDS) or diagnostic tools.

NANOTECHNOLOGY DEVICE	DEFINITION	THERAPEUTIC USE	REF.
Polymeric (functionalized) nanoparticles, nanocapsules and nanospheres	Polymeric nanoparticles (NP) are constituted of different biodegradable and biocompatible materials in which the chemical compound (drug or imaging agent) can be dissolved, entrapped, encapsulated or coated on the surface by adsorption or conjugation. Moreover, they can be functionalized with targeting ligands or antibodies.	DDS and diagnosis	[4,5]
(Nano) liposomes	These lipidic nanoparticulate systems are composed by concentric bilayers of phospholipid-based membranes. They can incorporate hydrophilic molecules in their internal water compartment and also hydrophobic compounds into the membrane. They can also be functionalized for specific brain targeting.	DDS	[6]
Solid lipid nanoparticles (SLN)	SLNs are formed by mono-, di-, tri- glycerides, fatty acids, steroids and waxes and stabilized physiologically compatible emulsifiers. They have some advantages such as; good biocompatibility, high drug loading capacity, high stability and the possibility of modify their surface for specific targeting.	DDS	[7]
Nanostructured Lipid Carriers (NLC)	A second generation of lipid nanocarriers, improved from SLNs. NLCs are composed by a mixture of solid and liquid lipids which improve the encapsulation efficiency and the release profile.	DDS	[8,9]
Gene therapy viral and non viral vectors	Gene therapy consists of specific gene or DNA compacted carriers to target cells or tissues, entering to the nucleus to be expressed. Viral and non viral gene deliver vectors have been developed.	DDS	[10,11]

Magnetic iron oxide nanoparticles	Iron oxide NPs have gained much interest due to their large surface area, magnetic properties and limited toxicity.	Diagnosis	[12]
Quantum dots	Quantum dots (QD) are nanoscale semiconductor crystals with a fluorescent response to absorbed light. Their fluorescent properties are advantageous in comparison with conventional fluorescent dyes. Their characteristics are minimal photo bleaching, optimal stability and high signal to noise ratio, among others. Moreover, their surface can be biofunctionalized.	Diagnosis	[2]
Nanowire	Nanowires have acquired much attention as innovative nanomaterials for the detection of CNS pathologies. They have the ability of receive and deliver electrical impulses which is a good value for the detection of various pathologies.	Diagnosis	[13]
Metal Nanoparticles	Gold and silver nanoparticles have been used for the detection of fluid biomarkers due to their accuracy and capacity for the detection of ultralow concentrations of different biomarkers.	Diagnosis	[14,15]

As it has been explained before, the complexity of the BBB makes difficult to cross or by pass it. Indeed, different strategies have been developed in order to obtain brain targeting. In the following section, we will describe different invasive and non invasive methods investigated for achieving this main goal.

2.1 Invasive methods for CNS delivery

2.1.1 Disruption of the BBB

In the past, several modifications of the BBB have been made using hyperosmotic solutions such as mannitol or urea to open tight junction network shortly enabling the drugs to cross the BBB. Although this strategy has had success in animals increasing permeability of the drugs to the CNS, there have also been reported some drawbacks such as neuronal damage, alteration in glucose uptake and microembolisms. Indeed, this procedure breaks down the defense mechanism of the brain and may permit the entrance of chemicals or toxins [17,21].

Moreover, biochemical disruption has also been investigated using different vasoactive agents such as histamine, bradykinin or other molecules to increase the permeability of the BBB [21].

2.1.2 Direct implantation to the brain

Direct local implantation is one of the simplest methods for brain drug delivery to avoid systemic side effects. However, drug diffusion is not always efficient since it depends on the location of the administered drug, liposolubility, molecular mass, polarity and tissue affinity.

On one hand, drugs and nanomedicine devices can be injected by stereotaxy in specific brain areas. This system enables the delivery of the drugs in functional and specific brain areas without damaging the surrounding zones. However, the dosage cannot be regulated after its implantation in the brain [17,22].

On the other hand, intrathecal or intraventricular administration has also been studied for brain delivery. It consists of a direct delivery of the drug to the cerebrospinal fluid (CSF) bypassing the BBB. Theoretically, solutes in the CSF can be freely transported into the brain; however, experimentally there have not been many successful results. In

addition, this administration is associated to a considerable risk and needs continuous infusion due to the CSF replacement [23,24].

2.2 Non-invasive methods for CNS delivery

2.2.1 Nasal delivery

The intranasal administration has been proposed as a non-invasive way to transport drugs directly to the brain through the olfactory and trigeminal nerve pathway, which enables the drugs to bypass the BBB [25]. In the case of nanomaterials, the main mechanism of uptake in nose to brain delivery is the transcellular pathway [26].

The transport of the drugs can be enhanced by the incorporation of mucoadhesive polymers into nasal formulation increasing the mucosal contact time. One of the most studied mucoadhesive polymers is chitosan [27]. In this sense, our research group developed chitosan coated NLC as a novel approach for brain delivery of proteins by intranasal administration. This formulation proved to be safe and non toxic. Moreover, it showed effective delivery to brain which could be interesting to decrease the dose and dosage frequency of drugs [28]. Other mucoadhesive polymers have been also studied. Indeed, lectins have been introduced as bioadhesive delivery systems to improve drug absorption on nasal mucosa [29].

2.2.2 Cell penetrating peptides (CPP)

Cell penetrating peptides (CPP) are short amphipatic and cationic peptides that unlike most peptides are rapidly internalized across cell membranes [30].

One of the first CPP described was the transactivator of transcription (TAT), from human immunodeficiency virus (HIV-1), which is commonly used for DDS modification in an attempt to improve their access to the brain [31]. *Gartziandia et al.* probed the suitability of NLC modification by TAT to increase the transport across *in vitro* cell monolayers for nose to brain delivery [32]. Other studies have confirmed that the modification of nanomaterials by CPPs increased the delivery into the brain, and therefore, maximize therapeutic effects and minimize systemic side effects [31,33].

2.2.3 Drug delivery systems (DDS)

As mentioned above, drug delivery systems (DDS) have been raised as a solution to reach the brain. They have some advantages to overcome some limitations of drugs such as poor solubility, lack of selectivity and development of multidrug resistance [17]. Currently, there are several types of DDS available for biomedical applications which have suitable physico-chemical characteristics to cross the BBB or may be functionalized to improve its brain access. They have positive features such as high chemical and biological stability, the possibility of incorporating both hydrophilic and hydrophobic molecules and they can also be administered by a variety of routes [1].

In the following sections we will widely describe different nanotechnology based approaches investigated for the diagnosis and treatment of the first and second most common neurodegenerative disorders, Alzheimer disease (AD) and Parkinson's disease (PD), respectively.

3. NANOTECHNOLOGY FOR THE DIAGNOSIS OF NEURODEGENERATIVE DISORDERS

3.1 Nanotechnology for AD diagnosis

AD is the most common form of dementia among the people over the age of 65 years. This neurodegenerative disorder is characterized by an irreversible neuronal loss and vascular toxicity due to the presence of amyloid beta ($A\beta$) peptide extracellular deposition in senile plaques, along with neurofibrillary tangles of phosphorylated tau protein. Clinically, it can be defined as a progressive loss of memory, deterioration of judgment decision, orientation to physical surrounding, and language area [34-37].

Currently, the diagnosis of AD is based on clinical criteria which include cognitive test and neuropsychological examination. Sometimes should also be requested a lumbar puncture to obtain (CSF) in order to analyze different biological markers such as $A\beta_{1-42}$ and phosphorylated tau protein. Moreover, imaging techniques such as magnetic resonance imaging (MRI) or positron emission tomography (PET) are sometimes required. However, the accuracy of these techniques is not much better than the clinical diagnostic criteria. Moreover, the results obtained from these methods cannot distinguish between AD and other forms of dementia for sure [38-40].

Early diagnosis of AD is a main priority for the scientific community as it is crucial for the actual therapies, which have shown their potency slowing the progression of the disease [12]. That is why, innovative methods have been developed.

3.1.1 Nanotechnology for fluid biomarker detection in AD

One of the most promising approaches for biomarker detection in CSF is the work realized by *Georganopoulou et al* [41]. They developed an ultrasensitive bio-barcode assay to measure the concentration of amyloid- β - derived diffusible ligands (ADDLs) in CSF. They used the 'sandwich process' involving both oligonucleotide-modified Au nanoparticles and magnetic microparticles, which have been previously functionalized with the antibodies of interest. By using this method they have been able to detect ADDLs at subfemtomolar concentrations, which is 6 orders higher sensitivity than the ELISA assay (Figure 4).

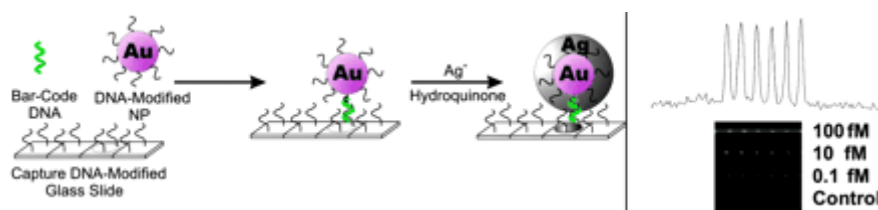


Figure 4: Schematic representation of scanometric detection. The method is based on capturing the barcode DNA on a microarray with spots of oligonucleotides that are complementary to half of the barcode DNA sequence. NPs with oligonucleotides that are complementary to the other half of the barcode DNA are hybridized to the captured barcode strands. The signal is enhanced by using silver amplification, and the results are recorded with the Verigene ID system, which measures scattered light intensity from each spot. Depending on the silver amplification time and the experimental conditions, the response can vary for each slide. For this reason, the grayscale intensity of the developed spots is then measured and averaged for each ADDL concentration (*Inset*) Reproduced with permission from [41]. © (2005) National Academy of Sciences, U.S.A.

Another procedure is the one proposed by *Haes et al.*, who designed a nanoscale optical biosensor based on localized surface plasmon resonance (LSPR) to ADDLs detection. They also used sandwich process with surface-confined Ag nanoparticles. The LSPR allowed the detection of biological species in a surfactant-free environment and has also shown its accuracy to detect ultralow concentrations of ADDLs in biological samples [14].

A further useful tool for the detection of amyloid- β peptides is the one developed by *Chikae et al.* They produced concurrently Au nanoparticles for the immobilization of biomolecules and bare carbon for electrochemical detection on the electrocode, which

enables the electrochemical sensing with easy fabrication and low cost [42]. Electrical detection methods have also been proposed to measure β -amyloid (1-42) fragments using scanning tunneling microscopy (STM). *Kang et al.* fabricate a biosurface containing a monoclonal antibodies fragment against β -amyloid and Au nanoparticles-antibodies conjugates for ultrasensitive electrical detection of β -amyloid (1-42). When an STM tip scanned the surface, the peak directly correlated with the applied concentration of the target molecule [43].

On the other hand, only one method has been published to the detection of biomarker tau protein using nanotechnology. *Neely et al.* developed Au nanoparticles based two-photon Rayleigh scattering (TPRS) assay for ultrasensitive and selective detection of tau protein in AD. This method enables to quantify this AD biomarker in 1pg/mL and it has also demonstrated its accuracy as it can distinguish from other proteins such as bovine serum albumin (BSA) [44].

3.1.2 Nanotechnology for image based diagnosis in AD

Magnetic iron oxide nanoparticles have been extensively studied for imaged based diagnosis in AD. These NPs selectively marks $A\beta_{40}$ fibrils which would be beneficial for the early detection of $A\beta$ plaques in AD patients. *Skaat et al.* synthesized a fluorescent-maghemite nanoparticle which recognizes $A\beta$ plaques in the brain enhancing the early detection of that hallmark using both MRI and fluorescent microscopy [45]. Another research group has also used magnetic iron oxide nanoparticles, chemically coupled with $A\beta_{1-42}$ peptide, to detect amyloid deposition in APP/PS1 mouse model using magnetic resonance microimaging (μ MRI) after femoral intravenous injection of the functionalized NP (Figure 5) [46]. *Cheng et al.*, used curcumin coated magnetic iron oxide nanoparticles conjugated with polyethylene glycol-poly(lactic acid), which selectively binds to $A\beta$ deposition, exhibiting lack of toxicity in either Madine Darby canine kidney (MDCK) or differentiated human neuroblastoma cells (SH-SY5Y). Moreover, they could visualized amyloid plaques *ex vivo* in T2*-weighted magnetic resonance imaging (MRI) of Tg2576 mouse brain [47].

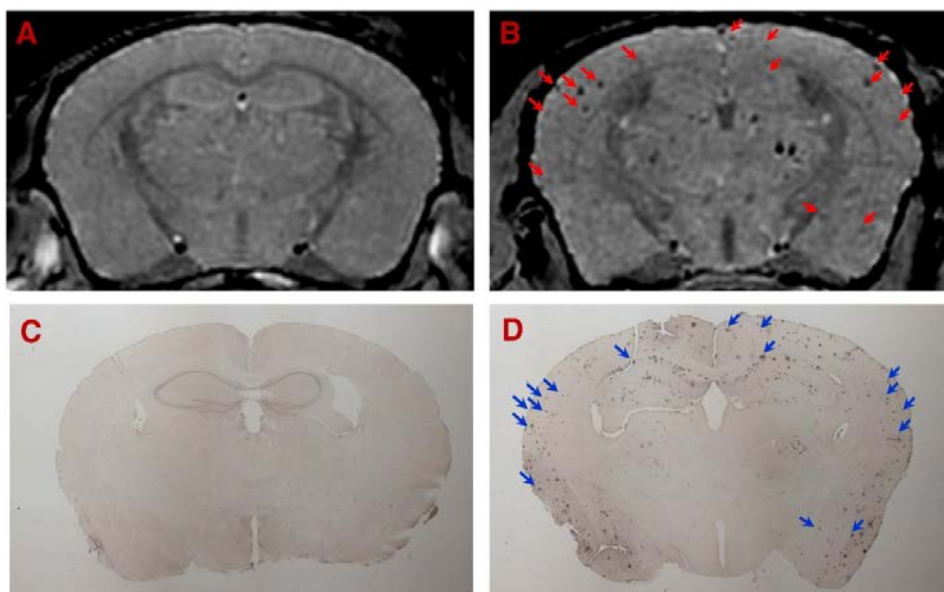


Figure 5: Amyloid plaques were detected with in vivo μ MRI after intravenous femoral injection of USPIO- $A\beta_{1-42}$ with mannitol. In vivo T2*-weighted MRI images show a 14-month-old wild-type (A) and APP/PS1 Tg (B) mouse brain. Note the matching of many large plaques (arrowheads) between immunohistochemistry (D) and μ MRI (B) in the APP/PS1 Tg mice. C shows the lack of plaque detection in a wild-type mouse following USPIO- $A\beta_{1-42}$ injection. Reproduced with permission from [46].

Quantum dots have also demonstrated their effectiveness recognizing β -amyloid precursor protein (APP) in cell culture by fluorescence imaging [48]. *Tokuraku et al.* developed quantum dot labeled amyloid- β peptide for monitoring the formation of fibrils and quantify the aggregates in solution and cell cultures [49].

Gold nanoparticles represented an useful device for monitoring $A\beta$ peptide assemblies at the early stage too. For this purpose, *Choi et al.* designed Co@Pt-Au nanoparticles, which have better magnetism and higher stability in aqueous media, to utilize in conjunction with MRI to monitor the structural evolution of $A\beta$ oligomers [15].

On the other hand, radioligands have also been encapsulated in PBCA-80 nanoparticles to enhance its specificity and affinity for $A\beta$ *in vitro* and *in vivo*. *Roney et al.* elaborated ^{125}I -clioquinol-PBCA nanoparticles as a promising tool for detection of $A\beta$ proteins using photon emission computed tomography (SPECT) imaging [50].

3.2 Nanotechnology for PD diagnosis

PD is a complex neurodegenerative disorder which affects 5 million of people worldwide. It is pathologically characterized by the progressive loss of dopaminergic neurons in the substantia nigra (SN) followed by the decrease of dopamine (DA) in the

striatum which is clinically manifested as resting tremor, bradykinesia, rigidity and postural instability [51-53]. The pathological hallmarks of PD are constituted of lewy bodies due to the aggregation of the abnormal protein alpha-synuclein (α -syn) [54].

PD diagnosis also relies on the evaluation on clinical symptoms and on the assessment of presynaptic nigrostriatal dopaminergic neurons via PET, SPECT based imaging represented by radiopharmaceuticals [55]. The major goal of the researchers is to determine a biomarker that could be associated with PD.

With the aim of determining a biomarker that could show the progression of the disease, *Yue et al.* fabricate ZnO nanowire arrays on 3D graphene which selectively detect uric acid (UA), DA and ascorbic acid (AA). After studying the serum of healthy individuals and PD patients, they could conclude that in PD patients there was a clear reduction in UA levels, which would be a promising biomarker to diagnose and monitor the progression of the disease [56]. Another research group has used Au nanoparticles for the quantitative colorimetric detection of neurotransmitters such as DA, L-DOPA, adrenaline or noradrenaline. They also probed the activity of tyrosin kinase, an important enzyme implied in PD [57]. Moreover, *Zhu et al.* have employed the nanotechnology for the detection of tyrosin kinase activity. They developed quantum dots functionalized with tyrosine and zwitteronic molecules to construct a nanometer scale scaffold to test tyrosin kinase activity with accuracy in vitro [58].

PD hallmark, α -syn protein, has also been studied for its detection. *An et al.* proposed Au-doped TiO₂ nanotube to design a photochemical immunosensor for the determination of α -syn. This new strategy showed high sensibility, stability, reproducibility and could become a promising technique for protein detection [59].

4. NANOTECHNOLOGY FOR THE TREATMENT OF NEURODEGENERATIVE DISORDERS.

4.1 Nanotechnology for AD treatment

Despite the efforts made by the scientific community, currently there is no cure for AD. So far, the drugs approved by the FDA for AD treatment are only symptomatic, without halting the progression of the disease. AchE (tacrine, donepezil, rivastigmine, galantamine) are mainly used for the treatment of the dementia phase. In moderate to

severe dementia memantine can be used, either in monotherapy or in combination with other approved drugs [60]. However, the clinical relevance of its use remains unclear [61].

In view of these limitations, new treatments are needed to prevent, delay or treat AD, addressing the main causes of this neurodegenerative process. To attain this purpose, in the last years new molecules such as neurotrophic factors (NTFs), antioxidant molecules and metal chelators have been raised as new therapeutical options. However, the clinical application of all these molecules is limited due to their short circulation half life and rapid degradation rate [62].

In an attempt to overcome all these drawbacks, new advances have been made in the field of nanotechnology for brain targeting. Here, we summarized the main investigated DDS for AD treatment (Table 2).

4.1.1 Polymeric nanoparticles

Polymeric nanoparticles have been used to encapsulate rivastigmine in order to enhance its brain entry and decrease frequent dosing, limiting cholinergic side effects. For instance, poly lactide-co-glycolide (PLGA) and poly (n-butylcyanoacrylate) nanoparticles (NP) coated with polysorbate (PBCA 80) have been prepared by *Joshi et al.* with favorable results in the *Morris Water Maze (MWM)* Test [63]. Moreover, Wilson et al. elaborated PBCA-80 NP loaded rivastigmine for brain targeting. The studies revealed the suitability of this nanoformulation improving the uptake 3.82 fold higher compared to the free drug (Figure 6) [64].

Table 2. Different drug delivery systems releasing therapeutic drug for AD treatment.

DDS	DRUG	MODEL	RESULTS	REF
PLGA and PBCA80 NP	Rivastigmine	<i>In vitro</i> ; Amnesic mice model	Increase brain concentrations; improve pharmacodynamic studies	[63,64]
Chitosan NP	Rivastigmine	<i>In vitro</i> , Wistar rats; Amnesic mice model	Improve memory activity; increase brain drug concentrations and decrease peripheral side effects	[65,66]
L-lactide depsipeptide NP	Rivastigmine	Amnesic rats	Improve pharmacodynamic and pharmacokinetic parameters	[67]
PLGA-80 NP	Donepezil	Sprague–Dawley rats	Increase brain concentration of AchE	[68]
PLGA NS	VEGF	<i>In vitro studies</i> APP/Ps1 mice	Increase cell viability and protect neurons from cytotoxicity; improve memory and behavioral studies	[69,70]
<i>Solanum tuberosum lectin</i> PEG-PLGA NP	bFGF	AD model induced by A β ₂₅₋₃₅	Improvement in behavioral, histochemical and biochemical studies	[71]
PBCA 80 NP	NGF	AD mouse model	Reverse induced amnesia	[72]
NP covalently conjugated with iron chelator	Various iron chelators	<i>In vitro studies</i>	Protect cortical neurons from A β toxicity	[73,74]
PEGylated liposomes	Galantamine	<i>In vitro studies</i>	Higher targeted brain delivery	[75]
Liposomes conjugated with cereport and Tf	NGF	BMVEC, <i>in vitro</i> BBB model; Sprague–Dawley rats; SK-N-MC cell culture	Correlation in <i>in vivo</i> and <i>in vitro</i> studies showing higher brain NGF levels; enhanced NGF neuroprotection	[76]
Liposomes conjugated with WGA and CL	NGF, curcumin	SK-N-MC cell line	Inhibit neurotoxicity	[77]

SLN	Galantamine	Rats	Higher bioavailability and improved behavioral studies	[78]
SLN	Memantine and α -lipoic acid	N2a cells; PHWB	Neuroprotection	[79]
NLC modified with lactoferrin	Curcumin	rats	Reduce the pathological impairment in AD rats hippocampus	[80]
NLC	Resveratrol	$A\beta_{1-42}$ induced AD rats	Recover short and long term memory	[81]
NLC	Curcumin, resveratrol	Mammalian cells	Enhance antioxidant activity	[82]
Lentiviral vectors	GDNF	3xTg-AD mice	Neuroprotective effect; improve spatial learning and memory	[83]
Sendai Virus Vector	BDNF	Tg2576 mouse model	Reduce neurons from synaptic degeneration	[84]

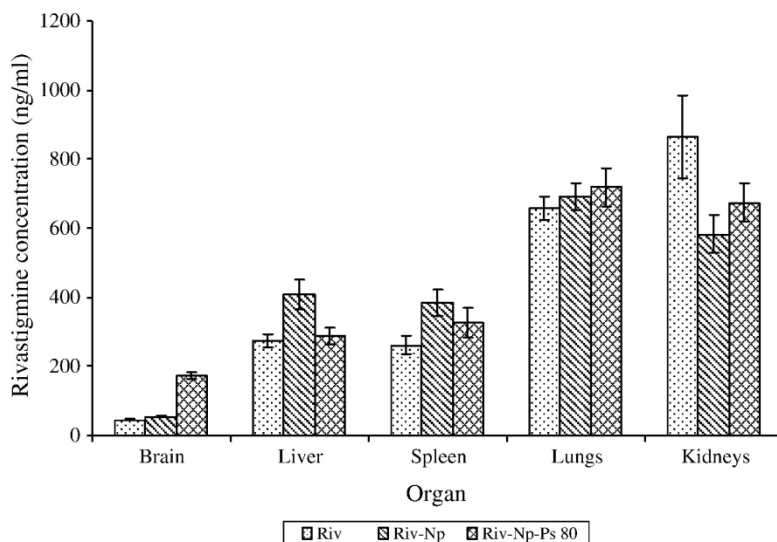


Figure 6: Rivastigmine concentrations (ng/ml) in different organs after intravenous injection of poly(*n*-butylcyanoacrylate) nanoparticles formulations. Riv = Rivastigmine solution. Riv-Np = Rivastigmine bound to nanoparticles. Riv-Np + Ps 80 = Rivastigmine bound to nanoparticles coated with 1% polysorbate 80. Reproduced with permission from [64].

Chitosan NP have also been developed to increase the rivastigmine therapeutic efficacy and tolerance profile. *In vivo* behavioral studies demonstrated an improvement in memory activity with chitosan NP after its intravenous administration [65]. The nasal route has also been investigated to deliver chitosan NP into the brain, showing less peripheral side effects and higher AchE brain concentrations compared to free rivastigmine [66].

L-lactide-depsipeptide polymeric nanoparticles have been developed by *Pagar et al.* in order to increase drug concentration in the targeted area. Pharmacodynamic and pharmacokinetic studies were performed showing faster regain of memory loss and an increase in brain concentrations together with a decrease in clearance after intravenous administration, respectively [67].

Another FDA approved inhibitor of acetylcholinesterase is donepezil. Donepezil loaded PLGA NP have been developed by *Bhavna et al.* The gamma scintigraphic image confirmed the higher brain accumulation of donepezil loaded NP. Furthermore, the coating process with Tween 80 improved the opening of the tight junctions enhancing brain drug delivery [68].

Not only the commercialized drugs, but also another investigated treatments such as NTFs, have been encapsulated in order to improve its biodistribution, hence, increasing their therapeutic levels at the brain and reducing the risk of suffering

systemic side effects. GFs are a promising group of proteins which are able to improve the growth, proliferation and differentiation of neuronal cells, moreover, they contribute in tissue morphogenesis, cell differentiation, angiogenesis and neurite outgrowth [85].

Among GFs, vascular endothelial growth factor (VEFG) was encapsulated in PLGA nanospheres (NS) by our research group as a novel therapeutic approach for AD. This novel nanotechnology based strategy showed to be effective in *in vitro* studies increasing cell viability and protecting neurons from A β toxicity. Moreover, VEFG loaded NS demonstrated its therapeutic potential promoting neurogenesis and improving exploratory memory and short-term memory in behavioral studies after its administration by craniotomy to APP/Ps1 mice [69,70].

In an attempt to use a less invasive route, *Zhang et al.* developed basic growth factor (bFGF) loaded PEG-PLGA NP conjugated with *Solanum tuberosum lectin* (STL) for nasal administration. This mucoadhesive compound selectively binds to nasal epithelium enhancing brain targeting. Behavioral, histochemical and biochemical studies confirmed the improvements obtained with this nanoformulation when compared to the control group [71].

Along with GF, *Kurakhmaeva et al.* developed neuronal growth factor (NGF) loaded PBCA NP coated with polysorbate 80 which demonstrated their effectiveness reversing the induced amnesia in an AD mouse model [72].

On the other hand, metal chelators have been suggested as a new therapeutic approach for AD since transition metals have been proposed to be responsible of neuronal damage in AD [86]. Furthermore, treatment with metal chelators in AD transgenic mouse has showed to be effective decreasing A β deposition and inhibiting τ phosphorylation [87]. However, their lack of efficiency crossing the BBB and neurotoxicity of many traditional metal chelators has limited their utility in AD. To overcome these disadvantages, *Liu et al.* developed a NP conjugated with iron chelator which showed its ability protecting cortical neurons from A β neurotoxicity [73,74].

4.1.2 (Nano) liposomes

Liposomes have also been proposed as promising nanocarriers for brain targeting. They can be functionalized with PEG for specific delivery into the brain.

With the aim of obtaining that main purpose, *Mufamadi et al.* prepared pegylated nanoliposomes loading galantamine; a reversible, competitive commercialized AchE inhibitor used in the treatment of AD. *In vitro* studies revealed higher targeted delivery of functionalized liposomes compared to non-functionalized nanoformulation [75].

Liposomes can also be conjugated with other molecules such as cereport and transferrin (Tf). RMP-7 (cereport) functionalized liposomes have been developed by *Xie et al.* demonstrating its capability crossing BBB in *in vitro* studies. These results were confirmed in an *in vivo* model where NGF distribution in the brain improved after the femoral administration of the functionalized liposomes (Figure 7) [76].

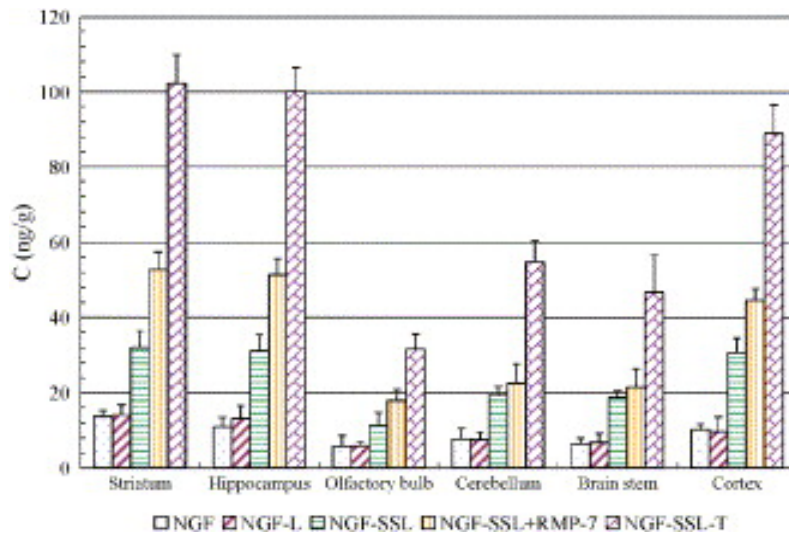


Figure 7: The distribution of NGF in each brain region of each group at 0.5 h (n = 6). SSL can favor NGF uptaken in the brain tissue. The concentration of NGF-SSL + RMP-7 and NGF-SSL-T was increased 2.07 and 3.19 times, respectively, more than that of NGF-SSL. Reproduced with permission from [76].

On the other hand, Tf has also been proposed as an useful tool to target brain cells. In line with this approach, *Kuo et al.* encapsulated NGF in cereport and Tf liposomes which demonstrated to be able to increase the width of tight junctions and open endothelial cells [88]. Moreover, the same research group encapsulated NGF along with curcumin in wheat germ agglutinin (WGA) and cardioplin (CL) conjugated liposomes. CL favored the ligand binding to A β and WGA enhanced the delivery of pharmaceuticals across the BBB [77]. Additionally, curcumin is known to increase β -amyloid degrading enzymes and protect against oxidation, which plays an important role in the pathophysiology of AD [89,90]. These liposomes loading

these two drugs demonstrated a synergistic effect inhibiting neurotoxicity in *in vitro* studies [77].

4.1.3 Lipid nanocarriers: Solid lipid nanoparticles (SLN) and Nanostructured lipid carriers (NLC).

Up to now, different studies have demonstrated the suitability of lipid nanocarriers to transport different pharmaceutical active agents to the brain tissue, providing therapeutic alternatives to treat AD [91,92].

Among others, *Misra et.al* developed SLN loading galantamine. After oral administration, the nanoformulation presented higher bioavailability than the free drug. Moreover, galantamine loaded SLN improved behavioral deficits presented in treated rats compared with the control group (Figure 8) [78].

Moreover, *Laserra et al.* loaded a codrug of memantine and (R)- α -lipoic acid (LAMEM) in SLN, which showed not only neuroprotective properties but also lack of toxicity in both N2a neuroblastoma (NB) cells and primary whole blood (PHWB) after MTT (3-(4,5-dimethylthiazol-2-yl)-2,5-diphenyltetrazolium) and LDH (lactate dehydrogenase) assays [79].

Another kind of lipid nanocarriers, NLCs, have also been investigated as a novel approach for brain targeting in AD. As mentioned above, curcumin may have clinical relevance in the treatment of AD, however, its poor bioavailability and rapid excretion makes difficult to obtain therapeutic levels in the brain. In an attempt to improve its pharmacokinetic properties, *Meng et al.* elaborated curcumin loaded NLC modified with lactoferrin. Biodistribution studies confirmed the suitability of this formulation enhancing brain uptake 2.78 times compared to non-modified NLC. Moreover, *in vivo* studies revealed a reduction in the pathological impairment in hippocampus of AD treated groups [80].

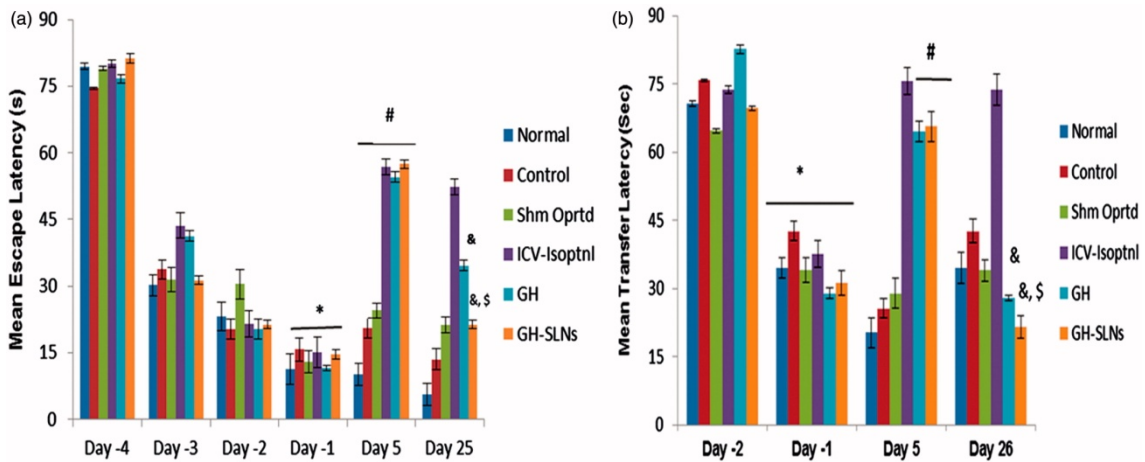


Figure 8. (a) Morris water maze test; effect of GH and GH-SLNs (5 mg/kg, p.o.) ($n = 6/\text{group}$) on escape latency of memory retrieval in ICV isoproterenol-treated rats after 25 days. Data are expressed as mean \pm S.E.M. * $p < 0.05$, as compared to day (-4) of the training; # $p < 0.05$, as compared to day (-1) of the training; & $p < 0.05$, as compared to isoproterenol group on day (25) of the training; \$ $p < 0.05$, as compared to GH group on day (25). (b) Effect of GH and GH-SLNs (5 mg/kg p.o.) treatment on mean transfer latency in elevated plus maze in ICV isoproterenol treated rats after 26 days. Data are expressed as mean \pm S.E.M. * $p < 0.05$, as compared to day (-1) of the training; # $p < 0.05$, as compared to isoproterenol group on day (26) of the training. ISOPTNL = Isoproterenol, GH= galantamine hydrobromide, SHM OPRTD=sham operated group. Reproduced with permission from [78].

Resveratrol is another antioxidant molecule which has demonstrated its ability to reduce A β pathway and attenuate cognitive decline [93]. *Frezza et al.* elaborated resveratrol loaded NLC showing their effectiveness to recover short-term and long-term memory. These promising results might be due to the higher resveratrol concentrations obtained in the brains of the animals treated with this nano-DDS [81]. In order to obtain a synergistic effect, *Coradini et al.* encapsulated both antioxidant drugs (resveratrol and curcumin) in NLC, which demonstrated to increase the stability of these two photosensible drugs, and therefore, enhanced the antioxidant activity in cell cultures [82].

4.1.4 Gene therapy

In AD, gene therapy has also been proposed to improve targeted drug delivery into the brain. In this sense, *Revilla et al.* developed lentiviral vectors engineered to overexpress GDNF as a promising strategy to treat AD. The result of their studies demonstrated GFP (green fluorescent protein) and GDNF expression in transduced astrocytes, which were confirmed by localization with the astrocyte marker GFAP (glial fibrillary acidic protein) [83]. Moreover, the neuroprotective effect of GDNF was demonstrated in hippocampus of 3xTg-AD mice since it improved spatial learning

and memory. In another research work, Sendai Virus Vector (SeV) mediated expression of BDNF in hippocampal reduces neurons from synaptic degeneration, thereby improving memory impairments in a Tg2576 mouse model of AD [84].

4.2 Nanotechnology for Parkinson disease treatment

Currently available therapies in clinical practice for PD treatment are focused on DA replacement to control motor symptoms. Nevertheless, the hydrophilic nature of DA together with its high hydrogen bonding potential limits its ability in terms of crossing the BBB. A more standard treatment is the administration of a DA prodrug, levodopa (L-DOPA) anyhow, the oral bioavailability of this compound is low and need to be combined with carbidopa to avoid peripheral degradation [94,95].

In any case, many PD patients become severely disabled due to the presence of non-motor symptoms, for example; sleep disorders, dementia or depression, along with the appearance of side effects such as fluctuations or dyskinesias, limiting the therapeutic use of these drugs [96]. In an attempt to produce a benefit on both non motor and motor symptoms, non ergotic agonist of DA such as pramipexol, ropinirole and rotigotine are currently used [97].

However, the lack of an effective treatment for PD has driven the investigations in the search for other useful molecules to address the main causes of this neurodegenerative process such as neurotrophic factors (NTFs) and antioxidants. However, as we have previously pointed out these molecules have limitations to obtain brain targeting. In order to overcome them, nanotechnology based approaches have been proposed as a novel strategy for PD treatment. In the following lines we have summarized the main investigated DDSs releasing both old and potential new treatments for PD (Table 3).

Table 3. Different drug delivery systems releasing therapeutic drug for PD treatment.

DDS	DRUG	MODEL	RESULTS	REF
NESD embedded in CAP NP	DA	Sprague-Dawley rats	Sustained release of DA	[98]
Chitosan NP	DA	Male Wistar rats	Increased neurotransmitter levels in the striatum	[99]
PLGA NP	DA	SH-SY5Y cell line, 6-OHDA rats	Internalization of DA; reversed neurochemical and neurobehavioral deficits	[100]
Chitosan NP	L-DOPA	Wistar rats	Increased L-DOPA concentrations	[101]
PLGA MS	L-DOPA- α -lipoic	Male Wistar	Improved pharmacokinetic parameters; limit PD motor syndrome	[102]
PLGA NP	L-DOPA	6-OHDA rat model	Motor function recovery	[103]
PLGA MS	L-DOPA/ benserazide	6-OHDA rat model	Reduced motor symptoms and decrease biochemical markers of PD	[104,105]
PLGA MS	Rotigotine	6-OHDA rat model	Sustained release and decrease dyskinesias	[106]
Chitosan NP	Ropinirole	Swiss albino rats	Brain targeted delivery	[107]
Chitosan NP	Bromocriptine	Swiss albino mice	Improved brain uptake; decreased catalepsia and oxidative stress levels	[108]
PLGA MS	GDNF	6-OHDA rat model	Improved behavioral studies, increase TH+ fibers and neuronal density	[109-112]
PLGA /collagen MS	GDNF	Neural/stem progenitor cells	Differentiation neuronal progenitor cells into mature neurons	[113]
PLGA MS	VEFG, GDNF	6-OHDA rat model	Neuroregeneration in behavioral and immunohistochemical tests	[114-116]
Nanoemulsion	Ropinirole	6-OHDA rat model	Increased bioavailability; restore biochemical changes	[117]
SLN	Ropinirole	Chlorpromazine induced male albino mice	Improved tremor activity and pharmacokinetic parameters	[118]

SLN	Bromocriptine	6-OHDA rat model	Decreased akynesias in pharmacodynamic studies	[119]
Liposomes	Resveratrol	6-OHDA rat model	Improved behavioral studies, TH+ cell levels and antioxidant capacity	[120]
Vitamin E nanoemulsion	Resveratrol	DPPH assay;Wistar rats	Enhanced antioxidant activity and pharmacokinetic parameters	[121]
Nanoemulsion	Coenzyme Q10	MPTP rat model	Offsetting neurotoxicity	[122]
Liposomes	GDNF	BBB <i>in vitro</i> model; rats	Improved bioavailability and obtain brain targeting	[123]
Adenoviral vector	GDNF	6-OHDA rat model, MPTP, 6-OHDA primate model	Improvement in behavioral test, increment in TH ⁺ fibers and DA levels.	[124-127]
Neurotensin polyplex carrier	GDNF	6-OHDA rat model	Functional and biochemical recovery	[128]
THLs liposomes conjugated with TfR Mab	GDNF	6-OHDA rat model	Improved behavioral studies and increases TH+ enzyme levels in the striatum	[11]
Lactoferrin modified NP	GDNF	6-OHDA rat model, rotenone induce PD model	Improve locomotor activity, reduce dopaminergic neural loss and increase monoamine neurotransmitter levels	[129,130]
Polyethylene imine grafted chitosan carrier	GDNF	293T cell line	Enhanced transfection efficiency	[131]

4.2.1 Polymeric nanoparticles

4.2.1.1 Polymeric nanoparticles for DA, L-DOPA and dopamimetic drug administration

Pillay et al. designed an intracranial nano-enabled scaffold device (NESD) embedded in stable DA loaded cellulose acetate phthalate NP in an attempt to avoid systemic side effect and increase DA levels in the brain, improving its therapeutic efficacy. *In vivo* studies confirmed a sustained release of the drug after implantation in the parenchyma of the frontal lobe of Sprague-Dawley rats [98]. Moreover, DA loaded chitosan NP have been developed by *Trapani et al.* showing lack of toxicity and improving the transport across the BBB according to the *in vitro* results. These outcomes were confirmed with *in vivo* biodistribution studies, where this nanoformulation showed to increase this neurotransmitter levels in the striatum after intraperitoneal administration [99].

PLGA based NP have also been studied for the targeted delivery of this neurotransmitter. *Pahuja et al.* research work confirmed the internalization of this NP in *in vitro* studies. Moreover, their *in vivo* assays revealed the suitability of this DDS reversing neurochemical and neurobehavioral deficits presented in PD [100].

NP based approaches have also been studied for the targeted delivery of L-DOPA. *Sharma et al.* encapsulated L-DOPA in chitosan NP in order to improve brain uptake and avoid carbidopa co-administration. These NP were then incorporated in a thermo reversible Pluronic F127 gel for intranasal administration. Although this nanoDDS increased L-DOPA concentrations at brain level, gel viscosity reduced NP uptake in comparison with NP dispersed in saline solution, since they exhibited higher drug brain levels [101]. The prodrug L-DOPA- α -lipoic acid was synthesized by *D'Aurizio et al.* in order to decrease enzymatic conversion hydrophilicity hence, promoting brain delivery. The encapsulation of this drug in PLGA-MS optimized L-DOPA pharmacokinetic profile, which could limit motor syndrome side effect associated in PD treatment [102].

L-DOPA treatment is commonly related with levodopa-induced dyskinesias. This main disadvantage can be overcome with sustained release provided by DDS. In an attempt to obtain that main purpose, *Gambaryan et al.* developed PLGA based L-DOPA delivery system. The regular intranasal administration of this nanosystem to

6-OHDA lesioned rats resulted in a lasting motor function recovery [103]. Moreover, *Ren et al.*, produced L-DOPA/benserazide loaded PLGA MS in order to obtain a sustained release profile. *In vivo* studies exhibited a decrease in apomorphine-induced turns and improved stepping of the lesion forepaw in a rat model of PD. Moreover, western-blot analysis showed a reduction in the levels of biochemical markers of PD [105]. These results are consistent with *Yang et al.* studies, where not only L-DOPA/benserazide loaded NP significantly reduced dyskinesias in a OHDA animal model of PD; but it also decreased biochemical markers [104].

As mentioned above, rotigotine is a non-ergoline dopaminergic drug used in PD therapy, however, it has an extensive first pass metabolism with low bioavailability through oral administration. In order to obtain higher brain levels, *Wang et al.* developed rotigotine loaded PLGA MS, which were able not only to obtain a sustained release with higher brain concentrations, but also decrease L-DOPA induced dyskinesias in a OHDA rat model [106]. The chronic administration of this formulation during 3 months to Cynomolgus monkeys and Sprague-Dawley rats demonstrated the lack of toxicity of this formulation *in vivo* [132]. *Jafarieh et al.* developed chitosan nanoparticles in order to obtain a nose to brain delivery. The mucoadhesive properties of the chitosan enable the delivery of ropinirole in the targeted brain area which was confirmed with gamma scintigraphy studies [107].

Bromocriptine is a widely used non-ergotic drug for PD treatment. *Shadab et al.* developed bromocriptine loaded chitosan NP for intranasal administration. These nanoformulation showed its ability not only improving brain uptake, as it showed in gamma scintigraphy imaging (Figure 9), but also decreasing catalepsia and oxidative stress levels [108].

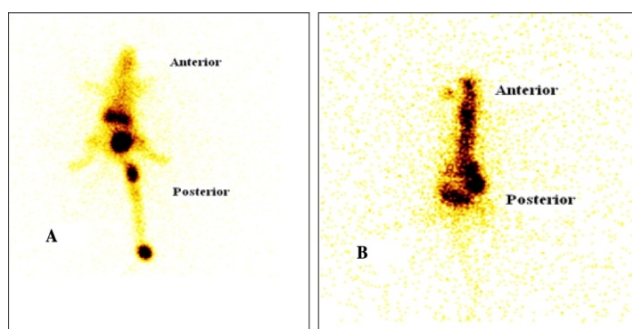


Figure 9: Gamma scintigraphy images of mice following (A) i.v. administration, (B) i.n. administration of bromocriptine loaded CS NPs. Reproduced with permission from [108].

4.2.1.1 Polymeric nanoparticles for growth factor administration

As well as in AD, GFs have been raised as a new therapeutic strategy to address the neurodegenerative process that occurs in PD [133,134]. In order to improve its brain targeting *Jollivet et al.* proposed for the first time the use of DDS to release NTFs in an attempt to treat NDs. They developed PLGA-MS for GFNF brain delivery in a partial lesioned rat model of PD. This formulation was able to stimulate the axonal regeneration of mesencephalic dopaminergic neurons, affected in PD, after its intrastriatal administration. Furthermore, the brain implantation of this glial derived neurotrophic factor (GDNF) loaded DDS increased TH⁺ fibers and neuronal density in the striatum and substantia nigra which may be associated with the functional improvement in the lesioned animals [109,110]. These results were confirmed with *Garbayo et al.* published research work, which reinforced the use of GDNF PLGA-MS both *in vivo* and *in vitro*. In fact, GDNF treated animals showed a reduction in apomorphine-induced rotational asymmetry test and in immunohistochemical analysis, together with an increase in the density of TH⁺ fibers at the striatal level (Figure 10). Moreover, this nanoformulation was able to increase dopaminergic striatal neurons and long-term neuroprotection and neurorestoration [111,112].

With the aim of obtaining a sustained release of GDNF, *Gujral et al.* developed PLGA/ collagen MS encapsulating GDNF fused with a collagen binding protein. After the collagenase action, the collagen phase degraded enabling the de-link of GDNF from the collagen and diffusing out of MS. Their studies revealed the differentiation of neuronal progenitors cells into mature neurons in *in vitro* studies, which are favorable results for PD treatment [113].

The co-administration of GDNF with other NTFs has also been investigated to obtain a synergistic effect of these drugs. In this sense, our research group developed PLGA MS loading VEGF, GDNF and their combination on severely and partially lesioned rat models. This work could demonstrate the neuroregenerative potential of this formulation in both behavioral and immunohistochemical tests in 6-OHDA lesioned rats with a reduction of the dose by a half due to the synergistic effect of NTFs [114-116].

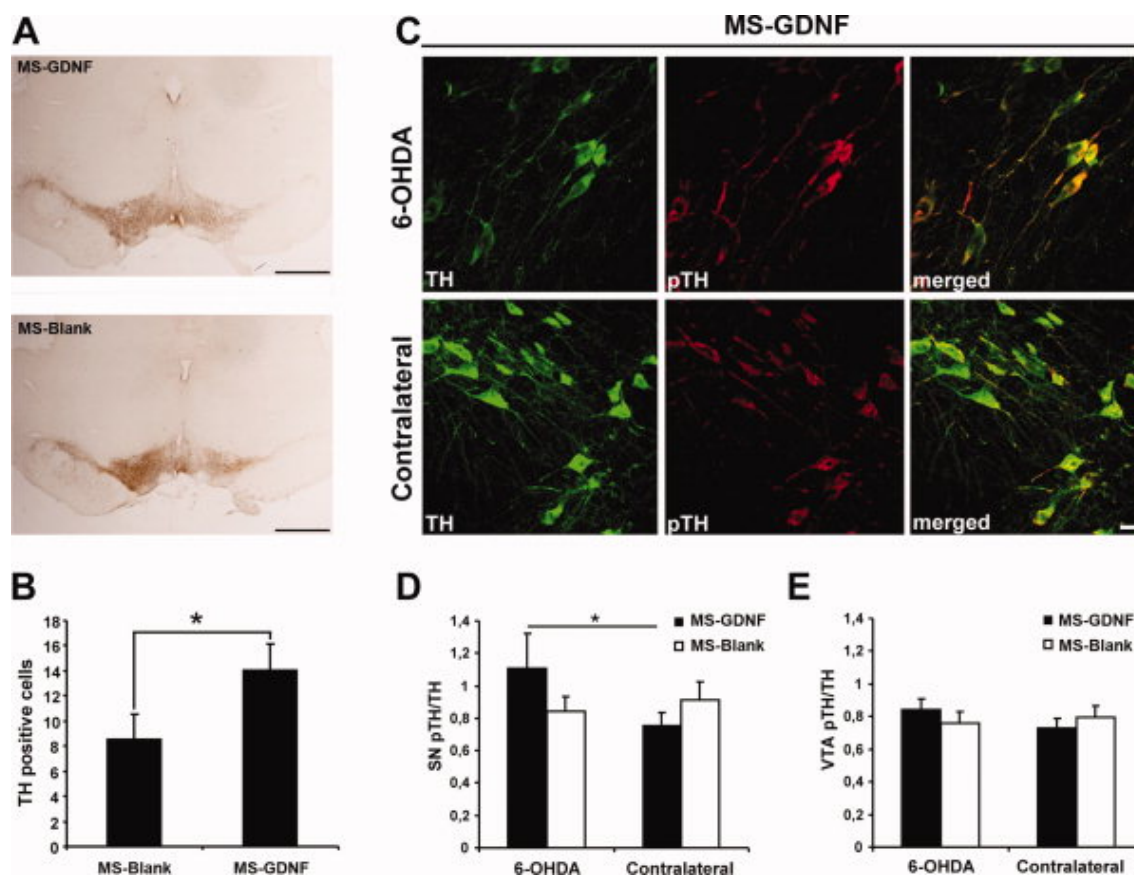


Figure 10. GDNF effect in the substantia nigra pars compacta. A: Immunohistochemistry for TH revealed an increase in the number of surviving cells in the SNpc of GDNF-treated compared with empty-microspheres-treated animals 30 weeks after the 6-OHDA lesion. B: Quantification of TH-positive neurons from the SNpc showed a statistically significant increase in the number of cells present in animals treated with GDNF microspheres compared with animals that received empty microspheres. Scale bar: 1 mm. Wilcoxon test: $*P < 0.05$. C: Double immunohistochemistry for TH and pTH showed that all cells were double labeled and presented an increase in pTH level. Quantification of fluorescence intensity of pTH, with respect to the total amount of TH at the level of SN (D) and VTA (E), showed a significant increase of pTH in TH-ir neurons from the SNpc of GDNF-treated animals, compared to the contralateral side. Scale bar: 20 μ m. Student's *t* test: $*P < 0.05$. Reproduced with permission from [112].

4.2.2 Liposomes and lipid nanocarriers

Besides polymer nanoparticles, oil based nanocarriers have been studied for non-ergoline DA agonist delivery. For example, *Azeem et al.* enhanced the bioavailability of ropirinole after the transdermal administration in a nanoemulsion formulation. They could also demonstrate to restore biochemical changes in a PD rat model [117]. Furthermore, SLN have also been developed loading ropirinole for intranasal delivery, showing to be effective improving pharmacokinetic parameters and without severe damage on the integrity of nasal mucosa [118]. SLN have also been studied for improving the bioavailability of another DA agonist, bromocriptine.

Moreover, the pharmacodynamic studies revealed the suitability of this formulation decreasing akinesias in 6-OHDA hemiparkinsonian rat model [119].

Although liposomes are a standard DDS, not many studies are reported with their use in PD. For instance, *Wang et al.* developed liposomes loading resveratrol, an antioxidant molecule known for improving the oxidative stress in PD and reducing dopaminergic neuronal loss, improving rotational behavior. The encapsulation of resveratrol showed more favorable effects in *in vivo* studies, such as an improvement in behavior, TH⁺ cells levels and antioxidant capacity [90]. Resveratrol has also been loaded in Vitamin E nanoemulsion enhancing its pharmacological activity, which were evaluated by DPPH (2, 2-diphenyl-1-picrylhydrazyl) assay [121]. Another well recognized antioxidant drug in PD is coenzyme Q10. However, there have been reported inconclusive results in clinical trials, due to the low solubility and poor brain penetration [135]. In order to improve its bioavailability, *Sikorska et al.* produced a nanomicellar formulation of coenzyme Q10, showing its capability offsetting the neurotoxicity before and after MPTP injection in a rat model [122]. Lately, *Wu et al.* developed GDNF loaded liposomes showing their effectiveness both *in vitro* and *in vivo*, enhancing the bioavailability of this growth factor [123].

4.2.3 Gene therapy

Last but not least, as in AD, gene therapy has also been raised as a promising strategy for PD treatment [136]. For example, *Kozłowski et al.* studied adenoviral (Ad) mediated GDNF gene transfer in a PD rat model, increasing the number of dopaminergic neurons in the substantia nigra and maintaining functional connections to the striatum [126]. Moreover, these results are supported with *Chen et al.* research work, as they could prove not only the protective effect of GDNF gene transfer but also, an improvement in behavioral tests and an increase in TH⁺ cells after the intracerebral administration of this nanosystem [125]. Moreover, the effectiveness of these Ad-GDNF have been performed in non-human primate models of PD. *Eslamboli et al.* and *Eberling et al.* demonstrated the suitability of this formulation increasing DA activity in the striatum, correlating it with clinical improvements and without any adverse effect in MPTP and 6-OHDA primate models, respectively [124,127].

Nevertheless, due to the risk of viral gene therapy related with immunogenicity and safety, safer and more successful non viral gene therapy have been proposed

for target brain tissue [137]. In this sense, *Gonzalez Barrios et al.* developed a neurotensin polyplex carrier for GDNF gene delivery to nigral dopamine neurons of hemiparkinsonian rats. The effective transfection was confirmed with both RT-PCR and western blot analysis [128]. With the aim of improving transfection efficiency, different modifications have been made on the surface of non viral vectors. For example, *Chung-Fang et al.* elaborated intravenous GDNF plasmid DNA using trojan horse liposomes (THLs) targeted with a monoclonal antibody (Mab) to the rat transferring receptor (TfR). Not only they could demonstrate a reduction in apomorphine-induced rotation, but also increased enzyme activity in striatum after the administration of encapsulated GDNF [11].

Additionally, *Huang et al.* elaborated a lactoferrin modified vector with an effective delivery of GDNF in the brain. *In vivo* studies performed in 6-OHDA and in rotenone-induced chronic PD model, showed to improve locomotor activity, reduce dopaminergic neuronal loss and enhance monoamine neurotransmitter after multiple intravenous administration and without brain toxicity [129,130]. Recently, a polyethylene imine grafted chitosan carrier has been developed by *Peng et al.* for GDNF gene delivery. This novel nanoformulation exhibited lack of toxicity and high transfection efficiency [131].

5. CONCLUSION

The application of nanotechnology to address the neurodegenerative disorders seems to change the future of neurology. As we have widely described in this chapter nanotechnology has shown to be a useful tool for crossing the BBB, a key aspect for an effective treatment of NDs, offering a brain target delivery and a sustained release profile. In addition, nanotechnology has exhibited more specificity and sensibility than current available diagnostic criteria for an accurate and early diagnosis of both AD and PD. Although the presented promising results, more investigations would be required in this field to permit the translation from preclinical state to clinical applications.

6. ACKNOWLEDGMENT

This project was partially supported by the “Ministerio de Economía y Competitividad” (SAF2013-42347-R), the University of the Basque Country

(UPV/EHU) (UFI 11/32), Basque Government (Saiotek S-PE13UN048),(GIC 10/127) and FEDER funds.

7. REFERENCES

1. Re F, Gregori M, Masserini M: Nanotechnology for neurodegenerative disorders. *Maturitas* 73(1), 45-51 (2012).
2. Amir Nazem and G. Ali Mansoori: Nanotechnology solutions for Alzheimer's disease: Advances in Research Tools, Diagnostic Methods and Therapeutic Agents. *Journal of Alzheimer Disease*, 199-223 (2013).
3. Modi G, Pillay V, Choonara YE: Advances in the treatment of neurodegenerative disorders employing nanotechnology. *Ann. N. Y. Acad. Sci.* 1184(1), 154-172 (2010).
4. Kreuter J: Drug delivery to the central nervous system by polymeric nanoparticles: What do we know? *Adv. Drug Deliv. Rev.* 71, 2-14 (2014).
5. Musyanovych A, Landfester K: Polymer Micro- and Nanocapsules as Biological Carriers with Multifunctional Properties. *Macromolecular Bioscience* 14(4), 458-477 (2014).
6. Lai F, Fadda AM, Sinico C: Liposomes for brain delivery. *Expert Opinion on Drug Delivery* 10(7), 1003-1022 (2013).
7. Gastaldi L, Battaglia L, Peira E *et al.*: Solid lipid nanoparticles as vehicles of drugs to the brain: Current state of the art. *European Journal of Pharmaceutics and Biopharmaceutics* 87(3), 433-444 (2014).
8. Beloqui A, Solinís MÁ, Rodríguez-Gascón A, Almeida AJ, Préat V: Nanostructured lipid carriers: Promising drug delivery systems for future clinics. *Nanomedicine: Nanotechnology, Biology and Medicine* 12(1), 143-161 (2016).
9. Müller RH, Radtke M, Wissing SA: Nanostructured lipid matrices for improved microencapsulation of drugs. *Int. J. Pharm.* 242(1-2), 121-128 (2002).
10. Schlachetzki F, Zhang Y, Boado RJ, Pardridge WM.: Gene therapy of the brain: the trans-vascular approach. *Neurology* 62, 1275-1281 (2004).
11. Xia C, Boado RJ, Zhang Y, Chu C, Pardridge WM: Intravenous glial-derived neurotrophic factor gene therapy of experimental Parkinson's disease with Trojan horse liposomes and a tyrosine hydroxylase promoter. *J. Gene Med.* 10(3), 306-315 (2008).
12. Brambilla D, Le Droumaguet B, Nicolas J *et al.*: Nanotechnologies for Alzheimer's disease: diagnosis, therapy, and safety issues. *Nanomedicine: Nanotechnology, Biology and Medicine* 7(5), 521-540 (2011).
13. Nunes A, Al-Jamal KT, Kostarelos K: Therapeutics, imaging and toxicity of nanomaterials in the central nervous system. *J. Controlled Release* 161(2), 290-306 (2012).
14. Amanda J. Haes ,Lei Chang , William L. Klein ,and Richard P. Van Duyne: **Detection of a Biomarker for Alzheimer's Disease from Synthetic and Clinical Samples Using a Nanoscale Optical Biosensor.** *Journal of the American Chemical Society*, 2264-2271 (2005).

15. Jin-sil Choi, Hyuck Jae Choi, Dae Chul Jung, bJoo-Hyuk Lee and Jinwoo Cheon: Nanoparticle assisted magnetic resonance imaging of the early reversible stages of amyloid β self-assembly. *Chem. Commun*, 2197-2199 (2008).
16. Chen Y, Liu L: Modern methods for delivery of drugs across the blood-brain barrier. *Adv. Drug Deliv. Rev.* 64(7), 640-665 (2012).
17. Garbayo E, Estella-Hermoso de Mendoza A, Blanco-Prieto MJ: Diagnostic and therapeutic uses of nanomaterials in the brain. *Curr. Med. Chem.* 21(36), 4100-4131 (2014).
18. Herve F, Ghinea N, Scherrmann JM: CNS delivery via adsorptive transcytosis. *AAPS J.* 10(3), 455-472 (2008).
19. Park K: Trojan monocytes for improved drug delivery to the brain. *J. Controlled Release* 132(2), 75 (2008).
20. Thuerauf N, Fromm MF: The role of the transporter P-glycoprotein for disposition and effects of centrally acting drugs and for the pathogenesis of CNS diseases. *Eur. Arch. Psychiatry Clin. Neurosci.* 256(5), 281-286 (2006).
21. Tajés M, Ramos-Fernandez E, Weng-Jiang X *et al.*: The blood-brain barrier: structure, function and therapeutic approaches to cross it. *Mol. Membr. Biol.* 31(5), 152-167 (2014).
22. Riley D, Lozano A: The fourth dimension of stereotaxis: timing of neurosurgery for Parkinson disease. *Neurology* 68(4), 252-253 (2007).
23. Blasberg RG, Patlak C, Fenstermacher JD: Intrathecal chemotherapy: brain tissue profiles after ventriculocisternal perfusion. *J. Pharmacol. Exp. Ther.* 195(1), 73-83 (1975).
24. Patel MM, Goyal BR, Bhadada SV, Bhatt JS, Amin AF: Getting into the brain: approaches to enhance brain drug delivery. *CNS Drugs* 23(1), 35-58 (2009).
25. Djupesland PG, Messina JC, Mahmoud RA: The nasal approach to delivering treatment for brain diseases: an anatomic, physiologic, and delivery technology overview. *Ther. Deliv.* 5(6), 709-733 (2014).
26. Ambikanandan Misra GK: Drug Delivery Systems from Nose to Brain. *Curr. Pharm. Biotechnol* 13(12), 2355-2379 (2012).
27. Wen MM: Olfactory targeting through intranasal delivery of biopharmaceutical drugs to the brain: current development. *Discov. Med.* 11(61), 497-503 (2011).
28. Gartzandia O, Herran E, Pedraz JL, Carro E, Igartua M, Hernandez RM: Chitosan coated nanostructured lipid carriers for brain delivery of proteins by intranasal administration. *Colloids Surf. B Biointerfaces* 134, 304-313 (2015).
29. Clark MA, Hirst BH, Jepson MA: Lectin-mediated mucosal delivery of drugs and microparticles. *Adv. Drug Deliv. Rev.* 43(2-3), 207-223 (2000).
30. Zou LL, Ma JL, Wang T, Yang TB, Liu CB: Cell-penetrating Peptide-mediated therapeutic molecule delivery into the central nervous system. *Curr. Neuropharmacol.* 11(2), 197-208 (2013).

31. Kanazawa T, Akiyama F, Kakizaki S, Takashima Y, Seta Y: Delivery of siRNA to the brain using a combination of nose-to-brain delivery and cell-penetrating peptide-modified nano-micelles. *Biomaterials* 34(36), 9220-9226 (2013).
32. Gartzandia O, Egusquiaguirre SP, Bianco J *et al.*: Nanoparticle transport across in vitro olfactory cell monolayers. *Int. J. Pharm.* 499(1–2), 81-89 (2016).
33. Qin Y, Chen H, Zhang Q *et al.*: Liposome formulated with TAT-modified cholesterol for improving brain delivery and therapeutic efficacy on brain glioma in animals. *Int. J. Pharm.* 420(2), 304-312 (2011).
34. Querfurth HW, LaFerla FM: Alzheimer's disease. *N. Engl. J. Med.* 362(4), 329-344 (2010).
35. Citron M.: Alzheimer's disease: strategies for disease modification. *Nat. Rev Drug Discov*, 387-398 (2010).
36. Desai AK GG: Diagnosis and treatment of Alzheimer's disease. *Neurology* 64, S34-9 (2005).
37. John Hardy KC: Amyloid at the blood vessel wall. *Nature Medicine* 12, 756-757 (2006).
38. Blennow K, Hampel H: CSF markers for incipient Alzheimer's disease. *The Lancet Neurology* 2(10), 605-613 (2003).
39. Fradinger EA, Bitan G: En route to early diagnosis of Alzheimer's disease – are we there yet? *Trends Biotechnol.* 23(11), 531-533 (2005).
40. Nasrallah IM, Wolk DA: Multimodality Imaging of Alzheimer Disease and Other Neurodegenerative Dementias. *Journal of Nuclear Medicine* 55(12), 2003-2011 (2014).
41. Georganopoulou DG, Chang L, Nam J *et al.*: Nanoparticle-based detection in cerebral spinal fluid of a soluble pathogenic biomarker for Alzheimer's disease. *Proceedings of the National Academy of Sciences of the United States of America* 102(7), 2273-2276 (2005).
42. Chikae M, Fukuda T, Kerman K, Idegami K, Miura Y, Tamiya E: Amyloid- β detection with saccharide immobilized gold nanoparticle on carbon electrode. *Bioelectrochemistry* 74(1), 118-123 (2008).
43. Kang D, Lee J, Oh B, Choi J: Ultra-sensitive immunosensor for β -amyloid (1–42) using scanning tunneling microscopy-based electrical detection. *Biosensors and Bioelectronics* 24(5), 1431-1436 (2009).
44. Adria Neely, Candice Perry, Birsan Varisli, Anant K. Singh, Tahir Arbnesi, Dulal Senapati, Jhansi Rani Kalluri, and Paresh Chandra Ray: Ultrasensitive and Highly Selective Detection Of Alzheimer's Disease Biomarker Using Two-Photon Rayleigh Scattering Properties of Gold Nanoparticle. *ACS Nano* 3(9), 2834-2840 (2009).
45. Skaat H, Margel S: Synthesis of fluorescent-maghemite nanoparticles as multimodal imaging agents for amyloid- β fibrils detection and removal by a magnetic field. *Biochem. Biophys. Res. Commun.* 386(4), 645-649 (2009).
46. Yang J, Zaim Wadghiri Y, Minh Hoang D *et al.*: Detection of amyloid plaques targeted by USPIO- $A\beta$ 1–42 in Alzheimer's disease transgenic mice using magnetic resonance microimaging. *Neuroimage* 55(4), 1600-1609 (2011).

47. Cheng KK, Chan PS, Fan S *et al.*: Curcumin-conjugated magnetic nanoparticles for detecting amyloid plaques in Alzheimer's disease mice using magnetic resonance imaging (MRI). *Biomaterials* 44, 155-172 (2015).
48. Feng L, Li S, Xiao B, Chen S, Liu R, Zhang Y.: Fluorescence imaging of APP in Alzheimer's disease with quantum dot or Cy3: a comparative study. *Zhong Nan Da Xue Xue Bao Yi Xue Ban* (2010).
49. Tokuraku K, Marquardt M, Ikezu T: Real-Time Imaging and Quantification of Amyloid- β Peptide Aggregates by Novel Quantum-Dot Nanoprobes. *PLoS ONE* (2009).
50. Celeste A. Roney, Veera Arora, Padmakar V. Kulkarni, Peter P. Antich, and Frederick J. Bonte: Nanoparticulate Radiolabelled Quinolines Detect Amyloid Plaques in Mouse Models of Alzheimer's Disease," *International Journal of Alzheimer's Disease. Journal of Alzheimer Disease* (2009).
51. Dauer W, Przedborski S: Parkinson's Disease: Mechanisms and Models. *Neuron* 39(6), 889-909 (2003).
52. Linazasoro G: A global view of Parkinson's disease pathogenesis: Implications for natural history and neuroprotection. *Parkinsonism Relat. Disord.* 15(6), 401-405 (2009).
53. Nussbaum RL, Ellis CE: Alzheimer's Disease and Parkinson's Disease. *N. Engl. J. Med.* 348(14), 1356-1364 (2003).
54. Spillantini MG, Schmidt ML, Lee VM, Trojanowski JQ, Jakes R, Goedert M.: **-Synuclein in Lewy bodies.** *Nature* 388, 839-840 (1997).
55. Perlmutter JS, Norris SA: Neuroimaging biomarkers for Parkinson disease: Facts and fantasy. *Ann. Neurol.* 76(6), 769-783 (2014).
56. Hong Yan Yue, Shuo Huang, Jian Chang, Chaejeong Heo, Fei Yao, Subash Adhikari, Fethullah Gunes, Li Chun Liu, Tae Hoon Lee, Eung Seok Oh, Bing Li, Jian Jiao Zhang, Ta Quang Huy, Nguyen Van Luan, and Young Hee Lee: ZnO Nanowire Arrays on 3D Hierarchical Graphene Foam: Biomarker Detection of Parkinson's Disease. *ACS Nano*, 1639-1646 (2014).
57. Ronan Baron, Maya Zayats, and Itamar Willner: Dopamine-, L-DOPA-, Adrenaline-, and Noradrenaline-Induced Growth of Au Nanoparticles: Assays for the Detection of Neurotransmitters and of Tyrosinase Activity. *Analytical Chemistry*, 1566-1571 (2005).
58. Authors Xianglong Zhu, Juan Hu, Zhenghuan Zhao, Mingjun Sun, Xiaoqin Chi, Xiaomin Wang, Jinhao Gao: Kinetic and Sensitive Analysis of Tyrosinase Activity Using Electron Transfer Complexes: In Vitro and Intracellular Study. *Small* (2015).
59. An Y, Tang L, Jiang X, Chen H, Yang M, Jin L, Zhang S, Wang C, Zhang W.: A photoelectrochemical immunosensor based on Au-doped TiO₂ nanotube arrays for the detection of α -synuclein. *Chemistry*, 14439-46 (2010).
60. Scheltens P, Blennow K, Breteler MMB *et al.*: Alzheimer's disease. *The Lancet*.
61. Howard R, McShane R, Lindsay J *et al.*: Donepezil and memantine for moderate-to-severe Alzheimer's disease. *N. Engl. J. Med.* 366(10), 893-903 (2012).

62. Begley DJ: Delivery of therapeutic agents to the central nervous system: the problems and the possibilities. *Pharmacol. Ther.* 104(1), 29-45 (2004).
63. Joshi SA, Chavhan SS, Sawant KK: Rivastigmine-loaded PLGA and PBCA nanoparticles: Preparation, optimization, characterization, in vitro and pharmacodynamic studies. *European Journal of Pharmaceutics and Biopharmaceutics* 76(2), 189-199 (2010).
64. Wilson B, Samanta MK, Santhi K, Kumar KPS, Paramakrishnan N, Suresh B: Poly(n-butylcyanoacrylate) nanoparticles coated with polysorbate 80 for the targeted delivery of rivastigmine into the brain to treat Alzheimer's disease. *Brain Res.* 1200, 159-168 (2008).
65. Nagpal K, Singh SK, Mishra DN: Optimization of brain targeted chitosan nanoparticles of Rivastigmine for improved efficacy and safety. *Int. J. Biol. Macromol.* 59, 72-83 (2013).
66. Fazil M, Md S, Haque S *et al.*: Development and evaluation of rivastigmine loaded chitosan nanoparticles for brain targeting. *European Journal of Pharmaceutical Sciences* 47(1), 6-15 (2012).
67. Pagar KP, Sardar SM, Vavia PR: Novel L-lactide-depsipeptide polymeric carrier for enhanced brain uptake of rivastigmine in treatment of Alzheimer's disease. *J. Biomed. Nanotechnol* 10(3), 415-426 (2014).
68. Bhavna , Shadab Md , Mushir Ali , Sanjula Baboota , Jasjeet Kaur Sahni , Aseem Bhatnagar , Javed Ali: Preparation, characterization, in vivo biodistribution and pharmacokinetic studies of donepezil-loaded PLGA nanoparticles for brain targeting. *Drug Development and Industrial Pharmacy* 40 (2014).
69. Herrán E, Pérez-González R, Igartua M, Pedraz JL, Carro E, Hernández RM: VEGF-releasing biodegradable nanospheres administered by craniotomy: A novel therapeutic approach in the APP/Ps1 mouse model of Alzheimer's disease. *J. Controlled Release* 170(1), 111-119 (2013).
70. E. Herran, R. Perez- Gonzalez, M. Igartua, J.L. Pedraz, E. Carro and R.M. Hernandez: Enhanced Hippocampal Neurogenesis in APP/Ps1 Mouse Model of Alzheimer's Disease After Implantation of VEGF-loaded PLGA Nanospheres. *Current Alzheimer Research* 12(10), 932-940 (2015).
71. Zhao Y, Li X, Lu C *et al.*: Gelatin nanostructured lipid carriers-mediated intranasal delivery of basic fibroblast growth factor enhances functional recovery in hemiparkinsonian rats. *Nanomedicine: Nanotechnology, Biology and Medicine* 10(4), 755-764 (2014).
72. Kamila B. Kurakhmaeva , Irma A. Djindjikhshvili , Valery E. Petrov , Vadim U. Balabanyan , Tatiana A. Voronina , Sergey S. Trofimov , Jörg Kreuter , Svetlana Gelperina , David Begley , Renad N. Alyautdin: Brain targeting of nerve growth factor using poly(butyl cyanoacrylate) nanoparticles. *Journal of Drug Targeting* 17(8) (2009).
73. Liu G, Men P, Harris PLR, Rolston RK, Perry G, Smith MA: Nanoparticle iron chelators: A new therapeutic approach in Alzheimer disease and other neurologic disorders associated with trace metal imbalance. *Neurosci. Lett.* 406(3), 189-193 (2006).
74. Liu G, Men P, Kudo W, Perry G, Smith MA: Nanoparticle–chelator conjugates as inhibitors of amyloid- β aggregation and neurotoxicity: A novel therapeutic approach for Alzheimer disease. *Neurosci. Lett.* 455(3), 187-190 (2009).
75. Mufamadi MS, Choonara YE, Kumar P *et al.*: Ligand-functionalized nanoliposomes for targeted delivery of galantamine. *Int. J. Pharm.* 448(1), 267-281 (2013).

76. Xie Y, Ye L, Zhang X *et al.*: Transport of nerve growth factor encapsulated into liposomes across the blood–brain barrier: In vitro and in vivo studies. *J. Controlled Release* 105(1–2), 106-119 (2005).
77. Yung-Chih Kuo CL: Rescuing apoptotic neurons in Alzheimer's disease using wheat germ agglutinin-conjugated and cardiolipin-conjugated liposomes with encapsulated nerve growth factor and curcumin. *International Journal of Nanomedicine*. (2015).
78. Shubham Misra , Kanwaljit Chopra , V. R. Sinha , Bikash Medhi: Galantamine-loaded solid–lipid nanoparticles for enhanced brain delivery: preparation, characterization, in vitro and in vivo evaluations. *Drug delivery* (2015).
79. Laserra S, Basit A, Sozio P *et al.*: Solid lipid nanoparticles loaded with lipoyl–memantine codrug: Preparation and characterization. *Int. J. Pharm.* 485(1–2), 183-191 (2015).
80. Meng F, Asghar S, Gao S *et al.*: A novel LDL-mimic nanocarrier for the targeted delivery of curcumin into the brain to treat Alzheimer's disease. *Colloids and Surfaces B: Biointerfaces* 134, 88-97 (2015).
81. Rudimar L. Frozza , Andressa Bernardi, Juliana B., André B. Meneghetti, Aline Matté, Ana M. O. Battastini, Adriana R. Pohlmann, Sílvia S. Guterres, Christianne Salbego: Neuroprotective Effects of Resveratrol Against A β Administration in Rats are Improved by Lipid-Core Nanocapsules. *Molecular Neurobiology* 47(3), 1066-1080 (2013).
82. Coradini K, Lima FO, Oliveira CM *et al.*: Co-encapsulation of resveratrol and curcumin in lipid-core nanocapsules improves their in vitro antioxidant effects. *European Journal of Pharmaceutics and Biopharmaceutics* 88(1), 178-185 (2014).
83. Revilla S, Ursulet S, Álvarez-López MJ *et al.*: Lenti-GDNF Gene Therapy Protects Against Alzheimer's Disease-Like Neuropathology in 3xTg-AD Mice and MC65 Cells. *CNS Neuroscience & Therapeutics* 20(11), 961-972 (2014).
84. Iwasaki Y, Negishi T, Inoue M, Tashiro T, Tabira T, Kimura N: Sendai virus vector-mediated brain-derived neurotrophic factor expression ameliorates memory deficits and synaptic degeneration in a transgenic mouse model of Alzheimer's disease. *J. Neurosci. Res.* 90(5), 981-989 (2012).
85. Ciesler J, Sari Y: Neurotrophic Peptides: Potential Drugs for Treatment of Amyotrophic Lateral Sclerosis and Alzheimer's disease. *Open J. Neurosci.* 3, 2 (2013).
86. Lovell MA, Robertson JD, Teesdale WJ, Campbell JL, Markesbery WR: Copper, iron and zinc in Alzheimer's disease senile plaques. *J. Neurol. Sci.* 158(1), 47-52 (1998).
87. Cherny RA, Atwood CS, Xilinas ME *et al.*: Treatment with a Copper-Zinc Chelator Markedly and Rapidly Inhibits β -Amyloid Accumulation in Alzheimer's Disease Transgenic Mice. *Neuron* 30(3), 665-676 (2001).
88. Kuo Y, Chou P: Neuroprotection Against Degeneration of SK-N-MC Cells Using Neuron Growth Factor-Encapsulated Liposomes with Surface Cereport and Transferrin. *J. Pharm. Sci.* 103(8), 2484-2497 (2014).
89. Stefani M, Rigacci S: Beneficial properties of natural phenols: Highlight on protection against pathological conditions associated with amyloid aggregation. *Biofactors* 40(5), 482-493 (2014).

90. Wang X, Wang W, Li L, Perry G, Lee H, Zhu X: Oxidative stress and mitochondrial dysfunction in Alzheimer's disease. *Biochimica et Biophysica Acta (BBA) - Molecular Basis of Disease* 1842(8), 1240-1247 (2014).
91. Gobbi M, Re F, Canovi M *et al.*: Lipid-based nanoparticles with high binding affinity for amyloid- β 1-42 peptide. *Biomaterials* 31(25), 6519-6529 (2010).
92. Smith A, Giunta B, Bickford PC, Fountain M, Tan J, Shytle RD: Nanolipidic particles improve the bioavailability and α -secretase inducing ability of epigallocatechin-3-gallate (EGCG) for the treatment of Alzheimer's disease. *Int. J. Pharm.* 389(1-2), 207-212 (2010).
93. Teng Ma, Meng-Shan Tan, Jin-Tai Yu, and Lan Tan: Resveratrol as a Therapeutic agent for Alzheimer's Disease. *Biomed Research International* 2014 (2014).
94. Garbayo E, Ansorena E, Blanco-Prieto MJ: Drug development in Parkinson's disease: From emerging molecules to innovative drug delivery systems. *Maturitas* 76(3), 272-278 (2013).
95. Rodríguez-Nogales C, Garbayo E, Carmona-Abellán MM, Luquin MR, Blanco-Prieto MJ: Brain aging and Parkinson's disease: New therapeutic approaches using drug delivery systems. *Maturitas* 84, 25-31 (2016).
96. Rascol O, Goetz C, Koller W, Poewe W, Sampaio C: Treatment interventions for Parkinson's disease: an evidence based assessment. *The Lancet* 359(9317), 1589-1598 (2002).
97. Sauerbier A, Jenner P, Todorova A, Chaudhuri KR: Non motor subtypes and Parkinson's disease. *Parkinsonism Relat. Disord.* 22, Supplement 1, S41-S46 (2016).
98. Pillay S, Pillay V, Choonara YE *et al.*: Design, biometric simulation and optimization of a nano-enabled scaffold device for enhanced delivery of dopamine to the brain. *Int. J. Pharm.* 382(1-2), 277-290 (2009).
99. Trapani A, De Giglio E, Cafagna D *et al.*: Characterization and evaluation of chitosan nanoparticles for dopamine brain delivery. *Int. J. Pharm.* 419(1-2), 296-307 (2011).
100. Pahuja R, Seth K, Shukla A *et al.*: Trans-blood brain barrier delivery of dopamine-loaded nanoparticles reverses functional deficits in parkinsonian rats. *ACS Nano* 9(5), 4850-4871 (2015).
101. Sumit Sharma, Shikha Lohan & R. S. R. Murthy: Formulation and characterization of intranasal mucoadhesive nanoparticulates and thermo-reversible gel of levodopa for brain delivery. *Drug Development and Industrial Pharmacy* (2013).
102. E. D'Aurizio, P. Sozio, L. S. Cerasa, M. Vacca, L. Brunetti, G. Orlando, A. Chiavaroli, R. J. Kok, W. E. Hennink, and A. Di Stefano: Biodegradable Microspheres Loaded with an Anti-Parkinson Prodrug: An in Vivo Pharmacokinetic Study. *Molecular Pharmaceutics* 8(6) (2011).
103. Gambaryan PY, Kondrasheva IG, Severin ES, Guseva AA, Kamensky AA: Increasing the Efficiency of Parkinson's Disease Treatment Using a poly(lactic-co-glycolic acid) (PLGA) Based L-DOPA Delivery System. *Exp Neurobiol* 23(3), 246-252 (2014).
104. Yang X, Zheng R, Cai Y, Liao M, Yuan W, Liu Z: Controlled-release levodopa methyl ester/benserazide-loaded nanoparticles ameliorate levodopa-induced dyskinesia in rats. *International Journal of Nanomedicine.*, 2077-2086 (2012).

105. Ren T, Yang X, Wu N, Cai Y, Liu Z, Yuan W: Sustained-release formulation of levodopa methyl ester/benserazide for prolonged suppressing dyskinesia expression in 6-OHDA-lesioned rats. *Neurosci. Lett.* 502(2), 117-122 (2011).
106. Wang A, Wang L, Sun K, Liu W, Sha C, Li Y.: Preparation of rotigotine-loaded microspheres and their combination use with L-DOPA to modify dyskinesias in 6-OHDA-lesioned rats. *Pharmaceutical Research* (2012).
107. Jafarieh O, Md S, Ali M *et al.*: Design, characterization, and evaluation of intranasal delivery of ropinirole-loaded mucoadhesive nanoparticles for brain targeting. *Drug Dev. Ind. Pharm.* 41(10), 1674-1681 (2015).
108. Md S, Khan RA, Mustafa G *et al.*: Bromocriptine loaded chitosan nanoparticles intended for direct nose to brain delivery: Pharmacodynamic, Pharmacokinetic and Scintigraphy study in mice model. *European Journal of Pharmaceutical Sciences* 48(3), 393-405 (2013).
109. Jollivet C, Aubert-Pouessel A, Clavreul A *et al.*: Long-term effect of intra-striatal glial cell line-derived neurotrophic factor-releasing microspheres in a partial rat model of Parkinson's disease. *Neurosci. Lett.* 356(3), 207-210 (2004).
110. Jollivet C, Aubert-Pouessel A, Clavreul A *et al.*: Striatal implantation of GDNF releasing biodegradable microspheres promotes recovery of motor function in a partial model of Parkinson's disease. *Biomaterials* 25(5), 933-942 (2004).
111. Garbayo E, Montero-Menei CN, Ansorena E, Lanciego JL, Aymerich MS, Blanco-Prieto MJ: Effective GDNF brain delivery using microspheres—A promising strategy for Parkinson's disease. *J. Controlled Release* 135(2), 119-126 (2009).
112. Garbayo E, Ansorena E, Lanciego JL, Blanco-Prieto MJ, Aymerich MS: Long-term neuroprotection and neurorestoration by glial cell-derived neurotrophic factor microspheres for the treatment of Parkinson's disease. *Movement Disorders* 26(10), 1943-1947 (2011).
113. Gujral C, Minagawa Y, Fujimoto K, Kitano H, Nakaji-Hirabayashi T: Biodegradable microparticles for strictly regulating the release of neurotrophic factors. *J. Controlled Release* 168(3), 307-316 (2013).
114. Herran,E, Requejo C, Ruiz-Ortega JA. *et al*: Increased antiparkinson efficacy of the combined administration of VEGF- and GDNF-loaded nanospheres in a partial lesion model of Parkinson's disease. *International Journal of Nanomedicine.* 9(1), 2677-2687 (2014).
115. Herrán E, Ruiz-Ortega JÁ, Aristieta A *et al.*: In vivo administration of VEGF- and GDNF-releasing biodegradable polymeric microspheres in a severe lesion model of Parkinson's disease. *European Journal of Pharmaceutics and Biopharmaceutics* 85(3, Part B), 1183-1190 (2013).
116. C. Requejo, J.A. Ruiz-Ortega, H. Bengoetxea *et al.*: Topographical Distribution of Morphological Changes in a Partial Model of Parkinson's Disease—Effects of Nanoencapsulated Neurotrophic Factors Administration. *Molecular Neurobiology* 52(2), 846-858 (2015).
117. Azeem A, Talegaonkar S, Negi LM, Ahmad FJ, Khar RK, Iqbal Z: Oil based nanocarrier system for transdermal delivery of ropinirole: A mechanistic, pharmacokinetic and biochemical investigation. *Int. J. Pharm.* 422(1–2), 436-444 (2012).

118. Pardeshi CV1, Rajput PV, Belgamwar VS, Tekade AR, Surana SJ.: Novel surface modified solid lipid nanoparticles as intranasal carriers for ropinirole hydrochloride: application of factorial design approach. *Drug delivery*, 47-56 (2013).
119. Lisabetta Esposito, Martina Fantin, Matteo Marti, Markus Drechsler, Lydia Paccamiccio, Paolo Mariani, Elisa Sivieri, Francesco Lain, Enea Menegatti et al.: Solid lipid nanoparticles as delivery systems for bromocriptine. *Pharmaceutical Research* 25(7) (2008).
120. Wang Y, Xu H, Fu Q, Ma R, Xiang J: Protective effect of resveratrol derived from *Polygonum cuspidatum* and its liposomal form on nigral cells in Parkinsonian rats. *J. Neurol. Sci.* 304(1–2), 29-34 (2011).
121. Rudra Pangeni, Sheshta Sharma, Gulam Mustafa et al.: Vitamin E loaded resveratrol nanoemulsion for brain targeting for the treatment of Parkinson's disease by reducing oxidative stress. *Nanotechnology* 25(48) (2014).
122. Sikorska M, Lanthier P, Miller H et al.: Nanomicellar formulation of coenzyme Q10 (Ubisol-Q10) effectively blocks ongoing neurodegeneration in the mouse 1-methyl-4-phenyl-1,2,3,6-tetrahydropyridine model: potential use as an adjuvant treatment in Parkinson's disease. *Neurobiol. Aging* 35(10), 2329-2346 (2014).
123. Wu S, Li G, Li X et al.: Transport of glial cell line-derived neurotrophic factor into liposomes across the blood-brain barrier: in vitro and in vivo studies. *Int. J. Mol. Sci.* 15(3), 3612-3623 (2014).
124. Eslamboli A, Georgievska B, Ridley RM et al.: Continuous Low-Level Glial Cell Line-Derived Neurotrophic Factor Delivery Using Recombinant Adeno-Associated Viral Vectors Provides Neuroprotection and Induces Behavioral Recovery in a Primate Model of Parkinson's Disease. *The Journal of Neuroscience* 25(4), 769-777 (2005).
125. Chen X, Liu W, Guoyuan Y et al.: Protective effects of intracerebral adenoviral-mediated GDNF gene transfer in a rat model of Parkinson's disease. *Parkinsonism Relat. Disord.* 10(1), 1-7 (2003).
126. Kozlowski DA, Connor B, Tillerson JL, Schallert T, Bohn MC: Delivery of a GDNF Gene into the Substantia Nigra after a Progressive 6-OHDA Lesion Maintains Functional Nigrostriatal Connections. *Exp. Neurol.* 166(1), 1-15 (2000).
127. Jamie L. Eberling, Adrian P. Kells, Philip Pivrotto et al.: Functional effects of AAV2-GDNF on the dopaminergic nigrostriatal pathway in parkinsonian rhesus monkeys. *Human Gene Therapy* 20(5), 511-518 (2009).
128. Juan A. Gonzalez-Barrios, Maria Lindahl, Michael J. Bannon et al.: Neurotensin polyplex as an efficient carrier for delivering the human GDNF gene into nigral dopamine neurons of hemiparkinsonian rats. *Molecular Therapy* 14(6), 857-865 (2006).
129. Huang R, Ke W, Liu Y et al.: Gene therapy using lactoferrin-modified nanoparticles in a rotenone-induced chronic Parkinson model. *J. Neurol. Sci.* 290(1–2), 123-130 (2010).
130. Huang R, Han L, Li J et al.: Neuroprotection in a 6-hydroxydopamine-lesioned Parkinson model using lactoferrin-modified nanoparticles. *J. Gene Med.* 11(9), 754-763 (2009).
131. Peng Y-S, Lai P-L, Peng S, et al.: Glial cell line-derived neurotrophic factor gene delivery via a polyethylene imine grafted chitosan carrier. *International journal of nanomedicine* 9, 3163-3174 (2014).

132. Tian J, Du G, Ye L *et al.*: Three-month subchronic intramuscular toxicity study of rotigotine-loaded microspheres in Cynomolgus monkeys. *Food and Chemical Toxicology* 52, 143-152 (2013).

133. Siegel GJ, Chauhan NB: Neurotrophic factors in Alzheimer's and Parkinson's disease brain. *Brain Res. Rev.* 33(2-3), 199-227 (2000).

134. Sullivan AM, Toulouse A: Neurotrophic factors for the treatment of Parkinson's disease. *Cytokine Growth Factor Rev.* 22(3), 157-165 (2011).

135. Shults CW: Therapeutic role of coenzyme Q10 in Parkinson's disease. *Pharmacol. Ther.* 107(1), 120-130 (2005).

136. Giridhar Murlidharan, Richard J. Samulski, and Aravind Asokan: Biology of adeno-associated viral vectors in the central nervous system. *Molecular Neuroscience* 7(76) (2014).

137. Francisco C. Perez-Martinez, Blanca Carrion and Valentin Ceña: The Use of Nanoparticles for Gene Therapy in the Nervous System. *J Alzheimer Dis* 31(4), 697-710 (2012).

The role of lipid nanoparticles and its surface modification in reaching the brain: an approach for neurodegenerative diseases treatment ³

Sara Hernando¹, Jose Luis Pedraz^{1,2}, Manoli Igartua^{1,2*}, Rosa Maria Hernandez^{1,2*}

¹NanoBioCel Group, Laboratory of Pharmaceutics, School of Pharmacy, University of the Basque Country (UPV/EHU), Vitoria-Gasteiz, 01006, Spain;

²Biomedical Research Networking Centre in Bioengineering, Biomaterials and Nanomedicine (CIBER-BBN), Vitoria-Gasteiz, 01006, Spain.

*Address correspondence Rosa Maria Hernandez and Manoli Igartua

³ Published in: Current Drug Delivery (2017)

IF: 1.645 (Q4)

<https://doi.org/10.2174/1567201815666180510103747>

Cat: Pharmacology and pharmacy

Nanomedicine is a field of science that employs materials in the nanometer scale. Specifically, the use of nanoparticles (NPs) has some medical applications due to their structure, for example, the ability to cross the biological barriers, and their effectiveness avoiding some drug delivery problems. Because of that, in the last years, the use of NPs has been raised as a workable solution for neurodegenerative diseases (ND) treatment [1,2]. NDs are characterized by a continuous structural and functional neuronal loss, usually correlated with neuronal death. Between NDs, Alzheimer disease (AD) and Parkinson's disease (PD) are the most common disorders worldwide, becoming a serious economic burden and public health problem [3].

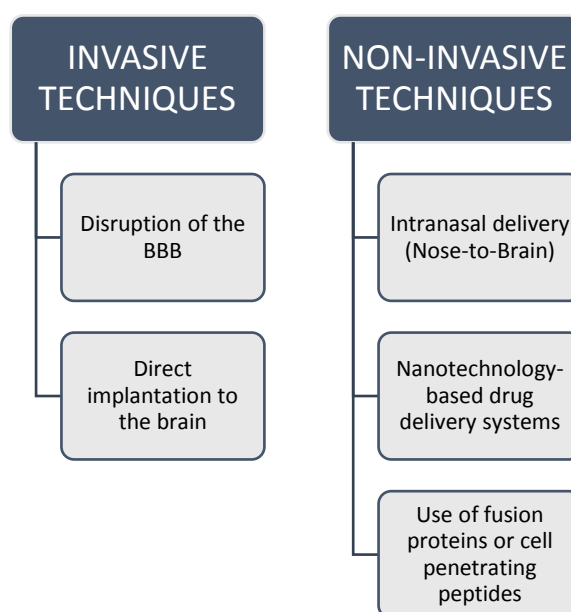


Figure 1. Schematic representation of some of the methods employed to deliver drugs to the brain.

One of the most challenging obstacles for an effective treatment of NDs is the low penetration of drugs to the central nervous system (CNS). The blood brain barrier (BBB) and the blood cerebrospinal fluid barrier (BCSFB) protect the brain against invading organism and unwanted substances with multispecific efflux transport proteins and detoxifying enzymes, limiting the entry of different compounds into the CNS [4,5]. Therefore, in the last years different strategies and approaches have been developed to obtain brain targeting [6]. In Figure 1 there have been summarized the most common techniques used to deliver drugs to the brain. More detailed information about different methods to bypass the BBB can be found in previous papers [7,8]

As previously pointed out, using nanoparticles opens the possibility to efficiently deliver a number of different drugs. Indeed, the use of surface-engineered nanoparticles is an emerging innovative method for the delivery of therapeutics into the CNS [9]. In this review, we will focus on lipid nanoparticles administration for ND treatment, focusing on the modifications of lipid nanoparticle surface for brain targeting. Figure 2 shows schematically lipid based nanoparticles.

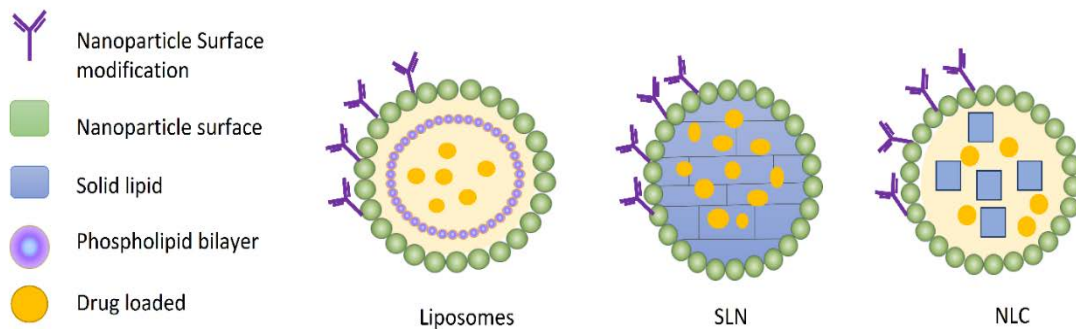


Figure 2. Schematic representation of lipid nanoparticulate systems with surface modification. NLC: nanostructured lipid carriers. SLN: solid lipid nanoparticles.

Among lipid nanoparticles, liposomes are synthetic small micelles formed by one or more concentric phospholipid bilayers. Regarding PD, glial derived neurotrophic factor (GDNF) loaded liposomes were developed by Wu et al. improving the bioavailability of the growth factor and obtaining brain targeting in rats after its intravenous (IV) administration [10]. Antioxidants, such as resveratrol, have been

encapsulated into liposomes for improving its bioavailability. Its administration to 6-OHDA animal model of PD improved locomotor activity, TH⁺ levels and the antioxidant capacity of the drug after two weeks treatment with daily intragastrically administration of the nanoformulation [11]. Liposomes can be surface engineered. For example, levodopa, the most commonly used drug in clinical practice, was encapsulated into chitosan (CS) modified liposomes. The controlled released of levodopa provided thanks to CS after its intragastric administration, decreased the levodopa induced dyskinesias (LID) compared to levodopa commercialized tablets [12]. GDNF loaded liposomes were also surface engineered by Xia et al with Trojan horses (TH). The IV administration of this nanosystem improved behavioral studies and increased TH⁺ enzyme levels in the striatum of treated rats [13]. On the other hand, Mufamadi et al. prepared pegylated nanoliposomes loading galantamine for AD treatment. Pegylation is known to reduce the opsonization and elimination of NP, increasing the time for reaching the brain before being cleared from the blood [14]. In vitro studies revealed higher targeted delivery of functionalized nanoliposomes in PC12 neuronal cells [15]. Liposomes can be functionalized with other molecules such as wheat germ agglutinin (WGA) and cardiolipin (CL). In line with this approach, neuronal growth factor (NGF) was loaded in WGA and CL modified liposomes. CL favored the ligand binding to A β peptide and WGA enhanced the delivery of pharmaceuticals across the BBB according to HBMECs/HA cell line [16].

The second lipidic nanoparticulate systems are the lipidic nanocarriers, which constitute nanometric colloidal drug carrier systems usually composed of fatty acids or mono-, di-, and tri- glycerides. Between others, nanostructured lipid carriers (NLC) and solid lipid nanoparticles (SLN) are widely used lipid nanosystems. These nanocarriers are highly stable systems, able to cross easily the BBB due to their lipophilic nature by endocytic mechanism, and without producing toxic degradation compounds. Moreover, unlike liposomes, they are highly stable remaining solid at body temperature and provide sustained release of drugs. On the other hand, NLCs present higher drug loading capacity, in contrast to SLNs, that is why the number of publications based on NLC formulations has considerably increased. [17, 18].

Up to now, different lipid nanocarriers have transported pharmaceutical active agents to the brain tissue, providing therapeutic alternatives to treat NDs. For example, a well-known dopamine agonist, bromocriptine, was encapsulated into

SLN decreasing akinesias in 6-OHDA hemiparkinsonian rat model after its intravenous administration [19]. *Azeem et al.* encapsulated ropirinole for intranasal administration, improving pharmacokinetic parameters without damage on the nasal mucosa [20]. *Gartziandia et al.* did also use the intranasal administration for the delivery of pharmaceuticals for PD treatment. Indeed, CS coated, GDNF loaded NLC administration to a 6-OHDA animal model of PD induced motor recovery and increased TH⁺ levels in both striatum and substantia nigra. CS is a cationic polysaccharide that increases the transmucosal transport across different mucosa, increasing time residence and maximizing brain targeting options [21]. In line with this approach, NLCs have also been coated with cell penetrating peptides (CPPs) for increasing brain targeting. Among CPPs, TAT is a short amphipatic and cationic peptide widely used for surface modification. TAT modified CS-NLC loading GDNF were intranasally administered to a MPTP mouse model of PD improving motor recovery, immunohistochemistry studies and decreased microglia activation [22].

Regarding AD, different studies have been conducted to test the lipid nanoparticles administration approach for this ND treatment. Among others, *Misra et al.* developed SLN loading galantamine. After oral administration, this nanosystem presented higher bioavailability than the free drug. Moreover, the oral administration of galantamine loaded SLN improved behavioral deficits presented in treated rats compared with the control group [23]. As in the case of PD, the use of resveratrol has been also highlighted for AD treatment. *Frezza et al.* *in vivo* conducted studies in A β ₁₋₄₂ induced rats showed the potential effect of resveratrol loaded NLCs recovering short and long-term memory. These promising results may be due to the higher resveratrol concentrations obtained in the brains of the animals treated with the intraperitoneally administration of this nanosystem [24]. Another powerful antioxidant for AD treatment is curcumin. However, its poor biavailability and rapid excretion makes difficult to obtain therapeutic levels in the brain. In an attempt to improve its pharmacokinetic properties, lactoferrin modified NLC encapsulating curcumin were used for an effective treatment of AD via IV route. Biodistribution studies confirmed the suitability of this nanoformulation enhancing brain uptake 2.78 folds compared to non-modified NLC. *In vivo* studies confirmed curcumin brain distribution reducing pathological impairment in hippocampus of AD treated groups [25].

CONCLUSIONS

In this review, we have highlighted the potential of lipid nanoparticles in reaching the brain, a challenging task in modern medicine. Based on the research articles published until today it is difficult to establish which lipid nanosystem or modification is the best one, since the administration route or animal models are different, among others. Anyway, it cannot be discussed the benefits obtained from lipid nanoparticle administration to obtain brain targeting, however, more research studies are needed to improve brain targeting and obtain an effective treatment for NDs.

CONFLICT OF INTEREST

The author(s) confirm that this article content has no conflict of interest.

ACKNOWLEDGMENTS

This project was partially supported by the “Ministerio de Economía y Competitividad” (SAF2013-42347-R), the University of the Basque Country (UPV/EHU) (UFI 11/32) and FEDER funds. The authors also wish to thank the intellectual and technical assistance from the ICTS “NANBIOSIS”, more specifically by the Drug Formulation Unit (U10) of the CIBER-BBN at the UPV/EHU. S. Hernando thanks the Basque Government for the fellowship grant.

REFERENCES

- [1] Re F, Gregori M, Masserini M: Nanotechnology for neurodegenerative disorders. *Maturitas* 73(1), 45-51 (2012).
- [2] Carradori D, Gaudin A, Brambilla D, Andrieux K: Applicatio of Nanomedicine to the CNS Diseases. *Int Rev Neurobiol* 130, 73-113 (2016).
- [3] Foster ER: Themes from the special issue on neurodegenerative diseases: what have we learned, and where can we go from here? *Am. J. Occup. Ther.* 68(1), 6-8 (2014).
- [4] Tajés M, Ramos-Fernandez E, Weng-Jiang X et al.: The blood-brain barrier: structure, function and therapeutic approaches to cross it. *Mol. Membr. Biol.* 31(5), 152-167 (2014).
- [5] Strazielle N, Ghersi-Egea JF: Potential Pathways for CNS Drug Delivery Across the Blood-Cerebrospinal Fluid Barrier. *Curr. Pharm. Des.* 22(35), 5463-5476 (2016).
- [6] Chen Y, Liu L: Modern methods for delivery of drugs across the blood–brain barrier. *Adv. Drug Deliv. Rev.* 64(7), 640-665 (2012).

[7] Gabathuler R: Approaches to transport therapeutic drugs across the blood–brain barrier to treat brain diseases. *Neurobiol Dis* 37(1), 48-57 (2010).

[8] Garbayo E, Estella-Hermoso de Mendoza A, Blanco-Prieto MJ: Diagnostic and therapeutic uses of nanomaterials in the brain. *Curr. Med. Chem.* 21(36), 4100-4131 (2014).

[9] Singh D, Kapahi H, Rashid M, Prakash A, Majeed AB, Mishra N: Recent prospective of surface engineered Nanoparticles in the management of Neurodegenerative disorders. *Artif. Cells Nanomed Biotechnol.* 44(3), 780-791 (2016).

[10] Wu S, Li G, Li X et al.: Transport of glial cell line-derived neurotrophic factor into liposomes across the blood-brain barrier: in vitro and in vivo studies. *Int. J. Mol. Sci.* 15(3), 3612-3623 (2014).

[11] Wang Y, Xu H, Fu Q, Ma R, Xiang J: Protective effect of resveratrol derived from *Polygonum cuspidatum* and its liposomal form on nigral cells in Parkinsonian rats. *J. Neurol. Sci.* 304(1–2), 29-34 (2011).

[12] Cao X, Hou D, Wang L et al.: Effects and molecular mechanism of chitosan-coated levodopa nanoliposomes on behavior of dyskinesia rats. *Biol. Res.* 49(1), 32 (2016).

[13] Xia C, Boado RJ, Zhang Y, Chu C, Pardridge WM: Intravenous glial-derived neurotrophic factor gene therapy of experimental Parkinson's disease with Trojan horse liposomes and a tyrosine hydroxylase promoter. *J. Gene Med.* 10(3), 306-315 (2008).

[14] Leyva-Gómez G, Cortés H, Magaña JJ, Leyva-García N, Quintanar-Guerrero D, Florán B: Nanoparticle technology for treatment of Parkinson's disease: the role of surface phenomena in reaching the brain. *Drug Discov Today* 20(7), 824-837 (2015).

[15] Mufamadi MS, Choonara YE, Kumar P et al.: Ligand-functionalized nanoliposomes for targeted delivery of galantamine. *Int. J. Pharm.* 448(1), 267-281 (2013).

[16] Yung-Chih Kuo CL: Rescuing apoptotic neurons in Alzheimer's disease using wheat germ agglutinin-conjugated and cardiolipin-conjugated liposomes with encapsulated nerve growth factor and curcumin. *Int J Nanomedicine* 10, 2653-2672 (2015).

[17] Müller RH, Radtke M, Wissing SA: Nanostructured lipid matrices for improved microencapsulation of drugs. *Int. J. Pharm.* 242(1–2), 121-128 (2002).

[18] Beloqui A, Solinís MÁ, Rodríguez-Gascón A, Almeida AJ, Prétat V: Nanostructured lipid carriers: Promising drug delivery systems for future clinics. *Nanomedicine* 12(1), 143-161 (2016).

[19] Lisabetta Esposito, Martina Fantin, Matteo Marti, Markus Drechsler, Lydia Paccamiccio, Paolo Mariani, Elisa Sivieri, Francesco Lain, Enea Menegatti et al.: Solid lipid nanoparticles as delivery systems for bromocriptine. *Pharm Res* 25(7), 1521-130 (2008).

[20] Pardeshi CV1, Rajput PV, Belgamwar VS, Tekade AR, Surana SJ.: Novel surface modified solid lipid nanoparticles as intranasal carriers for ropinirole hydrochloride: application of factorial design approach. *Drug Deliv.* 20(1) 47-56 (2013).

[21] O. Gartzandia, E. Herrán, J.A. Ruiz-Ortega, C. Miguelez, M. Igartua, J.V. Lafuente, J.L. Pedraz, L. Ugedo, R.M. Hernández: Intranasal administration of chitosan-coated nanostructured lipid carriers loaded with GDNF improves behavioral and histological recovery in a partial lesion model of Parkinson's disease. *J Biomed Nanotechnol.* 12, 1-11 (2016).

[22] Hernando S, Herran E, Figueiro-Silva J et al.: Intranasal Administration of TAT-Conjugated Lipid Nanocarriers Loading GDNF for Parkinson's Disease. *Mol. Neurobiol.* 55 (1), 145-155 (2018).

[23] Shubham Misra , Kanwaljit Chopra , V. R. Sinha , Bikash Medhi: Galantamine-loaded solid-lipid nanoparticles for enhanced brain delivery: preparation, characterization, in vitro and in vivo evaluations. *Drug Deliv.* 23(4) 1434-43 (2016).

[24] Rudimar L. Frozza , Andressa Bernardi, Juliana B., André B. Meneghetti, Aline Matté, Ana M. O. Battastini, Adriana R. Pohlmann, Sílvia S. Guterres, Christianne Salbego: Neuroprotective Effects of Resveratrol Against A β Administration in Rats are Improved by Lipid-Core Nanocapsules. *Mol. Neurobiol* 47(3), 1066-1080 (2013).

[25] Meng F, Asghar S, Gao S et al.: A novel LDL-mimic nanocarrier for the targeted delivery of curcumin into the brain to treat Alzheimer's disease. *Colloids Surf B Biointerfaces* 134, 88-97 (2015).

Intranasal administration of TAT conjugated lipid nanocarriers loading GDNF for Parkinson's Disease₄

Sara Hernando^{1#}, Enara Herran^{1,2#}, Joana Figueiro-Silva^{3,4}, José Luis Pedraz^{1,2}, Manoli Igartua^{1,2}, Eva Carro^{3,4}, Rosa Maria Hernandez^{1,2*}

¹NanoBioCel Group, Laboratory of Pharmaceutics, School of Pharmacy, University of the Basque Country (UPV/EHU), Vitoria-Gasteiz, 01006, Spain; ²Biomedical Research Networking Centre in Bioengineering, Biomaterials and Nanomedicine (CIBER-BBN), Vitoria-Gasteiz, 01006, Spain;

³Neuroscience Laboratory, Research Institute, Hospital 12 de Octubre, Madrid, Spain;

⁴Neurodegenerative Diseases Biomedical Research Centre (CIBERNED), Madrid, Spain.

*Corresponding author: Rosa Maria Hernandez

These two authors contributed equally to this work

⁴ Published in: Mol Neurobiol. (2018)

IF: 4.586 (Q1)

<https://doi.org/10.1007/s12035-017-0728-7>

Cat: Neuroscience

ABSTRACT

Parkinson's disease (PD) is the second most common neurodegenerative disorder (ND), characterized by the loss of dopaminergic neurons, microglial activation and neuroinflammation. Current available treatments in clinical practice cannot halt the progression of the disease. During the last few years, growth factors (GF) have been raised as a promising therapeutic approach to address the underlying neurodegenerative process. Among others, glial cell-derived neurotrophic factor (GDNF) is a widely studied GF for PD. However, its clinical use is limited due to its short half life, rapid degradation rate, and difficulties in crossing the blood brain barrier (BBB). Lately, intranasal administration has appeared as an alternative non-invasive way to bypass the BBB and target drugs directly to the central nervous system (CNS). Thus, the aim of this work was to develop a novel nanoformulation to enhance brain targeting in PD through nasal administration. For that purpose, GDNF was encapsulated into chitosan (CS)-coated nanostructured lipid carriers, with the surface modified with TAT peptide (CS-NLC-TAT-GDNF). After the physiochemical characterization of nanoparticles, the *in vivo* study was performed by intranasal administration to a 1-methyl-4-phenyl-1,2,3,6-tetrahydropyridine (MPTP) mouse model of PD. The CS-NLC-TAT-GDNF treated group revealed motor recovery which was confirmed with immunohistochemistry studies; showing the highest number of tyrosine hydroxylase (TH⁺) fibers in the striatum and TH⁺ neuron levels in the substantia nigra. Moreover, Iba-1 immunohistochemistry was performed, revealing that CS-NLC-TAT-GDNF acts as a modulator on microglia activation, obtaining values similar to control. Therefore, it may be concluded that the intranasal administration of CS-NLC-TAT-GDNF may represent a promising therapy for PD treatment.

Keywords: Parkinson's disease • nanostructured lipid carriers • glial derived neurotrophic factor (GDNF) • TAT peptide • neuroprotection

1. INTRODUCTION

Parkinson's disease (PD) is the second most common neurodegenerative disease (ND), affecting five million patients worldwide. Clinically it is characterized by resting tremor, bradykinesia, rigidity and postural instability. Non-motor features such as olfactory dysfunction, cognitive impairment, pain and sleep disorders are also common in early PD and are associated with reduced health related quality of life. Moreover, the pathological hallmarks of PD are progressive loss of dopaminergic neurons in the substantia nigra pars compacta (SNc) followed by decrease of dopamine (DA) and the presence of intraneuronal aggregations of abnormal protein alpha-synuclein (α -syn), called Lewy bodies (1-3). Neuroinflammation is another well-known feature of PD. Numerous studies have demonstrated the presence of an active inflammatory response in the brain mediated primarily by microglia and astrocytes. Microgliosis resulting from microglial activation occurs within the area of neurodegeneration, highlighting the link between neuroinflammation, PD and neuronal loss. Although the underlying mechanisms are not clear, it can be implied that reducing microglia activation is a reasonable target for neuroprotective therapies in PD (4-6).

Currently, the available treatments for PD focus on DA replacement to control motor symptoms. Although this approach can be initially effective in managing movement disorder symptoms, as the disease advances it is not useful in treating non-movement disorder symptoms. Moreover, side effects in long-term treatment (motor and non-motor fluctuations, dyskinesia and psychosis) are crucial challenges

in the clinical management of PD (3,7). This is why there is an urgent need of a disease modifying treatment capable of slowing down the progression of the disease. In an attempt to address neuronal degeneration, the use of growth factors (GF) has been raised as a promising alternative treatment. Among GFs, glial derived neurotrophic factor (GDNF) is known to be one of the most important for dopaminergic and motor neuronal survival due to its neuroprotective and neuroregenerative properties. However, GDNF's rapid degradation rate, structure, and molecular weight limits its ability to cross the blood brain barrier (BBB), making the search for alternative ways of bypassing the BBB necessary (8). In an attempt to deliver GDNF directly to the brain, intraventricular and intraparenchymal administrations have been proposed in both animals and human clinical trials, pointing out the therapeutic properties of this GF for PD (9-14). Lastly, due to the risks associated with these clinically less accepted administration routes, safer non-invasive ways have been proposed to reach the brain (15). Recent studies have described intranasal administration (i.n.) as a method to transport drugs directly to the central nervous system (CNS) through the olfactory and trigeminal pathways (16). Nevertheless, the disadvantages of this route of administration are the limited absorption across the nasal epithelium and the short residence time in the nasal cavity due to the mucociliary clearance; which leads to uncompleted drug absorption (17). In order to enhance the residence time in the nasal cavity, as well as protect these therapeutic proteins from being degraded, biodegradable nanocarriers have been used (18,19).

Moreover, the co-administration of nanoparticles (NP) with mucoadhesive polymers has shown to increase the contact time with nasal mucosa, hence, increasing brain concentrations. In fact, different experimental studies have confirmed the suitability of nanotechnology devices for target drug delivery to the CNS after i.n. administration. (20-26). In this regard, our research group developed chitosan (CS)-coated nanostructured lipid carriers (NLC) for the delivery of therapeutic proteins by i.n. administration. The NLC are improved second generation lipid carriers, derived from solid lipid nanoparticles (SLN), with higher entrapment efficiencies and a better safety profile. In this experimental research, CS-NLC was shown to be an effective nanocarrier for i.n. administration, obtaining brain targeting. However, less than expected concentrations of drug were obtained

in the brain (27). Thus, further modifications with this nanoformulation are needed in order to enhance CNS drug targeting after i.n. administration.

Another strategy to enhance NP target delivery into the brain is the use of cell-penetrating peptides (CPP). CPP are short amphipathic and cationic peptides which are rapidly internalized across cell membranes. They can be attached to the nanocarrier's surface in order to increase drug permeating efficiency and tissue targeting. Regarding nose-to-brain delivery, TAT and penetratin are well known CPP for enhancing CNS targeting. (28,29). Indeed, *Gartziandia et al.* confirmed the suitability of TAT modified lipid nanocarriers for nose-to-brain delivery in *in vitro* cell monolayers. Among the different studied formulations, TAT surface modified CS-NLC (CS-NLC-TAT) formulation exhibited the highest transport rate, confirming the appropriateness of this approach (30).

On the basis of the above mentioned results, the aim of this study was to assess the neuroprotective and neurorestorative potential of CS-NLC-TAT loading GDNF nanoformulation (CS-NLC-TAT-GDNF) intranasally administered to a MPTP (1-methyl-4-phenyl-1,2,3,6-tetrahydropyridine) mouse model of PD. Moreover, the ability of CS-NLC-TAT-GDNF to act as a regulator of the microglia activation process was studied due to the possible implication of this process in the pathogenesis of brain disorders associated with inflammation, such as PD.

2. MATERIALS AND METHODS

2.1 Materials

Precirol ATO[®]5 (glycerol disterate) and Mygliol[®] (caprylic/capric triglyceride) were a kind of gift from Gattefosé (France) and Sasol Germany GmbH, respectively. Tween 80 and Lutrol[®] F-68 (Poloxamer 188) were purchased from Panreac (Spain). Chitosan (CS) was obtained from NovaMatrix (Norway). Trehalose dihydrate, Triton X-110, 1-methyl-4-phenyl-1,2,3,6-tetrahydropyridine (MPTP), 3,3'-diaminobenzide (DAB), bovine serum albumin (BSA) and primary antibody anti-TH were acquired from Millipore Sigma Life Sciences (Germany). rhGDNF was purchased from Peptotech (UK), Depex mounting medium from BDH Gum[®] (UK), avidin-biotin-peroxidase complex (ABC kit) and DAPI mounting medium from Palex (Spain). Anti-rabbit Alexa fluor IgG 488 was purchased from Invitrogen[®] and Isoflurane Esteve from Maipe Comercial (Spain). Finally, TAT was obtained from ChinaPeptides.

2.2 CS-NLC-TAT-GDNF preparation

NLC were prepared using a previously described melt-emulsification technique (27). Firstly, a mixture of solid and liquid lipids (Precirol ATO[®] 5 2.5%, w/v and Mygliol[®] 0.25 % w/v) with GDNF (0.15%, w/v) were melted 5°C above their melting point (56°C). Then, an aqueous solution containing the surfactant combination of Tween 80 (3%, w/v) and Poloxamer 188 (2%, w/v) was heated at the same temperature to be added to the lipid phase under continuous stirring, for 60 seconds and at 50W (Bradson[®] Sonifier 250). The resulting emulsion was maintained with magnetic stirring for 15 minutes (min) at room temperature (RT) and immediately cooled at 4-8°C overnight to obtain the NLCs formation due to lipid solidification.

Prior to the NLC coating process, TAT was covalently linked to CS by a surface activation method previously described by our research group (30,31). Briefly, 250 μ l EDC (1-ethyl-3-(3-dimethylaminopropyl)carbodiimide hydrochloride) in solution (1mg/ml) and 250 μ l of sulfo NHS (*N*-hydroxysulfosuccinimide) in 0.02M phosphate buffered saline (PBS) were added dropwise to a 4 ml CS solution (0.5% w/v, in PBS 0.02M), under magnetic stirring (2 h at RT). For the coupling of TAT, 250 μ l TAT solution (1mg/ml) in PBS (0.02M; pH 7.4) was added dropwise to the activated CS, under gentle agitation. The TAT-CS solution was maintained under agitation for another 4 h at RT and then incubated 4°C overnight. The next day, the NLC were coated with TAT-CS; NLC dispersion previously prepared was added dropwise to the TAT-CS solution under continuous agitation for 20 min at RT. After the coating process, CS-NLC-TAT nanoformulation was centrifuged in Amicon filters (Amicon, "Ultracel-100k", Millipore, USA) at 908 G (MIXTASEL, P Selecta, Spain) for 15 min, washed three times with Milli Q water. Finally the nanoformulation was freeze-dried with the cryoprotectant trehalose at a final concentration of 15% (w/w) of the weighed lipid, and then it was lyophilized for 42 h (LyoBeta 15, Telstar, Spain).

2.3 NLC characterization: particle size, zeta potential, morphology and encapsulation efficiency

The mean particle size (Z-average diameter) and the polydispersity index (PDI) were measured by Dynamic Light Scattering (DLS), and the zeta potential was determined through Laser Doppler micro-electrophoresis (Malvern[®] Zetasizer Nano ZS, Model Zen 3600; Malvern instruments Ltd, UK). Three replicate analyses were

performed for each formulation. The data are represented as the mean \pm SEM. Nanoparticle surface characteristics and morphology were examined by transmission electron microscopy (JEOL JEM 1400 Plus).

The encapsulation efficiency (EE) of the NLC was determined by an indirect method, in which we measured the non-encapsulated GDNF presented in the supernatant obtained after the filtration/centrifugation process described in Materials. The EE (%) was determined by GDNF E_{max}[®] ImmunoAssay System (Promega Corporation, Madison, USA) and calculated using the following equation:

$$EE (\%) = \frac{\text{total GDNF content} - \text{free amount of GDNF}}{\text{total GDNF content}} \times 100$$

2.4 Animal model and treatments

Nine week-old male C57BL/6J mice supplied from Charles River Laboratory (Charles River, L'Arbresle, France) were used to produce the MPTP parkinsonian model. Mice were housed in standard conditions with a constant temperature of 22°C, a 12-h dark/light cycle and *ad libitum* access to water and food. All experimental procedures were performed in compliance with the Ethical Committee of Animal Welfare (CEBA) at the PROEX 343/14.

The MPTP lesion was carried out as described in previous reports (32,33). Fifty-three mice were used, 5 of which were treated with the saline solution as negative control. The other 48 were treated with the neurotoxin MPTP (30 mg/kg) intraperitoneally (i.p.) administered at 24 h intervals for five consecutive days in order to obtain a PD animal model for testing the different formulations. At the same time the lesion protocol was initiated the animals were divided into 7 groups (n=6). They got the following treatments on alternate days during 3 weeks, through nasal administration: negative control saline solution (saline i.p + saline i.n.), positive control saline solution (MPTP i.p + saline i.n.), GDNF (MPTP i.p + GDNF i.n.), empty CS-NLC (MPTP i.p + empty CS-NLC i.n.), CS-NLC-GDNF (MPTP i.p + CS-NLC-GDNF i.n.) and CS-NLC-TAT-GDNF (MPTP i.p + CS-NLC-TAT-GDNF i.n.) (Table 1). Mice were anesthetized with isoflurane and maintained in a supine position before the intranasal administration was realized. The corresponding treatments were suspended in 20 μ l of PBS for being administered to alternating nostrils (4 administrations of 2.5 μ l per nostril, leaving 3 minutes between administrations)

using an automatic micropipette. The final dose of GDNF after the three weeks treatment was 2.5 μ g per each animal group.

Table 1. Different experimental groups to perform the *in vivo* assay.

GROUP	TREATMENT	MPTP (+/-)
Control	Saline solution (0.9% w/v)	-
MPTP	Saline solution(0.9% w/v)	+
GDNF	2.5 μ g GDNF	+
CS-NLC blank	CS-NLC	+
CS-NLC-GDNF	CS-NLC-GDNF (2.5 μ g GDNF)	+
CS-NLC-TAT-GDNF	CS-NLC-TAT-GDNF(2.5 μ g GDNF)	+

2.5 Locomotor activity: Rotarod test

Locomotor activity of mice was assessed in a Rotarod apparatus (Ugo Basile, Italy) with increasing acceleration. The apparatus consisted of a horizontal motor-driven rotating rod in which the animals were placed perpendicular to the long axis of the rod. The mouse head was directed against the direction of rotation, so that the mouse has to progress forward to avoid falling. Once the animal has been positioned in the axis the test ends when the animal fell or after a maximum of 5 min. The time spent on the rotating rod was recorded for each animal and trial. On the test day each mouse is submitted to 5 consecutive trials with an interval of 30 min between each trial. However, the first 4 trials are discarded since they are pre-training sessions to familiarize mice with the procedure. Only the results from the fifth trial for each animal were used for statistical comparisons. The animals were tested in the locomotor activity assay before they were lesioned with MPTP, in the second and third week during the treatment and before they were sacrificed (Fig. 1).

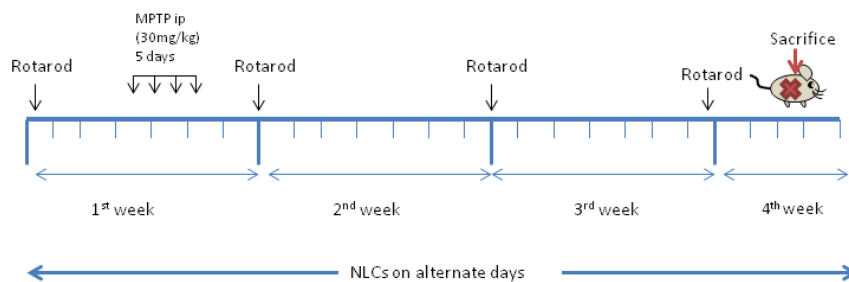


Fig. 1 Schematic illustration of *in vivo* assay

2.6 Tyrosine hydroxylase (TH) immunohistochemistry

Mice were transcardially perfused with 0.9% (w/v) and 4% (v/v) paraformaldehyde in 0.1 M PBS, pH 7.4. The brains were removed and post-fixed for 72 h in paraformaldehyde and then transferred to a PBS solution (0.1 M) for conservation and subsequent analysis. Hereafter, the fixed brains were coronally cut on a vibratome (Leica Microsystem) at 30 μ m, and batches of 6 tissue sections were collected in cold PBS with azide at 0.1% for further examination.

After selecting the brain areas of striatum (ST) and substantia nigra (SN), the TH⁺ (tyrosine hydroxylase positive) immunohistochemistry assay was performed. Fixed brain sections were washed with 0.1 M PBS. Endogenous peroxidases were quenched using 1% (v/v) H₂O₂ and 1% (v/v) ethanol in PBS, for 15 min at RT. After rinsing, brain sections were blocked with 2% BSA, 0.5% Triton-X in PBS. Then, they were incubated with primary antibody rabbit anti-tyrosine hydroxylase (1:2000) overnight under constant agitation at 4°C. The following day, brain slices were incubated with secondary biotinylated antibody (1:250) for 1 h. All brain sections were processed with an ABC kit for 90 min, and the reaction was visualized using DAB as the chromogen. Finally, slices were mounted on gelatin-coated slides, dehydrated, and mounted with fixed DPX medium.

2.7 Iba-1 immunohistochemistry

After selecting the brain areas of ST and SN, Iba-1 (ionizing calcium-binding adaptor molecule 1) immunohistochemistry was performed. Fixed brain sections were blocked with 2% (w/v) BSA solution and 0.5% (w/v) Triton-X in PBS. After rinsing, they were incubated in primary antibody Iba-1 (1:1000, Wako) overnight at 4°C. The following day brain slices were incubated with the secondary antibody: anti-rabbit Alexa Fluor IgG 488 (1:1000) in PBS with 0.1% BSA and 0.1% Triton-X for 2 h. Then the slices were washed and mounted on gelatin-coated slides and coverslipped with mounting medium with DAPI.

2.8 Integrated optical densitometry (IOD) of ST

The optical density of ST TH⁺ immunoreactive dopaminergic fibers was measured using a computerized analysis system (Image J), reading optical densities as grey levels. Images from sections including ST were taken at a 3200 ppp resolution digital scan (HP Photosmart C7200). The IOD reading was corrected for background

staining by subtracting the values of an area outside of the ST. Every sixth striatal section was immunolabeled for TH and a total of six sections were analyzed per animal.

2.9 Number of TH⁺ neurons in SN

The total number of TH⁺ neurons in SN was estimated by an unbiased stereology method. Images were taken using an inverted microscopy (Eclipse model TE2000-S, Nikon) at 20x magnification. Uniform, randomly chosen slices through the SN /every sixth section were analyzed for the total TH⁺ neurons in each mouse. TH⁺ neurons were scored as positive if their cell-body image included well defined nuclear counterstaining.

2.10 Iba-1 immunohistochemistry evaluation in ST and SN.

The analysis of activated microglia cells was performed by an unbiased stereology method similar to that described in the paragraph above. Images were taken using light microscopy (Leica TCS SP2 AOBS Spectral Confocal Scanner mounted on a Leica DM IRE2 inverted fluorescent microscope) at 20x magnification. Uniform, randomly chosen slices through the SN and ST /every sixth section were analyzed for the total of activated microglia cells in each mouse. Microglia cells were scored as positive if their cell-body image included well defined nuclear counterstaining. The images were processed with Image J win-64 Fiji.

2.11 Statistical analysis

Results are expressed as mean \pm SEM. Experimental data were analyzed using GraphPad Prism (v. 6.01, GraphPad Software, Inc.) One-way ANOVA was used for TH⁺ histological analysis evaluation. Student's t-test was applied for behavioral data and Iba-1 immunohistochemistry results, in both ST and SN. P values <0.05 were considered significant.

3. RESULTS

3.1 Nanoparticle characterization

As shown in Fig. 2, all formulations had a similar mean size. Moreover, they all exhibited positive zeta values, which indicated the CS coating process was successful. Regarding encapsulation efficiency, there were no statistically significant differences between both formulations, being about 87% for both of them.

In the external morphological study made by TEM, the nanoparticles showed uniform size without abnormalities.

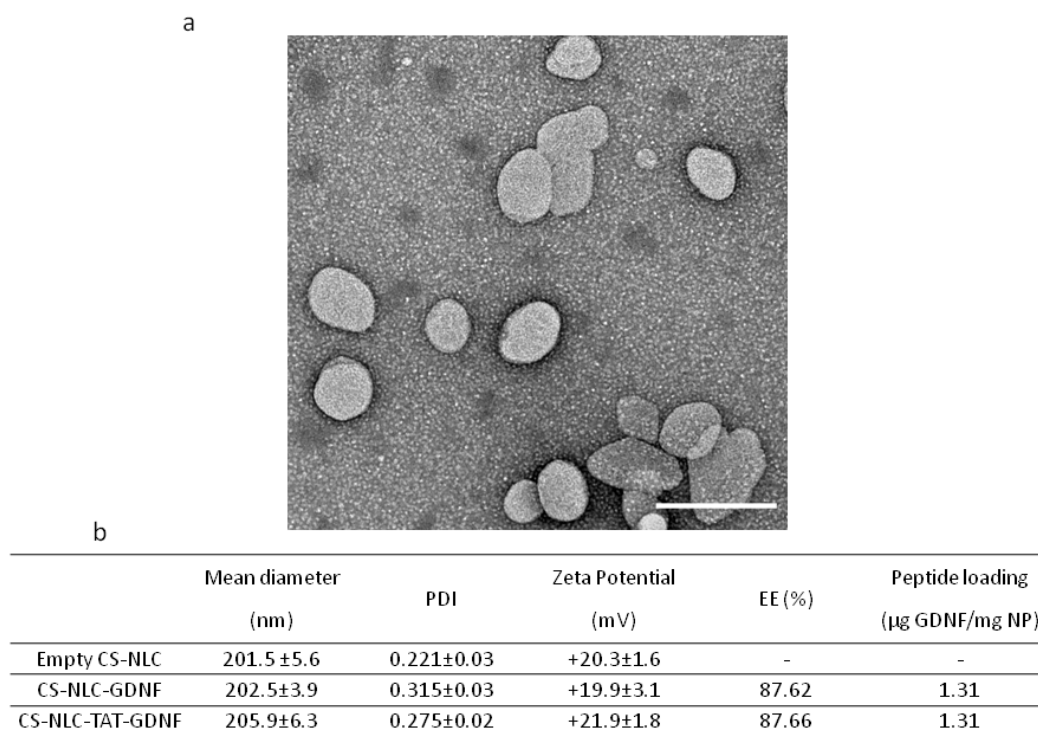


Fig. 2 (a) TEM photographs of NLC (scale bar 200nm). (b) Characterization of NLCs: mean size, PDI, zeta potential, EE (%) and peptide loading. Data are shown as the mean \pm SEM.

3.2 Study of locomotor activity in MPTP treated mice

In order to assess the capability of CS-NLC-TAT-GDNF to restore MPTP-induced locomotor impairment, the Rotarod test was performed (Fig. 3). Moreover, this test confirmed the suitability of the MPTP animal model; given that the administration of this toxin led to a statistically significant impairment on motor performance from the second week until the end of the study: MPTP (week 2: 37.17 \pm 6.1; week 3: 34.2 \pm 5.7; week 4: 44.8 \pm 6.7) vs Control (week 2: 93.8 \pm 26.3; week 3: 118.4 \pm 59.9; week 4: 107.3 \pm 21.84).

On the other hand, as shown in Fig. 3, the administration of CS-NLC-TAT-GDNF led to a significant improvement of the locomotor activity since this lipid NP administration was initiated. Whereas other groups exhibited a more attenuated recovery, mice treated with CS-NLC-TAT-GDNF displayed a statistically significant increase in motor performance since the beginning of the study at week 2

(191.8 ± 21.9 ; $^*p < 0.05$). This recovery was constant for the duration of the test; week 3 (175.3 ± 35.9 ; $^*p < 0.05$) and week 4 (176.4 ± 38.8 ; $^*p < 0.05$). The values of this group are comparable to the Control group. Although GDNF and CS-NLC-GDNF produce an improvement in locomotor activity, it was not statistically significant in any of the three weeks.

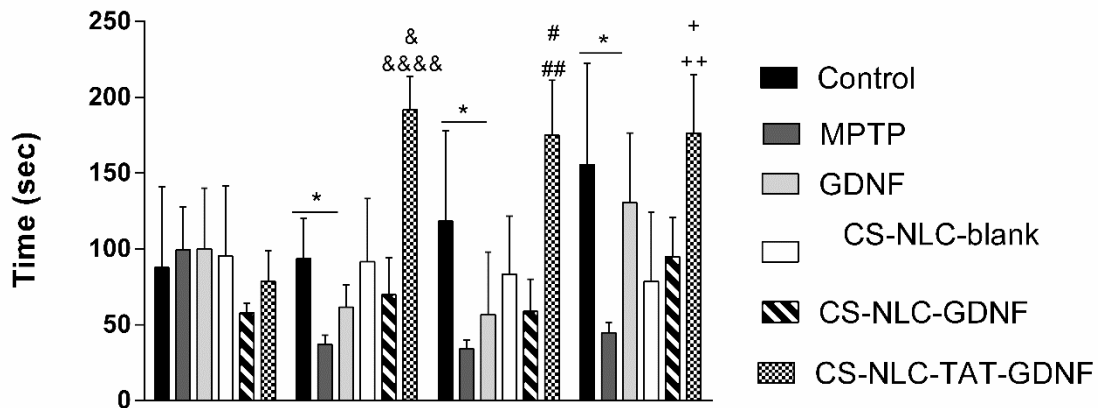


Fig. 3 Graphical representation of the data obtained from Rotarod test before and after MPTP administration, and treated with different formulations. The Rotarod test was performed before the MPTP lesion, at the second and third week after the lesion, and before sacrifice. The data are shown as the mean \pm SEM. ($^*p < 0.05$ Control vs MPTP ; $^{\&\&\&}p < 0.0001$ CS-NLC-TAT-GDNF vs MPTP ; $^{\&}p < 0.05$ CS-NLC-TAT-GDNF vs CS-NLC-blank, CS-NLC-GDNF; $^{\#\#}p < 0.05$ CS-NLC-TAT-GDNF vs MPTP; $^*p < 0.05$ CS-NLC-TAT-GDNF vs CS-NLC-blank; $^{++}p < 0.01$ CS-NLC-TAT-GDNF vs MPTP, CS-NLC-blank; $^+p < 0.05$ CS-NLC-TAT-GDNF vs CS-NLC-GDNF).

3.3 Histological evaluation

In addition to behavioral studies, immunohistochemical techniques were also used to analyze the efficacy of the treatments in a PD mouse model. For this purpose, three weeks after the treatment started, the animals were sacrificed in order to examine the presence of dopaminergic structures in both ST and SN. Fig. 4 (a-g) shows representative photomicrographs of TH immunostain in ST of the different treatment groups. It is remarkable the degeneration of TH⁺ fibers in the ST after MPTP administration (MPTP 93.22 ± 4.1 vs Control 136.1 ± 8.8 ; $^{\% \% \% \%}p < 0.05$), confirming the success of the lesion. The administration of GDNF did not statistically increase the density of TH fibers, (108.6 ± 5.03 ; $p > 0.05$) neither did the administration of CS-NLC-GDNF (88.64 ± 3.1 ; $p > 0.05$). In contrast, the administration of CS-NLC-TAT-GDNF resulted in the highest regeneration of TH⁺ fibers (141.18 ± 5.68 ; $^{\% \% \% \%}p < 0.05$).

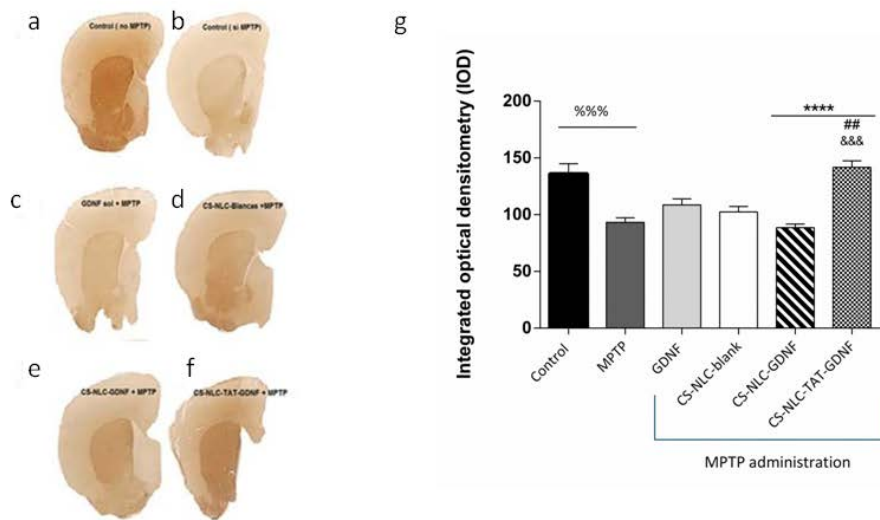


Fig. 4 Histological evaluation of the striatum. Representative photomicrographs of TH immunostain in ST in all mice groups: MPTP (a), Control (b), GDNF (c), CS-NLC-blank (d), CS-NLC-GDNF (e), CS-NLC-TAT-GDNF (f). The integrated optical density (IOD) of TH⁺ fibers in the ST of all groups (g). The data are shown as the mean \pm SEM. (%%% $p < 0.05$ Control vs MPTP; **** $p < 0.05$ CS-NLC-TAT-GDNF vs MPTP, CS-NLC-GDNF; &&& $p < 0.05$ CS-NLC-TAT-GDNF vs CS-NLC-blank; ## $p < 0.05$ CS-NLC-TAT GDNF vs GDNF, one way ANOVA).

On the other hand, the percentage of recovery of TH⁺ positive neurons was analyzed in the SN (Fig. 5). As in the ST, the percentage of TH⁺ neurons decreased after MPTP administration (25.02 ± 2.26 ; **** $p < 0.05$) compared to control, ratifying the lesion made by the parkinsonizing agent. The exogenous administration of GDNF did not statically increase the percentage of TH⁺ neurons. However, the encapsulation of this GF statically increased the percentage of TH⁺ neurons in both formulations (CS-NLC-GDNF and CS-NLC-TAT-GDNF). Moreover, the highest recovery of TH⁺ neurons was observed in the group of animals treated with CS-NLC-TAT-GDNF (91.46 ± 7.54 ; ##### $p < 0.05$), which is in accordance with the results obtained in the ST.

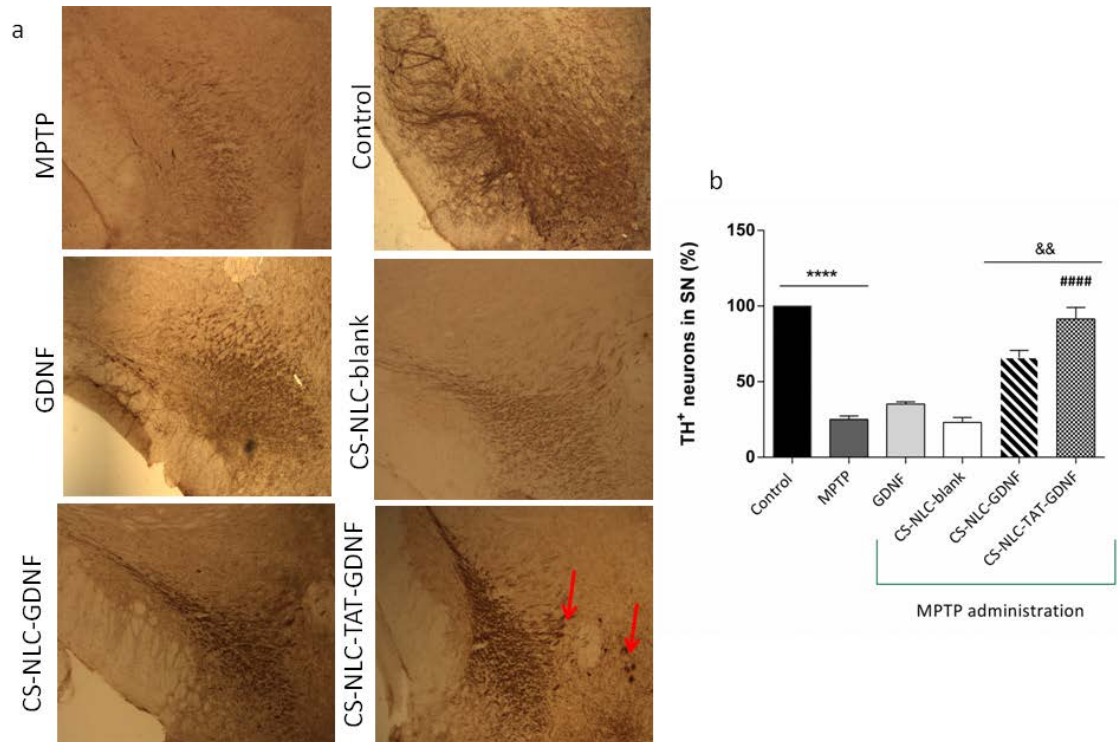


Fig. 5 Histological evaluation of the SN. Representative photomicrographs of TH immunostain in SN in all groups (a): MPTP, Control, GDNF, CS-NLC-blank, CS-NLC-GDNF, CS-NLC-TAT-GDNF. (b) TH⁺ neurons in SN (%). The data are shown as the mean \pm SEM. (**** p <0.05 Control vs MPTP; #### p <0.05 CS-NLC-TAT-GDNF vs MPTP, GDNF and CS-NLC-blank; && p < 0.05 CS-NLC-TAT-GDNF vs CS-NLC-GDNF, One-way ANOVA).

3.4 Microglial activation evaluation

Iba1 immunohistochemistry was performed in order to check the ability of our novel nanoformulation to decrease the number of activated microglia in both ST and SN (Fig. 6). First, the potential microglial toxicity of MPTP was confirmed in both ST and SN. Indeed, the number of activated microglia was markedly increased in ST; (144.8 ± 3.2 ; **** p < 0.0001) and in the SN it was almost duplicate; (188.1 ± 4.1 ; **** p < 0.0001).

Moreover, as seen in Fig. 6, the number of activated microglia after GDNF treatment (148.2 ± 3.2) is similar to that obtained after MPTP administration; therefore, the free GDNF administration did not produce a therapeutic effect as it did not decrease the level of activated microglia. However, when this GF was encapsulated into CS-NLC (CS-NLC-GDNF) the number of activated microglia was significantly decreased (105.6 ± 5.2 ; #### p <0.0001). In addition, in the group treated with CS-NLC-TAT-GDNF, activated microglia levels were still lower ($99.43.0 \pm 4.25$; #### p <0.0001). Although no significant differences were seen between these two

formulations (CS-NLC-GDNF vs CS-NLC-TAT-GDNF), a downward trend was observed.

Regarding the results obtained in SN, the tendency seen in the number of activated microglia is similar to the outcome achieved in ST. GDNF did not decrease the number of activated microglia (172.4 ± 6.4), but as we have previously pointed out in ST, the encapsulation into CS-NLC (CS-NLC-GDNF) led to a decrease of activated microglia levels (124.3 ± 3.2 ; $####p < 0.0001$). Contrary to the results obtained in ST, the CS-NLC-TAT-GDNF group exhibited a statistically significant decrease vs the CS-NLC-GDNF treated group ($&p < 0.05$), with the lowest levels of activated microglia (107.0 ± 6.2 ; $####p < 0.0001$).

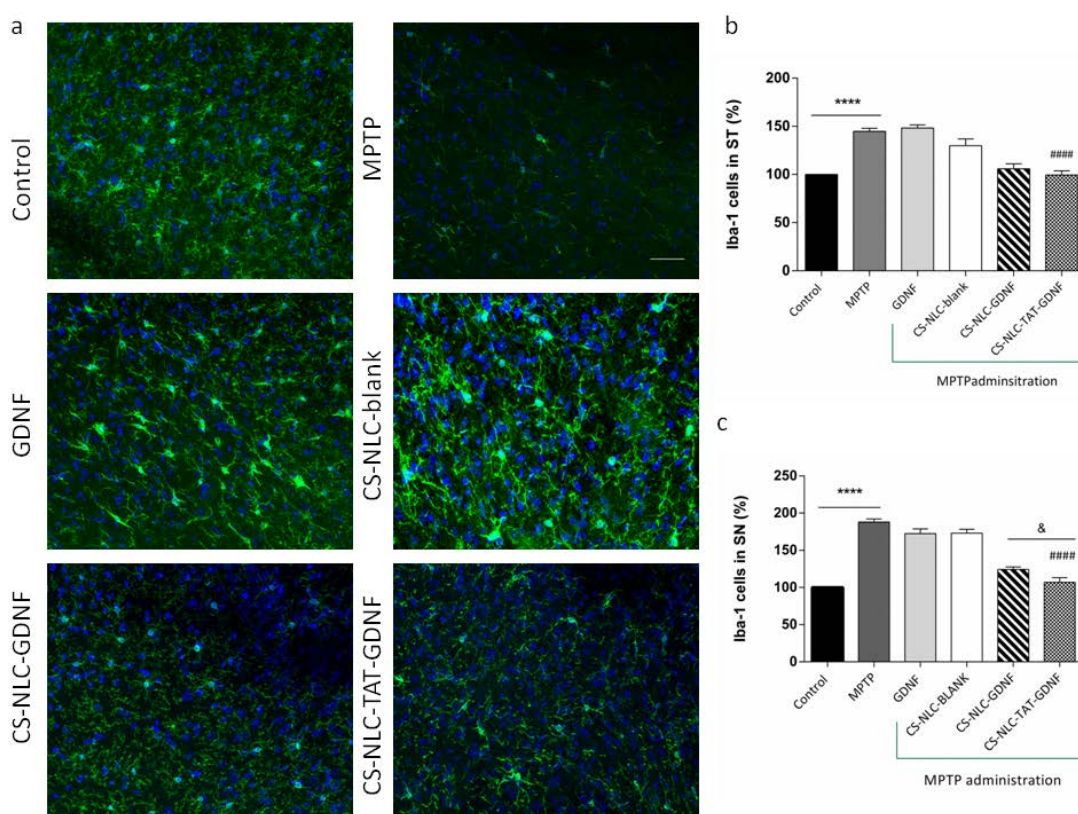


Fig. 6 Histological evaluation of activated microglia cells in both ST and SN. (a) Representative Iba-1 immunophotographs of all mice groups in the SN. (Control, MPTP, GDNF, CS-NLC-blank, CS-NLC-GDNF and CS-NLC-TAT-GDNF). (scale bar $50\mu\text{M}$) (b) Iba-1 cells in ST of all mice groups (%). The data are shown as the mean \pm SEM. ($****p < 0.0001$ MPTP vs. Control; $####p < 0.0001$ CS-NLC-TAT-GDNF vs MPTP and GDNF, Student's *t*-test) (c) Iba-1 cells in SN of all mice groups (%). The data are shown as the mean \pm SEM. ($****p < 0.001$ MPTP vs. Control, $####p < 0.0001$ CS-NLC-TAT-GDNF vs MPTP, GDNF and CS-NLC-blank; $&p < 0.05$ CS-NLC-TAT-GDNF vs CS-NLC-GDNF, Student's *t*-test).

4. DISCUSSION

Despite all the efforts made by the scientific community to obtain an effective therapy for PD, current available treatments cannot halt the progression of this disorder. In an attempt to address the neurodegenerative process, different disease modifying treatments are under investigation (34). Among others, GFs and specially the use of GDNF is particularly promising since it exhibits efficacy in the upregulation of the neurological mechanism involved in neurogenic processes, and therefore, modulates the progression of the disease (8). However, the hydrophilic nature of GDNF makes it difficult to cross the BBB, and for that reason, in the past few years numerous researchers have developed different nano and micro formulations loading GDNF as an approach for PD treatment (35-39). However, the invasive routes of administration used involve some risk which makes its translation to clinical practice difficult. In order to avoid them, new administration routes are under investigation, such as i.n. administration. In an attempt to increase the mucosal contact time and extend the residence time in the nasal cavity, NPs can be coated with mucoadhesive substances, such as CS. Many studies published in the past few years have developed CS-coated nanoparticles for the brain delivery of different drugs. Although in all these studies the obtained brain concentrations of drugs were less than desired, they were enough to obtain a significant pharmacodynamic effect (22,26,27,40). In light of these encouraging results, further modifications of nanoparticle surface should enhance brain concentrations, maximizing the therapeutic effect of this drug. Accordingly, in the present study a previously developed CS-NLC was coated with TAT peptide in light of our previous studies in *in vitro* cell monolayers, which confirmed the suitability of CS-NLC-TAT for nose-to-brain drug delivery (30). Thus, in the present work GDNF was encapsulated into TAT modified lipid nanocarriers (CS-NLC-TAT-GDNF) in order to enhance brain targeting.

Nanoparticle physicochemical characterization revealed values similar to those reported by us in previous work (30,40). Hereafter, the *in vivo* study was performed to prove the efficacy of our novel formulation by i.n. administration. For that main purpose, a MPTP animal model of PD was used. This model includes apoptotic cell death of DA neurons located in SNc and loss of striatal TH⁺ fibers. Moreover, this MPTP animal model mimics the clinical cardinal symptoms of PD in humans. For all

these reasons it is considered the gold standard animal model to screen neuroprotective and neurorestorative treatments for PD (33,41,42).

The Rotarod Test evidenced motor recovery soon after CS- NLC-TAT-GDNF i.n. administration and exhibited the best levels until the end of the study. In contrast, GDNF did not statistically improve the behavioral activity and neither did CS-NLC-GDNF, although a slight recovery can be seen. This finding was unexpected, since in our previous work the administration of CS-NLC-GDNF has been shown to reach the brain and improve locomotor activity (40). However, it should be noted that both the animal model and the administration frequency is different in this study. Indeed, in this research we used an MPTP mouse model with treatment on alternate days. In contrast, in the previous work, 6-hydroxydopamine partially lesioned rats with daily administration of CS-NLC-GDNF were used to assess the neuroprotective activity of the treatment.

In addition, the histological evaluation of the brains was performed. The injection of MPTP is directly related with degeneration of dopaminergic neurons; which means low density of TH⁺ structures in ST and SN, as seen in the results (Fig. 4, Fig. 5). The exogenous administration of GDNF did not lead to a statistically significant increase in either in the ST or SN. Indeed, it is a known fact that GDNF is a peptide which has difficulty crossing the BBB so it needs to be directly administered into the CNS (43). This is probably why the i.n. administration of this GF did not exhibit any therapeutic effect in this study. However, the CS-NLC-TAT-GDNF treated group increased the level of TH⁺ structures in both ST and SN, highlighting the improvement with GDNF brain targeting obtained after the lipid nanoparticle coated process with CS and TAT. Furthermore, the group treated with CS-NLC-GDNF did not increase TH⁺ fibers as expected, especially in ST, in light of *Gartziandia et al.* findings (40). As noted before, not only the animal model but also the administration frequency was different in this new *in vivo* assay, so it is difficult to extrapolate these results and make a reliable comparison. In any case, in the present study we determined that the surface modification with TAT maximized the therapeutic benefits of GDNF, inducing histological recovery not only in the SN but also in ST (28,29).

To date, investigations with GDNF for PD treatment have focused on the neuroprotective and neurorestorative potential of this GF. However, recently it has been highlighted the therapeutic effect of GDNF modulating microglial activation

process in the disease. Indeed, microglia mediated neuroinflammation has gained much attention in the development of PD and its treatment seems to be a key therapeutic option to prevent the progression of the neurodegenerative process. In the last few years research studies with primary rat microglia cultures and mouse microglial cell lines have demonstrated that GDNF decreases the synthesis and release of proinflammatory and neurotoxic molecules (44-46). Therefore, the exogenous administration of GDNF may not only have a protective effect on neurons, but may also modulate microglial activities to exert its therapeutic effect.

That is why in the present study, Iba-1 immunostaining was performed to assess the potential of the CS-NLC-TAT-GDNF formulation to decrease microglial activation in a MPTP mouse model of PD. Among different neurotoxic molecules, MPTP is known to produce an increase in microglial activation; which has been confirmed in monkeys, mice and even in humans (47-49). The data obtained in this study are in accordance with these results, since the subchronic administration of MPTP led to a statistically significant increase in the number of activated microglial cells. Moreover, microscopic photographs (Fig. 6) also illustrated the MPTP induced microglia activation.

The administration of GDNF did not decrease the activation of microglial cells. However, when encapsulated into surface modified lipid nanocarriers, the number of microglial activated cells decreased almost to control levels. These results were observed in both ST and SN. Moreover, the administration of CS-NLC-TAT-GDNF in SN was statistically significant when compared with CS-NLC-GDNF, which confirmed not only the suitability of the CS coating process but also the surface modification with TAT to bypass the BBB. Additionally, microglia is more numerous in the SN than in adjacent structures of the brain, resulting in an increase in apoptotic biomarkers and cytokines levels. These findings are supported by studies in both PD animal models and Parkinson's patients (50,51). Therefore, our results are encouraging since the exogenous administration of GDNF, encapsulated into our novel nanoformulation, targets microglia activation, modulating the neuroinflammatory component of PD.

5. CONCLUSION

Taking all these results into account, we can conclude that the *in vivo* administration of CS-NLC-TAT-GDNF improves the nose-to-brain delivery of GDNF. Both the behavioral studies and the immunohistochemistry data have confirm that i.n. administration of our novel nanoformulation may be a promising treatment for PD. In addition, the exogenous administration of GDNF in these biodegradable nanocarriers has demonstrated to reduce microgliosis in a MPTP mouse model of the disease. Although further studies are needed to ensure these findings, all in all it can be concluded that this nanoformulation approach is a step forward in PD therapy.

6. ACKNOWLEDGMENTS

This project was partially supported by the “Ministerio de Economía y Competitividad” (SAF2013-42347-R), the University of the Basque Country (UPV/EHU) (UFI 11/32) and FEDER funds. The authors thank SGIker of UPV/EHU and European funding (ERDF and ESF) for technical and human support. The authors also wish to thank the intellectual and technical assistance from the ICTS “NANBIOSIS”, more specifically by the Drug Formulation Unit (U10) of the CIBER-BBN at the UPV/EHU.

7. REFERENCES

1. Lees A.J., Hardy J Revesz T. (2009) Parkinson's disease. 373: 2055-66. doi: [http://dx.doi.org/10.1016/S0140-6736\(09\)60492-X](http://dx.doi.org/10.1016/S0140-6736(09)60492-X).
2. Nussbaum R.L., Ellis C.E (2003) Alzheimer's Disease and Parkinson's Disease. *N. Engl. J. Med.* 348: 1356-64. doi: 10.1056/NEJM2003ra020003.
3. Kalia L.V. and Lang AE (2015) Parkinson's disease. *The Lancet.* 386: 896-912. doi: [http://dx.doi.org/10.1016/S0140-6736\(14\)61393-3](http://dx.doi.org/10.1016/S0140-6736(14)61393-3).
4. Hirsch E.C. and Hunot S (2009) Neuroinflammation in Parkinson's disease: a target for neuroprotection? *The Lancet Neurology.* 8: 382-97. doi: [http://dx.doi.org/10.1016/S1474-4422\(09\)70062-6](http://dx.doi.org/10.1016/S1474-4422(09)70062-6).
5. Joers V., Tansey M.G., Mulas G., Carta A.R (2016) Microglial phenotypes in Parkinson's disease and animal models of the disease. *Prog. Neurobiol.* [Epub ahead of print] . doi: <http://dx.doi.org/10.1016/j.pneurobio.2016.04.006>.
6. Long-Smith CM, Sullivan AM, Nolan YM (2009) The influence of microglia on the pathogenesis of Parkinson's disease. *Prog. Neurobiol.* 89: 277-87. doi: <http://dx.doi.org/10.1016/j.pneurobio.2009.08.001>.
7. Oertel W, Schulz JB (2016) Current and experimental treatments of Parkinson disease: A guide for neuroscientists. *J. Neurochem.* 139 Suppl 1: 325-37. doi: 10.1111/jnc.13750 [doi].

8. Allen SJ, Watson JJ, Shoemark DK, Barua NU, Patel NK (2013) GDNF, NGF and BDNF as therapeutic options for neurodegeneration. *Pharmacol. Ther.* 138: 155-75. doi: <http://dx.doi.org/10.1016/j.pharmthera.2013.01.004>.
9. Sullivan AM, Toulouse A (2011) Neurotrophic factors for the treatment of Parkinson's disease. *Cytokine Growth Factor Rev.* 22: 157-65. doi: <http://dx.doi.org/10.1016/j.cytogfr.2011.05.001>.
10. Lapchak PA, Gash DM, Jiao S, Miller PJ, Hilt D (1997) Glial Cell Line-Derived Neurotrophic Factor: A Novel Therapeutic Approach to Treat Motor Dysfunction in Parkinson's Disease. *Exp. Neurol.* 144: 29-34. doi: <http://dx.doi.org/10.1006/exnr.1996.6384>.
11. Gill SS, Patel NK, Hotton GR, O'Sullivan K, McCarter R, Bunnage M, Brooks DJ, Svendsen CN, Heywood P (2003) Direct brain infusion of glial cell line-derived neurotrophic factor in Parkinson disease. *Nat. Med.* 9: 589-95. doi: 10.1038/nm850 [doi].
12. Lang AE, Gill S, Patel NK, Lozano A, Nutt JG, Penn R, Brooks DJ, Hotton G, Moro E, Heywood P, Brodsky MA, Burchiel K, Kelly P, Dalvi A, Scott B, Stacy M, Turner D, Wooten VG, Elias WJ, Laws ER, Dhawan V, Stoessel AJ, Matcham J, Coffey RJ, Traub M (2006) Randomized controlled trial of intraputamenal glial cell line-derived neurotrophic factor infusion in Parkinson disease. *Ann. Neurol.* 59: 459-66. doi: 10.1002/ana.20737 [doi].
13. Nutt JG, Burchiel KJ, Comella CL, Jankovic J, Lang AE, Laws ER, Jr, Lozano AM, Penn RD, Simpson RK, Jr, Stacy M, Wooten GF, ICV GDNF Study Group. Implanted intracerebroventricular. Glial cell line-derived neurotrophic factor (2003) Randomized, double-blind trial of glial cell line-derived neurotrophic factor (GDNF) in PD. *Neurology.* 60: 69-73.
14. Salvatore MF, Ai Y, Fischer B, Zhang AM, Grondin RC, Zhang Z, Gerhardt GA, Gash DM (2006) Point source concentration of GDNF may explain failure of phase II clinical trial. *Exp. Neurol.* 202: 497-505. doi: S0014-4886(06)00430-4 [pii].
15. Tajes M, Ramos-Fernandez E, Weng-Jiang X, Bosch-Morato M, Guivernau B, Eraso-Pichot A, Salvador B, Fernandez-Busquets X, Roquer J, Munoz FJ (2014) The blood-brain barrier: structure, function and therapeutic approaches to cross it. *Mol. Membr. Biol.* 31: 152-67. doi: 10.3109/09687688.2014.937468 [doi].
16. Djupesland PG, Messina JC, Mahmoud RA (2014) The nasal approach to delivering treatment for brain diseases: an anatomic, physiologic, and delivery technology overview. *Ther. Deliv.* 5: 709-33. doi: 10.4155/tde.14.41 [doi].
17. Costantino HR, Illum L, Brandt G, Johnson PH, Quay SC (2007) Intranasal delivery: Physicochemical and therapeutic aspects. *Int. J. Pharm.* 337: 1-24. doi: <http://dx.doi.org/10.1016/j.ijpharm.2007.03.025>.
18. Re F, Gregori M, Masserini M (2012) Nanotechnology for neurodegenerative disorders. *Maturitas.* 73: 45-51. doi: <http://dx.doi.org/10.1016/j.maturitas.2011.12.015>.
19. Shah B, Khunt D, Bhatt H, Misra M, Padh H (2015) Application of quality by design approach for intranasal delivery of rivastigmine loaded solid lipid nanoparticles: Effect on formulation and characterization parameters. *Eur J Pharm Sci* 78: 54-66. doi: <http://dx.doi.org/10.1016/j.ejps.2015.07.002>.
20. Sumit Sharma, Shikha Lohan & R. S. R. Murthy (2013) Formulation and characterization of intranasal mucoadhesive nanoparticulates and thermo-reversible gel of levodopa for brain delivery. *Drug Dev Ind Pharm.* 40 (7): 869-78 <http://dx.doi.org/10.3109/03639045.2013.789051>
21. Zhang C, Chen J, Feng C, Shao X, Liu Q, Zhang Q, Pang Z, Jiang X (2014) Intranasal nanoparticles of basic fibroblast growth factor for brain delivery to treat Alzheimer's disease. *Int. J. Pharm.* 461: 192-202. doi: <http://dx.doi.org/10.1016/j.ijpharm.2013.11.049>.

22. Md S, Khan RA, Mustafa G, Chuttani K, Baboota S, Sahni JK, Ali J (2013) Bromocriptine loaded chitosan nanoparticles intended for direct nose to brain delivery: Pharmacodynamic, Pharmacokinetic and Scintigraphy study in mice model. *Eur J Pharm Sci* 48: 393-405. doi: <http://dx.doi.org/10.1016/j.ejps.2012.12.007>.
23. Mistry A, Glud SZ, Kjems J, Randel J, Howard KA, Stolnik S, Illum L (2009) Effect of physicochemical properties on intranasal nanoparticle transit into murine olfactory epithelium. *J. Drug Target*. 17: 543-52. doi: 10.1080/10611860903055470 [doi].
24. Fazil M, Md S, Haque S, Kumar M, Baboota S, Sahni JK, Ali J (2012) Development and evaluation of rivastigmine loaded chitosan nanoparticles for brain targeting. *Eur J Pharm Sci* 47: 6-15. doi: <http://dx.doi.org/10.1016/j.ejps.2012.04.013>.
25. Zhao Y, Li X, Lu C, Lin M, Chen L, Xiang Q, Zhang M, Jin R, Jiang X, Shen X, Li X, Cai J (2014) Gelatin nanostructured lipid carriers-mediated intranasal delivery of basic fibroblast growth factor enhances functional recovery in hemiparkinsonian rats. *Nanomedicine*. 10: 755-64. doi: <http://dx.doi.org/10.1016/j.nano.2013.10.009>.
26. Jafarih O, Md S, Ali M, Baboota S, Sahni JK, Kumari B, Bhatnagar A, Ali J (2015) Design, characterization, and evaluation of intranasal delivery of ropinirole-loaded mucoadhesive nanoparticles for brain targeting. *Drug Dev. Ind. Pharm.* 41: 1674-81. doi: 10.3109/03639045.2014.991400 [doi].
27. Gartzandia O, Herran E, Pedraz JL, Carro E, Igartua M, Hernandez RM (2015) Chitosan coated nanostructured lipid carriers for brain delivery of proteins by intranasal administration. *Colloids Surf. B Biointerfaces*. 134: 304-13. doi: 10.1016/j.colsurfb.2015.06.054 [doi].
28. Qin Y, Chen H, Zhang Q, Wang X, Yuan W, Kuai R, Tang J, Zhang L, Zhang Z, Zhang Q, Liu J, He Q (2011) Liposome formulated with TAT-modified cholesterol for improving brain delivery and therapeutic efficacy on brain glioma in animals. *Int. J. Pharm.* 420: 304-12. doi: <http://dx.doi.org/10.1016/j.ijpharm.2011.09.008>.
29. Kanazawa T, Akiyama F, Kakizaki S, Takashima Y, Seta Y (2013) Delivery of siRNA to the brain using a combination of nose-to-brain delivery and cell-penetrating peptide-modified nano-micelles. *Biomaterials*. 34: 9220-6. doi: <http://dx.doi.org/10.1016/j.biomaterials.2013.08.036>.
30. Gartzandia O, Egusquiaguirre SP, Bianco J, Pedraz JL, Igartua M, Hernandez RM, Pr eat V, Beloqui A (2016) Nanoparticle transport across in vitro olfactory cell monolayers. *Int. J. Pharm.* 499: 81-9. doi: <http://dx.doi.org/10.1016/j.ijpharm.2015.12.046>.
31. Egusquiaguirre SP, Mangu an-Garc a C, Pintado-Berninches L, Iarriccio L, Carbajo D, Albericio F, Royo M, Pedraz JL, Hern andez RM, Perona R, Igartua M (2015) Development of surface modified biodegradable polymeric nanoparticles to deliver GSE24.2 peptide to cells: A promising approach for the treatment of defective telomerase disorders. *Eur J Pharm Biopharm.* 91: 91-102. doi: <http://dx.doi.org/10.1016/j.ejpb.2015.01.028>.
32. Anitua E, Pascual C, P erez-Gonzalez R, Orive G, Carro E (2015) Intranasal PRGF-Endoret enhances neuronal survival and attenuates NF- B-dependent inflammation process in a mouse model of Parkinson's disease. *J. Controlled Release*. 203: 170-80. doi: <http://dx.doi.org/10.1016/j.jconrel.2015.02.030>.
33. Blandini F, Armentero MT (2012) Animal models of Parkinson's disease. *FEBS J*. 279: 1156-66. doi: 10.1111/j.1742-4658.2012.08491.x [doi].
34. Kalia LV, Kalia SK, Lang AE (2015) Disease-modifying strategies for Parkinson's disease. *Mov. Disord.* 30: 1442-50. doi: 10.1002/mds.26354 [doi].

35. Herran,E, Requejo C, Ruiz-Ortega JA. et al (2014) Increased antiparkinson efficacy of the combined administration of VEGF- and GDNF-loaded nanospheres in a partial lesion model of Parkinson's disease. *Int J Nanomedicine*. 9(1): 2677-2687.
36. Herrán E, Ruiz-Ortega JÁ, Aristieta A, Igartua M, Requejo C, Lafuente JV, Ugedo L, Pedraz JL, Hernández RM (2013) In vivo administration of VEGF- and GDNF-releasing biodegradable polymeric microspheres in a severe lesion model of Parkinson's disease. *Eur J Pharm Biopharm*. 85: 1183-90. doi: <http://dx.doi.org/10.1016/j.ejpb.2013.03.034>.
37. Garbayo E, Montero-Menei CN, Ansorena E, Lanciego JL, Aymerich MS, Blanco-Prieto MJ (2009) Effective GDNF brain delivery using microspheres—A promising strategy for Parkinson's disease. *J. Controlled Release*. 135: 119-26. doi: <http://dx.doi.org/10.1016/j.jconrel.2008.12.010>.
38. Garbayo E, Ansorena E, Lanciego JL, Blanco-Prieto MJ, Aymerich MS (2011) Long-term neuroprotection and neurorestoration by glial cell-derived neurotrophic factor microspheres for the treatment of Parkinson's disease. *Mov Disord*. 26: 1943-7. doi: 10.1002/mds.23793.
39. Jollivet C, Aubert-Pouessel A, Clavreul A, Venier-Julienne M, Remy S, Montero-Menei CN, Benoit J, Menei P (2004) Striatal implantation of GDNF releasing biodegradable microspheres promotes recovery of motor function in a partial model of Parkinson's disease. *Biomaterials*. 25: 933-42. doi: [http://dx.doi.org/10.1016/S0142-9612\(03\)00601-X](http://dx.doi.org/10.1016/S0142-9612(03)00601-X).
40. O. Gartzandia, E. Herrán, J.A. Ruiz-Ortega, C. Miguelez, M. Igartua, J.V. Lafuente, J.L. Pedraz, L. Ugedo, R.M. Hernández (2016) Intranasal administration of chitosan-coated nanostructured lipid carriers loaded with GDNF improves behavioral and histological recovery in a partial lesion model of Parkinson's disease. *J Biomed Nanotechnol*. 12: 1-11. <https://doi.org/10.1166/jbn.2016.2313>
41. Schober A (2004) Classic toxin-induced animal models of Parkinson's disease: 6-OHDA and MPTP. *Cell Tissue Res*. 318: 215-24. doi: 10.1007/s00441-004-0938-y [doi].
42. Blesa J, Przedborski S (2014) Parkinson's disease: animal models and dopaminergic cell vulnerability. *Front. Neuroanat*. 8: 155. doi: 10.3389/fnana.2014.00155 [doi].
43. Barker RA (2009) Parkinson's disease and growth factors – are they the answer? *Parkinsonism Relat. Disord*. 15, Supplement 3: S181-4. doi: [http://dx.doi.org/10.1016/S1353-8020\(09\)70810-7](http://dx.doi.org/10.1016/S1353-8020(09)70810-7).
44. Chang YP, Fang KM, Lee TI, Tzeng SF (2006) Regulation of microglial activities by glial cell line derived neurotrophic factor. *J. Cell. Biochem*. 97: 501-11. doi: 10.1002/jcb.20646 [doi].
45. Rocha SM, Cristovão AC, Campos FL, Fonseca CP, Baltazar G (2012) Astrocyte-derived GDNF is a potent inhibitor of microglial activation. *Neurobiol. Dis*. 47: 407-15. doi: <http://dx.doi.org/10.1016/j.nbd.2012.04.014>.
46. Rickert U, Grampp S, Wilms H, Spreu J, Knerlich-Lukoschus F, Held-Feindt J, Lucius R (2014) Glial Cell Line-Derived Neurotrophic Factor Family Members Reduce Microglial Activation via Inhibiting p38MAPKs-Mediated Inflammatory Responses. *J. Neurodegener Dis*. 2014: 369468. doi: 10.1155/2014/369468 [doi].
47. Liberatore GT, Jackson-Lewis V, Vukosavic S, Mandir AS, Vila M, McAuliffe WG, Dawson VL, Dawson TM, Przedborski S (1999) Inducible nitric oxide synthase stimulates dopaminergic neurodegeneration in the MPTP model of Parkinson disease. *Nat. Med*. 5: 1403-9. doi: 10.1038/70978 [doi].
48. Langston JW, Forno LS, Tetrud J, Reeves AG, Kaplan JA, Karluk D (1999) Evidence of active nerve cell degeneration in the substantia nigra of humans years after 1-methyl-4-phenyl-1,2,3,6-tetrahydropyridine exposure. *Ann. Neurol*. 46: 598-605.

49. McGeer PL, Schwab C, Parent A, Doudet D (2003) Presence of reactive microglia in monkey substantia nigra years after 1-methyl-4-phenyl-1,2,3,6-tetrahydropyridine administration. *Ann. Neurol.* 54: 599-604. doi: 10.1002/ana.10728 [doi].

50. Lawson LJ, Perry VH, Dri P, Gordon S (1990) Heterogeneity in the distribution and morphology of microglia in the normal adult mouse brain. *Neuroscience.* 39: 151-70. doi: [http://dx.doi.org/10.1016/0306-4522\(90\)90229-W](http://dx.doi.org/10.1016/0306-4522(90)90229-W).

51. Mogi M, Kondo T, Mizuno Y, Nagatsu T (2007) p53 protein, interferon- γ , and NF- κ B levels are elevated in the parkinsonian brain. *Neurosci. Lett.* 414: 94-7. doi: <http://dx.doi.org/10.1016/j.neulet.2006.12.003>.

Beneficial effects of n-3 polyunsaturated fatty acids administration in a partial lesion model of Parkinson's disease: the role of glia and NRf2 regulation⁵

S. Hernando^{1,2}, C. Requejo^{1,6}, E. Herran³, J. A. Ruiz-Ortega^{4,5}, T. Morera-Herreras⁵, J. V. Lafuente^{6,7}, L. Ugedo⁵, E. Gainza³, J. L. Pedraz^{1,2}, M. Igartua^{1,2*} and R. M. Hernández^{1,2*}

¹NanoBioCel Group, Laboratory of Pharmaceutics, School of Pharmacy, University of the Basque Country (UPV/EHU), 01006, Vitoria-Gasteiz, Spain.

²Biomedical Research Networking Center in Bioengineering, Biomaterials and Nanomedicine (CIBER-BBN), Vitoria-Gasteiz, 01006, Spain.

³BioPraxis AIE, Hermanos Lumière 5, 01510 Miñano, Spain.

⁴Dept. Pharmacology, School of Pharmacy, University of the Basque Country (UPV/EHU), 01006, Vitoria-Gasteiz, Spain.

⁵Dept. Pharmacology, Faculty of Medicine and Nursing, University of the Basque Country (UPV/EHU), 48940, Leioa, Spain.

⁶LaNCE, Dept. Neurosciences, Faculty of Medicine and Nursing, University of the Basque Country (UPV/EHU), Leioa, 48940, Spain.

⁷Group Nanoneurosurgery, Institute of Health Research Biocruces, Barakaldo, 48903, Spain

*Co-corresponding author: Rosa Maria Hernández and Manoli Igartua

⁵ Published in : Neurobiol Dis. (2019)

<https://doi.org/10.1016/j.nbd.2018.10.001>

IF: 5.332 (Q1)

Cat:Neuroscience

ABSTRACT

Omega-3 polyunsaturated fatty acids (n-3 PUFAs) have been widely associated to beneficial effect over different neurodegenerative diseases. In the present study, we tested the potential therapeutic effect of docohexanoic acid (DHA) and its hydroxylated derivate, DHAH, in a partial lesion model of Parkinson's disease (PD). One month before and four months after the striatal lesion with 6-OHDA was made, the animals were daily treated with DHA (50 mg/kg), DHAH (50 mg/kg), vehicle or saline, by intragastric administration. Animal groups under n-3 PUFA treatments exhibited a trend to improve in amphetamine-induced rotations and cylinder test. The beneficial effect seen in behavioral studies were confirmed with TH immunostaining. TH⁺ fibers and TH⁺ neurons increased in the experimental groups treated with both n-3 PUFAs, DHA and DHAH. Moreover, the n-3 PUFAs administration decreased the astrogliosis and microgliosis, in both the striatum and substantia nigra (SN), with a higher decrease of GFAP⁺ and Iba-1⁺ cells for the DHAH treated group. This experimental group also revealed a positive effect on Nrf2 pathway regulation, decreasing the positive Nrf2 immunostaining in the striatum and SN, which revealed a potential antioxidant effect of this compound. Taking together, these data suggest a positive effect of n-3 PUFAs administration, and more concretely of DHAH, for PD treatment as it exhibited positive results on dopaminergic system, neuroinflammation and oxidative stress.

Keywords: Parkinson's disease •6-OHDA Polyunsaturated •fatty acids
•docohexanoic acid• neuroprotection• neuroinflammation

1. INTRODUCTION

Parkinson's disease (PD) is the second most common neurodegenerative disease, after Alzheimer disease (AD), which nowadays affect more than 5 million people worldwide. PD is characterized by the degeneration of dopaminergic neurons (Vivekanantham et al., 2015) in the *substantia nigra pars compacta* (SNpc). The resulted dopamine (DA) deficiency is the responsible of the classical parkinsonian motor symptoms: resting tremor, bradykinesia, rigidity and postural instability. However, non-motor symptoms are also present in the disease reducing health-related quality of life. These non-motor features include olfactory dysfunction, cognitive impairment, psychiatric symptoms, sleep disorders, autonomic dysfunction, pain and fatigue (Kalia and Lang, 2015, Lees et al., 2009, Chaudhuri et al., 2006, Schapira et al., 2017). Although the exact disease mechanisms underlying PD pathogenesis are not well understood, scientific evidences suggest that the nigral dopaminergic degeneration results from the convergence of different mechanism, including mitochondrial dysfunction, oxidative stress, apoptosis, excitotoxicity, altered protein handling and neuroinflammation (Gaki and Papavassiliou, 2014, Vivekanantham et al., 2015, Niranjana, 2014). Indeed, the presence of an active inflammatory response mediated by astrocytes and microglia has been long recognized but somewhat overlooked in PD. Reactive gliosis occurs within the area of neurodegeneration, highlighting the link between neurodegeneration and neuroinflammation (Hirsch and Hunot, 2009, Dexter and Jenner, 2013).

The most common treatments in clinical practice focus on DA replacement to control motor symptoms, however, its administration is related to disabling side effects such as; motor and non-motor fluctuations, dyskinesia and psychosis. Moreover, they are ineffective managing non-motor symptoms. The inefficacy of these treatments treating the symptomatology of the disease has aimed the research in the direction of novel therapies emphasizing neuroprotective activities (Oertel and Schulz, 2016, Hang et al., 2016). Among others, the use of antioxidants, polyunsaturated fatty acids (PUFAs) and polyphenols as nutraceuticals has gained great interest in the last years. The word “nutraceuticals” refers to compounds that derived from natural sources and the scientific data available support their beneficial role in the prevention and/or treatment of a disease. In the case of PD, different nutraceuticals have shown a positive effects managing the pathology of the disease; such as polyphenols from plant extract, food rich in vitamins (B,C,D and E) and PUFAs derived from fish oil (Zhao, 2009,Caruana and Vassallo, 2015,Chao et al., 2012, Dyall, 2015).

Omega-3 (n-3) and omega-6 (n-6) fatty acids are two major classes of PUFAS. n-3 PUFAs are essential nutrients in the development and functioning of brain and visual system. Moreover, there is growing evidence demonstrating that n-3 PUFAs remain important thorough our lifespan. The most abundant n-3 in the brain is docohexaeonic acid (DHA) that is required for normal neuronal function (Dyall, 2015). In addition, DHA is not only a structural membrane component but is also a modulator of crucial neurochemical processes, gene expression, synaptic plasticity and memory formation (Corsi et al., 2015). Recently, epidemiological studies have associated low levels of DHA consumption with a higher risk of suffering AD (Morris et al., 2003, Maclean et al., 2005). Moreover, a neuroprotective effect of DHA has been observed in different animal models of this disease (Boudrault et al., 2009). Although AD and PD have different clinical manifestations, both diseases shared mechanism of neurodegeneration: neuronal loss, deposit of insoluble protein filaments, oxidative stress, mitochondrial dysfunction and neuroinflammation (Xie et al., 2014). In fact, although much less scientific data is reported about DHA consumption and PD risk, recent epidemiological studies have suggested that high intake of unsaturated fatty acids decreases the risk of developing PD and protects from pesticides mediated toxicity (Kamel et al., 2014, de Lau et al., 2005). Moreover, in a recent clinical trial the effect of PUFAs and vitamin E coadministration was

evaluated demonstrating that this cosupplementation improved the clinical evaluation of the patients, decreased C-reactive protein sensitivity and increased total antioxidant capacity (Taghizadeh et al., 2017). Analysis in a MPTP animal model of PD have also shown the beneficial effect of PUFAs protection against the neurotoxicity caused by MPTP (Bousquet et al., 2008, Bousquet et al., 2009). Despite the mechanism of these fatty acids is not properly described, numerous papers have described the effect of PUFAs enhancing neurotrophic factors release, promoting the regulation of genes associated with oxidative stress or apoptosis and decreasing the inflammatory status related with PD (Bousquet et al., 2011a, Hashimoto et al., 2017).

Overall, we can conclude that there is an urgent need for the development of pharmaceuticals or nutraceuticals tools that could be implemented early to alter the natural progression of the disease. In the case of n-3 PUFAs, they are widely available and could represent an interesting nutraceutical option for PD treatment (Frédéric Calon, 2008). In the present study, we tested DHA and its hydroxylated derivate, DHAH, which is known to impede its β -oxidation increasing its half-life in cell membrane (Torres et al., 2014). In order to prove their potential neuroprotective and neurorestorative effect, 6-OHDA partially lesioned rats received chronic administration of these two kinds of PUFAs during a total of 5 months. Behavioral and immunohistochemical studies were performed in order to prove their potential therapeutic effect in PD.

2. MATERIAL AND METHODS

2.1 Materials

DHA and DHAH fatty acids in ethyl ester form were purchased from Medalchemy (Spain). They were aliquoted in topaz vials in N_2 inert atmosphere conditions ready for one unique use, in order to avoid its oxidation in the storage during the course of the experiment. Sodium phosphate dibasic (Na_2HPO_4), sodium phosphate monobasic (NaH_2PO_4), dibasic potassium phosphate (K_2HPO_4), potassium dihydrogen phosphate (KH_2PO_4), sucrose, sodium chloride (NaCl), p-formaldehyde, H_2O_2 , xylene and Tween[®] 80 were obtained from Panreac (Spain). 6-hydroxydopamine hydrochloride (6-OHDA), desipramine hydrochloride, chloral hydrate, amphetamine sulphate, carboxymethylcellulose sodium (CMC), 3,3'-diaminobenzidine (DAB), Triton X-100, sodium azide, bovine serum albumin (BSA),

MetOH, mouse anti-gliial fibrillary acidic protein antibody (GFAP), rabbit anti-tyrosine (TH) hydroxylase antibody, Fluoromount aqueous mounting medium and Depex (DPX) mounting medium were purchased from Sigma-Aldrich (Spain). 4',6-diamidino-2-phenylindole (DAPI), Donkey anti-mouse IgG (H+L) Cross-Adsorbed Secondary Antibody, Alexa Fluor 488, Donkey anti-rabbit IgG (H+L) Cross-Adsorbed Secondary Antibody, Alexa Fluor 488 were purchased from Termofisher Scientific (Spain). Normal goat serum (NGS), biotinylated goat α -rabbit and the avidin-biotin-peroxidase complex (ABC) kit from Palex (Spain). Polyclonal rabbit Iba-1 (ionized calcium-binding adapter molecule 1) antibody from Synaptic Systems (Germany), polyclonal rabbit Nrf2 (nuclear factor erythroid 2-related factor 2) antibody from Abcam (UK) and Isoflurane Esteve from Maipe Comercial (Spain).

2.2 Animals

Male albino Sprague-Dawley rats (170-220 g) were housed in groups of 4 under standard laboratory conditions ($22\pm 1^\circ\text{C}$, $55\pm 5\%$ relative humidity, and 12:12 h light/dark cycle) with food and water provided ad libitum. Every effort was made to minimize animal suffering and to use the minimum number of animals per group and experiment. Experimental protocols were reviewed and approved by the Local Ethical Committee for Animal Research of the University of the Basque Country (UPV/EHU, CEEA, ref.ES48/054000/6069). All of the experiments were performed in accordance with the European Community Council Directive on "The Protection of Animals Used for Scientific Purposes" (2010/63/EU) and with Spanish Law (RD 53/2013) for the care and use of laboratory animals.

2.3 6-hydroxidopamine (6-OHDA) lesion

The 6-OHDA lesion was performed according to previous studies (Gartziandia O. et al., 2016). Thirty minutes (min) before 6-OHDA injection, the rats were pre-treated with desipramine (25mg/kg, intraperitoneal (i.p)), and then, they were anesthetized with isoflurane inhalation (1.5-2%) and mounted on a Kopf stereotaxic instrument. The lesion was generated by the injection of $3\mu\text{g}/\mu\text{l}$ 6-OHDA solution into the striatum of the right hemisphere of the rats. Three injections of $2.5\mu\text{l}$ of 6-OHDA solution (a total volume of $7.5\mu\text{l}$) were administered at a rate of $0.5\mu\text{l}/\text{min}$ at three coordinates, relative to the bregma and dura, with the toothbar set at -2.4: AP + 1.3mm, ML +2.8mm, DV -4.5mm; AP -0.2mm, ML +3.0mm, DV -5.0mm and AP -0.6mm, ML +4.0mm, DV -5.5mm.

2.4 Experimental protocol

Fig. 1 shows the experimental protocol used. Before the 6-OHDA lesions were made to generate a partial lesion model of PD, the animals were randomly divided into four groups (n=8 animals, *per group*). During four weeks pre-lesion, two groups received intragastric daily treatment, with 18G gavage needle, of 50mg/kg of DHA or DHAH diluted in an aqueous solution with 0.5% of CMC and 0.05% of Tween 80. The other two groups received; one of them vehicle (aqueous solution with 0.5% CMC and 0.05% of Tween 80) and the other one just saline. These treatments were maintained during 15 weeks after the 6-OHDA surgery and, during this period, the behavioral tests were performed every 2 weeks. 15 weeks after the lesion was made, the animals were sacrificed and their brains processed for immunohistochemical evaluation.

Animals were included in the study when showed more than 3 turns per minute and less than 25 turns per minute in the amphetamine-induced rotational test in the first three weeks and in the last weeks after 6-OHDA injection. In addition, this criterion was supported by TH-immunostaining, in saline and vehicle groups, indicating that those animals showed less than 3 turns per minute in the beginning and in the end of the experiment did not show enough reduction of TH-immunoreactive (ir) fibers in the striatum (40% reduction in TH-ir fiber in the ipsilateral side respect to the contralateral one) to consider them as partially lesioned. On the other hand, animals showing more than 25 turns per minute in the beginning of the study were also excluded because the loss of TH-ir fibers in the striatum in the end of the experimental period was also almost complete (>90% loss of TH-ir fibers in the ipsilateral hemisphere). In short, 25 % of rats were discarded according to the exclusion criteria

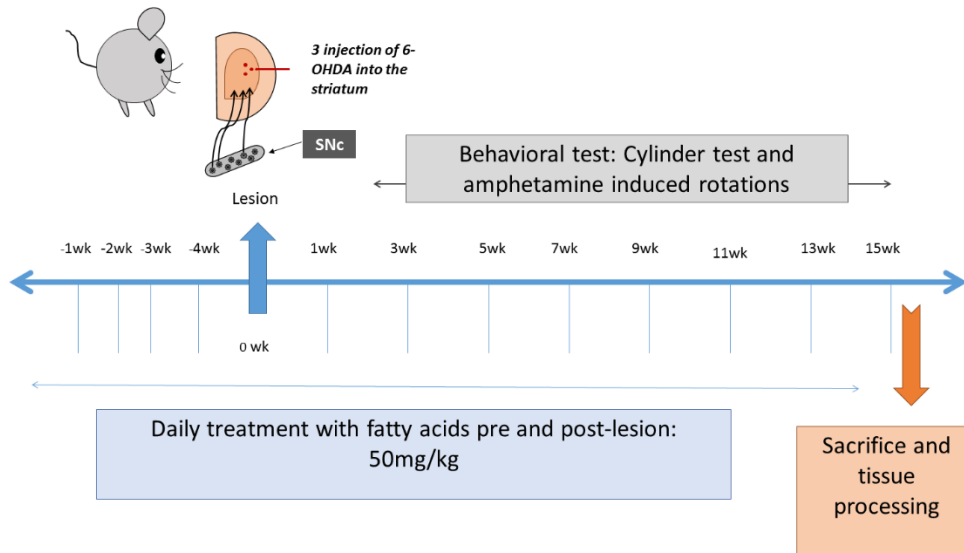


Fig 1. Schematic representation of the *in vivo* experimental study.

2.5 Amphetamine induced rotational test

Three weeks after inducing the 6-OHDA lesion, when the lesion with toxic is stabilized, the rats were tested in the amphetamine induced rotational test. This test was repeated once every two weeks. For this purpose, D-amphetamine (5 mg/kg (i.p.) in 0.9% NaCl; Sigma-Aldrich, St. Louis, USA) was intraperitoneally administered and, after 15 min of latency, in an individual cage for each animal, the total number of full ipsilateral rotations were recorded for 90 min with an automated rotameter (Multicounter LE3806; Harvard Apparatus, Holliston, MA, USA). The results are expressed as the % of ipsilateral turns per minute.

2.6 Cylinder test

Forelimb use asymmetry was assessed using the cylinder test fortnightly. Rats were individually placed in a 20cm diameter glass cylinder and allowed to explore freely. Mirrors were placed behind the cylinder to allow a 360° view of the exploratory activity. Each animal was left in place until at least 20 supporting front paw touches were done on the walls of the cylinder. The session was videotaped and later analyzed. Touches performed with the contralateral (injured side) or ipsilateral (uninjured side) front limb were counted and data are expressed as the percentage of ipsilateral placement, calculated as the following equation:

$$\% \text{ ipsilateral touches} = \frac{\text{ipsilateral paw placement}}{\text{ipsilateral} + \text{contralateral paw placement}} * 100.$$

2.7 Tissue preparation and postmortem analysis

The rats were transcardially perfused with 0.9% (w/v) NaCl and 4% (w/v) paraformaldehyde in 0.1M PBS, pH 7.4. The brains were removed and post-fixed for 24h in paraformaldehyde and then transferred to a 30% sucrose solution (w/v) in PBS 0.1 M for dehydration. After at least 3 days, brains were coronally sectioned on a freezing microtome (50 μ m) and kept in PBS 0.1 M solution with sodium azide 0.1% (w/v) at 4°C for further examination.

2.8 TH and Nrf2 immunohistochemistry

For TH and Nrf2 immunohistochemistry, sections were rinsed 3 times in potassium phosphate buffered saline (KPBS) (0.02M, pH 7.1), and then the endogenous peroxidases were quenched using 3% (v/v) H₂O₂ and 10% (v/v) methanol in KPBS for 30 min at room temperature (RT). After 3 rinsing steps in KPBS, the brain sections were preincubated in 1% (v/v) Triton X-100 with KPBS (KPBST) and NGS 5% (v/v) for 1 hour (h) at RT to block nonspecific binding sites. Then, they were incubated overnight (ON) with rabbit polyclonal antibody anti-TH (1:1000) or rabbit polyclonal antibody anti- Nrf2 (1:400) respectively, in 5% NGS (v/v) KPBST at RT. After, they were rinsed twice with KPBS and once with 2.5% NGS (v/v) in KPBST. Afterwards, the sections were incubated for 2h with a secondary biotinylated goat anti-rabbit IgG, which was diluted 1:200 in KPBST with 2.5% NGS (v/v). All sections were processed with ABC kit for 1h, and then the reaction was visualized using DAB as the chromogen. The reaction was stopped with successive rinsing steps with KPBS. Finally, the brain sections were mounted in gelatin-coated slides, dehydrated in ascending series of alcohols, cleared in xylene and coverslipped with DPX mounting medium.

2.9 Iba-1 and GFAP immunohistochemistry

After selecting the brain areas of the striatum and SN, Iba-1 (ionizing calcium-binding adaptor molecule 1) and glial fibrillary acidic protein (GFAP) immunohistochemistry were performed. Fixed brain sections were blocked with 2% (w/v) of BSA solution and 0.5% (v/v) Triton X-100 in PB during 1h at RT. After rinsing, they were incubated in rabbit polyclonal antibody Iba-1 (1:1000) or mouse monoclonal anti-GFAP (1:400), respectively with 0.1% (w/v) BSA and 0.1% Triton X-100 in PB with agitation ON at 4°C. The following day, brain slices were incubated with the secondary antibody: anti-rabbit Alexa Fluor IgG 488 (1:1000) or anti-mouse

Alexa Fluor IgG 488 (1:1000), respectively, in PB with 0,1% BSA and 0,1% Triton X-100 during 2h at RT. After three rinsing steps, the slices were incubated in DAPI (1:10.000) in PB during 10 min. Then, the slices were washed twice with PB and mounted on gelatin-coated slides and coverslipped with Fluoromount.

2.10 Integrated optical densitometry (IOD) of striatum

The optical density of the TH immunoreactive dopaminergic fibers in the striatum was measured using Image J win-64 Fiji and reading optical densities as grey levels. Images from section were taken with a 1200pp resolution digital scan (Epson). The IOD reading was corrected for background staining by subtracting the values of an area outside of the tissue from the obtained IOD of the striatum. For each animal eight slices were expressed as the percentage of IOD in the ipsilateral side respect to the contralateral non-lesioned side, which was set as 100%.

2.11 Number of TH⁺ neurons in SN

TH⁺ neuronal density in the SN was measured using a stereological tool (an optical fractionator) provided by the previously referred Mercator system. Probes of 50x50 μ m separated by 100 μ m were launched into the previously delimited area corresponding to the SN region. The counting was performed using a 40x objective. Positive cells that were present inside the probe or crossing on the right side of the X-Y axis were counted. A minimum of six histological sections per animal were used. Measurements from each slice were taken, and the mean value per animal was calculated.

2.12 Iba-1, GFAP and Nrf2 immunohistochemistry evaluation in striatum and SN.

The analysis of Iba-1, GFAP or Nrf2 positive cells was performed by an unbiased stereology method. Images were taken using a light microscopy (Zeiss Aniolab with a Olympus OP71 camera) at 20x magnification or a confocal microscopy (Zeiss Axiobserve Apotome 2, 20x Plan Aplochromat NA 0.8 objective). Six slices from each animal were used to represent the areas of interest for the analysis, striatum and SN. Images were taken on the contralateral and ipsilateral side. Iba-1, GFAP and Nrf2 cells were scored as positive if their cell-body image included well defined nuclear counterstaining. The data is expressed as the percentage of the contralateral non-lesioned side, which was set as 100%.

2.13 Statistical analysis

All results are expressed as means \pm SEM. Experimental data were analyzed using the computer program GraphPad Prism (v. 6.01, GraphPad Software, Inc.) Two-way ANOVA was used for analyzing animal body weight during experimental period and behavioral data. One-way ANOVA was used for analyze TH⁺, GFAP and Nrf2 histological evaluation in both the striatum and SN. Student's test was applied for Iba-1 immunohistochemistry. *P values* <0.05 were considered significant.

3. RESULTS

3.1 Animal health and survival

All animals appeared healthy during the experimental period. The success of the lesion was visible as a reduction on the body weight for all experimental groups at week 1 of the study; one week after the lesion was made (week 0). As seen in Fig 2. the variation of body weight between the four experimental groups during the study had no statistical significance, however, as previously pointed out one week after the lesion the body weight of all experimental groups decreased, being statistically significant (^{****} $p < 0.0001$, two-way ANOVA). The rats began the study with around 200g, week -4, (saline: 184.9g \pm 4.0, vehicle: 187.5g \pm 4.8, DHA 193.4g \pm 4.5, DHAH: 184.2g \pm 3.5) and gained weight gradually until almost 400g at the end point of this study, week 15 (saline: 385.9g \pm 9.2, vehicle: 364.9g \pm 7.3, DHA 403.7g \pm 10.9, DHAH: 374.7g \pm 11.2).

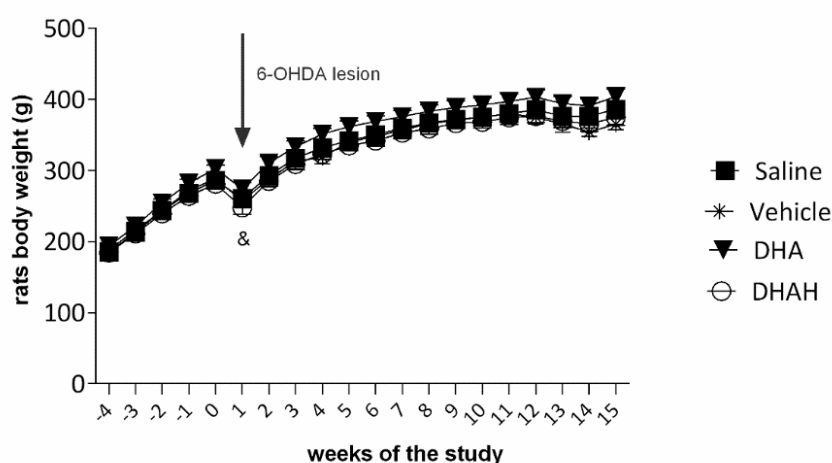


Fig 2. Evolution of rats' body weight during the study. [§] $p < 0.0001$ (week 1) between all the groups; Two-way ANOVA, Tukey's multiple comparisons test.

3.2 Effects of PUFAs treatment in the behavior of hemiparkinsonian rats

3.2.1 Amphetamine-induced rotations

The amphetamine-induced rotations evaluation was performed in all experimental groups to study the evolution on motor performance during the treatments. The first session was made three weeks after the lesion, when the 6-OHDA lesion was stabilized. Then, consecutive sessions were made once every two weeks until the end of the study. At the very beginning of the study all experimental animals exhibited very similar values, as the study advanced an improve trend in motor performance can be seen in the groups under PUFAs treatment (Fig. 3). However, this recovery was not statically significant at any point of the study.

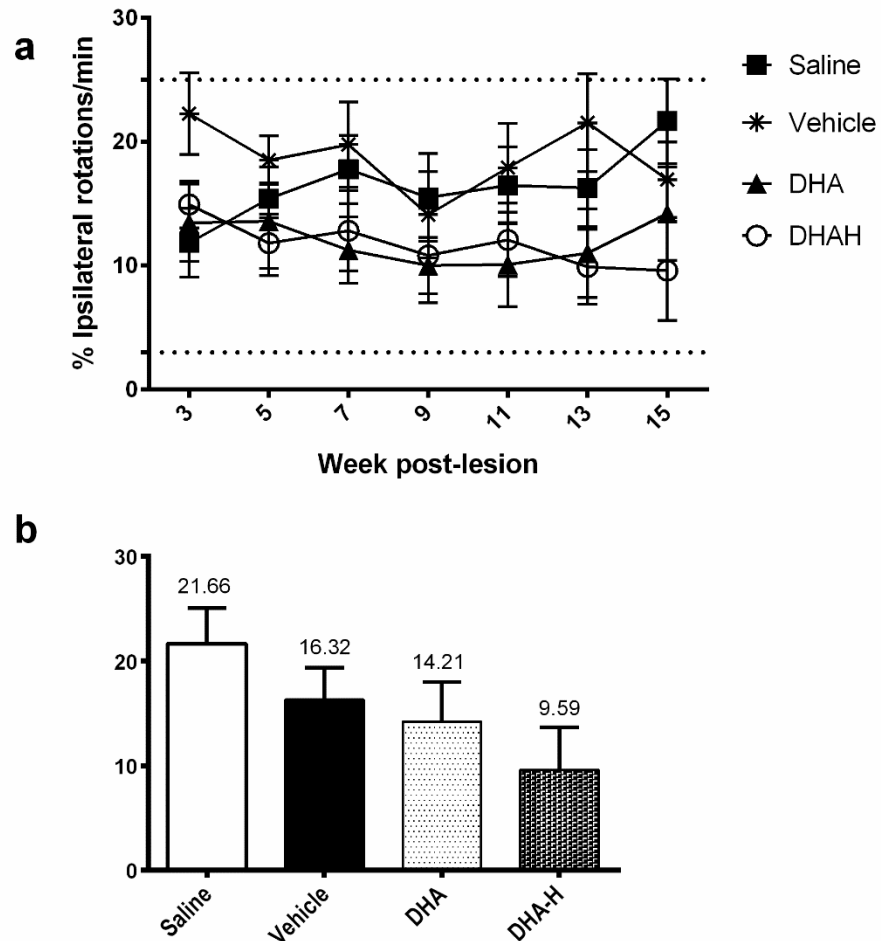


Fig 3. Amphetamine induced rotations. (a) Graphical representation of the evolution on amphetamine induced rotations during the study. (b) Graphical representation of the data obtained at week 15 in the study ($p > 0.05$, Two-way ANOVA, Tukey's multiple comparisons test).

3.2.2 Cylinder Test

The cylinder test was performed in all experimental groups to study the evolution in forelimb asymmetry. As seen in figure 4, the groups under the PUFAs treatment exhibited a recovery tendency but this was not statically significant at any point of the study. Although a statically significance cannot be seen, the percentage of ipsilateral touches decreased with the PUFAs treatment since the beginning of the study, being lowest at week 15 (saline: 95.83% \pm 3.22, vehicle; 92.32% \pm 6.19, DHA: 84.32% \pm 3.83, DHAH: 86.13% \pm 6.23; $p > 0.05$).

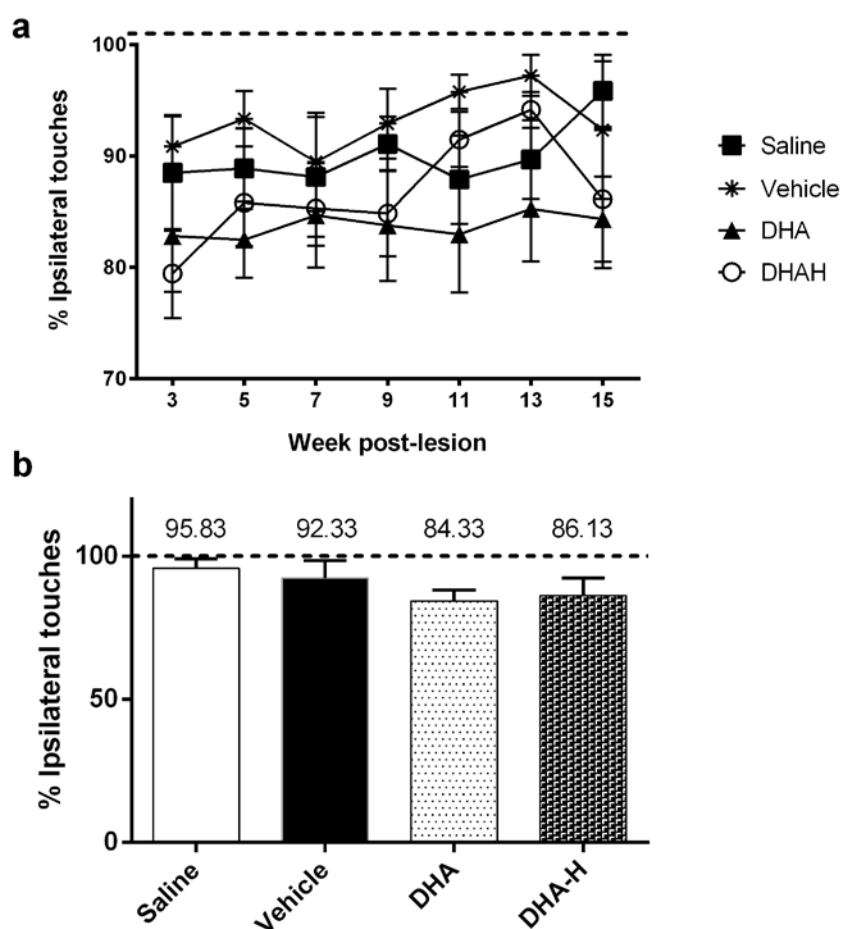


Fig 4. Cylinder test (a) Graphical representation of the evolution on the percentage of ipsilateral touches for all experimental groups. (b) Graphical representation of the data obtained at week 15 in the study ($p > 0.05$, Two-way ANOVA, Tukey's multiple comparisons test).

3.3 TH immunohistochemistry

Immunohistochemical techniques were also used to analyze the efficacy of PUFAs treatments in the 6-OHDA animal model. For this purpose, at week 15 of our study the animals were sacrificed in order to examine the changes in the nigrostriatal

system. Fig. 5 shows representative photomicrographs of the TH-immunostained striatum of all the different experimental groups. It is remarkable the degeneration of TH⁺ fibers in the striatum after 6-OHDA administration in both saline and vehicle groups (saline: 23.33% \pm 2.68, vehicle: 18.23% \pm 2.91), confirming the success of the lesion. A reduction higher than 40% in TH-ir fibers in the ipsilateral side respect to the contralateral side was considered to assess the success of the lesion and confirm a partial model of PD. The administration of DHA statistically increases the density of TH fibers (DHA: 29.34% \pm 3.03 vs vehicle: 18.23% \pm 2.91; * p <0.05). However, as seen in the Fig. 5, this increment on TH⁺ fibers was higher in the DHAH treated grouped (DHAH: 41.01% \pm 2.93 vs saline: 23.33% \pm 2.68, vehicle: 18.23% \pm 2.91; & p <0.0001).

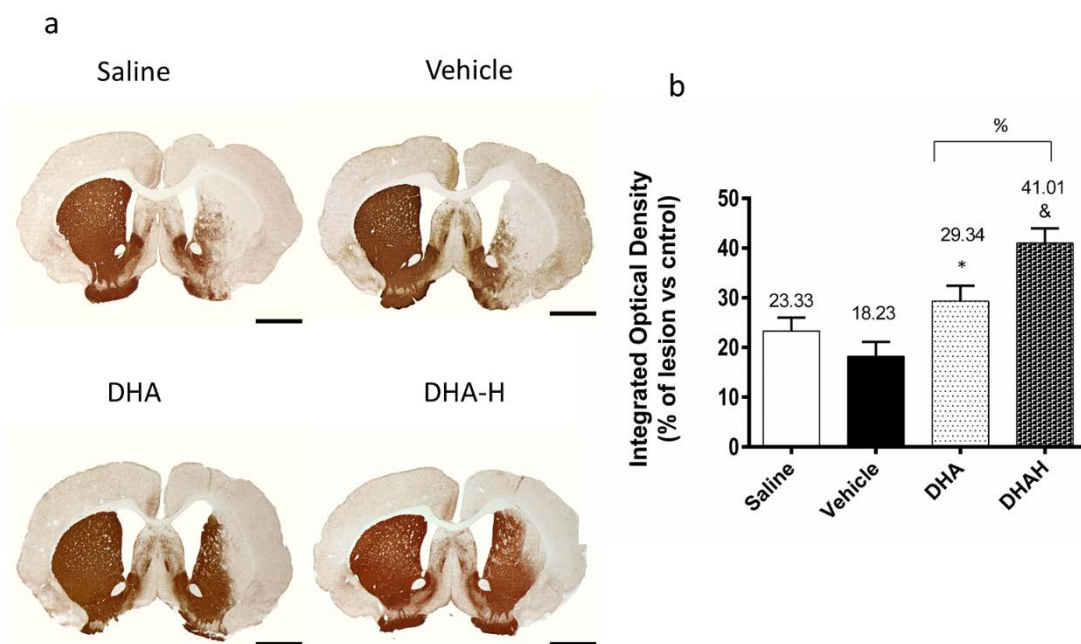


Fig. 5 (a) Representative photomicrographs of TH-immunostained striatum in all rat groups: saline, vehicle, DHA and DHAH (scale bar 2mm). (b) Graph depicts the integrated optical density (IOD) of TH⁺ fibers in the striatum of all groups. The data are shown as the mean \pm SEM. (* p <0.05 DHA vs Vehicle, & p <0.0001 DHAH vs Saline and Vehicle, * p <0.01 DHAH vs DHA), One-way ANOVA, Tukey's multiple comparisons test).

On the other hand, the percentage of recovery of TH⁺ positive neurons was analyzed in the SN (Fig. 6). As in the striatum, the percentage of TH⁺ neurons decreased after 6-OHDA injection (saline: 10.70 \pm 1.89, vehicle: 11.03 \pm 20.3), ratifying the lesion made by the parkinsonizing agent. As in striatum, the

administration of DHA increased the numbers of TH⁺ neurons in SN (DHA: 24.48±3.17 vs saline: 10.70% ± 1.89, #*p*<0.01 and vehicle: 11.03% ± 2.03, **p*<0.05). This augmentation of TH⁺ neurons in SN was also observed in the DHAH- treated group (DHAH: 31.01% ± 3.32 vs saline: 10.70% ± 1.89, %*p*<0.0001 and vehicle: 11.03% ± 2.03, &*p*<0.0001), showing a major recovery or preservation in the number of TH⁺ neurons than DHA-treated group. However, there was no statically significance between the administrations of the two kinds of PUFAs in the SN.

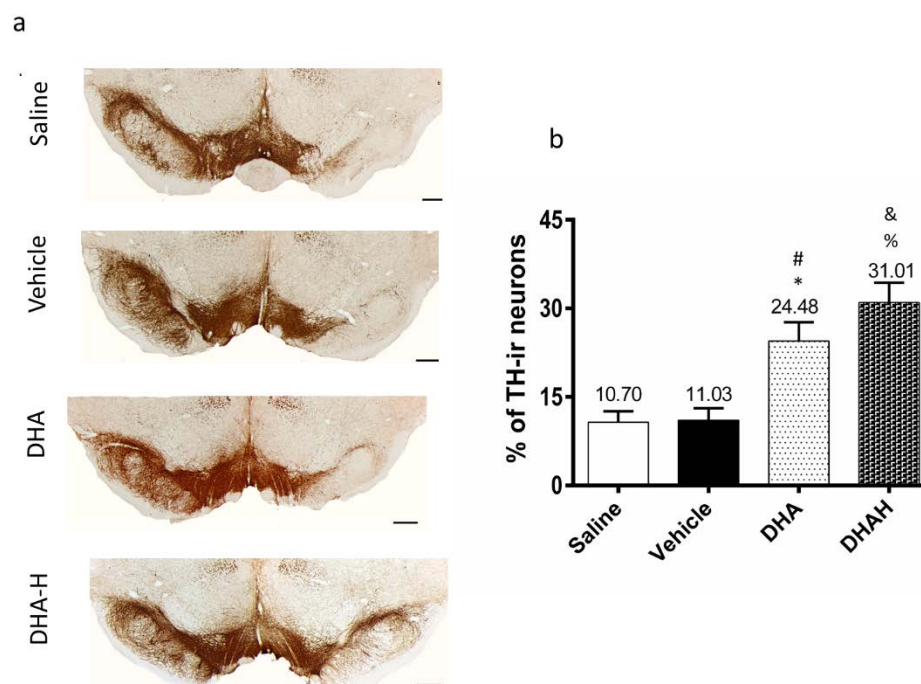


Fig 6. (a) Representative photomicrographs of TH immunostain in SN in all: saline, vehicle, DHA and DHAH (scale bar 500µm). (b) TH⁺ neurons in SN (%). The data are shown as the mean ± SEM. (&*p*<0.05 DHA vs vehicle, **p*<0.01 DHA vs saline, %*p*<0.0001 DHAH vs saline %*p*<0.001 DHAH vs vehicle), One-way ANOVA, Tukey's multiple comparisons test).

3.4 GFAP immunohistochemistry

GFAP immunohistochemistry was performed to test the ability of PUFAs treatment to modulate the neuroinflammatory component of the disease (Fig 7.). First, the potential astroglial toxicity of 6-OHDA was confirmed in both the striatum and SN as the administration of saline and vehicle duplicated the number of GFAP⁺ cells. The number of GFAP⁺ cells was markedly increased in striatum; (saline: 245.4%±27.8 and vehicle: 259.3%±40.37) and in the SN (saline: 214.6% ± 21.87, vehicle: 174.0% ± 11.08). In the striatum, the administration of DHA and DHAH statically decreased the number of GFAP⁺ cells (*p*<0.05 DHA: 143.4% ± 18.44 and **p*<0.05 DHAH: 129.0% ± 8.36). However, there was no difference between the administrations of

these two treatments. In SN, both DHA and DHAH decreased the number of GFAP⁺ cells, as seen in the striatum. ($^{\&}p < 0.0001$ DHA: 115.2% \pm 3.34 vs saline: 214.6% \pm 21.87) ($^{\#}p < 0.01$ DHA: 115.2% \pm 3.34 vs vehicle: 174.0% \pm 11.08) ($^{\&}p < 0.0001$ DHAH: 129.1% \pm 8.36 vs saline: 214.6% \pm 21.87); $^*p < 0.05$ DHAH: 129.1% \pm 8.36 vs vehicle: 174.0% \pm 11.08). The ability of these two different PUFAs to modulate the activation of astroglia in the striatum and SN was similar for both of them.

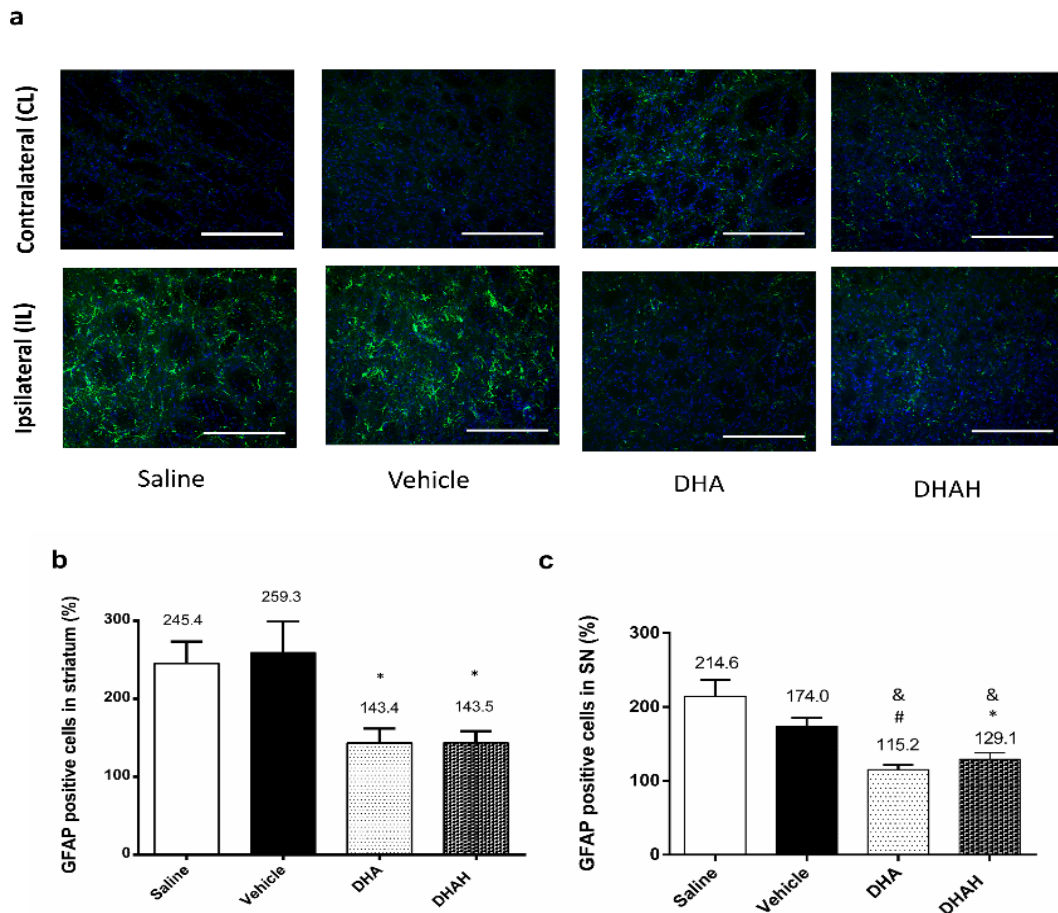


Fig 7. Histological evaluation of GFAP⁺ cells in both the striatum and SN (a) Representative GFAP immunophotographs of all rat groups in the striatum (saline, vehicle, DHA and DHAH) (scale bar 10 μ m). (b) GFAP⁺ cells in the striatum of all rat groups (%). The data are shown as the mean \pm SEM. ($^*p < 0.05$ DHA vs saline and vehicle) ($^*p < 0.05$ vs saline and vehicle). (c) GFAP⁺ cells in SN of all rat groups (%). The data are shown as the mean \pm SEM. ($^{\&}p < 0.0001$ DHA vs saline, $^{\#}p < 0.01$ DHA vs vehicle) ($^{\&}p < 0.0001$ DHAH vs saline, $^*p < 0.05$ DHAH vs vehicle), One-way ANOVA Tukey's multiple comparisons test). Blue stained for nucleus and green stained for GFAP⁺ cells.

3.5 Iba-1 immunohistochemistry

Together with GFAP immunohistochemistry, Iba-1 immunohistochemistry was realized to test how the PUFAs oral administration modulate other component of neuroinflammation in PD, the activated microglia cells (Fig 8.). As seen in GFAP

immunohistochemistry, the injection of 6-OHDA led to an increase of Iba-1⁺ cells in both the striatum and SN in non-treated groups, saline and vehicle, confirming the ability of this neurotoxin to increase the percentage of activated microglial cells (saline: 214.9% ± 19.62, vehicle: 221.2% ± 23.89 in the striatum; and saline: 191.5% ± 11.27, vehicle: 177.3% ± 10.25 in SN). In the striatum, the DHA administration led to a statistically decrease (142.7% ± 11.83 vs saline and vehicle, #*p*<0.01). This reduction was even higher in the DHAH treated group (110.4% ± 9.20 vs saline and vehicle, &*p*<0.0001), with a significance decrease when compared with DHA treated group (**p*<0.05). In the case of SN, they are similar to that seen in the striatum. The saline and vehicle groups exhibited the highest percentages of activated microglial cells (saline: 191.5% ± 11.27, vehicle: 177.3% ± 10.25) and the groups treated with PUFAs nutraceuticals statically decrease the level of activated microglial cells in this brain area (DHA: 122.8% ± 7.59 vs saline and vehicle, &*p*<0.0001 and DHAH: 113.6% ± 3.76 vs saline and vehicle, &*p*<0.0001). However, unlike in the striatum, there was no difference between these two groups.

3.6 Nrf2 immunohistochemistry

Nrf2 protein activation was evaluated in order to determine the ability of DHA and DHAH administration to modulate another well-known feature of the disease, the oxidative stress (Fig 9.). The injection of 6-OHDA to generate the PD model almost duplicate the expression of this marker in the control groups (saline and vehicle-treated groups) in both the striatum (saline: 176.6±15.44, vehicle: 162.0±12.68) and SN (saline: 180.4% ± 8.56, vehicle: 163.9% ± 7.34). In this case, the intragastric administration of DHA did not led to a statistically decrease of the expression in this protein neither in the striatum (133.9% ± 8.75) nor in SN (137.4% ± 4.72). Nevertheless, the group treated with DHAH exhibited better results with a statically decrease of Nrf2⁺ cells in both the striatum (115.3% ± 6.62 vs saline #*p*<0.0001 and vehicle **p*<0.001) and in SN (120.6% ± 4.54 vs saline &*p*<0.0001 and vehicle %*p*<0.001).

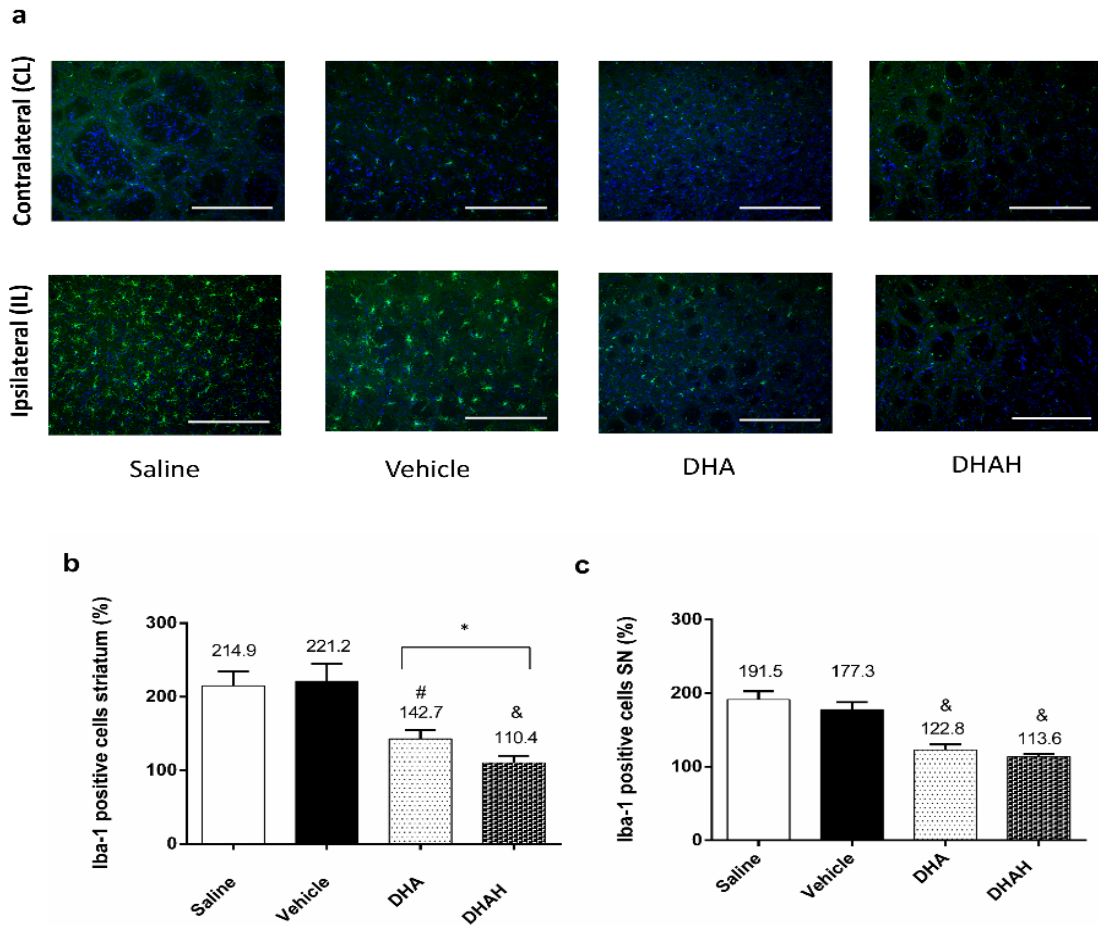


Fig 8. Histological evaluation of Iba-1⁺ cells in both the striatum and SN. (a) Representative Iba-1 immunophotographs of all rat groups in the striatum (saline, vehicle, DHA and DHAH) (scale bar 10 μ m). (b) Iba-1⁺ cells in the striatum of all rat groups (%). The data are shown as the mean \pm SEM. ($\#p < 0.01$ DHA vs saline and vehicle) ($\&p < 0.0001$ DHAH vs saline and vehicle) ($*p < 0.05$ DHAH vs DHA). (c) Iba-1⁺ cells in SN of all rat groups (%). The data are shown as the mean \pm SEM. ($\&p < 0.0001$ DHA vs saline, and vehicle) ($\&p < 0.0001$ DHAH vs saline and vehicle), unpaired Student's t-test. Blue stained for nucleus and green stained for Iba1⁺ cells.

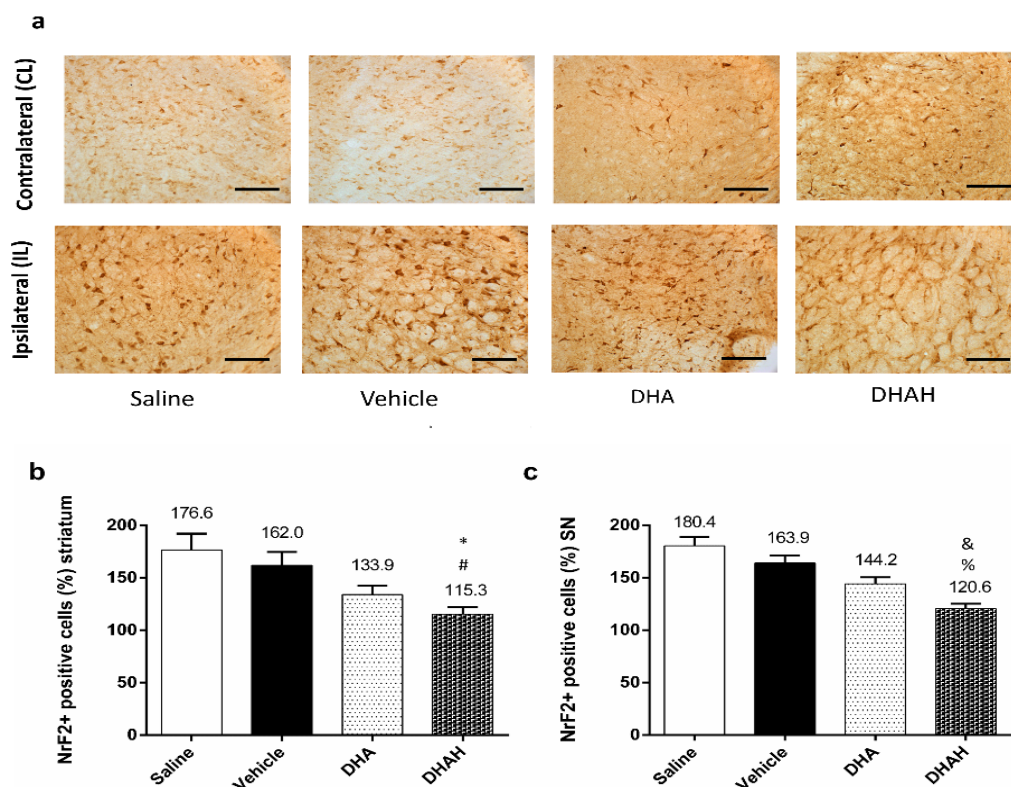


Fig 9. Histological evaluation of Nrf2⁺ cells in both the striatum and SN. (a) Representative Nrf2 immunophotographs of all rat groups in the SN (saline, vehicle, DHA and DHAH) (sale bar 2µm) (b) Nrf2⁺ cells in the striatum of all rat groups (%).The data are shown as the mean ± SEM. (*#p*<0.01 DHAH vs saline; **p*<0.05 DHAH vs vehicle). (c) Nrf2⁺ cells in SN of all rat groups (%). The data are shown as the mean ± SEM. (*&p*<0.0001 DHAH vs saline) (*%p*<0.001 DHAH vs vehicle), One-way ANOVA, Tukey's multiple comparisons test.

4. DISCUSSION

PD is a complex neurodegenerative disorder with multiple clinical manifestations and complex cellular and molecular pathology. Current available treatments based on traditional pharmacotherapeutic concepts are far from optimal. That is why in the last years scientists and pharmaceutical industry slowly, but progressively moved away from classical targets of pharmacotherapy to new compounds with neuroprotective properties to slow down the progression of the disease (Oertel and Schulz, 2016, Kalia and Lang, 2015). Accordingly, nutraceuticals such as flavonoids, vitamins, or n-3 PUFAs have gained the attention of the scientific community due to their potential effects modulating the pathological hallmarks of the disease: oxidative stress, neuroinflammation, mitochondrial dysfunction and excitotoxicity (Sutachan, et al., 2012, Magalingam et al., 2015, Dutta and Mohanakumar, 2015, Frédéric Calon, 2008). Moreover, recently the hydroxylation of polyunsaturated fatty acids have been proven to increase the half-life of its naturally

analog since they are not degraded by β - oxidation but by α - oxidation pathway. Therefore, the therapeutic effects of these hydroxylated molecules maybe increased (Ibarguren et al., 2014, Teres et al., 2012).

In this research article, we studied the beneficial effects of DHA and DHAH, a hydroxylated derivate of DHA. Up today, the beneficial effects of DHA in the treatment of NDs have been described in the scientific literature (Dyall, 2015, Bousquet et al., 2011b). Although the mode of action of DHA is not yet understood, numerous research papers have focused on the effects of DHA on cell membrane, concretely on lipid raft domains, which recently have been reported to be altered in NDs (Sonnino et al., 2014, Stillwell et al., 2005, Stillwell and Wassall, 2003). In the present study we studied these two kinds of PUFAS to elucidate if this molecule would equalize or increase, the beneficial effects already known for DHA in PD; testing the premise of an increase half-life and therefore, a therapeutic effect of this hydroxylated molecule. For achieving this purpose, these two kinds of n-3 PUFAs were evaluated in a 6-OHDA animal model of the disease.

6-OHDA-induced toxicity is extensively used to induce PD in murine animals. This toxin when injected in the striatum produces retrograde degeneration of nigrostriatal neurons. The lesion obtained with 6-OHDA is highly reproducible, which represents a considerable added value when new therapeutic strategies are to be investigated and clear neuroprotective effects must be demonstrated (Blandini and Armentero, 2012, Dauer and Przedborski, 2003). In the present study, amphetamine induced rotation was performed to evaluate the neuroprotective effect of n-3 PUFAs. First, the suitability of this animal model was assessed as in saline and vehicle treated groups the ipsilateral rotations per minute was higher than 10-15 turns per minute (Dunnett and Lelos, 2010). In the present study, the administration of nutraceuticals did not decrease ipsilateral induced rotations treatment and neither did the ipsilateral front paw touches in the cylinder test. Although a recovery trend can be seen in behavioral studies, these differences were not statically significant at any point of the study. The lack of statistical significance may be due to plasticity or compensatory mechanism, which may interfere with obtained rotational data. (Deumens et al., 2002) Indeed, the present work was a long study (15 weeks) and the behavioral tests were repeated several times, favoring the emergence of these processes (Schallert et al., 2000). In previous studies with chronic administration of

n-3 PUFAs, similar results were observed; without a statistical difference in behavioral tests (Barros et al., 2017, Delattre et al., 2010, Coulombe et al., 2016). In any case, the recovery trend saw in behavioral tests was confirmed with TH immunohistochemistry studies, supporting the beneficial effect of n-3 PUFAs on PD.

The DHAH supplementation increased up to 30% the density of TH⁺ fibers. Accordingly, the TH⁺ nigral neurons were higher in this experimental group. Similar results were obtained in previous studies with DHA supplementation supporting our finding (Bousquet et al., 2008, Ozsoy et al., 2011, Tanriover et al., 2010). Moreover, in this work, we confirm not only the neuroprotective and neurorestorative effect of DHA but also, of its hydroxylated derivate, DHAH, which had shown before positive effects in AD treatment; improving behavioral tests and decreasing A β oligomers and tau protein phosphorylation in cellular and animal models (Torres et al., 2014, Fiol-deRoque et al., 2013). The potential mechanism previously explained about the hydroxylation of these fatty acids may explain the differences observed in TH immunostaining for the two different groups of PUFAs.

On the other hand, the results obtained until today for PUFAs and PD treatment, have focused, in general, on behavioral studies, TH⁺ immunostaining and lipid peroxidation. Indeed, much less scientific data is published relating PUFAs treatment and its effect in neuroinflammation. n-3 PUFAs are known to have an anti-inflammatory effect, (Calder, 2015) and its administration may decrease the reactive gliosis shown in PD. Actually, the role of glia and neuroinflammation in PD has been disclosed as a potential target for neuroprotection (Hirsch and Hunot, 2009). Up to now, post-mortem studies provided evidence of neuroinflammation in PD with an increase in activated microglia and astroglial cells in the SN of PD patients (McGeer et al., 1988, Damier et al., 1993). The injection of 6-OHDA led to an increase of Iba-1⁺ and GFAP⁺ cells in both the striatum and SN. These data is in line with previous studies where a clear astrogliosis and microgliosis have been seen in this animal model (Long-Smith et al., 2009, Kitamura et al., 2010, Henning et al., 2008). The DHA and DHAH administration decreased the activated astroglial cells, reaching almost the values seen in the contralateral side.

Moreover, the results of DHA and DHAH modulating astrogliosis were similar to those seen in Iba-1 immunohistochemistry with a clear decrease of Iba-1⁺ cells after n-3 PUFAs administration. The exact mechanism by which n-3 PUFAs mediated their

anti-inflammatory properties are not still elucidated. Moreover, it is not clear if n-PUFAs inhibit glia activation directly or indirectly after enzymatic conversion to a variety of bioactive mediators. As previously pointed out, DHA is a major component of cell membrane having the ability to activate several interlinked pathways that may account their effects on cells. Among others, it is known the influence of n-3 PUFAs inhibiting the effects mediated by proresolving factors such as IL-1 β , downregulating the expression of several enzymes of arachidonic acid cascade in the brain or modifying membrane fluidity and therefore, inhibiting cytokine production or membrane ion channels (Sun et al., 2017, Hjorth and Freund-Levi, 2012, Bazinet and Laye, 2014). Indeed, the exogenous administration of DHA decreasing astrogliosis and microgliosis has been previously described in both *in vitro* and *in vivo* studies with different models of neuroinflammation (Paterniti et al., 2014, Harvey et al., 2015, Heras-Sandoval et al., 2016, Chang et al., 2015). Overall, the results obtained in this study confirmed this data and revealed a positive effect of DHAH supplementation decreasing astroglial and microglia positive cells and therefore, normalizing the activity of glia in PD injured brain.

Furthermore, in the last years, there has been a growing interest in the role of Nrf2 pathway in neurodegenerative diseases. The Nrf2 system is compromised by increased age and aging is the main risk factor for all neurodegenerative diseases, including PD. Moreover, as oxidative stress is a hallmark of PD, antioxidant therapy has been proposed as a reasonable therapeutic approach (Koppula et al., 2012). Under healthy conditions, the Nrf2-antioxidant response element (ARE) pathway is critical in order to maintain homeostasis. However, when there is an exposure to reactive oxygen species (ROS), Nrf2 dissociates from cytosolic and translocates to the nucleus where it binds to ARE which transcriptionally drive the expression of several detoxifying and antioxidant genes (Lim et al., 2014, Sandberg et al., 2014). In the case of PD, immunostaining for Nrf2 was observed in dopaminergic neurons in the SN of PD patients (Ramsey et al., 2007). The activation of Nrf2 pathway after 6-OHDA exposure has been seen both *in vivo* and *in vitro* studies (Siebert et al., 2009, Zhang et al., 2014, Jakel et al., 2005). The present study confirmed this data since saline and vehicle experimental groups exhibited positive Nrf2 immunostaining. Although scientific data have reported a decrease on Nrf2⁺ cells after DHA administration, we were not able to see that results neither in the striatum nor in SN. However, the studies were performed in cell culture or in other animal models of

neuroinflammation such as ischemia or traumatic brain injury (Ozkan et al., 2016). In this case, only the DHAH administration had a statically decrease after the chronic administration of this n-3 PUFA, maybe highlighting a higher potential antioxidant capacity for this compound.

Altogether, these results support the use of n-PUFAs, and more concretely the DHAH as a nutraceutical option for PD treatment. We demonstrated a positive effect of n-3 PUFAs supplementation on DAergic system, neuroinflammation and oxidative stress. As neurodegenerative diseases prevalence will continue to rise in the next decades, neuroprotective strategies have been widely studied and n-3 PUFAs have demonstrated to be a promising therapeutic approach. Moreover, those evidences have increased the development of new formulations and synthetic modifications from natural sources of n-3 PUFAs, such as DHAH. The synthetic modification of DHA to convert in DHAH have showed to increase the beneficial effects already known about DHA. Continue in this line of research should hopefully bring new nutraceuticals or pharmaceuticals options for an effective treatment of PD. However, larger clinical trials should be made in order to establish a clearer link between n-3 and PD. On the other hand, more studies are necessary to determine the action mechanism of n-3 PUFAs in PD, to stablish the therapeutic effective dosage and the state of the disease in which this treatment should have a beneficial effect.

5. ACKNOWLEDGMENTS

This project was partially supported by the Spanish Ministry of Economy and Competitiveness (RTC-2015-3542-1), the Basque Government (Consolidated Groups, IT 747-13 and IT 907-16). The authors thank for technical and human support provided by SGIker of UPV/EHU and European funding (ERDF and ESF). The authors also wish to thank the intellectual and technical assistance from the ICTS NANBIOSIS, more specifically by the Drug Formulation Unit (U10) of the CIBER-BBN at the UPV/EHU. S. Hernando thanks the Basque Government for the fellowship grant.

6. BIBLIOGRAPHY

Barros, A.S., Crispim, R.Y.G., Cavalcanti, J.U., et al., 2017. Impact of the Chronic Omega-3 Fatty Acids Supplementation in Hemiparkinsonism Model Induced by 6-Hydroxydopamine in Rats. *Basic Clin. Pharmacol. Toxicol.* 120, 523-531.

Bazinet, R.P., Laye, S., 2014. Polyunsaturated fatty acids and their metabolites in brain function and disease. *Nat. Rev. Neurosci.* 15, 771-785.

- Blandini, F., Armentero, M.T., 2012. Animal models of Parkinson's disease. *FEBS J.* 279, 1156-1166.
- Boudrault, C., Bazinet, R.P., Ma, D.W.L., 2009. Experimental models and mechanisms underlying the protective effects of n-3 polyunsaturated fatty acids in Alzheimer's disease. *J. Nutr. Biochem.* 20, 1-10.
- Bousquet, M., Gibrat, C., Saint-Pierre, M., et al., 2009. Modulation of brain-derived neurotrophic factor as a potential neuroprotective mechanism of action of omega-3 fatty acids in a parkinsonian animal model. *Prog Neuropsychopharmacol Biol Psychiatry* 33, 1401-1408.
- Bousquet, M., Saint-Pierre, M., Julien, C., et al., 2008. Beneficial effects of dietary omega-3 polyunsaturated fatty acid on toxin-induced neuronal degeneration in an animal model of Parkinson's disease. *FASEB J.* 22, 1213-1225.
- Bousquet, M., Calon, F., Cicchetti, F., 2011b. Impact of omega-3 fatty acids in Parkinson's disease. *Ageing Res Rev* 10, 453-463.
- Calder, P.C., 2015. Marine omega-3 fatty acids and inflammatory processes: Effects, mechanisms and clinical relevance. *Biochim Biophys Acta (BBA) - Molecular and Cell Biology of Lipids* 1851, 469-484.
- Caruana, M., Vassallo, N., 2015. Tea Polyphenols in Parkinson's Disease. *Adv. Exp. Med. Biol.* 863, 117-137.
- Chang, P.K., Khatchadourian, A., McKinney, R.A., et al., 2015. Docosahexaenoic acid (DHA): a modulator of microglia activity and dendritic spine morphology. *J. Neuroinflammation* 12, 34-015-0244-5.
- Chao, J., Leung, Y., Wang, M., et al., 2012. Nutraceuticals and their preventive or potential therapeutic value in Parkinson's disease. *Nutr. Rev.* 70, 373-386.
- Chaudhuri, K.R., Healy, D.G., Schapira, A.H., National Institute for Clinical Excellence, 2006. Non-motor symptoms of Parkinson's disease: diagnosis and management. *Lancet Neurol.* 5, 235-245.
- Corsi, L., Dongmo, B.M., Avallone, R., 2015. Supplementation of omega 3 fatty acids improves oxidative stress in activated BV2 microglial cell line. *Int. J. Food Sci. Nutr.* 66, 293-299.
- Coulombe, K., Saint-Pierre, M., Cisbani, G., et al., 2016. Partial neurorescue effects of DHA following a 6-OHDA lesion of the mouse dopaminergic system. *J Nutr Biochem* 30, 133-142.
- Damier, P., Hirsch, E.C., Zhang, P., et al., 1993. Glutathione peroxidase, glial cells and Parkinson's disease. *Neuroscience* 52, 1-6.
- Dauer, W., Przedborski, S., 2003. Parkinson's Disease: Mechanisms and Models. *Neuron* 39, 889-909.
- de Lau, L.M., Bornebroek, M., Witteman, J.C., et al., 2005. Dietary fatty acids and the risk of Parkinson disease: the Rotterdam study. *Neurology* 64, 2040-2045.
- Delattre, A.M., Kiss, Á, Szawka, R.E., et al., 2010. Evaluation of chronic omega-3 fatty acids supplementation on behavioral and neurochemical alterations in 6-hydroxydopamine-lesion model of Parkinson's disease. *Neurosci Res* 66, 256-264.
- Deumens, R., Blokland, A., Prickaerts, J., 2002. Modeling Parkinson's disease in rats: an evaluation of 6-OHDA lesions of the nigrostriatal pathway. *Exp. Neurol.* 175, 303-317.
- Dexter, D.T., Jenner, P., 2013. Parkinson disease: from pathology to molecular disease mechanisms. *Free Radic Biol Med.* 62, 132-144.

Dunnett, S.B., Lelos, M., 2010. Chapter 3 - Behavioral analysis of motor and non-motor symptoms in rodent models of Parkinson's disease. *Prog Brain Res* 184, 35-51.

Dutta, D., Mohanakumar, K.P., 2015. Tea and Parkinson's disease: Constituents of tea synergize with antiparkinsonian drugs to provide better therapeutic benefits. *Neurochem Int* 89, 181-190.

Dyall, S.C., 2015. Long-chain omega-3 fatty acids and the brain: a review of the independent and shared effects of EPA, DPA and DHA. *Front. Aging Neurosci.* 7, 52.

Fiol-deRoque, M.A., Gutierrez-Lanza, R., Teres, S., et al., 2013. Cognitive recovery and restoration of cell proliferation in the dentate gyrus in the 5XFAD transgenic mice model of Alzheimer's disease following 2-hydroxy-DHA treatment. *Biogerontology* 14, 763-775.

Frédéric Calon, F.C., 2008. Can we prevent Parkinson's disease with n-3 polyunsaturated fatty acids? *Future Lipidol* 3 (2), 133-137.

Gaki, G.S., Papavassiliou, A.G., 2014. Oxidative stress-induced signaling pathways implicated in the pathogenesis of Parkinson's disease. *Neuromolecular Med.* 16, 217-230.

Gartziandia O., Herrán E., Ruiz-Ortega J.A., et al., 2016. Intranasal administration of chitosan-coated nanostructured lipid carriers loaded with GDNF improves behavioral and histological recovery in a partial lesion model of Parkinson's disease. *J Biomed Nanotechnol* 12, 1-11.

Hang, L., Basil, A.H., Lim, K.L., 2016. Nutraceuticals in Parkinson's Disease. *Neuromolecular Med.* 18, 306-321.

Harvey, L.D., Yin, Y., Attarwala, I.Y., et al., 2015. Administration of DHA Reduces Endoplasmic Reticulum Stress-Associated Inflammation and Alters Microglial or Macrophage Activation in Traumatic Brain Injury. *ASN Neuro* 7.

Hashimoto, M., Hossain, S., Al Mamun, A., et al., 2017. Docosahexaenoic acid: one molecule diverse functions. *Crit. Rev. Biotechnol.* 37, 579-597.

Henning, J., Strauss, U., Wree, A., et al., 2008. Differential astroglial activation in 6-hydroxydopamine models of Parkinson's disease. *Neurosci Res.* 62, 246-253.

Heras-Sandoval, D., Pedraza-Chaverri, J., Perez-Rojas, J.M., 2016. Role of docosahexaenoic acid in the modulation of glial cells in Alzheimer's disease. *J. Neuroinflammation* 13, 61-016-0525-7.

Hirsch, E.C., Hunot, S., 2009. Neuroinflammation in Parkinson's disease: a target for neuroprotection? *The Lancet Neurology* 8, 382-397.

Hjorth, E., Freund-Levi, Y., 2012. Immunomodulation of microglia by docosahexaenoic acid and eicosapentaenoic acid. *Curr. Opin. Clin. Nutr. Metab. Care* 15, 134-143.

Ibarguren, M., López, D.J., Escribá, P.V., 2014. The effect of natural and synthetic fatty acids on membrane structure, microdomain organization, cellular functions and human health. *Biochim Biophys Acta (BBA) - Biomembranes* 1838, 1518-1528.

Jakel, R.J., Kern, J.T., Johnson, D.A., et al., 2005. Induction of the protective antioxidant response element pathway by 6-hydroxydopamine in vivo and in vitro. *Toxicol. Sci.* 87, 176-186.

Kalia, L.V., Lang, A.E., 2015. Parkinson's disease. *The Lancet* 386, 896-912.

Kamel, F., Goldman, S.M., Umbach, D.M., et al., 2014. Dietary fat intake, pesticide use, and Parkinson's disease. *Parkinsonism Relat Disord* 20, 82-87.

Kitamura, Y., Inden, M., Minamino, H., et al., 2010. The 6-hydroxydopamine-induced nigrostriatal neurodegeneration produces microglia-like NG2 glial cells in the rat substantia nigra. *Glia* 58, 1686-1700.

Koppula, S., Kumar, H., More, S.V., et al., 2012. Recent advances on the neuroprotective potential of antioxidants in experimental models of Parkinson's disease. *Int. J. Mol. Sci.* 13, 10608-10629.

Lees, A.J., Hardy, J., Revesz, T., 2009. Parkinson's disease. *The Lancet* 373, 2055-2066.

Lim, J.L., Wilhelmus, M.M., de Vries, H.E., et al., 2014. Antioxidative defense mechanisms controlled by Nrf2: state-of-the-art and clinical perspectives in neurodegenerative diseases. *Arch. Toxicol.* 88, 1773-1786.

Long-Smith, C.M., Sullivan, A.M., Nolan, Y.M., 2009. The influence of microglia on the pathogenesis of Parkinson's disease. *Prog. Neurobiol.* 89, 277-287.

Macleay, C.H., Issa, A.M., Newberry, S.J., et al., 2005. Effects of omega-3 fatty acids on cognitive function with aging, dementia, and neurological diseases. *Evid Rep. Technol. Assess. (Summ)* (114), 1-3.

Magalingam, K.B., Radhakrishnan, A.K., Haleagrahara, N., 2015. Protective Mechanisms of Flavonoids in Parkinson's Disease. *Oxid Med. Cell. Longev* 2015, 314560.

McGeer, P.L., Itagaki, S., Boyes, B.E., et al., 1988. Reactive microglia are positive for HLA-DR in the substantia nigra of Parkinson's and Alzheimer's disease brains. *Neurology* 38, 1285-1291.

Morris, M.C., Evans, D.A., Bienias, J.L., et al., 2003. Consumption of fish and n-3 fatty acids and risk of incident Alzheimer disease. *Arch. Neurol.* 60, 940-946.

Niranjan, R., 2014. The role of inflammatory and oxidative stress mechanisms in the pathogenesis of Parkinson's disease: focus on astrocytes. *Mol. Neurobiol.* 49, 28-38.

Oertel, W., Schulz, J.B., 2016. Current and experimental treatments of Parkinson disease: A guide for neuroscientists. *J. Neurochem.* 139 Suppl 1, 325-337.

Ozkan, A., Parlak, H., Tanriover, G., et al., 2016. The protective mechanism of docosahexaenoic acid in mouse model of Parkinson: The role of heme oxygenase. *Neurochem Int.* 101, 110-119.

Ozsoy, O., Seval-Celik, Y., Hacioglu, G., et al., 2011. The influence and the mechanism of docosahexaenoic acid on a mouse model of Parkinson's disease. *Neurochem. Int.* 59, 664-670.

Paterniti, I., Impellizzeri, D., Di Paola, R., et al., 2014. Docosahexaenoic acid attenuates the early inflammatory response following spinal cord injury in mice: in-vivo and in-vitro studies. *J. Neuroinflammation* 11, 6-2094-11-6.

Ramsey CP., Glass CA., Montgomery MB., et al., 2007. Expression of Nrf2 in Neurodegenerative Diseases. *J Neuropathol Exp Neurol.* 66, 75-85.

Sandberg, M., Patil, J., D'Angelo, B., et al., 2014. NRF2-regulation in brain health and disease: Implication of cerebral inflammation. *Neuropharmacology* 79, 298-306.

Schallert, T., Fleming, S.M., Leasure, J.L., et al., 2000. CNS plasticity and assessment of forelimb sensorimotor outcome in unilateral rat models of stroke, cortical ablation, parkinsonism and spinal cord injury. *Neuropharmacology* 39, 777-787.

Schapira, A.H.V., Chaudhuri, K.R., Jenner, P., 2017. Non-motor features of Parkinson disease. *Nat. Rev. Neurosci.* 18, 435-450.

Siebert, A., Desai, V., Chandrasekaran, K., et al., 2009. Nrf2 activators provide neuroprotection against 6-hydroxydopamine toxicity in rat organotypic nigrostriatal cocultures. *J. Neurosci. Res.* 87, 1659-1669.

Sonnino, S., Aureli, M., Grassi, S., et al., 2014. Lipid rafts in neurodegeneration and neuroprotection. *Mol. Neurobiol.* 50, 130-148.

Stillwell, W., Shaikh, S.R., Zerouga, M., et al., 2005. Docosahexaenoic acid affects cell signaling by altering lipid rafts. *Reprod. Nutr. Dev.* 45, 559-579.

Stillwell, W., Wassall, S.R., 2003. Docosahexaenoic acid: membrane properties of a unique fatty acid. *Chem Phys Lipids* 126, 1-27.

Sun, G.Y., Simonyi, A., Fritsche, K.L., et al., 2017. Docosahexaenoic acid (DHA): An essential nutrient and a nutraceutical for brain health and diseases. *Prostaglandins Leukot Essent Fatty Acids*

Sutachan J.J., Casas Z., Albarracin S.L., et al., 2012. Cellular and molecular mechanisms of antioxidants in Parkinson's disease. *Nutr Neurosci* 15, 120-126.

Taghizadeh, M., Tamtaji, O.R., Dadgostar, E., et al., 2017. The effects of omega-3 fatty acids and vitamin E co-supplementation on clinical and metabolic status in patients with Parkinson's disease: A randomized, double-blind, placebo-controlled trial. *Neurochem Int* 108, 183-189.

Tanriover, G., Seval-Celik, Y., Ozsoy, O., et al., 2010. The effects of docosahexaenoic acid on glial derived neurotrophic factor and neurturin in bilateral rat model of Parkinson's disease. *Folia Histochem. Cytobiol.* 48, 434-441.

Teres, S., Llado, V., Higuera, M., et al., 2012. 2-Hydroxyoleate, a nontoxic membrane binding anticancer drug, induces glioma cell differentiation and autophagy. *Proc. Natl. Acad. Sci. U. S. A.* 109, 8489-8494.

Torres, M., Price, S.L., Fiol-deRoque, M.A., et al., 2014. Membrane lipid modifications and therapeutic effects mediated by hydroxydocosahexaenoic acid on Alzheimer's disease. *Biochim Biophys Acta (BBA) - Biomembranes* 1838, 1680-1692.

Vivekanantham, S., Shah, S., Dewji, R., et al., 2015. Neuroinflammation in Parkinson's disease: role in neurodegeneration and tissue repair. *Int. J. Neurosci.* 125, 717-725.

Xie, A., Gao, J., Xu, L., et al., 2014. Shared mechanisms of neurodegeneration in Alzheimer's disease and Parkinson's disease. *Biomed. Res. Int.* 648740.

Zhang, N., Shu, H.Y., Huang, T., et al., 2014. Nrf2 signaling contributes to the neuroprotective effects of urate against 6-OHDA toxicity. *PLoS One* 9, e100286.

Zhao, B., 2009. Natural antioxidants protect neurons in Alzheimer's disease and Parkinson's disease. *Neurochem. Res.* 34, 630-638.

Nanostructured lipid carriers made of Ω -3 polyunsaturated fatty acids: *In vitro* evaluation of emerging nanocarriers to treat neurodegenerative diseases ⁶

Sara Hernando^{1,2,3}, Enara Herran ⁴, Rosa Maria Hernandez^{1,2,3*} and Manoli Igartua ^{1,2,3 *}

¹ NanoBioCel Research Group, Laboratory of Pharmaceutics, School of Pharmacy University of the Basque Country (UPV/EHU), 01006 Vitoria-Gasteiz, Spain; sara.hernando@ehu.eus

² Biomedical Research Networking Centre in Bioengineering, Biomaterials and Nanomedicine (CIBER-BBN), Institute of Health Carlos III, 28029, Madrid Spain

³ Bioaraba, NanoBioCel Research Group, 01006, Vitoria-Gasteiz, Spain

⁴ Biokeralty Research Institute, C/Albert Einstein 25 bajo, Edificio E-3 Miñano, 01510, Álava, Spain; enara.herran@keralty.com

*Correspondence: Rosa María Hernández and Manoli Igartua

⁶ Published in Pharmaceutics (2020)

IF: 4.421

<https://doi.org/10.3390/pharmaceutics12100928>

Cat: Pharmacology & Pharmacy science

ABSTRACT:

Neurodegenerative diseases (ND) are one of the main problems of public health systems in the 21st century. The rise of nanotechnology-based drug delivery systems (DDS) has become an emerging approach to target and treat these disorders related to the central nervous system (CNS). Among others, the use of nanostructured lipid carriers (NLCs) has increased in the last few years. Up to today, most of the developed NLCs have been made of a mixture of solid and liquid lipids without any active role in preventing or treating diseases. In this study, we successfully developed NLCs made of a functional lipid, such as the hydroxylated derivate of docoheptaenoic acid (DHAH), named DHAH-NLCs. The newly developed nanocarriers were around 100 nm in size, with a polydispersity index (PDI) value of <0.3, and they exhibited positive zeta potential due to the successful chitosan (CS) and TAT coating. DHAH-NLCs were shown to be safe in both dopaminergic and microglia primary cell cultures. Moreover, they exhibited neuroprotective effects in dopaminergic neuron cell cultures after exposition to 6-hydroxydopamine hydrochloride (6-OHDA) neurotoxin and decreased the proinflammatory cytokine levels in microglia primary cell cultures after lipopolysaccharide (LPS) stimuli. The levels of the three tested cytokines, IL-6, IL-1 β and TNF- α were decreased almost to control levels after the treatment with DHAH-NLCs. Taken together, these data suggest the suitability of DHAH-NLCs to attaining enhanced and synergistic effects for the treatment of NDs.

Keywords: nanostructured lipid carriers • nanocarrier • docoheptaenoic acid • neuroprotection • neuroinflammation

1. INTRODUCTION

Neurodegenerative diseases (ND) cause progressive loss of brain functions and overlapping clinical syndromes. Among the many risk factors associated with neurodegeneration, the aging process itself has by far the most impact. However, other environmental and genetic aspects are associated with the risk of suffering these diseases. Indeed, the NDs are the result of a combination of different environmental risk factors, such as vascular risk, tobacco consumption, alcohol and aging, together with different genes involved in the development of these central nervous system (CNS) disorders. For example, in Alzheimer's disease (AD), APOE4 (apolipoprotein E) is the major genetic risk factor. Moreover, mutations in APP, (amyloid precursor protein) PSEN1 (presenilin proteins) and PSEN2 probably accelerate the toxic accumulation of proteins that leads to the undergoing neurodegenerative process present in AD. Another example is mutation in GBA (glucocerebrosidase), which encodes β -glucocerebrosidase. Alterations in this gene lead to lysosomal enzyme deficiency and an increase in the prevalence of Parkinson diseases (PD). Other mutations in genes, such as LRRK2 (leucine-rich repeat kinase 2), parkin and SNCA, (alpha synuclein) which encodes the protein α -synuclein, are the most common causes of dominantly and recessively inherited PD. These NDs are age-dependent disorders that are becoming increasingly prevalent as life expectancy rises worldwide. This prevalence will increase, becoming a serious economic burden and public health problem. Despite AD and PD being the most common NDs, Huntington's disease (HD), amyotrophic lateral sclerosis (ALS),

frontotemporal dementia and the spinocerebellar ataxias are also examples of NDs, with aging as the main risk factor for all of them [1–3]. Although they have different clinical manifestations and symptoms, they share common features and mechanisms of neurodegeneration, highlighting protein deposits, mitochondrial homeostasis, stress granules and synaptic toxicity, together with a maladaptive innate immune response that converges in the form of chronic inflammation characterized by reactive gliosis and an increase in proinflammatory cytokines [4,5].

Despite the significant public health issues NDs have, to date, the treatments for these diseases remain symptomatic without halting the progression of the disease. Moreover, the lack of an overall positive effect on the clinical manifestation of the disease, together with the presence of systemic side effects, has prompted the patients to abandon their therapies [6,7]. Due to the lack of an effective treatment for NDs, in the last few years, promising new molecules, such as neurotrophic factors (NTFs), antioxidant molecules and polyunsaturated fatty acids (PUFAs), have been raised as a feasible therapeutic options to target the undergoing oxidative stress and inflammatory status or to enhance neurogenesis [8–10].

Nevertheless, no matter the treatment, one of the most challenging obstacles for an effective therapy for NDs is the low penetration efficiency of drugs to the CNS due to the presence of the blood brain barrier (BBB). In the last few years, different strategies have been developed in order to achieve brain targeting. These strategies include direct and indirect methods. The direct or invasive techniques include surgical methods to administer drugs directly into the brain and the disruption of the BBB to open it. Meanwhile, the indirect or noninvasive techniques include nonaggressive approaches to access the brain without affecting this barrier integrity [11,12]. These noninvasive techniques include alternative systemic administration routes like intranasal administration [13,14]. Gartziandia et al. conducted a study that successfully showed the brain delivery of therapeutics after intranasal administration with lipid nanoparticles coated with chitosan (CS) [15]. Moreover, the combination of the formulation with cell-penetrating peptides (CPP) has been disclosed as a useful strategy to enter the brain [16,17]. Anyway, one of the most studied approaches to attain this goal are nanotechnology-based drug delivery systems [18,19]. Among them, nanoparticles (NPs) have been widely used as a promising approach for ND treatment. NPs are highly stable 3D encapsulation

systems that can be loaded with drugs and functionalized with targeting ligands or antibodies, and they can be used as nanocarriers to deliver drugs to the CNS [20]. Among other materials, natural or synthetic polymers and lipids have been employed in NP development [11].

Indeed, numerous research papers have combined NPs with well-known treatments or therapeutic approaches that have recently appeared, such as growth factors (GFs), antioxidant molecules and PUFAs entrapped in the nanoformulation [21–24]. All these research papers support the use of nanoparticles, offering many advantages over traditional formulations, such as protecting the molecule from degradation, increasing the half-life of the therapeutic molecules and, therefore, limiting multiple dosing and decreasing side effects. Among others, the nanostructured lipid carriers (NLCs) are an unstructured solid lipid matrix made of a mixture of blended solid and liquid lipids and an aqueous phase with a mixture of surfactants [25]. In addition, they have gained the attention of researchers since they exhibit a lack of toxicity, high drug loading capacity of both hydrophobic and hydrophilic compounds and a natural tendency to pass across the BBB [26]. Moreover, the NLCs can be functionalized with different substances to increase their tendency to pass through the BBB [27]. Examples of these molecules are chitosan (CS) and the cationic cell-penetrating peptide TAT; both molecules have increased brain targeting of therapeutic molecules for NDs treatment, as we pointed out in previous publications [15,24].

Up to today, most of the lipids used for NLC formulation are inert excipients, without any active role in preventing or treating diseases [28]. Indeed, only a few research groups have described the use of functional lipids that could play a therapeutic role in forming the lipid matrix, i.e., Ω -9 oleic acid incorporated into a NLC formulation for dermal applications [29]. Other kinds of functional lipids are PUFAs, Ω -3 and Ω -6 polyunsaturated fatty acids. As previously pointed out, PUFAs have been raised as a promising new approach to target neurodegenerative diseases. Although the biochemical mechanism undergoing the beneficial effect in NDs is not clear at all, they have exhibited the positive effect of decreasing the neuroinflammation process undergoing NDs, improving memory in animal models of AD, sensory motor tests in PD animal models and inhibiting amyloid- β fibrils both in vitro and in vivo [30–32]. Such functional lipids, which are also called nutraceutical,

have proved to be a useful tool to manage NDs [33]; although they cannot totally restore brain functions, they may be beneficial to manage some symptoms of the disease or just as a coadjuvant treatment. Actually, in the last few years, numerous observational studies showed an association between a diet rich in PUFAs and a lower risk of PD. Moreover, dietary treatments with PUFAs have shown to decrease the inflammatory status of these NDs and decrease depressive symptoms, among others [34–36].

Therefore, taking into account the promising results obtained with PUFAs in ND treatment, along with the beneficial effects of NLCs modified with CS and TAT for brain targeting, the objective of this research article is to combine both strategies for ND treatment. More concretely, the goal of the present work is to develop NLC with a functional lipid, such as DHA (docohexaenoic acid) and its hydroxylated derivate (DHAH), so the nanoparticles themselves could exhibit neuroprotective and antiinflammatory effects. In summary, we aim to demonstrate the beneficial effect of PUFAs incorporated to the NLC matrix, generating a new functional nanocarrier for entrapping different therapeutic molecules in the future and acting as a synergetic therapy.

2. MATERIALS AND METHODS

2.1. Materials

Precirol ATO 5® (glycerol disterate) (pharma grade) and Mygliol® (caprylic/capric triglyceride) (pharma grade) were a kind gift from Gattefosé (Lyon, France) and IOI Oleo GmbH, respectively. DHA (80% purity) and DHAH (85.4% purity) fatty acids in ethyl ester and triglyceride form were purchased from Medalchemy (Alicante, Spain). They were aliquoted in topaz vials in N₂ inert atmosphere conditions ready for one unique use in order to avoid oxidation during storage over the course of the experiment. Tween 80, Tween 20 and 3.7% paraformaldehyde were purchased from Panreac (Barcelona, Spain). Lutrol® F-68 (Poloxamer 188) (FDA-approved excipient) was acquired from VWR Avantor (Barcelona, Spain). Chitosan (CS) was obtained from NovaMatrix (Sandvika, Norway). Trehalose dehydrate, Triton X-110, bovine serum albumin (BSA), poly-L-lysine hydrobromide (PLL), deoxyribonuclease I from a bovine pancreas (DNase I), 6-hydroxydopamine hydrochloride (6-OHDA), Cell Counting Kit-8 (CCK-8), 2,2'-Azino-bis(3-ethylbenzthiazoline-6-sulfonic acid) (ABTS) and Fluoromount™

Aqueous Mounting Medium were acquired from Millipore Sigma Life Sciences (Madrid, Spain). Additionally, 4',6-diamidino-2-phenylindole (DAPI), donkey anti-mouse IgG (H+L) cross-adsorbed secondary antibody, Alexa Fluor 555, goat anti-rabbit IgG (H+L) cross-adsorbed secondary antibody and Alexa Fluor 488 were purchased from Thermo Fisher Scientific (Madrid, Spain). Neurobasal TM medium, B-27 TM supplement, glutamine 100X, penicillin-streptomycin (P/S), fetal bovine serum (FBS), DMEM GlutaMAX TM, trypsin-EDTA 0.25% and Hank's Balanced Salt Solution (HBSS) were obtained from Gibco® by Life Technologies (Madrid, Spain). Anti-tyrosine-hydroxylase (TH) primary antibody and anti-glial fibrillary acidic protein (GFAP) primary antibodies were obtained from Abcam (Cambridge, UK). Anti-Iba1 (ionizing calcium-binding adaptor molecule 1) primary antibody was purchased from Synaptic Systems (Göttingen, Germany). Lipopolysaccharide (LPS) suitable for cell culture was bought from InvivoGen (Toulouse, France). Rat IL-6 Standard, Rat IL-1 β Standard and Rat TNF- α Standard ABTS ELISA Development Kits were obtained from Peprotech (London, UK). Finally, TAT (>95% purity) was obtained from ChinaPeptides (Suzhou, China). All reagents used were of analytical grade.

2.2. NLC Preparation and Optimization

NLC were prepared based on a previously described melt-emulsification technique [16,24]. Four different formulations were developed, combining solid and liquid lipids. The solid lipid Precirol ATO 5® (melting point: 56 °C) was used in all formulations; however, different liquid lipids in a different solid:lipid ratio were used, as shown Table 1. All nanoformulations shown in Table 1 were performed in triplicate.

DHA, its hydroxylated derivate in ethyl ester form (DHAH-EE) and Mygliol® (caprylic/capric glyceride) were liquid at room temperature; however, the hydroxylated derivate of DHA in triglyceride form (DHAH-TG) was slightly more viscous. We used two different variants of DHAH, its hydroxylated derivate in ethyl ester form (DHAH-EE) and triglyceride form (DHAH-TG) in order to select the most suitable one to develop our new nanocarrier.

The lipid phase, containing both the solid and the liquid lipid, was heated 5 °C above its melting point until a clear and homogeneous phase was obtained. The lipid phase was formed with a different solid:liquid lipid ratio, as described in Table 1. The aqueous solution was composed of Tween 80 (3% w/v) and poloxamer 188

(2% w/v) for a final volume of 4 ml. The aqueous phase was warmed and added to the melted oily phase and sonicated for 60 s at 50 W (Branson® Sonifier 250, Fisher Scientific, Madrid, Spain). The obtained nanoemulsion was maintained under magnetic stirring for 15 minutes (min) at room temperature and stored at 4 °C overnight to allow the recrystallisation of the lipid for NLC formation. On the following day, the nanoparticle dispersion was centrifuged in an Amicon filter (Amicon, “Ultracel-100k”, Millipore Sigma Life Sciences, Madrid, Spain) at 2500 rpm (MIXTASEL, JP Selecta, Barcelona, Spain) for 15 min and the nanoparticles were washed three times with milli Q water. Finally, 15% w/w trehalose was added as cryoprotectant, and the NLCs were lyophilized for 42 h (LyoBeta 15, Telstar, Spain).

Prior to the NLC coating process, TAT was covalently linked to CS by a surface activation method previously described by our research group [16]. The CS: TAT employed ratio was 1:0.01 (w/w). TAT conjugation with CS was prepared through a carbodiimide-mediated coupling reaction [37]. The reaction was made through the EDC/NHS technique, in which the reactive sulfo-NHS ester reacted with the amine functionality of proteins and peptides via the formation of an amide bond [38,39]. Briefly, 250 μ l EDC (1-ethyl-3-(3-dimethylaminopropyl) carbodiimide hydrochloride) in solution (1 mg/mL) and 250 μ l of sulfo-NHS (N-hydroxysulfosuccinimide) in 0.02 M phosphate buffered saline (PBS) were added dropwise to a 4 mL CS solution (0.5% w/v in PBS 0.02 M) under magnetic stirring (2 h at room temperature). For the coupling of TAT, a 250 μ l TAT solution (1 mg/mL) in PBS (0.02 M; pH 7.4) was added dropwise to the activated CS under gentle agitation. The TAT-CS solution was maintained under agitation for another 4 h at room temperature and then incubated at 4 °C overnight. The next day, the NLC were coated with TAT-CS; for that purpose, an NLC dispersion previously prepared was added dropwise to the TAT-CS solution under continuous agitation for 20 min at room temperature. After the coating process, CS-NLC-TAT nanoformulation was centrifuged in Amicon filters (Amicon, “Ultracel-100k”, Millipore, Millipore Sigma Life Sciences, Madrid, Spain) at 2500 rpm (MIXTASEL, JP Selecta, Barcelona, Spain) for 15 min and washed three times with Milli Q water. Finally, the nanoformulation was freeze-dried with the cryoprotectant trehalose at a final concentration of 15% (w/w) of the weighed lipid, and then it was lyophilized for 42 h (LyoBeta 15, Telstar, Terrassa, Spain). This final step, regarding the coating with CS and TAT, was only performed after the election of the lipid type and the solid:lipid ratio, resulting in the formulations named (CS-TAT) DHAH-NLC,

or just DHAH-NLC, and (CS-TAT) Mygliol-NLC, or just Mygliol-NLC, used in the following described studies in primary cell cultures.

Table 1. The composition of the different nanoparticles, using Precirol® ATO 5 and different Ω -3 fatty acids or Mygliol® as a liquid lipid with different solid:liquid lipid ratios.

LIQUID LIPID	FORMULATION	% PRECIROL ATO 5® (w/v)	% LIQUID LIPID (w/v)	% T80 (w/v)	% Poloxamer 188 (w/v)
MYGLIOL®	A1	2.5	0.25	3	2
	A2	2	0.75	3	2
	A3	1.75	1	3	2
	A4	1.5	1.25	3	2
DHA	B1	2.5	0.25	3	2
	B2	2	0.75	3	2
	B3	1.75	1	3	2
	B4	1.5	1.25	3	2
DHAH-EE	C1	2.5	0.25	3	2
	C2	2	0.75	3	2
	C3	1.75	1	3	2
	C4	1.5	1.25	3	2
DHAH-TG	D1	2.5	0.25	3	2
	D2	2	0.75	3	2
	D3	1.75	1	3	2
	D4	1.5	1.25	3	2

2.3. NLC Characterization

The mean particle size (Z-average diameter) and the polydispersity index (PDI) were measured by dynamic light scattering (DLS), and the zeta potential was determined through laser Doppler micro-electrophoresis (Malvern® Zetasizer Nano ZS, Model Zen 3600; Malvern Instruments Ltd., Malvern, UK). Three independent measurements were performed for each formulation. The data are represented as the mean \pm SD. Nanoparticle surface characteristics and morphology were examined by transmission electron microscopy (JEOL JEM 1400 Plus, Izasa Scientific, Madrid, Spain). The thermal behavior of the nanoparticles and the excipients and components themselves were studied using differential scanning calorimetry (DSC) (DSC-50, Shimadzu, Kyoto, Japan). Each sample was sealed in an aluminum pan and heated from 25 °C to 350 °C at a heating rate of 10 °C per minute. The sample size was 1–2 mg for each measurement. Finally, Fourier transform infrared (FTIR) spectra of Mygliol-NLC and DHAH-NLC with and without

CS and TAT coating were carried out on a Nicolet Nexus FTIR spectrometer using ATR Golden Gate (Thermo Scientific, Madrid, Spain) with a crystal ZnSe. The sample was placed directly onto the ATR crystal and the spectrum was obtained in transmittance mode. Each spectrum was the result of an average of 32 scans at 4 cm^{-1} resolution. Measurements were recorded in the wavelength range of 4000–750 cm^{-1} .

2.4. Cell Cultures

2.4.1. Primary Dopaminergic Cell Culture

Dopaminergic neuronal cultures were prepared from Wistar rat embryos at 15, 16 or 17 days of gestation (E15–E17). Animal procedures were reviewed and approved (3 April 2017) by the Local Ethical Committee for Animal Research of the University of the Basque Country (UPV/EHU, CEEA, ref. M20/2017/019). All of the experiments were performed in accordance with the European Community Council Directive on “The Protection of Animals Used for Scientific Purposes” (2010/63/EU) and with Spanish Law (RD 53/2013) for the care and use of laboratory animals.

To obtain primary dopaminergic cell cultures, the following protocols were followed with slight modifications [40,41] (Figure 1A). Pregnant rats were euthanized and, under no aseptic conditions, the whole brain was removed from the rat embryos and kept on ice in a Petri dish (10 cm \varnothing) with HBSS for removing the blood vessels and meninges. Petri dishes containing embryos' brains were put under the magnifying glass to select the brain areas of interest following Gaven et al. protocol [42]. The ventral portion of the mesencephalic flexure, a region of the developing brain rich in dopaminergic neurons, was used for cell preparations. After collecting the brain areas of interest, tissue was incubated with trypsin at 37 °C for 15 min under aseptic conditions. Then, it was also incubated with DNase for 30 s and, after that time, the trypsin was inactivated and the tissue was washed twice with DMEM GlutMAX™ FBS 10%, P/S. Then, the tissue was mechanically dissociated by several passages through a 5 and 2 mL pipette. Finally, the cell suspension was passed through a 100 μm nylon strainer and centrifuged for obtaining a cell pellet. The cell pellet was resuspended in neurobasal medium supplemented with 0.5 mM glutamine, 1% antibiotic and 3% B27. Cells were seeded in 96-well culture plates (for the cell viability assay, neuroprotective activity assay and 6-OHDA toxin-induced assay) and in 24-well culture plates with glass coverslips (for the

immunofluorescence assay), both previously coated with poly-L-lysine to promote cell adhesion, at a density of 40×10^3 cells/well and 150×10^3 cells/well, respectively.

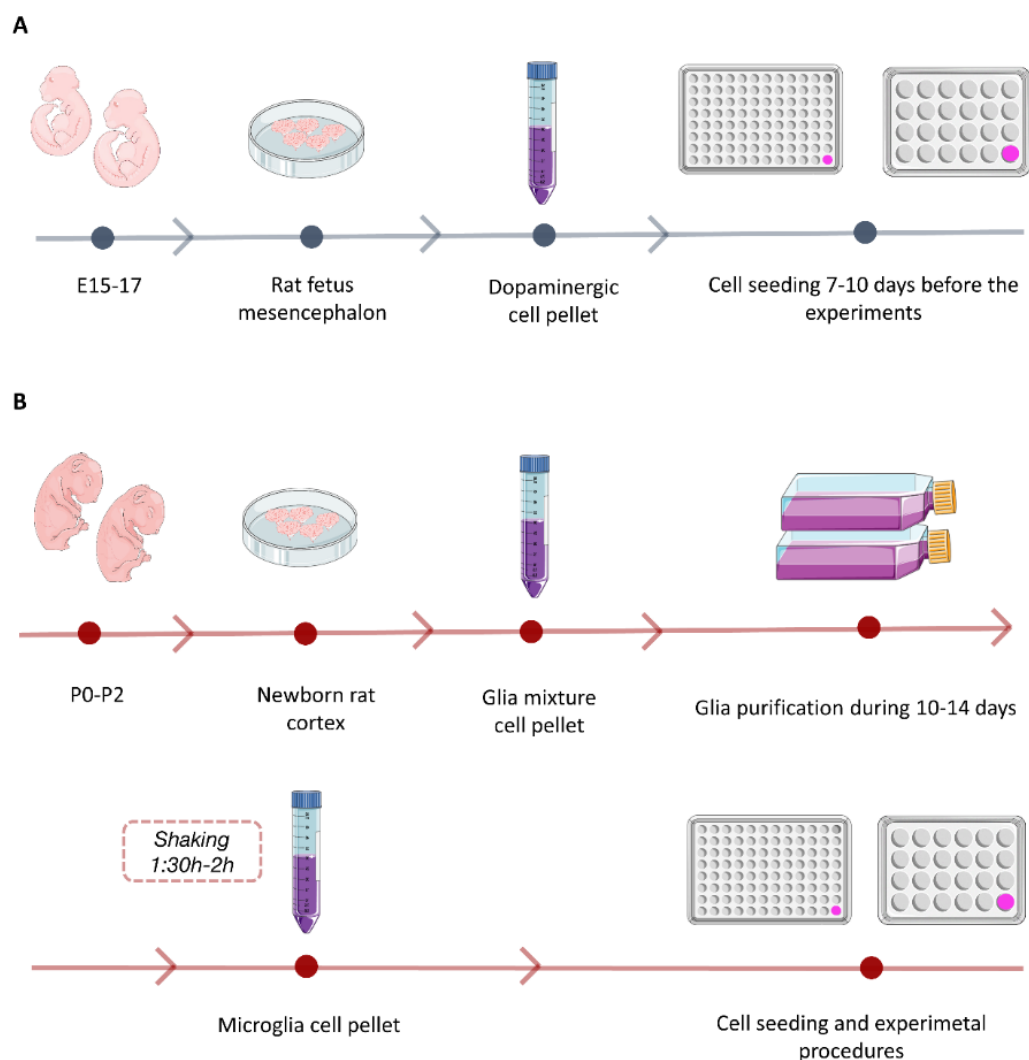


Figure 1. Schematic representation of primary cell culture protocols. (A) Primary dopaminergic neuron culture isolation and seeding. (B) Primary microglia cell culture isolation and seeding. This figure was created using Servier Medical Art templates, which are licensed under a Creative Commons Attribution 3.0 Unported License (<https://smart.servier.com>).

2.4.2. Primary Microglia Cell Culture

Microglia neuronal cultures were prepared from Wistar rat puppets at day 0 to 2 (P0–P2). Animal procedures were reviewed and approved by the Local Ethical Committee for Animal Research of the University of the Basque Country (UPV/EHU, CEEA, ref. M20/2017/035). All the experiments were performed in accordance with the European Community Council Directive on “The Protection of Animals Used for

Scientific Purposes" (2010/63/EU) (22 September 2010) and with Spanish Law (RD 53/2013) (8 February 2013) for the care and use of laboratory animals.

Primary microglia cell cultures were obtained following Chen et al. protocol with slight modifications [43] (Figure 1B). Puppets' brains were removed and kept on ice in a Petri dish (10 cm \varnothing) with HBSS under magnifying glasses for removing the meninges and selecting the brain area of interest. Then, the cortex of the brain was collected and incubated with trypsin for 15 min at 37 °C. The tissue was incubated with DNase for 30 s and, afterwards, the trypsin was inactivated and the tissue was washed twice with DMEM GlutMAX™ FBS 10%, P/S. Finally, the tissue was mechanically dissociated by several passages through a 5 and 2 mL pipette and, then, passed through a 70 μ m nylon strainer and centrifuged for obtaining a cell pellet. The obtained pellet was resuspended in DMEM GlutMAX™ FBS 15%, P/S and incubated in a poly-L-lysine-coated flask at 37 °C in a humidified 5% CO₂ atmosphere. After 3 days, full media were changed to DMEM GlutMAX™ FBS 10%, P/S. After this, half media changes were done every 2–3 days for maintaining this glia mixture culture for 10–14 days. After that period, the flask media were removed and replaced with DMEM GlutMAX™ FBS 15% P/S 24 h before microglia cell isolation started. Microglia cells were detached from the astroglia layer by shaking the flasks at 250 rpm for 1.5–2 h. Then, primary microglia cells were removed from the flask, resuspended in complete DMEM with FBS 15% and seeded in poly-L-lysine-precoated 96-well culture plates (for cell viability and cytokine release assays) and in 24-well culture plates with glass coverslips (for the immunofluorescence assay) at a density of 50×10^3 cells/well and 150×10^3 cells/well, respectively.

2.5. Immunofluorescence

Primary cells were seeded at a density of 150×10^3 cells/well in 24-well culture plates with glass coverslips precoated with poly-L-lysine. At the time of interest, cells were fixed with 3.7% paraformaldehyde (PFA) for 10 min and, then, washed three times in PBS. Then, they were blocked and permeabilized with 1% (w/v) of BSA solution and 0.1% (v/v) Triton X-100 in PBS for 1 h at room temperature. After rinsing, they were incubated in rabbit polyclonal antibody Iba-1 (1:1000), mouse monoclonal anti-GFAP (1:2000) or rabbit polyclonal antibody TH (1:1000), respectively, with 1% (w/v) BSA and 0.1% Triton X-100 in PBS with agitation on at 4 °C. The following day, cells were incubated with the secondary antibody: anti-rabbit Alexa Fluor IgG 488

(1:1000) or anti-goat Alexa Fluor IgG 555 (1:1000), respectively, in PBS with 1% BSA and 0.1% Triton X-100 for 2 h at room temperature. After three rinsing steps, the fixed cells were incubated in DAPI (1:10000) in PBS for 10 min. Then, they were washed twice with PBS and mounted with Fluoromount™.

2.6. Cell Viability Assay

As previously pointed out, for cell viability study, the cells were seeded in 40×10^3 cells/well in poly-d-lysine-precoated 96-well culture plates. Dopaminergic cells were maintained for 7–10 days before performing the experiments and the medium was changed every 3 days, if necessary. At a determined time point, the media from the cells were removed and new fresh media were added with the different nanoparticle concentrations, DHAH-NLCs or Mygliol-NLCs, (100, 75, 50, 25, 12.5 and 5 μ M) for 24 or 48 h. The concentration (μ M) refers to the quantity of DHAH present in the NLC formulation. For dosing Mygliol NPs, an equal amount of NLCs was used as an internal control to observe the difference between using a functional lipid, such as DHAH, versus an inert lipid, such as Mygliol®.

Afterwards, the viability was assessed using the CCK-8 kit. Briefly, 10 μ L of the CCK-8 reagent was added to the cells. After 4 h of incubation, the absorbance of the mixture was read at 450 nm, using 650 nm as the reference wavelength (Plate Reader Infinite M200, Tecan, Männedorf, Switzerland). The absorbance was directly proportional to the number of living cells in the culture. Cell viability for each condition is represented in a percentage related to the control positive (C+), where no treatment was added to the cell media.

In the case of microglia, slight modifications were done in the cell viability assay protocol. After obtaining a pure microglial cell culture, as previously pointed out, the microglia cells were seeded in 50×10^3 cells/well density. Some 24 h after cell attachment, the media were removed and the cells were incubated for 24 h or 48 h with the different concentrations of NLCs, as previously pointed out. Then, the viability CCK-8 test was performed as earlier described.

2.7. 6-OHDA Toxicity Assay

After 7–10 days of maintaining dopaminergic culture, the media were removed and different concentrations of 6-OHDA toxin were added (500, 100, 50, 25, 10 and 5 μ M) for 24 h to correlate neurotoxin concentration to cell viability; for C+, we just

changed the media and, for control negative (C⁻), DMSO 10% was added. To assess cell viability, after 24 h of incubation with 6-OHDA neurotoxin, the media were removed and the cells were fixed with 3.7% paraformaldehyde (PFA) for 10 min and, then, washed three times in PBS. DAPI staining (1:10000) in PBS for 15 min was used to determine viable cells. For cell viability quantification, fluorescence microscopy images were obtained by means of an inverted microscope (Nikon TMS, Hampton, NH). Two images per well and three wells were used for each group; in total, six images were taken per group. Dopaminergic cells were scored as positive if they exhibited defined nuclear counterstaining. The data are expressed as the percentage of the C⁺ group with no treatment, which was set as 100%.

2.8. Neuroprotective Assay

After 7–10 days of maintaining a dopaminergic culture, a neuroprotective assay was carried out with the developed nanocarriers (Figure 2A). The media were removed and different concentrations of DHAH-NLCs and Mygliol NLCs were added to the cells (50, 25 and 12.5 μ M) 24 h before the 6-OHDA neurotoxin was added to the culture. 24 h after, the media were removed and fresh media were added, with a final concentration of 25 μ M 6-OHDA neurotoxin and the previously tested concentrations for NLCs (50, 25 and 12.5 μ M). To assess the neuroprotective effect of DHAH-NLCs against 6-OHDA neurotoxin, the media were removed 24 h later and cells were fixed with 3.7% paraformaldehyde (PFA) for 10 min and, then, washed three times in PBS. DAPI staining (1:10000) in PBS for 15 min was used to determine viable cells. For cell viability quantification, fluorescence microscopy images were obtained by means of an inverted microscope (Nikon TMS, Hampton, NH). Two images per well and three wells were used for each group; in total, six images were taken per group. Dopaminergic cells were scored as positive if they exhibited defined nuclear counterstaining. The data are expressed as the percentage of the C⁺ group with no treatment but just media change, which was set as 100%.

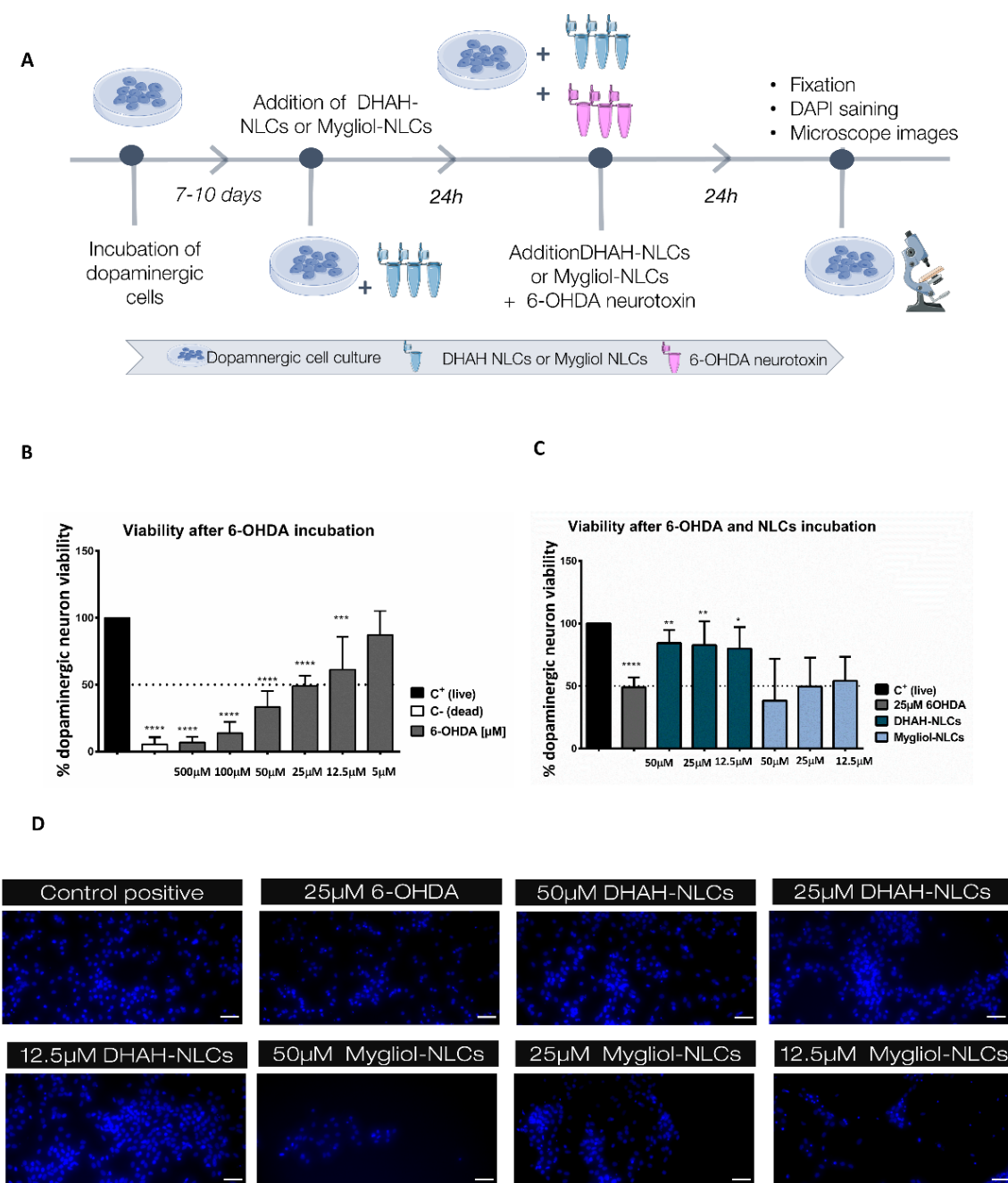


Figure 2. (A) Schematic representation of dopaminergic cell-based assays to evaluate the neuroprotective effects of DHAH-NLCs and Mygliol-NLCs. This figure was created using Servier Medical Art templates, which are licensed under a Creative Commons Attribution 3.0 Unported License (<https://smart.servier.com>). (B) Graphic representation of dopaminergic neuron viability after 24 h of incubation with different doses of 6-OHDA (**** $p < 0.0001$ C+ vs C-, 500 μ M, 100 μ M and 25 μ M *** $p < 0.001$ C+ vs 10 μ M); one-way ANOVA. (C) Graphic representation of the neuroprotective effect of DHAH-NLCs (** $p < 0.01$ 25 μ M 6-OHDA vs 50 μ M DHAH-NLCs and 25 μ M DHAH-NLCs, * $p < 0.05$ 25 μ M 6-OHDA vs 12.5 μ M DHAH-NLCs); One-way ANOVA. (D) Representative fluorescence images of the neuroprotective assay with DAPI staining. The scale bar indicates 50 μ M.

2.9. Proinflammatory Cytokine Release Quantification: TNF- α , IL-1 β and IL-6

DHAH-NLCs antiinflammatory effect against LPS (lipopolysaccharide) was carried out in microglia primary cells (Figure 3A). To perform the assay, cells were pretreated for 24 h with DHAH-NLCs and Mygliol-NLCs at different concentrations selected from studies previously carried out in section 2.6 (50 μ M, 25 μ M and 12.5 μ M) or just media change. After that treatment, media were removed and cells were incubated for another 24 h with LPS 50 ng/mL and the different concentration of the nanoparticles. After that 24 h, the cell media supernatant was collected and stored at -80 °C. The levels of TNF- α , IL-1 β and IL-6 were analyzed with ELISA assay (Peprotech, London, UK). The total amount of cytokine release was normalized according to cell viability measured with CCK-8 assay at the same time point.

2.10. Statistical Analysis

All results are expressed as mean \pm SD. The results obtained from the cell culture have been performed in $n = 3$ biological replicates for all the experiments described in this article. Experimental data were analyzed using the computer program GraphPad Prism (v. 6.01, GraphPad Software, San Diego, CA, USA). One-way ANOVA was used for analyzing all the data represented in this research article. P values <0.05 were considered significant.

3. RESULTS

3.1. Nanoparticle Characterization

The aim of the present work was to develop a new nanocarrier enriched in functional lipids, such as Ω -3 fatty acids, to form the lipid matrix of NLCs. For that purpose, we tried to substitute the lipids of the nanoformulation with different kinds of Ω -3 fatty acids. Precirol ATO 5® was maintained as solid lipid. All modifications in the optimization process of the nanoformulation were performed in the liquid lipid, DHA, DHA-TG and DHA-EE, modifying the liquid lipid type and also the ratio of solid:lipid to formulate NLCs, since the main goal of this research was to increase the percentage of these functional lipids up to the maximum to form this new nanocarrier. In order to achieve this aim, we increased the percentage of lipid liquid from the 0.25% that we used in previous studies with Mygliol® [44–46] to 1.25%, as described in Table 1.

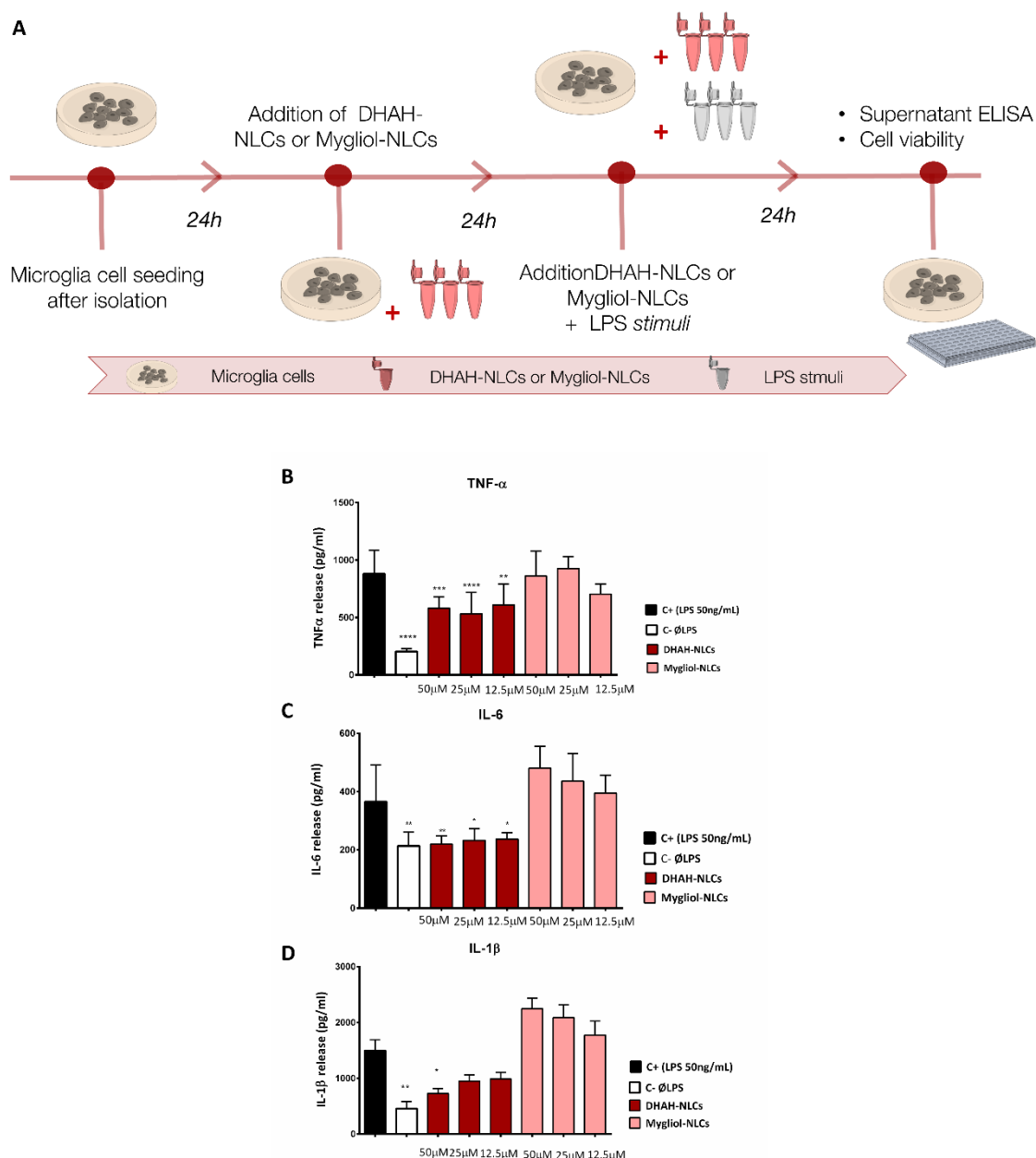


Figure 3. (A) Schematic representation of the anti-inflammatory assay with DHAH-NLCs and Mygliol-NLCs. This figure was created using Servier Medical Art templates, which are licensed under a Creative Commons Attribution 3.0 Unported License (<https://smart.servier.com>). (B) Graphic representation of TNF- α values (pg/mL) for all the different tested concentrations and formulations (****p < 0.0001 C+ vs C- and 25 μ M DHAH-NLCs, ***p < 0.001 C+ vs 50 μ M DHAH-NLCs, **p < 0.01 C+ vs 12.5 μ M DHAH-NLCs); one-way ANOVA. (C) Graphic representation of IL-6 values (pg/mL) for all the different tested concentrations and formulations (**p < 0.01 C+ vs C- and 50 μ M DHAH-NLCs, *p < 0.05 C+ vs 25 μ M DHAH-NLCs and 12.5 μ M DHAH-NLCs); one-way ANOVA. (D) Graphic representation of IL-1 β values (pg/mL) for all the different tested concentrations and formulations (**p < 0.01 C+ vs C- and *p < 0.05 C+ vs 5 μ M DHAH-NLCs); one-way ANOVA.

Between DHAH-EE and DHAH-TG, the ethyl ester form (DHAH-EE) was liquid at room temperature, and the obtained lyophilized NLCs were easy to handle. However, the NLCs prepared with DHAH-TG became a soggy and sticky powder at room temperature, and this was more difficult to handle after the lyophilization process. That is why the nanoformulations developed with DHAH-TG (C1–C4, Figure 4) were discarded to continue working.

We used DHA and two different types of DHAH to select the most suitable one to prepare the NLCs, and we worked with Mygliol®, the liquid lipid previously used in our research group for different clinical applications [15,47], as our control.

NLCs formed with DHA and DHAH-EE showed similar pharmaceutical characteristics; however, as we probed in a previous *in vivo* study, DHA and DHAH functional lipids showed different biological activity [31]. Therefore, taking into account the remarkably beneficial effects of DHAH, we chose DHAH-EE nanoformulations to continue working. Among the different nanoformulations developed with DHAH-EE (D1–D4, Figure 4), we selected D3 (51.40nm \pm 11.65 and 0.415 \pm 0.082 for PDI values) since it was the formulation with the highest percentage of Ω -3 fatty acid incorporated into the lipid matrix of NLCs with the best resuspension characteristics, qualitatively determined. In order to confirm the therapeutic effect of DHAH-EE in the newly developed NLCs, we also chose Mygliol-based NLCs in the same proportion of solid:liquid lipid (A3, Figure 4), with a particle size of 75.02 \pm 6.97 nm and 0.474 \pm 0.023 PDI value, as the control formulation.

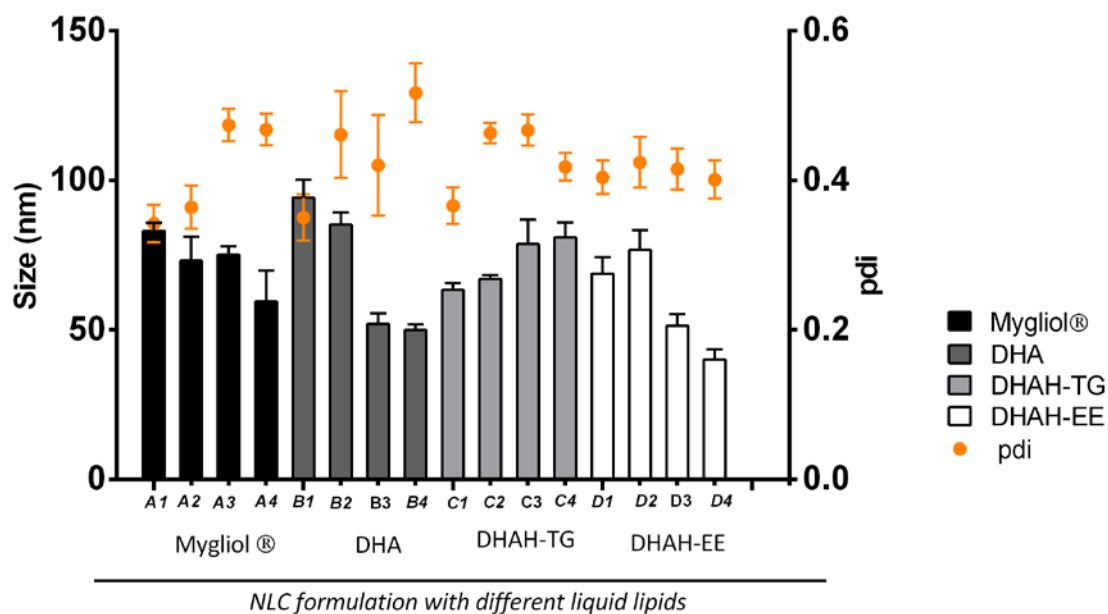


Figure 4. Characterization of the developed nanostructured lipids (NLCs) (n = 3 for all the nanoformulations).

All the data regarding size, PDI and Z potential of all the developed nanoformulations have been summarized in Table 2. As seen, the size of NLC decreased when the percentage of liquid lipid was higher. Moreover, the Z potential of all nanoformulations was negative, which was reverted after CS and TAT coating (Table 3).

In the next step, the CS and TAT coating process was performed. In Table 2, we can see the results from CS-TAT-NLC-DHAH-EE nanoformulation, called DHAH-NLCs, and from Mygliol-based nanoparticles with CS and TAT, called Mygliol-NLCs.

Both formulations were around 100 nm in size, with a PDI value below 0.5, and exhibited positive zeta values, indicating that the CS and TAT coating process has been successfully performed. In the external morphological study made by TEM (transmission electron microscopy), the nanoparticles showed a uniform size without irregularities (Figure 5). The DSC thermograms of the different excipients and formulations have been summarized in Appendix Figure A1.

Table 2. Characterization of the developed NLCs (n = 3 for all the nanoformulations). The data are presented in media \pm SD.

Formulation	Size after Lyoph (nm)	PDI	Z Potential (mV)
Formulation A1	83.07 \pm 36.54	0.342 \pm 0.061	-15.6 \pm 1.7
Formulation A2	73.11 \pm 19.51	0.364 \pm 0.071	-16.0 \pm 2.8
Formulation A3	75.02 \pm 6.97	0.474 \pm 0.023	-14.2 \pm 19.2
Formulation A4	59.38 \pm 25.39	0.468 \pm 0.052	-14.4 \pm 4.8
Formulation B1	94.19 \pm 18.01	0.350 \pm 0.092	-19.4 \pm 1.8
Formulation B2	85.20 \pm 12.20	0.461 \pm 0.174	-19.9 \pm 3.1
Formulation B3	51.98 \pm 10.70	0.420 \pm 0.202	-22.7 \pm 3.5
Formulation B4	49.93 \pm 5.36	0.587 \pm 0.118	-22.8 \pm 4.1
Formulation C1	63.34 \pm 6.95	0.366 \pm 0.073	-21.0 \pm 5.8
Formulation C2	67.02 \pm 4.10	0.463 \pm 0.031	-16.5 \pm 2.3
Formulation C3	78.63 \pm 24.66	0.467 \pm 0.062	-20.1 \pm 3.4
Formulation C4	80.87 \pm 15.15	0.418 \pm 0.056	-20.4 \pm 1.5
Formulation D1	68.62 \pm 16.70	0.404 \pm 0.068	-22.7 \pm 2.6
Formulation D2	76.68 \pm 20.12	0.425 \pm 0.101	-24.2 \pm 2.9
Formulation D3	51.40 \pm 11.65	0.415 \pm 0.082	-24.1 \pm 2.9
Formulation D4	39.98 \pm 10.39	0.401 \pm 0.076	-24.9 \pm 2.8

Table 3. Characterization of the final nanoformulations used for cell culture tests. (n = 2 independent experiments).

Formulation	Size after Lyoph (nm)	PDI	Z Potential (mV)
DHAH-NLC	97.80 \pm 2.00	0.274 \pm 1.26	12.63 \pm 1.26
Mygliol-NLC	94.31 \pm 0.43	0.454 \pm 0.007	14.13 \pm 0.21

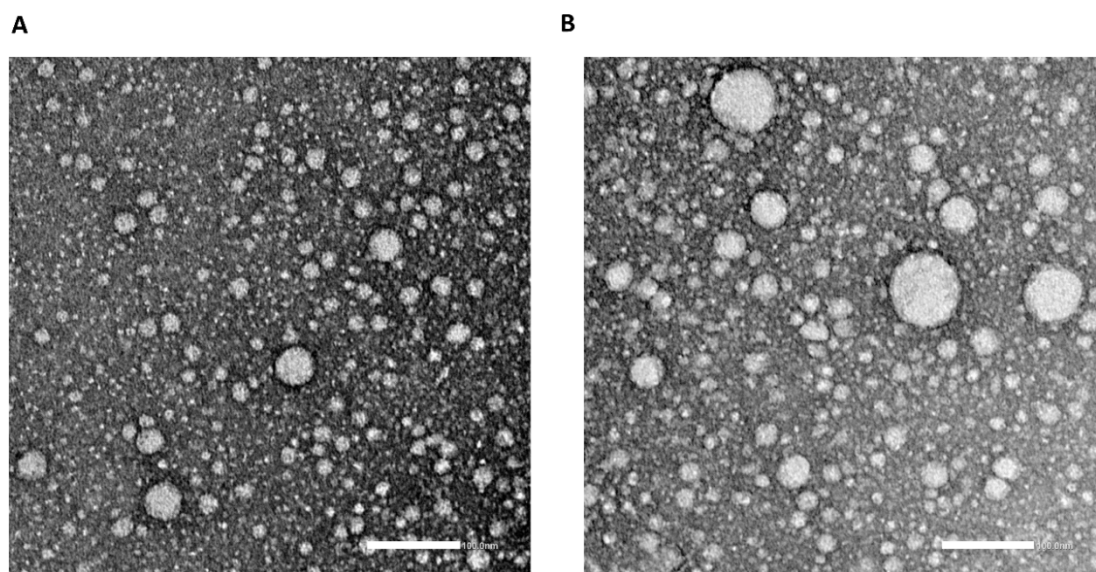


Figure 5. TEM (transmission electron microscopy) photographs of NLC (scale bar 100 nm). (A) hydroxylated derivate of docohexaenoic acid nanostructured lipids (DHAH-NLCs) (B) Mygliol-NLCs.

On the other hand, as seen in Figure A2, FTIR results exhibited a number of characteristic protein transmission bands (cm^{-1}). Mygliol-NLC and DHAH-NLC without CS and TAT coating showed typical peaks of lipid components, such as O–H stretching (3315), aliphatic C–H (2915, CH_3 and CH_2) asymmetrical stretching, aliphatic C–H (2852, CH_3 and CH_2) symmetrical stretching and C=O (1736, carboxylic group) stretching in addition to the vibrations associated with C–O and C–C (1150 and from 992 to 843) bonds. Moreover, CH_2 and CH_3 stretching (1466) and bending (1342) bands can be seen. Regarding nanoformulations with TAT and CS coating (CS-TAT-Mygliol-NLC and CS-TAT-DHAH-NLC), a new peak can be seen, concretely, in amide I (N–H stretching) (1645). This new peak is due to a chemical interaction. Indeed, it is related to the presence of the amide bond formed after TAT peptide conjugation through a cross linking reaction.

3.2. Cell Cultures

In order to assess the purity of our primary cultures, an immunofluorescence technique was performed in both dopaminergic and microglia cell cultures. The experiments were performed in triplicate and repeated at least three times independently ($n = 3$ biological replicates). Dopaminergic cell cultures were positive

for TH dopaminergic marker, as shown in Figure 6A. In the case of the microglia cell culture, we tested both the microglia marker Iba1 and the astroglia maker GFAP. The culture was shown to be specific in a high percentage to microglia marker (Figure 6B. iv). However, it must be noted that, after this isolation method, the culture is not 100% specific for microglia cells, and also some astrocytes can be seen in a non-noteworthy way.

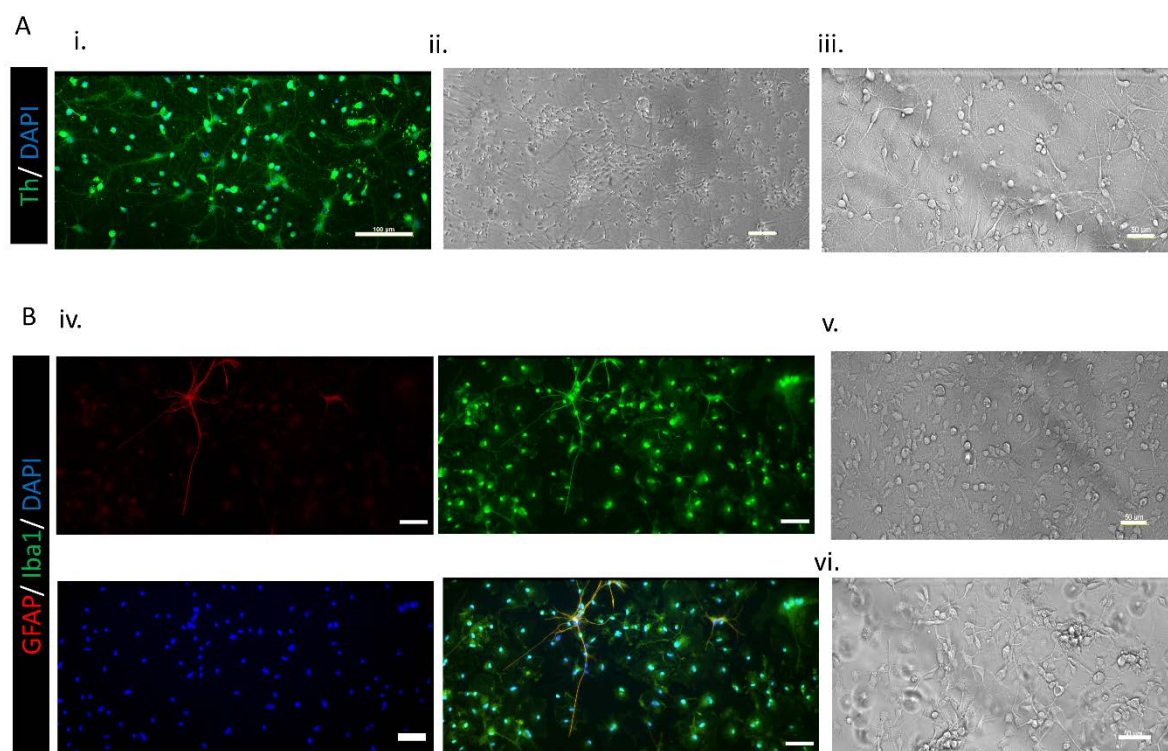


Figure 6. (A) Images of the primary dopaminergic cell culture. i: Immunofluorescence staining: positive for TH dopaminergic marker. (Scale bar 100 μ M) ii: (scale bar 100 μ M) and iii: (scale bar 50 μ M) Bright field images of primary dopaminergic cell cultures. (B) Images of the primary microglia cell culture. Iv: Immunofluorescence staining. (Scale bar 50 μ M) v: Bright field images of glia mix culture. (Scale bar 50 μ M). vi: Bright field images of the primary microglia cell culture after isolation. (Scale bar 50 μ M).

3.3. In Vitro Cell Viability Study

In order to assess the cytocompatibility of the nanoparticles, they were incubated with the dopaminergic and microglia cell cultures. After 24 and 48 h, cell viability was measured through the CCK-8 assay. Figure 7A,B illustrates the results obtained in the CCK-8 assay after incubating NLCs with a dopaminergic cell culture. None of the concentrations for the nanoformulations tested in dopaminergic cell cultures were cytotoxic, showing percentages of cell viability >70%. Indeed, as shown in Figure 7B, at 48 h, cell viability for the cultures treated with DHAH-NLCs was slightly

better at any of the tested concentrations compared to Mygliol-NLCs treated cells. The results of the viability assay for the microglia cell culture are, to some extent, different. As shown in Figure 7C,D, the tested concentrations of 100 and 75 μ M for the Mygliol-NLC formulation decreased cell viability below 70% at both tested time points; this effect was not seen with DHAH-NLC for any of the tested time points. This beneficial effect for DHAH-NLC was seen in any of the tested conditions, being more notorious at 50, 25 and 12.5 μ M concentrations (Figure 7C,D).

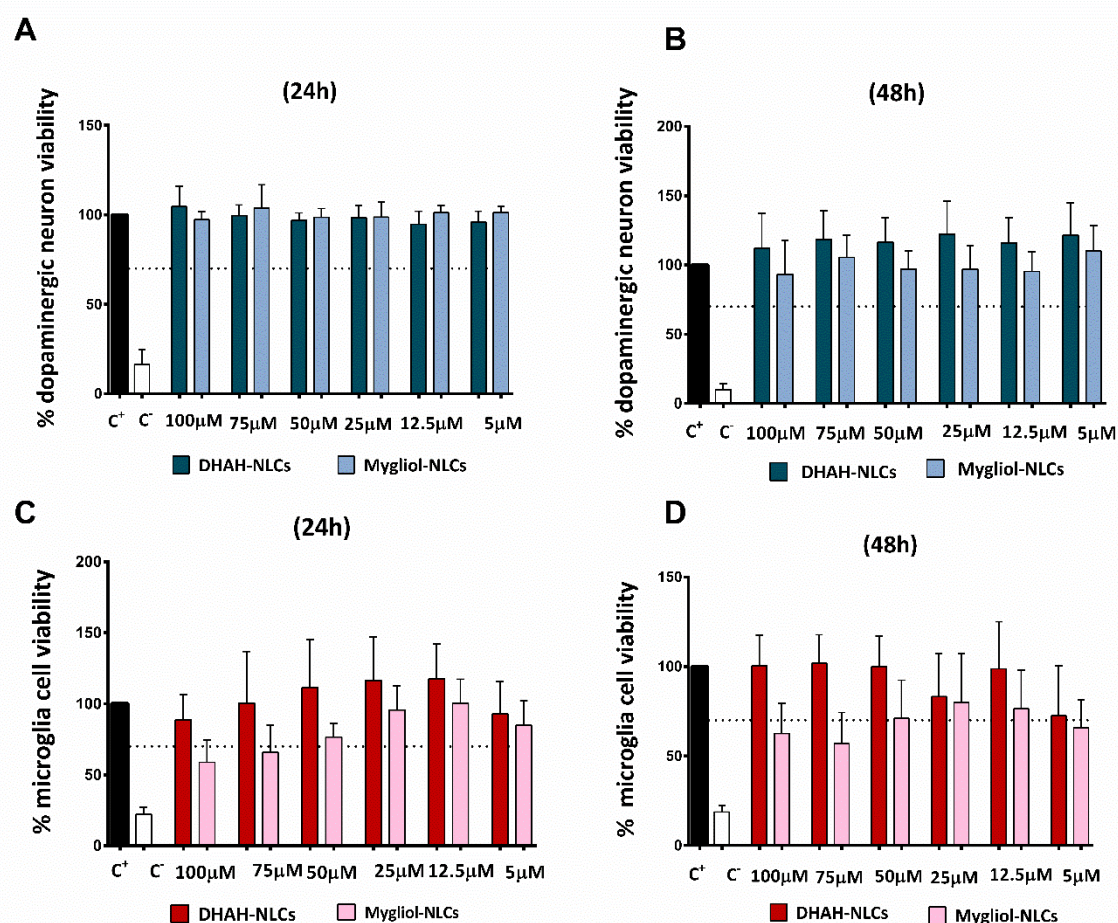


Figure 7. (A) Dopaminergic neuron viability at 24 h. (B) Dopaminergic neuron viability at 48 h. (C) Microglia cell viability at 24 h. (D) Microglia cell viability at 48 h. In all cases, different concentrations of DHAH-NLCs and Mygliol-NLCs were tested (the graphs show the results of three biological replicates media \pm SD).

3.4. 6-OHDA Neurotoxin Effect on Dopaminergic Culture

The incubation of dopaminergic neurons with 6-OHDA decreased cell viability in a dose-dependent manner (Figure 2B). The incubation of cells with 500 μ M of 6-OHDA resulted in only 6.78 ± 4.11 ($****p < 0.0001$) remaining living cells, which is similar to the values obtained after the incubation with our C⁻ (DMSO 10%) ($5.45 \pm$

5.2, **** $p < 0.0001$). In the following test concentrations, the values for 100 and 50 μM were below 50% of the remaining living cells; more specifically, for 100 μM (13.82 ± 8.24 , **** $p < 0.0001$) and for 50 μM (33.37 ± 11.87 , **** $p < 0.0001$), the values were obtained. In the case of 25 μM , the remaining living cells were around 50% (49.05 ± 7.79 , **** $p < 0.0001$), and, for 10 μM , it was slightly higher (60.37 ± 24.33 , *** $p < 0.001$). Finally, the incubation of dopaminergic cells with 5 μM 6-OHDA neurotoxin led to no statistical difference when compared to the C⁺ group, with 87.17 ± 18.02 remaining living cells.

3.5. DHAH-NLCs Exhibited a Neuroprotective Effect

After selecting the dose for generating a cell death of 50% after 24 h of incubation with 6-OHDA, 25 μM , we tried to demonstrate the neuroprotective effect of our DHAH-NLCs. The incubation of the dopaminergic neuron culture with DHAH-NLCs before and after 6-OHDA addition resulted in a neuroprotective effect in comparison to the neurotoxin itself (Figure 2C). The treatment with Mygliol-NLCs did not increase cell viability, with remaining living cell values similar to those obtained with just the neurotoxin incubation. The values for 50 μM Mygliol NLCs (38.35 ± 33.45), 25 μM Mygliol NLCs (49.49 ± 23.15) and 12.5 Mygliol NLCs (54.13 ± 19.11) were similar, without any neuroprotective effect. In contrast, for those cells treated with DHAH-NLCs, the values for the remaining living cells were similar to the control set as 100%. There were no statistical differences between the tested doses with the following values: 50 μM DHAH-NLCs (84.22 ± 10.58 , ** $p < 0.01$), 25 μM DHAH-NLCs (82.70 ± 18.96 , ** $p < 0.01$) and 12.5 μM DHAH-NLCs (79.92 ± 17.06 , * $p < 0.05$). The images taken with fluorescence microscopy showed the difference in living cells, comparing the ones treated with DHAH-NLCs with those treated Mygliol-NLCs (Figure 2D).

3.6. DHAH-NLCs Decreased Cytokine Proinflammatory Release

In order to assess the antiinflammatory effect of our DHAH-enriched nanoparticles (DHAH-NLCs), we performed the ELISA technique from a cell culture supernatant, as described in the Materials and Methods section. The results obtained from the cell supernatants for TNF- α , IL-1 β and IL-6 cytokines are summarized in Figure 3B–D.

Regarding TNF- α ELISA (Figure 2B), the basal levels of TNF- α , C⁻ (204.0 ± 23.96) statically increased ($****p < 0.0001$) after LPS treatment (50 ng/mL), named C⁺ (879.4 ± 204.0). In addition, although DHAH-NLCs were not able to obtain control levels of this cytokine, it is noteworthy that the effect of this treatment decreases this proinflammatory cytokine release, as seen in Figure 3B. This effect can be seen in all DHAH-NLCs concentrations: 50 μ M DHAH-NLCs (581.0 ± 100.1 , $***p < 0.001$), 25 μ M DHAH-NLCs (532.1 ± 186.0 , $****p < 0.0001$) and 12.5 μ M DHAH-NLCs (609.2 ± 55.1 , $**p < 0.01$), without any statistically significant differences between the different doses. In the case of Mygliol-NLCs, we could not see any positive effect decreasing cytokine levels for any of the tested concentrations ($p > 0.05$).

For the second tested cytokine, IL-6 (Figure 3C), we also observed the increase of basal levels (213.7 ± 47.3) up to almost double concentration (365.1 ± 125.9 , $***p < 0.001$) after the incubation with LPS. In this case, we could also see the decrease of this proinflammatory cytokine after the treatment with DHAH-NLCs. All the tested concentrations demonstrated a positive effect, decreasing IL-6 levels; indeed, 50 μ M DHAH-NLCs (219.3 ± 29.3 , $**p < 0.01$), 25 μ M DHAH-NLCs (232.7 ± 40.8 , $*p < 0.05$) and 12.5 μ M DHAH-NLCs (237.2 ± 15.4 , $*p < 0.05$) were the obtained values. However, no statistically significant differences were observed between the different concentrations. Regarding Mygliol-NLCs, no antiinflammatory effect was obtained after the treatment with these nanoparticles for any of the tested concentrations ($p > 0.05$).

Finally, we analyzed the levels of IL-1 β proinflammatory cytokine (Figure 3D). In this case, the LPS stimuli also increased the basal values (457.4 ± 125.8) more than three-fold, as we can see for the C⁺ values (1495.0 ± 518.1 , $**p < 0.01$). As seen before with the other two proinflammatory cytokines, the treatment with DHAH-NLCs decreased IL-1 β values. Actually, the values for DHAH-NLCs were the following: 50 μ M DHAH-NLCs (726.2 ± 256.6 , $*p < 0.05$), 25 μ M DHAH-NLCs (948.7 ± 301.6) and 12.5 μ M DHAH-NLCs (985.6 ± 301.0). Although in this case only the group treated with 50 μ M DHAH-NLCs showed a statistically significant difference, the trend to decrease this proinflammatory cytokine is notorious in all DHAH-NLCs concentrations. As in the previously analyzed proinflammatory cytokines, the levels of IL-1 β remained elevated for the cells treated with Mygliol-NLCs, for any of the tested conditions, showing values similar to the positive control.

4. DISCUSSION

NDs are one of the main problems of the public health system in the 21st century. Although they have different clinical manifestations and symptoms, they all share a complex mechanism of neurodegeneration, with aging as the main risk factor, and they are without an effective treatment [1,48]. In order to obtain an effective treatment for NDs, in the last few years, different therapeutic molecules have been raised as new clinical candidates. Among others, the use of functional lipids such as PUFAs and, more concretely, DHA and DHAH have been raised as a useful tool to treat NDs since they exhibit beneficial effects, decreasing neuroinflammation and protein deposit or increasing the release of neuroprotective agents [30,49]. However, no matter the treatment, one of the main issues with treating NDs is reaching the brain and passing through the BBB. That is why the use of nanotechnology and, more concretely, the NLCs, has exhibited promising results for targeting the brain, increasing bioavailability, protecting from oxidation and, therefore, maintaining the bioactivity of different molecules [19].

The main goal of this work was to combine both strategies to develop a new therapeutic nanocarrier enriched with PUFAs, more concretely, with DHAH, to generate a new type of NP that could target the brain and exhibit neuroprotective and antiinflammatory effects, therefore becoming a functional nanocarrier that could be combined with different molecules in the future to promote a synergistic therapy.

All the developed nanoformulations were 50–90 nm in size, with a PDI value below 0.5 indicating a homogenous suspension (Figure 4). The increment of the liquid lipid ratio led to a decrease in the size of the nanoparticles, as shown in previous publications (Table 2) [50,51]. Moreover, as seen in DSC thermograms (Figure A1), the addition of the liquid lipid to the solid lipid led to a slight reduction of the melting point of Precirol of 3–4 °C in all NLC thermograms, which is similar to previously conducted studies [50,52,53]. Anyway, the selected solid:liquid lipid ratio for the two different lipids, Mygliol and DHAH, was in the ratio normally used for NLC preparation [24]. After selecting the ratio and the lipid to constitute the new nanoformulation, the NPs' surface was modified with the addition of CS and TAT, resulting in two different formulations, named DHAH-NLCs and Mygliol-NLCs. The addition of CS and TAT peptide led to the conversion of Z potential from negative values to positive values (Tables 2 and 3), indicating that the undergoing process

was successfully performed. Moreover, the presence of amide I in FTIR spectra (Figure A2) confirmed that the coating process with TAT was successfully performed. As we have previously demonstrated, the addition of CS and TAT increased in vivo brain targeting after intranasal administration [16,24]. Moreover, TAT is a well-known CPP, usually used to enhance the delivery of different cargos into different types of cells, such as neurons [54,55]. The resulting NPs were similar in size (around 100 nm) and exhibited positive zeta values due to the successful CS coating process (Table 3).

Among the different NDs, in this research paper, we aim to study the effect of our newly developed nanocarriers in a cell model of PD by adding 6-OHDA neurotoxin, one of the most widely used neurotoxins, to a dopaminergic cell culture to mimic the destruction of catecholaminergic neurons and the degeneration of the nigrostriatal pathway [56]. The addition of 25 μ M 6-OHDA for 24 h led to a decrease in cell viability of 50%, as shown in Figure 2B. The dose and incubation time for this neurotoxin is variable, according to the scientific data available, varying from 5 to 100 μ M and from 30 min to 48 h [57–60]. That is why we incubated the neuronal cells with different doses for 24 h, an intermediate time point in the published articles, and selected the dose that generated 50% cell death so we could really see the effect of the neurotoxin on cell viability. In order to check the safety and effectiveness of the DHAH incorporated into our NLCs, we incubated the nanoformulations for 24 h and 48 h. All tested concentrations were shown to be safe (Figure 7A,B), with a viability up to 70% and showing better values for DHAH-NLCs at 48 h. Moreover, the effectiveness of DHAH-NLCs was also evaluated in dopaminergic cell cultures after the incubation with 6-OHDA. DHAH-NLCs were shown to be effective at protecting the cells from the neurotoxin compared to Mygliol-NLCs as the control group (Figure 2C and 2D). These data are in line with previous publications regarding the DHA neuroprotective effect shown in neuron cell cultures [61,62]. Moreover, it demonstrates the effectiveness of the DHAH functional lipid incorporated into the newly developed NLCs.

On the other hand, the neuroinflammatory process undergoing NDs and, more specifically, in PD is well known, being the consequence or the cause of the disease. Whatever the origin of the neuroinflammation, it is a fact that a therapeutic intervention downregulating this process could be great at halting the progression

of the disease [63]. Although different cell types and molecules are involved in the neuroinflammation, microglia cells are the primary initiators of the central inflammatory response to acute and chronic disorders related to NDs [64]. In order to treat this inflammatory response, PUFAs and, more concretely, DHA and DHAH have been raised as emerging candidates to downregulate this process and become a new therapeutic approach [9,31]. The DHAH-NLCs developed in this study were shown to be safe at any of the tested concentrations, with a viability up to 70%, in contrast to Mygliol-NLCs, where higher concentrations decreased cell viability (Figure 7C,D). Thus, these results demonstrated that the newly developed formulation with DHAH can be used in high concentrations without affecting cell viability.

In order to mimic the neuroinflammatory process in primary microglia cells, different molecules can be used. Among them, the gold standard stimuli for generating reactive gliosis and activating the neuroinflammation cascade is LPS. LPS has been widely used to generate animal models of neuroinflammation or induce it in cell culture, both primary and microglia cell lines [65–67]. The addition of LPS at 50 ng/mL concentration in this study generated the production of proinflammatory cytokines in similar levels to those in previously published scientific articles for microglia primary cell cultures isolated after the shaking method [66]. Regarding the potential antiinflammatory effect of our NPs, we showed that the ability of DHAH to decrease neuroinflammation was maintained in DHAH-NLCs, obtaining proinflammatory cytokine levels similar to C⁻ in IL-6 and IL-1 β , and decreasing TNF- α almost by half for any of the tested concentrations (Figure 3B–D). The ability of PUFAs to decrease the cytokine proinflammatory levels has previously been described [68]; thus, this study enforces the use of these kinds of PUFAs formulated in NLCs as an emerging tool to treat the undergoing inflammatory process in NDs.

5. CONCLUSIONS

Altogether, these results highlight that the newly developed nanocarriers can constitute a new therapeutic tool for treating NDs. The DHAH-NLCs were similar to previously developed NLCs in size, PDI, zeta values and TEM morphology. Moreover, they exhibited neuroprotective effects in a cell culture model of dopaminergic neurons and antiinflammatory properties, decreasing proinflammatory cytokine levels in primary microglia cell cultures. Although future

studies are needed to check its suitability in a different cell culture model or animal model of the disease, the results presented in this research article are promising for this new functional nanocarrier. Moreover, the combination of this new, safe and effective nanocarrier with different clinically approved or investigated therapeutic molecules could become in an emerging tool to treat, in a synergistic manner, the symptoms associated with NDs.

Author Contributions: Conceptualization, S.H., E.H., M.I. and R.M.H.; writing—original draft preparation, S.H.; writing—review and editing, S.H., E.H., M.I. and R.M.H.; visualization, S.H.; supervision, E.H, M.I. and R.M.H.; project administration, E.H., M.I. and R.M.H.; funding acquisition, M.I. and R.M.H. All authors have read and agreed to the published version of the manuscript.

Funding: This project was partially supported by the Spanish Ministry of Economy and Competitiveness (RTC-2015-3542-1) and the Basque Government (Consolidated Groups, IT 907–16).

Acknowledgments: The authors give thanks for the technical and human support provided by SGIker of UPV/EHU and European funding (ERDF and ESF). S. Hernando thanks the Basque Government for the fellowship grant.

Conflicts of Interest: The authors declare no conflict of interest.

APPENDIX

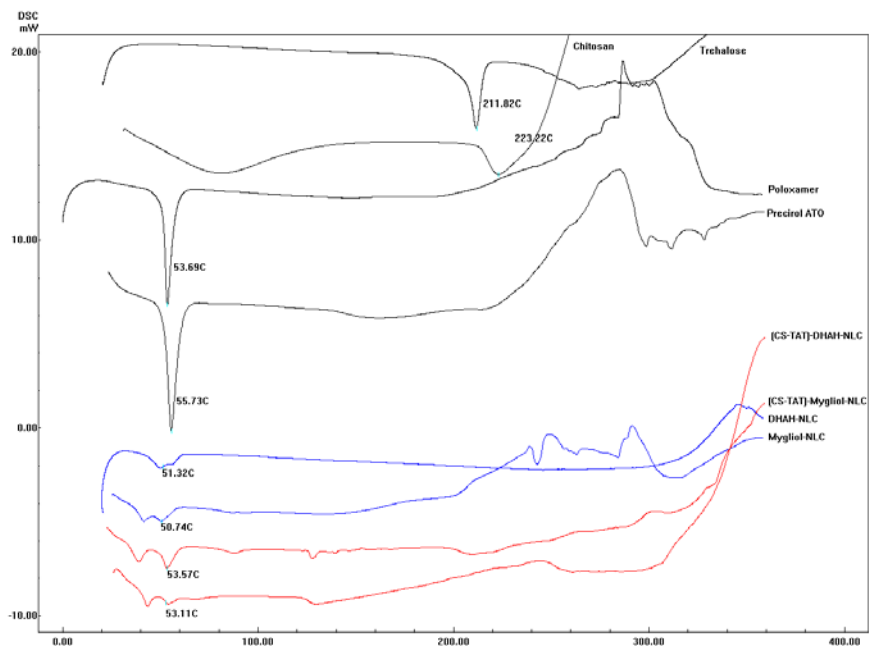


Figure A1. Differential scanning calorimetry (DSC) graphs of pure excipients (D-trehalose, Poloxamer 188, Precirol ATO 5, chitosan (CS) and the different developed nanoparticles).

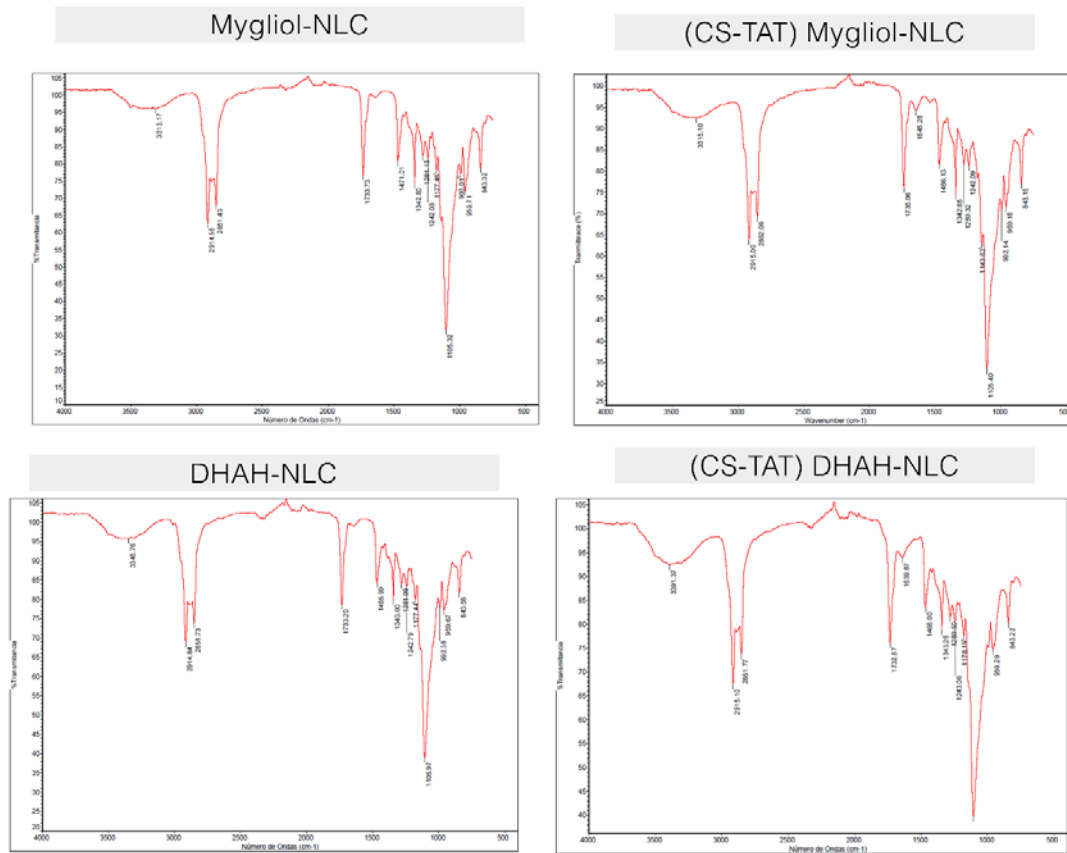


Figure A2. FTIR spectra of Mygliol-NLC, (CS-TAT) Mygliol-NLC, DHAH-NLC and (CS-TAT) DHAH-NLC.

6 REFERENCES

- [1] Hou, Y.; Dan, X.; Babbar, M.; Wei, Y.; Hasselbalch, S.G.; Croteau, D.L.; Bohr, V.A. Ageing as a risk factor for neurodegenerative disease. *Nat. Rev. Neurol.* 2019, 15, 565–581.
- [2] Kalia, L.V.; Lang, A.E. Parkinson's disease. *Lancet* 2015, 386, 896–912.
- [3] Scheltens, P.; Blennow, K.; Breteler, M.M.B.; de Strooper, B.; Frisoni, G.B.; Salloway, S.; Van der Flier, W.M. Alzheimer's disease. *Lancet* 2016, 388, 505–517.
- [4] Kalia, L.V.; Kalia, S.K.; Lang, A.E. Disease-modifying strategies for Parkinson's disease. *Mov. Disord.* 2015, 30, 1442–1450.
- [5] Xie, A.; Gao, J.; Xu, L.; Meng, D. Shared mechanisms of neurodegeneration in Alzheimer's disease and Parkinson's disease, *Biomed. Res. Int.* 2014, 2014, 648740.
- [6] Oertel, W.; Schulz, J.B. Current and experimental treatments of Parkinson disease: A guide for neuroscientists. *J. Neurochem.* 2016, 139 (Suppl. 1), 325–337.
- [7] Briggs, R.; Kennelly, S.P.; O'Neill, D. Drug treatments in Alzheimer's disease. *Clin. Med. (Lond).* 2016, 16, 247–253.
- [8] Sarubbo, F.; Moranta, D.; Asensio, V.J.; Miralles, A.; Esteban, S. Effects of Resveratrol and Other Polyphenols on the Most Common Brain Age-Related Diseases. *Curr. Med. Chem.* 2017, 24, 4245–4266.
- [9] Bazinet, R.P.; Laye, S. Polyunsaturated fatty acids and their metabolites in brain function and disease. *Nat. Rev. Neurosci.* 2014, 15, 771–785.
- [10] Allen, S.J.; Watson, J.J.; Shoemark, D.K.; Barua, N.U.; Patel, N.K. GDNF, NGF and BDNF as therapeutic options for neurodegeneration. *Pharmacol. Ther.* 2013, 138, 155–175.
- [11] Garbayo, E. Estella-Hermoso de Mendoza, A.; Blanco-Prieto, M.J. Diagnostic and therapeutic uses of nanomaterials in the brain. *Curr. Med. Chem.* 2014, 21, 4100–4131.
- [12] Hernando, S.; Herran, E.; Pedraz, J.L.; Igartua, M.; Hernandez, R.M.; Nanotechnology Based Approaches for Neurodegenerative Disorders: Diagnosis and Treatment. In *Drug and Gene Delivery to the Central Nervous System for Neuroprotection*; Sharma, H.S., Muresanu, D.F., Sharma, A., Eds.; Springer International Publishing: Cham, Switzerland, 2017; pp. 57–87.
- [13] Meredith, M.E.; Salameh, T.S.; Banks, W.A. Intranasal Delivery of Proteins and Peptides in the Treatment of Neurodegenerative Diseases. *AAPS J.* 2015, 17, 780–787.
- [14] Gambaryan, P.Y.; Kondrasheva, I.G.; Severin, E.S.; Guseva, A.A.; Kamensky, A.A. Increasing the Efficiency of Parkinson's Disease Treatment Using a poly(lactic-co-glycolic acid) (PLGA) Based L-DOPA Delivery System. *Exp Neurobiol.* 2014, 23, 246–252.
- [15] Gartzandia, O.; Herrán, E.; Ruiz-Ortega, J.A.; Miguelez, C.; Igartua, M.; Lafuente, J.V.; Pedraz, J.L.; Ugedo, L.; Hernández, R.M. Intranasal administration of chitosan-coated nanostructured lipid

carriers loaded with GDNF improves behavioral and histological recovery in a partial lesion model of Parkinson's disease. *J. Biomed. Nanotechnol.* 2016, 12, 1–11.

[16] Gartzandia, O.; Egusquiaguirre, S.P.; Bianco, J.; Pedraz, J.L.; Igartua, M.; Hernandez, R.M.; Pr at, V.; Beloqui, A. Nanoparticle transport across in vitro olfactory cell monolayers. *Int. J. Pharm.* 2016, 499, 81–89.

[17] Kanazawa, T.; Akiyama, F.; Kakizaki, S.; Takashima, Y.; Seta, Y.; Delivery of siRNA to the brain using a combination of nose-to-brain delivery and cell-penetrating peptide-modified nano-micelles. *Biomaterials.* 2013, 34, 9220–9226.

[18] Hernando, S.; Gartzandia, O.; Herran, E.; Pedraz, J.L.; Igartua, M.; Hernandez, R.M. Advances in nanomedicine for the treatment of Alzheimer's and Parkinson's diseases. *Nanomedicine (Lond)* 2016, 11, 1267–1285.

[19] Re, F.; Gregori, M.; Masserini, M.; Nanotechnology for neurodegenerative disorders. *Matur.* 2012, 73, 45-51.

[20] Srikanth, M.; Kessler, J.A. Nanotechnology-novel therapeutics for CNS disorders. *Nat. Rev. Neurol.* 2012, 8, 307-318.

[21] da Rocha Lindner, G.; Bonfanti Santos, D.; Colle, D.; Gasnhar Moreira, E.L.; Daniel Prediger, R.; Farina, M.; Khalil, N.M.; Mara Mainardes, R. Improved neuroprotective effects of resveratrol-loaded polysorbate 80-coated poly(lactide) nanoparticles in MPTP-induced Parkinsonism. *Nanomedicine (Lond)* 2015, 10, 1127–1138.

[22] Sharma, S.; Lohan, S.; Murthy, R.S.R. Formulation and characterization of intranasal mucoadhesive nanoparticulates and thermo-reversible gel of levodopa for brain delivery. *Drug Dev. Ind. Pharm.* 2014, 40 (7), 869-878.

[23] Shah, B.; Khunt, D.; Bhatt, H.; Misra, M.; Padh, H. Application of quality by design approach for intranasal delivery of rivastigmine loaded solid lipid nanoparticles: Effect on formulation and characterization parameters. *Eur. J. Pharm. Sci.* 2015, 78, 54–66.

[24] Hernando, S.; Herran, E.; Figueiro-Silva, J.; Pedraz, J.L.; Igartua, M.; Carro, E.; Hernandez, R.M. Intranasal Administration of TAT-Conjugated Lipid Nanocarriers Loading GDNF for Parkinson's Disease. *Mol. Neurobiol.* 2018, 55, 145–155.

[25] Beloqui, A.; Solin s, M. .; Rodr guez-Gasc n, A.; Almeida, A.J.; Pr at, V. Nanostructured lipid carriers: Promising drug delivery systems for future clinics. *Nanomedicine* 2016, 12, 143–161.

[26] In s Teixeira, M.; Lopes, C.M.; Helena Amaral, M.; Costa, P.C. Current insights on lipid nanocarrier-assisted drug delivery in the treatment of neurodegenerative diseases. *Eur. J. Pharm. Biopharm.* 2020, 149, 192–217.

[27] Pedraz, J.L.; Igartua, M.; Maria, R.; Hernando, S. The role of lipid nanoparticles and its surface modification in reaching the brain: An approach for neurodegenerative diseases treatment. *Curr. Drug Deliv.* 2018, 15, 1218–1220.

[28] Nanjwade, B.K.; Patel, D.J.; Udhani, R.A.; Manvi, F.V. Functions of lipids for enhancement of oral bioavailability of poorly water-soluble drugs. *Sci. Pharm.* 2011, 79, 705–727.

[29] Agrawal, Y.; Petkar, K.C.; Sawant, K.K. Development, evaluation and clinical studies of Acitretin loaded nanostructured lipid carriers for topical treatment of psoriasis. *Int. J. Pharm.* 2010, 401, 93–102.

[30] Hashimoto, M., Hossain, S., Mamun, A.A.; Matsuzaki, K.; Arai, H. Docosahexaenoic acid: One molecule diverse functions. *Crit. Rev. Biotechnol.* 2017, 37, 579–597.

[31] Hernando, S.; Requejo, C.; Herran, E.; Ruiz-Ortega, J.A.; Morera-Herrerias, T.; Lafuente, J.V.; Ugedo, L.; Gainza, E.; Pedraz, J.L.; Igartua, M.; et al. Beneficial effects of n-3 polyunsaturated fatty acids administration in a partial lesion model of Parkinson's disease: The role of glia and NRf2 regulation. *Neurobiol. Dis.* 2019, 121, 252–262.

[32] Boudrault, C.; Bazinet, R.P.; Ma, D.W.L. Experimental models and mechanisms underlying the protective effects of n-3 polyunsaturated fatty acids in Alzheimer's disease. *J. Nutr. Biochem.* 2009, 20, 1–10.

[33] Hang, L.; Basil, A.H.; Lim, K.L. Nutraceuticals in Parkinson's Disease. *Neuromol. Med.* 2016, 18, 306–321.

[34] Avallone, R.; Vitale, G.; Bertolotti, M. Omega-3 Fatty Acids and Neurodegenerative Diseases: New Evidence in Clinical Trials. *Int. J. Mol. Sci.* 2019, 20, 4256, doi:10.3390/ijms20174256.

[35] de Lau, L.M.; Bornebroek, M.; Witteman, J.C.; Hofman, A.; Koudstaal, P.J.; Breteler, M.M. Dietary fatty acids and the risk of Parkinson disease: The Rotterdam study. *Neurology* 2005, 64, 2040–2045.

[36] Morris, M.C.; Tangney, C.C.; Wang, Y.; Sacks, F.M.; Bennett, D.A.; Aggarwal, N.T. MIND diet associated with reduced incidence of Alzheimer's disease. *Alzheimers Dement.* 2015, 11, 1007–1014.

[37] Yadav, S.C.; Kumari, A.; Yadav, R. Development of peptide and protein nanotherapeutics by nanoencapsulation and nanobioconjugation. *Peptides* 2011, 32, 173–187.

[38] Layek, B.; Singh, J. Cell penetrating peptide conjugated polymeric micelles as a high performance versatile nonviral gene carrier. *Biomacromolecules* 2013, 14, 4071–4081.

[39] Costa, F.; Maia, S.; Gomes, J.; Gomes, P.; Martins, M.C. Characterization of hLF1-11 immobilization onto chitosan ultrathin films, and its effects on antimicrobial activity. *Acta Biomater.* 2014, 10, 3513–3521.

[40] Weinert, M.; Selvakumar, T.; Tierney, T.S.; Alavian, K.N. Isolation, culture and long-term maintenance of primary mesencephalic dopaminergic neurons from embryonic rodent brains. *J. Vis. Exp.* 2015, 96, 52475, doi: 10.3791/52475.

[41] Skaper, S.D.; Barbierato, M.; Ferrari, V.; Zusso, M.; Facci, L. Culture of Rat Mesencephalic Dopaminergic Neurons and Application to Neurotoxic and Neuroprotective Agents. *Methods Mol. Biol.* 2018, 1727, 107–118.

[42] Gaven, F.; Marin, P.; Claeysen, S. Primary culture of mouse dopaminergic neurons. *J. Vis. Exp.* 2014, 91, e51751.

[43] Chen, X.; Zhang, Y.; Sadadcharam, G.; Cui, W.; Wang, J.H.; Isolation, Purification, and Culture of Primary Murine Microglia Cells. *Bio-protocol* 2013, 3, e314, doi:10.21769/BioProtoc.314.

[44] Gainza, G.; Pastor, M.; Aguirre, J.J.; Villullas, S.; Pedraz, J.L.; Hernandez, R.M.; Igartua, M. A novel strategy for the treatment of chronic wounds based on the topical administration of rhEGF-loaded lipid nanoparticles: In vitro bioactivity and in vivo effectiveness in healing-impaired db/db mice. *J. Controlled Release* 2014, 185, 51–61.

[45] Garcia-Orue, I.; Gainza, G.; Girbau, C.; Alonso, R.; Aguirre, J.J.; Pedraz, J.L.; Igartua, M.; Hernandez, R.M. LL37 loaded nanostructured lipid carriers (NLC): A new strategy for the topical treatment of chronic wounds. *Eur. J. Pharm. Biopharm.* 2016, 108, 310–316.

[46] Pastor, M.; Basas, J.; Vairo, C.; Gainza, G.; Moreno-Sastre, M.; Gomis, X.; Fleischer, A.; Palomino, E.; Bachiller, D.; Gutiérrez, F.B.; et al. Safety and effectiveness of sodium colistimethate-loaded nanostructured lipid carriers (SCM-NLC) against *P. aeruginosa*: In vitro and in vivo studies following pulmonary and intramuscular administration. *Nanomedicine* 2019, 18, 101–111.

[47] Gartzandia, O.; Herran, E.; Pedraz, J.L.; Carro, E.; Igartua, M.; Hernandez, R.M. Chitosan coated nanostructured lipid carriers for brain delivery of proteins by intranasal administration. *Colloids Surf. B Biointerfaces* 2015, 134, 304–313.

[48] Gan, L.; Cookson, M.R.; Petrucelli, L.; La Spada, A.R. Converging pathways in neurodegeneration, from genetics to mechanisms. *Nat. Neurosci.* 2018, 21, 1300–1309.

[49] Sun, G.Y.; Simonyi, A.; Fritsche, K.L.; Chuang, D.Y.; Hannink, M.; Gu, Z.; Greenlief, C.M.; Yao, J.K.; Lee, J.C.; Beversdorf, D.Q. Docosahexaenoic acid (DHA): An essential nutrient and a nutraceutical for brain health and diseases. *Prostaglandins Leukot Essent. Fatty Acids* 2017, 136, 3–13.

[50] Saedi, A.; Rostamizadeh, K.; Parsa, M.; Dalali, N.; Ahmadi, N. Preparation and characterization of nanostructured lipid carriers as drug delivery system: Influence of liquid lipid types on loading and cytotoxicity. *Chem. Phys. Lipids* 2018, 216, 65–72.

[51] Gokce, E.H.; Korkmaz, E.; Deller, E.; Sandri, G.; Bonferoni, M.C.; Ozer, O. Resveratrol-loaded solid lipid nanoparticles versus nanostructured lipid carriers: Evaluation of antioxidant potential for dermal applications. *Int. J. Nanomed.* 2012, 7, 1841–1850.

[52] Thatipamula, R.; Palem, C.; Gannu, R.; Mudragada, S.; Yamsani, M. Formulation and in vitro characterization of domperidone loaded solid lipid nanoparticles and nanostructured lipid carriers. *DARU* 2011, 19, 23–32.

[53] Huguet-Casquero, A.; Moreno-Sastre, M.; Lopez-Mendez, T.B.; Gainza, E.; Pedraz, J.L. Encapsulation of Oleuropein in Nanostructured Lipid Carriers: Biocompatibility and Antioxidant Efficacy in Lung Epithelial Cells. *Pharm. 2020*, *12*, 429, doi: 10.3390/pharmaceutics12050429.

[54] Suk, J.S.; Suh, J.; Choy, K.; Lai, S.K.; Fu, J.; Hanes, J. Gene delivery to differentiated neurotypic cells with RGD and HIV Tat peptide functionalized polymeric nanoparticles. *Biomaterials 2006*, *27*, 5143–5150.

[55] Peng, L.; Niu, J.; Zhang, C.; Yu, W.; Wu, J.; Shan, Y.; Wang, X.; Shen, Y.; Mao, Z.; Liang, W.; et al. TAT conjugated cationic noble metal nanoparticles for gene delivery to epidermal stem cells. *Biomaterials 2014*, *35*, 5605–5618.

[56] Schober, A. Classic toxin-induced animal models of Parkinson's disease: 6-OHDA and MPTP. *Cell Tissue Res. 2004*, *318*, 215–224.

[57] Carrasco, E.; Werner, P. Selective destruction of dopaminergic neurons by low concentrations of 6-OHDA and MPP+: Protection by acetylsalicylic acid aspirin. *Parkinsonism Relat. Disord. 2002*, *8*, 407–411.

[58] Wang, G.Q.; Li, D.D.; Huang, C.; Lu, D.S.; Zhang, C.; Zhou, S.Y.; Liu, J.; Zhang, F. Icariin Reduces Dopaminergic Neuronal Loss and Microglia-Mediated Inflammation in Vivo and in Vitro. *Front. Mol. Neurosci. 2018*, *10*, 441.

[59] Yuan, W.J.; Yasuhara, T.; Shingo, T.; Muraoka, K.; Agari, T.; Kameda, M.; Uozumi, T.; Tajiri, N.; Morimoto, T.; Jing, M.; et al. Neuroprotective effects of edaravone-administration on 6-OHDA-treated dopaminergic neurons. *BMC Neurosci. 2008*, *9*, 75.

[60] Callizot, N.; Combes, M.; Henriques, A.; Poindron, P. Necrosis, apoptosis, necroptosis, three modes of action of dopaminergic neuron neurotoxins. *PLoS ONE 2019*, *14*, e0215277.

[61] Cao, D.; Xue, R.; Xu, J.; Liu, Z. Effects of docosahexaenoic acid on the survival and neurite outgrowth of rat cortical neurons in primary cultures. *J. Nutr. Biochem. 2005*, *16*, 538–546.

[62] Wang, P.-Y.; Chen, J.-J.; Su, H.-M. Docosahexaenoic acid supplementation of primary rat hippocampal neurons attenuates the neurotoxicity induced by aggregated amyloid beta protein (42) and up-regulates cytoskeletal protein expression. *J. Nutr. Biochem. 2010*, *21*, 345–350.

[63] Hirsch, E.C.; Hunot, S. Neuroinflammation in Parkinson's disease: A target for neuroprotection? *Lancet Neurol. 2009*, *8*, 382–397.

[64] Thurgur, H.; Pinteaux, E. Microglia in the Neurovascular Unit: Blood-Brain Barrier-microglia Interactions after Central Nervous System Disorders. *Neuroscience 2019*, *405*, 55–67.

[65] Fourrier, C.; Remus-Borel, J.; Greenhalgh, A.D.; Guichardant, M.; Bernoud-Hubac, N.; Lagarde, M.; Joffre, C.; Laye, S. Docosahexaenoic acid-containing choline phospholipid modulates LPS-induced neuroinflammation in vivo and in microglia in vitro. *J. Neuroinflamm. 2017*, *14*, 170.

[66] Lin, L.; Desai, R.; Wang, X.; Lo, E.H.; Xing, C. Characteristics of primary rat microglia isolated from mixed cultures using two different methods. *J. Neuroinflamm.* 2017, 14, 101.

[67] De Smedt-Peyrusse, V.; Sargueil, F.; Moranis, A.; Harizi, H.; Mongrand, S.; Laye, S. Docosahexaenoic acid prevents lipopolysaccharide-induced cytokine production in microglial cells by inhibiting lipopolysaccharide receptor presentation but not its membrane subdomain localization. *J. Neurochem.* 2008, 105, 296–307.

[68] Laye, S.; Nadjar, A.; Joffre, C.; Bazinet, R.P. Anti-Inflammatory Effects of Omega-3 Fatty Acids in the Brain: Physiological Mechanisms and Relevance to Pharmacology. *Pharmacol. Rev.* 2018, 70, 12–38.



© 2020 by the authors. Submitted for possible open access publication under the terms and conditions of the Creative Commons Attribution (CC BY) license (<http://creativecommons.org/licenses/by/4.0/>).

Dual effect of TAT functionalized DHAH lipid nanoparticles with neurotrophic factors in human BBB and microglia cultures ⁷

Sara Hernando^{ai}, Polyxeni Nikolakopoulou ^a, Dimitrios Voulgaris ^b, Rosa Maria Hernandez ^{c, d, e}, Manoli Igartua ^{c, d, e, *}, Anna Herland ^{a, b, *}

^a AIMES, Center for the Advancement of Integrated Medical and Engineering Sciences, Department of Neuroscience, Karolinska Institute, Stockholm, Sweden

^b Division of Micro and Nanosystems, KTH Royal Institute of Technology, Stockholm, Sweden

^c NanoBioCel Research Group, Laboratory of Pharmaceutics, School of Pharmacy University of the Basque Country (UPV/EHU), 01006 Vitoria-Gasteiz, Spain

^d Biomedical Research Networking Centre in Bioengineering, Biomaterials and Nanomedicine (CIBER-BBN), Institute of Health Carlos III, 28029, Madrid Spain

^e Bioaraba, NanoBioCel Research Group, 01006, Vitoria-Gasteiz, Spain

* Co-corresponding author: Manoli Igartua and Anna Herland

ⁱ Permanent adress:

^c NanoBioCel Research Group, Laboratory of Pharmaceutics, School of Pharmacy University of the Basque Country (UPV/EHU), 01006 Vitoria-Gasteiz, Spain

^d Biomedical Research Networking Centre in Bioengineering, Biomaterials and Nanomedicine (CIBER-BBN), Institute of Health Carlos III, 28029, Madrid Spain

^e Bioaraba, NanoBioCel Research Group, 01006, Vitoria-Gasteiz, Spain

⁷ Send to Acta Biomaterialia

IF: 7.242

Cat: Material Science & Biomaterials

ABSTRACT

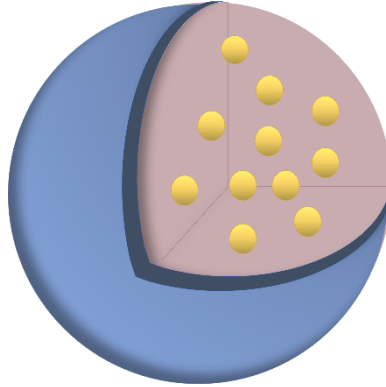
Neurodegenerative diseases (NDs) are an accelerating global problem, but we still lack routes to develop effective therapeutics. In this quest, it is crucial to identify novel drug candidates or drug carriers, which cross the blood-brain barrier (BBB) and reach the brain tissue. Neurotrophic factors (NTFs) and functional lipids, such as polyunsaturated fatty acids (PUFAs), have emerged as promising molecules to treat central nervous system (CNS) related disorders. Following a nanotechnology approach, we have previously developed PUFA-based nanostructured lipid carriers (NLC) named as DHAH-NLC that can entrap NTF and can be coated with chitosan (CS) and trans-activated transcription (TAT) peptide. Here, using human induced pluripotent stem cell (hiPSC)-derived brain microvascular endothelial-like cells (BMECs), we investigate if DHAH-NLCs can enter the brain via the BBB. Indeed, the TAT functionalized DHAH-NLCs successfully crossed the *in vitro* barrier, which exhibited high transepithelial/endothelial electrical resistance (TEER) values ($\approx 3000 \Omega \times \text{cm}^2$). The TAT functionalized DHAH-NLCs showed a permeability up to 0.1%. Next, to evaluate the therapeutic potency, we tested if our modified NLCs can regulate neuroinflammatory responses after lipopolysaccharide (LPS) treatment. Using human microglia (HMC3), we demonstrate that DHAH-NLCs successfully counteracted the inflammatory response in our cultures after LPS stimuli. Moreover, the encapsulation of glial cell-derived neurotrophic factor (GDNF) in our DHAH-NLCs (DHAH-NLC-GDNF) led to the activation of the Nrf2/HO-1 pathway, triggering the endogenous anti-oxidative system present in microglia. Overall, this work shows that the TAT functionalized DHAH-NLCs can cross the BBB, modulate immune responses, and serve as cargo carriers for GDNF; thus, becoming in a novel approach to treat CNS related disorders.

Keywords: BMECs • DHA • HMC3 microglia cell line • neuroinflammation • iPS Cells

GRAPHICAL ABSTRACT

Nanostructured lipid carriers (NLC) schematic representation

- NLC surface coating with TAT peptide
- NLC lipid matrix composed with DHAH functional lipid (DHAH-NLC)
- GDNF or VEGF NTFs encapsulated in the lipid matrix



Combinatory approach to target and treat neurodegenerative diseases

- DHAH-NLC with TAT peptide coating crossed the hiPSC derived BMCEs
- DHAH -NLC exhibited antiinflammatory properties in HMC3 human microglia cell line
- DHAH-NLCs with GDNF led to the activation of the Nrf2/HO-1 anti-oxidative pathway

1. INTRODUCTION

Neurodegenerative diseases (NDs) such as Alzheimer's disease (AD) and Parkinson's disease (PD) have escalated in prevalence; in fact, World Health Organization (WHO) forecasts that, in the years to come and as life expectancy increases, the number of patients suffering from NDs will increase considerably [1-3]. These devastating conditions are incurable, pose a socioeconomic burden for the public health system, families, and patients, and necessitate the development of effective therapeutics.

Neurodegeneration manifests with functional deterioration and ultimate loss of neurons; however, the molecular cues governing disease initiation and progression remain elusive. As a result, the development of effective medication is challenging. Notably, several agents have failed once they reached human clinical trials despite the promising results shown in pre-clinical studies using animal models [4-7]. Several factors contribute to these historical failures; among them, the lack of innovative treatments, reliable biomarkers, and, last but not least, the lack of predictive model systems to study the neurobiology of human brain disease [8].

The existing treatments only manage the symptoms and in some cases slow down disease progression; thus, the ongoing neurodegenerative process remains untreated [9,10]. Despite the differences in the clinical signature among the NDs, they all share some common characteristics of neurodegeneration such as neuronal loss, insoluble proteins deposits, oxidative stress, mitochondrial dysfunction, and

neuroinflammation [11-13]. The sustained neuroinflammation disrupts the balance between neurotrophic and neurotoxic factors; thus, growth factors (GFs) have emerged as putative candidates to treat neurodegeneration. GFs exhibit a neuroprotective character: they act on growth, proliferation, and differentiation while they regulate neuroinflammation, thereby promoting endogenous brain repair [14]. Among them, glial cell-derived neurotrophic factor (GDNF) and vascular endothelial factor (VEGF) have emerged as some of the best candidates for PD and AD, respectively [15,16]. More recently, polyunsaturated fatty acids (PUFAs) and especially omega (n)-3, have gained attention as functional lipids; recent data support the beneficial role of these natural compounds for the prevention and/or treatment of NDs due to their anti-inflammatory, anti-oxidative and neuroprotective properties. [17-19].

Nevertheless, most of these novel modalities are unable to cross the blood-brain barrier (BBB) and require an invasive administration route such as intrathecal or intracerebroventricular [20]. Nanotechnology-based drug delivery systems (DDS) comprise an alternative approach for brain targeting [21,22]. Nanostructured lipid carriers (NLCs), in particular, have gained popularity due to their ability to entrap highly lipophilic drugs and proteins, protect them from degradation, and enhance their stability [23-25]. Until recently, the lipids used for NLC formation were inert excipients without any active role in preventing or treating the symptomatology of the disease [26]. Lately, however, functional lipids such as oleic acid have been proposed as components of the lipid matrix of NLCs [27-29]. Following a similar approach, we have recently developed a new functional nanocarrier with the hydroxylated derivative of docosahexaenoic acid (DHAH), so that the nanoparticles (NPs) themselves could exhibit neuroprotective and anti-inflammatory effects (DHAH-NLCs) [30]. DHA is one of the most abundant PUFAs in the brain and, among other functions, regulates cell survival, neuroinflammation, and BBB permeability [31]. Moreover, the functionalization of the particles after surface modification leads to increased penetration via the BBB. For example, Chitosan (CS)- and cationic cell-penetrating trans-activated transcription (TAT)- coated particles showed enhanced barrier permeability and led to increased drug bioavailability in various brain regions [32-34]. Nevertheless, to assess the potential of these novel NPs to treat human disease, patient-oriented models are required.

Current disease modeling and drug screening *in vitro* platforms suffer from limited translatability to the clinic; studies in rodents suffer from interspecies differences and result in low relevance to humans, primary cells have limited availability while human endothelial cell lines show low transepithelial/endothelial electrical resistance (TEER) values [35-37]. Human brain microvascular endothelial cells (BMECs) form a tight barrier, which shows high selectivity [38,39]. Human induced pluripotent stem cell (hiPSC)-derived BMECs recapitulate most of the physiological properties of the brain endothelium, including tight, organized junctions and high TEER values, thereby providing an ideal platform for drug testing [40-42].

Microglia are the immune cells of the brain and play a crucial role in the neurodegenerative process [43-45]. They offer continuous tissue surveillance and react directly upon injury or infection. However, upon sustained neuroinflammation, microglia are activated, and they might impair BBB functionality, which results in aberrant cellular infiltration, increasing the levels of pro-inflammatory cytokines, proteases, and free radicals [46-48]. Thus, modulating microglia activation is vital for the development of effective therapeutics for NDs.

This study serves a dual scope. Initially, using hiPSC-derived BMECs, we investigated the ability of these newly generated, TAT-functionalized, DHAH-NLCs to cross the BBB. Next, using human microglia, we tested if our modified NPs could regulate inflammatory responses in our cultures. Moreover, we investigated if the encapsulation of VEGF or GDNF in our DHAH-NLCs would further enhance their neuroprotective and anti-inflammatory abilities of our particles.

2. MATERIALS AND METHODS

2.1 Materials

The references of the main products used in this work are summarized in Suppl. Table 1.

2.2 Nanostructured lipid carriers (NLCs) preparation

NLCs were prepared using a previously published melt-emulsification technique [34,49]. Firstly, a mixture of solid and liquid lipids (Precirol ATO @5 1.75%, w/v and Mygliol or DHAH 1% w/v) was melted 5°C above their melting point (56°C). Then, an aqueous solution containing Tween 80 (3%, w/v) and Poloxamer 188 (2%, w/v) was heated at the same temperature and added to the lipid phase under continuous

stirring, for 60 seconds, at 50W (Bradson Sonifier 250). The resulted emulsion was maintained under magnetic stirring for 15 minutes (min) at room temperature (RT) and immediately cooled at 4-8°C overnight to obtain the NLCs after lipid solidification.

NLCs surface was modified with CS only or with both CS and TAT. For the surface modification with CS, the NP dispersion was added dropwise to an equal volume (4 ml) of a CS solution (0.5%, w/v) under continuous agitation at RT for 20 min. After the coating process, the NLC dispersion was centrifuged in Amicon filters (Amicon, "Ultracel-100k", Millipore, USA) at 2,500 rpm (MIXTASEL, P Selecta, Spain) for 15 min, washed three times with Milli Q water and lyophilized for 42 h (LyoBeta 15, Telstar, Spain). TAT-peptide was covalently linked to the surface of CS coated NLCs by a surface activation method previously described by our research group [49,50]. Briefly, 250 μ l of EDC (1-ethyl-3-(3-dimethylaminopropyl) carbodiimide hydrochloride) in solution (1mg/ml) and 250 μ l of sulfo NHS (*N*-Hydroxysulfosuccinimide) in 0.02M PBS (1mg/ml) were added dropwise to a 4 ml CS solution (0.5% w/v, in PBS 0.02M), under magnetic stirring (2 h at RT). For the coupling of TAT, 250 μ l of the TAT solution (1 mg/ml) in PBS (0.02M; 7.4 pH) was added dropwise to the activated CS, under gentle agitation. The TAT-CS solution was maintained under stirring for another 4 h at RT and then incubated at 4°C overnight. On the day after, the NLCs were coated with TAT-CS; NLC dispersion previously prepared was added dropwise to the TAT-CS solution under continuous agitation for 20 min at RT. After the coating process, TAT-CS-NLC nanoformulation was centrifuged and lyophilized, as described in the previous paragraph.

Finally, the neurotrophic factors; glial cell-derived neurotrophic factor (GDNF) or vascular endothelial growth factor (VEGF) were loaded in the TAT-CS-NLCs previously developed formulation at a concentration of 0.125% (w/w) (DHAH-NLC GDNF and DHAH-NLC-VEGF) to probe the therapeutic effect of these nanoformulations in our microglial cultures after LPS *stimuli*. For the BBB transport assays, the lipophilic dye DiD was incorporated into the NLC (TAT-CS-NLC-DiD and CS-NLC-DiD), at a concentration of 0.5% (w/w). We developed these formulations following the previously described protocol with slight modifications; here, we included the relevant GF or dye, depending on the desired formulation, in the lipid phase, before the sonication process. Table 1 summarizes the six different

formulations -regarding the used lipid, the entrapped molecule, or the coating process with CS and TAT- that we developed and utilized in this study.

Table 1. Composition of the different NLCs used in the study.

<i>FORMULATION NAME</i>	<i>LIQUID LIPID</i>	<i>SURFACE MODIFICATION</i>	<i>ENTRAPPED MOLECULE (%) w/w</i>	<i>CELL MODEL TO PERFORM FUNCTIONAL ASSAYS</i>
CS-NLC-DiD	DHAH	CS	DiD (0.5)	hiPSCs derived BMECs
TAT-CS-NLC-DiD	DHAH	CS and TAT	DiD (0.5)	hiPSCs derived BMECs
Mygliol-NLC	Mygliol	CS and TAT	-	microglial cell line - HMC3
DHAH-NLC	DHAH	CS and TAT	-	microglial cell line - HMC3
DHAH-NLC- GDNF	DHAH	CS and TAT	GDNF (0.125)	microglial cell line - HMC3
DHAH-NLC-VEGF	DHAH	CS and TAT	VEFG (0.125)	microglial cell line - HMC3

2.3 NLC characterization: particle size, zeta potential, morphology, and encapsulation efficiency

The mean particle size (Z-average diameter), the polydispersity index (PDI), and the zeta potential were measured by Dynamic Light Scattering (DLS), through Laser Doppler micro-electrophoresis (Malvern Zetasizer Nano ZS, Model Zen 3600; Malvern Instruments Ltd, UK). For each formulation, we performed three replicate analyses. The data are expressed as the mean ±SEM. To investigate the morphology of the NPs, we performed transmission electron microscopy (TEM) with a JEOL JEM 1400 Plus.

The encapsulation efficiency (EE) of the NLCs was determined by an indirect method, in which we measured the non-encapsulated GDNF or VEGF presented in the supernatant obtained after the filtration/centrifugation process described in section 2.2. The EE (%) of the GF was determined by ELISA technique using the following equation:

$$EE (\%) = \frac{\text{total GF content} - \text{free amount of GF}}{\text{total GF content}} \times 100$$

The absence of DiD release from NLCs in transport buffer was assessed by our group previously [50,51]; thus, it is not described in the present work.

2.4 hiPSC differentiation to BMECs

2.4.1 hiPSCs maintenance

The hiPSC line that was used in this study was the Control 9 and it was obtained from the iPS Core at Karolinska Institutet [52]. hiPSCs were cultured in Matrigel-coated (0.5mg/6 well plate) six-well plates with mTeSR medium. When the confluence of hiPSCs was up to 80%, cells were passaged after 5 min incubation at 37°C with Versene solution. Then, using a 5ml pipette, cells were gently dissociated and passaged 1:3-1:8 split ratios onto Matrigel-coated six-well plates with mTeSR medium. For BMEC differentiation, we used hiPSCs up to passage 41, being in the typical passage range for BMEC differentiation [53].

2.4.2 BBB development

For BBB differentiation, we followed the protocol by *Neal et al.*, with slight modifications [42]. hiPSCs were maintained in mTeSR media as described above. One day before differentiation induction (D-1), cells were washed with Dulbecco's phosphate-buffered saline (DPBS), 500 μ l of TrypLE was added to each well and passaged after 5 min incubation at 37°C. Cells were diluted 1:5 in mTeSR media, centrifuged 3 min at 200 rcf, and resuspended in mTeSR media supplemented with ROCK inhibitor (10 μ M). hiPSCs were then seeded onto Matrigel-coated six-well plates at 16 K/cm² cell density. The day after (D0), mTeSR was removed and changed to E6 media. We repeated the procedure daily for four days (D0-D3). Then, media was switched to Human Endothelial Serum Free Media (hESFM media) supplemented with 1X B27, 20 ng/ml bFGF and 10 μ M RA called as, hESFM complete media. Cells were maintained in this media for two consecutive days without a media change. After those two days, the media was removed, wells were washed with DPBS and incubated with TrypLE for 20 min to 30 min at 37 °C until a single cell suspension was formed. The cells were then subcultured onto 6.5 mm Transwell filters with 0.4 μ m pore size, coated with a mixture of 400 μ g/mL collagen IV and 100 μ g/mL fibronectin in water; 3.3×10^5 cells were seeded in each Transwell with hESFM complete media.

24 h after subculture, TEER was measured using STX2 chopstick electrodes and an EVOM2 voltohmmeter (World Precision Instruments). Media was then switched to hESFM with B27 without bFGF and RA. The next day (48 h after subculture), TEER was measured and functional assays were performed.

2.4.3 BBB assessment: TEER measurement

All experiments performed in this study were carried out with one hiPSC cell line, Control 9; therefore, the TEER measurements presented are the results of one biological replicate (n=1). For each timepoint, the mean value of nine technical replicates (n=9) is shown. TEER was measured using an EVOM2 voltohmmeter (World Precision Instruments) with STX2 chopstick electrodes 24 h and 48 h post subculture and all values were corrected for the resistance of an empty, coated Transwell filter.

2.4.4 Immunocytochemistry

Transwell inserts with BMECs were washed twice with DPBS and incubated with 4% paraformaldehyde for 20 min. Cells were then washed three times with DPBS for a minimum of 5 min per wash. The fixed cells were blocked and permeabilized for a minimum of 1 h at RT in DPBS with 10% (v/v) goat serum and 0.1% (v/v) Triton X-100 in DPBS. After three washes, cells were then incubated with ZO-1 primary antibody (1:100) in staining solution containing 1% (v/v) goat serum and 0.01% (v/v) Triton X-100 in DPBS overnight at 4°C. The following day, cells were washed 3 times and incubated with the secondary antibody, an anti-Mouse IgG1 (γ 1), CF™488A antibody (1:1000) in staining solution for 1 h at RT. After three rinsing steps, the cells were incubated with 300 nM of 4',6-diamidino-2-phenylindole dihydrochloride (DAPI) for 10 min to label the nuclei. Inserts were then washed twice with DPBS, cut, and mounted with ProLong Glass Antifade Mountant on glass slides. Cells were visualized using a Zeiss laser scanning confocal microscope (LSM 710) using a 25X and a 40X objective.

2.4.5 NLC transport across BMECs differentiated from hiPSC

Transport of NLCs across BMECs was studied quantitatively by fluorescence measurement (Plate Reader Infinite M1000, Tecan, Switzerland) and qualitatively by confocal laser scanning microscopy (LSM 710), using DiD ($\lambda_{em} = 644$ nm, $\lambda_{ex} = 685$ nm) labeled NLCs. Here, two different types of formulations described in Table 1 were used, the CS-NLC-DiD and the TAT-CS-NLC-DiD.

hiPSC-derived BMECs were seeded on Transwell filters as described above (2.4.2 section, 3.3×10^5 cells per insert) and the transport of the different NLCs was evaluated 48 h after. The wells with TEER values above $3000 \Omega \text{cm}^2$ were selected to conduct the transport studies. The experiments were conducted at 37°C by adding $100 \mu\text{l}$ of 1 mg/ml NLC in hESFM with B27 on the apical side of the inserts. At different time points (0min, 30 min, 60 min, 90 min and 120 min), $50 \mu\text{l}$ of volume sample was collected from the basolateral side and $50 \mu\text{l}$ of fresh media was added to the same chamber. (The data are presented as the mean \pm SEM of nine technical replicates of this assay). The dilution factor was not compensated to calculate the final percentage of NLCs going through the BMEC monolayer since the dilution factor was negligible. The NLC concentration was determined by fluorescence measurement (Plate Reader Infinite M1000, Tecan, Switzerland). The relative fluorescent signal was correlated to a standard linear curve ($125\text{-}0 \mu\text{g/ml}$ in serial dilutions). The NLC transport rate is expressed as the mean of transported NLCs in percentage \pm SEM. After transport experiments, the supernatant was removed, and cell monolayers were fixed in PFA 4% for subsequent staining as described in 2.4.4. section. The NLCs that were not entrapped into BMECs were removed during washing and staining process. Images were captured using a Zeiss confocal microscope (LSM710).

2.5 HMC3 microglia cell culture

2.5.1 HMC3 cell line viability assay.

HMC3 cells were maintained in DMEM/F12 medium containing 10% (v/v) of FBS under standardized conditions (95% relative humidity, 5% CO_2 , 37°C). To evaluate the non-toxic and most effective dose to work, alamarBlue assay was carried out. Cells were seeded at $10\text{K}/\text{cm}^2$ in a 96-well plate for 24 h to allow cell attachment. The day after, different doses of the four different kind of NLC formulations described in Table 1 were added (DHAH-NLC, Mygliol-NLC, DHAH -NLC-GDNF and DHAH -NLC VEGF). The concentration for DHAH-NLCs refers to DHAH functional lipid concentration in μM : 12.5, 25, 50 and 100. (Suppl. Table 2). In order to check the differences in cell viability and functional assays between DHAH functional lipid and Mygliol lipid [30], an equal amount of Mygliol-NLCs was used equivalent to 15.5, 31, 62, 124, $\mu\text{g/ml}$ NPs concentration as internal control (M1-M4). For the two different tested GF: GDNF and VEGF (DAH-NLC-GNDNF) and (DHAH-NLC-VEGF) 12.5, 25,

50, and 100 μM for DHAH lipid content and 12.5, 25., 50 and 100 ng/ml for the GF concentration were used; (Suppl. Table 2). The different formulations and doses were incubated with HMC3 for 24 h and 48 h. Afterwards, the viability was assessed using the alamarBlue assay, following manufacturer's protocol. Briefly, 10 μL (1:10 in cell culture media) of the alamarBlue cell viability reagent was added to the cells. After 4 h of incubation the absorbance of the mixture was read at 570 nm, using 600 nm as reference wavelength (Plate Reader Infinite M1000, Tecan, Switzerland). The absorbance was directly proportional to the number of living cells in the culture. Cell viability for each condition is expressed as the percentage regarding to negative control (Control⁻) where no treatment was added to the cell media, which was set as 100%. For positive control (Control⁺), cells were treated with DMSO 10% for at least 24 h.

2.5.2.HMC3 activation with LPS

To test the efficacy of our NPs in modulating neuroinflammation, we treated our microglial cultures with LPS (100ng/ml, InvivoGen). Cells were seeded at 10K/cm² or 15K/cm², depending on the desired downstream analysis strategy; to investigate the genes involved in the neuroinflammatory process we performed gene expression analysis with RT-qPCR (seeding density 15K/cm²), whereas to assess cytokine responses we performed Multiplex assay (seeding density 10K/cm²). Our experimental design consisted of two experimental conditions (Suppl. Fig.1); in condition A, we tested if the NLCs themselves affected our microglia while in condition B, we tested if they could modulate inflammation following LPS treatment. The working concentration of NLCs was determined with the alamarBlue assay as described in 2.5.1 section.

Condition A: Test for effects of the NLCs on microglia

We tested the following formulations: DHAH-NLC (25 μM of DHAH lipid), DHAH-NLC-GDNF (25 μM of DHAH lipid and 25ng/ml GDNF), DHAH -NLC-VEGF (25 μM of DHAH lipid and 25ng/ml VEGF) and finally, Mygliol-NLC (an equal dose of NLCs was used as internal control, 31 $\mu\text{g/ml}$, (M2); to show the differences between formulating with Mygliol or DHAH functional lipid). Here, cells were treated with the NLCs 24 h after seeding and samples were collected the next day for downstream analysis. As positive control (LPS treated cells; Control⁺) we used cells that we treated with

100ng/ml LPS for 24 h, whereas as negative control (media change; Control⁻) we used cells that we performed only media change.

Condition B: Testing for effects of the NLCs on inflamed microglia

At this point, our cells were pre-treated with the various NLCs for 24 h, when they were challenged with LPS. Following LPS treatment, cells were treated again with the respective NLCs (same dose with condition A) and samples were collected 24 h after for downstream analysis. Similar to above, as positive control (LPS treated cells; Control⁺) we used cells that we treated with LPS for another 24 h, whereas as negative control (media change; Control⁻) we used cells that we performed only media change.

For both conditions, we analyzed six groups (Suppl. Fig.1).

2.5.2.1 RT-qPCR

Total RNA isolation and purification was performed using High pure RNA isolation Kit from Roche, following manufacturer's instructions. Subsequently, RNA quantity and quality were assessed by NanoDrop 1000 Spectrophotometer (Thermo Scientific). 500 ng RNA was used for cDNA synthesis using High-Capacity RNA-to-cDNA Kit according to manufacturer's instructions. TaqMan-based qPCR assay was used to perform gene expression analysis using a QuantStudio 5 Flex Real-Time PCR System. TaqMan Assay gene names (assay ID) are summarized in Suppl. Table 3. Samples were run in duplicates in 96 well plates. Relative gene expression was evaluated with the $\Delta\Delta$ Ct method after normalization to glyceraldehyde 3-phosphate dehydrogenase (GAPDH). All the experiments were run in triplicates.

2.5.2.2 Multiplex assay

Cytokine levels of cell culture supernatant were measured on the U-Plex MSD electrochemiluminescence multi-spot assay platform (MesoScale Diagnostics, Rockville USA). Concentration ranges 2,000 to 0.33 pg/ml for IL-6, 2,200 to 0.15 pg/ml for IL-8, 3,700 to 0.14 pg/ml for IL-10, 3,700 to 0.51 pg/ml for TNF- α , 3,800 to 0.15 pg/ml for IL-1 β and 17,000 to 1.7 pg/ml for IFN- γ were used. Cell viability in condition A and B (Suppl. Fig.1) was measured after DAPI staining (300 nM) with ImageXpress Pico Automated Cell Imaging System. No differences in HMC3 cell viability were observed after LPS and/or NLCs incubation ($p > 0.05$, One-way Anova) (Suppl. Fig.2). Thus, data are represented as pg/ml and have not been normalized to cell numbers. Cell viability for each condition (treated cells) is expressed as the

percentage of living cells when compared to the nontreated cells (media change; Control⁻), which was set as 100%. MSD assay was performed according to the manufacturer's instructions. MSD testing was conducted in a single laboratory by a single technician at the SciLifeLab (Stockholm, Sweden). All the experiments were run in triplicate.

2.6 Statistical analysis

All results are expressed as means \pm SEM. For hiPSC derived BMECS, TEER values are represented as the mean of nine technical replicates for three independent experiments. Experimental data were analyzed using GraphPad Prism (v. 6.01, GraphPad Software, Inc.). Two-way ANOVA followed by Bonferroni's posthoc test ($p < 0.05$) was used for analyzing the data. Gene expression analysis and cytokine release analysis are represented as mean \pm SEM for three independent experiments. Experimental data were analyzed using GraphPad Prism (v. 6.01, GraphPad Software, Inc.). One-way ANOVA followed by Bonferroni's posthoc test ($p < 0.05$) was used for analyzing the data. For the gene expression analysis, statistics were performed using the delta-Ct values. *P values* < 0.05 were considered significant.

3. RESULTS

3.1 Nanoparticle characterization

For this study, we developed several novel nanoformulations, which vary in the surface coating, the lipid used, or the encapsulated molecule. Our NLCs encapsulated either GFs (GDNF or VEGF) or the fluorescent tracer DiD, depending on the downstream experiments. Table 2 summarizes the mean particle size, polydispersity index (PDI), zeta potential and EE, for the GF-entrapping NLCs. Since, in our previous studies, we were not able to detect any release of the DiD tracer from NLCs, we assumed that the EE is 100% [50,51]. As shown in Table 2, all formulations were uniform in size (100-200nm) and had pDI values below 0.5, indicating a homogenous suspension. Moreover, they all exhibited positive zeta values, indicating that the CS and TAT coating process was successful. EE was around 85% for both GDNF and VEGF examined here. We utilized TEM to investigate the external morphology of our particles; our images show that our NPs showed uniform size without abnormalities (Fig. 1).

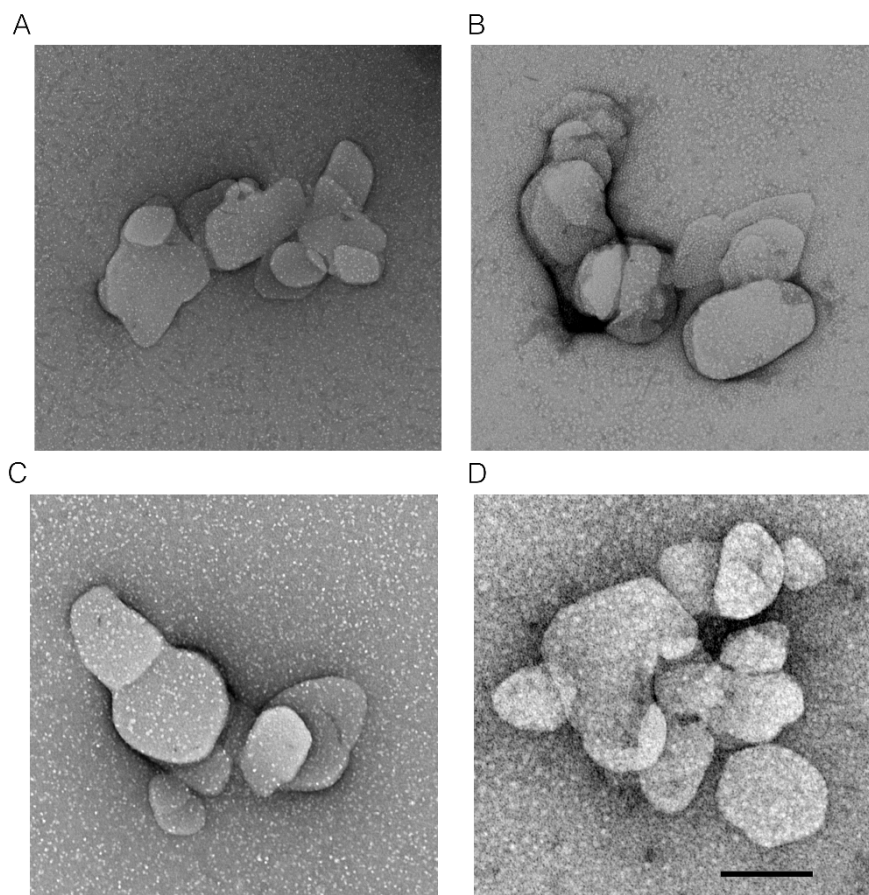


Fig. 1. TEM images of the NLCs. (A) Mygliol-NLC (B) DHAH-NLC (C) DHAH-NLC-GDNF (D) DHAH-NLC-VEGF. Scale bar 200 nm.

Table 2. Physicochemical characterization of NLC used in all the experimental studies (one batch). (*) The presence of a fluorescent dye (DiD) makes impossible to measure accurately the size, PDI and zeta potential of these two formulations.

FORMULATION	MEAN SIZE AFTER LYOPHI. (nm)	PDI	ZETA POTENTIAL (mV)	EE (%)
CS-NLC-DiD(*)				≈100
TAT-CS-NLC-DiD(*)				≈100
Mygliol-NLC	119.1±18.0	0.323±0.039	17.4±0.8	-
DHAH-NLC	105.4±25.6	0.400±0.032	20.9 ±0.5	-
DHAH-NLC- GDNF	257.1±3.5	0.338±0.022	18.0±0.4	82.01±1.67
DHAH-NLC-VEGF	264.1±16.0	0.471±0.076	20.5±0.8	88.74±0.37

3.2 Transport of the NLCs across the hiPSC-derived BBB

hiPSCs were differentiated to BMECs following the protocol described in Fig. 2A (protocol described by Neal *et al.*, 2019 [42] with slight modifications). Our hiPSC-derived BMECs showed the expected barrier phenotype; as shown in Fig. 2C, TEER values were around $3000 \Omega \times \text{cm}^2$ at 48 h post subculture for all the three experiments and cells expressed the BBB-specific tight junction protein ZO-1 (Fig. 2C, D). Once the barrier was established, we tested the permeability of our NPs across the BMEC monolayer. Specifically, we investigated if surface modification with TAT peptide would enhance the transport rate across the BBB. To do this, we compared the transport rate of TAT-CS-NLC-DiD (TAT modified NPs) versus CS-NLC-DiD (non-modified NPs). TAT-CS-NLC-DiD were detectable in the basolateral chamber already 90 min after we introduced the NPs to our cultures; nevertheless, 120 min after introducing the NPs to our cultures, $0.10\% \pm 0.01$ of TAT-CS-NLC-DiD were able to effectively cross BMEC monolayer (Fig. 3A). On the contrary, CS-NLC-DiD were not detectable in the basolateral chamber at any of the investigated time points. Confocal microscopy further confirmed these results, where only TAT-CS-NLC-DiD could be detected in the BMEC monolayer (Fig. 3B). Overall, our data demonstrate that our NPs crossed the hiPSC-derived BBB after surface modification with TAT peptide.

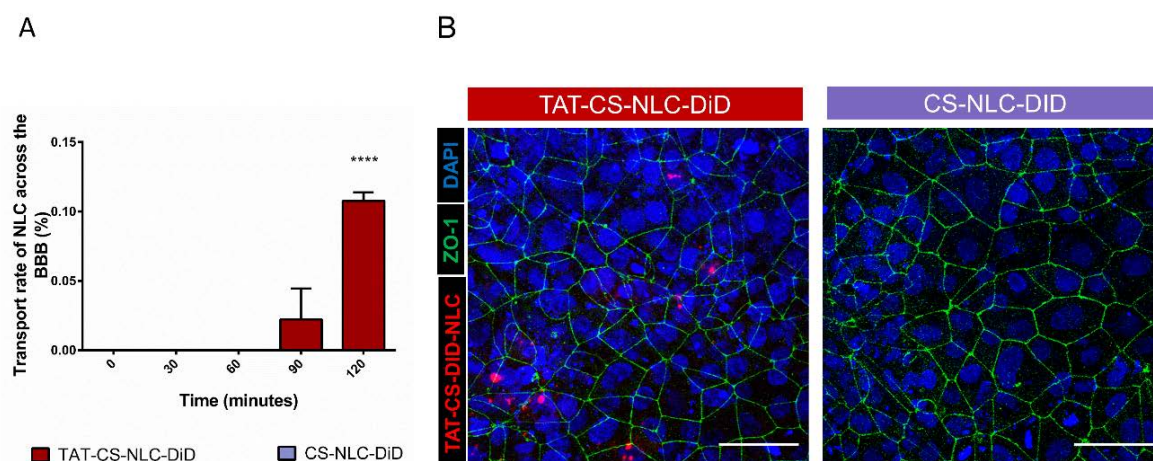


Fig.3. (A) TAT-CS-NLC-DiD successfully penetrated the BMEC monolayer as opposed to the CS-NLC-DiD. (Data are means \pm SEM of three individual experiments and nine technical replicates; **** $p > 0.0001$ TAT-CS-DiD-NLC vs CS-DiD-NLC, Two-way ANOVA, 120 min). (B) Representative images of the BMEC monolayer after treatment with our NPs. Blue shows the nuclei stained with DAPI, green shows the tight junctions stained with ZO-1, whereas the NLCs are shown in magenta (incorporated DiD). TAT-CS-NLC-DiD could be detected in our cell monolayer, while CS-NLC-DiD were not detectable. The images show the maximum intensity projection of a Z stack. Scale bar 50 μ m.

3.3 Microglia viability after incubation with NLCs

To assess the cytocompatibility as well as the working concentration for our NPs, we performed an AlamarBlue viability assay after 24 and 48 h incubation with the various NLCs. As shown in Fig.4, the incubation with the different NLCs led up to 70% cell viability at 24 h for all the tested conditions, except for when the highest concentration was used. However, at 48 h $> 70\%$ cell viability was only achieved in the low concentration range (25 and 12.5 μ M, for DHAH lipid and 25 and 12.5 ng/ml for GF Suppl. Table 2). Therefore, as working concentrations, we set 25 μ M for the functional lipid DHAH and 25 ng/ml for the GFs for all the different types of NLCs containing DHAH functional lipid and GDNF or VEGF. In the case of Mygliol-NLCs an equal dose of NLC was used, equivalent to 31 μ g/ml for NLC concentration (M2). (Suppl. Table 2).

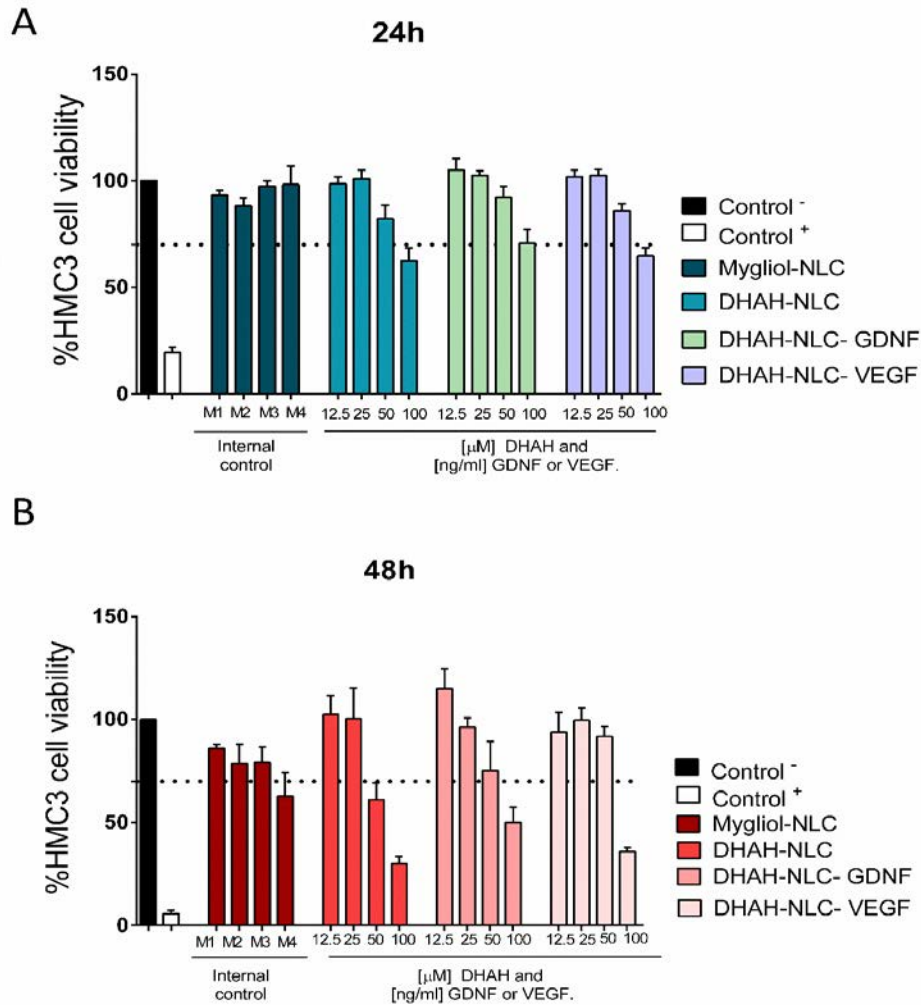


Fig.4. HMC3 cell viability study after incubation with the various NLCs (AlamarBlue reduction assay). (A) Cell viability after 24 h incubation with the various types and concentrations of NLCs. (B) Cell viability after 48 h incubation with the various types and concentrations of NLCs. In A and B, Control - denotes no treatment, media change and Control + denotes DMSO 10% for 24 h. Cell viability for each condition (treated cells) is expressed as the percentage of living cells when compared to the nontreated cells (media change; Control -), which was set as 100%. (Data are means \pm SEM of three individual experiments; the dashed line represents 70% viability).

3.4 DHAH-NLC modulate the microglial inflammatory response

3.4.1 Gene expression analysis (RT-qPCR)

To investigate if the NPs could modulate the inflammatory responses, we performed gene expression analysis in two different conditions. In condition A, we tested if the interaction between the microglia and the NPs would induce any inflammatory responses in the microglial cultures. Here, cells were treated with the various NLCs (Mygliol-NLC, DHAH-NLC, DHAH-NLC-GDNF, DHAH -NLC-VEGF) or LPS (Control +; control for inflammation induction) for 24 h and samples were

collected for gene expression analysis. As negative control (Control⁻) we used cells that only media change was performed (Methods 2.5.2 and Suppl. Fig.1A). In condition B, we tested if the NPs could modulate inflammation after LPS stimuli. In this case, the NLC pre-treated groups (Mygliol-NLC, DHAH-NLC, DHAH-NLC-GDNF, DHAH-NLC-VEGF) were challenged with LPS for 24 h. Similar to condition A, as control for the inflammatory state we used cells that received only LPS (Control⁺) and as negative those that we performed only media change (Control⁻) (Methods 2.5.2 and Suppl. Fig.1B).

As shown in the bright-field images in Suppl.Fig.1A, LPS stimulation resulted in a shift of the microglia towards an ameboid phenotype (Control⁺; Suppl. Fig.1A). Notably, this effect was not observable in the rest of the groups, which we treated with the various NLCs. Our analysis included both proinflammatory genes (IL6, TNF α , IL1- β , NF- κ B) as well as antioxidant genes (Nrf2, HO-1).

Condition A

Proinflammatory response: LPS treatment for 24 h upregulated IL-6, TNF- α , and IL-1 β (Fig.5), while the levels of COX-2 and NF- κ B remained unchanged (Suppl. Fig.3). In the case of IL-6, the LPS treated cells showed higher mRNA expression levels compared to the untreated, while treatment with the various NLCs did not result in significant changes. The Mygliol-NLC treated group showed a slight trend towards increase, but the effect did not reach significance. The DHAH-NLC, DHAH-NLC-GDNF, and DHAH-NLC-VEGF treated cells exhibited similar expression levels to the untreated cells with values significantly lower than the LPS treated cells (Fig.5A). For TNF- α , we observed a similar response with IL-6; LPS treatment resulted in the upregulation, whereas incubation with DHAH-NLC, DHAH-NLC-GDNF, and DHAH-NLC-VEGF did not induce any changes. Here, in the Mygliol-NLC treated group, we observed a significant increase compared to the untreated. The DHAH-NLC, DHAH-NLC-GDNF, and DHAH-NLC-VEGF treated cells exhibited similar expression levels to the untreated cells; values were significantly lower than both the LPS and the Mygliol-NLC treated cells (Fig.5B). Last but not least, IL-1 β mRNA levels increased following LPS stimulation, while none of the various NLCs, affected gene expression. The DHAH-NLC, DHAH-NLC-GDNF, and DHAH-NLC-VEGF treated cells exhibited similar expression levels to the untreated cells with values significantly lower than the LPS treated cells (Fig.5C).

Antioxidative response: Here, we investigated if our NPs could induce any antioxidative responses in our microglial cultures. Thus, we tested for alterations in the gene expression profile of the cultures for two traditional antioxidant genes, Nrf2 and HO-1. Administration of all the DHAH-enriched NLCs increased the levels of HO-1, but Nrf2 expression did not change. Both Nrf2 and HO-1 mRNA expression levels remained unchanged after treatment with Mygliol-NLC (Fig.5 D, Suppl. Fig.3C).

Condition B

Proinflammatory response: As expected, LPS stimuli resulted in IL-6 upregulation, which was not reverted after treatment with Mygliol-NLC. In contrast, incubation with DHAH-NLC, DHAH-NLC-GDNF, and DHAH-NLC-VEGF led to significant downregulation (Fig.5E). We observed a similar scheme for TNF- α ; LPS increased mRNA expression levels, while following treatment with Mygliol-NLC did not revert the effect. On the contrary, treatment with DHAH-NLC and DHAH-NLC-GDNF led again to downregulation, with TNF- α levels being significantly lower than both the LPS treated and the Mygliol-NLC group. We observed a similar trend for the DHAH-NLC-VEGF treated cells, but this effect did not reach significance (Fig.5F). Lastly, LPS treatment induced IL-1 β upregulation, and treatment with Mygliol-NLC did not normalize the values. Treatment with DHAH-NLC and DHAH-NLC-GDNF, however, reverted this effect; the levels were lower than the LPS treated cells and similar to the untreated cells. Moreover, in the case of IL-1 β , we observed a slight decrease in the DHAH-NLC-VEGF treated cells, but the effect was not significant (Fig.5G).

Antioxidative response: Here, only DHAH-NLC-GDNF incubation led to observable changes in HO-1 expression. For the other DHAH-enriched NLCs, although we observed a slight trend for an increase, it did not reach significance. Mygliol-NLC treated cells showed no change in HO-1 levels (Fig.5H). Nrf2 levels remained unchanged in all the tested groups (Suppl. Fig.3C).

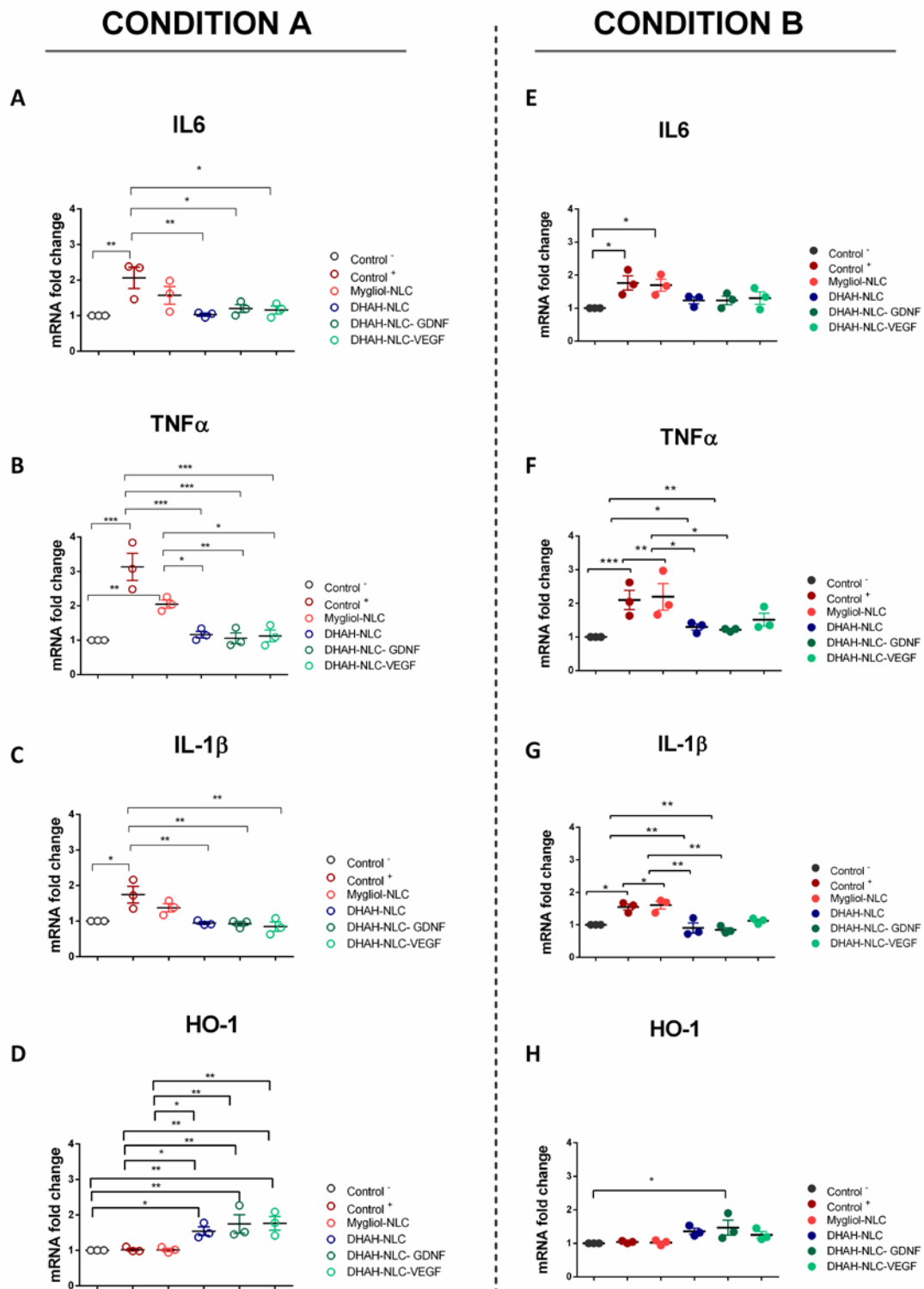


Fig.5. Gene expression analysis (RT-qPCR). (A) IL6 (B) TNF- α (C) IL-1 β and (D) HO-1 for condition A. (E) IL6 (F) TNF- α (G) IL-1 β and (H) HO-1 for condition B. Relative mRNA expression was normalized against GAPDH, and the gene expression of the group where only media change was performed (Control⁻) was used a reference (fold change 1). (Data are presented as fold change \pm SEM; N=3 independent experiments; Δ CT values were used for statistical analysis, *p<0.05 ** p<0.01 *** p<0.001, One- Way ANOVA).

3.4.2 Multiplex assay

From the U-plex assay, only IL-1 β , IL-6 and IL-8 could be detected in cell culture supernatant in all conditions.

Condition A:

In condition A, treatment with LPS for 24 h led to an increase in cytokine secretion of IL-6 and IL-8 (Control+; Fig. 1 A-C). IL-1 β showed a similar trend but it did not reach significance. Incubation with Mygliol-NLC did not alter cytokine secretion (Fig. 6 A-C) compared to the basal levels (Control-). Cells that were treated with the DHAH formulation (with or w/o GFs) secreted the same level of IL-1 β (Fig. 6A). Interestingly, secretion of IL-6 was significantly lower than the control (Fig. 6B), highlighting the potential anti-inflammatory properties of the DHAH enriched formulations (with or w/o GFs).

Condition B:

Cells pre-treated with the DHAH-enriched nanoformulations counteracted LPS-induced secretion of cytokines. All detected cytokines exhibited significantly reduced secretion (Fig. 6 D-F) when compared to treatment with LPS only (Control+). Mygliol-NLC pre-treated cells showed no significant difference upon stimulation when compared to LPS-only treated cells. Taken together, these results demonstrate the immunomodulatory effect that the DHAH formulation elicits. Encapsulation of GFs did not seem to have a pronounced effect on the inflammatory profile upon LPS stimulation (Fig.6 D-F). In detail, the secretion of all detected cytokines was on par with the DHAH-NLC treated group (Fig. 6 D-F).

4. DISCUSSION

The lack of effective treatments for NDs raises an urgent need to identify new drug candidates. In the last years, different treatments ranging from GFs to more natural compounds such as PUFAs have been suggested as feasible options to manage neurodegenerative processes [18,54]. However, brain targeting remains challenging as the BBB; with a precisely controlled transport mechanisms in tight barrier of the BMECs regulating fluxes in and out of the brain [55]. To achieve the delivery of neurotherapeutics into the brain, scientists have followed various strategies during the last decade [56,57]. Therefore, we developed improved nanocarriers for human CNS-targeting.

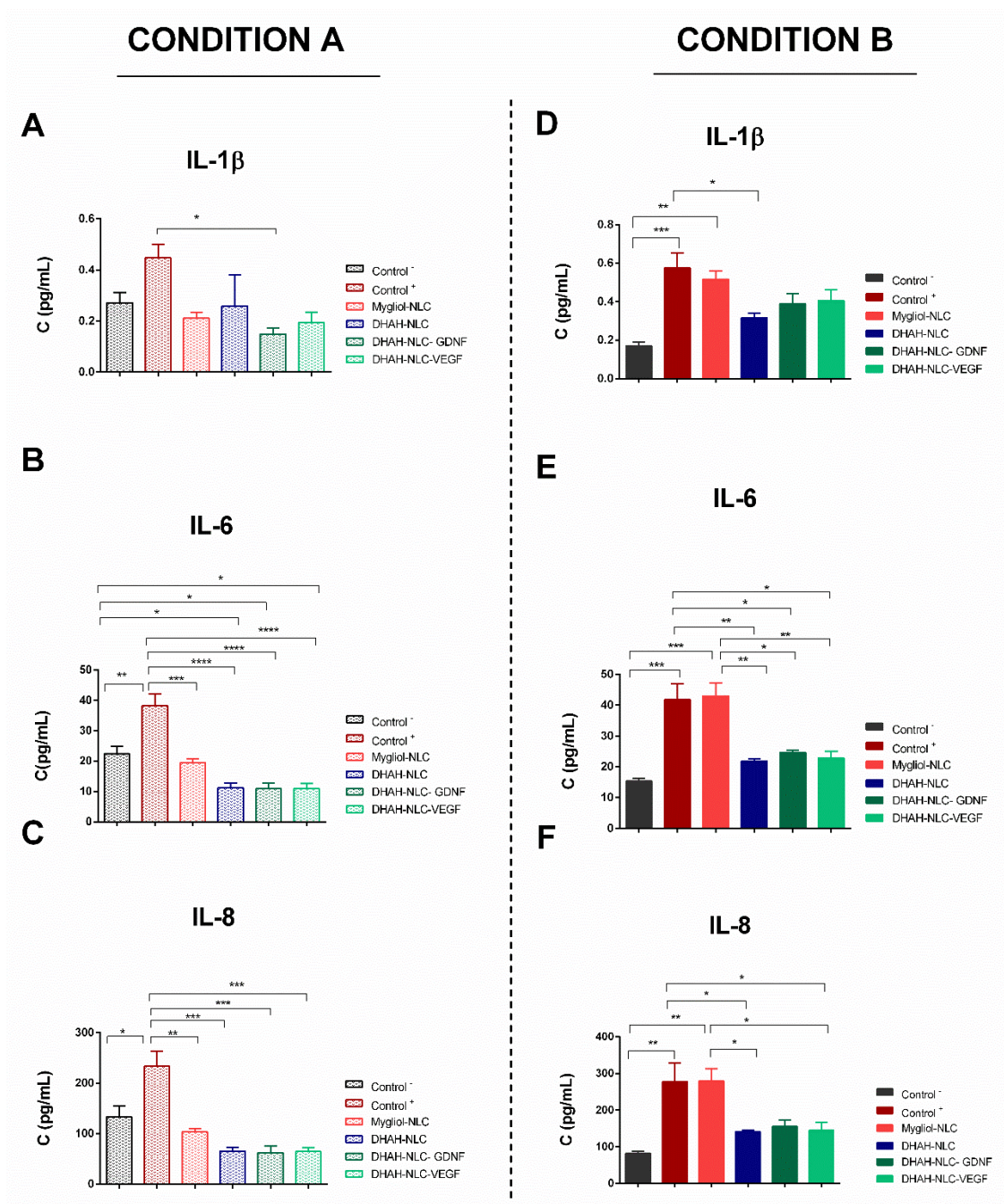


Fig.6. Cytokine secretion analysis (U-PLEX Assay) assay values. (A) IL-1 β (B) IL-6 and (C) IL-8 for condition A. (D) IL-1 β (E) IL-6 and (F) IL-8 for condition B. (Data are means \pm SEM of three individual experiments; * p <0.05 ** p <0.01 *** p <0.001, **** p <0.0001, One- Way ANOVA).

Initially, we developed and characterized the various NLCs used in this study. The obtained results are similar to those reported in our previous studies [34,58]. Moreover, all the formulations exhibited positive zeta potential due to the CS and TAT coating process. Besides, high encapsulation efficiency was obtained, around 85%, for both formulations loading the different GFs, GDNF, and VEGF. For particles

encapsulating the fluorescent tracer, we assumed $\approx 100\%$ for EE, similar to previous publications [51]. As shown by TEM photographs, the NLCs showed appeared uniform in size.

Transport studies in the brain via the BBB are challenging; the poor barrier properties of the majority of BBB models render transport studies virtually impossible. Among the different models to mimic the human BBB, BMECs derived from hiPSCs are good candidates for drug transport and screening assays, since hiPSC-derived BBB-like cells generate TEER close to *in vivo* conditions [59,60] The BMECs obtained in this research work act as a human BBB model showing high TEER values and ZO-1 staining. Indeed, the resultant BMECs exhibited a tight barrier with TEER values up to $3000 \Omega \times \text{cm}^2$, thereby being reliable for small and large molecules permeability studies. At the protein level, hiPSC-derived BBB-like cells expressed ZO-1, a tight junction protein prevalent in brain vasculature [55,61,62]. Importantly, similar have successfully been used to study transcytosis processes [63] .

This BBB *in vitro* model has been used previously to test the permeability of different substances, including atorvastatin-loaded NPs, without any difference between the drug in solution or the nanoformulation [59,63,64]. Here, we used this *in vitro* platform to test the permeability of our novel NLCs. To achieve the penetrance of the NPs across the barrier, we performed surface modification with TAT peptide. Indeed, our data show that TAT enrichment facilitated the penetrance of this lipid nanoformulation across the BMECs. 0.1% of the TAT-modified NLCs were detected in the basolateral chamber of our TW system two hours (120 min time point) after we introduced them to our BBB cultures; on the contrary, the NPs that were coated only with CS were not detectable at any of the examined time points. Although other permeability studies with functionalized NPs have exhibited better results [65-69], they were carried out in bEnd.3 cell model or in primary HBMECs with significantly lower TEER values, around $20\text{-}400 \Omega \times \text{cm}^2$, resulting in low relevance between the obtained permeability values and the clinical data [56,70]. Therefore, our findings show that surface modification with TAT peptide could lead to the development of patient-oriented therapeutics for the CNS.

Our next aim was to investigate if our newly developed NPs could modulate neuroinflammation in the human brain. To model neuroinflammation *in vitro* with

relevance to human physiology, we used HMC3, a human microglial cell line [71]. LPS has been widely used in both *in vivo* and *in vitro* models to induce inflammation in microglia [72-74]; others have previously shown that HMC3 also respond to LPS [75,76], thereby providing a good experimental model to study neuroinflammation. Indeed, our data show that HMC3 were responsive to LPS stimuli manifested by an altered gene expression profile and cytokine response when compared to basal conditions.

Our data show that in response to LPS, the HMC3 microglia shifted to the pro-inflammatory state; gene expression analysis showed significant upregulation of IL-6, TNF- α , and IL-1 β (Fig. 5 A-C), while cytokine secretion analysis showed IL-6, IL-1 β and IL-8 release in the media (Fig. 6 A-C). These data correlate with existing studies; IL-6 cytokine is the most responsive to various *stimuli* [71]. In our study, IL-8 cytokine exhibited the highest values with a three-fold upregulation after the incubation with LPS; this effect has been observed previously after the incubation with NS3 protein but not after LPS incubation [77]. Despite the observed upregulation of TNF- α at the gene expression level, we were not able to detect cytokine release in the media with the U-PLEX assay; this cytokine was below the threshold of the assay for both the basal and the LPS treated condition. Moreover, the qPCR analysis did not show any changes in terms of COX2 and NF- κ B genes (Suppl. Fig.3), which is in line with previous publications and different inflammatory stimuli [77,78]. Taken together, our data show that the HMC3 microglial cell line responds to LPS *stimuli*; therefore, we utilized these cells as an *in vitro* platform to test our NPs in terms of their ability to modulate inflammatory processes and provide data with human relevance.

Next, we investigated if treatment with various types of NLCs could modulate the LPS-induced inflammatory responses. Indeed, as shown in Fig. 5 E-G and Fig. 6 D-F, 24 h incubation with DHAH composed NLCs counteracted inflammatory response in the microglia; an effect that we did not observe after incubation with Mygliol-NLC. Our results highlight the potential anti-inflammatory properties of DHAH-NLC treatment and point to that the anti-inflammatory properties of Ω -3 fatty acids [79,80] are maintained when formulated in NLC lipid matrix. Previous studies suggest that GDNF and VEGF can inhibit neuroinflammation and, therefore, protect from neurodegeneration [81,82]. Hence, we hypothesized that the encapsulation of these

GFs in our DHAH-NLCs would further promote their anti-inflammatory potential. Surprisingly, the encapsulation of GDNF or VEGF in the DHAH enriched NLCs (DHAH-NLC-GDNF, DHAH-NLC-VEGF) did not seem to have a pronounced effect on the inflammatory profile upon LPS stimulation (Fig.6 D-F). In detail, the secretion of all detected cytokines was on par with the DHAH-NLC condition suggesting that either this specific microglia source is not responsive to GFs or that these GFs manifest their anti-inflammatory properties in other pathways [83,84]. While, to our knowledge, the effect of VEGF in activated microglia remains elusive [85], a recent study suggests that GDNF regulates microglia responses via the activation of the endogenous anti-oxidative system and not due the downregulation of pro-inflammatory markers such as TNF- α or IL-6 [86].

The antioxidant pathway Nrf2/HO-1 is a putative target against oxidative stress and neuroinflammation in NDs [87,88]. We, therefore, investigated if our NPs could show antioxidant abilities via this molecular cascade. Our data showed that treatment with all the DHAH enriched NLCs upregulated HO-1 in basal conditions (Condition A, Fig. 5D). In response to LPS *stimuli*, only DHAH-NLC-GDNF showed a significant upregulation in HO-1 levels (Fig 5H), while the rest of the DHAH enriched nanoformulations induced a slight increase that did not reach significance. Thus, we concluded that DHAH-NLC-GDNF activated the anti-oxidative system present in microglia, which is in line with recent studies [89,90].

5. CONCLUSION

Taken together, the present study shows that TAT functionalized NLCs can effectively cross the BBB and act as trojan horses for the transport of GFs in the human brain, thereby supporting their use as therapeutic agents for CNS disorders. Moreover, DHAH-NLCs could modulate neuroinflammatory and/or oxidative stress components, while additional encapsulation of GDNF further enhanced these effects. These findings suggest a novel, targeted synergistic strategy to enter the human CNS and regulate the aberrant microglial activation present in NDs.

6. ACKNOWLEDGEMENTS and FUNDING

A.H and D.V acknowledge support from Knut and Alice Wallenberg foundation (WAF 2015-0178). A.H and P.N. acknowledge the support from Swedish Research Council (2019-01803). R.H and M.I acknowledge support from the Spanish Ministry

of Economy and Competitiveness (RTC-2015-3542-1) and the Basque Government (Consolidated Groups IT 907–16). SH acknowledge the Basque Government for her fellowship grant.

7. BIBLIOGRAPHY

- [1] World Health Organization, Neurological Disorders: Public Health Challenges, 2020 (2020).
- [2] Alzheimer Disease International, World Alzheimer Report 2019: Attitudes to dementia, 2020 (2019).
- [3] C. Marras, J.C. Beck, J.H. Bower, E. Roberts, B. Ritz, G.W. Ross, R.D. Abbott, R. Savica, S.K. Van Den Eeden, A.W. Willis, C.M. Tanner, Parkinson's Foundation P4 Group, Prevalence of Parkinson's disease across North America, *NPJ Parkinsons Dis.* 4 (2018) 21-018-0058-0. eCollection 2018.
- [4] C.M. Henstridge, Modeling Alzheimer's disease brains in vitro, *Nat. Neurosci.* 21 (2018) 899-900.
- [5] M.A. Mofazzal Jahromi, A. Abdoli, M. Rahmanian, H. Bardania, M. Bayandori, S.M. Moosavi Basri, A. Kalbasi, A.R. Aref, M. Karimi, M.R. Hamblin, Microfluidic Brain-on-a-Chip: Perspectives for Mimicking Neural System Disorders, *Mol. Neurobiol.* 56 (2019) 8489-8512.
- [6] C.W. Olanow, K. Kieburtz, A.H. Schapira, Why have we failed to achieve neuroprotection in Parkinson's disease? *Ann. Neurol.* 64 Suppl 2 (2008) S101-10.
- [7] L.S. Schneider, F. Mangialasche, N. Andreasen, H. Feldman, E. Giacobini, R. Jones, V. Mantua, P. Mecocci, L. Pani, B. Winblad, M. Kivipelto, Clinical trials and late-stage drug development for Alzheimer's disease: an appraisal from 1984 to 2014, *J. Intern. Med.* 275 (2014) 251-283.
- [8] U. Marx, T.B. Andersson, A. Bahinski, M. Beilmann, S. Beken, F.R. Cassee, M. Cirit, M. Daneshian, S. Fitzpatrick, O. Frey, C. Gaertner, C. Giese, L. Griffith, T. Hartung, M.B. Heringa, J. Hoeng, W.H. de Jong, H. Kojima, J. Kuehnl, M. Leist, A. Luch, I. Maschmeyer, D. Sakharov, A.J. Sips, T. Steger-Hartmann, D.A. Tagle, A. Tonevitsky, T. Tralau, S. Tsyb, A. van de Stolpe, R. Vandebriel, P. Vulto, J. Wang, J. Wiest, M. Rodenburg, A. Roth, Biology-inspired microphysiological system approaches to solve the prediction dilemma of substance testing, *ALTEX.* 33 (2016) 272-321.
- [9] R. Briggs, S.P. Kennelly, D. O'Neill, Drug treatments in Alzheimer's disease, *Clin. Med. (Lond).* 16 (2016) 247-253.
- [10] W. Oertel, J.B. Schulz, Current and experimental treatments of Parkinson disease: A guide for neuroscientists, *J. Neurochem.* 139 Suppl 1 (2016) 325-337.
- [11] Y. Hou, X. Dan, M. Babbar, Y. Wei, S.G. Hasselbalch, D.L. Croteau, V.A. Bohr, Ageing as a risk factor for neurodegenerative disease, *Nat. Rev. Neurol.* 15 (2019) 565-581.
- [12] L. Gan, M.R. Cookson, L. Petrucelli, A.R. La Spada, Converging pathways in neurodegeneration, from genetics to mechanisms, *Nat. Neurosci.* 21 (2018) 1300-1309.
- [13] A.D. Gitler, P. Dhillon, J. Shorter, Neurodegenerative disease: models, mechanisms, and a new hope, *Dis. Model. Mech.* 10 (2017) 499-502.
- [14] S. Buch, Growth factor signaling: implications for disease & therapeutics, *J. Neuroimmune Pharmacol.* 9 (2014) 65-68.
- [15] S.J. Allen, J.J. Watson, D.K. Shoemark, N.U. Barua, N.K. Patel, GDNF, NGF and BDNF as therapeutic options for neurodegeneration, *Pharmacol Ther.* 138 (2013) 155-175.

- [16] A.M. Sullivan, A. Toulouse, Neurotrophic factors for the treatment of Parkinson's disease, *Cytokine Growth Factor Rev.* 22 (2011) 157-165.
- [17] G.Y. Sun, A. Simonyi, K.L. Fritsche, D.Y. Chuang, M. Hannink, Z. Gu, C.M. Greenlief, J.K. Yao, J.C. Lee, D.Q. Beversdorf, Docosahexaenoic acid (DHA): An essential nutrient and a nutraceutical for brain health and diseases, *Prostaglandins Leukot Essent Fatty Acids.* (2017).
- [18] R. Avallone, G. Vitale, M. Bertolotti, Omega-3 Fatty Acids and Neurodegenerative Diseases: New Evidence in Clinical Trials, *Int. J. Mol. Sci.* 20 (2019) 10.3390/ijms20174256.
- [19] P. Li, C. Song, Potential treatment of Parkinson's disease with omega-3 polyunsaturated fatty acids, *Nutr. Neurosci.* (2020) 1-12.
- [20] E. Garbayo, A. Estella-Hermoso de Mendoza, M.J. Blanco-Prieto, Diagnostic and therapeutic uses of nanomaterials in the brain, *Curr. Med. Chem.* 21 (2014) 4100-4131.
- [21] S. Hernando, O. Gartzandia, E. Herran, J.L. Pedraz, M. Igartua, R.M. Hernandez, Advances in nanomedicine for the treatment of Alzheimer's and Parkinson's diseases, *Nanomedicine (Lond).* 11 (2016) 1267-1285.
- [22] S. Hernando, E. Herran, J.L. Pedraz, M. Igartua, R.M. Hernandez, Nanotechnology Based Approaches for Neurodegenerative Disorders: Diagnosis and Treatment, in: Sharma H. S et al. (Ed.), *Drug and Gene Delivery to the Central Nervous System for Neuroprotection.* Springer International Publishing, Switzerland, 2017, pp. 57-87.
- [23] A. Khosa, S. Reddi, R.N. Saha, Nanostructured lipid carriers for site-specific drug delivery, *Biomed Pharmacother.* 103 (2018) 598-613.
- [24] M.I. Teixeira, C.M. Lopes, M.H. Amaral, P.C. Costa, Current insights on lipid nanocarrier-assisted drug delivery in the treatment of neurodegenerative diseases, *Eur J Pharm Biopharm.* 149 (2020) 192-217.
- [25] A. Beloqui, M.Á Solinís, A. Rodríguez-Gascón, A.J. Almeida, V. Préat, Nanostructured lipid carriers: Promising drug delivery systems for future clinics, *Nanomedicine.* 12 (2016) 143-161.
- [26] B.K. Nanjwade, D.J. Patel, R.A. Udhani, F.V. Manvi, Functions of lipids for enhancement of oral bioavailability of poorly water-soluble drugs, *Sci. Pharm.* 79 (2011) 705-727.
- [27] Y. Agrawal, K.C. Petkar, K.K. Sawant, Development, evaluation and clinical studies of Acitretin loaded nanostructured lipid carriers for topical treatment of psoriasis, *Int. J. Pharm.* 401 (2010) 93-102.
- [28] A. Huguet-Casquero, M. Moreno-Sastre, T.B. Lopez-Mendez, E. Gainza, J.L. Pedraz, Encapsulation of Oleuropein in Nanostructured Lipid Carriers: Biocompatibility and Antioxidant Efficacy in Lung Epithelial Cells, *Pharmaceutics.* 12 (2020) 10.3390/pharmaceutics12050429.
- [29] L.M. Negi, M. Jaggi, S. Talegaonkar, Development of protocol for screening the formulation components and the assessment of common quality problems of nano-structured lipid carriers, *Int. J. Pharm.* 461 (2014) 403-410.
- [30] S. Hernando, E. Herran, R.M. Hernandez, M. Igartua, Nanostructured Lipid Carriers Made of Omega-3 Polyunsaturated Fatty Acids: In Vitro Evaluation of Emerging Nanocarriers to Treat Neurodegenerative Diseases, *Pharmaceutics.* 12 (2020) 10.3390/pharmaceutics12100928.
- [31] R.J.S. Lacombe, R. Chouinard-Watkins, R.P. Bazinet, Brain docosahexaenoic acid uptake and metabolism, *Mol. Aspects Med.* 64 (2018) 109-134.
- [32] D. Zhang, J. Wang, D. Xu, Cell-penetrating peptides as noninvasive transmembrane vectors for the development of novel multifunctional drug-delivery systems, *J. Control. Release.* (2016).

- [33] D. Singh, H. Kapahi, M. Rashid, A. Prakash, A.B. Majeed, N. Mishra, Recent prospective of surface engineered Nanoparticles in the management of Neurodegenerative disorders, *Artif. Cells Nanomed Biotechnol.* 44 (2016) 780-791.
- [34] S. Hernando, E. Herran, J. Figueiro-Silva, J.L. Pedraz, M. Igartua, E. Carro, R.M. Hernandez, Intranasal Administration of TAT-Conjugated Lipid Nanocarriers Loading GDNF for Parkinson's Disease, *Mol. Neurobiol.* 55 (2018) 145-155.
- [35] H.C. Helms, N.J. Abbott, M. Burek, R. Cecchelli, P.O. Couraud, M.A. Deli, C. Forster, H.J. Galla, I.A. Romero, E.V. Shusta, M.J. Stebbins, E. Vandenhoute, B. Weksler, B. Brodin, In vitro models of the blood-brain barrier: An overview of commonly used brain endothelial cell culture models and guidelines for their use, *J. Cereb. Blood Flow Metab.* 36 (2016) 862-890.
- [36] B. Miccoli, D. Braeken, Y.E. Li, Brain-on-a-chip Devices for Drug Screening and Disease Modeling Applications, *Curr. Pharm. Des.* 24 (2018) 5419-5436.
- [37] P. Nikolakopoulou, R. Rauti, D. Voulgaris, I. Shlomy, B.M. Maoz, Anna Herland, Recent progress in translational engineered *in vitro* models of the central nervous system, *Brain.* awaa268 (2020).
- [38] B. Obermeier, R. Daneman, R.M. Ransohoff, Development, maintenance and disruption of the blood-brain barrier, *Nat. Med.* 19 (2013) 1584-1596.
- [39] B.V. Zlokovic, The blood-brain barrier in health and chronic neurodegenerative disorders, *Neuron.* 57 (2008) 178-201.
- [40] M.J. Workman, C.N. Svendsen, Recent advances in human iPSC-derived models of the blood-brain barrier, *Fluids Barriers CNS.* 17 (2020) 30-020-00191-7.
- [41] E.S. Lippmann, S.M. Azarin, J.E. Kay, R.A. Nessler, H.K. Wilson, A. Al-Ahmad, S.P. Palecek, E.V. Shusta, Derivation of blood-brain barrier endothelial cells from human pluripotent stem cells, *Nat. Biotechnol.* 30 (2012) 783-791.
- [42] E.H. Neal, N.A. Marinelli, Y. Shi, P.M. McClatchey, K.M. Balotin, D.R. Gullett, K.A. Hagerla, A.B. Bowman, K.C. Ess, J.P. Wikswo, E.S. Lippmann, A Simplified, Fully Defined Differentiation Scheme for Producing Blood-Brain Barrier Endothelial Cells from Human iPSCs, *Stem Cell. Reports.* 12 (2019) 1380-1388.
- [43] S. Hickman, S. Izzy, P. Sen, L. Morsett, J. El Khoury, Microglia in neurodegeneration, *Nat. Neurosci.* 21 (2018) 1359-1369.
- [44] V.H. Perry, J.A. Nicoll, C. Holmes, Microglia in neurodegenerative disease, *Nat. Rev. Neurol.* 6 (2010) 193-201.
- [45] A.D. Greenhalgh, S. David, F.C. Bennett, Immune cell regulation of glia during CNS injury and disease, *Nat. Rev. Neurosci.* 21 (2020) 139-152.
- [46] K. Haruwaka, A. Ikegami, Y. Tachibana, N. Ohno, H. Konishi, A. Hashimoto, M. Matsumoto, D. Kato, R. Ono, H. Kiyama, A.J. Moorhouse, J. Nabekura, H. Wake, Dual microglia effects on blood brain barrier permeability induced by systemic inflammation, *Nat. Commun.* 10 (2019) 5816-019-13812-z.
- [47] R.M. Ransohoff, How neuroinflammation contributes to neurodegeneration, *Science.* 353 (2016) 777-783.
- [48] Y. Shigemoto-Mogami, K. Hoshikawa, K. Sato, Activated Microglia Disrupt the Blood-Brain Barrier and Induce Chemokines and Cytokines in a Rat *in vitro* Model, *Front. Cell. Neurosci.* 12 (2018) 494.

[49] O. Gartzandia, S.P. Egusquiaguirre, J. Bianco, J.L. Pedraz, M. Igartua, R.M. Hernandez, V. Pr eat, A. Beloqui, Nanoparticle transport across in vitro olfactory cell monolayers, *Int. J. Pharm.* 499 (2016) 81-89.

[50] S.P. Egusquiaguirre, C. Mangu an-Garc a, L. Pintado-Berninches, L. Iarriccio, D. Carbajo, F. Albericio, M. Royo, J.L. Pedraz, R.M. Hern andez, R. Perona, M. Igartua, Development of surface modified biodegradable polymeric nanoparticles to deliver GSE24.2 peptide to cells: A promising approach for the treatment of defective telomerase disorders, *Eur J Pharm Biopharm.* 91 (2015) 91-102.

[51] O. Gartzandia, E. Herran, J.L. Pedraz, E. Carro, M. Igartua, R.M. Hernandez, Chitosan coated nanostructured lipid carriers for brain delivery of proteins by intranasal administration, *Colloids Surf. B Biointerfaces.* 134 (2015) 304-313.

[52] E. Uhlin, H. R onnholm, K. Day, M. Kele, K. Tammimies, S. B olte, A. Falk, Derivation of human iPS cell lines from monozygotic twins in defined and xeno free conditions, *Stem Cell Research.* 18 (2017) 22-25.

[53] M.J. Stebbins, H.K. Wilson, S.G. Canfield, T. Qian, S.P. Palecek, E.V. Shusta, Differentiation and characterization of human pluripotent stem cell-derived brain microvascular endothelial cells, *Methods.* 101 (2016) 93-102.

[54] J. Ciesler, Y. Sari, Neurotrophic Peptides: Potential Drugs for Treatment of Amyotrophic Lateral Sclerosis and Alzheimer's disease, *Open J. Neurosci.* 3 (2013) 2.

[55] Z. Zhao, A.R. Nelson, C. Betsholtz, B.V. Zlokovic, Establishment and Dysfunction of the Blood-Brain Barrier, *Cell.* 163 (2015) 1064-1078.

[56] Y. Zhou, Z. Peng, E.S. Seven, R.M. Leblanc, Crossing the blood-brain barrier with nanoparticles, *J. Control. Release.* 270 (2018) 290-303.

[57] Q. He, J. Liu, J. Liang, X. Liu, W. Li, Z. Liu, Z. Ding, D. Tuo, Towards Improvements for Penetrating the Blood-Brain Barrier-Recent Progress from a Material and Pharmaceutical Perspective, *Cells.* 7 (2018) 10.3390/cells7040024.

[58] O. Gartzandia, E. Herr an, J.A. Ruiz-Ortega, C. Miguelez, M. Igartua, J.V. Lafuente, J.L. Pedraz, L. Ugedo, R.M. Hern andez, Intranasal administration of chitosan-coated nanostructured lipid carriers loaded with GDNF improves behavioral and histological recovery in a partial lesion model of Parkinson's disease, *J Biomed Nanotechnol.* 12 (2016) 1-11.

[59] J.A. Brown, S.L. Faley, Y. Shi, K.M. Hillgren, G.A. Sawada, T.K. Baker, J.P. Wikswow, E.S. Lippmann, Advances in blood-brain barrier modeling in microphysiological systems highlight critical differences in opioid transport due to cortisol exposure, *Fluids Barriers CNS.* 17 (2020) 38-020-00200-9.

[60] E.K. Hollmann, A.K. Bailey, A.V. Potharazu, M.D. Neely, A.B. Bowman, E.S. Lippmann, Accelerated differentiation of human induced pluripotent stem cells to blood-brain barrier endothelial cells, *Fluids Barriers CNS.* 14 (2017) 9-017-0059-0.

[61] O. Tornavaca, M. Chia, N. Dufton, L.O. Almagro, D.E. Conway, A.M. Randi, M.A. Schwartz, K. Matter, M.S. Balda, ZO-1 controls endothelial adherens junctions, cell-cell tension, angiogenesis, and barrier formation, *J. Cell Biol.* 208 (2015) 821-838.

[62] F.L. Cardoso, D. Brites, M.A. Brito, Looking at the blood-brain barrier: Molecular anatomy and possible investigation approaches, *Brain Res Rev.* 64 (2010) 328-363.

[63] T.E. Park, N. Mustafaoglu, A. Herland, R. Hasselkus, R. Mannix, E.A. FitzGerald, R. Prantil-Baun, A. Watters, O. Henry, M. Benz, H. Sanchez, H.J. McCrea, L.C. Goumnerova, H.W. Song, S.P.

Palecek, E. Shusta, D.E. Ingber, Hypoxia-enhanced Blood-Brain Barrier Chip recapitulates human barrier function and shuttling of drugs and antibodies, *Nat. Commun.* 10 (2019) 2621-019-10588-0.

[64] M.M. Lubtow, S. Oerter, S. Quader, E. Jeanclos, A. Cubukova, M. Krafft, M.S. Haider, C. Schulte, L. Meier, M. Rist, O. Sampetean, H. Kinoh, A. Gohla, K. Kataoka, A. Appelt-Menzel, R. Luxenhofer, In Vitro Blood-Brain Barrier Permeability and Cytotoxicity of an Atorvastatin-Loaded Nanoformulation Against Glioblastoma in 2D and 3D Models, *Mol. Pharm.* 17 (2020) 1835-1847.

[65] A. Cox, D. Vinciguerra, F. Re, R.D. Magro, S. Mura, M. Masserini, P. Couvreur, J. Nicolas, Protein-functionalized nanoparticles derived from end-functional polymers and polymer prodrugs for crossing the blood-brain barrier, *Eur. J. Pharm. Biopharm.* 142 (2019) 70-82.

[66] B. Dos Santos Rodrigues, S. Lakkadwala, T. Kanekiyo, J. Singh, Development and screening of brain-targeted lipid-based nanoparticles with enhanced cell penetration and gene delivery properties, *Int. J. Nanomedicine.* 14 (2019) 6497-6517.

[67] Y. Kuo, H. Ko, Targeting delivery of saquinavir to the brain using 83-14 monoclonal antibody-grafted solid lipid nanoparticles, *Biomaterials.* 34 (2013) 4818-4830.

[68] Y. Xie, L. Ye, X. Zhang, W. Cui, J. Lou, T. Nagai, X. Hou, Transport of nerve growth factor encapsulated into liposomes across the blood-brain barrier: In vitro and in vivo studies, *J. Controlled Release.* 105 (2005) 106-119.

[69] X. Jiang, H. Xin, Q. Ren, J. Gu, L. Zhu, F. Du, C. Feng, Y. Xie, X. Sha, X. Fang, Nanoparticles of 2-deoxy-d-glucose functionalized poly(ethylene glycol)-co-poly(trimethylene carbonate) for dual-targeted drug delivery in glioma treatment, *Biomaterials.* 35 (2014) 518-529.

[70] D.J. Mc Carthy, M. Malhotra, A.M. O'Mahony, J.F. Cryan, C.M. O'Driscoll, Nanoparticles and the blood-brain barrier: advancing from in-vitro models towards therapeutic significance, *Pharm. Res.* 32 (2015) 1161-1185.

[71] C. Dello Russo, N. Cappoli, I. Coletta, D. Mezzogori, F. Paciello, G. Pozzoli, P. Navarra, A. Battaglia, The human microglial HMC3 cell line: where do we stand? A systematic literature review, *J. Neuroinflammation.* 15 (2018) 259-018-1288-0.

[72] W. Sheng, Y. Zong, A. Mohammad, D. Ajit, J. Cui, D. Han, J.L. Hamilton, A. Simonyi, A.Y. Sun, Z. Gu, J.S. Hong, G.A. Weisman, G.Y. Sun, Pro-inflammatory cytokines and lipopolysaccharide induce changes in cell morphology, and upregulation of ERK1/2, iNOS and sPLA(2)-IIA expression in astrocytes and microglia, *J. Neuroinflammation.* 8 (2011) 121-2094-8-121.

[73] I.C. Hoogland, C. Houbolt, D.J. van Westerloo, W.A. van Gool, D. van de Beek, Systemic inflammation and microglial activation: systematic review of animal experiments, *J. Neuroinflammation.* 12 (2015) 114-015-0332-6.

[74] C. Fourrier, J. Remus-Borel, A.D. Greenhalgh, M. Guichardant, N. Bernoud-Hubac, M. Lagarde, C. Joffre, S. Laye, Docosahexaenoic acid-containing choline phospholipid modulates LPS-induced neuroinflammation in vivo and in microglia in vitro, *J. Neuroinflammation.* 14 (2017) 170-017-0939-x.

[75] C. Lindberg, M. Crisby, B. Winblad, M. Schultzberg, Effects of statins on microglia, *J. Neurosci. Res.* 82 (2005) 10-19.

[76] H. Li, X. Zhang, M. Chen, J. Chen, T. Gao, S. Yao, Dexmedetomidine inhibits inflammation in microglia cells under stimulation of LPS and ATP by c-Fos/NLRP3/caspase-1 cascades, *EXCLI J.* 17 (2018) 302-311.

[77] A.R. Rajalakshmy, J. Malathi, H.N. Madhavan, Hepatitis C Virus NS3 Mediated Microglial Inflammation via TLR2/TLR6 MyD88/NF-kappaB Pathway and Toll Like Receptor Ligand Treatment Furnished Immune Tolerance, *PLoS One.* 10 (2015) e0125419.

[78] V.S. Jadhav, K.H. Krause, S.K. Singh, HIV-1 Tat C modulates NOX2 and NOX4 expressions through miR-17 in a human microglial cell line, *J. Neurochem.* 131 (2014) 803-815.

[79] S. Laye, A. Nadjar, C. Joffre, R.P. Bazinet, Anti-Inflammatory Effects of Omega-3 Fatty Acids in the Brain: Physiological Mechanisms and Relevance to Pharmacology, *Pharmacol. Rev.* 70 (2018) 12-38.

[80] E. Hjorth, M. Zhu, V.C. Toro, I. Vedin, J. Palmblad, T. Cederholm, Y. Freund-Levi, G. Faxen-Irving, L.O. Wahlund, H. Basun, M. Eriksdotter, M. Schultzberg, Omega-3 fatty acids enhance phagocytosis of Alzheimer's disease-related amyloid-beta42 by human microglia and decrease inflammatory markers, *J. Alzheimers Dis.* 35 (2013) 697-713.

[81] S.M. Rocha, A.C. Cristovão, F.L. Campos, C.P. Fonseca, G. Baltazar, Astrocyte-derived GDNF is a potent inhibitor of microglial activation, *Neurobiol. Dis.* 47 (2012) 407-415.

[82] Z. Xu, K. Han, J. Chen, C. Wang, Y. Dong, M. Yu, R. Bai, C. Huang, L. Hou, Vascular endothelial growth factor is neuroprotective against ischemic brain injury by inhibiting scavenger receptor A expression on microglia, *J. Neurochem.* 142 (2017) 700-709.

[83] Z.S. Katusic, S.A. Austin, Neurovascular Protective Function of Endothelial Nitric Oxide-Recent Advances, *Circ. J.* 80 (2016) 1499-1503.

[84] T. Tanaka, K. Oh-hashii, H. Shitara, Y. Hirata, K. Kiuchi, NF- κ B independent signaling pathway is responsible for LPS-induced GDNF gene expression in primary rat glial cultures, *Neurosci. Lett.* 431 (2008) 262-267.

[85] J.M. Bain, L. Moore, Z. Ren, S. Simonishvili, S.W. Levison, Vascular endothelial growth factors A and C are induced in the SVZ following neonatal hypoxia-ischemia and exert different effects on neonatal glial progenitors, *Transl. Stroke Res.* 4 (2013) 158-170.

[86] Y.P. Chang, K.M. Fang, T.I. Lee, S.F. Tzeng, Regulation of microglial activities by glial cell line derived neurotrophic factor, *J. Cell. Biochem.* 97 (2006) 501-511.

[87] M. Sandberg, J. Patil, B. D'Angelo, S.G. Weber, C. Mallard, NRF2-regulation in brain health and disease: Implication of cerebral inflammation, *Neuropharmacology.* 79 (2014) 298-306.

[88] S. Hernando, C. Requejo, E. Herran, J.A. Ruiz-Ortega, T. Morera-Herreras, J.V. Lafuente, L. Ugedo, E. Gainza, J.L. Pedraz, M. Igartua, R.M. Hernandez, Beneficial effects of n-3 polyunsaturated fatty acids administration in a partial lesion model of Parkinson's disease: The role of glia and NRF2 regulation, *Neurobiol. Dis e.* 121 (2019) 252-262.

[89] Y.P. Chang, K.M. Fang, T.I. Lee, S.F. Tzeng, Regulation of microglial activities by glial cell line derived neurotrophic factor, *J. Cell. Biochem.* 97 (2006) 501-511.

[90] P. Yue, L. Gao, X. Wang, X. Ding, J. Teng, Pretreatment of glial cell-derived neurotrophic factor and geranylgeranylacetone ameliorates brain injury in Parkinson's disease by its anti-apoptotic and anti-oxidative property, *J. Cell. Biochem.* 119 (2018) 5491-5502.

Supplementary information

Suppl. Table 1. Summary of the reagent used in this research article.

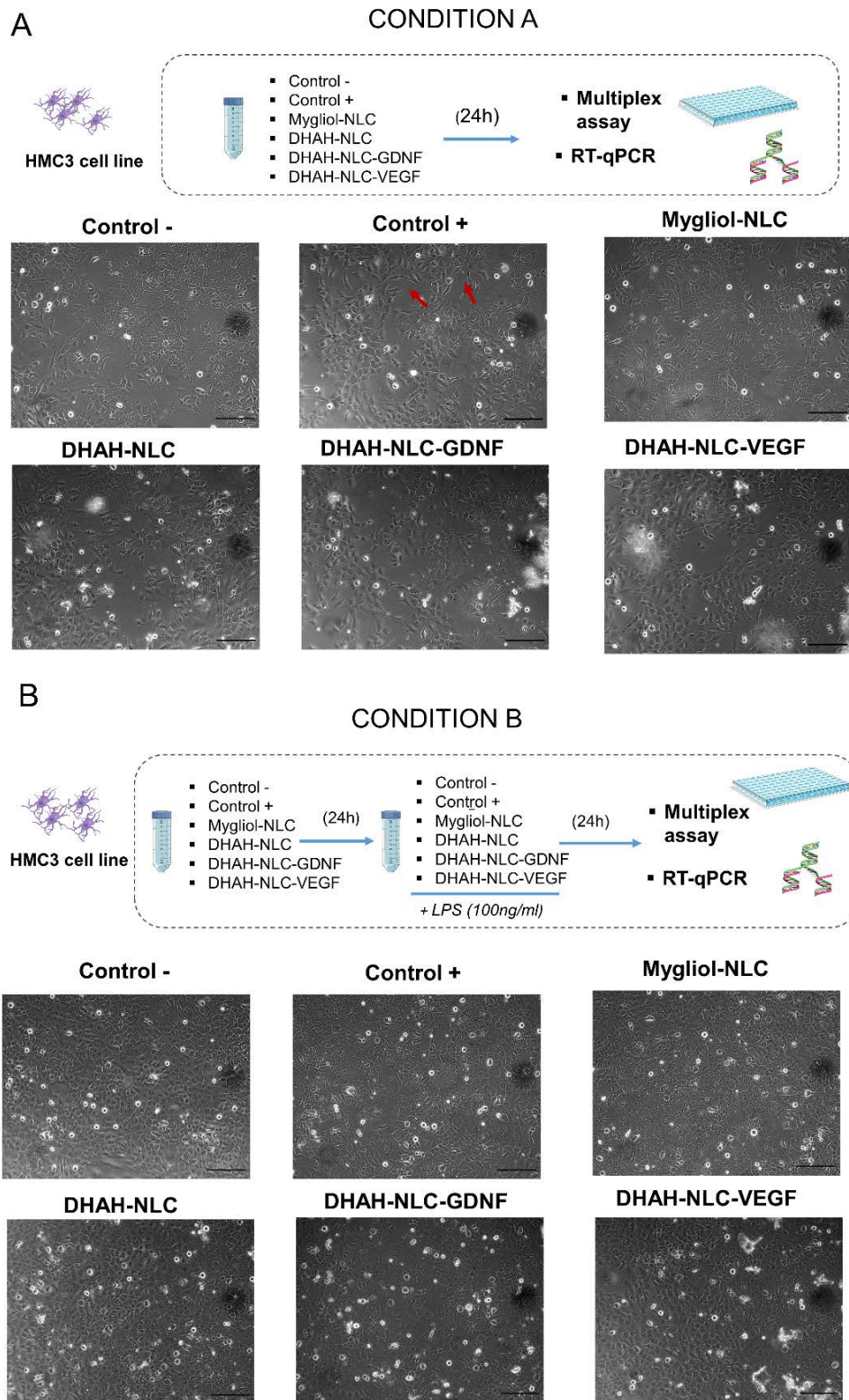
PRODUCT	Reference (company)
Precirol ATO®5 (glycerol distearate)	Gattefosé
Mygliol ® (caprylic/capric triglyceride)	Sasol Germany GmbH
DHAH fatty acid (ethyl ester form)	Medalchemistry
Tween 80	162050 (Panreac)
Tween 20	62312 (Panreac)
Lutrol ® F-68 (Poloxamer 188)	9003-11-6 (VWR)
Trehalose dehydrate	T5251 (Sigma)
Chitosan (Ultrapure)	4210021 (Novamatrix)
Matrigel	354230 (Corning)
mTeSR™ 1 media	85850 (Stem cell technologies)
ROCK inhibitor	1254 (TOCRIS)
Tryple Select	12563011 (Gibco)
Versene	15040066(Gibco)
E6 media (Essential 6 medium)	A1516401 (Gibco)
hESFM media (human endotelial serum free media)	11111044 (Gibco)
B27™ supplement (50X)	17504044 (Gibco)
bFGF (basic fibroblastic growth factor)	233-FB (R&D Systems)
RA (retinoic acid)	R2625 (Sigma)
Fibronectin	F1141 (Sigma)
Collagen type IV	C 5533 (Sigma)
DMEM/F-12, GlutaMAX™	31331028 (Gibco)
Fetal bovine serum (FBS)	A3840202 (Gibco)
Dulbecco's phosphate-buffered saline (DPBS), calcium, magnesium	14080048 (Gibco)
Dulbecco's phosphate-buffered saline (DPBS) no calcium, no magnesium	14190094 (Gibco)
4',6-diamidino-2-phenylindole (DAPI)	D1306 (Invitrogen)
1,1'-Dioctadecyl-3,3,3',3'-Tetramethylindodicarbocyanine Perchlorate	D307 (Invitrogen)
Paraformaldehyde (PFA)	441244 (Sigma)
Triton™ x-100	X100 (Sigma)
Normal Goat serum (NGS)	G9023 (Sigma)
β-Mercaptoethanol	31350-010 (Sigma)
ZO-1 antibody	33-9100 (Invitrogen)
Anti-Mouse IgG1 (γ1), CF™488A	SAB4600237 (Sigma)
LPS-EK Ultrapure	tlrl-pek1ps (InvivoGen)
RNA isolation kit	11 828 665 001 (Roche)
High-Capacity RNA-to-cDNA™ Kit	4387406 (Applied Biosystems)
TaqMan™ Fast Advanced Master Mix	4444557 (Applied Biosystems)
VEGF (vascular endothelial growth factor)	100-20 (Peprotech)
GDNF (glial derived growth factor)	450-10 (Peprotech)
VEGF ELISA Kit	900-K10 (Peprotech)
GDNF ELISA Kit	Ab100525 (Abcam)
TAT peptide	ChinaPeptides

Suppl. Table 2. Composition of the different type of NLCs and doses tested in HMC3 microglia cell line.

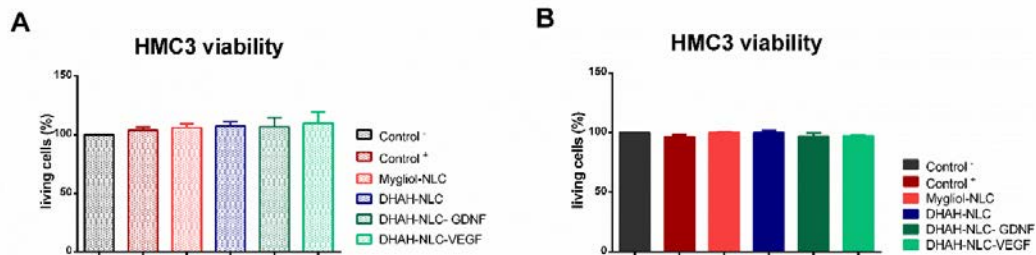
	Mygliol-NLC				DHAH-NLC				DHAH-NLC-GDNF				DHAH-NLC-VEGF			
	15.5	31	62	124	12.5	25	50	100	12.5	25	50	100	12.5	25	50	100
Internal control (M1-M4)(μ g/ml)	+	+	+	+	-	-	-	-	-	-	-	-	-	-	-	-
DHAH (μ M)	-	-	-	-	+	+	+	+	+	+	+	+	+	+	+	+
GDNF (ng/ml)	-	-	-	-	-	-	-	-	+	+	+	+	-	-	-	-
VEGF (ng/ml)	-	-	-	-	-	-	-	-	-	-	-	-	+	+	+	+

Suppl. Table 3. Taqman assay ID.

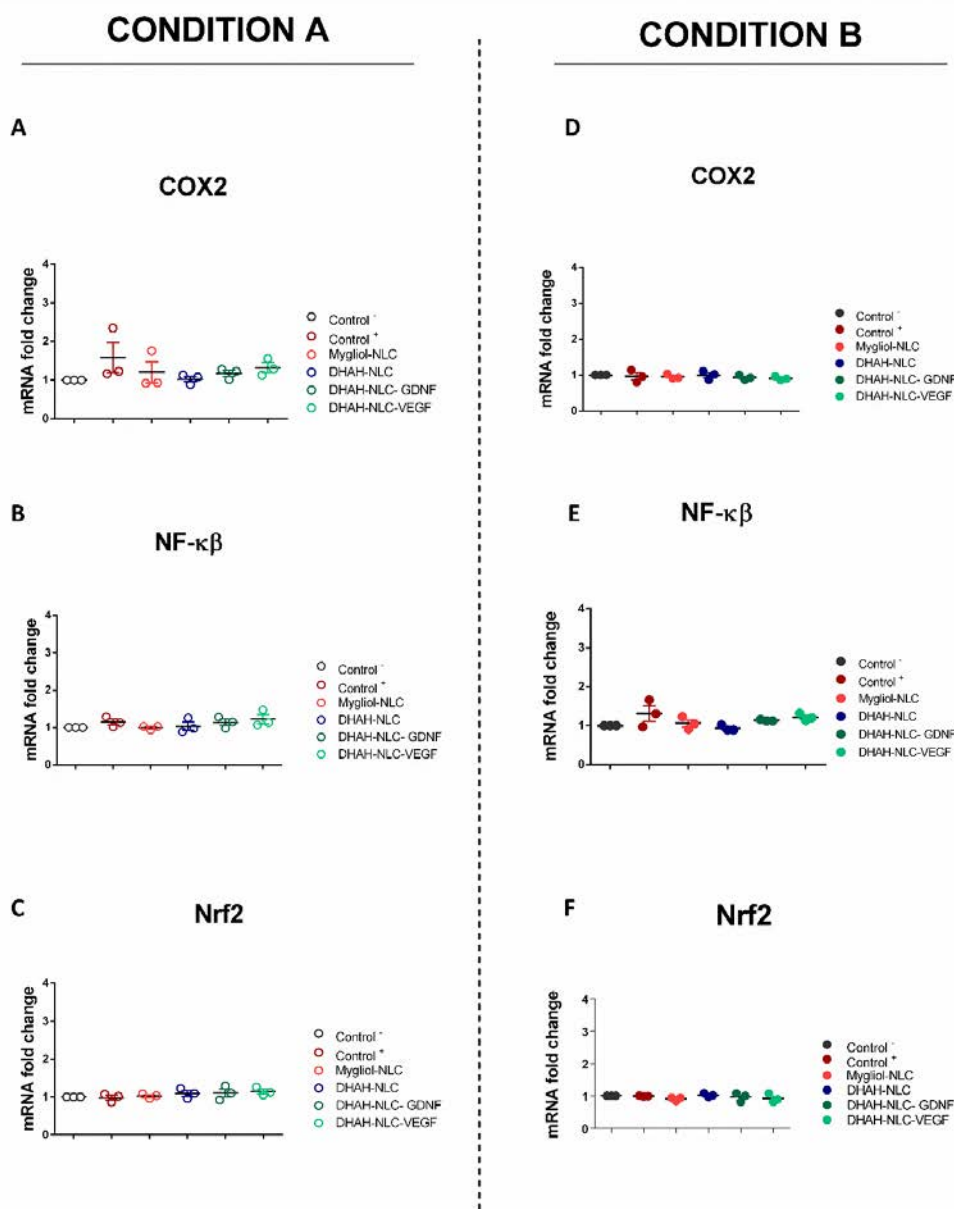
Gene name	Taqman assay ID
GADPH	Hs04420697_g1
NrF2	Hs00975961_g1
HO-1	Hs01110250_m1
NF- κ B	Hs00765730_m1
IL-1 β	Hs00174097_m1
IL-6	Hs00985639_m1
TNF- α	Hs00174128_m1
COX-2	Hs00153133_m1



Suppl. Fig.1. (A) Schematic representation of the experimental procedure in microglial culture and bright-field images 24h after treatment with our NPs. Control - (media change) Control + (LPS 50 ng/ml) for condition A. The arrows indicate the slightly change to amoeboid phenotype in microglia. Scale bar 240µm. (B) Schematic representation of the experiment conducted in HMC3 microglia and the obtained bright-field images at 48 h. Control - (media change) Control + (LPS 50 ng/ml) for condition B. Scale bar 40mm. This figure was created using Servier Medical Art templates, which are licensed under a Creative Commons Attribution 3.0 Unported License; <https://smart.servier.com>.

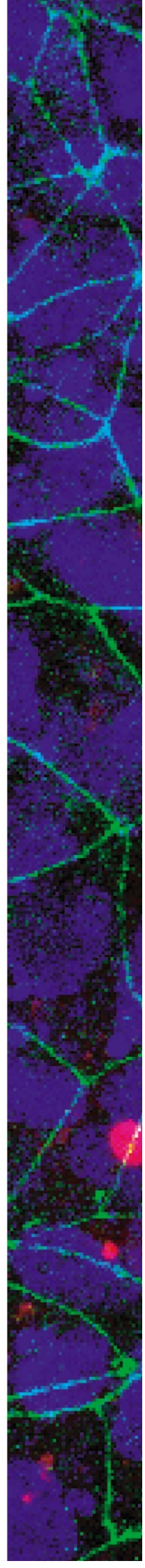


Suppl. Fig. 2. HMC3 cell viability after LPS treatment. (A) Remaining living cells for condition A. (B) Remaining living cells in condition B. Cell viability for each condition (treated cells) is expressed as the percentage of living cells when compared to the non-treated cells (media change; Control -), which was set as 100%. No differences in cell viability were detected ($p > 0.05$, One-way ANOVA).



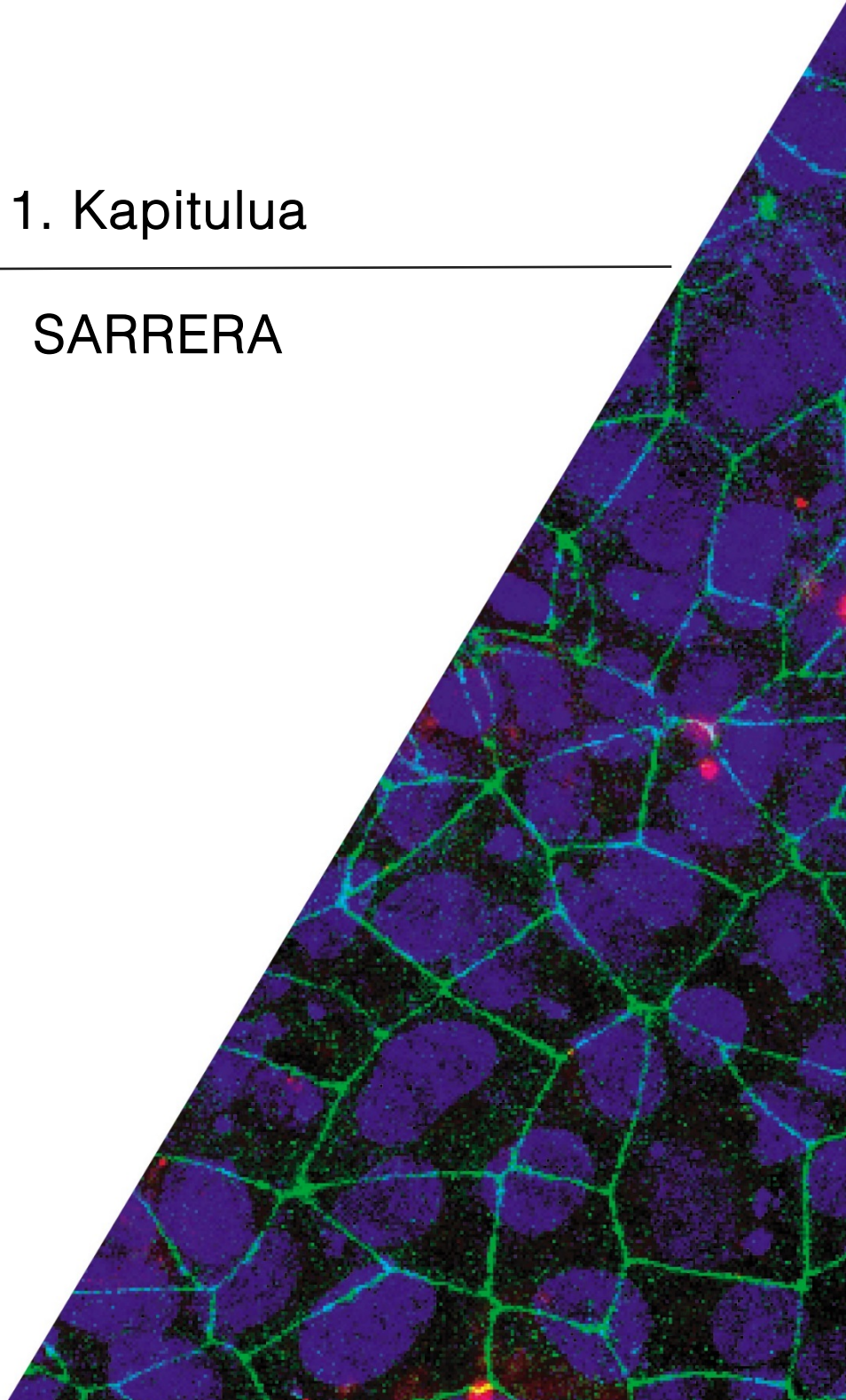
Suppl. Fig. 3. Gene expression analysis (RT-qPCR). (A) COX2 (B) NF- κ β (C) Nrf2 for condition A. (D) COX2 (E) NF- κ β (F) Nrf2 for condition B. Relative mRNA expression was normalized against GAPDH and the gene expression of the group that only media change was performed (Control-) was used for normalization (value 1). (Data are presented as fold change \pm SEM; N=3 independent experiments; Δ CT values were used for statistical analysis, One-Way ANOVA).

EUSKERAZKO BERTSIOA



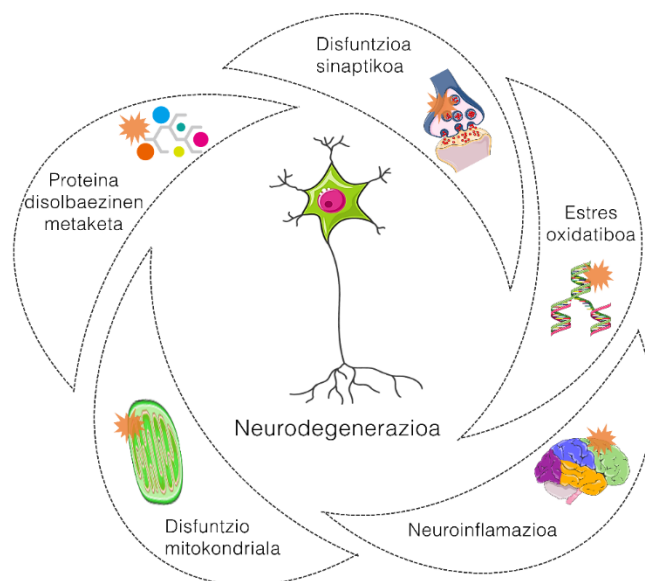
1. Kapituluu

SARRERA



1. Sarrera

Gaixotasun neurodegeneratiboak (*neurodegenerative diseases* edo ND) egoera neurologiko konplexuak dira, non sintoma kliniko desberdin agertu arren, kasu guztietan garuneko funtzioen galera progresiboa agertzen den. Gainera, neuronen galera selektiboa ematen da nerbio-sistema zentralean (*central nervous system* edo CNS) [1]. Kaltetutako zirkuitu neuronal ezberdinen arabera, sintoma kliniko ezberdinak agertzen dira, adibidez, oroimen-galera, muskulu dardara, gorputz-jarreraren ezegonkortasuna edo muskulu-tonuaren alterazio orokorrak. Nahiz eta sintoma kliniko ezberdinak eduki, gaixotasun hauek neurodegenerazioaren ezaugarri eta mekanismo komunak dituzte; non proteina disolbaezinen metaketak, disfuntzio mitokondrialak, estres granuluak, eta disfuntzio sinaptikoak, estres oxidatiboarekin batera, neuronen galera eta neurodegenerazioa eragiten dituzten [2,3] (1. Irudia). ND-ak faktore anitzeko gaixotasunak dira, arrisku-faktore eta kausa askorekin; hala ere, guztien artean, zahartzea da NDn eragin handiena duena [4]. Alzheimer gaixotasuna (*Alzheimer disease* edo AD) eta Parkinson gaixotasuna (*Parkinson disease* edo PD) ohikoenak dira adineko pertsonen artean. Izan ere, mundu osoko 43,7 milioi eta 6,1 milioi biztanlek, hurrenez hurren, pairatzen dituzte [5,6]. Biztanleriak zahartzen jarraituko duenez, NDen prebalentzia tasak gora egiten jarraituko du, eta ondorioz, NDak ekonomia eta osasun publikoarentzat arazo larri bihurtuko dira epe laburrean.

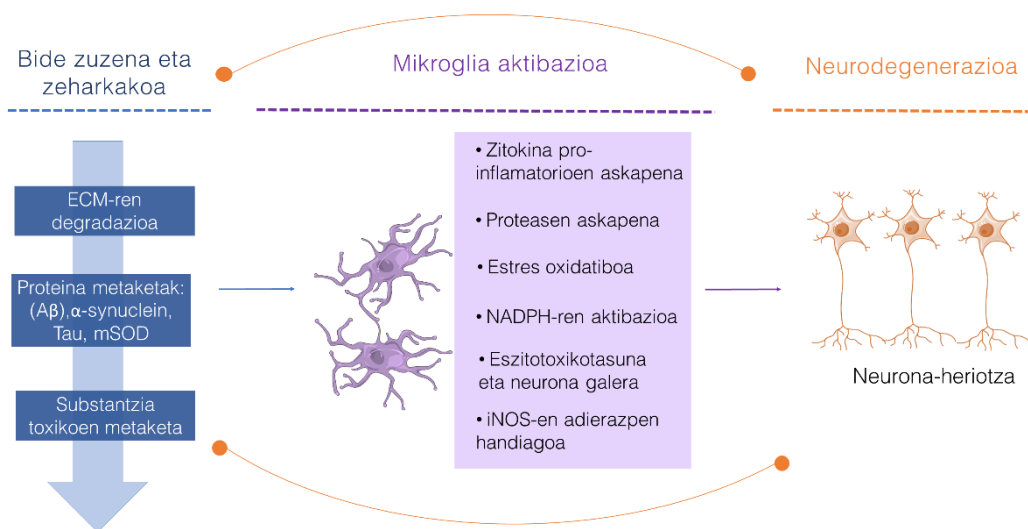


1. Irudia. Neurodegenerazioaren ezaugarri ezberdinak.

Gaur egungo terapiak ez dira optimoak, gaixotasunen sintomak tratatzen dituzte baina prozesu neurodegeneratiboan eragin gabe. Osasun publikorako arazo bat diren arren, praktika klinikoan tratamendu gutxi daude gaixotasunen hauen aurka. Esate baterako, AD kasuan bakarrik bi farmako mota daude: kolinesterasaren inhibitzaileak eta memantina, biek onura terapeutiko txikiekin. PDn kasuan gauza bera gertatzen da. L-dopa eta dopamina agonistek dopamina ordezkatzeko duten mugikortasun sintomatologia hobetuz, baina mugimenduari zerikusik ez duten sintometan inolako onurarik nabaritu gabe. Klinikari eragin positibo handiegirik ez izateak, albo-efektu sistemikoak agertzearekin batera, pazienteak tratamendua uztera bultzatu ditu [7,8]. Hori dela eta, prozesu neurodegeneratiboaren progresioa moteltzen duen tratamendu bat garatzea beharrezkoa bilakatu da. Zentzu honetan, zientzialariak eta baita farmazi industria ere, farmakoterapiako helburu klasikoetatik urrundu dira, gaixotasunaren aurkako tratamendu aldarazleetan zentratzeko. Horien artean, faktore neurotrofikoaren erabilera (*neurotrophic factors* edo NTF) estrategia itxaropentsua dela dirudi eta zientzialarien artean piztu du faktore hauen ezaugarri neurobirsortzaile eta neurobabesleengatik. NTFen gaixotasun neurologikoetan duten eragite mekanismoa guztiz ulertu ez arren, *in vitro* eta *in vivo* ikerketa ezberdinetan efektu terapeutikoak lortu dituzte, neuronon biziraupena luzatuz baita gaixotasunaren sintomatologia gutxituz ere. Hazkuntza faktore (*growth factor* edo GF) ezberdinen artean, gliatik eratorritako faktore neurotrofikoa (*glial derived neurotrophic factor* edo GDNF) erreferentziazko NTF da PD-rako, motoneuronetan eta neurona dopaminergikoetan eragin garrantzitsuak erakusten baititu. Halaber, endotelio baskularreko hazkunde faktorea (*vascular endothelial growth factor* edo VEGF) ND-rako tratamendurik onena da, neuronon hazkunde eta neurobabesa hobetzen baititu. Gainera, angiogenesisia eta endotelioko zelulena garapena sustatzen ditu, ADri lotutako toxikotasun neurobaskularra hobetuz [9,10].

Tratamendu gehienak galera neuronala leheneratzean zentratu dira gaixotasunaren bilakaera aldatzeko. Dena den, azken urteotan jakin da NDak pentsatzen ziren baino konplexuagoak direla eta neuronetan oinarritutako terapiak ez direla nahikoak gaixotasun hauen aurka. Izan ere, NDetan bestelako zelula mota batzuek ere parte hartzen dute, batez ere, glia. Astrozitoak, oligodendrozitoak eta mikroglia dira CNSan aurkitzen diren glia mota nagusiak [11,12]. Denen artean, mikroglia neurodegenerazioa eragiten duen neuroinflamazio faktore garrantzitsuena da. 2. irudian ikusten den bezala, mikroglia, bide zuzen edo

zeharkoen bidez aktibatzen da, zitokina edota proteasak askatuz, horrela, estres oxidatiboa eta eszitotoxikotasuna eraginez. Erantzun honek prozesu neurodegeneratiboa handitzen du, neuronen galera eta substantzia toxikoen metaketa dakarrena, eta beraz prozesu amaigabea bihurtuz. Prozesu degeneratibo autoeragile hau neurodegenerazioaren eremuan gertatzen da, neuroinflamazioaren eta neurodegenerazioaren arteko lotura azpimarratuz [13,14].



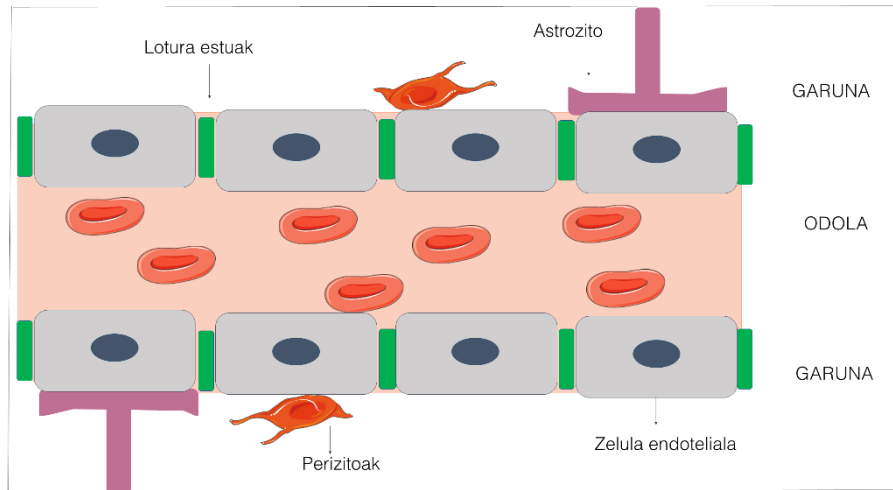
2. Irudia. Mikrogliak aktibazioaren eginkizuna neurodegenerazioan. (ECM: matritz extrazelularra; mSOD: dismutasa superoxidoa; NADPH: nikotinamida adenina dinukleotido fosfatoa; iNOS: oxido nitriko sintasa induzigarria).

NDen konplexutasunak, berezko dituen neurona-galerarekin, neuroinflamazioarekin eta estres-oxidatiboarekin, tratamendu ezberdinen konbinazioa behar du, garunean gertatzen diren degenerazio mekanismo ezberdinak tratatzeko. Azken urteotan, konposatu natural berriak agertu dira, neuroinflamazio eta estres-oxidatiboaren aurrean emaitza positiboak aurkeztu dituztenak. Fitokimiko ezberdinak tratamendu gisa erabili daitezke NDen aurka; erresberatrola, kurkumina edo gantz-azido poliasegabeak (*polyunsaturated fatty acids* edo PUFAk) besteak beste. Konposatu hauen mekanismoa argi ez dagoen arren, haien efektu terapeutikoak antioxidatzaile eta antiinflamatorio gisa frogatuta daude [15].

Hala ere, tratamendu eraginkor bat lortzeko erronka handienetariko bat barrera hematoentzefalikoa (*blood brain barrier* edo BBB) zeharkatzea da (3. Irudia). Barrera dinamikoa honek substantzia eta molekula neurotoxikoen fluxua garunean kontrolatzen du, beraz, terapia berrien eraginkortasuna mugatuz. BBB zelula

Lipido-garraiatzaile nanoegituratu berriak Ω -3 gantz-azido poliinsaturatuetan eta TAT peptidotan oinarritutakoak gaixotasun neurodegeneratiboak tratatzeko

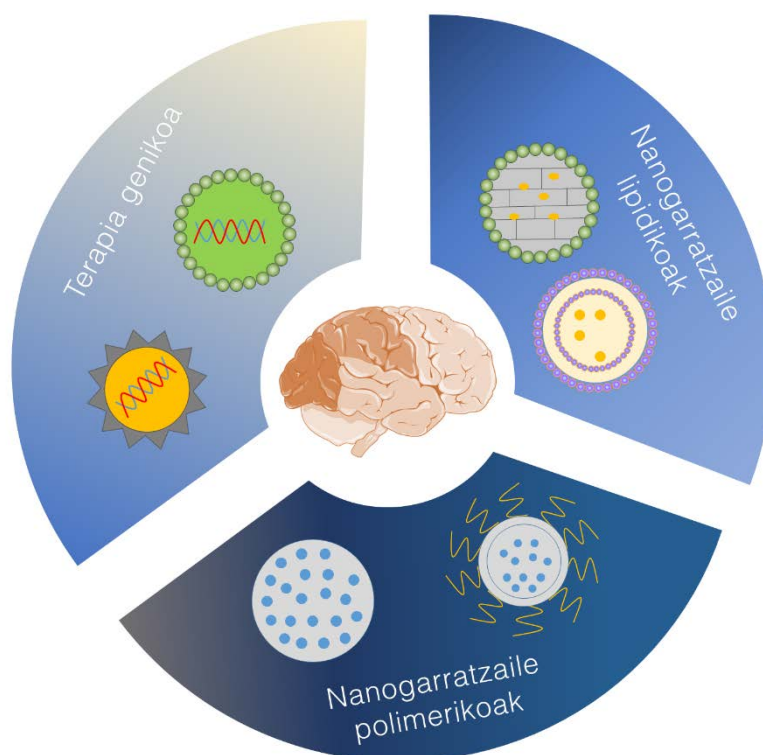
endotelial oso espezializatuak osatzen dute, garuneko zelula mikrobaskularrak (*brain microvascular endothelial cells* edo BMECak) izena dutenak, zeinek perizito eta astrozitoekin batera unitate neurobaskularra (*neurovascular unit* edo NVU) osatzen duten, barrera dinamiko honi berariazko ezaugarriak emanez [16,17].



3. Irudia. Barrera hematoentzefalikoa (BBB) eta unitate neurobaskularraren beste osagai batzuen irudikapen eskematikoa.

Barrera hau zeharkatzeko, estrategia ezberdinak erabil daitezke. Azken urteotan estrategia zuzen desberdinak ikertu dira. (Artikulu honetan BBB zeharkatzeko estrategia ezberdinei buruzko informazio gehiago aurki daiteke [18]. Doktorego-tesi honen *Appendix 2an*). Kirurgia edo barreraren haustura lortzen duten estrategiak teknika zuzenak dira, non farmakoak garunean bertan kokatzen diren haien efektu terapeutikoa lortzeko. Berriz, zeharko estrategietan barreraren osotasuna mantentzen da. Zeharkakoa estrategia hauen artean, administrazio bide alternatiboak daude, esaterako, sudurreko administrazioa, baita farmakoen konbinaketa zeluletan barnera daitezkeen peptidoekin ere (*cell penetrating peptides* edo CPP) edota farmakoen kapsularatzea nanoteknologian oinarritutako farmakoak askatzeko sistemetan (*drug delivery system* edo DDS). DDSak farmakoak garunera eramateko gaitasuna duten nano-tamaineko garratzaileak dira. Gainera, farmakoak degradazio entzimatikotik babesten ditu eta BBB zeharkatzeko aukera hobetzen dute [19]. (Artikulu honetan AD eta PD tratatzeko nanomedikuntzaren erabilerari buruzko informazio gehiago aurki daiteke [20] Doktorego-tesi honen *Appendix 1* (4. irudia)). Gehien erabiltzen diren DDSetako batzuk nanopartikulak (nanoparticles edo NPak) dira. NPak partikula solidoak dira, non konposatu aktiboa disolbatu, sartu edo

kapsularatzen den, edo zeini printzipio aktiboa adsorbatzen edo itsasten zaien. Gainera, administrazio bide ezberdinak erabil daitezke haien bideratzeko. NPen garapenean, besteak beste, polimero eta lipido natural edo sintetikoak erabili dira [21]. Azken urteotan, ikerketa-talde askok NPen erabilera tratamendu ezagunekin edo orain dela gutxi agertutako tratamendu berrieekin konbinatu dute, hala nola, aurrez aipatutako GFekin edo fitokimikoekin [22-25]. Ikerketa hauek guztiek NPak formulazio tradizionalak baino ezaugarri hobekak eskaintzen dituztela azpimarratzen dute, molekulak degradaziotik babestuz edo molekula terapeutikoen erdi-bizitza areagotuz, beraz, dosifikazioaren maiztasuna mugatuz eta albo-ondorioak murriztuz [26]. Haien artean, nanoegituratutako garratzaile lipidikoak (*nanostructured lipid carriers* edo NLCak) daude, zeinak lipidoetan oinarritutako lipido-matrize solidoak dira. Matrize hauek lipido nahaste batez (lipido solido eta likido) eta tentsioaktiboak dituen fase urtsu batez osatuta daude. [27]. Azkenik, haien toxikotasun falta, farmakoen dosi handiak eramateko ahalmena eta BBB zeharkatzeko berezko joera azpimarratu behar dira [28].



4.Irudia. Nanomedikuntzan oinarritutako tresnak CNSra bideratzeko terapiak gaixotasun ezberdinen aurka.

Halaber, NPen gainazala estekatzailerik ezberdinekin funtzionalizatu daiteke, BBB eta neuronekin dituzten elkarrekintzak kontrolatzeko eta haien sarrera CNSra errazteko. Horrela, farmakoen bioerabilgarritasuna hobetuko da, bestelako gertaera fisiologikorik aldatu gabe [29]. Estekatzailerik artean, polietilenglikola (PEG) erabilienetako bat da. Dena den, azken urteetan glikoproteina, polisakarido edo peptido berriak agertu dira, farmakoak CNSra bideratzeko helburuarekin. (Informazio gehiago izateko, ikusi NPen gainazalaren eraldaketari buruzko berrikuspen hedatua [30]. Doktorego-tesi honen *Appendix 3*). CPPak edo kitosanoa (*chitosan* edo CS) haien arteko adibideak dira. CS ezaugarri kimiko eta biologiko bereziak dituen polisakaridoa da, besteak beste, biobateragarritasuna, toxikotasun baxua eta biodegradagarritasuna. Horrez gain, farmakoen askapena garunean hobetzen du [31]. CPPei dagokionez, peptido anfiopatiko eta kationiko laburrak dira, gainerako peptido gehienak ez bezala, mintz zelularren bidez azkar internalizatzen direnak. Hauek, NPen gainazalera itsas daitezke, zelula ezberdinen sarrera ahalbidetuz, eta beraz, farmakoen kontzentrazio terapeutikoa eta eraginkortasuna maximizatuz [32].

Orain arte, NLCen matrize lipidikoaren eraketarako erabiltzen ziren lipido gehienak inerteak ziren, gaixotasunak prebenitu edo tratatu barik [33]. Izatez, ikerketa gutxi deskribatu dute lipido funtzionalen erabilera; haien arteko adibide bat, aplikazio dermikoetan erabiltzeko, Ω -9 azido oleikoa da, NLCren matrizea osatzeko [34]. Beste lipido funtzional mota bat PUFAk dira. Lehen adierazi dugun bezala, beste fitokimiko batzuen artean NDak tratatzeko edo eragozteko erabili daitezke. PUFAen artean, Omega-3 (Ω -3) eta Omega-6 (Ω -6) espezie nagusiak dira. Ω -3 PUFak garunaren eta ikusmen sistemaren garapenerako eta funtzionamendurako funtsezko elikagaiak dira. PUFA guztien artean, azido dokohexaenoikoak (*docohexaenoic acid* edo DHA) %90a baino gehiago osatzen du. Bestalde, garunean %10 eta %20ko tartean agertzen da DHA gainontzeko lipidoen artean. Nahiz eta konposatu hauen efektu terapeutikoa lortzeko erabiltzen dituzten mekanismo zehatzak ezezagunak izan, *in vitro* eta *in vivo* egindako ikerketek haien eragina frogatu dute neurobabesean, neuroinflamazioan eta neurotransmisoreen zein geneen adierazpena aldatzen.[38]. Horrez gain, emaitza positiboak izan dituzte memoria hobetzen animalia ereduetan, PD ereduetan, zentzumen-motor probetan, edo amiloide proteinaren metaketa gutxituz *in vitro*, zein *in vivo* [39-41]. Gainera, azken urteetan argitaratutako ikerlan epidemiologikoetan frogatu denez, PUFAen

osagarriek eragin positiboa dute PD edo ADren intzidentzia gutxitzen. Efektu positibo hau saiakuntza klinikoetan baieztatu da DHarentzako eta beste Ω -3rentzako ere bai. Beste sintoma batzuen artean, narriadura kognitiboa txikitu dute, baita gaixotasun hauetan dagoen inflamazio prozesua murriztu ere, adibidez, depresioaren sintomak gutxituz. Laburbilduz, efektu positibo hauek Ω -3aren erabilera lipido funtzional gisa indartzen dute, gaixotasunaren sintoma batzuk moldatuz, tratamendu bakar bezala, baita terapia sinergiko batean adjubante bezala ere [48].

Dena den, komunitate zientifikoak eta industria farmazeutikoak NDentzat tratamendu eraginkor bat lortzeko egindako ahalegin guztiek proba klinikoetan huts egin dute, II. eta III. faseetan, translazio klinikoa lortu gabe [49,50]. Neuroterapeutiko ezberdinen tratamenduaren hutsegitea biomarkatzaile fidagarrien eta animalia gaixotasun eredu faltarengatik da. Hori dela eta, *in vitro* eredu berrien beharra adierazi da, zeinek NDn giza garunaren baldintzak imitatuko dituen farmakoen fidagarritasuna aztertzeko tresna bezala.

In vitro brain-on-chip plataformak sortzeko ereduaren artean, giza zelula pluripotenzialak (*human induced pluripotential cells* edo hIPSCak) nerbio-sistema modelatzeko eta giza garuneko ingurunean lan egiteko gaitasuna daukaten tresna egokia dirudite. Lehen adierazi dugun bezala, NDn tratamenduan arrakasta izateko alderdi garrantzitsuenetariko bat BBB zeharkatzea da. Horregatik, hIPSCtatik BMCEak sortzea funtsezko bihurtu da sendagai berrien eta nanoterapeutikoen toxikotasuna eta garunean zeharreko iragazkortasuna aztertzeko. *In vitro* tresna berri honek animalien erabilera murriztu lezake, gainera, lortutako emaitzen fidagarritasun handituz. Nahiz eta 3. irudian ikusten den bezala mikroglia NVUaren parte ez izan, NVUak kontrolatutako prozesu garrantzitsuetan parte hartzen du, BBB erregulatzen osasun zein gaixotasun garaian. Lehen ikusi dugun bezala, mikroglia neuronekin harremanetan dago eta NDn berezko neuroinflamazioan parte hartzen du. Gainera, mikroglia BBBaren hausturan laguntzen du, zelulen infiltrazio aberrantea ahalbidetuz eta zitokina inflamatorioen, proteinen eta erradikal askeen mailak handituz [55]. Egia esan, mikroglia eta BBBa etengabeko komunikazio biokimikoan daude eta zelula horien alterazioak NDn patofisiologiarekin erlazionatzen dira. BBB-mikroglia elkarrekintza dinamiko hau NDetako

neuroinflamazioan agertzen da, diana terapeutiko berri batean bihurtu daitekeena etorkizunean [56].

Laburtzeko, NDen konplexutasunak estrategia eta molekula ezberdinak konbinatzea eskatzen du, CNSra heltzeko eta NDekin erlazionatutako patologia ezberdinak tratatzeko. Nanomedikuntzak estrategia ezberdinak konbinatzeko aukera ireki du. Izan ere, nanofomulazio baten barnean sendagai ezberdinak konbina daitezke. Gainera, nanopartikulen gainazala alda daiteke garuna hobeto zeharkatzeko. Honek guztiak ikuspegi berri bat ireki dezake NDen tratamendurako.

2. Metodoak

2.1 NLCen ekoizpena

NLCak urtze-emulsifikazio metodoaren bidez prestatu ziren, gure ikerketa taldeak aurretik deskribatutako prozedura erabiliz [31]. Hasteko, lipido solido (Precirol ATO® 5 (Gattefosé, Frantzia) eta likidoen (Mygliol® (Sasol, Alemania GmbH) edo bestelako PUFAen (Medalchemy, Espainia)) nahasteka erabili zen NLCen matrize-lipidikoa prestatzeko. Lipido solidoen eta likidoen ratioa % 0,25tik % 1,25ra aldatu zen (1. Taula). Fase lipidikoa fusio tenperaturaren 5 °C gaineratik (56 °C) urtu zen. Bestalde, fase urtsua Tween 20 (% 3 b/b) eta Poloxamer 188 (% 2 b/b) tentsioaktiboekin berotu zen, tenperatura berean fase lipidikora gehitzeko eta jarraian, nahasketa 60 segunduz emulsifikatu zen 50 W-etara (Bradson® Sonifier 250). Lortutako emulsioa 4 °C-tara biltegitatu zen hurrengo egunera arte, lipidoaren ber-kristalizazioa eta NLCen eraketa bideratzeko. NPen gainazala aldatzeko, NLCen dispersioa CS disoluziora (% 0,5 p/b) tantaka gehitu zen 20 minutuz irabiatuz. Estaldura prozesua eta gero, partikulak zentrifugatu ziren (Amicon, "Ultracel-100k", Millipore, USA). Hiru zentrifugazio egin ziren 2.500 rpm-tara (MIXTASEL, P Selecta, Spain) 10 minutuz, haien artean partikulak MilliQ urarekin garbituz. Azkenik, 42 orduz liofilizatu ziren (LyoBeta 15, Telstar, Espainia). TAT peptidoa NLC gainazalean lotura kobalente baten bidez lotu zen [57]. CS disoluziora (% 0,5 p/b, PBS-an 0.02 M) honakoak tantaka gehitu ziren 2 orduz irabiatuz giro tenperaturan: 250µl EDC (1-ethyl-3-(3-dimethylaminopropyl) carbodiimide hydrochloride) (Millipore Sigma Life Sciences, Germany) (1mg/ml) disoluzioa eta 250µl sulfo NHS (N-Hydroxysulfosuccinimide) (Millipore Sigma Life Sciences, Germany) disoluzioa 0.02 M-eko gantz-fosfatu indargetzailean (*phosphate buffer saline* edo PBS) (1 mg/ml).

CSaren aktibazioa eta gero, TAT peptidoa gehitu zen gainazalera. Horretarako, 250 µl TAT peptidoaren disoluzioa (1 mg/ML, PBS-en, 7.4pH) tantaka gehitu zen aktibatutako CS disoluziora 20 minutuz irabiatuz. Partikulen estaltze prozesuaren ondoren, formulazioa zentrifugatu eta liofilizatu zen lehen azaldu dugun bezala. Amaitzeko, GDNF edo VEGF NTFak (Peprotech, UK) % 0,125 do % 0,15 (p/p) kontzentrazioan kapsulatu ziren formulazio lipidikoaren barnean. Ikerketaren arabera, GFen kontzentrazio ezberdina erabili zen. Modu berean, DiD (1,1'-Diocetadecyl-3,3,3',3'-Tetramethylindodicarbocyanine Perchlorate) (Termofisher Scientific, Espainia) izenekoa trazatzaile fluoreszente bat, % 0,5 (p/p) kontzentrazioan kapsularatu zen formulazio lipidikoaren barnean. Formulazio hauek guztiak aurretik azaldutako protokoloa jarraituz prestatu ziren. Baina, GFa edo trazatzaile fluoreszentea gehituz fase lipidokoarekin emulsifikatu aurretik. Doktorego-tesi honetan erabili diren formulazioa guztiak 1. taulan laburtu dira.

2.2 NLCen karakterizazioa: partikulen tamaina, zeta potentziala, morfologia eta kapsularazte eraginkortasuna.

Partikulen batezbesteko tamaina eta polidispersio indizea (*polydispersity index* edo *PDI*) argi dispersio dinamikoaren (*Dynamic light scattering* edo *DLS*) bidez neurtu ziren eta zeta potentziala Laser Doppler mikroelektroforesiaren bidez (Malvern® Zetasizer Nano ZS, Model Zen 3600; Malvern instruments Ltd, UK). Neurketa bakoitza hirutan burutu zen nanopartikulen liofilizazioaren ostean. Haien morfologia transmisioko mikrokopia elektronikoaren bidez aztertu zen (TEM, Philips EM208S). NLCen kapsularatze eraginkortasuna (*encapsulation efficiency* edo *EE*) zeharka neurtu zen 2.1 atalean azaldutako iragazpen/zentrifugazio prozesuan lortutako gainjalkinaren GF (GDNF edo VEGF) askea neurtuz. ELISA kit baten bidez GF kantitatea kuantifikatu zen eta hurrengo ekuazioaren bidez kalkulatu zen EEa:

1. Taula. Doktorego-tesi honetan erabilitako NLC ezberdinen konposizioa.

IKERLANA	FORMULAZIOA	PRECIROL ATO5 @ % (w/v)	LIPIDO LIKIDOA (%) (w/v)	GAINAZALAREN ALDAKETA	KAPSULARATUTAKO MOLEKULA (%) p/b	ANIMALIA EDO ZELULA EREDUA	
I. Ikerlana	CS-NLC-blank	2,5	Mygliol ®	0,25	CS	-	
	CS-NLC-GDNF	2,5	Mygliol ®	0,25	CS	GDNF (0,15)	
	CS-NLC-TAT-GDNF	2,5	Mygliol ®	0,25	CS and TAT	GDNF (0,15)	
II. Ikerlana	Mygliol-NLC	2,5	Mygliol ®	0,25	-	-	
		2		0,75	-	-	
		1,75		1	-	-	
		1,5		1,25	-	-	
	DHA-NLC	2,5	DHA	0,25	-	-	
		2		0,75	-	-	
		1,75		1	-	-	
		1,5		1,25	-	-	
	DHA-EE-NLC	2,5	DHA-EE	0,25	-	-	
		2		0,75	-	-	
		1,75		1	-	-	
		1,5		1,25	-	-	
	DHA-TG-NLC	2,5	DHA-TG	0,25	-	-	
		2		0,75	-	-	
		1,75		1	-	-	
		1,5		1,25	-	-	
Mygliol-NLC	1,75	Mygliol ®	1	CS and TAT	-	Neurona eta mikroglia zelulen kultiboa	
DHAH-NLC	1,75	DHAH	1	CS and TAT	-		
IV. Ikerlana	CS-NLC-DiD	1,75	DHAH	1	CS	DiD	hIPSCtik BMCEtara desberdintzatutako zelulak
	TAT-CS-NLC-DiD	1,75	DHAH	1	CS and TAT	DiD	
	Mygliol-NLC	1,75	Mygliol ®	1	CS and TAT	-	HMC3 mikroglia zelula lerroa
	DHAH-NLC	1,75	DHAH	1	CS and TAT	-	
	DHAH-NLC- GDNF	1,75	DHAH	1	CS and TAT	GDNF (0,125)	
	DHAH-NLC- VEGF	1,75	DHAH	1	CS and TAT	VEGF (0,125)	

$$EE (\%) = \frac{GF_{\text{aren kantitate teorikoa}} - GF_{\text{askea}}}{GF_{\text{aren kantitate teorikoa}}} \times 100$$

NLCtik DiD trazatzailearen askapen falta beste ikerketa batean frogatu zen [31]. Horregatik, ez da ikerketa honen barnean azaldu.

2.3 Animalia ereduak

2.3.1 MPTP Animalia eredu eta tratamendua

Bederatzi asteko C57BL/6J sagu arrak erabili ziren (Charles River, L'Arbresle, Frantzia) MPTP parkinson eredu sortzeko (I. ikerlana). Animaliak 12 orduko argi-ilun zikloan mantendu ziren, 22 °C-ko tenperaturarekin eta karraskari pentsua zein ura *ad libitum* eman zitzaien. Animaliekin egiten den Esperimentaziorako Etika Batzordeak onartutako protokoloak jarraituz burutu ziren prozedura guztiak (prozedura zenbakia PROEX 343/14). I. Ikerlanean 53 sagu erabili ziren. Horietatik, bost gatz disoluzioaren tratatu ziren kontrol negatibo (*control*) bezala. Beste 48 saguak MPTP toxikoarekin tratatu ziren (30 mg/kg) (Millipore Sigma Life Sciences, Alemania) administrazio intraperitonealarekin (*intraperitoneally edo i.p*) bost egunetan zehar 24 orduko tartearrekin. Lesio protokoloa hasten zen momentu berean, animaliak sei talde (n=6) ezberdinetan banatu ziren 2. Taulan agertzen diren tratamendua jaso zuten bi egunetan behin, 3 astetan zehar. Tratamendua administratzeko sudur-bidea erabili zen. GDNFaren azkeneko dosia 2.5 µg izan zen animalia bakoitzarentzat. Animalien aktibitate lokomotorea ikerketaren astero aztertu zen lau asteetan zehar. Ikerketak amaitu ondoren, saguak sakrifikatu ziren eta garun ehunak batu eta fixatu ziren immunohistokimika bidezko ebaluaziorako.

2. Taula. Talde esperimental ezberdinak *in vivo* saioan, I. ikerlana.

TALDEA	TRATAMENDUA	MPTP (+/-)
<i>Control</i>	Gatz Disoluzioa (NaCl %0,9 p/b)	-
MPTP	Gatz Disoluzioa (NaCl %0,9 p/b)	+
GDNF	2,5 µg GDNF NaCl disoluzioan	+
CS-NLC blank	CS-NLC	+
CS-NLC-GDNF	CS-NLC-GDNF (2,5 µg GDNF)	+
CS-NLC-TAT-GDNF	CS-NLC-TAT-GDNF(2,5 µg GDNF)	+

2.3.2 6-OHDA arratoi lesio protokoloa eta tratamenduak

32 Sprague-Dawley arratoi ar (170-220 g) karioletan launaka ostatu ziren laborategiko baldintza estandarrekin (22 ± 1 °C, % 55 \pm 5 hezetasuna eta 12 orduko argi/ilun zikloarekin) eta karraskari pentsua zein ura *ad libitum* eman zitzaizen (II. Ikerlana). Saio guztiak Euskal Herriko Unibertsitateko Animaliekin egiten den Esperimentaziorako Etika Batzordeak onartutako protokoloak jarraituz burutu ziren (prozedura zenbakia: CEEA, ref: ES48/054000/6069). Esperimentu guztiak Europako Erkidegoko Kontseiluaren Erabakiaren arabera egin ziren, "Helburu Zientifikoetarako animalien babesari buruzko Europako Zuzentaraua" (2010/63/EB) eta laborategiko animalientzako zaintza eta erabilerarako Espainiako Zuzenbidearekin (RD 53/2013) bat etorritz.

6-OHDA animalia eredu lortzeko hurrengo protokoloa erabili zen [30]. 6-OHDA (Termofisher Zientifikoa, Espainia) 30 minutu administratu baino lehenago, arratoiak desipraminarekin tratatu ziren (25 mg/kg) i.p. administrazioaren bidez. Ondoren, isoflurano inhalazioarekin anestesiatu ziren (% 1,5-2) eta Kopf tresna estereotaxiko batean jarri ziren lesioa gauzatzeko [25]. 6-OHDA injekzioa eman baino lau aste lehenago, animaliak lau taldetan banatu ziren, jasoko zuten tratamenduaren arabera (n=8). Tratamenduak egunero administratu ziren kanula baten bidez, urdailean kokatzeko. 6-OHDAko lesioa izan baino lau aste lehenago hasi zen tratamendua. Ondoren, 15 aste gehiago jarraitu zen tratamendua. Gainera, bi astetik behin, entsegu lokomotoriak ezberdinak egiten zitzaizkien, administratutako PUFAen eraginkortasuna egiaztatzeko. Ikerketak amaitu ondoren, arratoiak sakrifikatu ziren eta garun ehunak batu eta fixatu ziren immunohistokimika bidezko ebaluaziorako.

3. Taula. Talde esperimental ezberdinak *in vivo* saioan, II. ikerlana. (CMC: karboximetilzelulosa; DHA: azido dokohexaenoikoa; DHAH-EE: DHAren etil ester egoera).

TALDEA	TRATAMENDUA	6-OHDA
<i>Saline</i>	Gatz disoluzioa (NaCl 0,9% p/b)	+
<i>Vehicle</i>	Urtsu disoluzioa CMC % (p/b) 0,5rekin eta Tween 80 %(p/b) 0,05rekin	+
DHA	DHA <i>vehicle</i> urtsu disoluzioan formulatuta	+
DHAH	DHAH-EE <i>vehicle</i> urtsu disoluzioan formulatuta	+

2.4. Entsegu lokomotoreak PD-ko animalia ereduetan

2.4.1 Rotarod entsegua

Saguen aktibitate lokomotorea *Rotarod* aparatu batean (5A irudia) ebaluatu zen, gero eta azelerazio handiagoarekin. Saguen burua biraketaren norabidearen kontra zegoen zuzenduta, eta, beraz, saguek aurrera egin behar zuten ez erortzeko. Honelako bost proba egin ziren, 30 minutuko tarteekin. Proba animalia erortzen zenean amaitzen zen, edo gehienez 5 minutu igaro ondoren. Animalia eta proba bakoitzeko, *Rotarodean* emandako denbora grabatu egin zen. Hala ere, animalia bakoitzeko bosgarren probaren emaitzak bakarrik erabili ziren konparazio estatistikoak egiteko. Gainerako lau saioak baztertuak izan ziren pre-entrenamendu saioak baitziren, saguak prozedura ezagutzeko. Animalia guztiei aktibitate lokomotorea ebaluatu zitzairen MPTP toxikoaren administrazioaren aurretik eta lesioaren ondoren, astero lau asteetan zehar.

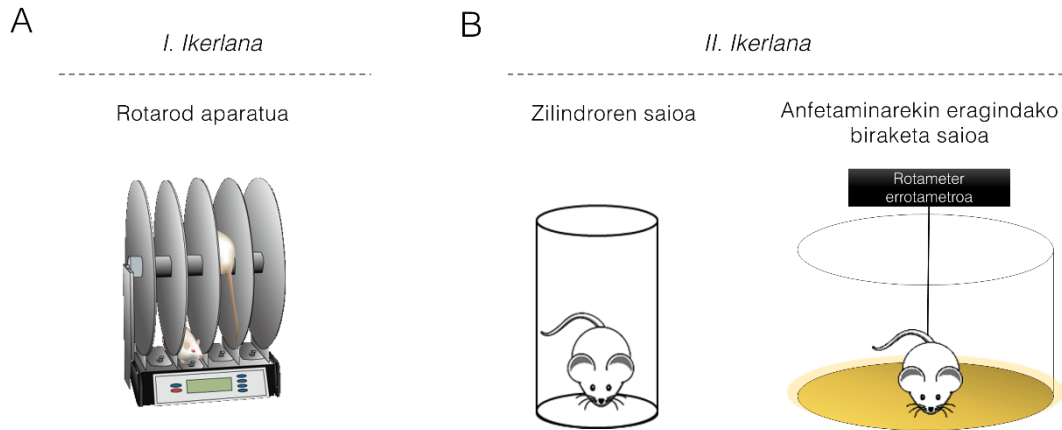
2.4.2 Zilindroren saioa

Entsegu honetan aurreko gorputz adar asimetria ebaluatu zen, bi astetan behin, 15 astetan zehar. Lehen saioa, behin 6-OHDA lesioa (2.3.2 atala) egonkortu 3 aste ondoren egin zen. Arratoiak 20 cm diametroko kristalezko zilindro batean jarri ziren libre esploratzeko (5B irudia). Ispiluak jarri ziren zilindroaren atzean, esplorazio-jarduera 360° -tan ikusteko. Animalia bakoitza bertan mantendu zen, zilindroa hankarekin 20 aldiz ukitu arte. Saioa bideokamerarekin grabatu zen ondoren aztertzeko. Aurreko gorputz-adarrarekin, kontralateralekin, (zauritutako aldea) edo ipsilateralekin (kalterik gabeko aldea) egindako ukituak zenbatu ziren eta datuak ukituen ipsilateralaren portzentaje gisa adierazten dira, hurrengo ekuazioa erabiliz:

$$\% \text{ ipsilateral ukituak} = \frac{\text{ipsilateral ukituak}}{\text{ipsilateral} + \text{kontralateral ukituak}} * 100$$

2.4.3 Anfetaminak eragindako biraketa saioa

6-OHDArekin lesioa egin eta 3 aste ondoren, arratoiei anfetaminak eragindako biraketa entsegua egin zitzairen. Bi astetan behin errepikatu zen proba hau. Horretarako, D-anfetamina (5 mg/kg % 0,9 NaCl-tan; Sigma-Aldrich, Saint Louis, AEB) i.p administratua izan zen eta, 15 minutu igaro ondoren, animalia bakoitza kaiola batean, biraketa ipsilateral osoen kopurua erregistratu zen 90 minutuz errotometro automatiko batekin (Multicounter LE3806, Harvard Apparatus). Emaitzek minutuko biraketa portzentajea adierazten dute.



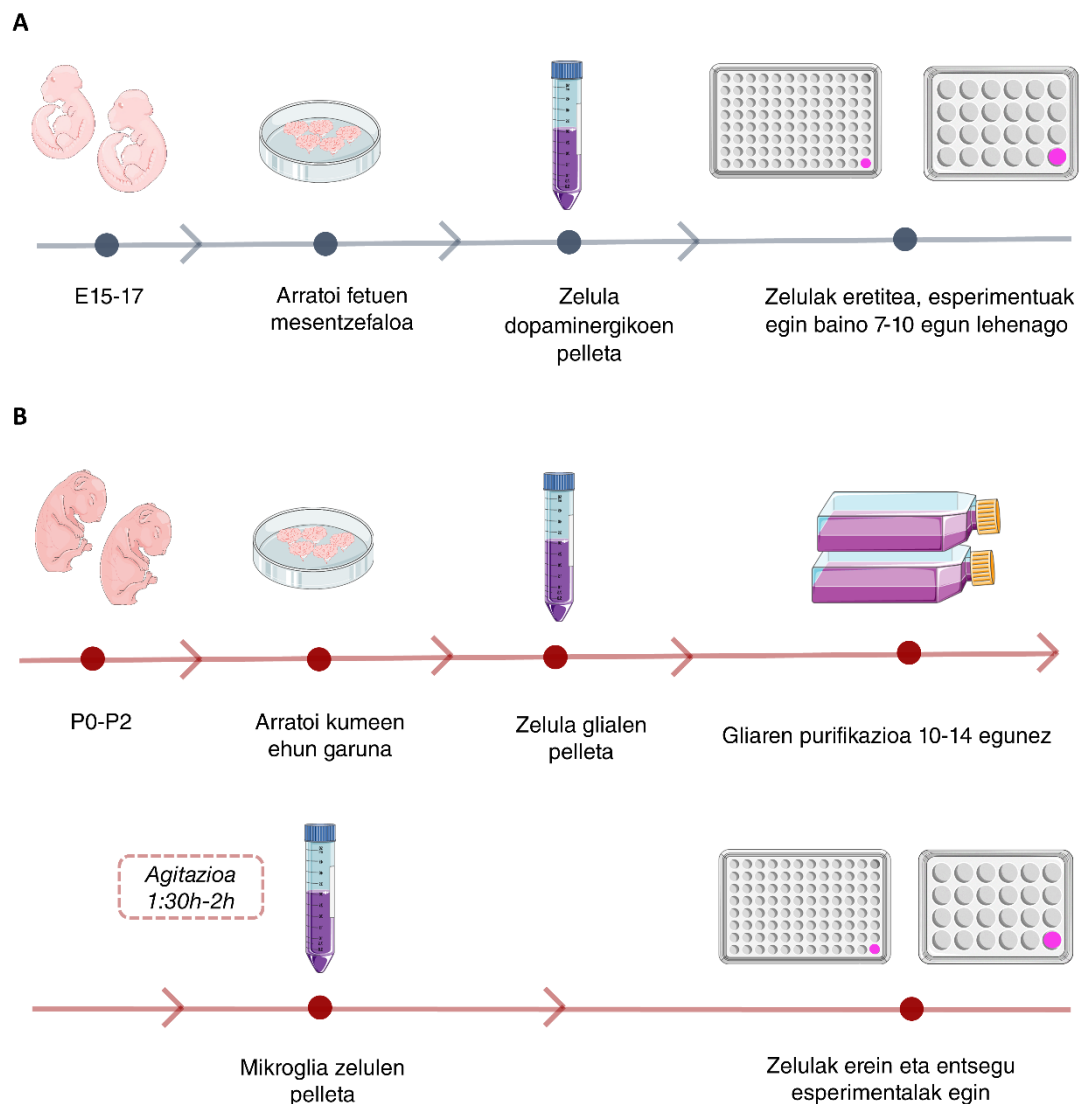
5. Irudia. Doktorego-tesi honetan egindako entsegu lokomotorren irudikapen eskematikoa (A) *Rotaroden* saioa I. Ikerlanean egin zen (B) Zilindroaren saioa eta anfetaminarekin eragindako biraketa saioak II. ikerlanean egin ziren.

2.5 In vitro ereduak eta kultibo zelularrak

2.5.1 Neurona dopaminergiko kultiboa

Neurona dopaminergiko kultiboak Wistar arratoi enbrioietatik (15, 16 edo 17 egunekoak (E15-E17)) prestatu ziren doktorego-tesi honen hirugarren ikerlana egiteko. Animalia-prozedurak Euskal Herriko Unibertsitateko Animaliekin egiten den Esperimentaziorako Etika Batzordeak (UPV/EHU, CEEA, Erref. M20/2017/019) jarraituz egin ziren. Esperimentu guztiak "Helburu Zientifikoetarako Animaliak Babesteko Europako Erkidegoko Zuzentarauari (2010/63/EB) eta laborategiko animaliak zaintzeko eta erabiltzeko Espainiako Zuzenbideari (RD 53/2013) jarraituz egin ziren. Neurona dopaminergiko kultiboak lortzeko, ondorengo protokoloak jarraitu ziren, aldaketa txiki batzuekin [58,59] (6. irudia). Haurdun zeuden arratoiak sakrifikatu ziren eta, baldintza aseptikorik gabe, garun guztia arratoi-enbrioietatik atera zen izotzetan mantenduz Petri plaka batean (10 cm), HBSSan (*Hank's Balanced Salt Division*) (Gibco, Life Technologies, Espainia) odol-hodiak eta meningeak kentzeko. Ondoren, zelula mesentzefalikoaren zati bat aukeratu zen Gaven et al. protokoloa jarraituz [60]. Garuneko interes guneak bildu eta gero, ehuna tripsinarekin (Gibco, Life Technologies, Espainia) inkubatu zen, 15 minutuz, baldintza aseptikoetan. Geroago, DNAsa entzimekin ere inkubatu zen (deoxierribonukleasa I, behi areatik (DNase I) (Millipore Sigma, Alemania) 30 segundoz, eta, horren ostean tripsina inaktibatzen eta ehuna bi aldiz garbitu zen

DMEM disoluzioarekin (*Dulbecco 's Modified Eagle Medium*). Hurrengo urratsean, ehuna mekanikoki txikitu zen, 5 ml eta 2 mL-ko pipeta batetik zenbait aldiz pasatuz. Azkenik, zelula suspentsioa iragazi zen 100 milimetroko Nylon iragazki batekin eta zelula pelleta lortzeko zentrifugatu zen. Zelula pelleta Neurobasal kultibo ingurunean berreseki zen, 0,5 Mm glutaminarekin, % 1 antibiotikoarekin (P/S) eta % 3 B27-rekin (Gibco, Life Technologies, Espainia), eta zelulak saioe funtzionaletarako erein ziren.



6. Irudia. Kultibo primarioen irudikapen eskematikoa. (A) Neurona dopaminergikoen isolamendua eta kultiboa. (B) Zelula mikroglialen isolamendua eta kultiboa.

2.5.1.1 Zelulen bideragarritasun saioa

2.5.1 sekzioan lortutako zelula suspentsioa poli-lisina – 96-putzuko kultibo plakan erein zen 40×10^3 zelula/putzuko dentsitatearekin. Zelula dopaminergikoak 7-10 egunez mantendu ziren esperimentuak egin aurretik eta kultibo-ingurunea 3

egunetik behin aldatu zen, behar izanez gero. Hautatutako denbora puntuan, zelulen kultibo-ingurunea kendu, eta kultibo-ingurune berria gehitu zitzairen nanopartikulen kontzentrazio ezberdinekin: DHAH-NLCak edo Mygliol-NLCak (1. Taula, III. ikerlana) (100, 75, 50, 25, 12,5 eta 5 μ M) 24 orduz edo 48 orduz. Kontzentrazioa (μ M) NLCen formulazioan dagoen DHAH kantitateari dagokio. Mygliol NPak dosifikatzeko, NLCen kopuru berdina erabili zen barne kontrol bezala, DHAH lipido funtzionala edo Mygliol bezalako lipido inerte bat erabiltzearen arteko ezberdintasunak aztertzeko. Gero, bideragarritasuna ebaluatu zen, CCK-8 kitaren protokoloa jarraituz. Baldintza bakoitzerako zelularen bideragarritasun portzentajea kontrol positiboaren arabera adierazten da, non zelulei tratamendurik gehitu ez zitzairen.

2.5.1.2 6-OHDA toxikotasun saioa: neurotoxikotasun eredia in vitro

Esekidura zelularra (2.5.1 atala) 40×10^3 zelula/dentsitatearekin erein zen 96 putzuko kultibo plaketan. Zelula dopaminergikoen kultiboa 7-10 egunetan mantendu zen, kultibo-ingurunea hiru egunetik behin aldatuz. Orduetik aurrera, kultibo-ingurunea kendu zen eta 6 OHDA toxinen kontzentrazio ezberdinak gehitu ziren (500, 100, 50, 25, 10 eta 5 μ M) 24 orduz, neurotoxinaren kontzentrazioa zelulen bideragarritasunarekin erlazionatzeko. Kontrol positibo gisa (C⁺), zelulak soilik kultibo-ingurunearekin erabili ziren eta kontrol negatiboarentzako (C⁻) DMSO (*dimetyl sulfoxide*) %10 portzentajearen gehitu zen. Zelulen bideragarritasuna egiaztatzeko, 6-OHDA neurotoxinarekin 24 orduko inkubazioaren ondoren, kultibo-ingurunea kendu zen eta zelulak %3,77 paraformaldehidoarekin (PFA) (Panreac, Espainia) fixatu ziren 10 minutuz, ondoren, 3 aldiz garbitu ziren PBSrekin. Horren ondoren, DAPI (4',6-diamidino-2-fenilindole) (Termofisher Scientific, Espainia) PBS disoluzioarekin inkubatu ziren 15 minutuz, zelulen bideragarritasuna zehazteko. Datuak C⁺ taldearen portzentajearen arabera adierazten dira, tratamendurik ez zuena.

2.5.1.3 Neurobabes saioa

Lehen bezala, zelulak 40×10^3 dentsitatearekin erein ziren 7-10 egunez inkubatuz. Ondoren, DHAH-NLCekin edo Mygliol NLCekin tratatu ziren, (50, 25 eta 12.5 μ M), 6-OHDA neurotoxina kulturari gehitu aurretik. 24 ordu geroago, kultibo-ingurunea kendu egin zen, eta beste kultibo-ingurune berri bat gehitu zen, honako kontzentrazioarekin: 25 μ M 6-OHDA neurotoxina eta aurretik gehitutako NLCren

kontzentrazio berberekin (50, 25 eta 12,5 μ M). DHAH-NLCak neurotoxinaren aurka neurobabesleak ziren ala ez egiaztatzeko, kultibo-ingurunea 24 ordu beranduago kendu zen eta zelulak fixatu eta DAPIrekin inkubatu ziren, 2.5.1.2 atalean deskribatu den bezala.

2.5.2 Mikrogliaaren kultibo zelularra

Mikroglia kultiboak Wistar arratoi kumeetatik prestatu ziren (P0-P2), doktorego-tesi honen hirugarren ikerketa esperimentalala egiteko. Animalia-prozedurak Euskal Herriko Unibertsitateko Animaliekin egiten den Esperimentaziorako Etika Batzordea (UPV/EHU, CEEA, Erref. M20/2017/035). Esperimentu guztiak "Helburu Zientifikoetarako Animaliak Babesteko Europako Erkidegoko Zuzentarauari (2010/63/EB) eta laborategiko animaliak zaintzeko eta erabiltzeko Espainiako Zuzenbideari (RD 53/2013) jarraituz egin ziren. Chen et al.-en protokoloa jarraitu zen mikroglia zelulen kultiboa lortzeko [6]. Kumeei garuna kendu eta Petri plaka batean (10 cm) izotzarekin mantendu ziren, meningeak eta odol hodiak kentzeko eta garun eremu zehatza hautatzeko. Geroago, garun-kortexa bildu eta tripsinarekin inkubatu zen 37 °C-tara, ehuna DNAsa entzimarekin inkubatu zen 30 segundoz eta, ondoren, tripsina inaktibatu zen ehuna bi aldiz DMEM GluatMAX™ FBS % 10, P/Srekin garbituz. Jarraitzeko, ehuna mekanikoki txikitu zen, 5 ml eta 2 mLko pipeta banatik ehuna zenbait aldiz pasatuz. Lortutako zelula suspentsioa DMEM GlutaMAX™ FBS %15, P/San berreseki zen, eta poli-lisine *flask*-etan inkubatu zen 37° C-tara, % 5 CO₂ atmosferan. Hiru egun pasa ondoren, kultibo-ingurune osoa DMEM GlutaMAX™ FBS %10-rekin aldatu zen, honen ondoren, kultibo-ingurunearen erdia 2-3 egunez behin aldatu zen glia nahaste hau 10-14 egunez mantentzeko. Mikroglia zelulen isolamendua egiteko, *flaskoen* kultibo ingurunea kendu eta DMEM GlutaMAX™ FBS % 15 P/S-rekin ordezkatu zen, isolamendua hasi baino 24 ordu aurretik. Horren ostean, mikroglia *flaskoak* irabiagailu batean jarri ziren 250 rpm-tara 1:30-2 orduz, mikroglia zelulak astroglia geruzatik askatzeko. Geroago, mikroglia zelulak irabiagailutik atera ziren, DMEM FBS % 15-ekin berreseki ziren, eta poli-lisina-96 putzuko kultibo plaketan erein ziren ikasketa desberdinetarako.

2.5.2.1 Zelulen bideragarritasun saioa

Mikroglia zelulen bideragarritasun saioa 2.5.1.1. atalean deskribatutakoaren antzekoa da. Hala ere, kasu honetan, mikroglia zelulak 50 x 10³ zelula/putzu dentsitatean erein ziren. 24 orduz inkubatu ondoren, kultibo-ingurunea kendu eta

Lipido-garraiatzaile nanoegituratu berriak Ω -3 gantz-azido poliinsaturatuetan eta TAT peptidotan oinarritutakoak gaixotasun neurodegeneratiboak tratatzeko

zelulak NLCen kontzentrazio ezberdinekin inkubatu ziren 24 edo 48 orduz. Azkenik, bideragarritasuna ebaluatu zen, CCK-8 kit-aren protokoloa jarraituz.

2.5.2.2 Zitokina pro-inflamatorioen askapenaren kuantifikazioa: TNF- α , IL-1 β eta IL-6

DHAH-NLCen antiinflamazio efektua LPSaren aurka mikroglia kultibo zelularretan aztertu zen. Saioa egiteko, zelulak 24 orduz DHAH-NLCen eta Mygliol-NLCen kontzentrazio desberdinekin (50 μ M, 25 μ M eta 12,5 μ M) tratatu ziren. Ondoren, beste 24 orduz LPSarekin (50ng/ml) eta nanopartikulen kontzentrazio ezberdinekin inkubatu ziren. 24 ordu pasa ondoren, putzuen gainjalkina hartu zen, TNF- α , IL-1 β eta IL-6-aren mailak ELISA saioarekin kuantifikatzeko (Peprotech (UK)). Askatutako zitokina kopuru osoa CCK-8 saioarekin neurtutako bideragarritasun zelularren arabera normalizatu zen.

2.5.3 BMCEen desberdintzapen protokoloa: BBB eredia

Doktoretza tesi honen 4. Ikerlanean hIPSCa BMCEtara desberdintzatu ziren BBB giza eredu bat sortzeko. Horretarako, hIPSCak Matrigel (Corning®, AEB) estaldura zuten sei putzuko kultibo plaketan kultibatu ziren mTeSR™1 (STEMCELL Technologies, Frantzia) kultibo-ingurunearekin. Doktorego-tesi honetan, BBB eredia lortzeko, Neal et al.-ek garatutako protokoloa erabili zen, baina aldaketa txikiekin [62]. Desberdintzapen prozesua hasi aurretik (D-1), zelulei kultibo-ingurunea kendu zitzaien eta DPBSarekin (*Dulbecco's Phosphate-Buffered Saline* edo DPBS) garbitu ziren. Ondoren, TrypLE (Gibco, Life Technologies, Suedia) disoluzioaren 500 μ l-rekin inkubatu ziren 5 minutuz. Jarraian, ingurunea 1:5 diluitu zen mTeSR kultibo ingurunearekin eta zelulak 3 minutuz zentrifugatu ziren 200 rcf-tara, mTeSRan berreskitzeko ROCK inhibitzailearekin (Y-27632 dihidrokloridoa) (Bio-Techne, AEB). hIPSCak 16 K/cm²-ko dentsitatearekin erein ziren matrigel estaldura zuten sei putzuko kultibo plaketan. 24 ordu geroago, mTeSR kultibo ingurunea kendu eta E6 (*Essential 6™ medium*) (Gibco, Life Technologies, Suedia) kultibo-ingurunearekin ordezkatu zen; lau egunetan zehar egunero aldatuz (D0-D3). Ondoren, kultibo-ingurunea hESFMra (giza endotelial seruma librea) (Gibco, Life Technologies, Suedia) aldatu zen: honako gehigarriekin: B27 1X, FGF (fibroblast hazkuntza faktorea) (Bio-Techne, AEB) 20ng/ml eta RA (All-trans retinoic azidoa) (Millipore Sigma Life Science, Alemania) 10 μ M. Ingurune honetan zelulak bi egun gehiagoz mantendu ziren, kultibo-ingurunea aldatu gabe. Denbora horren ostean,

ingurunea kendu, zelulak garbitu eta TrypLEekin 20-30 minutuz inkubatu ziren zelula suspentsio bat eratu zen arte. Zelulak zentrifugazio prozedura jarraituz jaso ziren eta subkultibatzeko. 3.3×10^3 zelula/putzu dentsitatearekin erein ziren Transwell plaketan, zeinak 400 $\mu\text{g}/\text{mL}$ IV. motako kolageno eta 100 $\mu\text{g}/\text{mL}$ fibronektina (Millipore Sigma Life Sciences, Alemania) estaldura zuten, eta hESFM kultibo-ingurunearekin. 24 ordu ondoren, TEER (*transendothelial electrical resistance*) neurtu zen STX2 chopstick elektrodoak eta EVOM2 voltmetro bat (World Precision Instruments) erabiliz. Prozedura hau ere errepikatu egin zen 48 ordu pasa eta gero. Zelulak edozein entsegu funtzionalerako erabili aurretik, kultibo-ingurunea hESFM ingurunera aldatu zen, zeinak B27 zuen baina bFGF edo RA gehitu gabe. Iragazkortasun saiorako, zelulei bFGF eta RA 24 ordu lehenago kendu zitzairen.

2.5.3.1 NLCen iragazkortasuna hPSCtik desberdintzatutako BMCEtan

NLCen garraioa BBB *in vitro* eremuan zehar kuantitatiboki aztertu zen fluoreszentsia neurketaren bidez (*Plate Reader Infinite M1000*, Tecan, Suitza) eta kualitatiboki laser-ekorketa bidezko mikroskopiaren bidez (LSM 710), zeinarentzat DiDarekin (TSM = 644 nm, FLS = 685 nm) markatutako NLCak erabili ziren BMECtan zehar garraioa ebaluatzeko. Zelulak Transwell™ plaketan 48 orduz inkubatu ondoren, 2.5.3 atalean azaldu den bezala, 3000 $\Omega \times \text{cm}^2$ -tik gorako TEER balioa izan zuten BMCEak aukeratu ziren iragazkortasun saioak egiteko. Esperimentuak 37 °C-tara egin ziren, eta 100 mg/ml NLCko (CS-NLC-DiD edo TAT-CSNLC-DiD, 1. Taula) kontzentrazioa gehitu zen B27dun hESFM ingurunera. Denbora une desberdinetan (0 min, 30 min, 1 ordu, 1 ordu 30 min eta 2 ordu), 50 μL -ko laginak bildu ziren ganbera basolateraletik, eta 50 μL ingurune berri gehitu ziren ganbera berean. NLCen kontzentrazioa fluoreszentsia neurketen bidez aztertu zen (*Plate Reader Infinite M1000*, Tecan, Suitza). Seinale fluoreszentea kalibraketa-zuzenarekin (125-0 – $\mu\text{g}/\text{ml}$ serieko diluzioetan) erlazionatua baitzegoen. Iragazkortasun esperimentuen ondoren, zelulak PFArekin fixatu ziren, ondorengo entseguetarako.

2.5.4 HMC3 mikrogliaren kultibo zelularra

2.5.4.1 HMC3ren bideragarritasun saioa

HMC3 zelulak %10 FBS zuen DMEM/F12 kultibo ingurunean (Gibco, Life Technologies (Suedia) mantendu ziren baldintza estandarizatuetan (% 95 hezetasun erlatiboa, %5 CO_2 , 37°C). NLCen dosi ez toxiko eta efektiboena ebaluatzeko,

alarBlue™ saioa gauzatu zen. Zelulak 10 K/cm²-ko dentsitatean kultibatu ziren 24 orduz. Hurrengo egunean, lau formulazio desberdinetako NLCak (DHAH-NLC, Mygliol-NLC, DHAH-NL-GDNF eta DHAH-NLC VEGF, 1. Taula) zeluletara gehitu ziren, 24 eta 48 orduz inkubatu. Gero, bideragarritasuna egiaztatu zen alarBlue™ kit-a erabiliz, fabrikatzailearen protokoloa jarraituz. Baldintza bakoitzaren bideragarritasun zelularra, kontrol negatiboaren (C⁻) portzentajearen arabera adierazten da, C⁻ %100 izanez. Kontrol positiboarentzako (C⁺) zelulak DMSO %10-rekin tratatu ziren 24 orduz.

2.5.4.2 HMC3 aktibaketa LPSarekin

Zelulak 10 K/cm² edo 15 K/cm²-n dentsitatean erein ziren ondoren zelula horiekin egingo zen saioaren arabera, Multiplex saioa, zitokina-maila egiaztatzeko edo RT-qPCR, neuroinflamazio prozesuaren geneak zehazteko, hurrenez hurren. Bi baldintza ezberdin probatu ziren entsegu honetan. Lehenengoan (A baldintza) zelulak NPekin inkubatu genituen (1. Taula) 24 orduz. NLCen kontzentrazioak aurretik egindako alarBlue™ saioan lortutako emaitzen arabera aukeratu ziren; 25 μ M lipido funtzionalerako (DHAH) eta 25 ng/ml GFrako (VEGF eta GDNF) (Mygliol-NLCentzako NLCen dosi berdina erabili zen, barne kontrola bezala). Baldintza honetan, kontrol positiboa (Control⁺) (LPS 100 ng/ml 24 orduz) eta kontrol negatiboa (Control⁻) (zelulak soilik kultibo ingurunearekin) jarri ziren. Bigarren baldintzan (B baldintzan), zelulak NLCen lau formulazio ezberdinekin (1. Taula) tratatu ziren 24 orduz. Denbora horren ondoren, LPS (100 ng/ml) eta NP ezberdinekin 24 ordu gehiagoz inkubatu ziren. Control-arentzako ingurunea egunero aldatu zen. 24 ordu pasa ondoren, zelulen gainjalkina Multiplex saiorako bildu zen (2.8 atala), edo zelulak lisatu ziren RNAREN estrakziorako (2.7 atala).

2.6 Immunohistokimika eta immunofluoresentzia teknikak

2.6.1 Immunohistokimika

2.6.1.1 Peroxidasa teknika

Lehen azaldu dugun bezala, animalien lokomotzio saioak amaitu ondoren, (I. eta II. ikerlanak) sakrifikatu egin ziren. Bi ikerketa ezberdin horietan immunohistokimika proba ezberdinak egin ziren. Tirosina hidroxilasa (TH) immunohistokimika saioa bi ikerlanetan egin zen. Bestalde, eritroide 2 nukleoaren faktorearen (Nrf2) immunohistokimika bigarren ikerlanetan bakarrik egin zen, PUFAen tratamendua jaso zuten animalietan bakarrik. Kasu bietan antzeko protokoloa jarraitu zen. Izan ere,

sakrifikatuak izan ondoren, burmuineko ehuna, zehazki, estriatua (ST) eta substantzia nigra (SN) aukeratu ziren TH eta Nrf2 immunohistokimikak egiteko. Garuneko ehun xaflak indargetzaile ezberdinekin garbitu ziren. Ondoren, peroxidasa endogenoak blokeatu ziren 15-30 minutuz. Garbitu ondoren, ehun xaflak blokeatu eta iragazkortu ziren ordu batez. Jarraian, antigorputz primarioekin inkubatu izan ziren, TH edo Nrf2-ren aurkako antigorputzekin, etengabeko irabiaketarekin, 4°C-tara. Hurrengo egunean antigorputz sekundarioarekin inkubatu ziren. Amaitzeko, ABC kit-arekin (Palex, Espainia) inkubatu ziren eta DAB kromogenoarekin ere bistaratzeko. Azkenik, garun xaflak muntatu, deshidratatu eta DPXarekin (BDH Gum, UK) fixatu ziren. Teknika honetan erabili ziren erreaktiboak eta prozedurak 4. taulan laburbildu dira eskematikoki.

2.6.1.2 Immunofluoreszentzia teknika

Iba1 eta GFAP mikroglia eta astrogliaren markatzaileak aztertzeko, aurretik azaldutako protokolo eta teknikaren desberdina den prozedura bat erabili zen. ST eta SNren garun xaflak garbitu ondoren, antigorputz primarioekin inkubatu ziren 4°C-tara gau osoan zehar. Hurrengo egunean, garun xaflak antigorputz sekundarioekin inkubatu ziren 2 orduz. Gero, xaflak garbitu eta DAPIrekin inkubatu ziren nukleoa tindatzeko; amaitzeko muntatzeko ingurunearekin muntatu ziren. (DAPIren tindaketa egin ezean, erabiltzen zen muntatzeko inguruneak DAPI zeukan barneratua). 4. taulan indargetzaile, antigorputzak eta prozedurak laburtu dira.

2.6.2 Immunofluoreszentzia teknika zeluletan

BMCen kasuan, ZO-1ren (*zonula occludens-1*) tindaketa egin zen, gure BBB ereduaren fidagarritasuna egiaztatzeko ZO-1aren presentziarekin. Immunofluoreszentzia (IF) Transwell plakan bertan egin zen. Zelulak fixatu eta garbitu ondoren, blokeatu ziren, % 10 ahuntz serumarekin eta % 0,1 Triton X-100aren (Millipore Sigma Life Science, Alemania) disoluzioarekin DPBSn. Hiru alditan garbitu ondoren, zelulak ZO-1ren kontrako antigorputzarekin inkubatu ziren (1:100) ahuntz serumarekin (% 1) eta Triton X-100 (% 0,01) DPBS-ko disoluzioan, 4°C-tara. Hurrengo egunean, zelulak antigorputz sekundarioarekin inkubatu ziren, antisagu IgG1 (γ 1), CF[™] 488A antigorputza (Millipore Sigma Life Science, Alemania) ahuntz-serumarekin (% 1) eta Triton X-100 (% 0,01) disoluzioarekin DPBSn. Hiru aldiz garbitu ondoren, zelulak fixatu eta DAPIrekin inkubatu ziren. Azkenik, Transwell plakak moztu eta ProlongGlass Antifade (Invitrogen[™], Termofisher Scientific, Suedia) ingurunearekin muntatu ziren.

4. Taula. Immunhistokimika saioen eta erabilitako teknika ezberdinen laburpena (I. Ikerlana eta II. Ikerlana. PB: fosfato indargetzailea BSA: behi serum albumina, TH: tirosina hidroxilasa, ON: gau osoa KPBS: potasio fosfato tanpoia NGS: ahuntz normal serum; KPBST: potasio fosfato tanpoia %1 Triton-Xr-ekin; Nrf2: eritroide 2 nukleoaren faktorearen; Iba-1: kaltzio lotzailea molekula egokitzaila ionizatzailea edo *ionizing calcium-binding adaptor molecule 1*; GFAP: glial fibrilar proteina azidoa edo *glial fibrillary acidic protein*; DAPI: *4',6-diamidino-2-phenylindole*.

Peroxidasa teknika					
		<i>Peroxidoak blokeatu</i>	<i>Blokeatu eta iragazkortu</i>	<i>Antigorputz primarioa</i>	<i>Antigorputz sekundarioa</i>
I.	<i>Ikerlana</i>	% 1 H ₂ O ₂ (b/b) eta % 1 (b/b) etanol Panreac (Espainia) PBen, 15 min, RT.	% 2 (p/b) BSA (Millipore Sigma Life Sciences, Alemania), % 0,5 (b/b) Triton-X (Millipore Sigma Life Sciences, Alemania) PB disoluzioan.	untzi poliklonala anti-TH (1:2000) (Millipore Sigma Life Sciences, Alemania) BSA % 0,1 (p/b), Triton-X %0,5 (b/b), ON, 4°C.	Antigorputz sekundarioa biotilinatua (1:250) (Palex, Espainia), PBen, 1 h, RT.
II.	<i>Ikerlana</i>	%1 H ₂ O ₂ (b/b) eta % 10 (b/b) metanol (Panreac, Espainia) KPBSen, 30 min, RT.	%5 (b/b) NGS (Palex, Espainia) eta % 1 (b/b)Triton X-100 (Millipore Sigma Life Sciences, Alemania) KPBSen, 1h, RT	untzi poliklonaal anti-TH (1:1000) (Millipore Sigma Life Sciences, Alemania) or untzi poliklonala anti-Nrf2 (Abcam, UK) (1:400) in in % 5 NGS (b/b) KPBSTen, RT, ON, 4°C	Ahuntz antigorputz sekundarioa biotilinatua anti-untzi IgG (1:200), % 2,5 NGS (b/b) KPBSTen, 2 h, RT.
Immunofluorestzia teknika					
		<i>Blokeatu eta iragazkortu</i>	<i>Antigorputza primarioa</i>	<i>Antigorputza sekundarioa</i>	DAPIren inkubazioa
I.	<i>Ikerlana</i>	% 2 (p/b) BSA disoluzioa eta % 0,5 (p/b) Triton-Xrekin PBen, 1 h, RT.	untzi poliklonala anti- Iba-1 (1:1000, Wako) BSA % 0,1 (p/b), Triton-X %0,5 (b/b), PBen, ON, 4°C.	anti-untzia Alexa Fluor IgG 488 (1:1000) (Termofisher Scientific, Espainia) % 0,1 (p/b) BSArekin eta %0,1 Triton-Xrekin (b/b) PBen, 2 h RT.	Xaflak Vectashiel® DAPIrekin montatu ziren (Vector Laboratories, Espainia)
II.	<i>Ikerlana</i>	% 2 (p/b) BSA disoluzioa eta % 0,5 (p/b) Triton-Xrekin PBen, 1 h, RT.	untzi poliklonala anti- Iba-1 (1:1000) (Synaptic Systems, Alemania) edo sagu anti GFAP (1:400) (Termofisher Scientific, Espainia) BSA % 0,1 (p/b), Triton-X % 0,5 (b/b), PBen, ON, 4°C.	anti-untzia Alexa Fluor IgG 488 (1:1000); anti-sagurra Alexa Fluor IgG 488 (1:1000) (Termofisher Scientific, Espainia) %0.1 (p/b) BSArekin eta % 0.1 Triton-Xrekin (b/b) PBen, 2 h RT.	DAPI (1:10.000) (Termofisher Scientific, Espainia) eta FluoroMount™ ingurunearekin montatu (Millipore Sigma Life Sciences, Alemania)

2.7 RTqPCR

HMC3 mikrogliia zeluletatik, RNA guztiaren isolamendu eta purifikazioa (2.5.4.2 atala) *High RNA pure* isolamendu kita (Roche, Suitza) erabiliz egin zen, fabrikatzailearen azalpenak jarraituz. Ondoren, RNAREN kantitatea eta kalitatea NanoDrop™ 1000 espektrofotometroarekin (Thermo Scientific) ebaluatu zuen. TaqMan Master Mix, TaqMan entseguarekin batera (Thermo Scientific, Suedia) erabili zen genak amplifikatzeko. Ondoren, QuantStudio Flex 5 Flex Real-Time PCR tresna erabili zen gene errelebanteen kopurua neurtzeko. 96 putzuko plakak erabili ziren eta lagin bakoitza bikoiztuta jarri zen RTqPCR saioa egiteko. Geneen adierazpen erlatiboa delta Ct metodoa erabiliz kalkulatu zen, erreferentziazko gene bezala glizeraldehido 3-fosfato dehidrogenasa (GAPDH) erabiliz.

2.8 Multiplex saioa

Zitokina maila zelulen gainjalkinetan neurtzeko (2.5.4.2 atala) U-Plex MSD puntu-nitzeko elektrokimiluminiszentzia plataforma (MesoScale Diagnostics, Rockville USA) erabili zen. MSD saioa fabrikatzaileen azalpenen arabera egin zen. MSD saioa laborategi bakar batean SciLifeLabeko laborategian (Stockholm, Suedia) eta teknikari bakar batekin egin zen.

2.9 Analisi estatistikoa eta irudiak

Datu esperimentalak GraphPad Prism (6.01, *GraphPad Software, Inc.*) programa informatikoa erabiliz aztertu ziren. $P < 0.05$ zeuden balioak estatistikoki esanguratsu bezala onartu ziren. Grafiko guztiak egiteko GraphPad Prism erabili ziren (6, 01, GraphPad Software, Inc.) Irudi guztiak Servier Medical Artetik hartutako ereduak erabiliz sortu ziren (*Creative Commons Attribution 3.0 Unported License* <https://smartart.servier.com>).

3. Hipotesi eta helburuak

Gaixotasun neurodegeneratiboak egoera neurologiko konplexuak dira. Bizitxaropenak gora egiten duen heinean, haien prebalentziak ere gora egin du, eta gaur egun ez dute tratamendu efektiborik gaixotasunaren progresioa moteltzeko. Terapia eraginkor bat lortzeko, ikerketak gaixotasunaren eraldaketa estrategietan zentratu dira, batez ere. Beste batzuen artean, GFak aukera terapeutiko posible gisa agertu dira, zelulen desberdintzapena areagotzen baitute, baita neurogenesia eta axoietan hazkundera sustatu ere. Hala ere, gero eta ebidentzia handiagoek adierazten dute NDen patogenesisia ez dagoela neurona-konpartimentura mugatuta, baizik eta gliarekin oso erlazionatuta dagoela. Egia esan, mikroglia jokalaria giltzarri bat da NDeko neuroinflamazioan eta haren modulazioa tresna baliagarri bat izan daiteke NDen tratamendurako. Horregatik, azken urteotan, PUFak bezalako molekula mota batzuk NDen estres oxidatiboa eta neuroinflamazioa moldatzeko egokiak direla dirudi.

GFen kasuan, NDen aurka tratamendu eraginkor bat lortzeko arazorik handiena BBBa zeharkatzea da. Hori gainditzeko ahaleginean, estrategia ezberdinak garatu dira azken urteotan. Aztertutako estrategien artean, nanoteknologian oinarritutako DDSak erabiltzea da garrantzitsuenetarikoa, CNSren gaixotasunak kontrolatu eta tratatzeko. Horien artean, NLCak lipidoetan oinarritutako matrizeak dira, lipido solido eta likidoen nahasketa eta tentsioaktiboak dituen fase urtsu batekin nahastu ondoren sortzen direnak. Nanopartikula lipidiko hauek lipido inerteekin garatzen dira, gaixotasunaren tratamenduan edo prebentzioan inolako efekturik izan gabe. Hala ere, azken urteotan, lipido funtzional ezberdinak txertatu dira NLCen matriz lipidikoa sortzeko; beraz, nanopartikulak berak ondorio onuragarriak izan ditzake. Gainera, NLCen gainazala peptido eta polisakarido ezberdinekin aldatu daiteke garunera bideratzeko, BBBa zeharkatuz. Horren ondorioz, garunean molekula terapeutikoen kontzentrazioa handituko da, NDak tratatzeko gaitasuna indartuz.

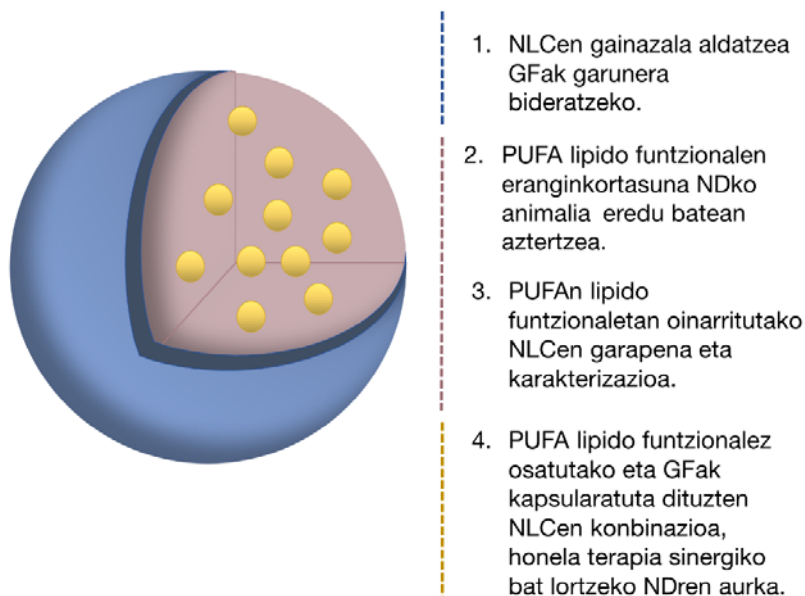
Aurreko guztia kontuan hartuta, doktorego-tesi honen helburu nagusia lipido funtzionalez osaturiko NLCen garapena izango da, bere gainazala osagai ezberdinekin eraldatuz. Garatutako formulazioak CNSrekin lotutako gaixotasunak tratatzera bideratuko dira. Beraz, tesi honen helburu zehatzak honakoak dira:

1. CS-TAT estaldura duten NLC partikulak garatu, karakterizatu eta *in vivo* aztertzea. NLC hauek animalia eredu bati sudur-bidetik eman ondoren garunera bideratzeko eta GDNFaren efektu terapeutikoa handitzeko ahalmena ezagutzeko. [63]. (I. Ikerlana, doktorego- tesi honen *Appendix 4*-an ikus daiteke)

2. DHA eta DHAH lipido funtzionalek Parkinson gaixotasunaren 6-OHDA arratoi ereduari dituzten eraginak aztertzea, hain zuzen, sistema dopaminergikoan, neuroinflamazioan eta estres oxidatiboan duten eragina ikertuz [40]. (II. Ikerlana, doktorego-tesi honen *Appendix 5*-an ikus daiteke)

3. DHAH lipido funtzionalez osatutako NLCen garapena eta karakterizazioa, haien gaitasun neurobabesle eta antiinflamatorioak mantenduz neurona eta mikroglia kultibo zelularretan [64]. (III. Ikerlana, doktorego-tesi honen *Appendix 6*-an ikus daiteke)

4. DHAH lipido funtzionalez osatutako eta GDNF edo VEGF kapsularatua duten NLCen garapena eta karakterizazioa, NDren aurkako tratamendu sinergiko bat lortzeko. Formulazioa berri hau *in vitro* giza ereduari aztertuko da, non gizakiaren baldintzak imitatuko diren, animalia ereduari alternatiba gisa. (IV. Ikerlana, doktorego-tesi honen *Appendix 7*-an ikus daiteke)



7. Irudia. Doktorego-tesi honen helburuen irudikapen eskematikoa. (NLC: garratzaile lipiko nanoegituratuak; GF: hazkuntza faktoreak; PUFA: gantz azido poliinsaturatuak; ND: gaixotasun neurodegeneratiboak).

4. Emaitzak eta eztabaida

Lehen aipatu dugun bezala, parkinson gaixotasuna bigarren ND arruntena da. Egoera neurodegeneratibo konplexua da non dardara, bradizinesia, zurruntasuna eta ezegonkortasun posturala ezaugarri nagusiak diren. Komunitate zientifikoak azken urteotan egindako ahalegin guztien arren, orain arte ez dago tratamendurik gaixotasunaren progresioa moteltzeko [64,65]. NTF terapiak, GDNFa zehazki, PDren neurodegenerazioa moteltzeko gaitasuna du. Nahiz eta azken proba klinikoetan izan dituen ondorioei buruzko eztabaida egon, GDNFak PDrentzako NTF terapia onena izaten jarraitzen du [66,67]. GDNFaren traslazio kliniko arrakastatsua lortzeko garraio eta administrazioa bide eraginkorrak lortu behar dira. Alderdi honi dagokionez, gure ikerketa taldean burututako aurreko ikerketetan, GDNFa kapsularatua zuten mikropartikula polimerikoak eta nanosferak garatu genituen. Animalia ereduetan administratu ondoren, aktibitate lokomotorea hobetu zutelarik [68,69]. Hala ere, erabilitako administrazio-bide inbaditzaileak, administrazio intraestriatalak, partikula hauen aplikazio klinikoa mugatzen du. Beraz, administrazio bide alternatiboen bidez administratu daitezkeen nano-garraiatzaileen garapena beharrezkoa da.

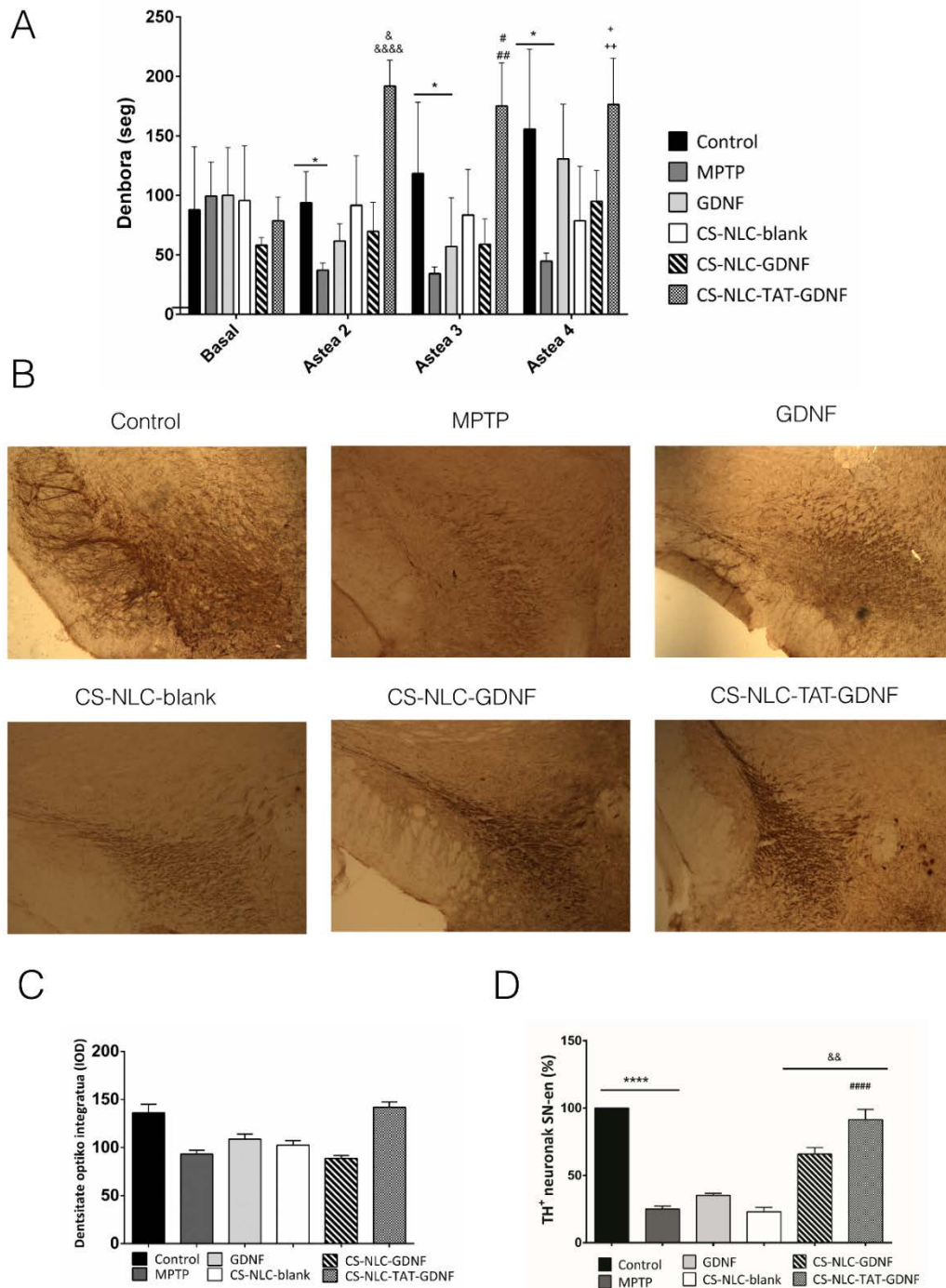
Doktorego-tesi honen lehen ikerlanean, CS eta TATekin eraldatutako garraiatzaile funtzional bat garatu genuen. Zeina saguei sudur bidetik eman ondoren GDNF molekula terapeutikoa garunera arrakastaz bideratzeko gai izan zen. Sudurreko administrazioaren bidez molekula terapeutikoak garunera bideratzea lor daiteke, teknika inbaditzaileak erabili gabe. Helburu hori lortzeko, NPen gainazalean aldaketak egin daitezke. Gure ikerketa taldeak egindako ikerketa baten arabera, gainazala CSrekin eraldatu zuten NLCak GDNFa garunera bideratzeko eta lesionatutako arratoien sintomatologia motorea hobetzeko gai izan ziren [25]. Ikerlan honetan, CSrekin ez ezik, garunera hobeto heltzeko, TATrekin ere eraldatu genuen NPen gainazala, GDNFaren kontzentrazioa handitzeko garunean. Izan ere, TAT peptidoa jadanik erabilia izan da sudurreko administrazioaren bidez molekula terapeutikoak garunera bideratzeko [70,71] eta doktorego-tesi honetan lortutako emaitzek datu horiek baieztatzen dituzte.

CS eta TAT peptidoarekin eraldatutako GDNF dun NLCen formulazioak (CS-NLC-TAT-GDNF), zeta potentzial balio positiboak (+21,9, +1,8 mV) zituzten, TAT eta CS gainazalean itsasteko prozesua arrakastaz burutu zela agerian utziz. CS-NLC-GDNF

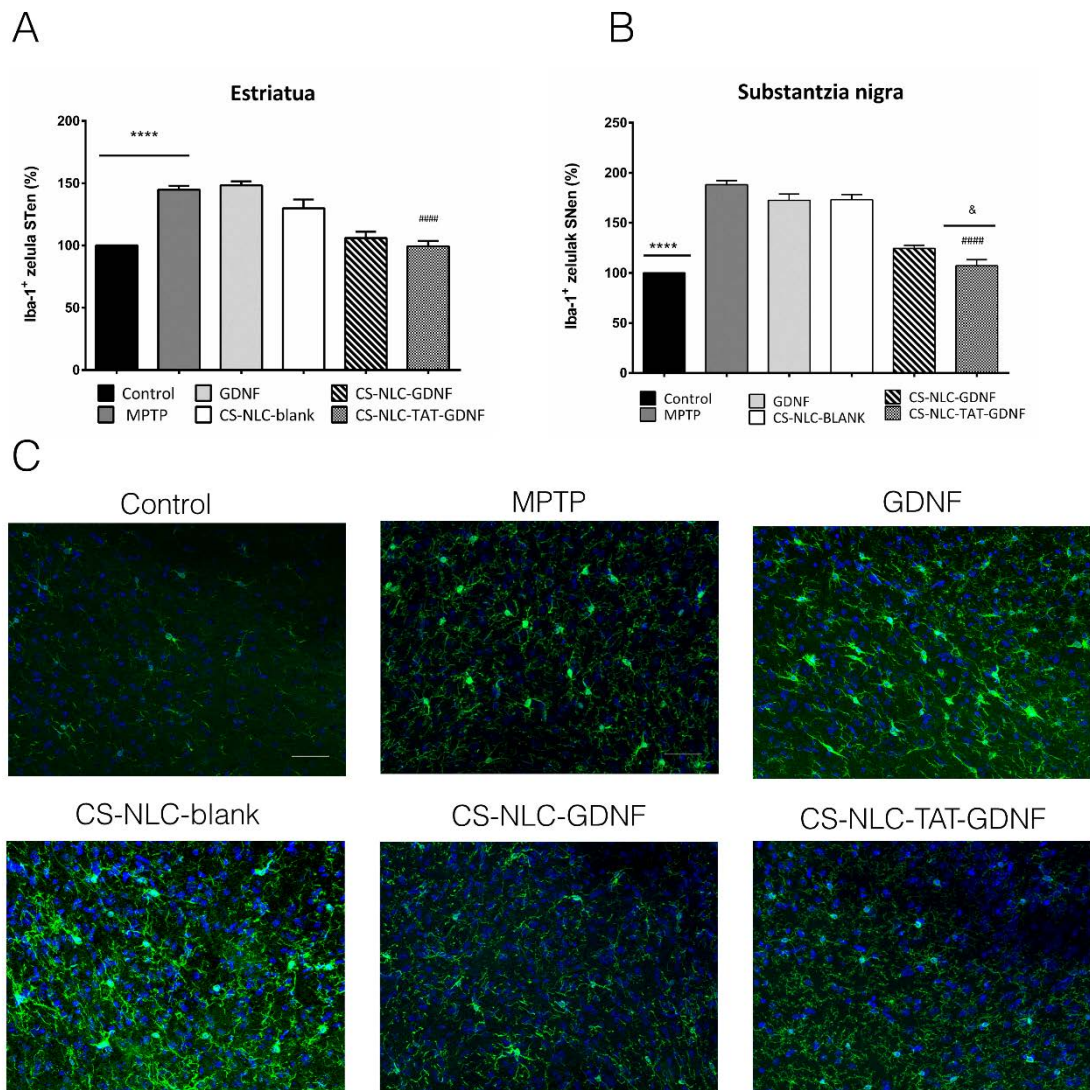
eta CS-NLC-TAT-GDNFen kapsularatze eraginkortasuna (EE) altua izan zen, %87 gutxi gora behera bi formulazioentzako. Gainera, partikulen tamainak ($205,9 \pm 6,3$ nm) (PDI $0,275 \pm 0,02$) sudurreko administrazioarentzako egokiak ziren [31]. MPTP animalia-ereduan CS-TAT-NLC-GDNF nanoformulazioaren administrazioak aktibitate lokomotorea berrezarri zuen, ikerketaren hasieratik amaieraino emaitzarik onenak aurkeztu zituelarik (8.irudia A) ($191,8 \pm 21,9$; * $p < 0,05$ eta $176,4 \pm 38,8$; * $p < 0,05$, hurrenez hurren). Ondorio onuragarri hau ebaluazio immunohistokimikoarekin berretsi zen. 8B-D irudian ikusten den bezala, CS-NLC-TAT-GDNFen administrazioak TH zuntz positiboan mailak handituz STean. Efektu hau CS-NLC-GDNF taldean hein txikiagoan ere ikusi zen, NLCak garunera bideratzeko eta bertan GDNFaren kontzentrazio terapeutikoa handitzeko TAT peptidoaren eraginkortasuna agerian utziz.

Gainera, duela gutxi GDNFak gaixotasun neurodegeneratiboetan agertzen den mikroglia aktibazioa modulatu duen efektu terapeutikoa behatu da [72-74]. Lehen azaldu dugun bezala, mikroglia faktore giltzarri bat da NDe tan gertatzen den neuroinflamazioan, eta bere modulazioa onuragarria izan daiteke NDe tan tratamenduan. Azken urteotan, GDNFak molekula proinflamatorio eta neurotoxikoen askapena murrizten dituela frogatu da mikroglia zelularretan eta animalia eredu ezberdinetan [72-74]. Ikerlan honetan, GDNFaren administrazioak, neuronetan eragin babeslea izateaz gain, mikroglia aktibazioa modulatu ere efektu terapeutikoa izan dezakeela ondorioztatzen da. Izan ere, CS-NLC-TAT-GDNF nanoformulazioaren administrazioak mikroglia aktibazioa murriztu zuen, Iba-1⁺ zelulen porzentajea (%) gutxituz, kontrol taldean agertzen diren antzeko balioetaraino; STean ($99,43 \pm 4,25$; ##### $p < 0,0001$) eta SNen ($107,0 \pm 6,2$; ##### $p < 0,0001$). (9. irudia) Disoluzioan zegoen GDNFaren administrazioak ez zuen mikroglia aktibazioa gutxitu. Horregatik, emaitza hauek berretsi dute CS eta TAT NPen gaitasuna GDNFren garun-mailak handitzeko; eta beraz, efektu terapeutikoa lortzeko. Hain zuzen ere, formulazio honek aktibitate lokomotorea hobetu zuen, THren adierazpena garuneko bi interes-eremuetan handitu zuen, eta, horrez gain, PDari lotutako mikroglia gutxitu zuela frogatu genuen.

Lipido-garraiatzaile nanoegituratu berriak Ω -3 gantz-azido poliinsaturatuetan eta TAT peptidotan oinarritutakoak gaixotasun neurodegeneratiboak tratatzeko



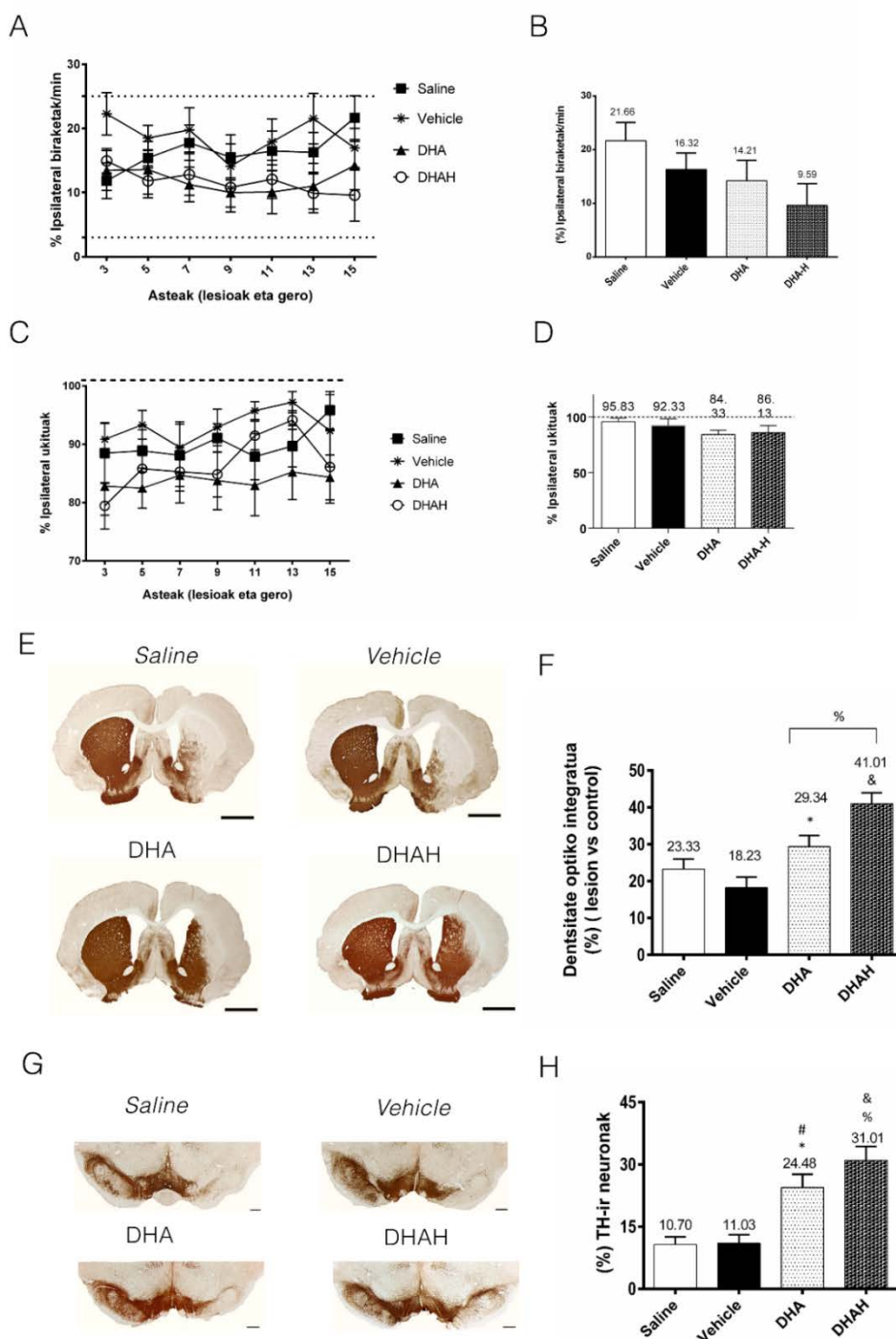
8. Irudia. (A) Aktibitate lokomotorea (* $p < 0,05$ Control vs MPTP; &&&& $p < 0,0001$ CS-NLC-TAT-GDNF vs MPTP; & $p < 0,05$ CS-NLCTAT- GDNF vs CS-NLC-blank, CS-NLC-GDNF; ## $p < 0,05$ CS-NLCTAT- GDNF vs MPTP; # $p < 0,05$ CS-NLC-TAT-GDNF vs CS-NLC-blank; ++ $p < 0,01$ CS-NLC-TAT-GDNF vs MPTP, CS-NLC-blank; + $p < 0,05$ CS-NLC-TAT-GDNF vs CS-NLC-GDNF), *Students t test*. (B) TH immunohistokimika saioaren irudi adierazgarriak SNen arratoi talde guztiarentzako. (C) Dentsitate optiko integratua (IOD) TH zuntza positiboak STen. (%% $p < 0,05$ Control vs MPTP; **** $p < 0,05$ CS-NLC-TAT-GDNF vs MPTP, CS-NLC-GDNF; &&& $p < 0,05$ CS-NLS-TAT-GDNF vs CS-NLC blank; ## $p < 0,05$ CS-NLC-TAT GDNF vs GDNF, *One-way ANOVA*). (D) TH⁺neuronak SNen(%) (**** $p < 0,05$ Control vs MPTP; #### $p < 0,05$ CS-NLCTAT- GDNF vs MPTP, GDNF and CS-NLC-blank; && $p < 0,05$ CS-NLCTAT- GDNF vs CS-NLC-GDNF, *One-way ANOVA*) Datuak batezbestekoa \pm SEM erakusten dira.



9. Irudia. (A) Iba-1⁺ zelua STen irudikapen grafikoa. (****p < 0,0001 MPTP vs Control; #####p < 0,0001 CS-NLC-TAT-GDNF vs MPTP and GDNF. (B) Iba-1⁺ zelula SNen irudikapen grafikoa (****p < 0,001 MPTP vs Control, #####p < 0.0001 CSNLC- TAT-GDNF vs MPTP, GDNF and CS-NLC-blank; &p < 0,05 CSNLC- TAT-GDNF vs CS-NLC-GDNF (*Student's t test*). Datuak batezbestekoa ± SEM erakusten dira. (C) Iba 1⁺ irudi adierazgarriak SNen (irudien eskalak 50µM).

Doktorego-tesi honen bigarren urratsean, NDen neuroinflamazioa hobeto kudeatzeko tratamendu ezberdinak aztertzen jarraitu genituen. Beste molekulen artean, PUFA bezalako lipido funtzionalak erabiltzeak arreta piztu du gaixotasunen prebentzio edota tratamenduan duten paper onuragarriaren ondorioz. Ondorio onuragarrien mekanismo zehatza ezagutzen ez den arren, emaitza positiboak eman dituzte gaixotasunen ezaugarri patologikoak modulatz: estres oxidatiboa, neuroinflamazioa, disfuntzio mitokondrial eta eszitotoxikotasuna [36,39]. Gainera, egindako ikerketa epidemiologikoez, AD eta PD animalia ereduekin batera, euren erabilerari eusten diote [43,75,76]. Lipido funtzional ezberdinen artean, doktorego-

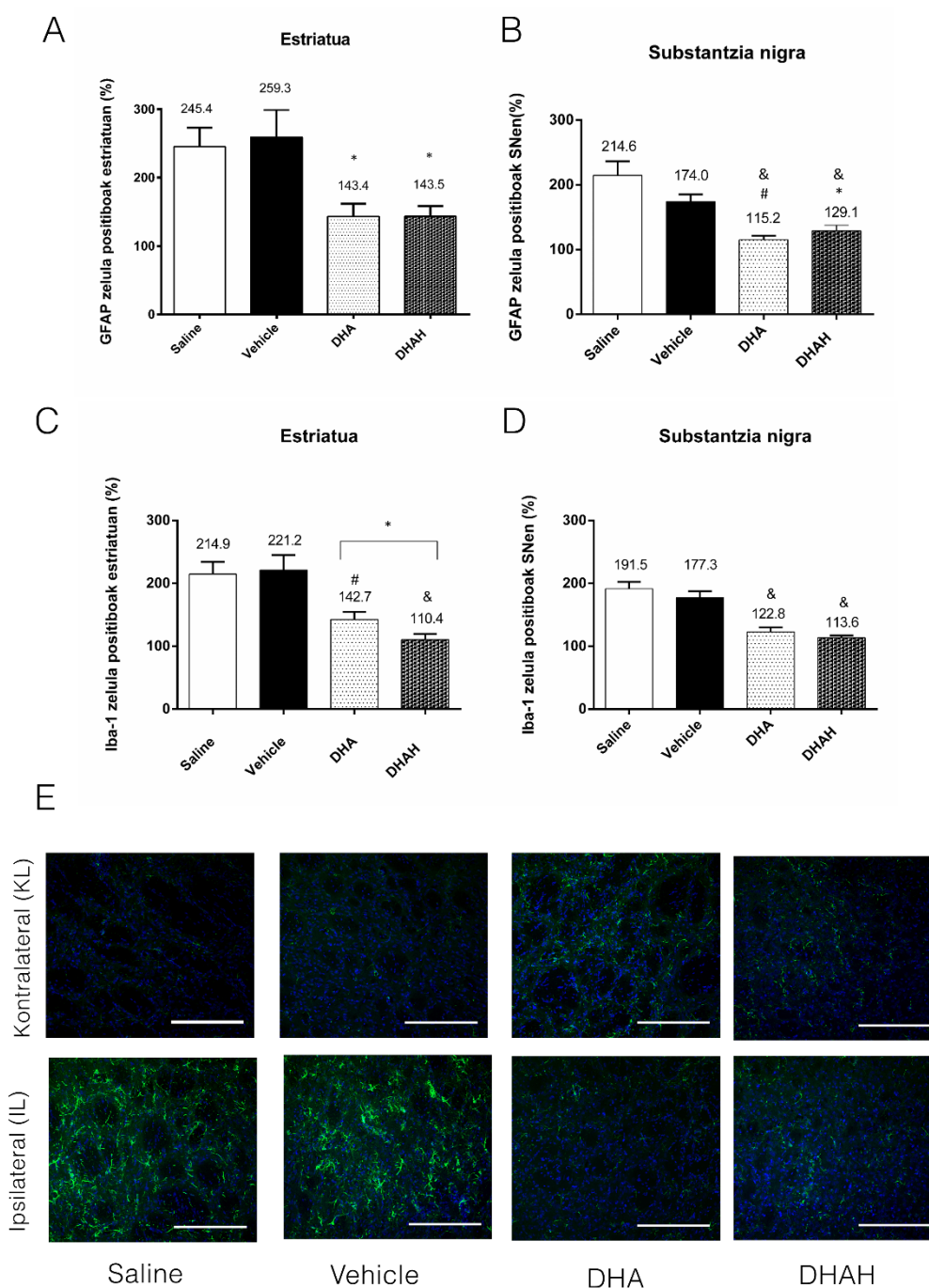
tesi honen ikerlanean DHAn eta bere hidoxilazioaren ondorioz deribatutako DHAHan zentratuko gara. Bi lipido funtzional hauen administrazio kronikoak, DHA eta DHAH eguneroko administrazioak, 6-OHDA lesio neurotoxikoaren aurretik eta ondoren, animalien jokaeraren hobekuntza erakutsi zuen. Nahiz eta eragin positiboa izan, 15 astetan zehar egindako entseguetan ez ziren emaitza estatistikoki esanguratsuak (*Two-way Anova*) lortu; ez anfetamina eragindako biraketa saioan ezta zilindroen saioan ere. PUFAen administrazio kronikoa egiten duten aurreko ikerlanetan honelako emaitzak ikusi ziren ere bai [77,78] (10. A-D Irudia). Hala eta guztiz ere, funtzio lokomotorren hobekuntzaren joera azterketa immunohistokimikoekin berretsi zen, lipido funtzional hauen eragin onuragarria bermatuz. DHAH osagarriak TH⁺ zuntzen dentsitatea handitu zuen (%) ($41,01 \pm 2,93$) ($41,93$), DHA taldearekin konparatuta ($29,4 \pm 3,03$) balio altuagoak erakutsiz. Diferentzia hau handiagoa izan zen *saline* taldearekin, ia bikoiztu egiten baitzituen balioak ($23,33 \pm 2,68$) (10. E-F irudia). Antzeko eran, TH⁺ neurona nigralen balioak altuagoak izan ziren esperimendu talde honetan ($31,0 \pm 3,32$), eta emaitzak antzekoak baina txarragoak izan ziren DHAekin tratatutako taldearentzat ($24,48 \pm 3,17$). Kasu honetan, DHAH tratamenduan zehar zihoan taldearen TH⁺ balioak *saline* ($10,70 \pm 1,89$) taldearenak baino hiru aldiz altuagoak izan ziren (10. G-H. irudia).



10. Irudia. (A) Anfetamina eragindako saioa eboluzioaren irudikapen grafikoa. (B) 15. astean lortutako emaitzen irudikapen grafikoa. (C) Zilindro saioaren irudikapen grafikoa (D) 15. astean lortutako emaitzen irudikapen grafikoa ($p > 0.05$, *Two-way ANOVA*, *Tukey's multiple comparisons test*) (E) THren zuntza positiboak STen. irudikapen grafikoa (irudien eskala 2mm). (F) Dentsitate optiko integratua (IOD) THr zuntza positiboak STen. Datuak batezbestekoa \pm SEM erakusten dira. ($*p < 0.05$ DHA vs Vehicle, $\&p < 0.0001$ DHAH vs Saline eta Vehicle, $\%p < 0.01$ DHAH vs DHA), *One-way ANOVA*, *Tukey's multiple comparisons test*). (G) TH⁺ zelulak SNen irudikapen grafikoa (irudien eskala 500µm). (H) TH⁺ neuronak in SN (%). Datuak batezbestekoa \pm SEM erakusten dira. ($\&p < 0.05$ DHA vs vehicle, $*p < 0.01$ DHA vs saline, $\&p < 0.0001$ DHAH vs saline $\%p < 0.001$ DHAH vs vehicle), *One-way ANOVA*, *Tukey's multiple comparisons test*.

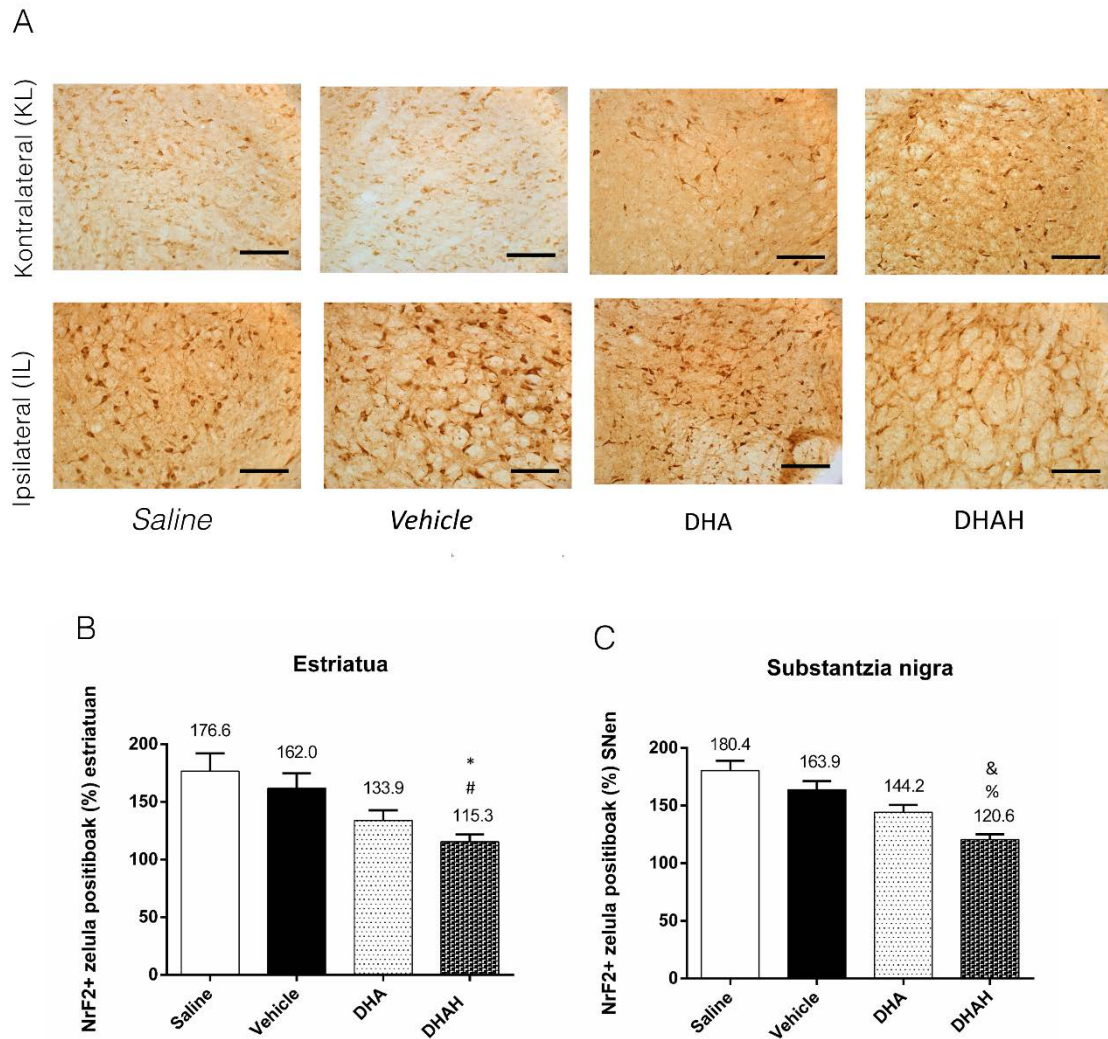
Gainera, PUFAek neuroinflamazioaren aurkako efektua dutela ezagutzen da [79]. Horregatik, hain zuzen ere, bere administrazioak gliosi errektiboa gutxitu dezake, PDan dagoen neuroinflamazioa moldatuz [80]. Ikerketa honetan, PUFAak 6-OHDA animalia ereduaren dagoen astrogliosisia eta mikrogliosisia gutxitzeko dituen gaitasuna berretsi dugu. Astrogliaren GFAP markatzailea DHAREN ($143,4 \pm 18,4$) ($115,2 \pm 3,3$) eta DHAHAREN ($129,0 \pm 8,4$) ($129,1 \pm 8,4$) tratamenduaren ondoren murriztu egin zen, ST eta SN garuneko interesdun bi eremuetan, hurrenez hurren (11. A-B, E irudia). Gainera, aurreko ikerketan bezala, lipido funtzional horiek mikroglia aktibazioan duten eragina ere egiaztatu genuen. Kasu honetan, DHAREN eguneroko tratamenduak 6-OHDA toxikoaren ondoren dagoen mikrogliosisia murriztu zuen, bai STean ($142,7 \pm 11,8$) zein SNn ($122,8 \pm 7,59$) (11. C-D irudia). Iba-1⁺ zelulen beharokada agerikoagoa izan zen DHAH tratamenduaren ondoren STan ($110,4 \pm 9,2$) eta SNan ($113,6 \pm 3,8$) kontrol taldeko antzeko balioekin. Izan ere, DHAK astrogliosisia eta mikrogliosisia murrizteko duen ahalmena aurretik deskribatu da *in vitro* eredu desberdinekin [81-84]. Orokorrean, ikerketa honetan lortutako emaitzak aurreko argitalpenekin bat datoz, DHAH administrazioaren ondoriozko eragin positiboa erakutsiz, astrogliosisia eta mikroglia zelula positiboak gutxituz. Hori dela eta, gliaren jardura normalizatzen dute PDak zauritutako garunean.

Azkenik, lipido funtzional horien eragina bide antioxidatzailean (ARE / Nrf2) aztertu genuen. Izan ere, estres oxidatiboa PDaren ezaugarria da eta, beraz, terapia antioxidatzailea tratamendu gisa proposatu da [85]. 6-OHDA neurotoxinaren ondoren ikusitako Nrf2 bidearen aktibazioa DHAH administrazioaren ondoren gutxitu egin zen STan ($115,3 \pm 6,6$) eta SNan ($120,6 \pm 4,8$) antzeko balioak lortuz (12. irudia). Kasu honetan, DHAREN administrazioak Nrf2⁺ zelulak gutxitu zituen intereseke bi guneetan. Hala ere, ez zen estatistikoki esanguratsua izan, kultibo zelularretan edo neuroinflamazioaren animalia ereduaren ikusitakoaren kontrara [86,87]. Laburbilduz, bigarren ikerketa esperimental honetan lortutako emaitza guztiek DHAHa lipido funtzional gisa erabiltzea onartzen dute, sistema dopaminergikoan, neuroinflamazioan eta estres oxidatiboan eragin positiboa izan baitzuen.



11. Irudia. (A) GFAP⁺ zelulak estriatuan arratoi talde guztientzako (%). (* $p < 0,05$ DHA vs saline and vehicle) (* $p < 0,05$ vs saline and vehicle). (B) GFAP⁺ zelulak SNen arratoi talde guztientzako (%). (& $p < 0,0001$ DHA vs saline, # $p < 0,01$ DHA vs vehicle) (& $p < 0,0001$ DHAH vs saline, * $p < 0,05$ DHAH vs vehicle). Datuak batezbestekoa \pm SEM erakusten dira (*One-way ANOVA Tukey's multiple comparisons test*) (C) Iba-1⁺ zelulak estriatuan arratoi talde guztientzako (%). (* $p < 0,01$ DHA vs saline and vehicle) (& $p < 0,0001$ DHAH vs saline and vehicle) (* $p < 0,05$ DHAH vs DHA). (D) Iba-1 zelulak SNen arratoi talde guztientzako (%). (& $p < 0,0001$ DHA vs saline, and vehicle) & $p < 0,0001$ DHAH vs saline and vehicle), *unpaired Student's t-test*. Datuak batezbestekoa \pm SEM erakusten dira. (E) GFAP⁺ STen irudi adierazgarriak (irudien eskala 10 μ m). Urdina nukleoak tindatzen ditu eta berdea GFAP⁺ zelulak tindatzen ditu.

Lipido-garraiatazaille nanoegituratu berriak Ω -3 gantz-azido poliinsaturatuetan eta TAT peptidotan oinarritutakoak gaixotasun neurodegeneratiboak tratatzeko

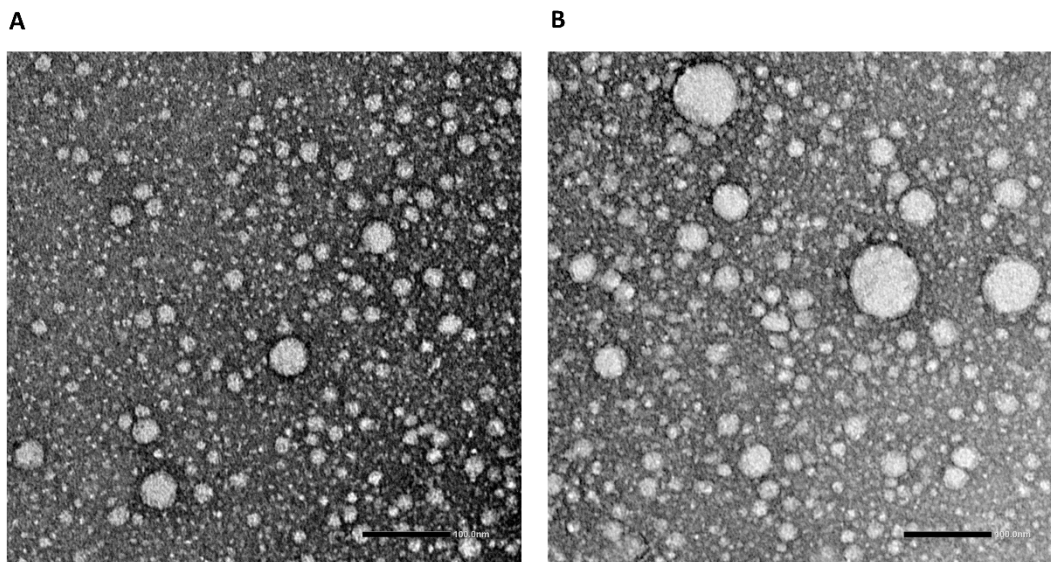


12. Irudia. (A) Nrf2 SNen irudi adierazgarriak. (irudien eskala $2\mu\text{m}$) (B) Nrf2⁺ zelulak STen arratoi talde guztientzako. (* $p < 0.01$ DHAH vs saline; * $p < 0.05$ DHAH vs vehicle). (C) Nrf2⁺ zelulak SNen arratoi talde guztientzako (%) (& $p < 0.0001$ DHAH vs saline) (% $p < 0.001$ DHAH vs vehicle), Datuak batezbestekoa \pm SEM erakusten dira. (One-way ANOVA, Tukey's multiple comparisons test).

Behin DHAH NDtan dagoen neuroinflamazioa eta estres oxidatzailea modulatzeko lipido funtzional egokia zela frogatu genuenean, hirugarren ikerketa esperimentalak diseinatu genuen DHAHa nanoformulazio lipidikoen matrizean sartzeko, NLC berria garatuz.

Garatutako nanoformulazio guztiek (1. taula) 50-90 nm bitarteko tamaina zuten, PDIaren balioa 0.5etik beherakoa izanik, suspentsioa homogenea zela baieztatuz. Mygliol eta DHAH, bi lipido desberdinetarako hautatutako solido:likido ratioa NLCak prestatzeko erabiltzen den proportzio normalean zegoen [27]. Garatutako NPEk antzeko tamaina zuten, 100 nm ingurukoa, eta zeta potentziala balio positiboak

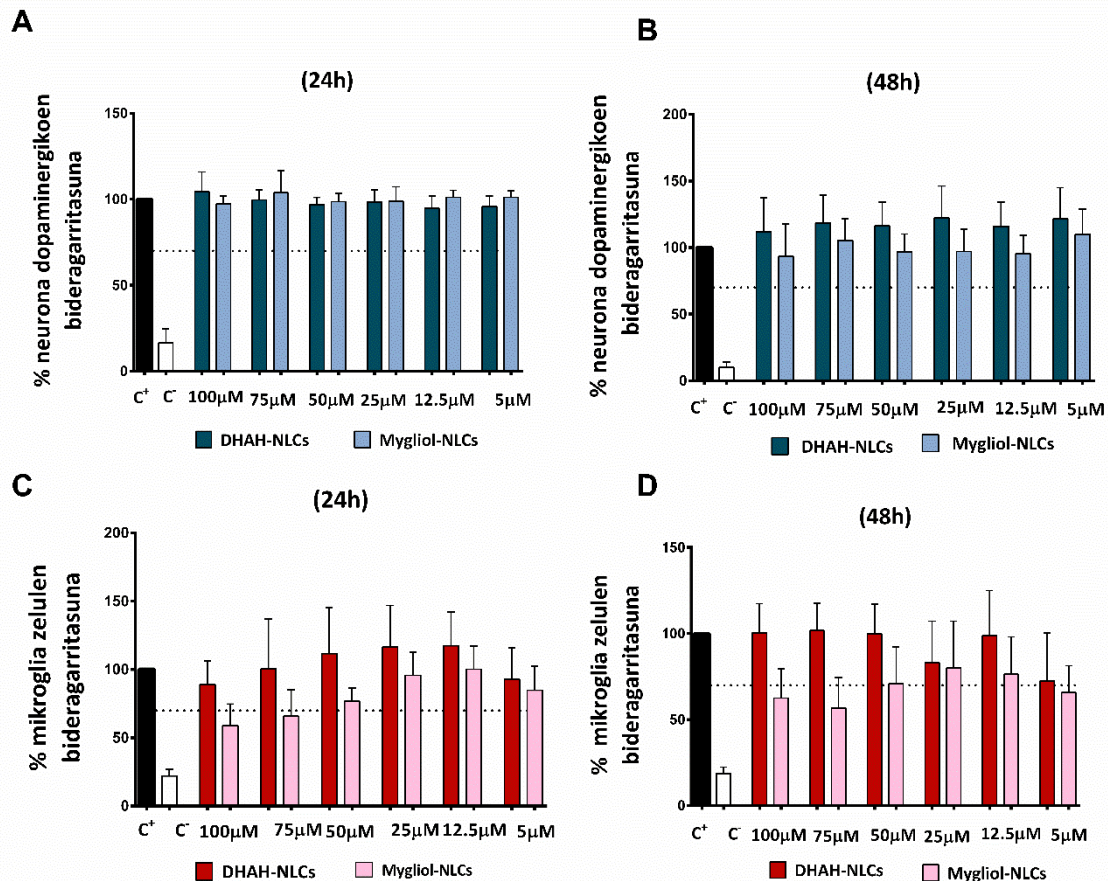
erakutsi zituzten, CS eta TAT estaldura prozesua arrakastatsua izan zela adieraziz. TEM irudiek erakutsi zuten NPak uniformeak zirela morfologian eta tamainaren dispersioetan (13. irudia).



13. Irudia. NLCen TEM irudiak (irudien eskala 100 nm). (A) DHAH-NLCak (B) Mygliol-NLCak.

Hirugarren ikerlanean saio desberdinak egin ziren *in vitro* zelula kultiboetan, DHAHren ezaugarri onuragarriak mantentzen dituzten nanoformulazio horien eraginkortasuna ebaluatzeko. Hasteko, DHAHrekin garatutako NLCak neurona dopaminergikoen kultibo zelularretan probatu ziren. Nanoformulazioak frogatutako kontzentrazio guztietan seguruak zirela ikusi zen (100 μ M, 75 μ M, 50 μ M, 25 μ M, 12,5 μ M eta 5 μ M) % 70-erainoko bideragarritasun emaitzekin. Gainera, DHAH-NLCtek balio hobeak erakusten zituzten 48 ordutan neurona dopaminergikoen kultibo zelularretan (14. A-B irudia). Bestalde, DHAH-NLCen eraginkortasuna agente neurobabesle gisa egiaztatzeko, zelula dopaminergikoak formulazio honekin tratatu ziren 25 μ M 6-OHDA neurotoxinarekin inkubatu aurretik eta ondoren. DHAH-NLCek zelulak neurotoxinatik babesteko eraginkorrak zirela erakutsi zuten, Mygliol-NLCekin alderatuta (15. A, E irudia). Datu hauek bat datoz neurona zelulen kultiboetan DHAK duen efektu neurobabeslearekin [88,89]. Beraz, aurreko ikerlanak baieztatutako (II. Ikerlana) DHAHri buruz ezagutzen diren efektu neurobabesleak DHAH-NLCtan mantentzen direla esan dezakegu.

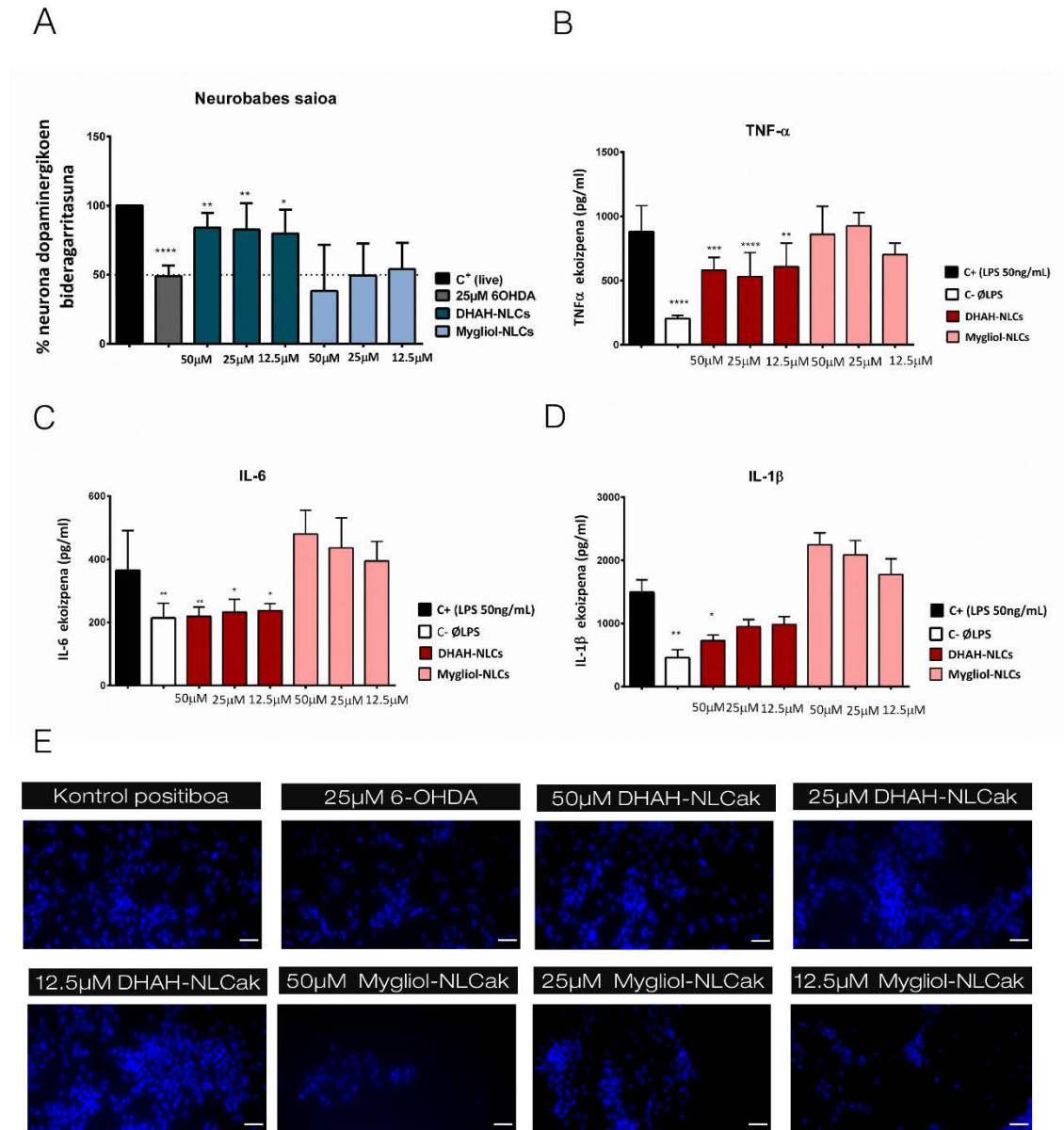
Bestalde, lehen bezala, gure nanoformulazioak NDetan agertzen den neuroinflamazioa gutxitzeko duen gaitasuna egiaztatzea dugu helburu. Lehenik eta behin, bi nanoformulazioen segurtasuna frogatzeko (DHAH-NLC eta Mygliol-NLC) lehen aipatutako kontzentrazio guztietan probatu zen mikroglia kultibo zelularretan. Saio honetan, DHAH-NLCak seguruak direla erakutsi zen, % 70erainoko bideragarritasuna izan baitzuten edozein kontzentrazioetan, Mygliol-NLCek, berriz, kontzentrazio handienetan zelulen bideragarritasuna gutxitu zuten (14. C-D irudia).



14. Irudia. (A) Neurona dopaminergikoen bideragarritasuna 24 ordutan (24h) (B) Neurona dopaminergikoen bideragarritasuna 48 ordutan (48h). (C) Mikroglia zelulen bideragarritasuna 24 ordutan (24h) (D) Mikroglia zelulen bideragarritasuna 48 ordutan (48h). Kasu guztietan, DHAH-NLCren eta Mygliol-NLCren kontzentrazio ezberdinak testatu ziren Hiru erreplikazio biologikoren emaitzak agertzen dira grafikoan (batezbestekoa \pm SEM).

Kontzentrazioak zehaztu ondoren, nanoformulazio hauek LPS estimuluarekin aktibatutako mikrogliaekin inkubatu genituen. LPSa gehien erabiltzen den estimulu pro-inflamatorioa da, gliosia sortu eta neuroinflamazio-jauzia aktibatzen baititu. [90-92]. LPSa 50 ng/ml-tako kontzentrazioan erabiliz, zitokina inflamatorioen askapenaren maila jadanik argitaratutakoaren antzekoa izan zen [91]. Goranzko

erregulazio hori DHAH-NLCak administratu ondoren leheneratu zen. Hori dela eta, DHAH-NLCen barnean, DHAHak neuroinflamazioa gutxitzeko duen gaitasuna mantendu zuela esan dezakegu, IL-6 eta IL-1 β en zitokinen mailak C⁻ren antzeko balioak izan baitzuten eta TNF- α ren balioak ia erdira murriztu baitziren probatutako edozein kontzentrazioetan. (15. B-D irudia). Beste PUFA batzuek, hala nola, DHA edo EPA (azido eikosapentaenoikoa), zitokina inflamatorioen mailak gutxitzeko duten gaitasuna aurretik azaldu da [93]. Horrela, ikerketa honek NLCTan formulatutako lipido funtzional mota horien erabilera indartzen du, NDtan gertatzen den neuroinflamazio prozesua tratatzeko tresna baliogarri gisa. Orokorrean, emaitza hauek agerian uzten dute garatutako nanoformulazio berri hau NDak tratatzeko tresna terapeutiko berria izan daitekeela. DHAH-NLCen tamaina, PDla, zeta potentzialaren balioa eta TEMen behatutako morfologia antzekoak ziren aurretik garatutako NLCKin konparatuta. Gainera, neurona dopaminergikoen kultibo zelular eredu batean eragin neurobabesleak erakutsi zituzten eta mikroglia kultibo zelularretan neuroinflamazioaren aurkako ezaugarriak behatu ziren, zitokinen mailak gutxituz.



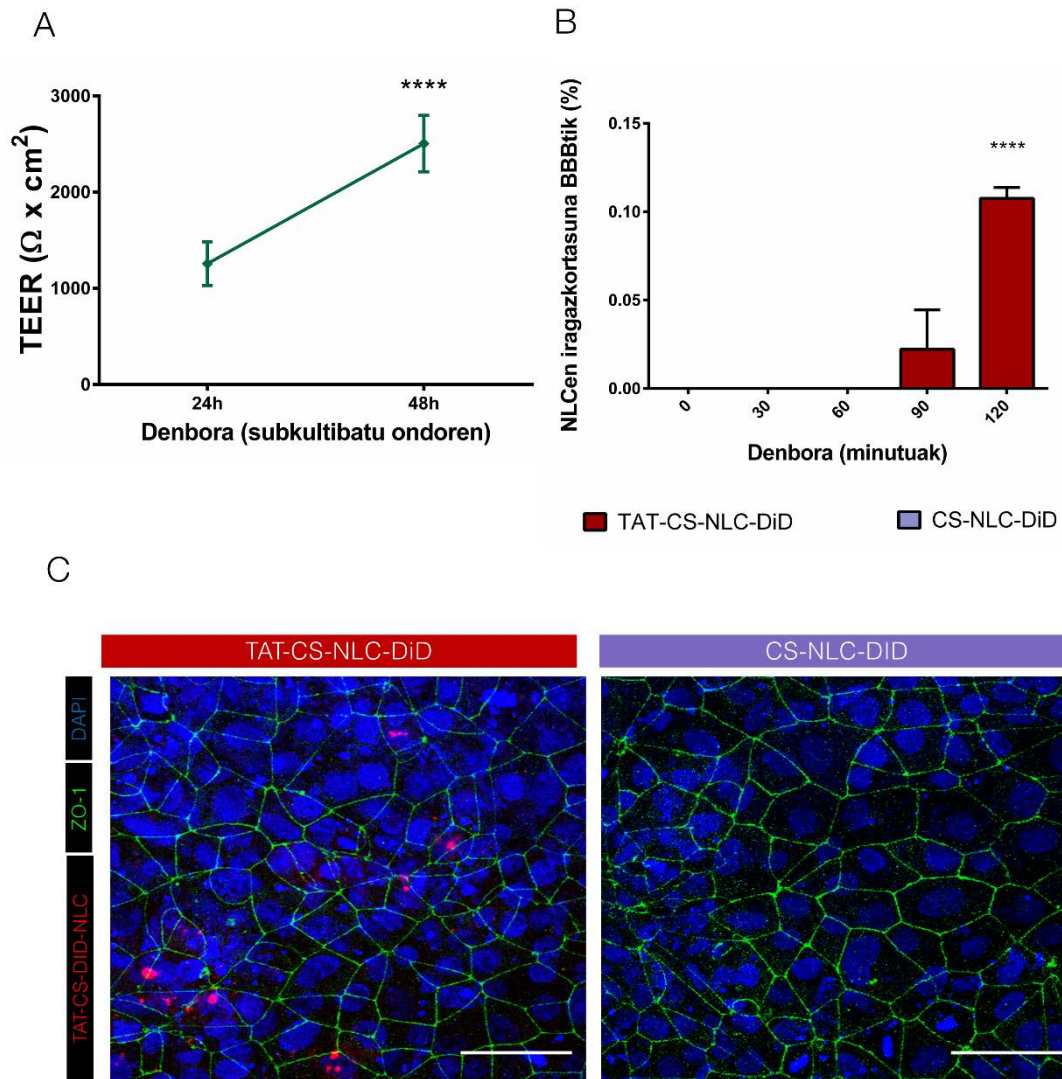
15. Irudia (A) DHAH-NLCen neurobabes saioaren irudikapen grafikoa. (** $p < 0,01$ 25 μ M 6-OHDA vs 50 μ M DHAH-NLCak and 25 μ M DHAH-NLCak, * $p < 0,05$ 25 μ M 6-OHDA vs 12.5 μ M DHAH-NLCak), *One-way ANOVA*. (B) TNF- α -ren balioak (pg/ml) NLC ebaluatutako kontzentrazio ezberdinarentzako. (**** $p < 0,0001$ C⁺ vs C⁻ and 25 μ M DHAH-NLCak, *** $p < 0,001$ C⁺ vs 50 μ M DHAH-NLCak, ** $p < 0,01$ C⁺ vs 12.5 μ M DHAH-NLCak), *One-way ANOVA* (C) IL-6-en balioak (pg/ml) NLC ebaluatutako kontzentrazio ezberdinarentzako. (** $p < 0,01$ C⁺ vs C⁻ and 50 μ M DHAH-NLCak, * $p < 0,05$ C⁺ vs 25 μ M DHAH-NLCak and 12,5 μ M DHAH-NLCak), *One-way ANOVA*. (D) IL-1 β -ren balioak (pg/ml) NLC ebaluatutako kontzentrazio ezberdinarentzako. (** $p < 0,01$ C⁺ vs C⁻ and * $p < 0,05$ C⁺ vs 5 μ OM DHAH-NLCak), *One-way ANOVA*. (E) Neurobabesle saioaren irudi adierazgarriak DAPI tindaketarekin. (irudien eskala 50 μ M).

Amaitzeko, doktorego-tesi honen azken lan esperimentalean, nano-garraiatzaile (DHAH-NLC) seguru eta eraginkor berri honen konbinazioa GDNF edo VEGF bezalako molekula terapeutikoekin aztertu genuen. Honela, modu sinergikoan

jokatuz NDak tratatzeko tresna berri batean bihurtu daitekeen frogatu nahi genuen. Gainera, garatutako nano-garraiatzaile berri honen igarotzea BMCE kultibo zelularrean zehar aztertu genuen, giza BBB *in vitro* eredu batean. Nanoteknologian oinarritutako DDSak emaitza itxaropentsuak erakutsi baditu ere, tratamendu farmazeutiko guztiek azterketa prekliniko zorrotzak behar dituzte haien toxikotasuna eta eraginkortasuna ebaluatzeko. *Organ-on-chip* plataformak giza fisiologiaren alderdi garrantzitsuak barneratuta dituzten saioentzako euskarri bat dira, honela sendagaien efektua eta toxikotasuna ikertzeko tresna fidagarriago bat lor daitekeelarik [52,94].

Giza BBBa imitatzeke eredu desberdinen artean, hIPSCetatik desberdintzatsutako BMCEak hautagai onak dira, BBBaren azterketa preklinikoak egiteko, baita molekula ezberdinen BBBa zeharkatzeko duten gaitasuna aztertzeke ere [95,96]. Ikerketa honetan lortutako TEER balioek, $3.000 \Omega \times \text{cm}^2$ ingurukoak, (16. A irudia) eredu honen egokitasuna berretsi zuten, molekula txiki eta handien BBBaren igarotzea ikertzeko [97]. Ikerketa honetan, frogatu genuen TAT peptidoarekin eraldatutako NLC nanoformulazioak BMCEetan zehar igarotzeke ahalmena zuela, 16B irudian kuantitatiboki eta 16C irudian kualitatiboki ikusten den bezala. NPen gainazala TAT bezalako peptido batekin eraldatzeak, zeina normalean zelulen mintzetan zehar molekula desberdinen igarotzea handitzeke erabiltzen den ohiko estrategia dena [98], NP horien igarotzea hobetu zuen BBB *in vitro* eredu honetan. Funtzionalizatutako NPekin egindako beste iragazkortasun azterketek emaitza hobek erakutsi badituzte ere [99-102], hauek bEnd.3D zelula ereduak edota TEER balio baxuagoak, $200 \Omega \times \text{cm}^2$ ingurukoak, dituzten HBMCE zeluletan egin ziren, lortutako datu klinikoak eta iragazkortasun balioak fidagarriak ez direla agerian uzten duena [103.104]. Hori dela eta, burututako iragazkortasunaren azterketa fidagarriagoa da erabilitako giza BBB ereduak eta, gainera TAT peptidoarekin partikulen gainazala eraldatzeak garunera iristeko duen egokitasuna berresten du.

Lipido-garraiatzaile nanoegituratu berriak Ω -3 gantz-azido poliinsaturatuetan eta TAT peptidotan oinarritutakoak gaixotasun neurodegeneratiboak tratatzeko

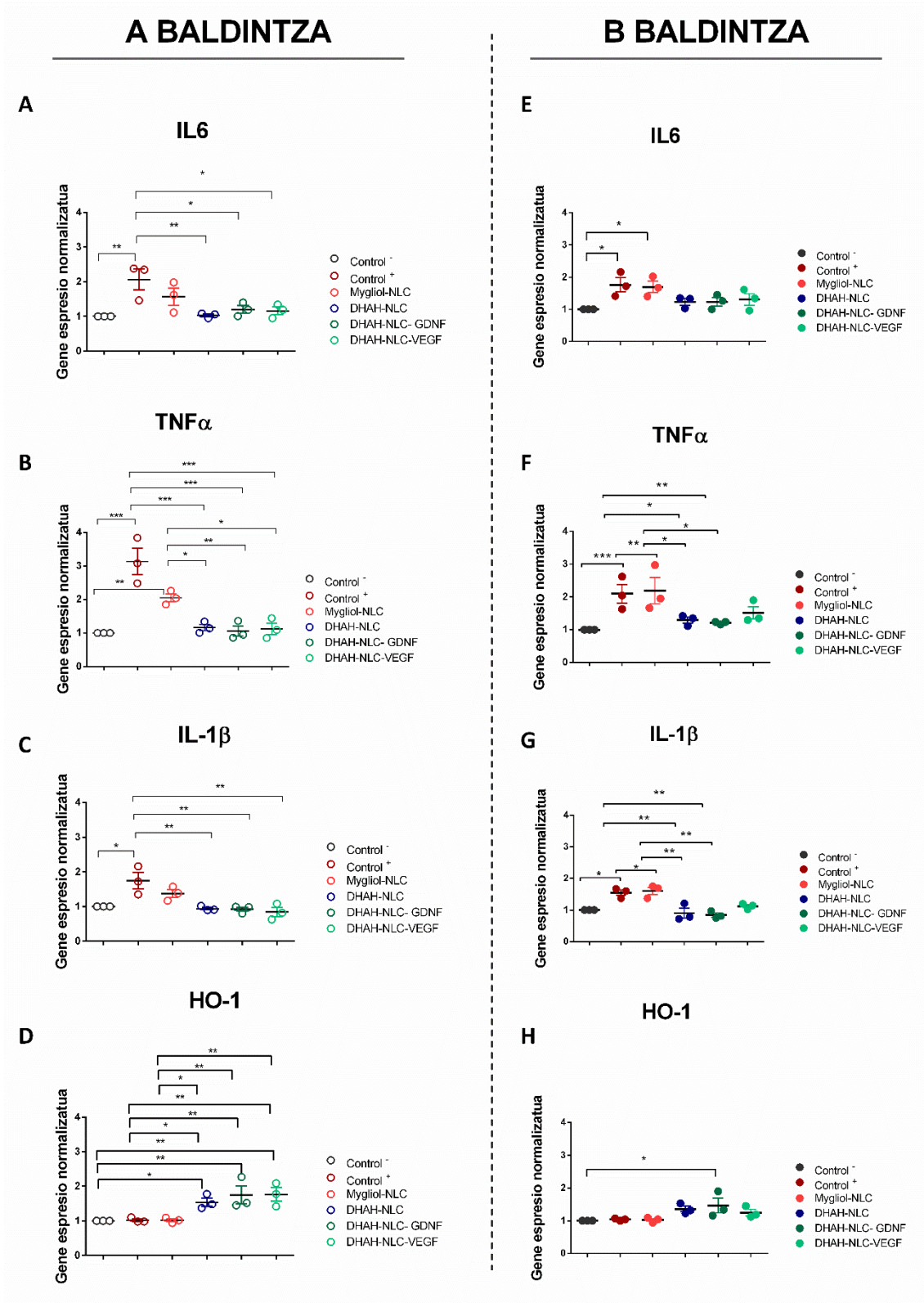


16. Irudia. (A) TEERen balioak subkultibatu ondoren *Transwell*[®] plaketan bi denbora une ezberdinetan (24h) (48h) (**** $p < 0.0001$ TEER balioak 24 h vs. TEER balioak 48 h). (B) NLCak BMCEtik egindako iragazkortasun saioaren irudikapen grafikoa. (%) (**** $p > 0.0001$ TAT-CS-DiD-NLC vs CS-DiD-NLC, *One way ANOVA*) 2 ordu (2h) denbora unean. (C) Immunofluoreszentiako irudiak ZO-1 eta DAPI tindaketak. TAT-CS-DiD-NLCak BMCEan ikus daitezke kualitatiboki. (Irudien eskala 50 μ M).

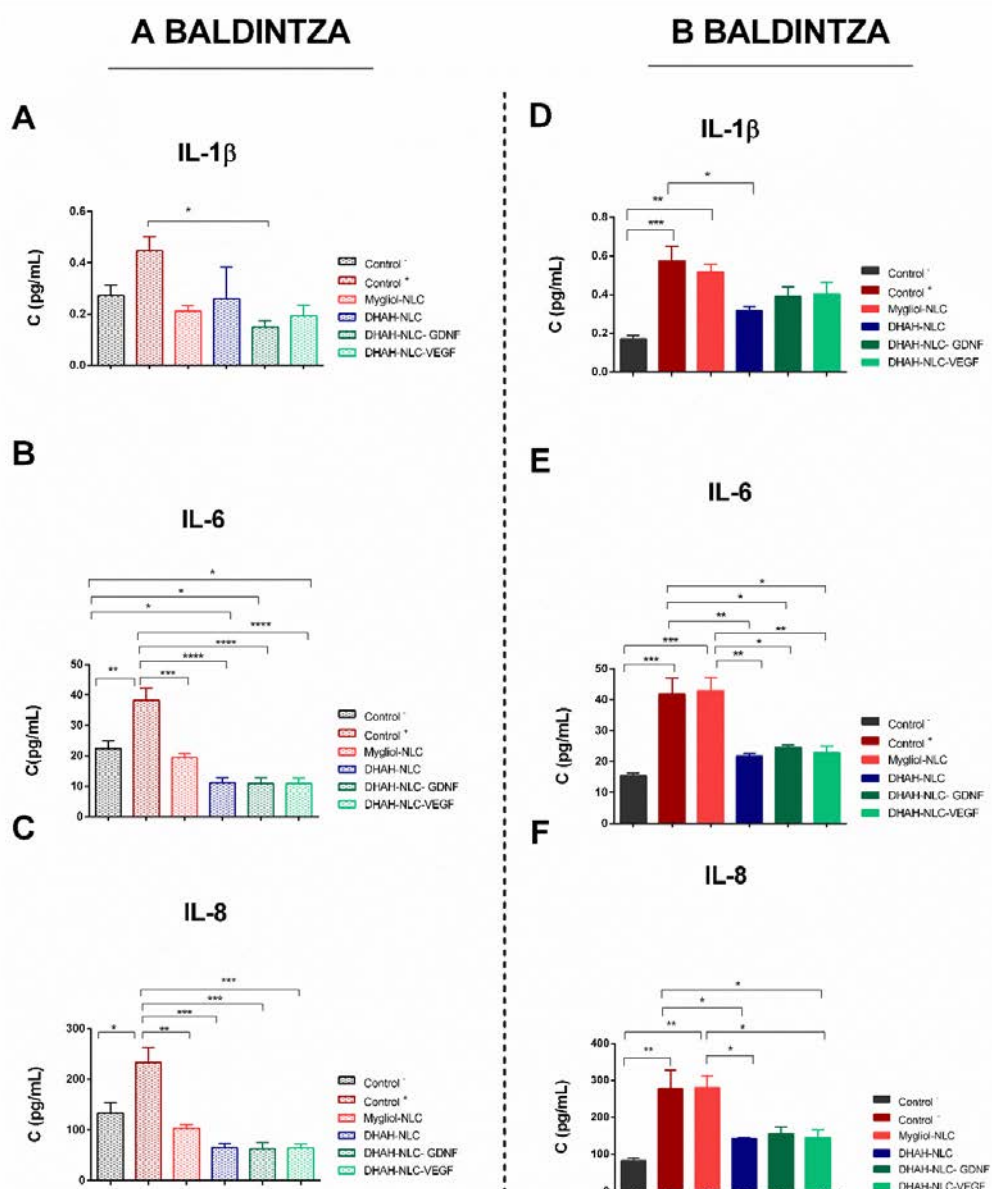
Bestalde, aurretik azaldu bezala, mikroglia etengabeko kalte neuronala areagotzen duen faktore eragile giltzarri gisa planteatu da [105]. Gainera, mikroglia buruzko ikerketek agerian utzi dute funtsezko alderdia dela NVUa ulertzeko osasunean zein gaixotasunean. Azterketa esperimetal honetan, LPS estimuluaren ondorioz sortutako neuroinflamazioa HMC3 giza zelula mikroglialean leheneraztea da gure helburua. LPS estimuluarekin inkubatu aurretik, garatutako nanoformulazio berriak zelula mikroglial eredu honekin inkubatu genituen. Probatutako

nanoformulazioetako batek ere ez zuen HMC3 zelulen inflamazio patroia aldatu (17. A-C irudia eta 18. A-C irudia); beraz, ondoriozta dezakegu LPSaren ondorioz sortutako neuroinflamazio egoera estimulu horren emaitza dela, ez NLC ezberdinekin inkubatzearagatik. DHAH-NLC tratamenduarekin LPSren ondoren sortutako neuroinflamazioa gutxitu egin zen; hala ere, efektu hori ez zen Mygliol-NLCekin ikusi (17. E-G irudia eta 18. D-F irudia). Datu hauek DHAH lipido funtzionalarekin garatutako nanoformulazioaren efektu antiinflamatorioa nabarmentzen dute. Jadanik Ω -3 gantz azidoek neuroinflamazioaren aurkako efektuak dituztela ezagutzen zen [93,106], eta lan esperimental honekin egiaztatuz NLC matrizean formulatu ondoren mantentzen direla. GDNF edo VEGF eta DHAHaren arteko efektu sinergikoa ikusi nahian, DHAH-NLC-GDNF eta DHAH-NLC-VEGF formulazioak garatu genituen, bi terapeutikoak batera administratzeko. Nahiz eta GDNF eta VEGFak mikroglian efektu onuragarriak dituztela ezagutzen den,[72,107] (9. irudia) kasu honetan ez genuen efektu sinergikorik ikusi (17. E-G irudia eta 18. D-F irudia). Neuroinflamazio egoeraren murriztea ikus zitekeen arren, VEGFak ezta GDNFak ere ez zituzten DHAH-NLC tratamenduaren ondoren lortutako emaitzak hobetu. Egia esan, mikrogliaren aktibazioa gutxitzean VEGFak duen paperari buruz argitaratutako lanak ez dira erabakigarriak [108]. GDNFari dagokionez, azken ikerketa batek azpimarratzen du GF honek mikroglian sortzen duen efektu antiinflamatorioa oxidazio-sistema endogeno baten aktibazioagatik izan daitekeela, ez TNF- α edo IL-6 bezalako zitokina inflamatorioen murrizketagatik [109].

Hipotesi hau gure datuekin bat dator. Izan ere, ikerketa honetan NR2 / HO-1 bide anti-oxidatiboa aztertu da, NDtan sortzen den estres oxidatiboa eta neuroinflamazioa tratatzeko estrategia gisa planteatu baita [110]. 17. H irudian agertzen den bezala, DHAH-NLC-GDNFrekin egindako tratamenduak gene horren adierazpena areagotu zuen, baita neuroinflamazio testuinguru batean ere. DHAHak bide hori indartzeko duen gaitasuna jada deskribatu da arratoi hemiparkisonianoetan egindako lan batean [40] (12. irudia). HO-1 geneen adierazpena DHAH nanoformulazio guztiekin handitu zen arren (17. H irudia), GDNFarekin batera emandako administrazioak soilik lortu zituen emaitza esanguratsuak. Emaitza horietan, GDNFaren efektua sistema anti-oxidatzailearen aktibazioan agerian uzten da eta bat dator argitaratutako azken lan esperimentalekin [109,111].



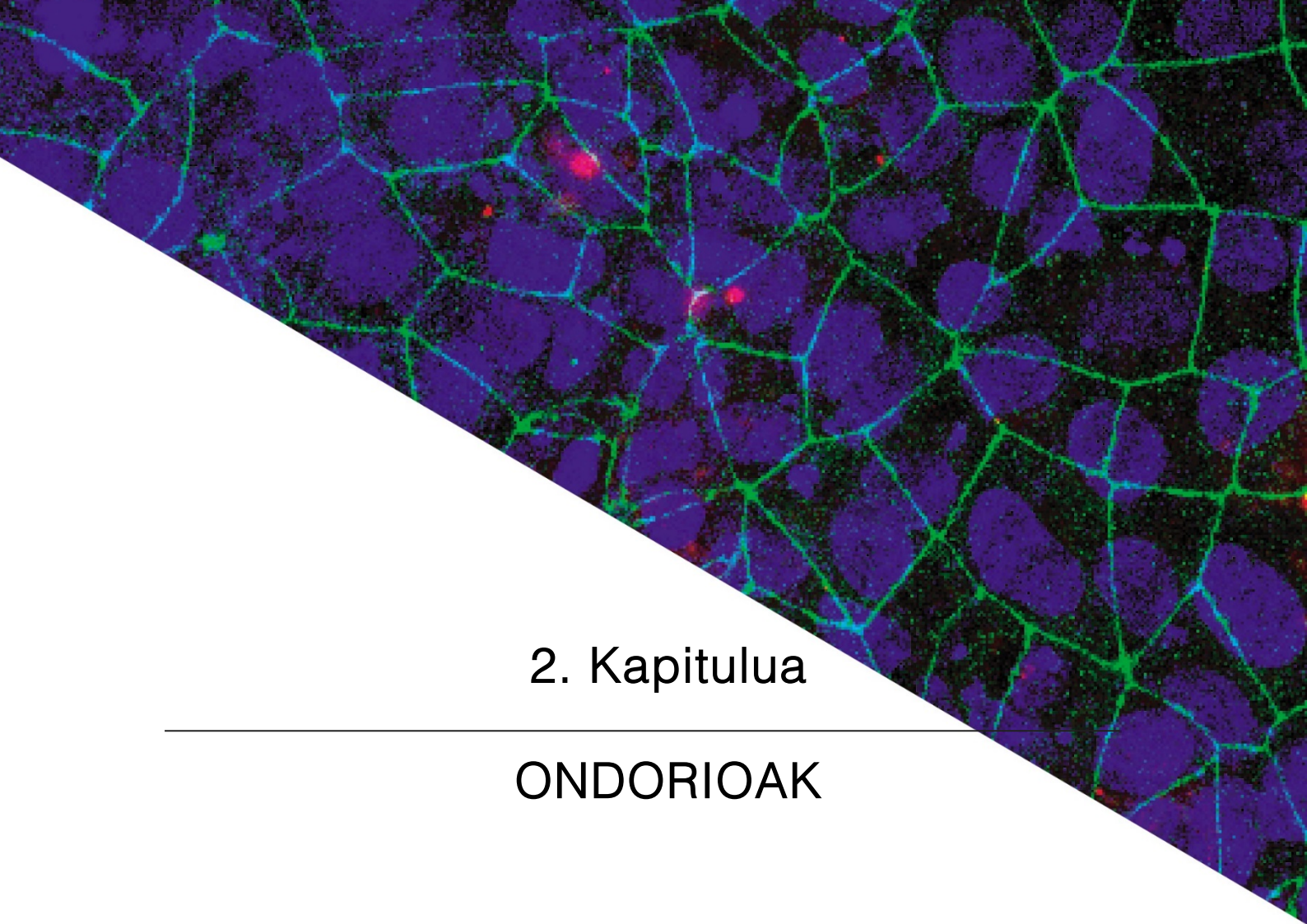
17. Irudia. Gene espresioaren analisia (RT-qPCR). mRNA irudikapen grafikorako erabili zen eta analisi estatistikoa egiteko Δ CTren balioak erabili ziren. Normalizazioa egiteko GAPDH genea erabili zen (A) IL6 (B) TNF- α (C) IL-1 β eta (D) HO-1 A baldintzarako. (E) IL6 (F) TNF- α (G) IL-1 β eta (H) HO-1 B baldintzarako. * p <0.05 ** p <0.01 *** p <0,001, *One- Way ANOVA*.



18. Irudia. Multiplex saioaren balioak. (A) IL-1 β (B) IL-6 and (C) IL-8 A baldintzarako. (D) IL-1 β (E) IL-6 and (F) IL-8 B baldintzarako. * $p < 0,05$ ** $p < 0,01$ *** $p < 0,001$, **** $p < 0,0001$; *One-Way ANOVA*.

Laburbilduz, ikerketa honek TATren bidez funtzionalizatutako NLCak BBBa zeharkatuz garunera heltzeko eta horrela CNSari loturiko gaixotasunak tratatzeko tresna eraginkor gisa erabiltzea indartzen du. Gainera, DHAH lipido funtzionalarekin osatutako NLCek efektu positiboak erakutsi zituzten NDetan agertzen den neuroinflamazioa eta estres oxidatiboa modulatuaz giza mikroglia zelula lerroan. Efektu onuragarri hori GDNFaren administrazioarekin batera hobetu zen, estrategia sinergiko bideratua ahalbidetuz ND desberdinetan dagoen neuroinflamazioa eta BBB-mikroglia elkarreragina tratatzeko.

Erreferentzia zerrenda 46-52 orrialdeetan aurkitzen da



2. Kapituluua

ONDORIOAK

Doktorego-tesi honetako ikerketa esperimentaletan lortutako emaitzetatik honako ondorioak eratorri daitezke.

1. CS eta TATrekin gainazala eraldatuta duten NLCen garapena arrakastaz administratu zen sudur bidetik PD animalia-ereduan, haien aktibitate lokomotorea berreskuratuz, garuneko interes eremuetan THren adierazpena areagotuz eta gaixotasunari lotutako mikrogliosia gutxituz.

2. DHAH lipido funtzionalaren eguneroko administrazio kronikoak 6-OHDA PD arratoi ereduan aktibitate lokomotorea hobetzeko joera erakutsi zuen. Efektu hau animalien sistema dopaminergikoan izan zituen eragin positiboekin baieztatu zen, hau da, TH adierazpena handitzearekin. Gainera, DHAHaren administrazioak PD animalia eredu honetan agertzen diren neuroinflamazioa eta estres oxidatiboa modulatu zituen.

3. DHAH lipido funtzionalarekin eta CS eta TAT estaldura erabiliz garatutako NLCen tamaina, Z potentziala eta TEM irudien bidez behatutako morfologia, aurretik garatutako NLCen antzekoak izan ziren. Gainera, nano-garraiatazaila berri hauek DHAH lipido funtzionalaren gaitasuna mantentzen dute, neurona eta mikroglia kultibo zelularretan dituzten ezaugarri neurobabesle eta antiinflamatorioei dagokienez.

4. CS eta TATrekin DHAHan oinarritutako nanopartikulen funtzionalizazioa giza BBBaren *in vitro* eredua zeharkatzeko tresna baliagarria dela frogatu zen, eredu hori hIPSCetatik desberdintzatutako BMCEetan oinarrituta zegoelarik. Iragazkortasunaren emaitzak erakutsi dute nanoformulazio berri hau CNSrekin lotutako gaixotasunak bideratzeko eta tratatzeko hautagai ona dela.

5. DHAH lipido funtzionala NLC lipidoen matrizerara gehitzeak eragin positiboa erakutsi du giza mikroglia kultiboan dagoen neuroinflamazioa eta estres oxidatiboa modulatzuz. Efektu onuragarri hau GDNFa NLCtan kapsularatu zenean areagotu zen, eta itxaropenezko terapia sinergikoa izan liteke farmakoak CNSra bideratzeko eta NDCtan dauden BBB-mikrogliaelkarrekintzak tratatzeko.

